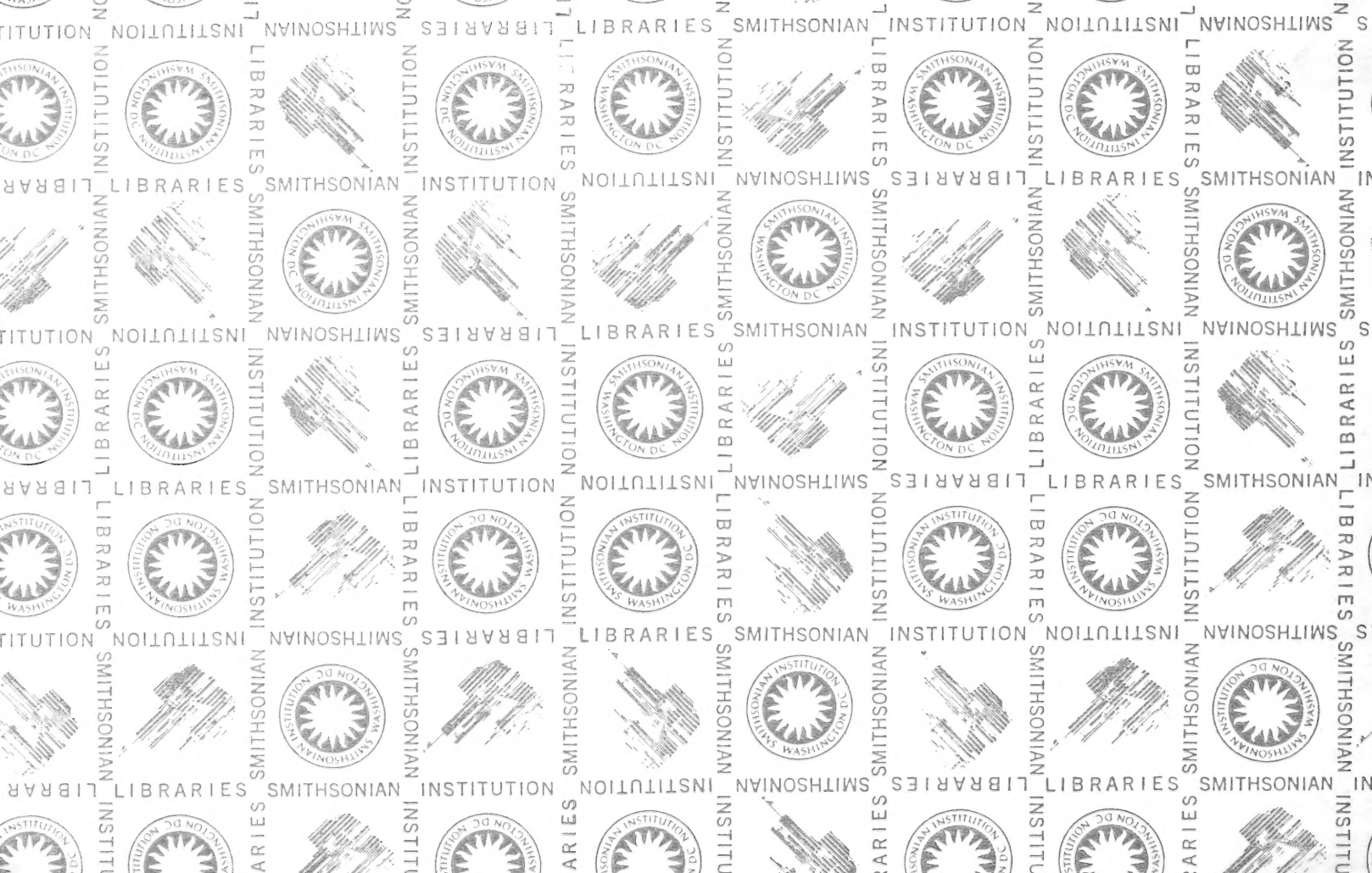
SMITHSONIAN INSTITUTION LIBRARIES

BULLETINS

OF

AMERICAN PALEONTOLOGY

★

VOL. LX

★

1971

Paleontological Research Institution
Ithaca, New York 14850
U. S. A.

IN MEMORIAM

Edwin C. Allison
1925-1971

Miss Winifred Goldring
1888-1971

William B. Heroy, Sr.
1883-1971

Floyd L. Hodson
1893-1971

Max J. Kopf
1893-1971

Malcolm MacLeod
1901-1970

Norman L. Thomas
1897-1971

Miss E. C. Williams
1885-1971

CONTENTS OF VOLUME LX

Bulletin No.		Pages	Plates
264.	**Jurassic and Cretaceous Hagiastridae from the Blake-Bahama Basin (Site 5A, Joides Leg I) and the Great Valley Sequence, California Coast Ranges.** By Emile A. Pessagno, Jr.	1-84	1-19
265.	**A New Species of Coronula (Cirripedia) from the Lower Pliocene of Venezuela.** By Norman E. Weisbord	85-98	20
266.	**Palynology and the Independence Shale of Iowa.** By James B. Urban	99-190	21-45
267.	**Trepostomatous Ectoprocta (Bryozoa) from the Lower Chickamauga Group (Middle Ordovician), Wills Valley, Alabama.** By Frank K. McKinney	191-337	46-68

INDEX

No separate index is included in the volume. Each number is indexed separately. Contents of the volume are listed in the beginning of the volume.

BULLETINS
OF
AMERICAN
PALEONTOLOGY
(Founded 1895)

Vol. 60

No. 264

JURASSIC AND CRETACEOUS HAGIASTRIDAE FROM THE BLAKE-BAHAMA BASIN (SITE 5A, JOIDES LEG I) AND THE GREAT VALLEY SEQUENCE, CALIFORNIA COAST RANGES

By

EMILE A. PESSAGNO, JR.

1971

Paleontological Research Institution
Ithaca, New York 14850 U. S. A.

BULLETINS
OF
AMERICAN
PALEONTOLOGY
(Founded 1895)

Vol. 60

No. 264

JURASSIC AND CRETACEOUS HAGIASTRIDAE FROM THE BLAKE-BAHAMA BASIN (SITE 5A, JOIDES LEG I) AND THE GREAT VALLEY SEQUENCE, CALIFORNIA COAST RANGES

By

EMILE A. PESSAGNO, JR.

April 29, 1971

Paleontological Research Institution
Ithaca, New York 14850 U. S. A.

Library of Congress Card Number: 75-128176

Printed in the United States of America
Arnold Printing Corporation

CONTENTS

Abstract ... 5

Introduction ... 5

Acknowledgments ... 7

Discussion ... 7

Method of study ... 8

Locality descriptions ... 8

Notations on the integration of radiolarian range zones with planktonic foraminiferal zonation ... 14

Terminology ... 15

Systematic paleontology ... 16

Superfamily Spongodiscacea Haeckel ... 16

Family Hagiastridae Riedel ... 19

Subfamily Amphibrachiinae, n. subfam. ... 20

Subfamily Patulibracchiinae, n. subfam. ... 22

Subfamily Hagisastrinae Riedel ... 51

References cited ... 57

Plates ... 61

JURASSIC AND CRETACEOUS HAGIASTRIDAE FROM THE BLAKE-BAHAMA BASIN (SITE 5A, JOIDES LEG I) AND THE GREAT VALLEY SEQUENCE, CALIFORNIA COAST RANGES

Emile A. Pessagno, Jr.

ABSTRACT

The Hagiastridae Riedel include Spongodiscacea with two, three, or four-rayed tests comprised of layered spongy meshwork lacking concentric rings or spirals. This family appears to be restricted to the Mesozoic. It has a lengthy geologic history which extends at least as far back as the Jurassic. The majority of hagiastrid species are distinctive and short ranging.

Twenty-four new species and four new genera are described herein from the Upper Cretaceous portion of the Great Valley Sequence, California Coast Ranges. Four new species are described from the late Jurassic (Tithonian) strata of the Blake-Bahama Basin (Site 5A, JOIDES Leg I).

In this report Spumellariina with spongy meshwork, irregardless of test shape, have been placed in the superfamily Spongodiscacea Haeckel.

INTRODUCTION

In the thick, monotonous flysch succession comprising most of the Great Valley Sequence, Radiolaria are far more abundant than any other kind of invertebrate fossils. During the course of the investigation a rich, diversified, well-preserved assemblage of Radiolaria was recovered from the Upper Cretaceous portion of the Great Valley Sequence. Samples were collected in this study from measured sections from Contra Costa County in the south to Tehama County in the north. In general, the best preserved Radiolaria occur in limestone nodules and concretions associated with the mudstones, shales, and siltstones of this flysch succession. The mudstones, shales, and siltstones often contain abundant Radiolaria. However, the Radiolaria extracted from these lithotypes are not nearly so well preserved as those occurring in the limestones.

This is the third in a series of reports dealing with the Upper Cretaceous Radiolaria of the California Coast Ranges (cf. Pessagno, 1969b, 1970). The present report differs somewhat in content from previous reports (Pessagno, *ibid.*) in that it also includes some Radiolaria from the Jurassic (Tithonian) strata of the Blake-Bahama Basin (JOIDES Leg I).

It is clear that faunal change displayed by the Upper Cretaceous Radiolaria of the California Coast Ranges is sufficiently great to allow establishing a detailed system of zonation. The Hagiastridae Riedel like the Neosciadiocapsidae Pessagno are a key group in fa-

Contribution Number 155, Geosciences Division, University of Texas at Dallas, P.O. Box 30365, Dallas, Texas 75230

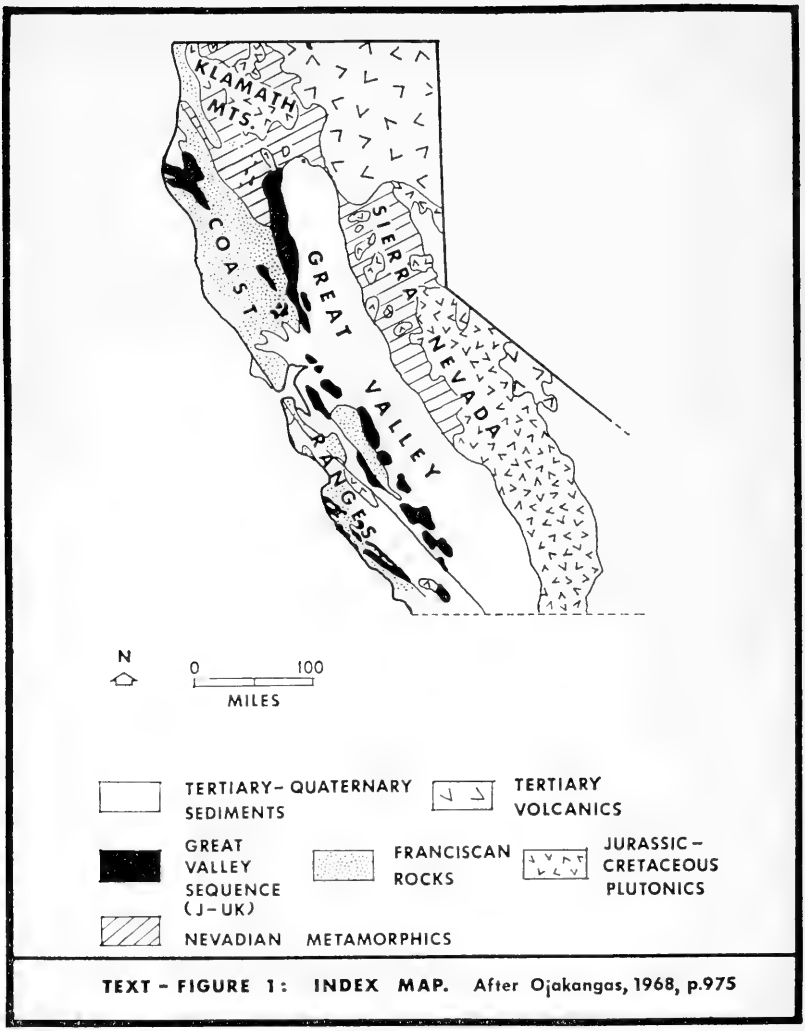

TEXT - FIGURE 1: INDEX MAP. After Ojakangas, 1968, p.975

cilitating the development of such a system of zonation. The Hagiastridae, in fact, appear to be one of the most important groups for biostratigraphic correlation in the Mesozoic. They have a geologic history which extends at least as far back as the Jurassic. Furthermore, the Hagiastridae include a number of short ranging and highly distinctive species.

Numerous species assignable to the Hagiastridae were figured by the early workers on Mesozoic Radiolaria. Hagiastrid species were figured by Rüst (1885, 1898), Parona, (1890), Squinabol (1903, 1914), and various other workers who pioneered in the study of European Mesozoic Radiolaria.

ACKNOWLEDGMENTS

This work has been supported by grants from the National Science Foundation: GA-4043 to the University of California, Davis, GA-1224 to the Southwest Center for Advanced Studies, Dallas, Texas, GA-15998 to the University of Texas at Dallas, and by the general NASA grant (NGL - 44 - 004 - 001) to the Southwest Center for Advanced Studies. The writer wishes to thank Verne Harlan for his assistance in the field; to Walter Brown, Allen White, Charles Smith, and Mrs. Sheila Martin for their care in taking the scanning electron micrographs and preparing the illustrations; and to Miss Maria Bilelo for her help in the laboratory. He particularly wishes to thank William R. Riedel (Scripps Institution of Oceanography) for his helpful comments regarding the manuscript. Numerous megafossils were kindly identified for the writer by David L. Jones, Paleontology and Stratigraphy Branch, U.S. Geological Survey, Menlo Park, California.

DISCUSSION

The inclusion of all Spumellariina with primarily spongy tests in the superfamily Spongodiscacea should lead to a more phylogenetic classification. Previous workers have relied largely on test shape and symmetry in their classificatory schemes. Hence, Spumellariina whose tests are constructed out of the same sort of spongy meshwork were placed in radically different family or superfamily groupings largely dependent on their test shape. For example, Haeckel (1887, pp. 284-286; pp. 339-341) placed *Spongoprunum* Haeckel in the "Pronoidea" largely on the basis of the ellipsoidal or cylindrical character of its test. Whereas *Spongoprunum* has (exclusive of polar spines) a completely spongy test, it is placed

with other genera such as *Ellipsostylus* Haeckel and *Xiphatractus* Haeckel which possess one or more latticed shells. Many such examples can be cited from the literature.

It is clear that the present classification at the superfamily level cross-cuts Haeckelian classification. Yet it relates a large group of Spumellariina which build their tests out of spongy meshwork and hopefully represents a more natural classification. If the shape of the test is to be emphasized, this investigator feels that it should be emphasized at the family or subfamily level.

The Spongodiscacea as defined herein have been subdivided into the Spongodiscilae Haeckel and the Pseudoaulophacilae Riedel. The former group includes forms which possess irregular spongy meshwork lacking any semblance of symmetrical arrangement; the latter group includes forms which possess spongy meshwork arranged in a more orderly, symmetrical fashion (*i.e.*, in spirals, concentric rings, layers). The Hagistridae Riedel, the primary subject of this report, are included in the Pseudoaulophacilae Riedel.

Criteria for the classification of the Hagiastridae at the family, subfamily, generic, and specific levels are summarized in Text-figure 4.

METHOD OF STUDY

The dense, spongy meshwork of the hagiastrid test makes it difficult to illustrate effectively with light optics. In this investigation a JEOL JSM-1 scanning electron microscope equipped with a goniometer stage was used as the primary means of illustrating and studying hagiastrid morphology (cf. Honjo and Berggren, 1967, pp. 393-404, pls. 1-4; Hay and Sandberg, 1967, pp. 407-418, pls. 1,2).

Gold palladium or gold used in shadow casting can be removed, if desired, with a drop of aqua regia. However, in some cases it was found that shadow casting actually enhances specimen detail for optical observation. Specimens were mounted in caedax or hyrax for optical analysis with transmitted light. The number of air bubbles in the mounting medium can be appreciably reduced by degasing the hyrax or caedax under vacuum.

LOCALITY DESCRIPTIONS

NSF 32-B. Lower part of the Forbes Formation ("Dobbins Shale" Member): 15 feet above contact between Forbes Formation and the underlying Guinda Formation. Gray calcareous mudstone

with abundant limestone nodules; sample from limestone nodules. Tributary to Petroleum Creek, Yolo County, California. U.S.G.S. Rumsey Quad. (7.5′). T12N, R3W, Sect. 10; 1.5 miles N43°W of VABM Guinda 1798. This locality occurs at about the same horizon as NSF 134-B. See planktonic foraminiferal and megafossil data presented under NSF 55-B.

NSF 55-B. Lower part of the Forbes Formation (upper part of so-called "Dobbins Shale" Member); 424 feet above contact between Forbes Formation with underlying Guinda Formation. Gray calcareous mudstone with sparse limestone nodules. Tributary to Petroleum Creek, Yolo County, California USGS Rumsey Quad. (7.5′). T12N, R3W, Sect. 10; 1.5 miles N35°W of VABM Guinda 1798. Associated planktonic Foraminifera recorded by the writer from this horizon include *Globotruncana arca* (Cushman), *Globotruncana rosetta* (Carsey), *Globotruncana loeblichi* Pessagno, *Rugoglobigerina* sp. aff. *R. rugosa* (Plummer), *Globotruncana linneiana s. s.* (d'Orbigny), *Globotruncana lapparenti s. s.* Brotzen, and *Ventilabrella ornatissima* (Cushman and Church). The lack of *Globotruncana hilli* Pessagno and *Globotruncana churchi* Martin in this assemblage suggests an early Campanian age (see data presented by Douglas, 1969, p. 154 and Pessagno, 1967, 1969a, text-figure 5). *"Inoceramus orientalis"* (identified by D. L. Jones, U. S. Geol. Survey, Menlo, Park, California) was collected by the writer at NSF 40-B in the lower Forbes ("Dobbins Shale" Member). According to Jones this species is indicative of an early Campanian age. NSF 40-B is situated 295 feet below NSF 55-B and 128 feet above the Forbes - Guinda contact.

NSF 134-B. Lower part of the Forbes Formation ("Dobbins Shale" Member); 60 feet above contact between Forbes Formation and the underlying Guinda Formation. Gray calcareous mudstone with abundant limestone nodules; sample from limestone nodules. Tributary to Petroleum Creek, Yolo County, California. USGS Rumsey Quadrangle (7.5′). T12N, R3W, Sect. 15; 1.1 miles N36°W of VABM Guinda 1798. Planktonic Foraminifera recovered from mudstones (NSF 134-A) at this locality include *Globotruncana arca* (Cushman), *Globotruncana rosetta* (Carsey) *s. l., Globotruncana lapparenti* Brotzen.

NSF 291-B. Yolo Formation [Upper part of type Yolo at north

bank of Cache Creek, Yolo County]. Limestone nodules interbedded with dark gray calcareous mudstones and siltstones; 140 feet below the contact of the Yolo Formation with the overlying Sites Formation. USGS Glascock Mountain Quad. (7.5′); T12N, R4W, Sect. 2; 0.15 miles downstream from northwest end of Rt. 16 bridge over Cache Creek. An ammonite collected from this locality by the writer and identified by D. L. Jones (USGS, Menlo Park, Calif.) as "*Kossmaticeras* aff. *K. japonicum*" indicates (*fide* Jones) that NSF 291-B is Coniacian in age.

NSF 316-B. Middle part of the Sites Formation at Cache Creek, Yolo County, California. Gray calcareous shales and siltstones with small limestone nodules. Sample from north side of creek, six feet away from large fault zone. USGS Glascock Mountain Quadrangle (7.5′); T12N, R4W, Sect. 2; 0.4 miles downstream from the Rt. 16 bridge over Cache Creek. About 1293 feet above the contact between the Sites Formation and the underlying Yolo Formation. See biostratigraphic data presented under NSF 319-B.

NSF 319-B. Upper part of the Sites Formation at Cache Creek, Yolo County, California. Sample from limestone nodules occurring in gray siliceous mudstones cropping out along Rt. 16. USGS Glascock Mountain Quad. (7.5′); T12N, R4W, Sect. 2; 0.25 miles due north of Camp Haswell (Boy Scouts of Amer.); about 1961.0 feet above the base of the Sites Formation. A Coniacian ammonite, collected by the writer and identified by D. L. Jones (USGS) as "*Kossmaticeras* aff. *K. japonicum*" was recovered from the upper part of the underlying Yolo Formation. Coniacian planktonic Foraminifera (correlative with the *Marginotruncana renzi* Assemblage Zone of Pessagno, 1967, 1969a) have been recovered by the writer from the lower portion of the overlying Funks Formation at nearby Rumsey Canyon.

NSF 327-C. Upper part of the Sites Formation at Cache Creek, Yolo County, California. Sample from limestone nodules occurring in gray siliceous mudstones cropping out along Rt. 16. USGS Glascock Mountain Quad. (7.5′); T12N, R4W, Sect. 2; 0.22 miles due north of Camp Haswell (Boy Scouts of Amer.); about 2675.0 feet above the base of the Sites. See biostratigraphic data presented for NSF-319-B.

NSF 350. Limestone nodule from the lower portion of the "Antelope Shale"/"Fiske Creek Formation" cropping out along

the north bank of Cache Creek, Yolo County, California. USGS Glascock Mountain Quad. (7.5′); T12N, R4W, Sect. 4; 0.13 miles S35°W of Rayhouse Road crossing of Cache Creek at "Low Water Bridge." NSF 350 occurs 542 feet above a horizon containing common *Praeglobotruncana stephani* (Gandolfi) and 658 feet below beds containing *Rotalipora greenhornensis* (Morrow) and *Rotalipora appenninica* (O. Renz). NSF 350 likewise occurs 1,047 feet below beds containing *Calycoceras sp.* (late Cenomanian form), *Rotalipora cushmani* (Morrow), *Rotalipora appenninica* (O. Renz), and *Hedbergella brittonensis* Loeblich and Tappan. (Planktonic forminiferal identifications are the writer's; ammonite identificaton by D. L. Jones, U.S. Geological Survey, Menlo Park, California.) The planktonic foraminiferal data indicate that NSF 350 is definitely of Cenomanian age. In that NSF 350 appears to occur below the *R. cushmani* (Morrow) datum point (cf. Text-figure 2), it is most likely correlative with the *Rotalipora evoluta* Subzone of Pessagno, 1967, 1969. Data presented by Renz, Luterbacher, and Schneider (1963, pp. 1073-1116) indicate that *R. cushmani* makes its first appearance within the upper part of the *Mantelliceras mantelli* Zone (early Cenomanian) of the Neuenburger Jura.

NSF 405. Limestone nodule from the late Cenomanian portion of "Antelope Shale"/"Fiske Creek" Formation; 0.6 miles southwest of Monticello Dam on Route 128; USGS Monticello Dam Quad. (7.5′). T8N, R2W, Sect. 29. Ammonites identified for the writer from this locality by D. L. Jones (U.S. Geol. Survey, Menlo Park, Calif.) include *Acanthoceras* sp. and *Puzosia* sp. A preliminary report by Jones indicates that the ammonites are of late Cenomanian age.

NSF 440. Yolo Formation. Limestone nodules interbedded with dark gray shales. Monticello Dam Quad. (7.5′); T8N, R2W, Sect. 28. North side of Putah Creek, Yolo County; mouth of Thompson Canyon; 0.35 miles due east of north end of Monticello Dam.

NSF 450 — NSF 451. Limestone nodules associated with light gray calcareous mudstones. Upper part of Panoche Group (undifferentiated). Exploration Adit number 1: 110-270 feet. California Dept. of Water Resources. Div. of Design and Construction;

Del Valle Dam and Reservoir Damsite Foundation Exploration. U.S. Army Corps of Engineers, Tesla Quad. (15′). Coordinates E1,639,000; N408,250. Associated planktonic Foraminifera at this horizon include *Globotruncana churchi* Martin, *Globotruncana hilli* Pessagno, *Globotruncana linneiana* (d'Orbigny), *Globotruncana arca* (Cushman), *Globotruncana bulloides* Vogler, *Globotruncana rosetta* (Carsey) and *Ventilabrella ornatissima* (Cushman and Church). Data presented by Pessagno (1967, 1969a) demonstrate that *Globotruncana hilli* Pessagno first appears at the base of the *Globotruncana calcarata* Zonule. Douglas (1969, p. 154) indicated that *G. churchi* is restricted to the late Campanian.

NSF 482. Forbes Formation; lower part of "Dobbins Shale" Member near contact with underlying Guinda Formation. Abundant limestone nodules associated with dark gray mudstones. USGS Brooks Quad. (7.5′); R2W, T10N, Sect. 30; 0.22 miles N20°E of Big Spring, Yolo County, California. Associated megafossils collected at this locality by the writer and identified by D. L. Jones (USGS, Menlo Park, California) include *"Inoceramus orientalis, Bostrychoceras* sp. and *Anagaudryceras* sp." Jones indicated that the megafossils are of early Campanian age.

NSF 483. Yolo Formation. Horizon of small limestone nodules in a sequence of dark gray mudstones, siltstones, and sandstones. Monticello Dam Quad. (7.5′); T8N, R2W, Sect. 28. Route 128 (Solano County) at southeast side of horseshoe bend in road; Cold Canyon; 0.23 miles southwest of Route 128 highway bridge over Putah Creek.

NSF 531. Lower part of the Forbes Formation ("Dobbins Shale" Member). Gray calcareous mudstones with limestone nodules; sample from limestone nodule. Exposure in bluff on west side of Salt Creek, Colusa County, California. USGS Rumsey Quadrangle (7.5′); T13N, R3W, Sect. 7. Adjacent to Dobbins Ranch; 0.2 miles S60°W from BM 584. Campanian ammonites, chiefly *Patagoniosites arbucklensis* (Anderson) were collected at this locality by the writer and identified by D. L. Jones (U.S. Geological Survey, Menlo Park). Matsumoto (1960, p. 83) reported this species together with *Gaudryceras* sp. cf. *G. striatum* (Jimbo), and *Inoceramus schmidti* Michael from the same locality.

NSF 568-B, 572-B. "Marsh Creek Formation." Samples from

limestone nodules interbedded with dark gray siliceous to calcareous mudstones. Antioch South Quad. (7.5′); T1N, R2E, Sect. 32. South bank of Marsh Creek, Deer Valley Road crossing of Marsh Creek, Contra Costa County, California. NSF 568-B by bridge; NSF 572-B 0.10 to 0.15 miles downstream from bridge. Associated planktonic Foraminifera present at this horizon include *Globotruncana churchi* Martin, *G. arca* (Cushman) and *Gublerina ornatissima* (Cushman and Church). This data with biostratigraphic data from the Putah Creek, Pleasants Valley, and Tesla areas indicate that the radiolarian assemblage present at NSF 568-B, and NSF 572 is assignable to the upper part of the *G. calcarata* Zonule of Pessagno (1967, 1969a).

NSF 584. "Antelope Shale"/"Fiske Creek Formation." Limestone nodules occurring in rhythmically bedded sandstones and mudstones/shales. USGS Sites Quad. (7.5′); T17N, R4W, Sect. 8 (northeast corner); Funks Creek, Colusa County. Cenomanian planktonic Foraminifera have been figured from this locality by Küpper (1956, pp. 40-47, pl. 8) and Douglas (1968, pp. 151-209, pl. 1). The presence of *Rotalipora cushmani* (Morrow) and *Rotalipora greenhornensis* (Morrow) suggests a middle to late Cenomanian age. Ammonites collected by the writer at this outcrop were identified by D. L. Jones (USGS, Menlo Park, California) as "*Calycoceras* sp." Matsumoto (1960, p. 36) recorded middle to late Cenomanian ammonites *Calycoceras boulei* Collignon and *Calycoceras* cf. *stoliczkai* Collignon from this same locality and other localities in its vicinity.

NSF 591. "Antelope Shale"/"Fiske Creek Formation." Limestone nodule associated with gray siltstones, mudstones, and sandstones; 223 feet below the contact with the overlying Venado Formation. USGS Sites Quadrangle (7.5′); T17N, R4W, Sect. 4 (S.W. corner); 1.05 miles west of Patterson Road. 2.9 miles N8°W of BM 261 (Section 20) on Sites-Maxwell Road. The radiolarian astemblage at this locality is essentially the same as that occurring in the upper part of the "Antelope Shale"/"Fiske Creek Formation" at Cache Creek. At Cache Creek (NSF 383-B) this assemblage is associated with early Turonian megafossils, *(i.e., Inoceramus labiatus* (Schlotheim) and *Kanabiceras* (?) sp.; identified by D. L. Jones, USGS, Menlo Park, Calif.) occurring in strata situated about 218 feet below the contact with the overlying Venado Formation.

NSF 697. Venado Formation. Thick shale interval interbedded with massive sandstones; sample from limestone nodules in shales. USGS Glascock Mountain Quad. (7.5′); T12N, R4W, Sect. 3; south bank of Cache Creek, Yolo County; 0.9 miles due west of BM 527 in southern part of Section 2. Early Turonian megafossils (*i.e., Inoceramus labiatus* (Schlotheim) and *Kanabiceras* (?) sp. were collected by the writer from the "Antelope Shale"/"Fiske Creek Formation" 242 feet below the base of the Venado Formation (megafossils identified by D. L. Jones, USGS, Menlo Park, Calif.).

NSF 705-B. "Marsh Creek Formation"; 0.5 miles north of Contra Costa-Alameda County line on Vasco Road (Kellog Creek section). USGS Bryon Hot Springs Quadrangle (7.5′).

NOTATIONS ON THE INTEGRATION OF RADIOLARIAN RANGE ZONES WITH PLANKTONIC FORAMINIFERAL ZONATION

(1) *Rotalipora evoluta datum (first appearance).* — Corresponds to base of *R. evoluta* Subzone (Pessagno, 1967, 1969a) which in turn corresponds approximately to the lower part of the *Mantelliceras mantelli* Zone of ammonite workers; earliest Cenomanian.

(2) *Rotalipora cushmani datum (first appearance).* — Corresponds to base of *R. cushmani-greenhornensis* Subzone (Pessagno, 1967, 1969a) which in turn corresponds to upper part of *Mantelliceras mantelli* Zone of ammonite workers; late early Cenomanian. See Renz, Luterbacher, and Schneider (1963, pp. 1073-1116, pls. 1-9).

(3) *Planomalina buxtorfi datum (extinction).* — Corresponds to the lower part of *R. cushmani-greenhornensis* Subzone (Pessagno, *ibid.*). Data available appear to indicate that this datum point occurs within the *Acanthoceras rhotomagense* Zone (middle Cenomanian) of ammonite workers.

(4) *First appearance of double-keeled Globigerinacea.* — Corresponds to base of *M. sigali* Subzone (Pessagno, *ibid.*) and to base of *Actinocamax plenus* Subzone in the Anglo-Parisian Basin (Jefferies, 1961, p. 618, pl. 79, figs. 30 a-c). Jefferies considered the *A. plenus* Subzone early Turonian. (See discussion of Cenomanian-Turonian boundary problem in Pessagno, 1969a).

(5) *First appearance of double-keeled Marginotruncanidae/Globigerinacea with curved, raised sutures umbilically.* — Corresponds

to the base of *W. archaeocretacea* Subzone (Pessagno, *ibid.)* Impossible at present to integrate precisely with ammonite zonation.

(6) *M. helvetica — M. sigali datum (extinction).* — Corresponds to top of *M. helvetica* Assemblage Zone, *W. archaeocretacea* Subzone (Pessagno, *ibid.*). Late Turonian ammonites such as *Prionocyclus, Prionotropis,* and *Coilposceras* occur in the upper part of the *W. archaeocretacea* Subzone. For more detailed discussion see Pessagno (1969a).

(7) *Marginotruncanidae datum (extinction).* — Corresponds to top of *M. concavata* Subzone (Pessagno, *ibid.);* early Santonian. See Pessagno (1969a) for integration of planktonic foraminiferal and megafossil data.

(8) *Globotruncana arca datum (first appearance).* — Corresponds to base of *G. fornicata-stuartiformis* Assemblage Zone (Pessagno, *ibid.);* basal Campanian. See Pessagno (1969a) for integration of megafossil and planktonic foraminiferal data and for discussion of Santonian — Campanian boundary problem.

(9) *Rugoglobigerina datum (first appearance).* — Corresponds to the base of the *Planoglobulina glabrata* Zonule of Pessagno (1969a); late early Campanian. Not possible to integrate with megafossil zonation at present.

(10) *Globotruncana hilli datum (first appearance).* — Corresponds to base of *G. calcarata* Zonule of Pessagno *(ibid.)* and to base of *Bostrychoceras polyplocum* Zone of ammonite workers latest Campanian. See Pessagno (1969a) for a more detailed discussion.

(11) *Globotruncana linneiana—bulloides datum (extinction).* — Corresponds to the top of the *G. fornicata—stuartiformis* Assemblage Zone of Pessagno *(ibid.);* latest early Maestrichtian. No precise data available for the integration of planktonic foraminiferal and megafossil zonation.

(12) *Globotruncana datum (extinction).* — Corresponds to top of *G. contusa-stuartiformis* Assemblage Zone, *A. mayaroensis* Subzone (Pessagno, *ibid.).* No precise data available for the integration of planktonic foraminiferal zonation with megafossil zonation.

TERMINOLOGY

Bar. Rodlike structure forming component part of polygonal pore frame. Pl. 2, fig. 1.

Bracchiopyle. Cylindrical, porous tube extending in a distal direc-

tion from the center of the tip of the primary ray. Only known to date in *Halesium,* n. gen. and *Patulibracchium,* n. gen. Pl. 1, figs. 1, 2.

Central area. Area situated at juncture of rays. Pl. 1, fig. 1.

Central spine. Long spine extending distally from center of ray tip. Pl. 1, fig. 5.

Lacuna. Cavity occurring in central area of some species of *Crucella,* n. gen. Pl. 18, fig. 1. Sometimes covered by thin veneer of spongy meshwork.

Lateral spines. Short spines flanking central spine, usually one to either side. Pl. 1, fig. 5.

Node. See Pl. 2, fig. 1.

Patagium. Delicate spongy meshwork surrounding rays; comprised of polygonal pore frames consisting of bars lacking nodes at pore frame vertices. Pl. 2, fig. 5.

Pore frame. Polygonal structure formed of bars or tabulae and bars usually connected (except with patagium) by nodes at vertices.

Primary ray. In *Halesium,* n. gen. and *Patulibracchium,* n. gen. Ray possessing bracchiopyle. Pl. 1, fig. 1, Text-fig. 4.

Secondary ray. In *Halesium,* n. gen. and *Patulibracchium,* n. gen. Ray to left of primary ray. Pl. 1, fig. 1, Text-fig. 4.

Tabula, -ae. Vertical, porous, sheetlike structures occurring with *Halesium,* n. gen. Pl. 2, figs. 1.

Tertiary ray. In *Halesium,* n. gen. and *Patulibracchium,* n. gen. Ray to right of primary ray. Pl. 1, fig. 1, Text-fig. 4.

SYSTEMATIC DESCRIPTIONS

Phylum PROTOZOA

Subphylum SARCODINA

Class ACTINOPODEA

Subclass RADIOLARIA

Order POLYCYSTIDA

Remarks. — Riedel (1967, p. 291) emended the Polycystida Ehrenberg to include only those Radiolaria having a skeleton comprised of opaline silica lacking admixed organic compounds.

Suborder **SPUMELLARIINA**

Superfamily **SPONGODISCACEA** Haeckel

Definition. — Spumellariina with spongy tests of variable shape

TEXT-FIGURE 3: CRITERIA FOR CLASSIFICATION

Family Level	Subfamily Level	Generic Level	Specific Level
Presence of a layered, spongy test with polygonal pore frames arranged in a linear fashion. Presence of two, three, or four unchambered, spongy rays extending out from small central area.	Number of rays. Symmetry of test.	Presence or absence of bracchiopyle. Presence or absence of spines on ray tips. Detailed structure of meshwork: a. Presence of pore frames comprised only of bars. b. Presence of pore frames comprised of bars and tabulae.	Type of meshwork on rays and central area. Shape of rays and ray tips longitudinally and axially. Structure of spines and bracchiopyle when present. Angles between rays. Length, width and height of rays. Length of spines. Number of rows of pore frames per ray. Presence or absence of nodes at vertices of pore frames. Et Cetera.

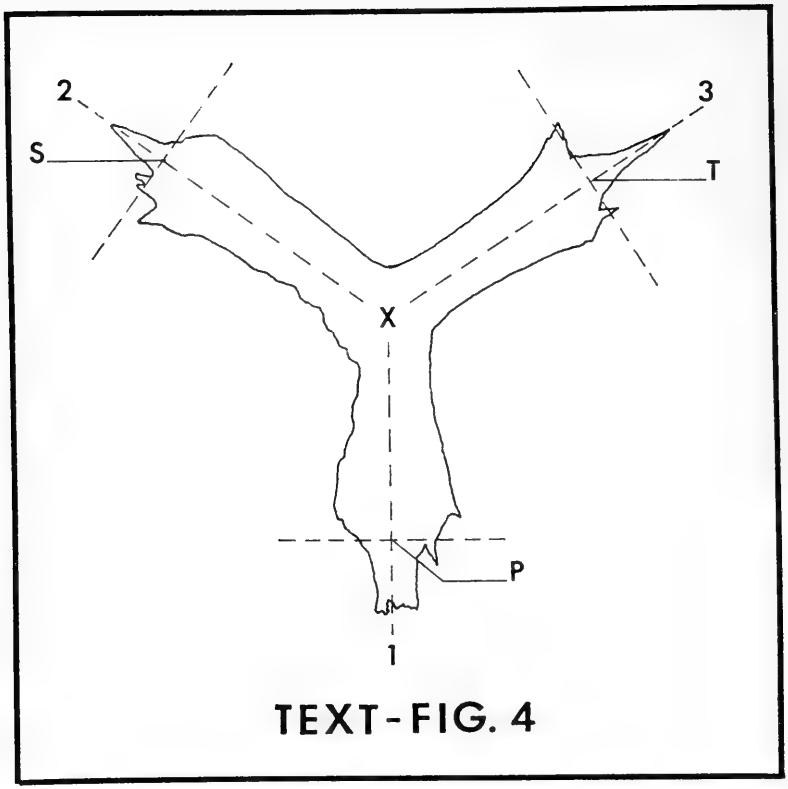

TEXT-FIGURE 4

X = point at center of central area.
P = point at end of primary ray and at center of ray tip.
S = point at end of secondary ray and center of ray tip.
T = point at end of tertiary ray and at center of ray tip.
1 = primary ray.
PX = length of primary ray exclusive of bracchiopyle.
2 = secondary ray.
SX = length of secondary ray exclusive of central spine.
3 = tertiary ray.
TX = length of tertiary ray exclusive of central spine.
Angle PXS = angle formed by lines SX and PX.
Angle SXT = angle formed by lines SX and TX.
Angle TXP = angle formed by lines TX and PX.

lacking sieve plates, lattice shells, or chambered rays; with or without spines. Pore frames comprising spongy meshwork arranged with or without symmetry.

Remarks. — The Spongodiscacea as defined above include all Spumellariina with spongy tests. The shape of the test and its symmetry are not regarded as important at the superfamily level.

The Spongodiscacea are divided into two subsuperfamilies: the Spongodiscilae Haeckel and the Pseudoaulophacilae Riedel. The Spongodiscilae include all Spongodiscacea showing spongy meshwork with no semblance of symmetry in the arrangement of their pore frames. The Pseudoaulophacilae include all Spongodiscacea with spongy meshwork arranged in some symmetrical fashion (*e.g.*, in concentric rings, spirals, or parallel layers).

Range. — Paleozoic to Recent.

Occurrence. — World-wide.

Subsuperfamily **SPONGODISCILAE** Haeckel

Definition. — Spongodiscacea with irregular spongy meshwork with pore frames arranged unsymmetrically. Overall test shape varying with family or subfamily.

Range. — Paleozoic to Recent.

Occurrence. — World-wide.

Subsuperfamily **PSEUDOAULOPHACILAE** Riedel

Definition. — Spongodiscacea with spongy meshwork comprised of pore frames arranged symmetrically in concentric rings, spirals, parallel layers, and so forth. Overall test shape varying with family or subfamily.

Range. — Paleozoic? Mesozoic to Recent.

Occurrence. — World-wide.

Family **HAGIASTRIDAE** Riedel, emended

Type genus. — *Hagiastrum* Haeckel.

Emended definition. — Spongodiscacea with two, three, or four arms or rays. Meshwork arranged in parallel to subparallel layers axially. Individual layers comprised of pore frames arranged linearly or sublinearly.

Remarks. — This definition corresponds closely to Riedel's (1970) original definition of the Hagiastrinae. The Hagiastrinae

Riedel are restricted in this report to forms showing four rays arranged at right angles along two axes.

The Hagiastridae are divided herein into three subfamilies on the basis of the number and arrangement of rays: (1) the Amphibrachiinae, n. subfam., (2) the Patulibracchiinae, n. subfam., and (3) the Hagiastrinae Riedel. These subfamilies are characterized by having two, three, and four rays respectively.

Range. — Mesozoic.

Occurrence. — World-wide.

Subfamily **AMPHIBRACHIINAE,** new subfamily

Type genus. — *Amphibrachium* Haeckel.

Description. — Test as with family. Comprised of two straight, opposing, unchambered rays arranged along one axis and extending outward from small central area.

Remarks. — The Amphibrachiinae, n. subfam., differ from the Patulibracchiinae, n. subfam., by possessing two rather than three rays.

Range and occurrence. — Jurassic; Early Cretaceous of Europe. Jurassic (Tithonian) of Blake-Bahama Basin.

Genus **AMPHIBRACHIUM** Haeckel emended

1881. *Amphibrachium* Haeckel, Jenaische Zeitsch. Naturw., vol. 15 (n. ser., vol. 18), No. 3, p. 460.

1954. *Amphibrachium* Haeckel, Campbell, Treatise on Invert. Paleont., Pt. D, Protista 3, p. D86. [Inadvertently designated *A. diminutum* Rüst, 1885 (p. 296, pl. 7, fig. 5) as type species.]

Type species. — *Amphibrachium diminutum* Rüst, 1885. *A. diminutum* appears to have been inadvertently designated as the type species by Campbell in 1954. No mention was made by Campbell *(ibid.)* that this represented a subsequent designation.

Emended definition. — Test as with subfamily. Comprised of two opposing rays extending out from a minute, often asymmetrical central area. Rays with expanded, somewhat bulbous tips lacking large spines, but sometimes possessing irregularly distributed small spines. With or without patagium.

Range and occurrence. — As defined above, *Amphibrachium* appears to be restricted to strata of Jurassic and Early Cretaceous (Neocomian) age. Jurassic — Neocomian of Europe; Late Jurassic (Tithonian) of the Blake-Bahama Basin (JOIDES DSD) Leg 1, Site 5A, Core 7, Section 1: 274.3 meters).

Amphibrachium petersoni, Pessagno n. sp. Pl. 19, figs. 1,8

Description. — Test as with genus. Rays subequal in length. Shorter ray with expanded triangularly shaped tip; other ray with rounded tip. Both rays terminating in short spines; rays elliptical in cross-section. Meshwork with square to rectangular pore frames arranged in three markedly linear rows. Central area small.

Remarks. — *Amphibrachium petersoni,* n. sp. differs from *A. sansalvadorensis,* n. sp. (1) by having wider, shorter rays which are subequal in length; (2) by having one ray with a bulbous tip and the other with an expanded triangular tip.

This species is named for Dr. M. N. A. Peterson (Scripps Institution of Oceanography), Chief Scientist of the JOIDES Deep Sea Drilling Project.

Measurements.—

	Length of rays microns	Width of rays microns
Holotype (USNM 165578)	370 430	80
Paratype (USNM 165580)	350 370	60
Paratype (USNM 165580)	320 380	80
Paratype (USNM 165579)	390 460	80
Paratype (Pessagno Coll.)	340 400	70

Type locality. — JOIDES (DSD), Leg I, Site 5A, Core 7, Section 1: 274.3 meters. Blake-Bahama Basin.

Deposition of types. — Holotype = USNM 165578. Paratypes = USNM 165579 — 165580 and Pessagno Collection, University of Texas at Dallas.

Range and occurrence. — Late Jurassic (Tithonian) of Blake-Bahama Basin in so far as known.

Amphibrachium sansalvadorensis Pessagno, n. sp. Pl. 19, figs. 9, 10

Description. — Test as with genus. One ray slightly shorter than other; both rays elliptical in axial section. Meshwork with square pores frames arranged in a markedly linear fashion in three rows. Rays with bulbous tips with several irregularly distributed short spines. Central area small.

Remarks. — *A. sansalvadorensis,* n. sp. differs from *A. diminutum* Rüst (1) by having proportionately longer rays; (2) by

having markedly straight rays with square meshwork; and (3) by having short spines on its ray tips.

This species is named for the island of San Salvador in the Bahama Islands.

Measurements. —

	Length of rays microns	Width of rays microns
Holotype (USNM 165568)	500 550	40
Paratype (USNM 165569)	470 560	60
Paratype (USNM 165570)	450 560	50
Paratype (Pessagno Coll.)	410 460	50
Paratype (Pessagno Coll.)	380 480	50

Type locality. — JOIDES (DSD), Leg I, Site 5A, Core 7, Section 1 (top) : 274.3 meters. Blake-Bahama Basin.

Deposition of types. — Holotype = USNM 165568. Paratypes = USNM 165569 — 165570 and Pessagno Collection, University of Texas at Dallas.

Range and occurrence. — To date, this species has only been found in strata of Late Jurassic (Tithonian) age at its type locality.

Subfamily **PATULIBRACCHIINAE,** new subfamily

Type genus. — *Patulibracchium,* n. genus.

Description. — Test as with family. Comprised of three straight, unchambered rays extending out from a small central area.

Remarks. — The Patulibracchiinae, n. subfam., differ from the Amphibrachiinae, n. subfam., by possessing three rather than two rays and from the Hagiastrinae Riedel by possessing three rather than four rays.

The majority of the species occurring in this subfamily belong to *Patulibracchium,* n. gen. This genus together with *Halesium,* n. gen., is characterized by having a cylindrical tube, the *bracchiopyle,* on one of the three rays. The ray possessing the bracchiopyle is termed the *primary ray;* the ray to the left of the primary ray is termed the *secondary ray;* and the ray to the right of the primary ray is termed the *tertiary ray.* Usually all three rays are of different length with different interradial angles. The system of form analysis shown in Text-figure 4 is primarily proposed for measurement of specimens assignable to either *Patulibracchium* or *Halesium. Paron-*

aella, n. gen., differs from the forementioned genera by lacking a bracchiopyle and having rays of equal length with subequal interradial angles.

Range. — Jurassic? Cretaceous.

Occurrence. — World-wide.

Genus **HALESIUM,** new genus

Type species. — *Halesium sexangulum* Pessagno, n. sp.

Description. — Test in horizontal view with rays comprised of triangular to rectangular/square pore frames always arranged in two markedly linear rows. Marked linearity of meshwork due to three prominent vertical parallel tabulae (central and lateral tabulae) which merge in central area. Tabulae with massive nodes which intersect with bars to form either triangular or square frames. Meshwork in central area triangular. Meshwork arranged in horizontal, parallel layers. Rays subequal in length. Primary ray always with massive, cylindrical bracchiopyle. Secondary and tertiary rays usually terminating in two prominent lateral spines and one prominent central spine.

Remarks. — *Halesium,* n. gen. differs from *Patulibracchium,* n. gen. (1) in having pore frames always arranged in two parallel rows on its rays (exclusive of ray tips); (2) by having pore frames comprised of tabulae as well as bars; (3) by the uniform character of its meshwork; and (4) by the arrangement of its meshwork in parallel, horizontal layers. Both genera share bracchiopyles on their primary rays.

The triangular meshwork of *Halesium* differs from that of *Pseudoaulophacus* Pessagno by being comprised of bars and tabulae instead of just bars and by being arranged in parallel instead of concentric layers.

This genus is named for Dr. Anton L. Hales, University of Texas at Dallas, in honor of his contributions to deep earth studies.

Range. — Early Cenomanian to middle Turonian. Range zone may extend into Early Cretaceous. Early Cretaceous not extensively studied during this project.

Occurrence. — Great Valley Sequence, California Coast Ranges.

Halesium quadratum Pessagno, n. sp. Pl. 3, figs. 1-6; Pl. 4, figs 1,2

Description. — Test as with genus. Rays exclusive of tips with square pore frames and circular pores; nodes of central and lateral

tabulae parallel; interconnected by bars which extend at right angles to axis of rays (Pl. 3, fig. 2; Pl. 4, fig. 2). Central area with triangular pore frames. Meshwork in longitudinal view tetragonal/rectangular with circular to elliptical pores; pore frames arranged in parallel layers. Seconday and tertiary rays with short imperforate lateral spines and short somewhat more massive and perforate central spines. Primary ray with cylindrical bracchiopyle; bracchiopyle perforate proximally and imperforate distally; pores circular to elliptical in shape. Lateral spines of primary ray essentially the same as those of seconday and tertiary rays. Rays rectangular in axial view except for tips which are wedge-shaped. Patagium well developed on most specimens; often tends to obscure primary meshwork.

Remarks. — *H. quadratum,* n. sp. is compared with *H. sexangulum,* n. sp. below.

Quadratus (Latin) = square.

Measurements. — See Text — figure 4 for explanation of designations.

Holotype (USNM 165547)

∢ PXS = 120 degrees PX = 307 microns
∢ SXT = 120 degrees SX = 332 microns
∢ TXP = 120 degrees TX = 332 microns

Length of central spine at S = 80 microns.
Length of central spine at T = 110 microns.

Paratype (USNM 165549)

∢ PXS = 114 degrees PX = 208 microns
∢ SXT = 113 degrees SX = 237 microns
∢ TXP = 133 degrees TX = 231 microns

Length of brachiopyle = 56 microns.
Length of central spine at S = 56 microns.
Length of central spine at T = not measureable; spine broken.

Paratype (Pessagno Coll.)

∢ PXS = 126 degrees PX = 311 microns
∢ SXT = 121 degrees SX = 360 microns
∢ TXP = 113 degrees TX = 336 microns

Length of central spine at S = 80 microns.
Length of cental spine at T = 80 microns.
Bracchiopyle broken.

Paratype (Pessagno Coll.)

∢ PXS = 120 degrees PX = 230 microns
∢ SXT = 125 degrees SX = 210 microns
∢ TXP = 115 degrees TX = 210 microns

Length of bracchiopyle = 60 microns.
Length of central spine at S = 70 microns.
Length of central spine at T = 60 microns.

Paratype (Pessagno Coll.)

∢ PXS = 119 degrees	PX = 290 microns
∢ SXT = 112 degrees	SX = 290 microns
∢ TXP = 129 degrees	TX = 290 microns

Central spines and bracchiopyle broken.

Type locality. — NSF 350. See Locality. Descriptions and Text-figure 5.

Deposition of types. — Holotype = USNM 165547. Paratypes = USNM 165548 — 165549 and Pessagno Collection, University of Texas at Dallas.

Range. — Early Cenomanian to middle Turonian. Range zone may extend into Albian. Strata of Early Cretaceous age not extensively sampled during this study.

Occurrence. — See Text-figure 5 and Locality Descriptions.

Halesium sexangulum Pessagno, n. sp. Pl. 1, figs. 5-6; Pl. 2, figs. 1-6

Description. — Test as with genus. Rays and central area with well-developed triangular meshwork horizontally. Nodes of central tabulae staggered with respect to nodes on lateral tabulae; bars connecting nodes forming equilateral triangular frames between a given lateral tabula and central tabula; forming hexagonal areas comprised of equilateral triangular frames between lateral tabulae (Pl. 2, figs. 1,6). Tips of rays with tetragonal meshwork. Meshwork in longitudinal section comprised of parallel layers of subrectangular pores frames with circular to elliptical pores. Tertiary and secondary rays with short imperforate central spines and massive lateral spines. Primary ray with massive lateral spines and large cylindrical bracchiopyle (Pl. 1, figs. 5,6); bracchiopyle with circular to elliptical pores arranged between six diverging ridges. Rays rectangular in axial view except for tips which become markedly wedge-shaped distally. Patagium often well developed (Pl. 2, figs. 4,6).

Remarks. — *H. sexangulum,* n. sp. differs from *H. quadratum,* n. sp. (1) by having triangular rather than square pore frames; (2) by having a more highly perforate bracchiopyle; (3) by possessing longer, more massive lateral spines; and (4) by having proportionately shorter rays.

Sexangulum-a-um (Latin) = hexagonal.

Measurements. — (For explanation of designations see Text-figure 4).

Holotype (USNM 165544)

$\measuredangle$ PXS = 118 degrees PX = 200 microns
$\measuredangle$ SXT = 122 degrees SX = 200 microns
$\measuredangle$ TXP = 120 degrees TX = 170 microns
Length of bracchiopyle = 50 microns.
Length of central spine at S = 40 microns.
Length of central spine at T = 40 microns.

Paratype (USNM 165545)

$\measuredangle$ PSX = 117 degrees PX = 220 microns
$\measuredangle$ SXT = 123 degrees SX = 210 microns
$\measuredangle$ TXP = 120 degrees TX = 210 microns
Length of bracchiopyle; not measureable; bracchiopyle broken.
Length of central spine at S = 40 microns.
Length of central spine at T; Not measureable; spine broken.

Paratype (USNM 165546)

$\measuredangle$ PSX = 110 degrees PX = 210 microns
$\measuredangle$ SXT = 128 degrees SX = 210 microns
$\measuredangle$ TXP = 122 degrees TX = 210 microns
Length of bracchiopyle = 45 microns.
Length of central spine at S; not measureable; spine broken.
Length of central spine at T = 45 microns.

Paratype (Pessagno Coll.)

$\measuredangle$ PXS = 117 degrees PX = 210 microns
$\measuredangle$ SXT = 123 degrees SX = 220 microns
$\measuredangle$ TXP = 120 degrees TX = 210 microns
Bracchiopyle broken.
Length of central spine at S = 57 microns.
Length of central spine at T = 40 microns.

Paratype (Pessagno Coll.)

$\measuredangle$ PXS = 115 degrees PX = 160 microns
$\measuredangle$ SXT = 125 degrees SX = 186 microns
$\measuredangle$ TXP = 120 degrees TX = 172 microns
Length of bracchiopyle = 50 microns.
Length of central spine at S = 50 microns.
Length of central spine at T = 45 microns.

Type locality. — NSF 350. See Locality Descriptions and Text-figure 5.

Deposition of types. — Holotype = USNM 165544. Paratypes = USNM 165545 — 165546 and Pessagno Collection, University of Texas at Dallas.

Range. — Early Cenomanian to middle Turonian. The range zone of this species may extend into the Albian. Strata of Early Cretaceous age were not extensively sampled during the course of this study.

Occurrence. — See Text-figure 5 and Locality Descriptions.

Genus **PATULIBRACCHIUM,** new genus

Type species. — *Patulibracchium davisi,* n. sp.

Description. — Test in horizontal view with rays and central

area comprised of square, rectangular, polygonal, or triangular pore frames; pore frames comprised of bars connected to nodes at vertices and arranged in linear to sublinear fashion in several rows. Primary rays with porous, centrally placed bracchiopyle (Pl. 1, figs. 1,2); bracchiopyle in most cases flanked by two (rarely more) subsidiary spines. Secondary and tertiary rays terminating in central spines and flanking lateral spines (usually two). Rays variable in length always widening at tips; circular, elliptical, to subrectangular in axial section. Primary ray usually somewhat shorter and more massive.

Remarks. — *Patulibracchium,* n. gen. differs from *Halesium,* n. gen. by having pore frames comprised solely of bars rather than tabulae and bars; by having pore frames (on rays exclusive tips) that are arranged sublinearly in numerous rows rather than consistently two rows; and by lacking meshwork arranged in planiform layers. Both genera possess bracchiopyles.

Patulus (Latin) = extended, spreading + *bracchium* (Latin, N.) = arm. *Bracchium* is preferred in most Latin dictionaries to *brachium.*

Range. — Late Cretaceous. ?Early Cretaceous. ?Late Jurassic.

Occurrence. — Great Valley Sequence, California Coast Ranges. Upper Cretaceous of Eurasia.

Patulibracchium arbucklensis Pessagno, n. sp.
Pl. 15, fig. 6; Pl. 16, figs. 1-3

Description. — Test as with genus. Pore frames on all rays polygonal (dominantly tetragonal); arranged in a linear to sublinear fashion. Pore frames in central area predominantly polygonal (tetragonal); triangular pore frames rare. Tips of all rays rounded, with small circular pores; not greatly expanded laterally. Secondary and tertiary rays with centrally placed spines. Spines finely perforate with circular to elliptical pores situated between ridges that converge distally. Primary ray with much broader tip having nearly imperforate, massive, cylindrical bracchiopyle; a few circular to elliptical pores occurring ony at the base of the bracchiopyle. Fragments of patagium usually present.

Remarks. — *P. arbucklensis,* n. sp. differs from *P. teslaensis,* n. sp. (1) by having a wide primary ray with a more rounded tip; (2) by having more irregular meshwork comprised of variously shaped polygonal pore frames; (3) by having narrower tips on its secondary

and tertiary rays; (4) by the less linear arrangement of pore frames on its rays; and so forth. *P. arbucklensis,* n. sp. appears to be closely related to *"Rhopalastrum" attenuatum* Lipman. It differs from the latter species by having narrower rays and a smaller central area. Lipman (1952, pl. 3, fig. 2) showed a tubular structure (probably a bracchiopyle) on the shorter and wider of the three rays. It is likely that *"R." attenuatum* Lipman should be included in *Patulibracchium,* n. gen. A comparison of *P. arbucklensis* with *P. petroleumensis,* n. sp., is given under the latter species.

This species is named for the town of Arbuckle, Colusa County, California.

Measurements. — See Text-figure 4 for explanation of designations.

Holotype (USNM 165523)

∢ PXS	= 114 degrees	PX = 200 microns
∢ SXT	= 122 degrees	SX = 290 microns
∢ TXP	= 124 degrees	TX = 310 microns

Spines and bracchiopyle broken.

Paratype (USNM 165523)

∢ PXS	= 120 degrees	PX = 290 microns
∢ SXT	= 112 degrees	SX = 320 microns
∢ TXP	= 128 degrees	TX = 320 microns

Spines and bracchiopyle broken.

Paratype (Pessagno Coll.)

∢ PXS	= 126 degrees	PX = 270 microns
∢ SXT	= 118 degrees	SX = 350 microns
∢ TXP	= 116 degrees	TX = 370 microns

Spines and bracchiopyle broken.

Paratype (Pessagno Coll.)

∢ PXS	= 116 degrees	PX = 250 microns
∢ SXT	= 130 degrees	SX = ————
∢ TXP	= 114 degrees	TX = 360 microns

Type locality. — NSF 32-B. See Locality Descriptions and Text-figure 5.

Deposition of types. — Holotype = USNM 165523. Paratypes = USNM 165524 and Pessagno Collection, University of Texas at Dallas.

Range. — Early Campanian.

Patulibracchium sp. aff. **P. arbucklensis,** n. sp. Pl. 16, fig. 4

Remarks. — This form is similar in most respects to *P. arbucklensis,* n. sp. but has shorter rays and different interradial angles.

Range. — Early Campanian.

Occurrence. — NSF 32-B. See Locality Descriptions and Text-figure 5.

Patulibracchium californiaensis Pessagno, n. sp.
Pl. 11, fig. 6; Pl. 12, figs. 1,2

Description. — Test as with genus. Rays short and broad; flaring to form wide tips. Meshwork on rays and central area comprised of equilateral triangular frames with nodules at vertices. Secondary and tertiary rays with centrally placed spine flanked by two lateral spines. Primary ray with somewhat wider tip; having fragile bracchiopyle with rectangular meshwork; bracchiopyle flanked by two lateral spines. Detailed structure of bracchiopyle not known. Spines on all three rays, imperforate lacking spongy structure. Rays in longitudinal section somewhat wedge-shaped; tapering from central area toward tips; sides of rays planiform. Central area occasionally somewhat raised. Fragments of patagium observed on some specimens.

Remarks. — *Patulibracchium californiaensis,* n. sp. may be related to *Patulibracchium ungulae,* n. sp. It can be distinguished from the latter species by its shorter, broader rays with greatly widened tips and by its completely triangular meshwork.

Measurements. — See Text-figure 4 for explanation of designations.

Holotype (USNM 165520)

∢ PXS = 120 degrees	PX = 150 microns
∢ SXT = 110 degrees	SX = 150 microns
∢ PXT = 130 degrees	TX = 150 microns

Spines and bracchiopyle broken.

Paratype (Pessagno Coll.)

∢ PXS = 120 degrees	PX = 109 microns
∢ SXT = 120 degrees	SX = 125 microns
∢ PXT = 120 degrees	TX = 140 microns

Topotype (lost in SEM)

∢ PXS = 120 degrees	PX = 152 microns
∢ SXT = 110 degrees	SX = 132 microns
∢ TXP = 130 degrees	TX = 132 microns

Bracchiopyle broken.
Central spine at S = 4.8 microns.
Central spine at T = 4.0 microns.

Paratype (Pessagno Coll.)

∢ PXS = 120 degrees	PX = 420 microns
∢ SXT = 120 degrees	SX = 430 microns
∢ TXP = 120 degrees	TX = ————

Spines and bracchiopyle broken.

Type locality. — NSF 32-B. See Locality Descriptions.

Deposition of types. — Holotype = USNM 165520. Paratypes = USNM 165521 and Pessagno Collection, University of Texas at Dallas.

Range. — Early Campanian.

Occurrence. — See Text-figure 5 and Locality Descriptions.

Patulibracchium davisi Pessagno, n. sp. Pl. 1, figs. 1-4

Description. — Test as with genus. Pore frames on rays exclusive of tips square with inset circular pores arranged in a markedly linear fashion. Central area with triangular pore frames. Rays widening somewhat distally, terminating in broad tips. Secondary and tertiary rays with large central spines having circular to elliptical pores; central spines flanked by two (sometimes more) small, imperforate lateral spines (Pl. 1, fig. 1). Primary ray with well-developed cylindrical bracchiopyle. Bracchiopyle with nine or ten subparallel ridges separating rows of circular to elliptical pores (Pl. 1, fig. 2); two small imperforate lateral spines flanking bracchiopyle.

Remarks. — *P. davisi,* n. sp. differs from *P. woodlandensis,* n. sp. (1) by having a narrower bracchiopyle; (2) by having pore frames on its rays which are consistently square and arranged in a markedly linear fashion; and (3) by having narrower rays. *P. davisi* is compared to *P. ruesti,* n. sp. under the latter species.

P. davisi, n. sp. is named for E. F. Davis in honor of his work on the radiolarian cherts of the Franciscan Complex.

Measurements. — See Text-figure 4 for explanation of designations.

Holotype (USNM 165499)

$\measuredangle$ PXS = 124 degrees PX = 290 microns
$\measuredangle$ SXT = 120 degrees SX = 320 microns
$\measuredangle$ TXP = 116 degrees TX = 320 microns
Length of bracchiopyle = 110 microns.
Length of central spine at S = 80 microns.
Length of central spine at T = 80 microns.

Paratype (USNM 165500)

$\measuredangle$ PXS = 115 degrees PX = 270 microns
$\measuredangle$ SXT = 120 degrees SX = 270 microns
$\measuredangle$ TXP = 125 degrees TX = 270 microns
Bracchiopyle and central spine at S broken.
Central spine at T = 80 microns.

Paratype (USNM 165501)

$\measuredangle$ PXS = 118 degrees PX = 240 microns
$\measuredangle$ SXT = 117 degrees SX = 210 microns
$\measuredangle$ TXP = 125 degrees TX = 270 microns
Length of bracchiopyle = 70 microns.
Length of central spine at S = 70 microns.
Central spine at T broken.

Paratype (Pessagno Coll.)

∢ PXS = 119 degrees	PX = 190 microns
∢ SXT = 117 degrees	SX = 210 microns
∢ TXP = 124 degrees	TX = 210 microns

Length of bracchiopyle = 50 microns.
Length of central spine at S = 50 microns.
Central spine at T broken.

Paratype (Pessagno Coll.)

∢ PXS = 119 degrees	PX = 250 microns
∢ SXT = 123 degrees	SX = 250 microns
∢ TXP = 118 degrees	TX = 250 microns

Length of bracchiopyle = 80 microns.
Length of central spine at S = 100 microns.
Length of central spine at T = 100 microns.

Type locality. — NSF 350. See Locality Descriptions.

Deposition of types. — Holotype = USNM 165499. Paratypes = USNM 165500 — USNM 165501 and Pessagno Collection, University of Texas at Dallas.

Range. — Early Cenomanian.

Occurrence. — See Text-figure 5 and Locality Descriptions.

Patulibracchium delvallensis Pessagno, n. sp. Pl. 13, figs. 2,3

Descriptions. — Test as with genus. Pore frames on all three rays dominantly square to rectangular. Central area consistently with well-developed triangular meshwork. Secondary and tertiary rays slender; considerably longer than somewhat more robust primary ray. Secondary and tertiary rays with fragile, spongy central spines; only fragments of basal portions of spines preserved. Primary ray with somewhat wider tip; bracchiopyle fragmentary, structure not documented. Rays elliptical in axial section.

Remarks. — *P. delvallensis,* n. sp., is closely related to *P. teslaensis,* n. sp. It differs from the latter species (1) by having secondary and tertiary rays which are about one and one-half times as long as the primary ray; (2) by having slender rays; (3) by having a greater interradial angle between its secondary and tertiary rays; and so forth. Both species share similar meshwork on their rays and central area. *P. delvallensis* appears to have arisen from *P. teslaensis,* n.sp. during late Campanian times. Transitional forms are common in late Campanian samples. *P. delvallensis,* n.sp., is compared to *P. taliaferroi,* n.sp., under the latter species.

This species is named for Arroyo del Valle, Alameda County, California.

Measurements. — See Text-figure 4 for explanation of designations.

	Degrees	Microns
Holotype (USNM 165529)		
	∢ PXS = 122	PX = 300
	∢ SXT = 123	SX = 420
	∢ TXP = 115	TX = 420
Paratype (USNM 165530)		
	∢ PXS = 115	PX = 280
	∢ SXT = 128	SX = 440
	∢ TXP = 117	TX = 420
Paratype (USNM 165531)		
	∢ PXS = 118	PX = 290
	∢ SXT = 130	SX = 470
	∢ TXP = 112	TX = 500
Paratype (Pessagno Coll.)		
	∢ PXS = 113	PX = 220
	∢ SXT = 134	SX = 360
	∢ TXP = 113	TX = 350
Paratype (Pessagno Coll.)		
	∢ PXS = 125	PX = 280
	∢ SXT = 117	SX = 390
	∢ TXP = 118	TX = 390

Note: Bracchiopyles and spines on all specimens broken and incomplete.

Type locality. — NSF 451. See Locality Descriptions.

Deposition of types. — Holotype = USNM 165529. Paratypes = USNM 165530 — USNM 165531 and Pessagno Collection, University of Texas at Dallas.

Range. — Late Campanian. See Text-figure 2.

Occurrence. — See Text-figure 5 and Locality Descriptions.

Patulibracchium dickinsoni Pessagno, n. sp. Pl. 17, figs. 3-6

Descriptions. — Test as with genus. Three rays about equal in length; always tending to bifurcate; bifurcations terminating in imperforate spines. Meshwork on rays tetragonal to pentagonal, arranged in a similar fashion. Meshwork in central area with triangular tetragonal, or pentagonal pore frames. Primary ray difficult to distinguish from tertiary and secondary rays. Fragments of delicate bracchiopyle with subrectangular pores situated between bifurcating portions of primary ray (Pl. 17, fig. 5). Rays elliptical in axial section. Portions of patagium preserved.

Remarks. — This species differs from all other species of *Patulibracchium* by virtue of its bifurcating rays. The structure of its meshwork and shape of its rays in axial section suggests a phylogenetic relationship to *P. delvallensis,* n. sp.

P. dickinsoni, n. sp. is named for Dr. William P. Dickinson, Department of Geology, Stanford University, in honor of his contri-

butions to the study of the Great Valley Sequence, California Coast Ranges.

Measurements. — See Text-figure 4 for explanation of designations.

Note: PX, SX, and TX measured from center of central area to end of bifurcating rays (exclusive of spines).

Holotype (USNM 165541)

∢ PXS = 117 degrees PX = 250 microns
∢ SXT = 127 degrees SX = 300 microns
∢ TXP = 116 degrees TX = 290 microns

Length of spines (when entire) on bifurcating ray tips = 70 microns.

Paratype (USNM 165542)

∢ PXS = 125 degrees PX = 260 microns
∢ SXT = 117 degrees SX = 270 microns
∢ TXP = 118 degrees TX = 270 microns

Length of spines (when entire) on bifurcating ray tips = 40 microns.

Paratype (USNM 165542)

∢ PXS = 125 degrees PX = 230 microns
∢ SXT = 113 degrees SX = 250 microns
∢ TXP = 122 degrees TX =————

Spines broken.

Paratype (Pessagno Coll.)

∢ PXS = 122 degrees PX = 280 microns
∢ SXT = 105 degrees SX = 280 microns
∢ TXP = 133 degrees TX = 280 microns

Length of spines (when entire) on bifurcating ray tips = 40 microns.

Paratype (Pessagno Coll.)

∢ PXS = 122 degrees PX = 290 microns
∢ SXT = 119 degrees SX = 290 microns
∢ TXP = 119 degrees TX = 290 microns

Spines broken.

Type locality. — NSF 568-B. See Locality Descriptions.

Deposition of types. — Holotype = USNM 165541. Paratypes = USNM 165542 — 165543 and Pessagno Collection, University of Texas at Dallas.

Range. — Latest Campanian. Although it is certain that the range zone of this species does not extend below the latest Campanian, it may well extend into the Maestrichtian. The Maestrichtian is poorly represented or absent in the Coast Ranges of northern California.

Occurrence. — See Text-figure 5 and Locality Descriptions.

Patulibracchium inaequalum Pessagno, n. sp. Pl. 4, figs. 3-6; Pl. 5, fig. 1

Description. — Test as with genus. Primary ray nearly at right angles to secondary and tertiary rays. Primary ray considerably shorter than other rays; possessing a cylindrical bracchiopyle with indeterminate number of subparallel imperforate ridges. Pore

frames on rays, spines, and bracchiopyle rectangular, square, to variously polygonal in shape. Centrally placed spines on secondary and tertiary rays spongy in character; lateral spines lacking on ray tips.

Remarks. — *Patulibracchium inaequalum,* n. sp., differs from *P. davisi,* n. sp. (1) by having a shorter primary ray which is oriented nearly at right angles to its secondary and tertiary rays; (2) by possessing single large, spongy central spines not flanked by lateral spines; (3) by the markedly different length of its rays; (4) by the more irregular character of its meshwork; and so forth. It is likely that the spongy spines of *P. inaequalum* terminate in imperforate tips. To date, however, imperforate tips have not been observed.

Inaequalis (Latin) = unequal, irregular.

Measurements. — See Text-figure 4 for explanation of designations.

Holotype (USNM 165502)

∢ PXS = 101 degrees	PX = 220 microns
∢ SXT = 158 degrees	SX = 670 microns
∢ TXP = 101 degrees	TX = 540 microns

Bracchiopyle and spines broken.

Paratype (USNM 165503)

∢ PXS = 101 degrees	PX = 230 microns
∢ SXT = 157 degrees	SX = 460 microns
∢ TXP = 102 degrees	TX = ————

Length of bracchiopyle = 80 microns. Central spines broken.

Paratype (USNM 165504)

∢ PXS = 123 degrees	PX = 250 microns
∢ SXT = 143 degrees	SX = 350 microns
∢ TXP = 94 degrees	TX = 400 microns

Bracchiopyle and spines broken.

Paratype (Pessagno Coll.)

∢ PXS = 95 degrees	PX = 200 microns
∢ SXT = 160 degrees	SX = 430 microns
∢ TXP = 105 degrees	TX = 500 microns

Bracchiopyle and spines broken.

Topotoype (destroyed in mounting)

∢ PXS = 115 degrees	PX = 160 microns
∢ SXT = 142 degrees	SX = 760 microns
∢ TXP = 103 degrees	TX = 760 microns

Length of bracchiopyles = 152 microns. Central spines broken.

Type locality. — NSF 350. See Locality Descriptions.

Deposition of types. — Holotype = USNM 165502. Paratypes = USNM 165503 — 165504 and Pessagno Collection, University of Texas at Dallas.

Range. — Early Cenomanian.

Occurrence. — See Locality Descriptions and Text-figure 5.

Patulibracchium lawsoni, Pessagno, n. sp. Pl. 13, figs. 4-6; Pl. 14, fig. 1

Description. — Test as with genus. Rays nearly equal in length; widening distally to form wedge-shaped, broad tips. Meshwork on rays with triangular, tetragonal, or pentagonal pore frames arranged in a sublinear fashion. Central area with meshwork comprised of triangular pore frames. Tips of all three rays with two pronounced, imperforate lateral spines; secondary and tertiary rays with minute central spines. Primary ray with large, fragile bracchiopyle having coarse rectangular pore frames; rays subrectangular in axial section (Pl. 13, fig. 5); with or without patagium.

Remarks. — *P. lawsoni,* n. sp. is closely related to *P. torvitatis,* n. sp. It can be easily distinguished from the latter species by having minute central spines on its secondary and tertiary rays rather than long central spines as in the case of *P. torvitatis.* It is likely that *P. lawsoni,* n. sp. arose from *P. torvitatis* during Campanian times through the atrophy of the latter form's central spines and through a widening of the bracchiopyle.

This species is named after Andrew C. Lawson in honor of his contributions to the geology of the California Coast Ranges.

Measurements. — See Text-figure 4 for explanation of designations.

Holotype (USNM 165532)

Degrees	Microns
∢ PXS = 115	PX = 200
∢ SXT = 110	SX = 220
∢ TXP = 135	TX = 210

Bracchiopyle broken.

Paratype (USNM 165533)

∢ PXS = 123	PX = 200
∢ SXT = 114	SX = 180
∢ TXP = 123	TX = 190

Bracchiopyle broken.

Paratype (USNM 165534)

∢ PXS = 128	PX = 170
∢ SXT = 114	SX = 170
∢ TXP = 118	TX = 180

Bracchiopyle broken.

Paratype (Pessagno Coll.)

∢ PXS = 123	PX = 210
∢ SXT = 114	SX = 240
∢ TXP = 123	TX = 230

Bracchiopyle broken.

Paratype (Pessagno Coll.)

∢ PXS = 118	PX = 170
∢ SXT = 110	SX = 220
∢ TXP = 132	TX = 230

Bracchiopyle broken.

Type locality. — NSF 451. See Locality Descriptions.

Deposition of types — Holotype = USNM 165532. Paratypes = USNM 165533 — USNM 165534 and Pessagno— Collection, University of Texas at Dallas.

Range. — Early to latest Campanian. See Text-figure 2.

Occurrence. — See Text-figure 5 and Locality Descriptions.

Patulibracchium marshensis Pessagno, n. sp. Pl. 15, figs. 2-5

Description. — Test as with genus. Rays exclusive of central spines and bracchiopyle nearly equal in length; primary ray slightly shorter. Meshwork on rays and central area polygonal; pore frames variable in size and shape, varying from tetragonal to pentagonal to hexagonal. Secondary and tertiary rays with long porous spines (Pl. 15, figs. 3,5) with rows of circular to elliptical pores situated between six (?) ridges that converge toward the imperforate spine tips. Primary rays with long, cylindrical bracchiopyle lacking ridges; bracchiopyle with circular to elliptical pores. Rays elliptical in axial section. Fragments of patagium present on some specimens.

Remarks. — This species may be related to *P. petroleumensis,* n. sp. of the early Campanian. Both species have elliptically shaped ray tips and show similarity in meshwork. *P. marshensis,* n. sp. differs from *P. petroleumensis,* n. sp. (1) by lacking triangular meshwork in its central area; (2) by the less linear nature of the meshwork on its rays; and so forth.

This species is named for Marsh Creek, Contra Costa County, California.

Measurements. — See Text-figure 4 for explanation of designations.

Holotype (USNM 165535)

∢ PXS = 116 degrees	PX = 170 microns
∢ SXT = 123 degrees	SX = 190 microns
∢ TXP = 121 degrees	TX = 190 microns

Length of bracchiopyle = 80 microns.
Length of central spine at S = 90 microns.
Length of central spine at T = 80 microns.

Paratype (USNM 165536)

∢ PXS = 125 degrees	PX = 180 microns
∢ SXT = 106 degrees	SX = 200 microns
∢ TXP = 129 degrees	TX = 200 microns

Length of bracchiopyle = 60 microns.
Length of central spine at S = 80 microns.

Paratype (Pessagno Coll.)

∢ PXS = 120 degrees	PX = 220 microns
∢ SXT = 110 degrees	SX = 240 microns
∢ TXP = 130 degrees	TX = 240 microns

Type locality. — NSF 568-B. See Locality Descriptions.

Deposition of types. — Holotype = USNM 165535. Paratypes = USNM 165536 and Pessagno Collection, University of Texas at Dallas.

Range. — Latest Campanian. See Text-figure 2.

Occurrence. — See Text-figure 5 and Locality Descriptions.

Patulibracchium petroleumensis Pessagno, n. sp. Pl. 11, figs. 2-5

Description. — Test as with genus. Rays short with greatly expanded spongy tips; meshwork exclusive of tips with rectangular to square pore frames predominating; pore frames arranged in a linear fashion. Meshwork on ray tips comprised of pentagonal to hexagonal pore frames. Central area with a predominance of triangular pore frames. Secondary and tertiary rays with centrally placed spongy spines comprised of pentagonal to hexagonal pore frames; spines fragmentary, usually not preserved in their entirety. Primary ray with somewhat broader tip and poorly preserved cylindrical bracchiopyle whose detailed structure is indeterminate. With or without patagium.

Remarks. — *P. petroleumensis,* n. sp. differs from *P. arbucklensis,* n. sp. (1) by having much shorter rays with much wider tips; (2) by having spongy, more porous central spines on its secondary and tertiary rays; (3) by the proportionately greater width of its rays; and so forth. *P. petroleumensis,* n. sp. seems closely related to *P. marshensis,* n. sp. A comparison of the two species is given under *P. marshensis.*

This species is named for Petroleum Creek in the Rumsey Hills, Yolo County, California.

Measurements. — See Text-figure 4 for explanation of designations.

Holotype (USNM 165517)

Degrees	Microns
∢ PXS = 110	PX = 176
∢ SXT = 112	SX = 230
∢ TXP = 128	TX = 200

Paratype (USNM 165518)

∢ PXS = 120	PX = 180
∢ SXT = 116	SX = 190
∢ TXP = 124	TX = 190

Paratype (USNM 165519)		
	∢ PXS = 130	PX = 170
	∢ SXT = 119	SX = 200
	∢ TXP = 111	TX = 200
Paratype (Pessagno Coll.)		
	∢ PXS = 125	PX = 250
	∢ SXT = 125	SX = 250
	∢ TXP = 110	TX = 250
Topotype (broken in mounting)		
	∢ PXS = 113	PX = 176
	∢ SXT = 127	SX = 180
	∢ TXP = 120	TX = 168

Bracchiopyle and spines broken on all specimens.

Type locality. — NSF 32-B. See Locality Descriptions.

Deposition of types. — Holotype = USNM 165517. Paratypes = USNM 165518 — USNM 165519.

Occurrence. — See Text-figure 5 and Locality Descriptions.

Patulibracchium sp. aff. **P. petroleumensis,** n. sp. **Pl. 16, fig 5**

Remarks. — This form is similar to *P. petroleumensis,* n. sp. but has coarser, more irregular meshwork.

Range and occurrence. — NSF 32-B. See Locality Descriptions and Text-figure 2. Early Campanian.

Patulibracchium ruesti Pessagno, n. sp. **Pl. 7, fig. 6; Pl. 8, figs. 1-4**

Description. — Test as with genus. Rays narrow proximally; flaring distally to form moderately broadened tips. Pore frames on rays square to rectangular; sometimes irregularly tetragonal. Central area with triangular meshwork. Tips of secondary and tertiary rays with three spines; a central spine and two short lateral spines. Central spine massive, spongy for the most part with large circular to elliptical pores; terminating in an imperforate tip on well-preserved specimens. Shorter lateral spines predominantly imperforate. Primary ray with fragile, subcylindrical bracchiopyle; bracchiopyle with five ridges framing two rows of large circular to elliptical pores. Fragments of patagium present on some specimens.

Remarks. — *P. ruesti,* n. sp. differs from *P. torvitatis* n. sp. (1) by possessing rays with narrower tips; (2) by having finer meshwork; (3) by possessing a larger, more massive central spine on its secondary and tertiary rays; (4) by having much shorter lateral spines on its rays; and so forth. *P. ruesti,* n. sp. appears closely related to *P. davisi,* n. sp. It differs from the latter species by having

(1) somewhat larger and more spongy central spines; (2) a more coarsely perforate bracchiopyle; and (3) coarser meshwork with well-developed triangular frames in its central area.

P. ruesti, n. sp. is named for David Rüst in honor of his contributions to the study of Mesozoic Radiolaria in the latter part of the nineteenth century.

Measurements. — See Text-figure 4 for explanation of designations.

Holotype (USNM 165511)
∢ PXS = 120 degrees PX = 200 microns
∢ SXT = 116 degrees SX = 200 microns
∢ TXP = 124 degrees TX = 230 microns
Length of bracchiopyle = 60 microns.
Length of central spine at S = 70 microns.
Length of central spine at T= 65 microns.

Paratype (USNM 165512)
∢ PXS = 116 degrees PX = 180 microns
∢ SXT = 126 degrees SX = 220 microns
∢ TXP = 118 degrees TX = 220 microns
Bracchiopyle broken.
Length of central spine at S = 80 microns.
Length of central spine at T = 70 microns.

Paratype (USNM 165513)
∢ PXS = 122 degrees PX = 220 microns
∢ SXT = 121 degrees SX = 260 microns
∢ TXP = 117 degrees TX = 260 microns
Bracchiopyle and central spines broken.

Paratype (Pessagno Coll.)
∢ PXS = 111 degrees PX = 190 microns
∢ SXT = 123 degrees SX = 170 microns
∢ TXP = 126 degrees TX = 180 microns
Bracchiopyle and central spines broken.

Paratype (Pessagno Coll.)
∢ PXS = 125 degrees PX = 170 microns
∢ SXT = 119 degrees SX = 200 microns
∢ TXP = 116 degrees TX = 210 microns
Bracchiopyle and central spine at T broken.
Central spine at S = 70 microns.

Type locality. — NSF 483. See Locality Descriptions.

Deposition of types. — Holotype = USNM 165511. Paratypes = USNM 165512 — USNM 165513 and Pessagno Collection, University of Texas at Dallas.

Range. — Late Turonian/Coniacian-Coniacian. See Text-figure 2.

Occurrence. — See Text-figure 5 and Locality Descriptions.

Patulibracchium taliaferroi Pessagno, n. sp. Pl. 14, figs. 2-6; Pl. 15, fig. 1

Description. — Test as with genus. Pore frames on all three rays dominantly rectangular; arranged in three to four markedly linear rows. Pores frames of central area tetragonal to pentagonal. Secondary and tertiary rays long and narrow; gradually widening from central area to ray tips; sides of rays straight but not parallel; ray tips with spongy central spines which are seldom preserved in their entirety. Primary ray with parallel, straight sides, about three-quarters the length of the secondary and tertiary rays with a large subcylindrical bracchiopyle which tends to flare outwardly (Pl. 14, figs. 3,4); bracchiopyle with large circular pores. Rays elliptical in axial section. Fragments of a patagium present on some specimens.

Remarks. — *P. taliaferroi,* n. sp. appears to be closely related to *P. delvallensis,* n. sp. It differs from *P. delvallensis,* n. sp. (1) by lacking triangular meshwork in its central area; (2) by having slender rays with three to four as opposed to six rows of pores; (3) by having secondary and tertiary rays which gradually widen in a distal direction; and (4) by having a more triangularly shaped central area.

This species is named for N. L. Taliaferro in honor of his contributions to the geology of the California Coast Ranges.

Measurements. — See Text-figure 4 for explanation of designations.

Holotype (USNM 165538)

$\measuredangle$ PXS = 115 degrees PX = 300 microns
$\measuredangle$ SXT = 127 degrees SX = 390 microns
$\measuredangle$ TXP = 118 degrees TX = 400 microns
Bracchiopyle and central spines broken.

Paratype (USNM 165539)

$\measuredangle$ PXS = 125 degrees PX = 200 microns
$\measuredangle$ SXT = 110 degrees SX = ————
$\measuredangle$ TXP = 125 degrees TX = ————
Length of bracchiopyle = 50 microns.
Central spines broken.

Paratype (Pessagno Coll.)

$\measuredangle$ PXS = 125 degrees PX = 250 microns
$\measuredangle$ SXT = 109 degrees SX = 320 microns
$\measuredangle$ TXP = 126 degrees TX = 330 microns
Bracchiopyle and central spines broken.

Paratype (Pessagno Coll.)

∢ PXS = 122 degrees	PX = 300 microns
∢ SXT = 111 degrees	SX = ————
∢ TXP = 127 degrees	TX = 450 microns

Paratype (Pessagno Coll.)

∢ PXS = 116 degrees	PX = 250 microns
∢ SXT = 121 degrees	SX = ————
∢ TXP = 123 degrees	TX = ————

Type locality. — NSF 568-B. See Locality Descriptions.

Deposition of types. — Holotype = USNM 165538. Paratypes = USNM 165539 — USNM 165540 and Pessagno Collection, University of Texas at Dallas.

Range. — Latest Campanian. See Text-figure 2 and comment under range of *P. dickersoni,* n.sp.

Occurrence. — See Text-figure 5 and Locality Decriptions.

Patulibracchium teslaensis Pessagno, n. sp. Pl. 12, figs. 3-6; Pl. 13, fig. 1

Description. — Test as with genus. Pore frames on all three rays dominantly square or rectangular; sometimes irregularly tetragonal. Central area with well-developed triangular meshwork. Primary, secondary, and tertiary rays nearly equal in length, with relatively narrow heart-shaped tips; tip of primary ray often slightly wider than those of secondary and tertiary rays. Secondary and tertiary rays with long centrally placed spines which are spongy and fragile; spines rarely preserved. Primary ray with cylindrical bracchiopyle (Pl. 12, figs. 5,6) with circular to elliptical pores. Rays elliptical in axial section.

Remarks. — *P. teslaensis,* n. sp. differs from *P. arbucklensis,* n. sp. (1) by having rays which are more equal in length; (2) by having well-developed triangular meshwork in its central area and rays with predominantly square or rectangular meshwork; (3) by having heart-shaped ray tips of nearly uniform size. Both species appear to show converging ridges on their spine tips. This may perhaps suggest a phylogenetic link.

This species is named after the Tesla Quadrangle, Alameda and San Joaquin Counties, California.

Measurements. — See Text-figure 4 for explanation of designations.

Holotype USNM 165526)
∢ PXS = 125 degrees PX = 290 microns
∢ SXT = 120 degrees SX = 320 microns
∢ TXP = 115 degrees TX = 290 microns
Bracchiopyle and central spine at S broken.
Length of central spine at T = 70 microns.

Paratype (USNM 165527)
∢ PXS = 120 degrees PX = 280 microns
∢ SXT = 110 degrees SX = 290 microns
∢ TXP = 130 degrees TX = 300 microns
Bracchiopyle and central spines broken.

Paratype (USNM 165528)
∢ PXS = 120 degrees PX = 250 microns
∢ SXT = 125 degrees SX = 280 microns
∢ TXP = 115 degrees TX = 300 microns
Bracchiopyle and central spines broken.

Paratype (Pessagno Coll.)
∢ PXS = 118 degrees PX = 250 microns
∢ SXT = 118 degrees SX = 330 microns
∢ TXP = 124 degrees TX = 290 microns
Bracchiopyle and central spines broken.

Paratype (Pessagno Coll.)
∢ PXS = 118 degrees PX = 250 microns
∢ SXT = 118 degrees SX = 330 microns
∢ TXP = 124 degrees TX = 290 microns
Bracchiopyle and central spines broken.

Type locality. — NSF 451. See Locality Descriptions.

Deposition of types. — Holotype = USNM 165526. Paratypes = USNM 165527 — USNM 165528 and Pessagno Collection, University of Texas at Dallas.

Range. — Early to late Campanian. See Text-figure 2.

Occurrence. — See Text-figure 5 and Locality Descriptions.

Patulibracchium torvitatis, n. sp. Pl. 6, figs. 4-6; Pl. 7, figs. 1,2

Description. — Test as with genus. Rays markedly narrow proximally; flaring distally to form broad tips. Pore frames on rays rectangular, variously tetragonal, or triangular. Central area with markedly triangular pore frames. Pore frames on both rays and central area with massive nodes at vertices. Tips of secondary and tertiary rays with three prominent spines: two lateral spines and one central spine; central spine always the longest on well-preserved specimens (Pl. 6, fig. 4). Primary ray have cylindrical bracchiopyle with relatively large circular to elliptical pores arranged in a linear fashion between six (?) parallel ridges; bracchiopyle flanked to either side by short lateral spines. Spines on all three rays lacking

pores. Occasional specimens with shorter spines interspersed between centrally placed spines and laterally placed spines. Secondary ray somewhat longer than primary and tertiary rays. Primary ray with broader tip than those of other rays. Rays wedge-shaped in longitudinal section, widening in a distal direction; subrectangular in axial section. With or without patagium.

Remarks. — *P. torvitatis,* n.sp. differs from *P. davisi,* n.sp. by possessing (1) rays with wider tips; (2) coarser meshwork with a larger number of triangular pore frames; (3) a more coarsely perforate bracchiopyle; (4) longer, more massive lateral spines at the termination of rays; and so forth. *P. torvitatis* is compared to *P. lawsoni,* n.sp. under the latter species.

Torvitas, -atis (Latin, F.) = savageness, wildness (of appearance or character).

Measurements. — See Text-figure 4 for explanation of designations.

Holotype (USNM 165508)

∢ PXS = 120 degrees PX = 170 microns
∢ SXT = 120 degrees SX = 190 microns
∢ TXP = 120 degrees TX = 190 microns
Bracchiopyle and central spine at T broken.
Length of central spine at S = 70 microns.

Paratype (USNM 165509)

∢ PXS = 123 degrees PX = 190 microns
∢ SXT = 112 degrees SX = 200 microns
∢ TXP = 125 degrees TX = 190 microns

Paratype (USNM 165510)

∢ PXS = 126 degrees PX = 190 microns
∢ SXT = 117 degrees SX = 210 microns
∢ TXP = 117 degrees TX = 220 microns
Central spines and bracchiopyle broken.

Paratype (Pessagno Coll.)

∢ PXS = 117 degrees PX = 170 microns
∢ SXT = 123 degrees SX = 160 microns
∢ TXP = 120 degrees TX = 170 microns
Central spines broken.
Length of bracchiopyle = 50 microns.

Paratype (Pessagno Coll.)

∢ PXS = 118 degrees PX = 210 microns
∢ SXT = 118 degrees SX = 230 microns
∢ TXP = 124 degrees TX = 230 microns
Central spines and bracchiopyle broken.

Type locality. — NSF 483. See Locality Descriptions.

Deposition of types. — Holotype = USNM 165508. Paratypes =

USNM 165509 – 165510 and Pessagno Collection, University of Texas at Dallas.

Range. – Middle Turonian to early Campanian.

Occurrence. – See Locality Descriptions and Text-figure 5.

Patulibracchium ungulae Pessagno, n. sp. Pl. 7, figs. 3-5

Description. – Test as with genus. Rays relatively broad, flaring distally to form clawlike tips. Pore frames large; dominantly rectangular or square on rays but sometimes irregularly tetragonal to pentagonal. Central area with triangluar meshwork. Secondary and tertiary rays with massive central spines having circular to elliptical pores; two shorter lateral spines flanking central spine; lateral spines likewise having circular to elliptical pores. Primary ray with bracchiopyle flanked by two lateral spines resembling those of other rays. Bracchiopyle cylindrical, wide with subrectangular pores. Rays nearly equal in length. Tip of primary ray somewhat wider than tips of secondary and tertiary rays. With or without patagium.

Remarks. – *P. ungulae,* n. sp. is similar to *P. torvitatis,* n. sp. It differs from the latter species by having rays with porous, spongy spines; by having rays which are nearly equal in length; and by having broader and proportionately shorter rays with wider tips. It is likely that these two species are closely related. A comparison of *P. ungulae* with *P. californiaensis,* n. sp. is given under the latter species.

Ungula, ae (Latin F.) = claw or talon.

Measurements. – See Text-figure 4 for explanation of designations.

Holotype (USNM 165514)

∢ PXS = 123 degrees PX = 170 microns
∢ SXT = 117 degrees SX = 170 microns
∢ TXP = 120 degrees TX = 170 microns
Length of central spine at S = 40 microns.
Length of central spine at T = 40 microns.
Bracchiopyle broken.

Paratype (USNM 165515)

∢ PXS = 119 degrees PX = 120 microns
∢ SXT = 110 degrees SX = 120 microns
∢ TXP = 131 degrees TX = 130 microns
Central spines and bracchiopyle broken.

Paratype (USNM 165516)

$\measuredangle$ PXS = 118 degrees PX = 140 microns
$\measuredangle$ SXT = 114 degrees SX = 140 microns
$\measuredangle$ TXP = 128 degrees TX = 140 microns
Central spine at T and bracchiopyle broken.
Length of central spine at S = 60 microns.

Paratype Pessagno Coll.)

$\measuredangle$ PXS = 110 degrees PX = 150 microns
$\measuredangle$ SXT = 125 degrees SX = 150 microns
$\measuredangle$ TXP = 125 degrees TX = 160 microns
Central spines and bracchiopyle broken.

Paratype (Pessagno Coll.)

$\measuredangle$ PXS = 123 degrees PX = 150 microns
$\measuredangle$ SXT = 117 degrees SX = 150 microns
$\measuredangle$ TXP = 120 degrees TX = 140 microns
Central spines and bracchiopyle broken.

Type locality. — NSF 483. See Locality Descriptions.

Deposition of types. — Holotype = USNM 165514. Paratypes = USNM 165515 — USNM 165516 and Pessagno Collection, University of Texas at Dallas.

Range. — Middle Turonian to Coniacian.

Occurrence. — See Text-figure 5 and Locality Descriptions.

Patulibracchium woodlandensis, n. sp. Pl. 5, figs. 2-6

Description. — Test as with genus. Rays with square to rectangular pore frames intermixed with some tetragonal, pentagonal, or hexagonal pore frames. Central area with triangular or irregularly tetragonal pore frames. Secondary and tertiary rays with large central spines flanked to either side by a variable number (often as many as eight on both sides) of lateral spines. Central spines with coarse square to polygonal pore frames basally, terminating in imperforate tips. Lateral spines imperforate. Primary ray with large cylindrical bracchiopyle divided into six segments by six parallel ridges; each of six segments with two rows of circular to elliptical pores. Rays broad with greatly expanded tips; elliptical in axial section. With or without patagium.

Remarks. — *P. woodlandensis,* n. sp. differs from *P. davisi,* n. sp. (1) by having broader rays with wider tips; (2) by having pore frames which are more irregular in their size, shape, and distribution as opposed to those of *P. davisi,* which are predominantly square or rectangular and arranged linearly; (3) by having a wider bracchiopyle; and so forth.

This species is named for the town of Woodland, Yolo County, California.

Measurements. — See Text-figure 4 for explanation of designations.

Holotype (USNM 165505)

∢ PXS = 112 degrees PX = 310 microns
∢ SXT = 123 degrees SX = 310 microns
∢ TXP = 115 degrees TX = 310 microns
Length of bracchiopyle = 70 microns.
Length of central spine at S = 90 microns.
Central spine at T broken.

Paratype (USNM 165506)

∢ PXS = 124 degrees PX = 230 microns
∢ SXT = 124 degrees SX = 240 microns
∢ TXP = 112 degrees TX = 260 microns
Length of bracchiopyle = 60 microns.
Length of central spine at S = 60 microns.
Central spine at T broken.

Paratype (USNM 165507)

∢ PXS = 120 degrees PX = 240 microns
∢ SXT = 120 degrees SX = 260 microns
∢ TXP = 120 degrees TX = 260 microns
Length of bracchiopyle = 60 microns.
Central spines broken.

Paratype (Pessagno Coll.)

∢ PXS = 120 degrees PX = 210 microns
∢ SXT = 117 degrees SX = 200 microns
∢ TXP = 123 degrees TX = 200 microns
Bracchiopyle and central spines broken.

Paratype (Pessagno Coll.)

∢ PXS = 121 degrees PX = 230 microns
∢ SXT = 114 degrees SX = 230 microns
∢ TXP = 125 degrees TX = 270 microns
Length of bracchiopyle = 60 microns.
Central spines broken.

Type locality. — NSF 350. See Locality Descriptions.

Deposition of types. — Holotype = USNM 165505. Paratypes = USNM 165506 — 165507 and Pessagno Collection, University of Texas at Dallas.

Range. — Early Cenomanian. See Text-figure 2.

Occurrence. — See Text-figure 5 and Locality Descriptions.

Genus **PARONAELLA,** new genus

Type species. — *Paronaella solanoensis,* n. sp.

Description. — Test lack rays with bracchiopyle. Rays always of nearly equal in length; expanded or thickened ray tips lacking.

Meshwork linear to sublinear; comprised of irregular polygonal pore frames. Pore frames comprised of bars connected to weakly developed nodes.

Remarks. — *Paronaella,* n. gen. differs from *Patulibracchium,* n. gen. and *Halesium,* n. gen. by lacking a bracchiopyle and expanded ray tips and by always having rays which are nearly equal length.

This genus is named for C. F. Parona, one of the early students of Mesozoic Radiolaria.

Range. — Upper Cretaceous in so far as known. Forms possibly assignable to this genus occur in the Jurassic.

Occurrence. — Upper Cretaceous of the California Coast Ranges.

?Paronaella ewingi, n. sp. Pl. 19, figs. 2-5

Description. — Test with extremely elongate, slender rays of nearly equal length having expanded ellipsoidal tips. Ray tips terminating in five to seven minute spines. Meshwork on rays comprised of square to rectangular frames arranged in two markedly linear rows. Rays subrectanglar in axial section.

Remarks. — *?Paronaella ewingi,* n. sp., is tentatively assigned to *Paronaella,* n. gen. Although it lacks a bracchiopyle as do all species of *Paronaella,* the strong linearity of its pore frames suggests the presence of tabulae similar to those of *Halesium,* n. gen. It is likely that this species should be assigned to a new and yet undescribed genus.

?P. ewingi, n. sp. is analagous to *"Chitonastrum" tricuspidatum* Rüst (1885, p. 9, fig. 8) from the "Kieselkalke von Cittiglio." Like the latter species it possesses markedly linear rows of pore frames and three slender, straight, long rays. However, *?P. ewingi,* n. sp. possesses five to seven spines on its ray tips whereas *"C." tricuspidatum* Rüst possesses two long lateral spines and one long central spine on each ray.

?P. ewingi, n. sp. is one of the most abundant and distinctive species occurring in the Tithonian sediments of the Blake-Bahama Basin.

This species is named for Dr. Maurice Ewing (Lamont-Doherty Geological Observatory), Co-Chief Scientist of JOIDES Leg I.

Measurements. —

	Interradial angles. Degrees	Length of rays. Microns
Holotype (USNM 165559)	∢ 113, 124, 123	390, 400, 400
Paratype (USNM 165560)	∢ 118, 124, 118	310, 330, 330
Paratype (Pessagno Coll.)	∢ 116, 122, 122	420, 450, 450
Paratype (Pessagno Coll.)	∢ 121, 112, 127	380, 410, 420
Paratype (Pessagno Coll.)	∢ 120, 108, 132	400, 380, 380

Type locality. — JOIDES Leg I, Site 5A, Core 7, Section 1: Top 274.3 meters (900 feet). Blake-Bahama Basin.

Deposition of types. — Holotype = USNM 165559. Paratypes = USNM 165560 – 165561 and Pessagno Collection, University of Texas at Dallas.

Range and occurrence. — Late Jurassic (Tithonian) of the Blake-Bahama Basin.

Paronaella solanoensis Pessagno, n. sp. Pl. 10, figs. 2,3

Description. — Rays and central area with tetragonal, pentagonal, and hexagonal pore frames. Rays elliptical in axial section, relatively wide with two prominent lateral spines and one prominent central spine at ray tips; irregularly dispersed short spines occurring on ray tips or occasionally on sides of ray.

Remarks. — *P. solanoensis,* n. sp. differs form *P. venadoensis,* n. sp. (1) by its coarser, more massive meshwork and (2) by possessing both well-developed lateral and central spines.

This species is named for Solano County, California.

Measurements. —

	Interradial angles.	Length of rays.
Paratype (USNM 165580)	∢ 110, 125, 125 degrees	110, 120, 110 microns
Holotype (USNM 165551)	∢ 115, 125, 120 degrees	140, 140, 140 microns
Paratype (USNM 165552)	∢ 121, 119, 120 degrees	130, 130, 120 microns

Length of central spine when complete = 40 microns.

Paratype (Pessagno Coll.)
∢ 132, 115, 113 degrees 160, 160, 160 microns
Length of central spine when complete = 50 microns.
Paratype (Pessagno Coll.)
∢ 118, 128, 114 degrees 140, 160, 120 microns
Length of central spines when entire = 50 microns.

Type localities. — Holotype and some paratypes from NSF 483. Remaining paratypes from NSF 291-B. See Locality Descriptions.

Deposition of types. — Holotype = USNM 165550. Paratypes = USNM 165551 — 165552 and Pessagno Collection, University of Texas at Dallas.

Range. — Late Turonian/Coniacian — Coniacian.

Occurrence. — See Text-figure 5 and Locality Descriptions.

Paronaella venadoensis Pessagno, n. sp. Pl. 10, figs. 4-6; Pl. 11, fig. 1

Description. — Rays and central area with tetragonal, pentagonal, and hexagonal pore frames. Rays elliptical in axial section; rays exclusive of spines with square tips. Relatively long (for genus) central spines with triradiate bases occurring on ray tips; central spines flanked by short lateral spines and irregularly placed small spines occurring on ray tips and on sides of rays.

Remarks. — A comparison of *P. venadoensis,* n. sp., with *P. solanoensis,* n. sp., is given under the latter species.

This species is named for the ghost town of Venado (Mountain House), Colusa County, California.

Measurements. —

Holotype (USNM 165553)
Interradial angles. Length of rays.
∢ 115, 125, 120 degrees 150, 160, 150 microns
Paratype (USNM 165554)
∢ 120, 120, 120 degrees 110, 130, 120 microns
Length of central spine when entire = 60 microns.
Paratype (USNM 165555)
∢ 118, 124, 118 degrees 140, 140, 130 microns
Length of central spine when entire = 40 microns.
Paratype (Pessagno Coll.)
∢ 115, 135, 110 degrees 140, 140, ——microns
Length of central spine when complete = 50 microns.

Type locality. — NSF 483. See Locality Descriptions and Text-figure 5.

Deposition of types. — Holotype = USNM 165553. Paratypes = USNM 165554 — 165555 and Pessagno Collection, University of Texas at Dallas.

Range. — Late Turonian/Coniacian — Coniacian.

Occurrence. — See Text-figure 5 and Locality Descriptions.

?Paronaella worzeli Pessagno, n. sp. Pl. 19, fig. 6

Description. — Test with three rays of nearly equal length ending with heart-shaped tips. Pore frames square to variously tetragonal; arranged in three markedly linear rows on rays. Rays terminating in prominent central spines. Rays subrectangular in axial section. Patagium not observed.

Remarks. — *?P. worzeli,* n. sp. is tentatively placed in *Paronaella,* n. gen., even though it lacks a bracchiopyle. Like *?P. ewingi,* n. sp. *?P. worzeli* possesses meshwork on its rays arranged in three markedly linear rows. This suggests the presence of tabulae as with *Halesium, n. gen.* (See *?P. ewingi,* n. sp.). *?P. worzeli,* n. sp. appears to be closely related to *"Rhopalastrum" trixiphus* Rüst (1885, p. 27, pl. 8, fig. 14) from the "Kiesellkalke von Cittiglio". It differs from the latter species by having distinctly heart-shaped ray tips. It is likely that both of these species will have to be placed in a new genus once their morphology is better understood. The somewhat recrystallized nature of the JOIDES material (Leg I, Site 5A, Core 7) prohibits establishing a new genus at the present time.

This species is named for Dr. J. Lamar Worzel (Lamont-Doherty Geological Observatory), Co-Chief Scientist of JOIDES Leg I.

Measurements. —

	Interradial angles.	Length of rays.
Holotype (USNM 165556)	∢ 123, 117, 120 degrees	310, 350, 310 microns
Paratype (USNM 165557)	∢ 124, 131, 105 degrees	340, 340, 340 microns
Paratype (Pessagno Coll.)	∢ 114, 123, 123 degrees	430, 400, 430 microns

Type locality. — JOIDES Leg I, Site 5A, Core 7, Section 1 : 274.3 meters (900 feet). Blake-Bahama Basin. See Locality Descriptions.

Deposition of types. — Holotype = USNM 165556. Paratypes =

USNM 165557 and Pessagno Collection, University of Texas at Dallas.

Range and occurrence. — Late Jurassic (Tithonian) of the Blake-Bahama Basin in so far as known.

?Paronaella sp. 1 Pl. 17, fig. 1

Remarks. — This form differs from *P. venadoensis,* n. sp. and *P. solanoensis,* n. sp. by having rays with linearly arranged rectangular meshwork and considerably longer central spines.

The generic assignment of *?P.* sp. 1 is questioned in that spines have not been noted on all three rays of any one specimen. In theory, a bracchiopyle could be present.

Range. — Middle Turonian.

Occurrence. — NSF 432. See Locality Descriptions.

Paronaella sp. 2 Pl. 17, fig. 2

Remarks. — This form is similar to *P. solanoensis.* It possesses two massive central spines on each ray. The central spines seem to be somewhat shorter than the lateral spines. *T.* sp. 2 differs from *P. solanoensis,* n. sp. by having well-developed rectangular meshwork on its rays and by having spines that merge or are interconnected at their bases.

Range. — Late Turonian/Coniacian — Coniacian.

Occurrence. — NSF 319B and NSF 483. See Locality Descriptions.

Subfamily **HAGIASTRINAE** Riedel, emended

Type genus. — *Hagiastrum* Haeckel.

Description. — Test as with family but comprised of four rays. Rays extending from small central area along two axes at right angles to one another.

Remarks. — The Hagiastrinae Riedel are restricted to forms having four rays arranged along two axes at right angles. The Hagiastrinae differ from the Patulibracchinae, n. subfam., by having four rather than three rays.

The Hagiastrinae as defined in the restricted sense above include two genera: *Hagiastrum s.s.* and *Crucella,* n. gen. The Hagiastrinae show a lengthy geologic history which extends back at least to the Jurassic. Rüst (1885, 1898) and Parona (1890) figured forms assignable to *Hagiastrum s.s.* and *Crucella* from the

Jurassic of Italy. Poorly preserved specimens assignable to *Crucella* have been observed by the writer from the Jurassic (Tithonian) of the Blake-Bahama Basin (see Pl. 19, fig. 7).

Range. — Jurassic to Cretaceous.

Occurrence. — World-wide.

Genus **Hagiastrum** Haeckel, Emended definition

1881. *Hagiastrum* Haeckel, Jenaische Zeitsch. Naturw., vol. 15, (n. ser. vol. 8), No. 3, 460.

1954. *Hagiastrum* Haeckel, Campbell, Treatise on Invert. Paleont., Pt. D. Protista, 3, p. D86 [Designated *Hagiastrum plenum* Rüst 1885 as type species.]

Type species. — *Hagiastrum plenum* Rüst, 1885. *H. plenum* Rüst appears to have been designated as the type species by Campbell in 1954.

Emended definition. — Test as with subfamily. Comprised of four rays situated at right angles to one another. Rays sometimes longer along one axis than other and terminating in bulbous, rounded tips lacking spines. Central areas small. With or without patagium.

Remarks. — *Hagiastrum s.s.* Haekel as defined here is compared with *Crucella* below.

Range and occurrence. — As defined in the sense above, *Hagiastrum* is restricted to strata of Jurassic to Late Cretaceous age. To date *Hagiastrum* is known from the siliceous chalks of Cittiglio and from the Upper Cretaceous portion of the Great Valley Sequence, California Coast Ranges.

Hagiastrum sp. Pl. 10, fig. 1

Remarks. — This form has three rows of rectangular/square to variously tetragonal pore frames on its rays. The meshwork in the central area is tetragonal to triangular. The four rays are long and slender with small, bulbous tips. It differs from *Hagiastrum plenum* Rüst by having slender rays with proportionately smaller ray tips.

Range and occurrence. — A few specimens of the form figured here were encountered in the Middle Turonian portion of the Marsh Creek Formation at NSF 705-B.

Genus **CRUCELLA,** new genus

Type species. — *Crucella messinae,* Pessagno, n. sp.

Description. — Test as with subfamily. Four rays, elliptical to rectangular in cross-section with polygonal meshwork arranged linearly to sublinearly; rays equal in length; tapering distally; terminating in centrally placed spines. Central area with polygonal (often triangular) meshwork; sometimes with a lacuna, with or without patagium.

Remarks. — *Crucella,* n. gen., differs from *Hagiastrum* Haeckel (1) by possessing rays of nearly equal length; (2) by possessing rays with tapered rather than bulbous tips; and (3) by having prominent spine at the tip of each ray.

Crux, Crucis (Latin, F.) = cross.

Range. — Late Jurassic to Late Cretaceous.

Occurrence. — World-wide.

Crucella cachensis Pessagno, n. sp. Pl. 9, figs. 1-3

Description. — Test as with genus. Rays with tetragonal pore frames. Central area markedly elevated with well-developed lacuna; lacuna sometimes covered by thin veneer of tetragonal meshwork. Rays cylindrical in shape longitudinally; elliptical axially with spines that are circular in cross-section.

Remarks. — This species differs from *C. messinae,* n. sp. (1) by the straight, cylindrical character of its rays longitudinally; (2) by possessing a lacuna in its central area; and (3) by lacking prominent triradiate spines.

C. cachensis, n. sp. is named after Cache Creek, Yolo County, California.

Measurements. —

	Length of rays microns	Length of spines when entire
Holotype (USNM 165562)	160	———
Paratype (USNM 165563)	150	———
Paratype (Pessagno Coll.)	150	———
Paratype (Pessagno Coll.)	160	———
Paratype (Pessagno Coll.)	150	70 microns

Type locality. — NSF 697. See Locality Descriptions.

Deposition of types. — Holotype = USNM 165562. Paratypes = USNM 165563 — 165564 and Pessagno Collection, University of Texas at Dallas.

Range and occurrence. — Early to middle Turonian. See Text-figure 5 and Locality Descriptions.

Crucella espartoensis Pessagno, n. sp. Pl. 18, figs. 1-4

Description. — Test as with genus. Meshwork on rays with coarse triangular, tetragonal, pentagonal, and hexagonal pore frames; tetragonal pore frames predominating. Central area with large lacuna. Terminal spines on rays short, massive, circular in axial section. Rays elliptical in axial section; in longitudinal view narrow proximally, flaring to become somewhat elliptical distally. Usually with patagium.

Remarks. — *C. espartoensis,* n. sp. appears to be closely related to *"Hagiastrum" tumeniensis* Lipman (1960, p. 130) from the Santonian — Campanian of Russia. It differs from the species named by Lipman by consistently possessing a large lacuna and having terminal spines lacking ridges. *C. espartoensis,* n. sp. is the most distinctive species of *Crucella* in the California Upper Cretaceous.

This species is named for the town of Esparto, Yolo County, California.

Measurements. —

	Length of rays Microns	Length of spines when entire Microns
Holotype (USNM 165565)	110	80
Paratype (USNM 165566)	120	100
Paratype (USNM 165567)	150	———
Paratype (USNM 165567)	140	60
Paratype (Pessagno Coll.)	130	70

Type locality. — NSF 32B. See Locality Descriptions.

Deposition of types. — Holotype = USNM 165565. Paratypes =

USNM 165566 — 165567 and Pessagno Collection, University of Texas at Dallas.

Range. — Early Santorian to early Campanian. Obsolete data in Text-figures 2 and 5.

Occurrence. — See Text-figure 5 and Locality Descriptions.

Crucella irwini Pessagno, n. sp. Pl. 9, figs. 4-6

Description. — Test as with genus. Rays with coarse tetragonal, pentagonal, or hexagonal pore frames arranged sublinearly. Central area with shallow lacuna and tetragonal to hexagonal pore frames. Rays slender; cylindrical longitudinally with relatively short spines which are circular in cross-section.

Remarks. — This species differs from *C. messinae,* n. sp. (1) by having proportionately coarser pore frames lacking nodes; (2) by the proportionately longer and slender character of its rays; (3) by possessing a lacuna in its central area; and (4) by having spines which are circular rather than triradiate in axial section.

C. irwini, n. sp. is named for William P. Irwin (USGS, Menlo Park, California) in honor of his contributions to the study of the geology of the California Coast Ranges.

Measurements. —

	Length of rays Microns	Length of spines Microns
Holotype (USNM 165582)	170	50
Paratype (USNM 165583)	200	———
Paratype (USNM 165584)	190	50
Paratype (Pessagno Coll.)	200	50
Paratype (Pessagno Coll.)	200	80

Type locality. — NSF 705-B. See Locality Descriptions.

Deposition of types. — Holotype = USNM 165582. Paratypes = USNM 165583 — 165584 and Pessagno Collection, University of Texas at Dallas.

Range. — Middle Turonian.

Occurrence. — See Text-figure 5 and Locality Descriptions.

Crucella messinae Pessagno, n. sp. Pl. 6, figs. 1-3

Description. — Test as with genus. Rays with tetragonal to pentagonal pore frames arranged sublinearly; pore frames with massive nodes at vertices. Central area with some triangular pore frames. Rays cylindrical longitudinally with long triradiate spines; with or without patagium.

Remarks. — A comparison of this species with *C. cachensis,* n.sp. and *C. plana,* n.sp. is given under these species.

C. messinae, n. sp. is named for the late Angelina R. Messina in honor of her contributions to micropaleontology.

Measurements. —

	Length of rays Microns	Length of spines Microns
Holotype (USNM 165569)	170	90
Paratype (USNM 165570)	160	80
Paratype (USNM 165571)	130	———
Paratype (Pessagno Coll.)	170	———
Paratype (Pessagno Coll.)	110	60

Type locality. — NSF 350. See Locality Descriptions and Text-figure 5.

Deposition of types. — Holotype = USNM 165569. Paratypes = USNM 165570 — 165571 and Pessagno Collection, University of Texas at Dallas.

Range. — Early to late Cenomanian. (Incorrect in Text-figure 2.)

Occurrence. — See Text-figure 5 and Locality Descriptions.

Crucella plana Pessagno, n. sp. Pl. 8, figs. 5,6

Description. — Test as with genus. Rays and central area with dominantly tetragonal pore frames. Rays and central area planiform horizontally; rays subcylindrical longitudinally; somewhat more inflated distally; terminating in spines lacking ridges; spines circular in axial section. Rays square in axial section. Test with or without patagium.

Remarks. — *C. plana,* n. sp. differs from *C. messinae,* n. sp.

(1) by lacking triradiate spines (2) by having rays and a central area which are planiform horizontally; and (3) by possessing tetragonal rather than triangular pore frames in its central area.

Planus-a-um (Latin) = flat.

Measurements. —

	Length of rays Microns	Length of spines Microns
Holotype (USNM 165562) 166693	150	———
Paratype (USNM 165563) 166694	150	———
Paratype (Pessagno Coll.)	150	———
Paratype (USNM 165564) 166695	130	———
Paratype (Pessagno Coll.)	160	70

Type locality. — NSF 483. See Locality Descriptions.

Deposition of types. — Holotype = USNM 165562. Paratypes = USNM 165563 — 165564 and Pessagno Collection, University of Texas at Dallas.

Range. — Late Turonian/Coniacian — Coniacian.

Occurrence. — See Text-figure 5 and Locality Descriptions.

REFERENCES CITED

Campbell, A. S.
1954. *Radiolaria. In* Treatise on Invertebrate Paleontology, Pt. D, Protista 3, pp. 11-163, text-figs. 6-86.

Douglas, R. G.
1969. *Upper Cretaceous planktonic Foraminifera in northern California. Part-I — Systematics.* Micropaleontology, vol. 15, No. 2, pp. 151-209, pls. 1-11.

Haeckel, E. H. P. A.
1881. *Entwurf eines Radiolarien-Systems auf Grund von Studien der "Challenger" Radiolarien.* Jenaische Zeitsch. Naturw., vol. 15, pp. 418-472.
1887. *Report on the Radiolaria collected by H. M. S. Challenger during the years 1873-1876.* Rept. Voyage Challenger, Zool., vol. 18, pp. i-cxxxviii, 1803, pls. 140.

Hay, W. W., and Sandberg, P. A.
1967. *The scanning electron microscope, a major break through for micropaleontology.* Micropaleontology, vol. 13, No. 4, pp. 407-418, pls. 1,2.

Honjo, S., and Berggren, W. A.
1967. *Scanning electron microscope studies of planktonic Foraminifera.* Micropaleontology, vol. 13, No. 4, pp. 393-406, pls. 1-4.

Jefferies, R. P. S.

1961. *The paleoecology of the Actinocamax plenus Subzone (Lowest Turonian) in the Anglo-Paris Basin.* Paleont., vol. 4, pt. 4, pp. 609-647, pls. 77-79.

Küpper, Klaus

1956. *Upper Cretaceous pelagic Foraminifera from the "Antelope Shale", Glenn and Colusa Counties, California.* Cushman Found. Foram. Research, Contr., vol. 7, pt. 2, pp. 40-47, pl. 8.

Lipman, R. Kh.

1952. *Materially morphographicheskomu izucheniyu radiolyarii verkhnemelovykh otlozhenii russkoi platformy.* Paleontologiya i Stratigrafiya. Trudy VSEGEI, pp. 24-51, 3 pls.

1960. *Radiolaria. In* Stratigrafiya i fauna melovykl otlozkenii zapadno — sibirskoi nizmenmosti. Trudy VSEGEI, n. ser., vol. 29, pp. 124-134, pls. 26-32.

Matsumoto, Tatsuro

1960. *Upper Cretaceous ammonites of California — Part III.* Mem. Faculty of Science, Kyushu Univ., Series D, Geology, Spec. Vol. II, pp. 1-204.

Ojakangas, R. W.

1968. *Cretaceous sedimentation, Sacramento Valley, California.* Geol. Soc. Amer., Bull., vol. 79, No. 8, pp. 973-1008, 11 figs., 5 pls.

Parona, C. F.

1890. *Radiolarie nei noduli selciosi del calcare giurese di Cittiglio presso Laveno.* Boll. Soc. Geol. Ital., vol. 9, pt. 1, pp. 1-46, pls. 1-6.

Pessagno, E. A., Jr.

1967. *Upper Cretaceous planktonic Foraminifera from the Western Gulf Coastal Plain.* Palaeont. Americana, vol. 5, No. 37, pp. 245-445, pls. 48-101, text-figures 1-63.

1969a. *Upper Cretaceous stratigraphy of the Western Gulf Coast area of Mexico, Texas, and Arkansas.* Geol. Soc. Amer., Mem. 111, pp. 1-139, pls. 1-60.

1969b. *The Neosciadiocapsidae, a new family of Upper Cretaceous Radiolaria.* Bull. Amer. Paleont., vol. 56, No. 253, pp. 377-439, pls. 23-38, text figs. 1-4.

1970. *The Rotaformidae, a new family of Upper Cretaceous Nassellariina (Radiolaria) from the Great Valley Sequence. California Coast Ranges.* Bull. Amer. Paleont., vol. 58, No. 257, pp. 5-32.

Renz, O., Luterbacher, H., and Schneider, A.

1963. *Stratigrapisch — palaontologische Untersuchungen im Albien und Cenomanien des Neuenburger Jura.* Ecologae Geol. Helv., vol. 56, No. 2, pp. 1073-1116, pls. 1-9.

Riedel, W. R.

1967. *In* The fossil record. A symposium with documentation. Chapter 8 (Protozoa), pp. 291-332.

1971. *Systematic Classification of Polycystine Radiolaria.* SCOR Symposium on Micropaleontology of Marine Bottom Sediments — Cambridge, September, 1967. Cambridge University Press, Ms. pp. 1-47, (In Press).

Rüst, David

1885. *Beitrage zur Kenntniss der fossilen Radiolarien aus Gesteinen des Jura.* Palaeontographica, vol. 31, (ser. 3, vol. 7), pp. 269-321, pls.26-45.

1898. *Neue Beitrage zur Kenneniss der fossilen Radiolarien aus Gesteinen des Jura und der Kreide.* Palaeontographica, vol. 45, pp. 1-67, pls. 1-19.

Squinabol, Senofonte

1903. *Le radiolarie dei noduli selciosi nella Scaglia degli Euganei.* Riv. Italiana Paleontologia, vol. 9, pp. 105-150, pls. 8-10.

1904. *Radiolarie cretacee degli Euganei.* Atti. Mem. R. Accad. Sci. Lett. Arti Padova, n. ser., vol. 20, pp. 171-244, pls. 1-10.

1914. *Contributo alla conoscenza dei Radiolarii fossili del veneto.* Appendice *Di un genere di Radiolarii caratteristico del Secondario.* Mem. 1st. R. Univ. Padova, vol. 2, pp. 249-306, pls. 20-24.

PLATES

EXPLANATION OF PLATE 1

All figures except figures 3-4 are scanning electron micrographs.

Figure Page

1,2. **Patulibracchium davisi** Pessagno, n. sp. 30
Holotype (USNM 165499). NSF 350. Early Cenomanian part of the "Fiske Creek Formation"/"Antelope Shale". Fig. 1. View showing primary ray (P) with bracchiopyle (BR), secondary ray (S), and tertiary ray (T). Marker = 100 microns. Fig. 2
Tip of primary ray with bracchiopyle taken at higher magnification. Note cylindrical nature of bracchiopyle. Marker = 50 microns.

3,4. **Patulibracchium davisi** Pessagno, n. sp. 30
Paratype (USNM 165501). NSF 350. Early Cenomanian part of the "Fiske Creek Formation"/"Antelope Shale". Markers in both light photomicrographs = 100 microns.

5,6. **Halesium sexangulum** Pessagno, n. sp. 25
Holotype (USNM 165544). NSF 350. Early Cenomanian part of the "Fiske Creek Formation"/"Antelope Shale". Fig. 5. View showing primary ray with well-developed bracchiopyle (BR), secondary ray, and tertiary ray. CS = central spine; LS = lateral spine. Marker = 100 microns. Fig. 6. Tip of primary ray and bracchiopyle taken at higher magnification.

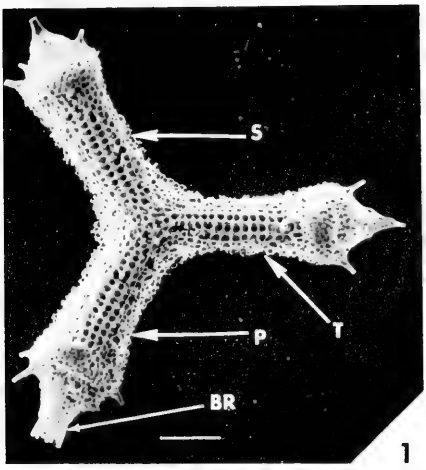

1

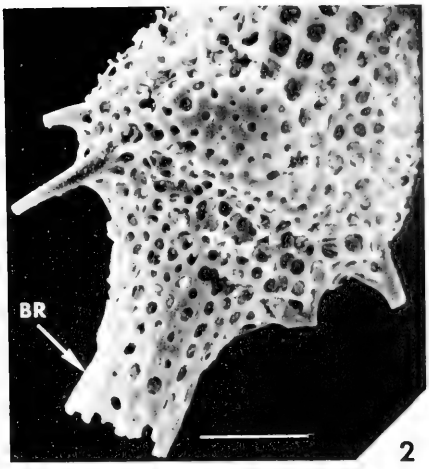

2

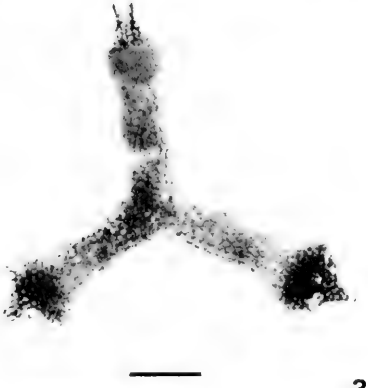

3

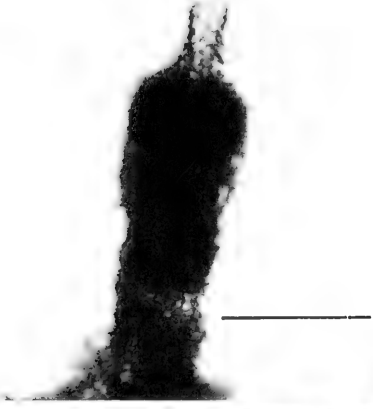

4

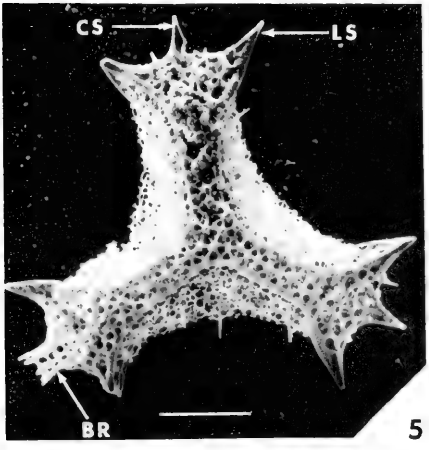

5

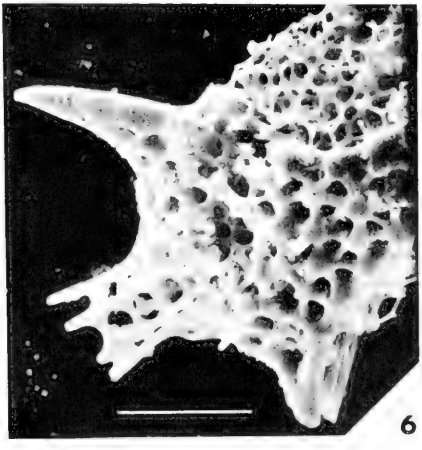

6

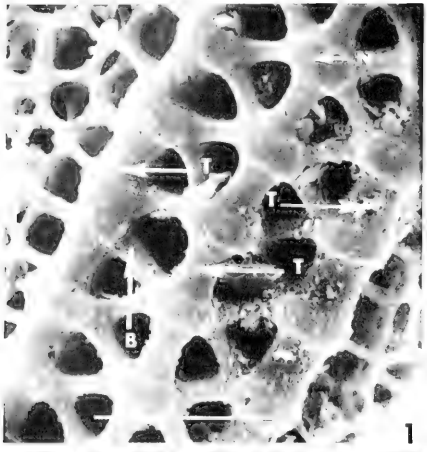
T
T
T
B
1

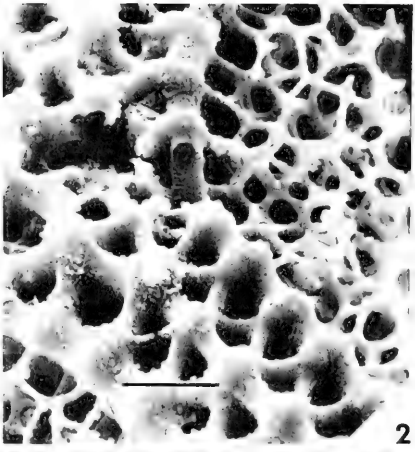
2


3

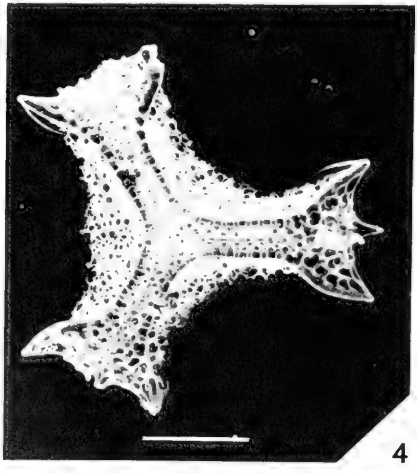
4

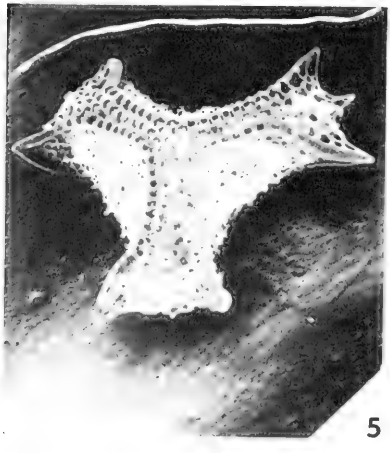
5

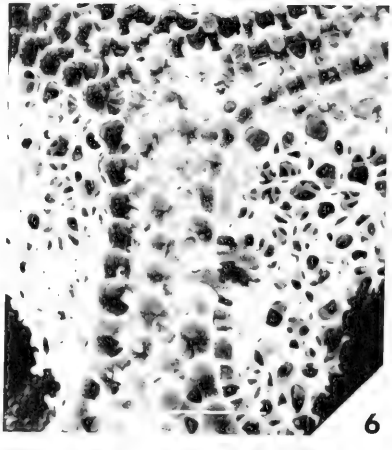
6

EXPLANATION OF PLATE 2

All figures are scanning electron micrographs.

Figure Page

1-3. **Halesium sexangulum** Pessagno, n. sp. 25
Paratype (Pessagno Collection). NSF 350. Early Cenomanian portion of "Fiske Creek Formation"/"Antelope Shale." Fig. 1. View of ray showing hexangular meshwork, comprised of equilateral triangular pore frames. Note patagium in upper left and lower right. T = tabulae; B = bar; N = node; marker equals 10 microns . Fig. 2. Marker = 20 microns. Fig. 3. Cross-section of tabula (T) taken at higher magnification; same view shown at lower magnification n fgure 2. Marker = 100 mcrons.

4-6. **Halesium sexangulum** Pessagno, n. sp. 25
Paratype (USNM 165545). NSF 350. Early Cenomanian portion of "Fiske Creek Formation"/"Antelope Shale." Fig. 4. Horizontal view; Marker = 100 microns. Fig. 5. Specimen somewhat tilted; Note wedge-shaped character of rays and well-developed patagium. Marker = 100 microns. Fig. 6. Hexagonal meshwork comprised of triangular pore frames taken at higher magnification. Marker = 50 microns.

EXPLANATION OF PLATE 3

All photographs are scanning electron micrographs.

Figure — Page

1,2. **Halesium quadratum** Pessagno, n. sp. 23
Holotype (USNM 165547). NSF 350. Early Cenomanian part of the "Fiske Creek Formation"/"Antelope Shale". Fig. 1. Primary ray with broken bracchiopyle pointed upward (twelve o'clock). Marker = 100 microns. Fig. 2. Central area and portions of rays taken at higher magnification; note square pore frames, with recessed circular pores. Marker = 10 microns.

3. **Halesium quadratum** Pessagno, n. sp. 23
Paratype (Pessagno Collection). Patagium somewhat better developed than with holotype; bracchiopyle broken. Marker = 100 microns.

4,5. **Halesium quadratum** Pessagno, n. sp. 23
Paratype (Pessagno Collection). Fig. 4. Irregular meshwork of patagium tending to mask primary meshwork of rays; bracchiopyle well developed (positioned at tip of primary ray at three o'clock). Fig. 5. View of bracchiopyle at higher magnification; note lack of pores. Marker = 20 microns.

6. **Halesium quadratum** Pessagno, n. sp. 23
Paratype (Pessagno Collection). Lateral view of ray at high magnification. Note layered character of ray. Marker = 20 microns.

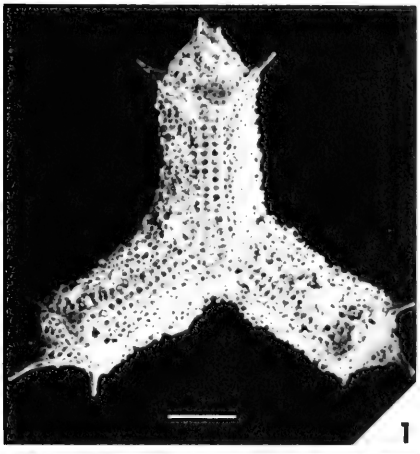
1

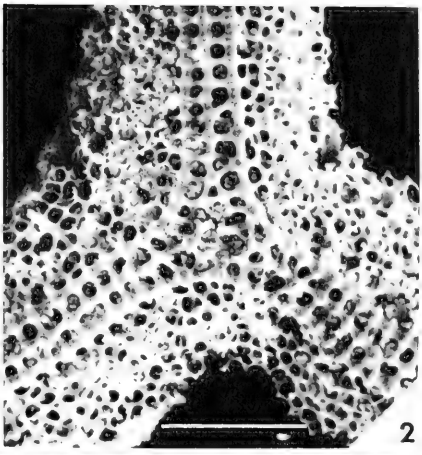
2

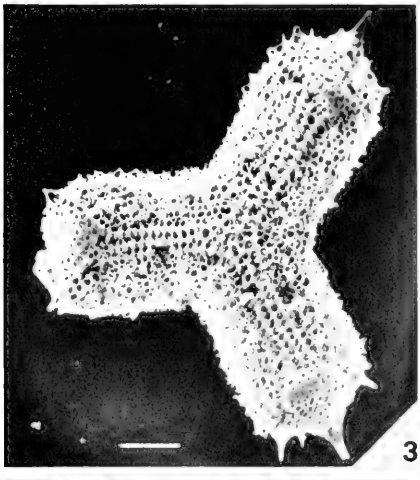
3

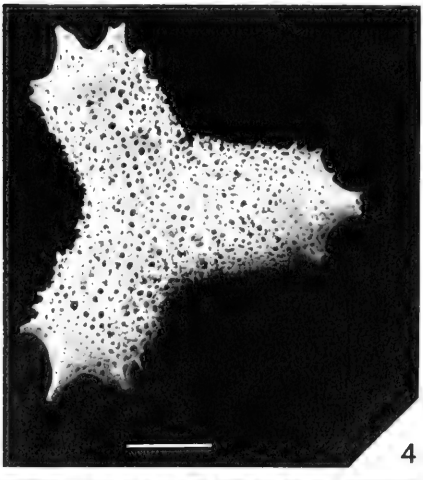
4

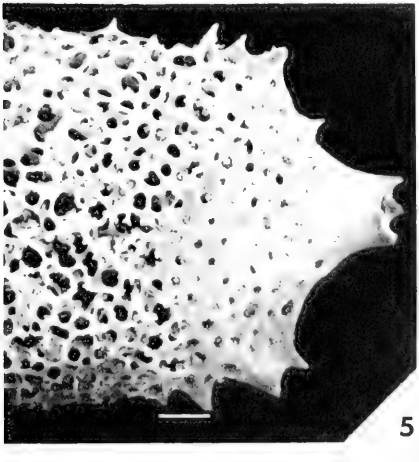
5

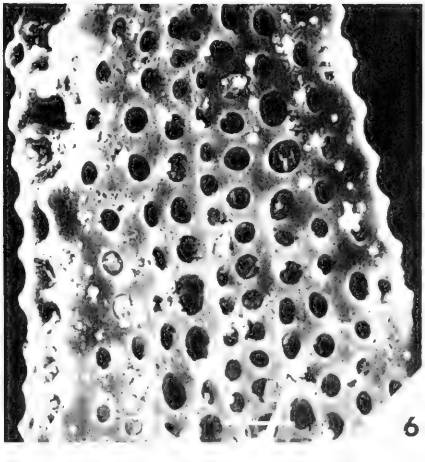
6

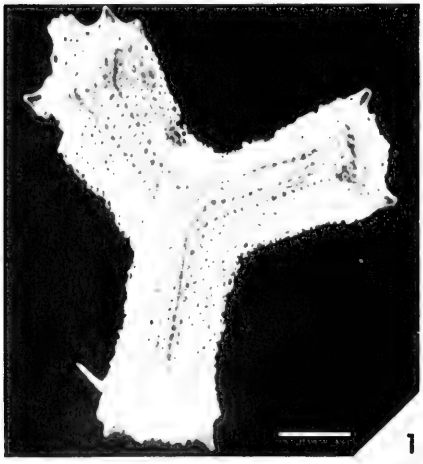
1

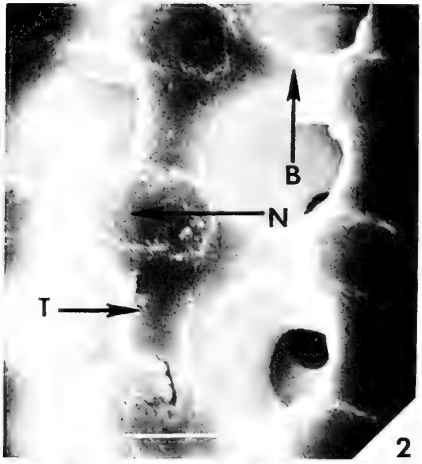

2

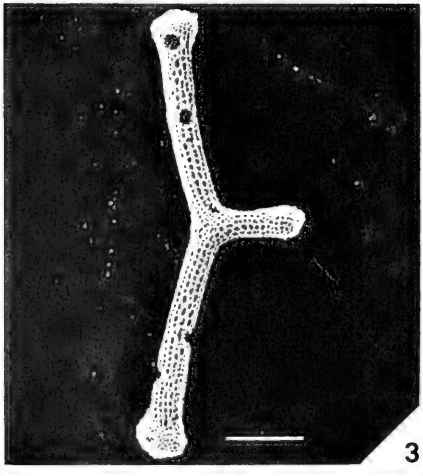
3

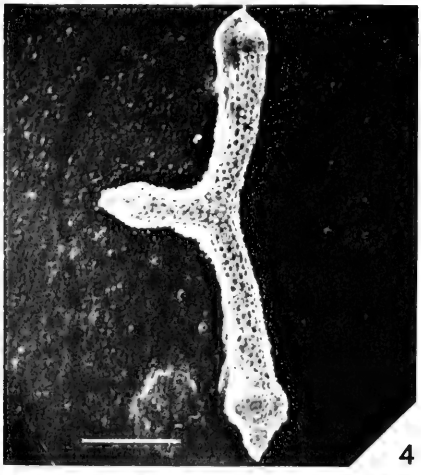
4

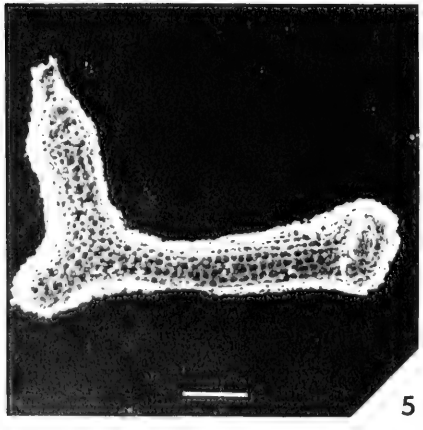
5

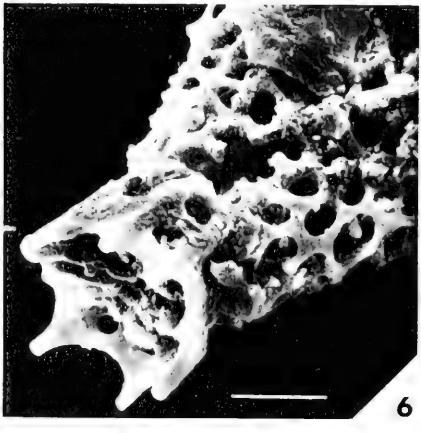
6

EXPLANATION OF PLATE 4

All figures are scanning electron micrographs.

Figure — Page

1,2. **Halesium quadratum** Pessagno, n. sp. 23
NSF 405. Late Cenomanian portion of the "Fiske Creek Formation"/"Antelope Shale." Fig. 1, Whole specimen view; primary ray with bracchiopyle at eleven o'clock; marker = 100 microns. Fig. 2. View at higher magnification showing square pore frames with nodes (N) at vertices and recessed circular pores; T = tabula; B = bar; marker = 10 microns.

3. **Patulibracchium inaequalum** Pessagno, n. sp. 33
Holotype (USNM 105502). NSF 350. Early Cenomanian portion of "Fiske Creek Formation"/"Antelope Shale"; primary ray is short ray. Marker = 200 microns.

4. **Patulibracchium inaequalum** Pessagno, n. sp. 33
Paratype (Pessagno Collection). NSF 350. Early Cenomanian portion of "Fiske Creek Formation"/"Antelope Shale." Primary ray is short ray. Marker = 200 microns.

5,6. **Patulibracchium inaequalum** Pessagno, n. sp. 33
Paratype (USNM 165503). NSF 350. Early Cenomanian portion of "Fiske Creek Formation"/"Antelope Shale." Fig. 5. Primary ray with bracchiopyle is short ray. Marker = 100 microns. Fig. 6. View of bracchiopyle at higher magnification. Marker = 20 microns.

EXPLANATION OF PLATE 5

All figures are scanning electron micrographs.

Figure — Page

1. **Patulibracchium inaequalum** Pessagno, n. sp. 33
Topotype (specimen destroyed in mounting). NSF 350. Early Cenomanian portion of "Fiske Creek Formation"/"Antelope Shale." Marker = 100 microns.

2,3. **Patulibracchium woodlandensis** Pessagno, n. sp. 45
Holotype (USNM 165505). NSF 350. "Fiske Creek Formation"/"Antelope Shale." Fig. 2: Primary ray with bracchiopyle at three o'clock. Marker = 100 microns. Fig. 3. View of bracchiopyle at higher magnification. Marker = 50 microns.

4,5. **Patulibracchium woodlandensis** Pessagno, n. sp. 45
Paratype (USNM 165507). NSF 350. Early Cenomanian portion of "Fiske Creek Formation"/"Antelope Shale." Fig. 4. Primary ray with bracchiopyle at seven o'clock. Marker = 100 microns. Fig. 5. View of ray tip and bracchiopyle at higher magnification. Marker = 50 microns.

6. **Patulibracchium woodlandensis** Pessagno, n. sp. 45
Paratype (Pessagno Collection). NSF 350. Early Cenomanian portion of "Fiske Creek Formation"/"Antelope Shale." View of bracchiopyle. Marker = 50 microns.

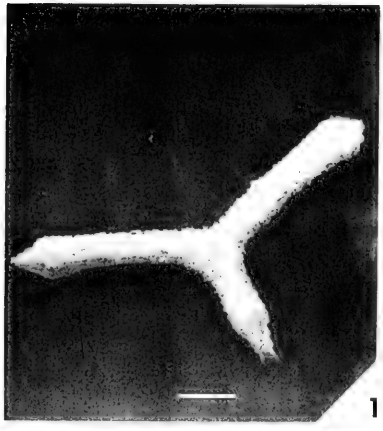
1

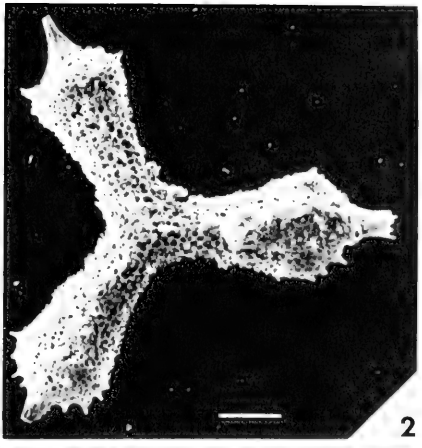
2


3

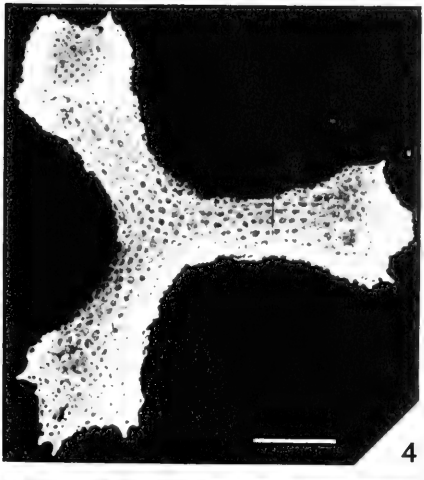
4

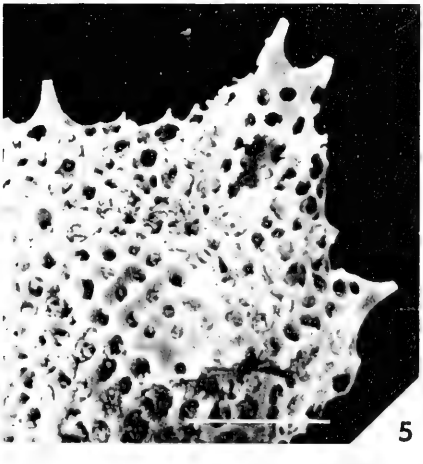
5

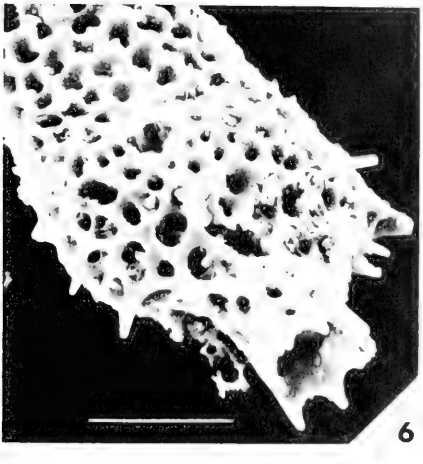
6

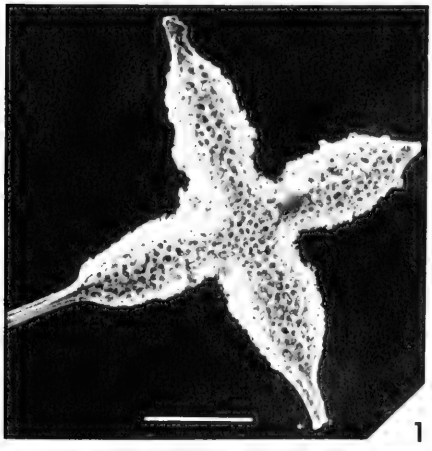
1

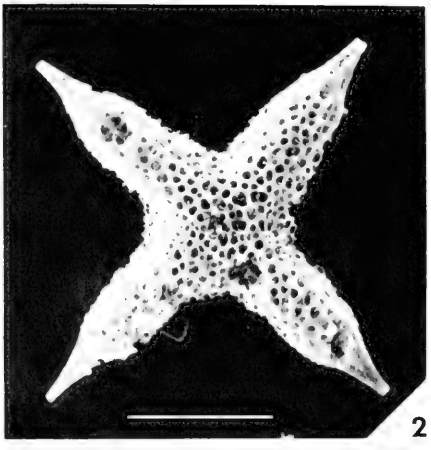
2

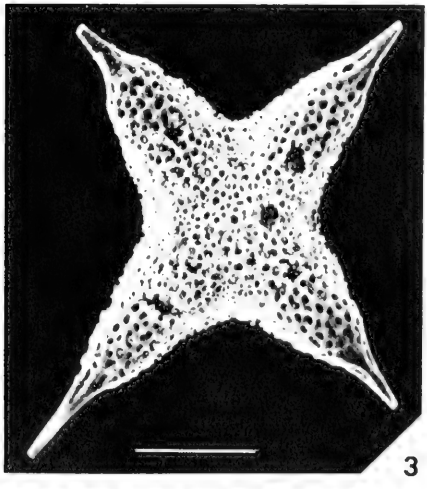
3

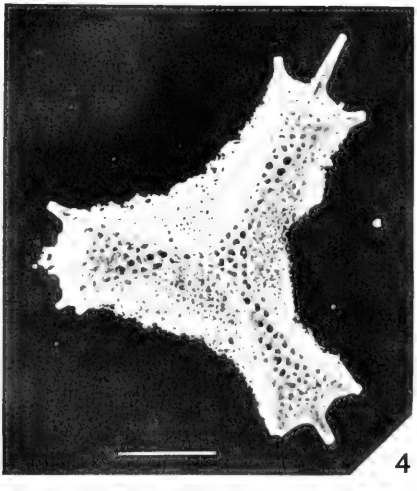
4

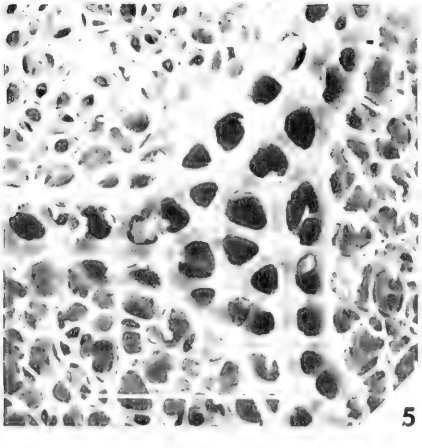
5

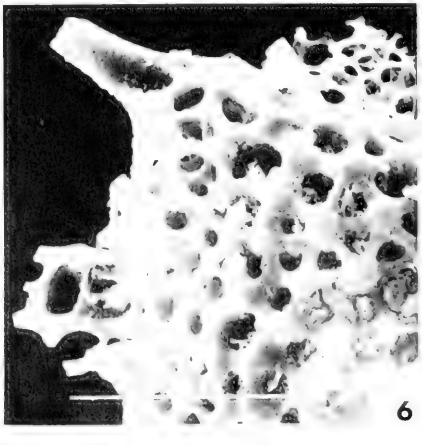
6

EXPLANATION OF PLATE 6

All figures are scanning electron micrographs.

Figure — Page

1. **Crucella messinae** Pessagno, n. sp. — 55
   Holotype (USNM 165569). NSF 350. Early Cenomanian portion of "Fiske Creek Formation"/"Antelope Shale." Marker = 100 microns.

2. **Crucella messinae** Pessagno, n. sp. — 55
   Paratype (USNM 165571). NSF 350. Early Cenomanian portion of "Fiske Creek Formation"/"Antelope Shale." Marker = 100 microns.

3. **Crucella messinae** Pessagno, n. sp. — 55
   Paratype (USNM 165570). NSF 350. Early Cenomanian portion of "Fiske Creek Formation"/"Antelope Shale." Marker = 100 microns.

4. **Patulibracchium torvitatis** Pessagno, n. sp. — 42
   Holotype (USNM 165508). NSF 483. Late Turonian/Coniacian portion of Yolo Formation. Fig. 4. Primary ray with broken bracchiopyle at nine o'clock; note well-developed patagium. Marker = 100 microns. Fig. 5. Central area and proximal portions of rays with surrounding patagium. Marker = 50 microns. Fig. 6. View of distal portion of primary ray with fragmental patagium.

EXPLANATION OF PLATE 7

All figures are scanning electron micrographs.

Figure — Page

1. **Patulibracchium torvitatis** Pessagno, n. sp. 42
Paratype (USNM 165510). NSF 483. Yolo Formation. Late Turonian/Coniacian. Marker = 100 microns.

2. **Patulibracchium torvitatis** Pessagno, n. sp. 42
Hypotype (Pessagno Collection). NSF 32-B. Forbes Formation "Dobbins Shale Member." Early Campanian. Marker = 100 microns.

3. **Patulibracchium ungulae** Pessagno, n. sp. 44
Holotype (USNM 165514). NSF 483. Yolo Formation. Late Turonian/Coniacian. Marker = 100 microns.

4. **Patulibracchium ungulae** Pessagno, n. sp. 44
Paratype (USNM 165515). NSF 483. Yolo Formation. Late Turonian/Coniacian. Marker = 100 microns.

5. **Patulibracchium ungulae** Pessagno, n. sp. 44
Paratype (USNM 165516). NSF 483. Yolo Formation. Late Turonian/Coniacian. Marker = 100 microns.

6. **Patulibracchium ruesti** Pessagno, n. sp. 38
Holotype (USNM 165511). NSF 483. Yolo Formation. Late Turonian/Coniacian. Primary ray with bracchiopyle at eleven o'clock. Marker = 100 microns.

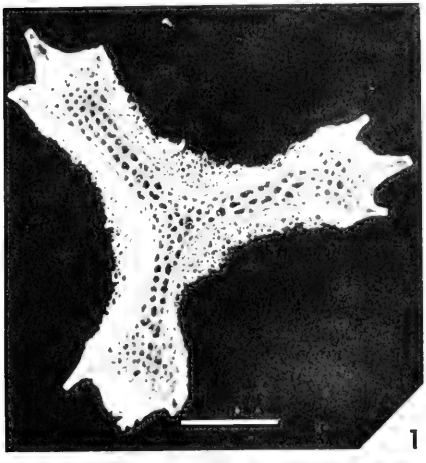
1

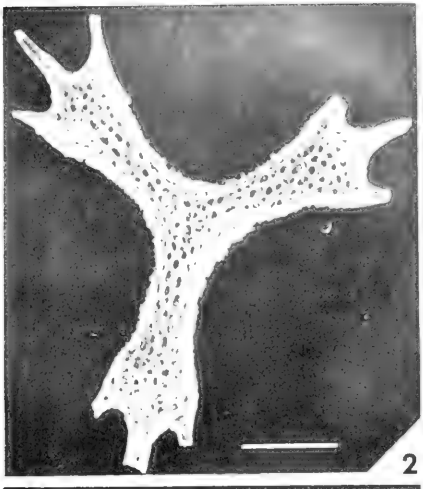
2

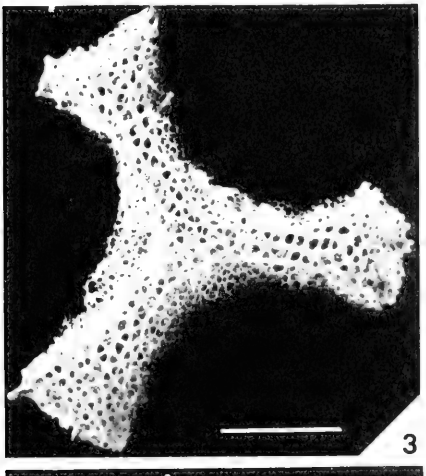
3

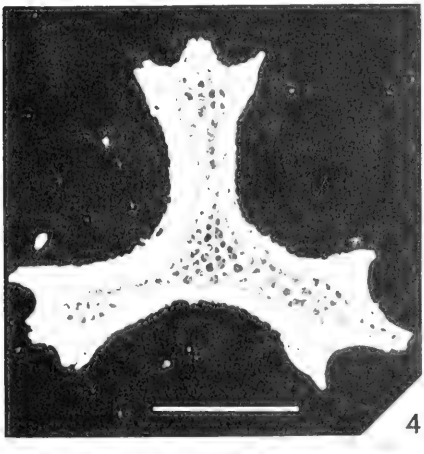
4

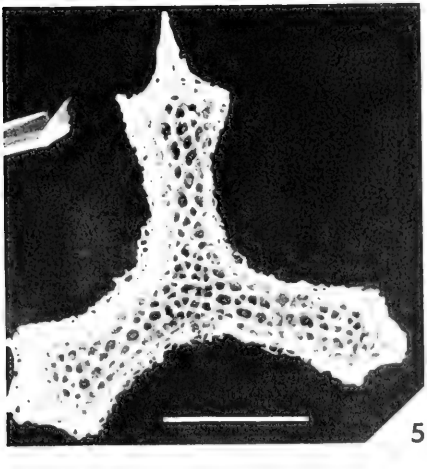
5

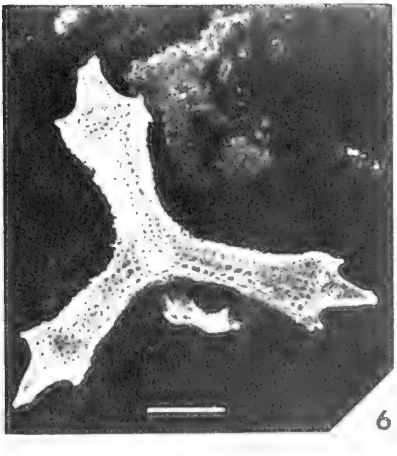
6

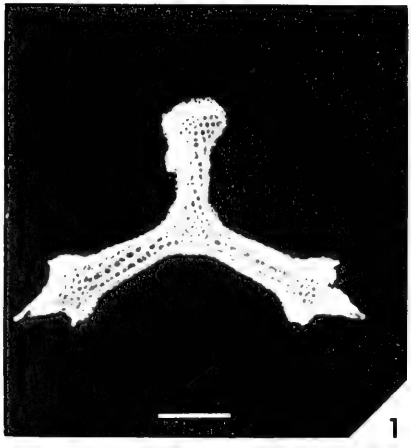
1

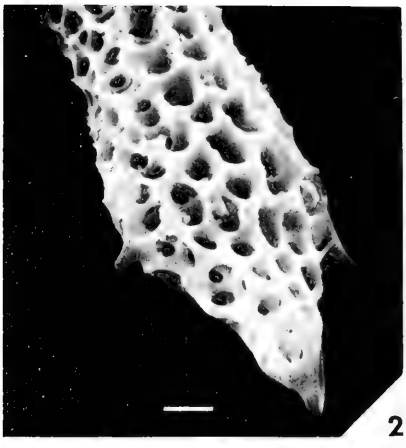
2

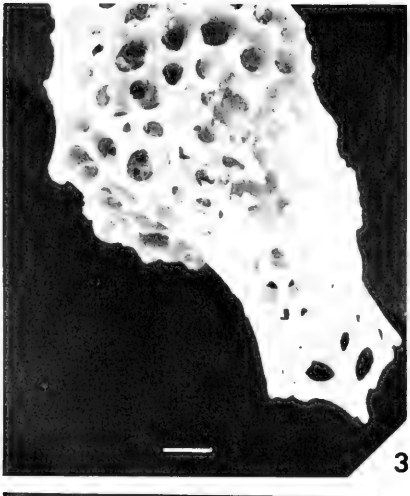
3

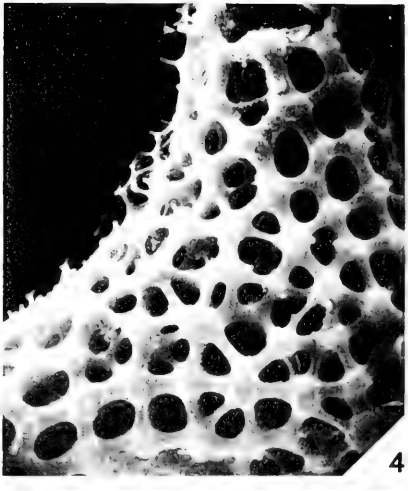
4

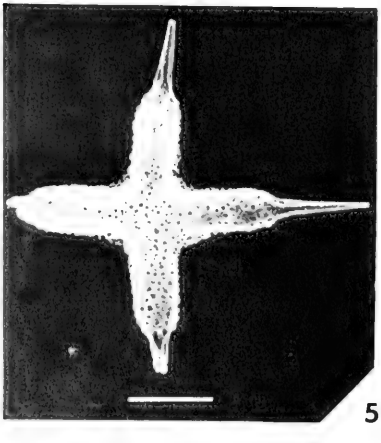
5

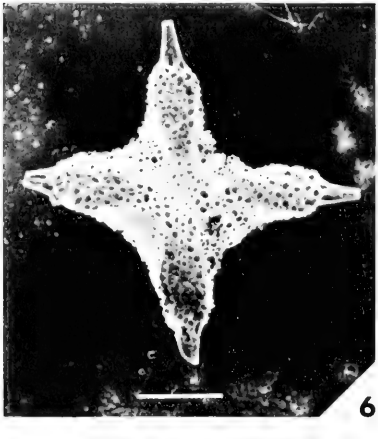
6

EXPLANATION OF PLATE 8

All figures are scanning electron micrographs.

Figure — Page

1,4. **Patulibracchium ruesti** Pessagno, n. sp. 38
Paratype (USNM 165512). NSF 483. Yolo Formation. Late Turonian/Coniacian. Fig. 1. Marker = 100 microns. Fig. 4. View of portion of central area of higher magnification. Marker = 10 microns.

2,3. **Patulibracchium ruesti** Pessagno, n. sp. 38
Paratype (Pessagno Collection). Yolo Formation. Late Turonian/Coniacin. Fig. 2. View of a ray at high magnification. Marker = 10 microns. Fig. 3. View of bracchiopyle at higher magnification. Marker = 10 microns.

5. **Crucella plana** Pessagno, n. sp. 56
Holotype (USNM 165562). NSF 483. Yolo Formation. Late Turonian/Coniacian. Marker = 100 microns.

6. **Crucella plana** Pessagno, n. sp. 56
Paratype (USNM 165563). NSF 483. Yolo Formation. Late Turonian/Coniacian. Marker = 100 microns.

EXPLANATION OF PLATE 9

All figures are scanning electron micrographs.

Figure — Page

1. **Crucella cachensis** Pessagno, n. sp. 53
Holotype (USNM 165562). NSF 697. Middle Turonian portion of Venado Formation. Note lacuna (L) in position of arrow. Marker = 100 microns.

2,3. **Crucella cachensis** Pessagno, n. sp. 53
Paratype (Pessagno Collection). NSF 697. Middle Turonian portion of Venado Formation. In figure 3 note marked raised area around lacuna. Markers in both figures = 100 microns.

4. **Crucella irwini** Pessagno, n. sp. 54
Holotype (USNM 165582). NSF 705B. Middle Turonian portion of the "Marsh Creek Formation." Marker = 100 microns.

5,6. **Crucella irwini** Pessagno, n. sp. 54
Paratype (USNM 165558; 165584. NSF 705B. Middle Turonian portion of the "Marsh Creek Formation." Marker = 100 microns.

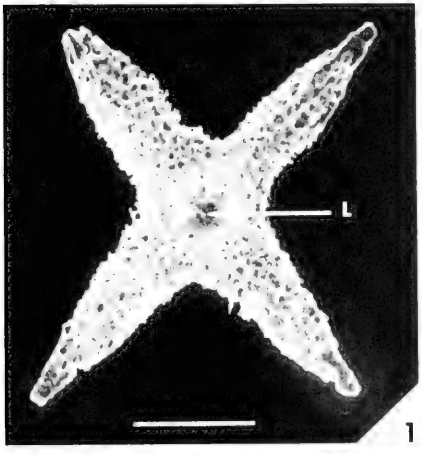

1

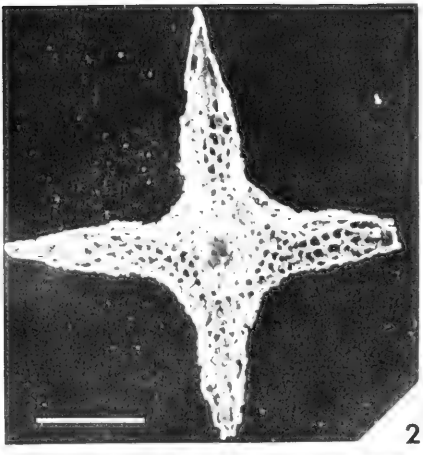

2

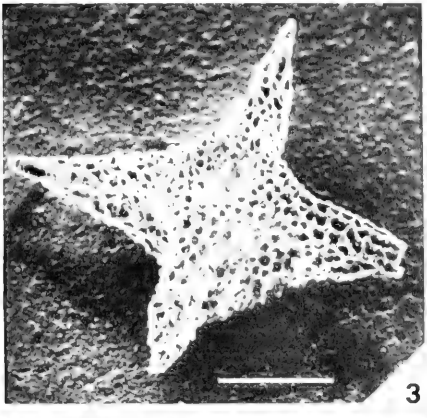

3

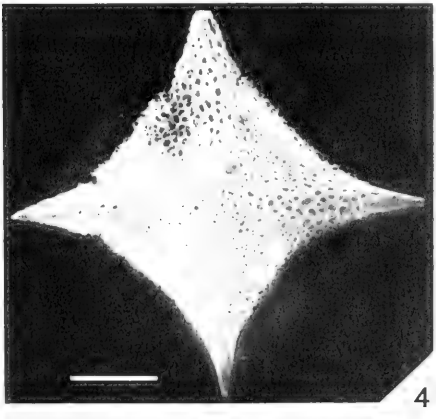

4

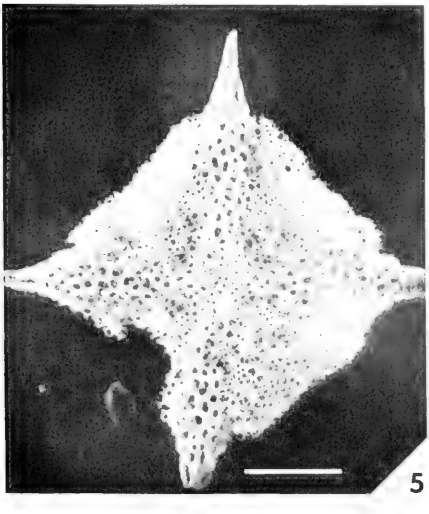

5

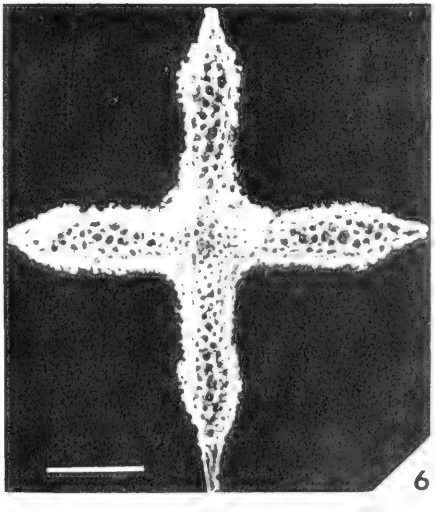

6

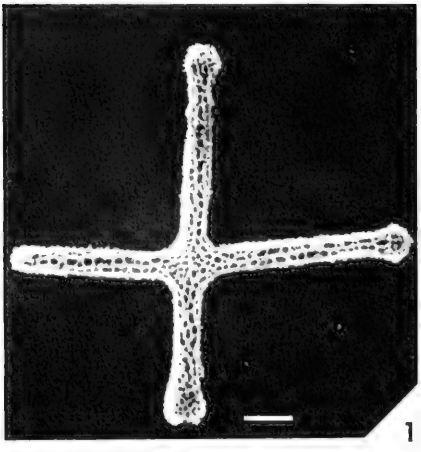
1

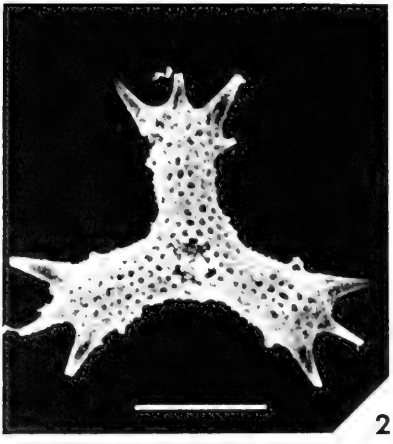
2

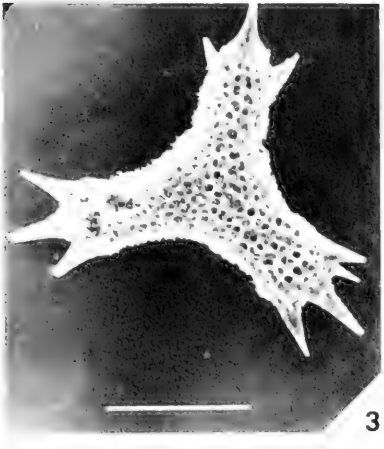
3

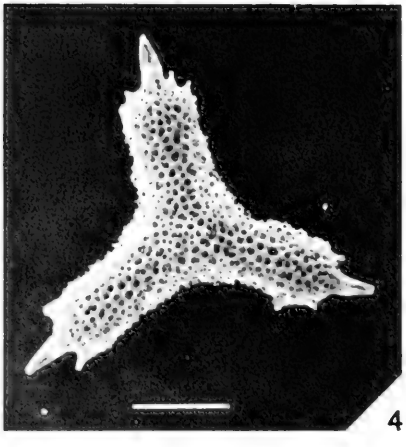
4

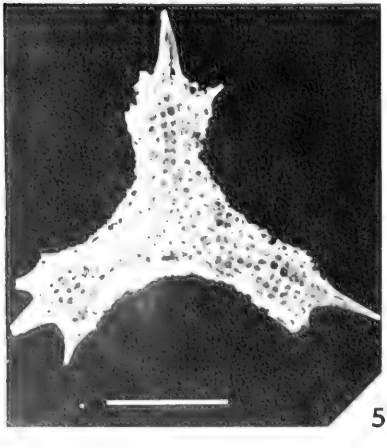
5

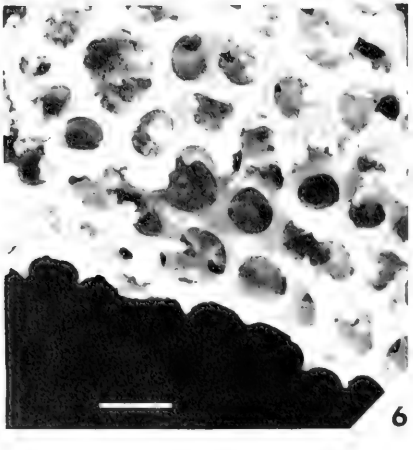
6

EXPLANATION OF PLATE 10

All figures are scanning electron micrographs.

Figure — Page

1. **Hagiastrum,** sp. 52
   NSF 705-B. Middle Turonian portion of "Marsh Creek Formation." Marker = 100 microns.

2. **Paronaella solanoensis** Pessagno, n. sp. 48
   Holotype (USNM 165550). NSF 483. Late Turonian/Coniacian. Yolo Formation. Marker = 100 microns.

3. **Paronaella solanoensis** Pessagno, n. sp. 48
   Paratype (USNM 165551). NSF 483. Late Turonian/Coniacian. Yolo Formation. Marker = 100 microns.

4. **Paronaella venadoensis** Pessagno, n. sp. 49
   Holotype (USNM 165553). NSF 483. Late Turonian/Coniacian. Yolo Formation. Marker = 100 microns.

5,6. **Paronaella venadoensis** Pessagno, n. sp. 49
   Paratype (USNM 165554). NSF 483. Late Turonian/Coniacian. Yolo Formation. Fig. 5. Marker = 100 microns. Fig. 6. View of side of ray showing layering. Marker = 10 microns.

EXPLANATION OF PLATE 11

All figures except 3 and 4 are scanning electron micrographs.

Figure — Page

1. **Paronaella venadoensis** Pessagno, n. sp. 49
   Paratype (USNM 165555). NSF 483. Late Turonian/Coniacian part of the Yolo Formation. Marker = 100 microns.

2. **Patulibracchium petroleumensis** Pessagno, n. sp. 37
   Holtype (USNM 165517). NSF 32-B. Forbes Formation "Dobbins Shale" Member; early Campanian. Marker = 100 microns.

3. **Patulibracchium petroleumensis** Pessagno, n. sp. 37
   Paratype (USNM 165518). NSF 32-B. Forbes Formation "Dobbins Shale" Member; early Campanian. Light photomicrograph. Marker = 100 microns.

4. **Patulibracchium petroleumensis** Pessagno, n. sp. 37
   Paratype (Pessagno Collection). NSF 32-B. Forbes Formation "Dobbins Shale" Member; early Campanian Light photomicrograph. Marker = 100 microns.

5. **Patulibracchium petroleumensis** Pessagno, n. sp. 37
   Topotype (specimen destroyed in SEM work). NSF 32-B. Forbes Formation "Dobbins Shale" Member; early Campanian. Marker = 100 microns.

6. **Patulibracchium californiaensis** Pessagno, n. sp. 29
   Holotype (USNM 165520). NSF 32-B. Forbes Formation ("Dobbins Shale" Member; early Campanian. Marker = 100 microns.

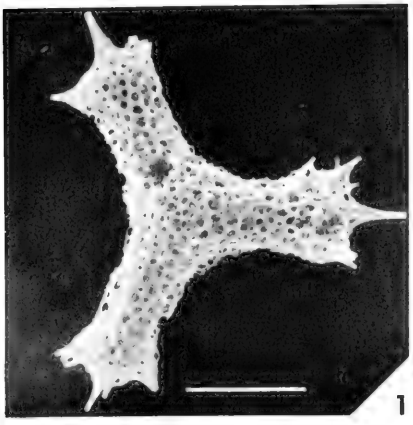
1

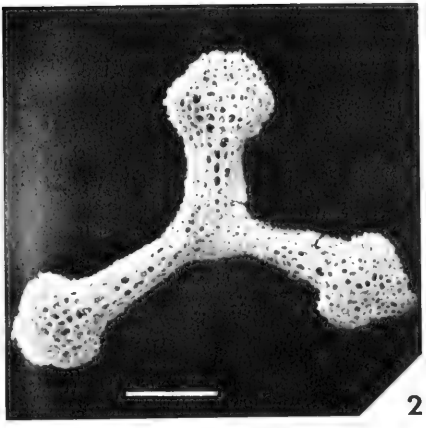
2

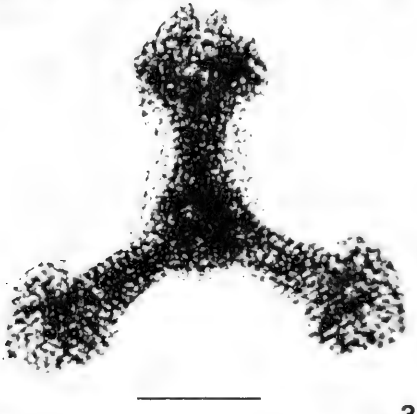
3

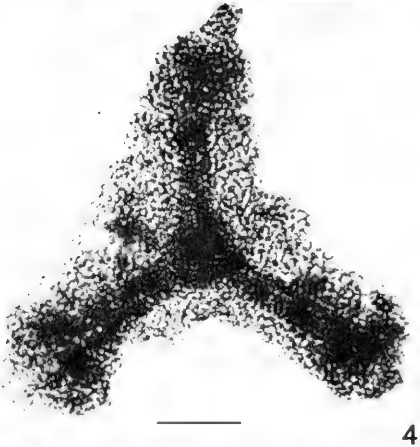
4

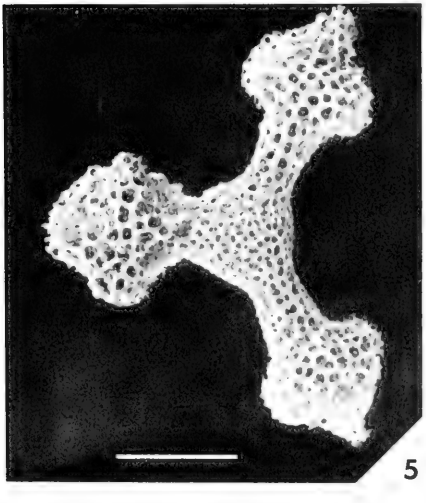
5

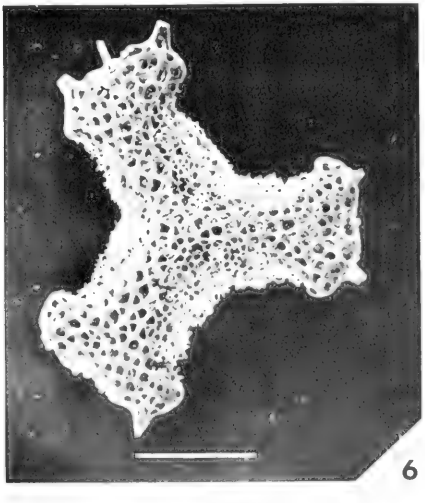
6

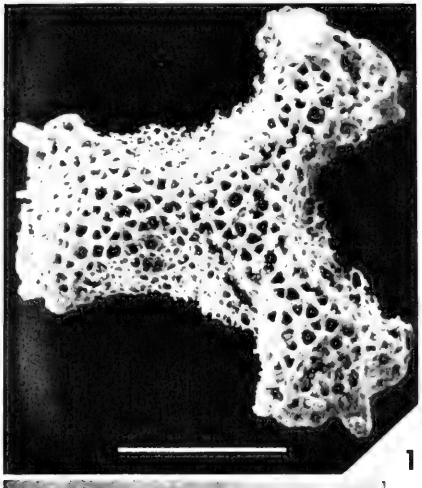
1

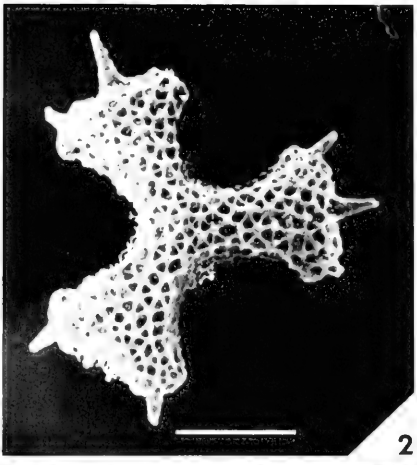
2

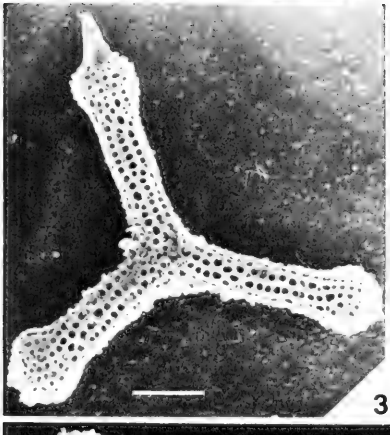
3

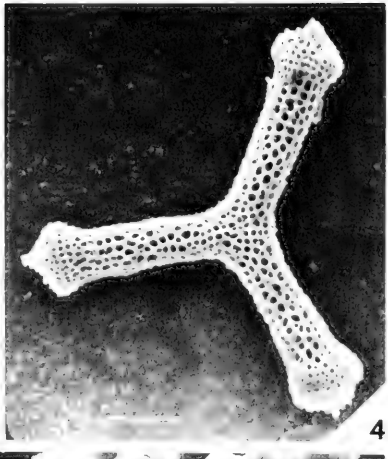
4

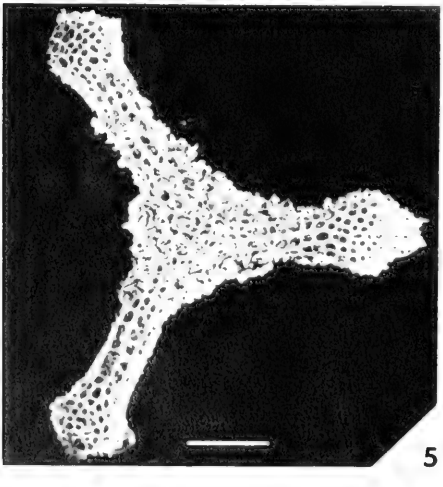
5

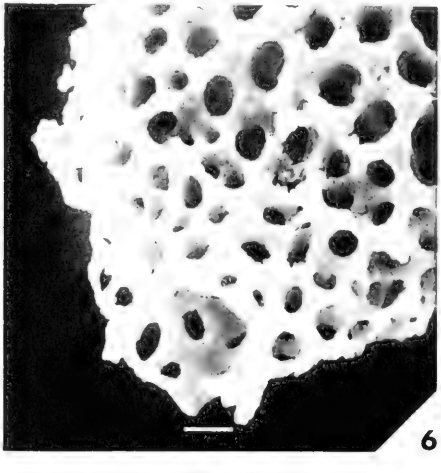
6

EXPLANATION OF PLATE 12

All figures are scanning electron micrographs.

Figure — Page

1. **Patulibracchium californiaensis** Pessagno, n. sp. 29
Paratype (USNM 165521). NSF 32-B. Forbes Formation ("Dobbins Shale" Member); early Campanian. Marker = 100 microns.

2. **Patulibracchium californiaensis** Pessagno, n. sp. 29
Topotype (lost in SEM work). NSF 32-B. Forbes Formation ("Dobbins Shale" Member). Marker = 100 microns.

3. **Patulibracchium teslaensis** Pessagno, n. sp. 41
Holotype (USNM 165526). NSF 451. Panoche Group (undifferentiated); late Campanian. Marker = 100 microns.

4. **Patulibracchium teslaensis** Pessagno, n. sp. 41
Paratype (USNM 165527). NSF 451. Panoche Group (undifferentiated); late Campanian. Marker = 100 microns.

5,6. **Patulibracchium teslaensis** Pessagno, n. sp. 41
Paratype (USNM 165528). NSF 451. Panoche Group (undifferentiated); late Campanian. Fig. 5. Primary ray with bracchiopyle at three o'clock. Marker = 100 microns. Fig. 6. View of bracchiopyle. Marker = 10 microns.

EXPLANATION OF PLATE 13

All figures except figure 1 are scanning electron micrographs

Figure — Page

1. **Patulibracchium teslaensis** Pessagno, n. sp. 41
Hypotype. NSF 55-B. Forbes Formation ("Dobbins Shale" Member); early Campanian. Marker = 100 microns.

2. **Patulibracchium delvallensis** Pessagno, n. sp. 31
Holotype (USNM 165529). NSF 451. Panoche Group (undifferentiated); late Campanian. Short ray is primary ray. Marker = 100 microns.

3. **Patulibracchium delvallensis** Pessagno, n. sp. 31
Paratype (USNM 165530). NSF 451. Panoche Group (undifferentiated); late Campanian. Marker = 100 microns.

4,5. **Patulibracchium lawsoni** Pessagno, n. sp. 35
Holotype (USNM 165532). NSF 451. Panoche Group (undifferentiated; late Campanian. Marker = 100 microns.

6. **Patulibracchium lawsoni** Pessagno, n. sp. 35
Paratype (USNM 165534). NSF 451. Panoche Group (undifferentiated). Late Campanian. Marker = 100 microns.

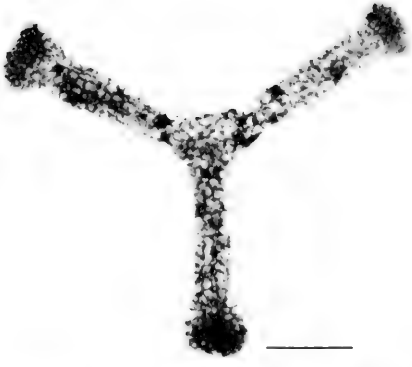

1

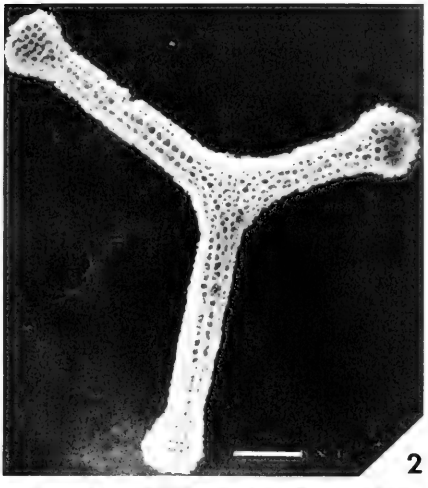

2

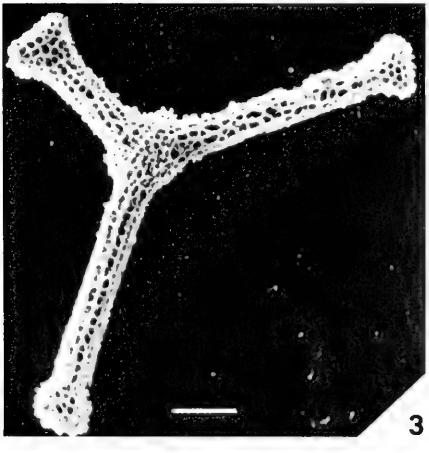

3

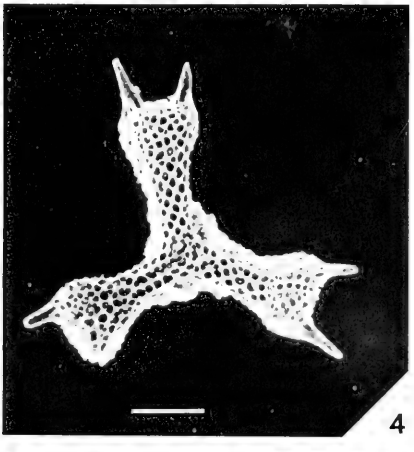

4

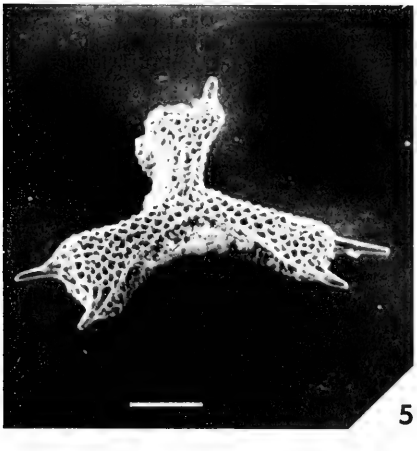

5

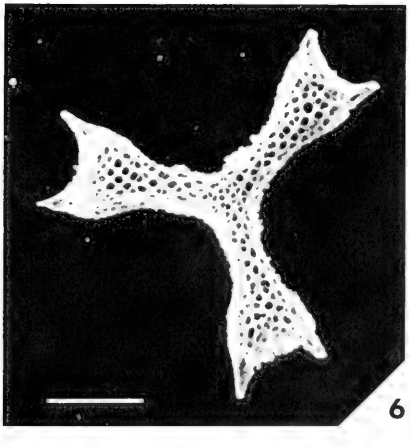

6

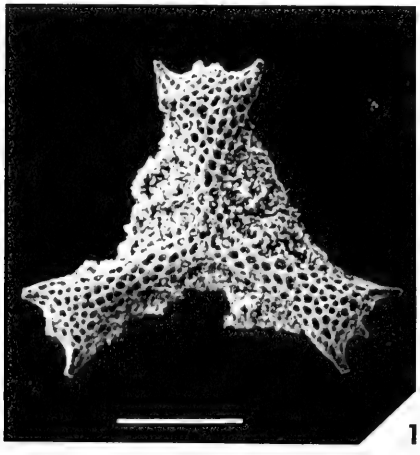
1


2

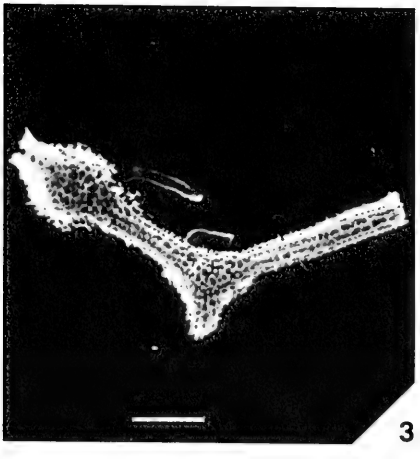
3

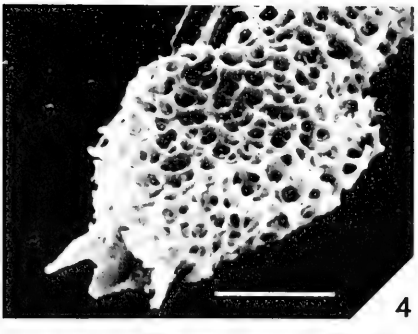
4

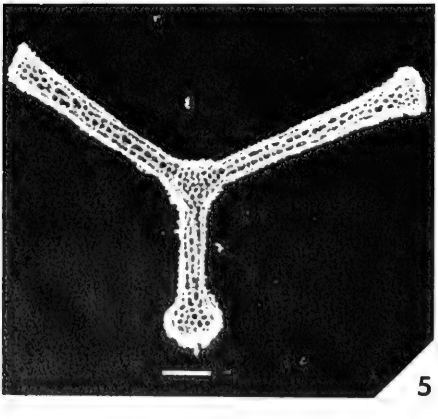
5

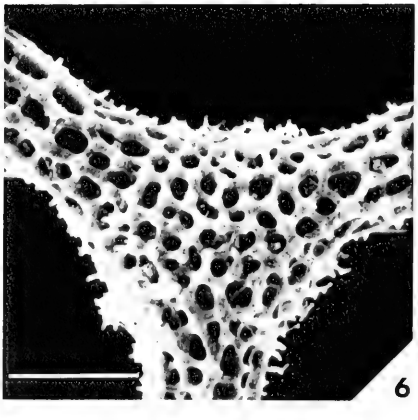
6

EXPLANATION OF PLATE 14

All figures except 2 are scanning electron micrographs.

Figure — Page

1. **Patulibracchium lawsoni** Pessagno, n. sp. 35
Paratype (Pessagno Collection). NSF 451. Panoche Group (undifferentiated; late Campanian. Marker = 100 microns.

2. **Patulibracchium taliaferroi** Pessagno, n. sp. 40
Holotype (USNM 165538). NSF 568-B. Latest Campanian portion of the "Marsh Creek Formation." Primary ray at nine o'clock. Marker = 100 microns.

3,4. **Patulibracchium taliaferroi** Pessagno, n. sp. 40
Paratype (USNM 165539). NSF 568-B. Latest Campanian portion of the "Marsh Creek Formation." Fig. 3. Marker = 100 microns. Fig. 4. View of bracchiopyle at higher magnification. Marker = 50 microns.

5,6. **Patulibracchium taliaferroi** Pessagno, n. sp. 40
Paratype (Pessagno Collection). NSF 568-B. Latest Campanian portion of the "Marsh Creek Formation." Fig. 5. Marker = 100 microns. Fig. 6. View of central area at higher magnification. Marker = 50 microns.

EXPLANATION OF PLATE 15

All figures except 2 are scanning electron micrographs.

Figure — Page

1. **Patulibracchium taliaferroi** Pessagno, n. sp. 40
Paratype (Pessagno Collection). NSF 568-B. Latest Campanian portion of "Marsh Creek Formation." Marker = 100 microns.

2. **Patulibracchium marshensis** Pessagno, n. sp. 36
Holotype (USNM 165535). Latest Campanian portion of "Marsh Creek Formation." Primary ray with well-developed bracchiopyle at eleven o'clock. Marker = 100 microns.

3-5. **Patulibracchium marshensis** Pessagno, n. sp. 36
Paratype (USNM 165536). NSF 568-B. Latest Campanian portion of "Marsh Creek Formation." Fig. 3. Primary ray at nine o'clock; marker = 100 microns. Fig. 4. View of tip of primary ray and bracchiopyle at higher magnification. Marker = 50 microns.

6. **Patulibracchium arbucklensis** Pessagno, n. sp. 27
Holotype (USNM 165523). NSF 32-B. Forbes Formation ("Dobbins Shale" Member). Marker = 100 microns.

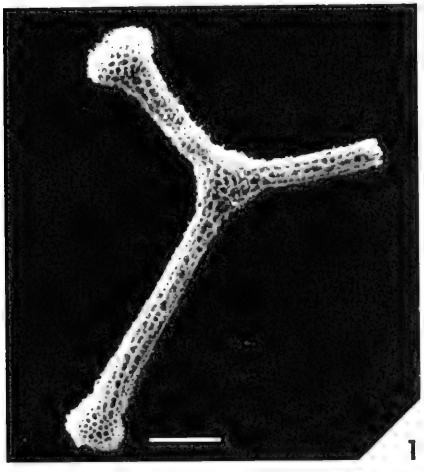
1


2

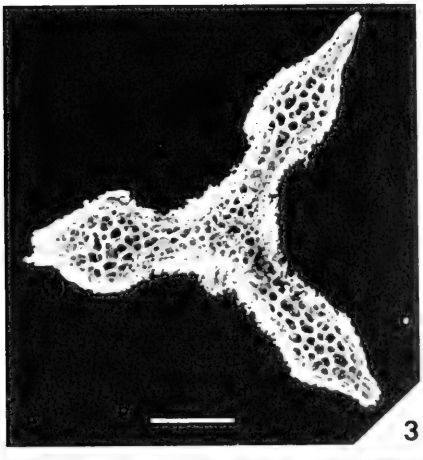
3

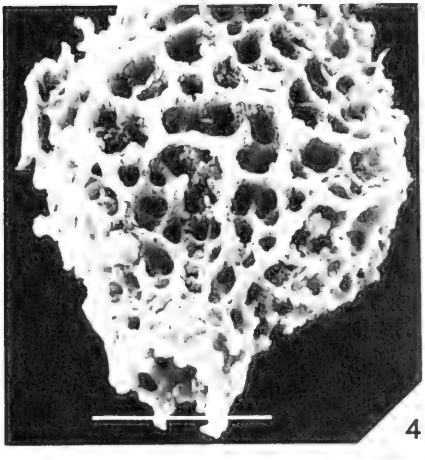
4

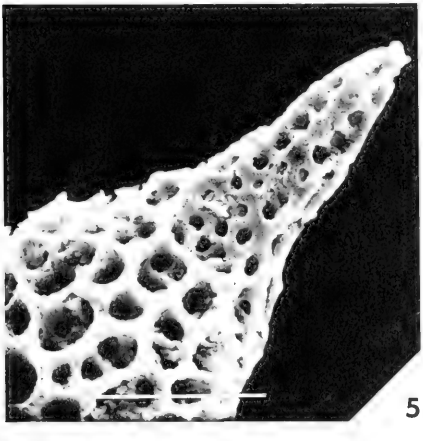
5

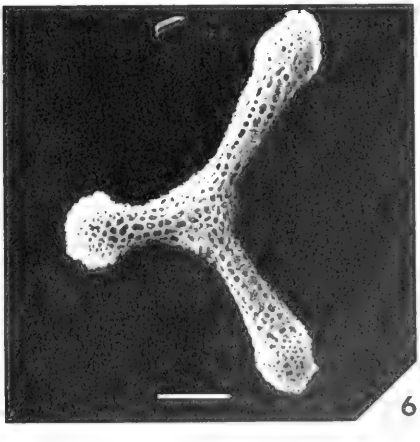
6

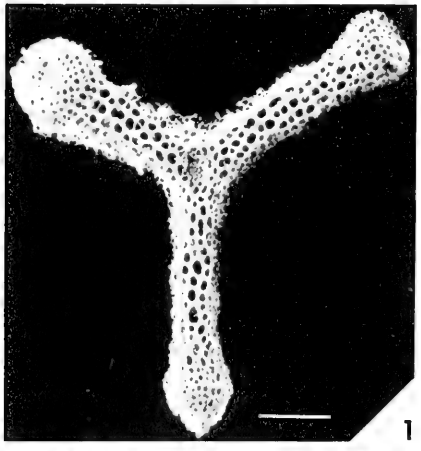
1

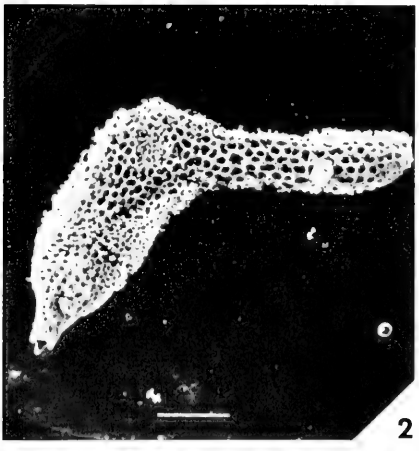
2

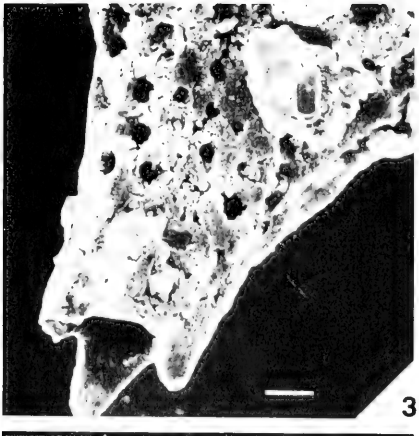
3

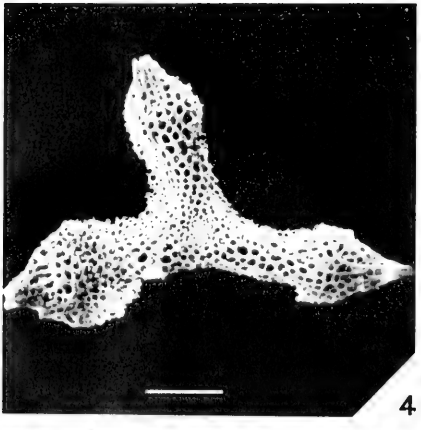
4

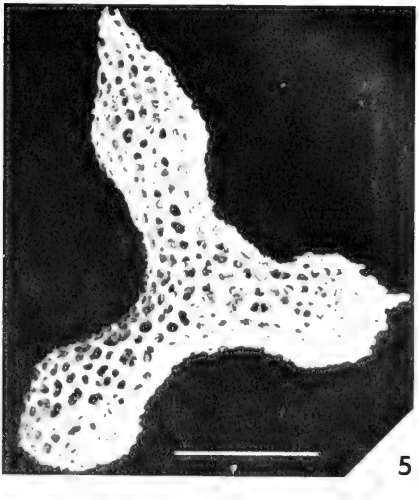
5

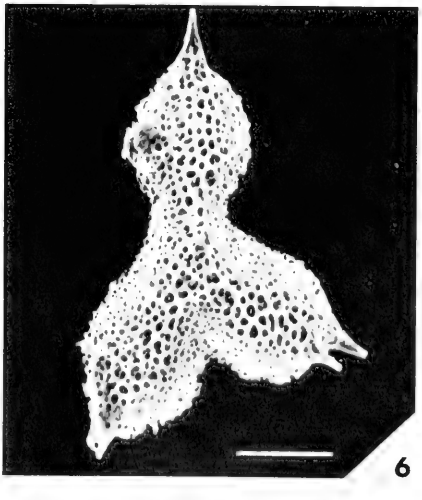
6

EXPLANATION OF PLATE 16

All figures are scanning electron micrographs.

Figure — Page

1. **Patulibracchium arbucklensis** Pessagno, n. sp. 27
   Paratype (Pessagno Collection). NSF 32-B. Forbes Formation ("Dobbins Shale" Member); early Campanian. Marker = 100 microns.

2,3. **Patulibracchium arbucklensis** Pessagno, n. sp. 27
   Paratype (Pessagno Collection). NSF 32-B. Forbes Formation ("Dobbins Shale" Member); early Campanian. Fig. 2. Marker = 100 microns. Fig. 3. View of bracchiopyle at higher magnification. Marker = 100 microns.

4. **Patulibracchium** sp. aff. **P. arbucklensis,** n. sp. 28
   NSF 32-B. Forbes Formation ("Dobbins Shale" Member); early Campanian. Marker = 100 microns.

5. **Patulibracchium** sp. aff. **P. petroleumensis,** n. sp. 38
   NSF 32-B. Forbes Formation ("Dobbins Shale" Member); early Campanian. Marker = 100 microns.

6. ?**Patulibracchium** sp. .....
   NSF 32-B. Forbes Formation ("Dobbins Shale" Member); early Campanian. Marker = 100 microns.

EXPLANATION OF PLATE 17

All figures except 3-5 are scanning electron micrographs.

Figure — Page

1. **Paronaella** sp. 1 50
   NSF 432. Middle Turonian portion of Venado Formation. Marker = 100 microns.

2. **Paronaella** sp. 2 51
   NSF 483. Late Turonian/Coniacian portion of Yolo Formation. Marker = 100 microns.

3. **Patulibracchium dickinsoni** Pessagno, n. sp. 32
   Holotype (USNM 165541). NSF 568-B. Latest Campanian portion of the "Marsh Creek Formation." Marker = 100 microns.

4,5. **Patulibracchium dickinsoni** Pessagno, n. sp. 32
   Paratype (USNM 165542). NSF 568-B. Latest Campanian portion of the "Marsh Creek Formation." Fig. 4. Primary ray at ten o'clock. Marker = 100 microns. Fig. 5. Tip of primary ray with remnants of bracchiopyle (BR) indicated by arrow. Marker = 100 microns.

6. **Patulibracchium dickinsoni** Pessagno, n. sp. 32
   Paratype (USNM 165543). NSF 568-B. Latest Campanian portion of the "Marsh Creek Formation." Marker = 100 microns.

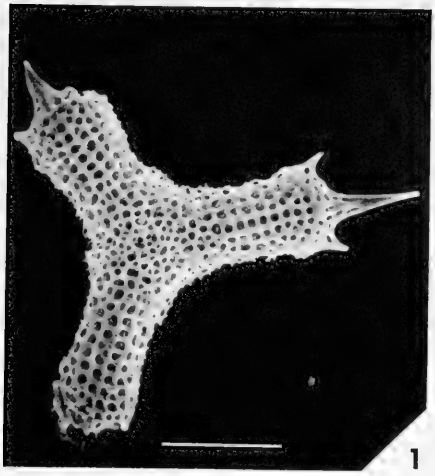

1

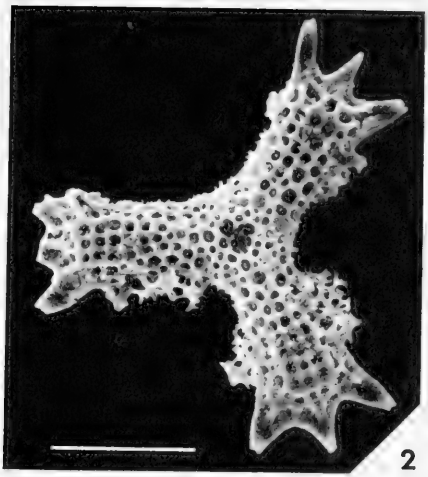

2

3

4

5

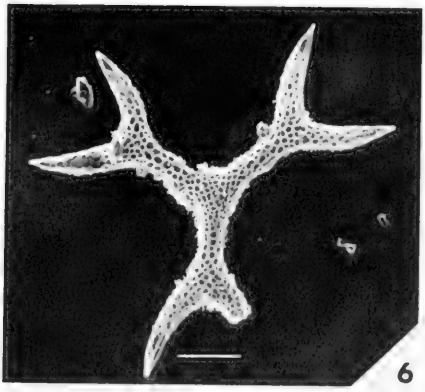

6

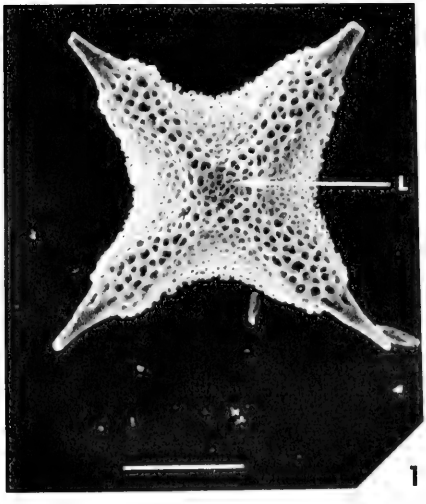
L
1

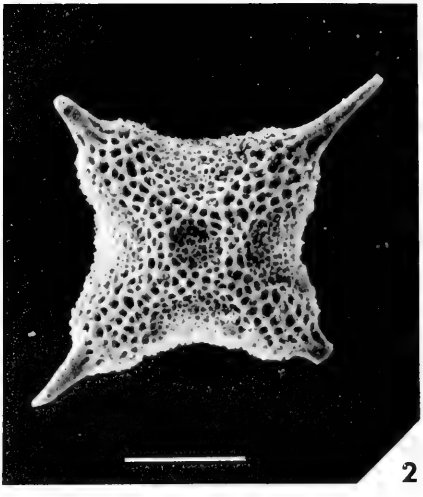
2

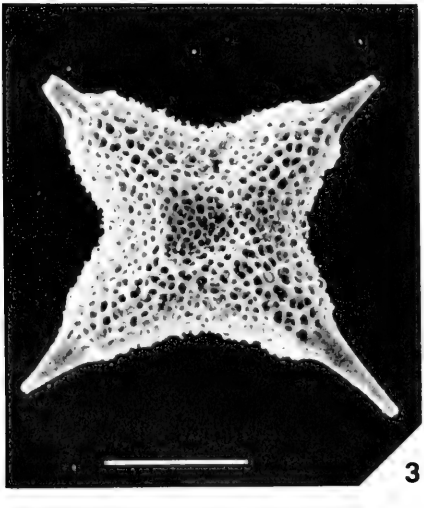
3

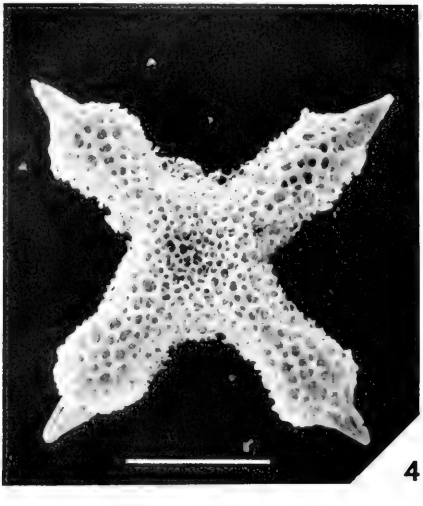
4

EXPLANATION OF PLATE 18

All figures are scanning electron micrographs. All specimens from NSF 32-B. Forbes Formation ("Dobbins Shale" Member); early Campanian.

Figure — Page

1. **Crucella espartoensis** Pessagno, n. sp. 53
Holotype (USNM 165565). Lacuna (L) marked by arrow. Marker = 100 microns.

2. **Crucella espartoensis** Pessagno, n. sp. 53
Paratype (USNM 165566). Marker = 100 microns.

3,4. **Crucella espartoensis** Pessagno, n. sp. 53
Paratype (Pessagno Collection). Marker = 100 microns.

EXPLANATION OF PLATE 19

All figures are scanning electron micrographs of Jurassic (Tithonian) Radiolaria from Blake-Bahama Basin. JOIDES (DSD) Leg I, Site 5A, Core 7, Section 1: top.

Figure — Page

1. **Amphibracchium petersoni** Pessagno, n. sp. 21
Paratype (USNM 165579). Marker = 100 microns.

2. ?**Paronaella ewingi** Pessagno, n. sp. 47
Holotype (USNM 165559). Marker = 200 microns.

3-5. ?**Paronaella ewingi** Pessagno, n. sp. 47
Paratypes. Fig. 3. (USNM 165560). Fig. 4 (Pessagno Collection). Fig. 5. (Pessagno Collection); note small spines on ray tips and linear nature of pore frames suggesting presence of tabulae. Markers = 200 microns.

6. ?**Paronaella worzeli** Pessagno, n. sp. 49
Holotype (USNM 165556). Marker = 200 microns.

7. **Crucella,** sp. .....
Marker = 200 microns.

8. **Amphibracchium petersoni** Pessagno, n. sp. 21
Holotype (USNM 165578). Marker = 200 microns.

9. **Amphibracchium sansalvadorensis** Pessagno, n. sp. 21
Holotype (USNM 165568). Marker = 200 microns.

10. **Amphibracchium sansalvadorensis** Pessagno, n. sp. 21
Paratype (USNM 165569). Marker = 200 microns.

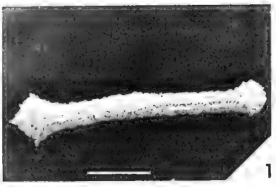
1

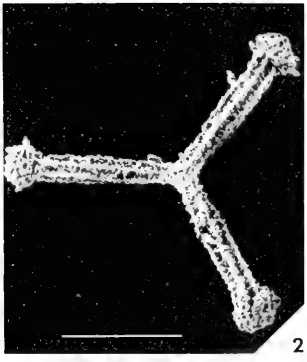
2

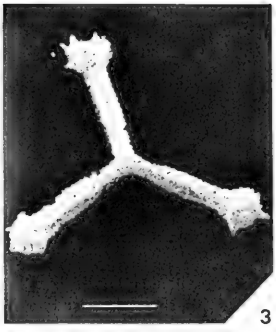
3

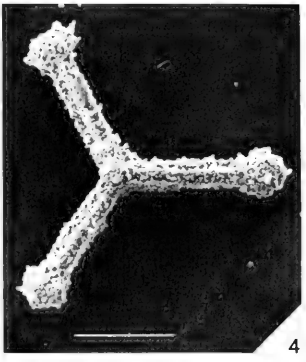
4

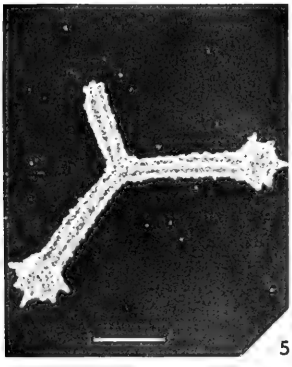
5

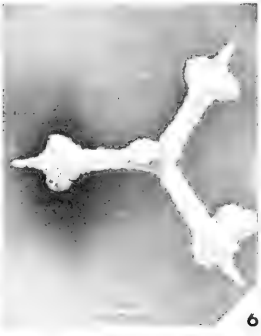
6

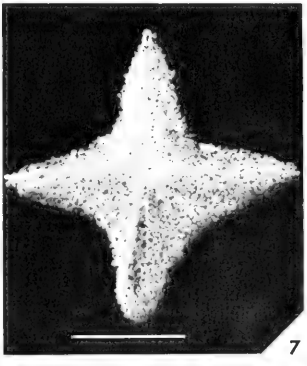
7

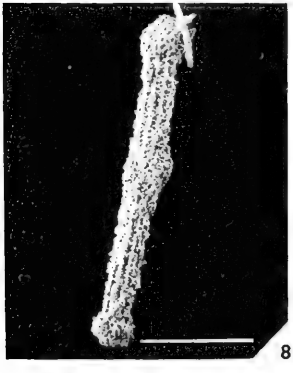
8

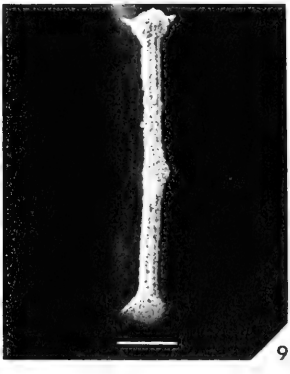
9

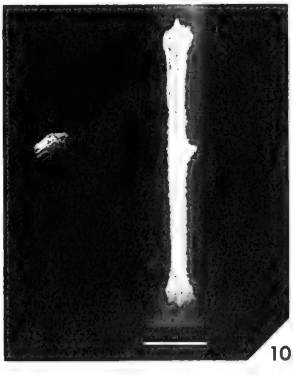
10

INDEX

Note — Light face type refers to pages. Bold face type refers to plates.

A

Abathomphalus mayaroensis Subzone 15
Acanthoceras 11
Acanthoceras rhotomagense Zone 14
Actinocamax plenus Subzone 14
Amphibrachium 20
"Antelope Shale" 10, 13
appenninica, Rotalipora 11
arbucklensis, n. sp., Patulibracchium **15, 16** 27, 41
arca, Globotruncana 9, 13
attenuatum, "Rhopalastrum" 28

B

Blake-Bahama Basin 5, 47, 48
Bostrychoceras polyplocum Zone 15
boulei, Calycoceras 13
brittonensis, Hedbergella 11

C

cachensis, n. sp., Crucella **9** 53, 56
californiaensis, n. sp., Patulibracchium **11, 12** 29, 44
Calycoceras 13
"Chitonastrum" 47
churchi, Globotruncana 9, 12
Crucella, n. gen. 51
cushmani, Rotalipora 11, 13

D

davisi, Patulibracchium **1** 26, 30, 34, 43, 45
delvallensis, n. sp., Patulibracchium **13** 31, 32, 40
dickinsoni, n. sp. Patulibracchium **17** 32
diminutum, Aphibracchium 20, 21
"Dobbins Shale" Member 8, 9

E

Ellipsostylus 8
espartoensis, n. sp., Crucella **18** 54
ewingi, n. sp., Paronaella **19** 47, 50

F

"Fiske Creek Formation" 10, 13
Forbes Formation 8, 9

G

Globotruncana 9, 11
Globotruncana arca datum (first appearance) 15
Globotruncana calcarata Zonule 13, 15
Globotruncana contusastuartiformis Assemblage Zone 15
Globotruncana datum (extinction) 15
Globotruncana fornicata-stuartiformis Assemblage Zone 15
Globotruncana linneiana-bulloides datum (extinction) 15
greenhornensis, Rotalipora 11, 13
Guinda Formation 8, 9

H

Haeckel, E. 7
Hagiastrum 19, 51, 53
Halesium, n. gen. 16, 22, 23, 27, 47
Hedbergella 11
hilli, Globotruncana 9, 12

I

inaequalum, n. sp., Patulibracchium **4, 5** 33

Inoceramus 9, 13
irwini, n. sp., Crucella **9** 55

J

"aff. japonicum, Kossmaticeras" 10

K

Kanabiceras 13
"Kieselkalke von Cittiglio" 47
Kossmaticeras 10

L

labiatus, Inoceramus . 13
lapparenti, s.s., Globotruncana 9
lawsoni, n. sp., Patulibracchium **13, 14** 35, 43
linneiana, s.s, Globotruncana 9
loeblichi, Globotruncana 9

M

Mantelliceras mantelli Zone 11, 14
Marginotruncana concavata Subzone 15
Marginotruncana helvetica-Marginotruncana sigali datum (extinction) . 15
Marginotruncana renzi Assemblage Zone 15
Marginotruncanidae datum (extinction) 15
"Marsh Creek Formation" 14
marshensis, n. sp., Patulibracchium .**15** 36
messinae, n. sp., Crucella **6** 52, 53, 56

O

"orientalis, Inoceramus" 9
ornatissima, Ventilabrella 9, 13

P

Panoche Group 11
Parona, C. F. 7
Paronaella, n. gen. 22, 23, 46
Patulibracchium, n. gen. 16, 22, 23, 27, 28, 47
petersoni, n. sp., Amphibrachium .**19** 21
Petroleum Creek 9
petroleumensis, n. sp., Patulibracchium .**11** 28, 36, 37
plana, n. sp., Crucella **8** 56
Planomalina buxtorfi datum (extinction) 14
Praeglobotruncana 11
Prionocyclus 15
Prionotropis 15
"Prunoidea" 7
Puzosia 11

Q

quadratum, n. sp., Halesium **3, 4** 23

R

"Rhopalastrum" 28, 50
Riedel, W. R. 7
rosetta, Globotruncana 9
Rotalipora 11, 13
Rotalipora cushmani datum (first appearance) 14
Rotalipora cushmani-greenhornensis Subzone 14
Rotalipora evoluta datum (first appearance) 14
Rotalipora evoluta Subzone 11,14
ruesti, n. sp., Patulibracchium **7, 8** 30, 38
Rugoglobigerina datum (first appearance) .. 15
Rüst, D. 7

S

San Salvador 22

sansalvadorensis, n. sp.
Amphibrachium **19** 21
sexangulum, n. sp.,
Halesium **1, 2** 23, 24, 25
Sites Formation 10
solanoensis, n. sp.
Paronaella **10** 46, 48, 51
Spongoprunum 7
Squinabol, S. 7
stephani, Praeglobo-
truncana 11
stoliczkai cf.,
Calycoceras 13

T

taliaferroi, n. sp.,
Patulibracchium
14, 15 31, 40
teslaensis, n. sp.,
Patulibracchium
12, 13 27, 31, 41
torvitatis, n. sp.,
Patulibracchium **6, 7** 35, 42, 44
tricuspidatum,
"Chitonastrum" 47
trixiphus,
"Rhopalastrum" 50
tumeniensis,
"Hagiastrum" 54

U

ungulae, n. sp.,
Patulibracchium **7** 29, 44

V

Venado Formation 13, 14
venadoensis, n. sp.,
Paronaella **10, 11** 48, 49, 51
Ventilabrella 9, 13

W

Whiteinella archaeo-
cretacea Subzone 15
woodlandensis, n. sp.,
Patulibracchium **5** 30, 45

X

Xiphotractus 8

Y

Yolo Formation 9, 10

XLV. (No. 204). 564 pp., 63 pls. 18.00
Venezuela Cenozoic pelecypods

XLVI. (Nos. 205-211). 419 pp., 70 pls. 16.00
Large Foraminifera, Texas Cretaceous crustacean, Antarctic Devonian terebratuloid, Osgood and Paleocene Foraminifera, Recent molluscan types.

XLVII. (Nos. 212-217). 584 pp., 83 pls. 18.00
Eocene and Devonian Foraminifera, Venezuelan fossil scaphopods and polychaetes, Alaskan Jurassic ammonites, Neogene mollusks.

XLVIII. (No. 218). 1058 pp., 5 pls. 18.00
Catalogue of the Paleocene and Eocene Mollusca of the Southern and Eastern United States.

XLIX. (Nos. 219-224). 671 pp., 83 pls. 18.00
Peneroplid and Australian forams, North American carpoids, South Dakota palynology, Venezuelan Miocene mollusks, *Voluta*.

L. (Nos. 225-230). 518 pp., 42 pls. 18.00
Venezuela and Florida cirripeds, Antarctic forams, Linnaean Olives, Camerina, Ordovician conodonts, Niagaran forams.

LI. (Nos. 231-232). 420 pp., 10 pls. 18.00
Antarctic bivalves, Bivalvia catalogue.

LII. (Nos. 233, 236). 387 pp., 43 pls. 18.00
New Zealand forams, Stromatoporoidea, Indo-Pacific, Miocene-Pliocene California forams.

LIII. (Nos. 237-238). 488 pp., 45 pls. 18.00
Venezuela Bryozoa, Kinderhookian Brachiopods.

LIV. (Nos. 239-245). 510 pp., 50 pls. 18.00
Dominican ostracodes, Texan pelecypods, Wisconsin mollusks, Siphocypraea, Lepidocyclina, Devonian gastropods, Miocene Pectens Guadaloupe.

LV. (Nos. 246-247). 657 pp., 60 pls. 18.00
Cenozoic corals, Trinidad Neogene mollusks.

LVI. (Nos. 248-254). 572 pp., 49 pls. 18.00
American Foraminifera, North Carolina fossils, coral types, Belanski types, Venezuelan Cenozoic Echinoids, Cretaceous Radiolaria, Cymatiid gastropods.

LVII. (Nos. 255-256). 321 pp., 62 pls. 18.00
Alaskan Jurassic ammonites, Pt. II, Jurassic Ammonitina New Guinea.

LVIII. (Nos. 257-262). 305 pp., 39 pls. 18.00
Cretaceous Radiolaria, Cretaceous Foraminifera, Pacific Silicoflagellates, North American Cystoidea, Cincinnatian Cyclonema, new species Vasum.

LIX. (No. 263). 314 pp. 18.00
Bibliography of Cenozoic Echinoidea.

Palaeontographica Americana

Volume I. See Johnson Reprint Corporation, 111 Fifth Ave., New York, N. Y. 10003
Monographs of Arcas, Lutetia, rudistids and venerids.

II. (Nos. 6-12). 531 pp., 37 pls. 23.00
Heliophyllum halli, Tertiary turrids, Neocene Spondyli, Paleozic cephalopods, Tertiary Fasciolarias and Paleozoic and Recent Hexactinellida.

III. (Nos. 13-25). 513 pp., 61 pls. 28.00
Paleozoic cephalopod structure and phylogeny, Paleozoic siphonophores, Busycon, Devonian fish studies, gastropod studies, Carboniferous crinoids, Cretaceous jellyfish, Platystrophia and Venericardia.

IV. (Nos. 26-33). 492 pp., 72 pls. 28.00
Rudist studies Busycon, Dalmanellidae, Byssonychia, Devonian lycopods, Ordovican eurypterids, Pliocene mollusks.

V. (Nos. 34-37). 445 pp., 101 pls. 32.00
Tertiary Arcacea, Mississippian pelecypods, Ambonychiidae, Cretaceous Gulf Coastal forams.

VI. (Nos. 38-41). 444 pp., 83 pls. 35.00
Lycopsids and sphenopsids of Freeport Coal, Venericardia, Carboniferous crinoids, Trace fossils.

VII. (Nos. 42-44). 153 pp., 26 pls. 15.00
Torreites Sanchezi, Cancellariid Radula, Ontogeny, sexual dimorphism trilobites.

Vols. I-XXIII. See Kraus Reprint Corp., 16 East 46th St., New York, N. Y. 10017, U.S.A.

XXIV. (Nos. 80-87). 334 pp., 27 pls. 12.00
Mainly Paleozoic faunas and Tertiary Mollusca.

XXV. (Nos. 88-94B). 306 pp., 30 pls. 12.00
Paleozoic fossils of Ontario, Oklahoma and Colombia, Mesozoic ehinoids, California Pleistocene and Maryland Miocene mollusks.

XXVI. (Nos. 95-100). 420 pp., 58 pls. 14.00
Florida Recent marine shells, Texas Cretaceous fossils, Cuban and Peruvian Cretaceous, Peruvian Eogene corals, and geology and paleontology of Ecuador.

XXVII. (Nos. 101-108). 376 pp., 36 pls. 14.00
Tertiary Mollusca, Paleozoic cephalopods, Devonian fish and Paleozoic geology and fossils of Venezuela.

XXVIII. (Nos. 109-114). 412 pp., 34 pls. 14.00
Paleozoic cephalopods, Devonian of Idaho, Cretaceous and Eocene mollusks, Cuban and Venezuelan forams.

XXIX. (Nos. 115-116). 738 pp., 52 pls. 18.00
Bowden forams and Ordovician cephalopods.

XXX. (No. 117). 563 pp., 65 pls. 16.00
Jackson Eocene mollusks.

XXXI. (Nos. 118-128). 458 pp., 27 pls. 16.00
Venezuelan and California mollusks, Chemung and Pennsylvanian crinoids, Cypraeidae, Cretaceous, Miocene and Recent corals, Cuban and Floridian forams, and Cuban fossil localities.

XXXII. (Nos. 129-133). 294 pp., 39 pls. 16.00
Silurian cephalopods, crinoid studies, Tertiary forams, and Mytilarca.

XXXIII. (Nos. 134-139). 448 pp., 51 pls. 16.00
Devonian annelids, Tertiary mollusks, Ecuadoran stratigraphy paleontology.

XXXIV. (Nos. 140-145). 400 pp., 19 pls. 16.00
Trinidad Globigerinidae, Ordovician Enopleura, Tasmanian Ordovician cephalopods and Tennessee Ordovician ostracods and conularid bibliography.

XXXV. (Nos. 146-154) 386 pp., 31 pls. 16.00
G. D. Harris memorial, camerinid and Georgia Paleocene Foraminifera, South America Paleozoics, Australian Ordovician cephalopods, California Pleistocene Eulimidae, Volutidae, and Devonian ostracods from Iowa.

XXXVI. (Nos. 155-160). 412 pp., 53 pls. 16.00
Globotruncana in Colombia, Eocene fish, Canadian Chazyan Antillean Cretaceous rudists, Canal Zone Foraminifera, fossils, foraminiferal studies.

XXXVII. (Nos. 161-164). 486 pp., 37 pls. 16.00
Antillean Cretaceous Rudists, Canal Zone Foraminifera, Stromatoporoidea.

XXXVIII. (Nos. 165-176). 447 pp., 53 pls. 18.00
Venezuela geology, Oligocene Lepidocyclina, Miocene ostracods, and Mississippian of Kentucky, turritellid from Venezuela, larger forams, new mollusks, geology of Carriacou, Pennsylvanian plants.

XXXIX. (Nos. 177-183). 448 pp., 36 pls. 16.00
Panama Caribbean mollusks, Venezuelan Tertiary formations and forams, Trinidad Cretaceous forams, American-European species, Puerto Rico forams.

XL. (No. 184). 996 pp., 1 pls. 18.00
Type and Figured Specimens P.R.I.

XLI. (Nos. 185-192). 381 pp., 35 pls. 16.00
Australian Carpoid Echinoderms, Yap forams, Shell Bluff, Ga. forams. Newcomb mollusks, Wisconsin mollusk faunas, Camerina, Va. forams, Corry Sandstone.

XLII. (No. 193). 673 pp., 48 pls. 18.00
Venezuelan Cenozoic gastropods.

XLIII. (Nos. 194-198). 427 pp., 29 pls. 16.00
Ordovician stromatoporoids, Indo-Pacific camerinids, Mississippian forams, Cuban rudists.

XLIV. (Nos. 199-203). 365 pp., 68 pls. 16.00
Puerto Rican, Antarctic, New Zealand forams, Lepidocyclina, Eumalacostraca.

BULLETINS
OF
AMERICAN
PALEONTOLOGY

(Founded 1895)

Vol. 60

No. 265

A NEW SPECIES OF CORONULA (CIRRIPEDIA) FROM THE LOWER PLIOCENE OF VENEZUELA

By

NORMAN E. WEISBORD

June 1, 1971

Paleontological Research Institution
Ithaca, New York 14850, U.S.A.

Library of Congress Card Number: 77-158088

Printed in the United States of America
Arnold Printing Corporation

A NEW SPECIES OF *CORONULA* (CIRRIPEDIA) FROM THE LOWER PLIOCENE OF VENEZUELA

Norman E. Weisbord*
Department of Geology
The Florida State University

ABSTRACT

Coronula macsotayi, a new species of whale barnacle from the Mare Formation of Venezuela, is described, compared, and illustrated. Its nearest relative is *Coronula bifida* Bronn, 1831, which occurs in the Pliocene and Pleistocene of Italy. The genus *Coronula* is reported for the first time from Venezuela.

INTRODUCTION

On March 10th, 1969 the writer received from Oliver Macsotay Izak a nearly whole and excellently preserved whale barnacle of the genus *Coronula.* The single specimen was collected by Macsotay from the basal sand of the Mare Formation at its type locality, which is on the hillside above the west bank of Quebrada Mare Abajo, Distrito Federal, Venezuela, approximately 22 kilometers by road north of Caracas. The species is new and is given the name *Coronula macsotayi.*

ACKNOWLEDGMENTS

I wish to express my appreciation to the National Science Foundation for its support of my research on the late Cenozoic invertebrates of Venezuela. This contribution is one of a number of books and papers, most of them published by the Paleontological Research Institution, resulting from that support. I wish also to thank Gerrit Mulders of Tallahassee for photographing many of the Venezuelan specimens, including the *Coronula* described in this article.

MARE FORMATION

The Mare Formation was first described by Frances de Rivero (1956, p. 120) as a discrete unit within the Cabo Blanco Group. The Mare is highly fossiliferous, and contains not only a host of exceptionally well-preserved marine invertebrates, but also, as pointed out by Macsotay (1968, pp. 303,304), some equally well-preserved freshwater and land shells which were washed into the marine accumulation during Mare time. From a preliminary inspection of the fossils, Dr. Rivero tentatively regarded them as "probably Pleistocene although some species [of mollusks] suggest a possible older age, especially the presence of *Strombina.*"

During 1955 and 1956 the writer spent a number of weekends mapping the geology of the Cabo Blanco area, and in 1957 (Weisbord, pp. 18-20) re-described the Mare Formation as follows:

*Research Associate, Paleontological Research Institution.

The Mare formation is a shallow-water marine deposit. It is about 40 feet thick at the type locality but attains a thickness of perhaps 60 feet elsewhere. The lower 10 to 15 feet are made up of incoherent grits and sands containing many well-preserved fossils. This lower member starts as a pebble to granule gravel or "grit" (with occasional stringers of cobbles) and grades upward to a sand of decreasing coarseness. The upper 30 feet or so of the Mare formation consists of tan, homogeneous, and slightly compacted silts of a fine and even texture. These silts conformably overlie the coarser sediments at the base of the Mare formation, but the contact between them is usually rather sharp. Like the grits, the silts of the Mare formation are also highly fossiliferous, albeit more so below than above, and, at the top of the formation, the silts may be barren of fossils.

Weisbord was inclined to consider the Mare Formation as Pliocene in age, an opinion that was reinforced after his study of the Mollusca (1962, 1964a, 1964b). That study included the identification and establishing the range of 230 species of Mare mollusks. Of that number, 26 to 41 per cent were found to have survived to Recent time, a ratio that would suggest, applying Lyell's extinction criterion, an early Pliocene age rather than late Miocene or late Pliocene. The spread of 26 to 41 per cent indicates the lowest to highest percentages permissible, and takes into consideration the judgment factor in deciding whether fossil species are the same as, or different than, closely related living ones. It was also thought that certain newly described Mare species would eventually be found living in Venezuelan waters, and such indeed is proving to be the case. It is anticipated that ultimately about a third, or 33 per cent, of the Mare mollusks will be recorded as having survived to Recent time.

The stratigraphic succession within the Cabo Blanco Group, and the relationship of the Mare Formation to other divisions of the Group, are shown in the following table.

CABO BLANCO GROUP

SUBRECENT

Bench-forming beach rock, and reworked clays, sands, and gravels. Thickness 3 meters max.

Disconformity

ABISINIA FORMATION (Lower Pleistocene)

Clays, silts, sands, and gravels, the latter locally with marine fossils. Thickness 13 meters max.

Disconformity

MARE FORMATION (Middle-Lower Pliocene)

Uniformly coarse friable sandstone at base grading upward to soft siltstone. Highly fossiliferous. Thickness 19 meters max.

Angular unconformity to disconformity

PLAYA GRANDE FORMATION (MAIQUETIA MEMBER)—Lower Pliocene

Shales, siltstones, calcareous sandstones, and conglomerates. Bioherms and biostromes of calcareous algae. Fossils moderately abundant throughout. Thickness 68 meters.

Fault

PLAYA GRANDE FORMATION (CATIA MEMBER)—Lower Pliocene

Calcareous siltstones and sandstones, conglomerates, some shales and impure limestones, and rare lentils of barnacle coquinas. Fossils moderately abundant, in places as casts and molds. Thickness 156-233 meters.

Angular unconformity

LAS PAILAS FORMATION (Middle Tertiary)

Unfossiliferous mudstones, siltstones, sandstones, and conglomerates. Thickness 375 meters +.

Including *Coronula macsotayi,* n. sp. described in this paper, ten species of fossil Cirripedia are now known from the Cabo Blanco Group of Venezuela (Weisbord, 1965). Six of the ten barnacles occur in the Mare Formation, and of the six, one, and possibly two (17 to 33 per cent) of the Mare barnacles are living today. As the four remaining species are related to known late Neogene species, the early Pliocene age of the Mare Formation as indicated by the Mollusca, is not controverted by the seemingly low survival rate of the Cirripedia. Longevity, or the survival capability of Cenozoic invertebrates, differs greatly among the classes of organisms, but once a standard "mortality table" has been established for one biologic hierarchy (Lyell, 1833, etablished his epochs of the Tertiary by the per cent of species of Mollusca that survived to Recent time), then the percentage for all other biologic hierarchies also becomes a standard providing a sufficient number of species are available to insure statistical validity.

As the concepts enunciated above were nurtured by the writer's study of the Cabo Blanco Group of Venezuela, there is presented in the following tabulation a roundup, under the hierarchy of Class or Order, all of the fossil species identified in each formation of the

Group and the percentage of those species that are also living today. Included in the tabulation are the fossils collected in the Guaiguaza Clay, a formation 115 kilometers west of Cabo Blanco, the stratigraphic position of which is not yet known.

The age determinations are based, with modification, on Lyell's subdivision of the Tertiary period by the per cent of fossil Mollusca that have survived to Recent time. Complementing the Mollusca as age indicators are 1) the percentages in the Recent of other classes of organisms, 2) the local stratigraphy and the succession of beds, and 3) the dating of the Abisinia Formation (the absolute age of which is in excess of 300,000 years) as determined by the Ionium disequilibrium method (see Osmond, *in* Weisbord, 1965, footnotes pp. 11,12).

PERCENTAGE OF RECENT SPECIES BY CLASS AND FORMATION

Abisinia Formation (Lower Pleistocene)

Class or Order	Total number of species	Number of fossil species in Recent	Per cent of species in Recent
Anthozoa (Scleractinia)	2	2	100
Echinoidea	1	1	100
Gymnolaemata (Cheilostomata)	1	1	100
Polychaetia (Sedentarida)	1	1	100
Cirripedia	1	1	100
Gastropoda (MOLLUSCA)	34	26-31	76-91
Pelecypoda (MOLLUSCA)	18	15-16	83-90
TOTAL	58	47-53	81-91
MOLLUSCA ONLY	52	41-47	80-90

Guaiguaza Clay (Upper Pliocene)

Class or Order	Total number of species	Number of fossil species in Recent	Per cent of species in Recent
Anthozoa (Scleractinia)	2	2	100
Scaphopoda (MOLLUSCA)	2	1	50
Gastropoda (MOLLUSCA)	25	9	36
Pelecypoda (MOLLUSCA)	14	11	79
TOTAL	43	23	53
MOLLUSCA ONLY	41	21	51

Mare Formation (Middle-Lower Pliocene)

Class or Order	Total number of species	Number of fossil species in Recent	Per cent of species in Recent
Foraminiferida[1]	72	60	83
Anthozoa (Scleractinia)	3	3	100
Echinoidea	1	1	100
Gymnolaemata (Cheilostomata)	10	6	60
Polychaetia (Sedentarida)	2	1	50
Cirripedia	6	1-2	17-33
Scaphopoda (MOLLUSCA)	8	4-5	50-63
Gastropoda (MOLLUSCA)	140	23-52	16-37
Pelecypoda (MOLLUSCA)	82	32-58	39-46
TOTAL	324	131-168	40-52
MOLLUSCA ONLY	230	58-95	26-41

Playa Grande Formation Undifferentiated (Lower Pliocene)

Class or Order	Total number of species	Number of fossil species in Recent	Per cent of species in Recent
Chlorophyceae (Dasycladales)	1	0	0
Foraminiferida[1]	140	106	76
Anthozoa (Scleractinia)	5	4	80
Echinoidea	5	5	100
Gymnolaemata (Cheilostomata)	7	4	57
Polychaetia (Sedentarida)	4	0	0
Cirripedia	8	2	25
Scaphopoda (MOLLUSCA)	9	3-5	33-55
Gastropoda (MOLLUSCA)	84	9-20	11-24
Pelecypoda (MOLLUSCA)	72	30-37	42-52
TOTAL	335	163-183	49-54
MOLLUSCA ONLY	165	42-62	25-37

[1]Data obtained from Bermúdez (1966), and Bermúdez and Fuenmayor (1966).

SYSTEMATIC DESCRIPTION

Coronula macsotayi, n. sp. Pl. 20, figs. 1-4

Diagnosis. — A coronoform balanid, formerly attached to a cetacean, characterized by its large elongated orifice and exceptionally thick radii and sheath, both of which are constructed of numerous fine quadrangular tubules. The radii are horizontally disposed from the summit to the base. This differentiates the species from the Pliocene *Coronula barbara* Darwin of England and Italy, on which the summit of the radii is oblique.

Description. — The shell is large, crownlike, longer than high, tumid about the middle, and angularly suboval in outline. The

height is about five-sevenths the length. The six compartments are similar in appearance, but the carina is slightly attenuated and the carinolateral parietes somewhat wider below than the others. The orifice is large, sharply hexagonal at the summit, its length a little over one half, and the width two-fifths that of the shell. The membrane of the basis is missing, but judging from the configuration of the base of the shell, the basis was as long as, and somewhat wider than the orifice, and obtusely hexagonal in outline.

The parietes are convex, with prominent convexly arched longitudinal ribs. The ribs are crossed by numerous strong transverse folds, generally slightly arcuate and in places flexuous, traversed by sturdy, vertically aligned, closely spaced growth ridges of nearly equal size. The transverse folds become crowded and recumbent at the base, and from the base upward to within 5 mm of the apex on the largest rib, there are 60 folds in a length of 48.5 mm. On this same rib, at the base where it is the widest and fortuitously bifid, there are 34 vertical ridges in a width of 6.5 mm. The vertical ridges are squarish and nodulated, the nodulations more pronounced on the crest and underside of the folds. Where fully developed the ridges are wider than their interspaces. Within and along the crest of the transverse folds there is a row of tiny elliptical pores, the pores representing a cross section of the small interconnected longitudinal canals running through the interspaces of the vertical ridges. A strong, erect, longitudinal, laminar plate is present underneath each of the middle longitudinal ribs of a paries. The plate occurs midway between the sutures of each rib and is the keel on which the transverse folds are developed. Each laminar plate, as well as the wall of the sheath to which it is connected, is scored by numerous fine vertical striae. The space between the laminae is 1 mm at the apex to 5 mm at the base of the ribs.

There are four longitudinal ribs on the carina and rostrum, and five on each of the other parietes. On the carina and rostrum only three of the four ribs reach the apex of the paries, and on the sides only four of the five. The shorter fourth rib of the carina and fifth rib of the carinolaterals appear some distance down from the apex and widen to the basis on the margin of the parietes facing the rostrum; similarly the fourth rib of the rostrum and fifth of the laterals on the other side of the shell is introduced on the margin of the

parietes facing the carina. The two or three middle ribs of each paries are the largest, the outermost ones the smallest; the latter are fused with the outer ribs of the neighboring compartment at the base of the shell and diverge rapidly therefrom to form the characteristic wide "V" of the compartments. The ribs are locked together at their sutures in an alternating zigzag array by toothlike projections from the ends of the transverse folds on each longitudinal rib. Several of the ribs are bifid or split toward the base, a character that seems to have arisen from fracturing, as the faint cleft dividing them is not sutured by interlocking teeth.

The radii are thick, broadly triangular, and horizontally lineated on the outer surface. In section the radius is seen to be made up of a number of plys of thin, closely spaced laminae separated by microscopic vertical partitions, producing in effect a system of small cellular tubules, quadrate in form and horizontal in alignment. The margin of the radius facing the carina overrides and merges with the upper surface of the nearest longitudinal rib, whereas the margin of the radius facing the rostrum continues under its nearest rib and interlocks with it below the first parietal suture. The summit of the radii is horizontal or parallel with the base, and this horizontality is one of the distinguishing characters of the species.

The inner surface of the radii is tightly appressed against but not calcified to the opposed surface of the sheath at the summit of the shell. The sheath is thick, and though not visible in its entirety, is inferred to be as long as the internal shell wall. The interior of the sheath proper is constructed of horizontal tubules similar to those of the radii, but the inner surface of the sheath is thickly calcified and smooth. The summit of the sheath is thin and essentially horizontal, rising slightly above the summit of the radii. As seen within the body cavity of the shell, the lateral plates of the sheath overstep the rostral plate; the laterals and carinolaterals are joined evenly at the sutures; and the carinolaterals pass smoothly under the narrow carinal plate. The cavity for the body is large and deeply cup-shaped.

The opercular valves are not known, and the alae are hidden from view.

Dimensions. — Specimen I689a, (not 1689a) PRI 28292 (holotype) length of shell 71 mm, width 56 mm, height 52 mm; length of orifice 38 mm, width 25 mm; length of base 42 mm, width 32 mm.

Type locality. — Basal sand member of Mare Formation at W-13, on hillside above west bank of Quebrada Mare Abajo, Distrito Federal, Venezuela. Lower Pliocene. Collected and donated by Oliver Macsotay Izak of the Instituto Oceanográfico, Cumaná, Venezuela.

Comparisons. — There are four species of *Coronula* with which *Coronula macsotayi* may be compared — the Recent and cosmopolitan *Coronula diadema* (Linnaeus), the Pliocene *Coronula barbara* Darwin from England and Italy, the Pliocene and Pleistocene *Coronula bifida* Bronn from Italy, and the Pliocene *Coronula dormitor* Pilsbry and Olsson from Ecuador. The most closely related of the four is *Coronula bifida* Bronn as described and illustrated by Alessandri (1894, pp. 302,303, pl. 3, figs. 7a,7b; 1906, pp. 315-317, pl. 18, figs. 8-11). The shell of *C. bifida,* however, is subcircular and subcylindrical in form and is nearly as high as long; the orifice is only slightly longer than wide and is less than half the length of the shell compared with the relatively longer and larger orifice of *C. macsotayi;* the carinal plate and paries are much wider than on *C. macsotayi,* but the compartments of *C. bifida* are not so widely triangular as on the Venezuelan shell.

The principal difference between *Coronula barbara* Darwin and *Coronula macsotayi,* n. sp., is that the summit of the radii is definitely oblique on *C. barbara* but horizontal on *C. macsotayi,* and it is this obliquity, according to Alessandri (1894, pp. 303,304, pl. 3, figs. 8a,8b; 1906, p. 317, pl. 18, figs. 12a,12b), that distinguishes *C. bifida* Bronn (1831, p. 126) from *C. barbara* Darwin (1854a, pp. 421-423, pl. 15, fig. 6; 1954b, pp. 38-40, pl. 2, figs. 8-8e). *Coronula diadema* (Linnaeus) (see Darwin, 1854a, pp. 417-419, pl. 15, figs. 3-3b; pl. 16, figs. 1,2,7; 1854b, pp. 39,40; Pilsbry, 1916, pp. 273, 274, pl. 65, figs. 3,4; and Zullo, 1969, p. 22) is differentiated from *C. bifida* Bronn, *C. barbara* Darwin, and *C. macsotayi,* n. sp., by, among other characters, its form which is that of a slightly swollen cask whose diameter is less than its height. *C. dormitor* Pilsbry and Olsson (1951, p. 202, pl. 11, figs. 1-5) differs from *C. macsotayi* in lacking the interlocking teeth between the external ribs.

Comments. — This whale barnacle is named for Oliver Macsotay, stratigrapher and paleontologist, who is actively engaged in research on the Neogene deposits of eastern Venezuela.

The holotype PRI 28292, is in the Paleontological Research Institution, Ithaca, New York, 14850, U.S.A.

LITERATURE CITED

Alessandri, Giulio de

1894. *Contribuzione allo studio dei Cirripedi fossili d'Italia.* Soc. Geol. Italiana, Boll., vol. 13, No. 3, pp. 234-314, pls. 3-5, text-figs. 1-3.

1906. *Studi monografici sui Cirripedi fossili d'Italia.* Palaeontogr. Italica, vol. 12, pp. 207-324, pls. 13-18, text-figs. 1-9.

Bermúdez, Pedro J.

1966. *Consideraciones sobre los sedimentos del Miocene Medio al Reciente de las costas central y oriental de Venezuela. Primera parte.* Bol. Geol. [Venezuela], vol. 7, No. 14, pp. 333-411, 4 tables, correlation chart.

Bermúdez, Pedro J., and Fuenmayor, Angel N.

1966. *Consideraciones sobre los sedimentos del Miocene Medio al Reciente de las costas central y oriental de Venezuela. Segunda parte. Los foraminiferos bentónicos.* Bol. Geol. [Venezuela], vol. 7, No. 14, pp. 412-611, pls. 1-4.

Bronn, Heinrich Georg

1831. *Italiens Tertiär-Gebilde und deren organische Einschlüsse.* Pp. i-xii, 1-176, 1 pl.

Darwin, Charles Robert

1854a. *A monograph on the sub-class Cirripedia, with figures of all the species.* Ray Society London, Publ., pp. i-viii, 1-684, pls. 1-30, text-figs. 1-11.

1854b. *A monograph of the fossil Balanidae and Verrucidae of Great Britain.* Palaeontogr. Soc. London, Mon., vol. 8, pp. 1-44, pls. 1,2, text-figs. 1-6.

Linnaeus, Carl

1766-67. *Systema Naturae per Regna Tria Naturae.* Stockholm, ed. 12, vol. 1, pt. 1, *Regnum Animale,* pp. 1-532 (1766); pt. 2, pp. 533-1327 (1767).

Lyell, Charles

1833. *Principles of Geology.* Vol. III, 109 pp.

Macsotay, Oliver

1968. Edad y paleocología de las formaciones Tuy y Siguire a base de *su fauna de moluscos fósiles.* Bol. Geol. [Venezuela], vol. 9, No. 19, pp. 297-305, pl. 1.

Pilsbry, Henry A.

1916. *The sessile barnacles (Cirripedia) contained in the collection of the U.S. National Museum; including a monograph of the American species.* U.S. Nat. Mus., Bull. 93, pp. i-xi, 1-366, pls. 1-76, text-figs. 1-99.

Pilsbry, Henry A., and Olsson, Axel A.

1951. *Tertiary and Cretaceous Cirripedia from northwestern South America.* Acad. Nat. Sci. Philadelphia, Proc., vol. 103, pp. 197-210, pls. 8-11.

Rivero, Frances de

1956. *Cabo Blanco, Grupo. Léxico Estratigráfico de Venezuela.* Bol. Geol. [Venezuela], Publ. Especial, vol. 1, pp. 116-121.

Weisbord, Norman E.

1957. *Notes on the geology of the Cabo Blanco area, Venezuela.* Bull. Amer. Paleont., vol. 38, No. 165, pp. 1-25, geol. map.

1962. *Late Cenozoic gastropods from northern Venezuela. Ibid.,* vol. 42, No. 193, pp. 1-672, pls. 1-48, text-figs. 1,2.
1964a. *Late Cenozoic pelecypods from northern Venezuela. Ibid.,* vol. 45, No. 204, pp. 1-564, pls. 1-59. photo-figs. 1-8.
1964b. *Late Cenozoic scaphopods and serpulid polychaetes from northern Venezuela. Ibid.,* vol. 47, No. 214, pp. 110-203, pls. 16-22.
1965. *Some late Cenozoic cirripeds from Venezuela and Florida. Ibid.,* vol. 50, No. 225, pp. 1-45, pls. 1-12.

Zullo, Victor A.

1969. *Thoracic Cirripedia of the San Diego Formation, San Diego County, California.* Los Angeles County Mus., Contrib. Sci., No. 159, pp. 1-25, figs. 1-77.

PLATE

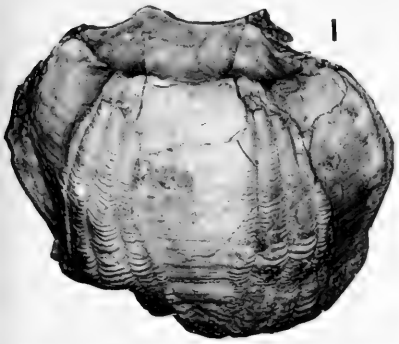

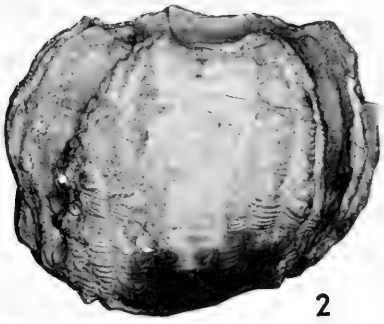

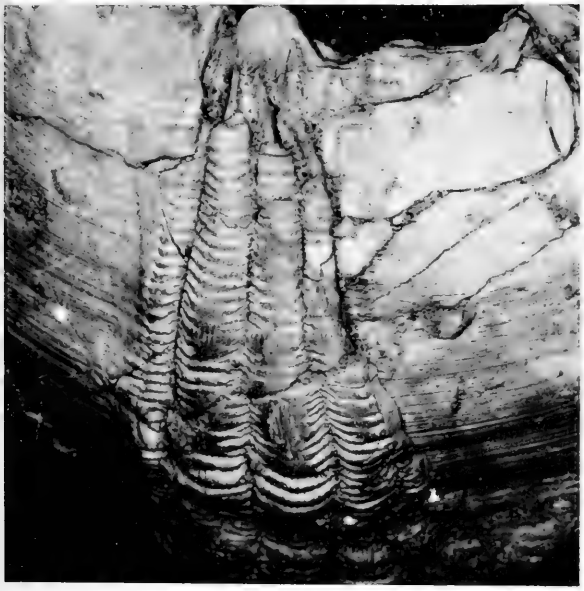

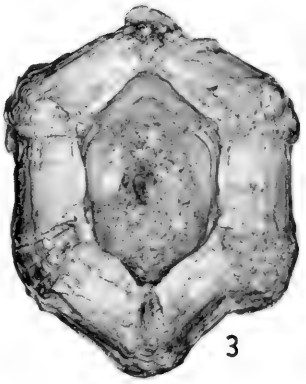

Figs. 1-4, *Coronula macsotayi*, n. sp. Holotype (1689a). PRI 28292. Figs. 1-3, X 0.7; fig. 4, X 1.9. Fig. 1, side view, carina right; fig. 2, side view, carina left; fig. 3, orifice, carina facing observer; fig. 4, enlargement of carinolateral paries (see fig. 1 directly above).

INDEX

Number 265

Note: Light face figures refer to the page numbers. Bold face figures refer to the plate numbers.

A

Abisinia Formation .. 88, 90
Alessandri, Giulio de 94, 95

B

barbara, Coronula 91, 94
Bermúdez, Pedro J..... 91, 94
bifida, Coronula 94
Bronn, Heinrich Georg 94, 95

C

Cabo Blanco 87, 90
Cabo Blanco Group .. 88, 89
Caracas 87
Catia Member 89

D

Darwin, Charles Robert 94, 95
diadema, Coronula 94
Distrito Federal 87, 94
dormitor, Coronula 94

F

Fuenmayor, Angel N. 91, 95

G

Guaiguaza Clay 90

I

Instituto Oceanográfico, Cumaná 94

L

Las Pailas Formation 89
Linnaeus, Carl 94, 95
Lyell, Charles 88, 89, 90, 91

M

Macsotay, Oliver, Izak 87, 94, 95
macsotayi, Coronula **20** 87, 89, 91-95
Mare Formation 87, 89, 91, 94
Maiquetía Member 89
Mulders, Gerrit **87**

N

National Science Foundation 87

O

Olsson, Axel A. 94, 95
Osmond, John Kenneth 90

P

Pilsbry, Henry A. 94, 95

Q

Quebrada Mare Abajo 87, 94

R

Rivero, Frances de 87, 95

S

Strombina 87

W

Weisbord, Norman E. 87, 88, 90, 95

Z

Zullo, Victor A. 94, 96

BULLETINS
OF
AMERICAN
PALEONTOLOGY
(Founded 1895)

Vol. 60

No. 266

PALYNOLOGY AND THE INDEPENDENCE SHALE OF IOWA

By

James B. Urban

1971

Paleontological Research Institution
Ithaca, New York 14850 U. S. A.

BULLETINS
OF
AMERICAN
PALEONTOLOGY
(Founded 1895)

Vol. 60

No. 266

PALYNOLOGY AND THE INDEPENDENCE SHALE OF IOWA

By

JAMES B. URBAN

August 5, 1971

Paleontological Research Institution
Ithaca, New York 14850 U. S. A.

Library of Congress Card Number: 70-135053

Printed in the United States of America
Arnold Printing Corporation

CONTENTS

Abstract 103

Introduction 103

Acknowledgments 105

Methods 106

Systematic palynology 106

Discussion 150

Conclusions 154

References cited 156

Plates 161

PALYNOLOGY AND THE INDEPENDENCE SHALE OF IOWA

James B. Urban*

ABSTRACT

A diverse palynomorph assemblage has been recovered from a shale believed to be identical to the Independence Shale of Iowa. Preservation and stratigraphic age of the fossils suggest two cycles of deposition. The assemblage indicates the Independence Shale was derived from rocks of Upper Devonian age and deposited during Late Mississippian time. Fourteen new species and four new genera are described in this report.

INTRODUCTION

The Independence Shale of Iowa has been the object of considerable study and debate since Calvin (1878) reported dark shale below the Devonian (Cedar Valley) Limestone (Table 1) from a quarry at Independence, Iowa. He reported finding 14 species of brachiopods of which six were common to the Rockford (Lime Creek) Shale. His interpretation suggested a close temporal relationship with the Lime Creek Shale with the intervening limestone interruption being due to facies variation.

Subsequently, a number of researchers (Savage, 1920), (Stookey, 1932, 1933, 1938, 1939), and (Scobey, 1940) have expressed the opinion that the Independence Shale is Lime Creek Shale deposited in depressions or caves in the Cedar Valley Limestone. However, Stainbrook (1935) reported several sections of shale which he maintained were conformably below the Cedar Valley Formation and equivalent to the type Independence Formation. He also stated that the presence of *Hypothyridina* and *Manticoceras* in some of the shales indicated that they should be placed in the Upper Devonian. It should be noted that neither of these fossils were recovered from the type section. Again in 1944, Stainbrook reiterated his belief that the Independence Shale was immediately subjacent to the Cedar Valley Limestone. A fauna (principally brachiopod) was listed that was considered to be characteristic of the formation.

Primarily as a result of Stainbrook's work, the Independence Shale has become reasonably well established as a shale interval between the Cedar Valley Formation and Wapsipinicon Formation. Although the origin of the shale has been a subject of much debate, most workers have agreed on an Upper Devonian age assignment. Müller and Müller (1957) studied the conodonts from a number of

Contribution No. 142, The University of Texas at Dallas.
*Geoscience Division, The University of Texas at Dallas, P.O. Box 30365, Dallas, Texas 75230.

DEVONIAN SYSTEM	UPPER DEVONIAN	YELLOW SPRING GROUP	ENGLISH RIVER FM. MAPLE MILL FM. APLINGTON FM. SHEFFIELD FM.	
			LIME CREEK FM.	OWEN MBR. CERRO GORDO MBR. JUNIPER HILL MBR.
			SHELL ROCK FM.	NORA MBR. ROCK GROVE MBR. MASON CITY MBR.
	MIDDLE DEVONIAN		CEDAR VALLEY FM.	CORALVILLE MBR. RAPID MBR. SOLON MBR.
			WAPSIPINICON FM.	DAVENPORT MBR. KENWOOD MBR. OTIS MBR. COGGEN MBR. BERTRAM MBR.
	LOWER DEVONIAN		LAPORTE CITY FM.	

TABLE 1. STRATIGRAPHIC SECTION OF THE DEVONIAN SYSTEM OF IOWA.

sections that they believed to be the Independence Formation. The conodonts indicated an Early Upper Devonian age. However, none of the type section rock was available for study except as debris thrown out of the original quarry operation. Samples of the debris failed to yield any conodonts or other fossils considered diagnostic of the formation.

Dorheim (1967) reported a shale containing an Upper Devonian conodont fauna exposed below Middle Devonian rocks of the Wapsipinicon Formation in a quarry at Springville, Iowa. On the basis of the conodont information and the lithologic similarity, he equated the shale with the Independence Formation and was of the opinion that the lower stratigraphic position supported the interpretation of the Independence as a stratigraphic leak. Finally, he concluded that the shale was deposited during Upper Devonian time on a karst topography developed in the Middle Devonian rocks.

The sample which is the basis for this investigation was an outcrop sample collected from an active limestone quarry (Brooks Quarry) located NE cor. sec. 3 and NW cor. sec. 2, T88N, R9W along the south side of Highway 20, Buchanan County, Iowa. Sixteen samples were collected as segments of a continuous channel of the Solon Member of the Cedar Valley Formation. A shale interval 2.5 feet thick, 6 feet wide and completely surrounded by the carbonate rock was collected approximately 15 feet above the base of the Cedar Valley Limestone. There is no visible vertical extension of the shale which exhibited an alteration of light gray-green layers with dark gray, carbonaceous layers.

An exceptionally well-preserved and diversified assemblage of palynologic fossils was recovered from the shale. The palynomorphs present suggest an alternative interpretation for the Independence shales.

ACKNOWLEDGMENTS

Appreciation is expressed to Garland Hershey, former Director, Iowa Geologic Survey, and Fred Dorheim, Chief Economic Geologist, Iowa Geologic Survey, for providing the samples used in this investigation. Thanks also to Charles Felix, Sun Oil Co. for making the slides of the Springer study available. Gratitude is due Charles Smith for photographic work and assistance in making plates and to Miss Sheila Moiola and Miss Danielle Heder for draft-

ing the text figures. Anton L. Hales and E. A. Pessagno, University of Texas at Dallas, L. R. Wilson, University of Oklahoma and Al Traverse, Bob Sanders and H. T. Ames, Pennsylvania State University made constructive and appreciated criticisms of the manuscript. Special thanks are due Mrs. Elaine Padovani for preparation and photography of the fossils with the scanning electron microscope. The investigator also acknowledges partial financial support for this study from the National Aeronautics and Space Administration Grant NGL-44-004-001.

METHODS

The maceration techniques discussed in Urban and Kline (1970) were used. Fifteen strew mount microscope slides were prepared of the residue using Clearcol for the mounting medium and the method of Wilson (1959b). Individual specimens were prepared for examination with the scanning electron microscope using the procedures outlined in Urban and Padovani (1970). Approximately 3000 scanning electron micrographs were made of palynomorphs in this study.

Slides containing the type specimens have been deposited in the palynological repository of the University of Oklahoma, Norman, Oklahoma. The number sequence for type specimens refers to sample number, slide number, and ring number on the slide.

SYSTEMATIC PALYNOLOGY

Numerous suprageneric classification systems of fossil spores have been proposed. The best known are the combined works of Potonié and Kremp (1954, 1955, 1956a,b) and Potonié (1956, 1958, 1960) who proposed a classification of the *Sporae dispersae*. Numerous other systems have been proposed as well as many modifications of each system. Consequently, the suprageneric classification is in such a state of flux that the objective becomes poorly defined. In addition, the systems proposed to date are so superficial that they hinder an understanding of natural relationships. Therefore, the taxa have been placed in alphabetical order by genus strictly for purposes of retrieval and ease of reference.

The increased definition made possible by the scanning electron microscope has provided additional information about the mor-

phology of Carboniferous spores. The new information has commonly resulted in considerable difficulty in comparison with previously described taxa. The principal difficulty seems to be due to most taxonomic descriptions being based on gross shape characteristics rather than morphologic relationships determining the various shapes.

The term "*cingulum*" illustrates the difficulty. Potonié and Kremp (1955, p. 15) referred to a cingulum as "a massive ridge present in the equatorial region of spores (Zonales), which often is wedge-like in cross section, and which distinctly enlarges the equatorial diameter and circles the entire equator . . .". *Lycospora* and *Densosporites* were given as examples of a wedge-shape cingulum. Couper (1958, p. 102) defined cingulum as "a flange-like extension of the exine around the equatorial region of the spore." Couper and Grebe (1961, p. 5) defined cingulum as "a surrounding structural feature more or less confined to the equator in which the exine is relatively thicker than any other part of the spore . . . ". Staplin and Jansonius (1964, p. 98) used "zona" in reference to the equatorial structure of *Densosporites,* which they defined as "the outer layer (exoexine) as seen in polar view, appearing as a relatively wide rim extending beyond the margin of the inner layer (intexine), including equatorial centrifugal extensions in excess of the normal exoexinal thickness." They also stated that the "dark" appearance of the typical densospore structure is not necessarily a function of thickness.

Other definitions could be added but similar differences are present in them also. The only agreement among the definitions appears to be the equatorial position of the structure. Examination of numerous specimens of "densospores" in this investigation as well as other work in progress indicate the "typical" *Densosporites* cingulum is not defined morphologically by any of the aforementioned. Instead, it appears the "*Densosporites* cingulum" is a thickened inner layer (inner exoexine) which is enveloped by a thin outer layer (outer exoexine). The absolute morphology cannot be determined without an examination of *Densosporites covensis* Berry.

One of the most readily recognized differences between observations with the scanning electron microscope and published descriptions is the nature of the proximal surface. Most commonly,

the conspicuous proximal sculpture is all that is described, features such as "suture" length and the presence or absence of lips. Yet, examination of spores in this investigation demonstrate that it is rare when there is not a characteristic sculpture on the proximal surface. These preliminary studies also suggest that the proximal sculpture is more consistent in character than the ornament of the distal surface.

A common feature of the proximal surface that is included in many descriptions are the so-called "lips." A number of variations exist that may be referred to as lips: They may be (1) optical sections of the exine due to the proximal surface being preserved in its original pyramidal form, (2) internal or external thickening of the exine adjacent to the trilete suture or (3) ornament on the proximal surface adjacent to the triradiate structure. Although the three are morphologically distinct, they are most commonly grouped together, in simple shape terms, as lips.

Perhaps the most striking observation relates to the "trilete" or "monolete" suture. Spores in this investigation plus other fossil as well as modern material examined in this laboratory suggest that all spores are tectate (*sensu* Potonié, 1934). Approximately 573 descriptions were referred to in this work. Only 19 mentioned a tectate condition of the sutures and those were in fossils with conspicuous morphology such as *Cirratriradites*.

A solution of the descriptive problems is not readily available. Nevertheless, it must be realized that thorough *morphologic* descriptions are absolutely necessary if spores and pollen are to attain maximum utility in phylogenetic or stratigraphic studies.

Genus **ACANTHOTRILETES** Naumova, emend Potonié and Kremp, 1954

Type species, *A. ciliatus* (Knox), Potonié and Kremp, 1964.

Acanthotriletes echinatus Hoffmeister, Staplin and Malloy Pl. 22, figs. 1, 2

1955. *Acanthotriletes echinatus* Hoffmeister, Staplin, and Malloy. Jour. Paleont., vol. 29, p. 379, pl. 38, figs. 1,2.

Genus **AHRENSISPORITES** Potonié and Kremp, 1954

Type species, *Ahrensisporites guerickei* (Horst), Potonié and Kremp, 1954.

Ahrensisporites beeleyensis Neves, 1961 Pl. 22, figs. 3-7

1961. *Ahrensisporites beeleyensis* Neves, Palaeontology, vol. 4, p. 262, pl. 32, fig. 10.

Remarks. — Inclusion of this species in the genus *Ahrensisporites* represents an extension of the concept of the genus. Neves (1961, p. 263) stated "The presence of a composite kyrtome . . . distinguishes the spores of this species." The kyrtome as defined by Potonié and Kremp (1954, p. 13) is an exine fold of characteristic shape. The composite kyrtome of *A. beeleyensis* is actually a thickening over the distal surface, which has an outline form similar to the kyrtome of *A. guerickei.*

Considerable morphologic variation occurs within this species in the samples studied. The proximal surface may have only a simple triradiate scar with some scattered cones in the interradial areas or in many instances, the cones in the interradial regions may be aligned essentially parallel to the triradiate mark and give rise to some proximal ridges. A similar situation exists with the distal ornamentation. The cones may be essentially absent and resulting in a simple thickened distal "kyrtomeform" or the cones may be completely free, giving rise to the "dentate kyrtome."

Ahrensisporites halesi, Urban, n. sp. Pl. 22, figs. 8-12

Derivation of name. — In honor of Dr. Anton L. Hales, Chairman, Division of Geosciences, University of Texas at Dallas, particularly for his special interest in paleontology.

Description. — Spores radial, trilete; equatorial outline is triangular with straight to markedly concave sides. Triradiate structure is tectate with simple rays extending to a point at the base of the auriculae. Exine appears to be a single layer. The proximal exine is considerably thinner than the distal except along the triradiate scar and results in the interradial areas of the proximal surface commonly sagging below the equator. Exine is uniformly 2-3 microns thick except at the apices where the exine is three or more times thicker forming auriculae, outer margins of the auriculae are curved toward the distal side and are continuous with a thickened, serrated ridge which curves inward toward the distal pole then outward to the adjacent auriculum forming a characteristic kyrtome. The surface of the exine is laevigate.

Size. — Holotype 40 microns measured from the interradial margin to the tip of the auriculum. Variation in size of spore, 32 to 48 microns; mean 42 microns; 36 specimens measured.

Types. — Holotype, 147F12-1; paratype 147F17-1.

Type locality. — Brooks Quarry, NE cor. sec. 3 and NW cor. sec. 2, T88N, R9W along side of Highway 20, Buchanan County, Iowa.

Remarks. — The species exhibits several common variations; the distal ridges may be only slightly serrated, but this condition occurs only in smaller forms with strongly concave interradial margins. The auriculae may be slightly partate. Occasionally the distal curving portion of the auriculae is terminated on the distal surface by a prominent cone where each kyrtome ridge would begin. Another frequent variation is a form with typical kyrtome plus one, two, or three cones at the distal pole.

Although some variation is present in this species, the auriculae always exhibit the pronounced distal arching. *A. guerickei* lacks the prominently serrated kyrtome ridges plus it is roundly triangular in form. *A. beeleyensis* has a "composite kyrtome" and does not have the prominent auriculae.

Genus **ANAPICULATISPORITES** Potonié and Kremp, 1954

Type species, *Anapiculatisporites isselburgensis* Potonié and Kremp, 1954.

Anapiculatisporites minor Butterworth and Williams, 1958 Pl. 23, figs. 2, 3

1958. *Anapiculatisporites minor* Butterworth and Williams, Roy. Soc. Edinburgh, Trans., vol. 63, p. 365, figs. 32-34.

Genus **CALAMOSPORA** Schopf, Wilson, and Bentall, 1944

Type species, *Calamospora hartungiana* Schopf *in* Schopf, Wilson, and Bentall, 1944.

Calamospora hartungiana Schopf, 1944 Pl. 23, figs. 1, 4

1944. *Calamospora hartungiana* Schopf *in* Schopf, Wilson, and Bentall, Illinois Geol. Sur., Report of Investigations, No. 91, p. 51, text fig. 1.

Genus **CAMPTOTRILETES** Naumova emend Potonié and Kremp, 1954

Type species, *Camptotriletes corregatus* (Ibrahim), Potonié and Kremp, 1954.

Camptotriletes cf. **C. bacculentus** (Loose), Potonié and Kremp, 1955 Pl. 23, figs. 8, 9

1934. *Verrucosi-sporites bacculentus* Loose, Inst. Paläobot. u Petrog. d. Brennsteine Arb., vol. 4, No. 3, p. 154, pl. 7, fig. 15.
1944. *Punctati-sporites bacculentus* (Loose), Schopf, Wilson, and Bentall, Illinois Geol. Sur., Report of Investigations, No. 91, p. 30.
1950. *Verrucoso-sporites bacculentus* (Loose), Knox, Bot. Soc. Edinburgh, Trans., vol. 35, p. 317.
1955. *Camptotriletes bacculentus* (Loose), Potonié and Kremp, Teil I, Palaeontographica, Abt. B, Bd. 98, Nos. 1-3, p. 104, pl. 16, figs. 287, 288.

Camptotriletes cristatus Sullivan and Marshall, 1966 Pl. 23, figs. 5-7

1966. *Camptotriletes cristatus* Sullivan and Marshall, Micropaleontology, vol. 12, No. 3, p. 270, pl. 1, fig. 25.

Remarks. — Specimens referred to *C. cristatus* compare closely to the description of Sullivan and Marshall except they show some reduction of ornament on the proximal surface.

Genus **CINCTURASPORITES** Hacquebard and Barss, emend.

Type species, *Cincturasporites altilis* Hacquebard and Barss, 1957.

Emended description. — Spores radial, trilete; equatorial outline subtriangular, rounded at the apices and nearly straight sides. Trilete structure tectate, elevated and often appearing as wide lips; commissure rays extend to the inner margin of the equatorial structure. The equatorial structure is thick, broad (20-40 percent of the diameter) and zoned. The zones consist of an outer light zone and an inner dark zone. The equatorial structure is essentially uniform in thickness throughout and parallel to the central area. Exine laevigate to punctate.

Remarks. — The emendation proposed above is intended to conform to the diagnosis of the type species. The above description refers to a thick zoned equatorial structure which is believed to be synonymous with the cingulum and overlap of Hacquebard and Barss (1957). However, Bharadwaj and Venkatachala (1962) pointed out that if the inner zone were an overlap of the central area, it should be a thinner area and probably lighter in color. The equatorial structure is interpreted as a solid structure and the zones as probably representing different thicknesses with the outer being slightly thinner due to the curvature of the structure. The zoned condition is obvious in the illustration of the holotype.

Considerable controversy exists over the status of the genus *Cincturasporites*. Potonié (1960) reported a similarity between *Cincturasporites* and *Murospora*. However, Somers (1952) did not illustrate or describe a zoned cingulum in *Murospora*. Playford (1962a) believed that *Cincturasporites* embraced the concepts of several genera *(Knoxisporites, Stenozonotriletes* and *Lophozonotriletes)* and should not be recognized. Playford's contention that the generic concepts are too widely circumscribed is certainly a valid

statement. Consequently, it is proposed that the genus be conserved in a form more closely restricted to the type species.

Bharadwaj and Venkatachala (1962) contended the holotype is an overmacerated specimen and consequently does not represent the morphology of other specimens from the assemblage slide containing the holotype. They figured other specimens which they thought showed the morphology better. However, the forms chosen by the latter authors had distal ornament not reported in the holotype and did not have the zoned (overlapping) cingulum considered by the original authors to be most significant. Forty seven specimens were examined in this study. All exhibited excellent preservation as evidenced by the clear cut exine showing no pits or other degradation. In view of the forementioned facts, the emendation of Bharadwaj and Venkatachala is not considered justified.

Cincturasporites altilis Hacquebard and Barss, 1957 Pl. 23, figs. 10-12

1957. *Cincturasporites altilis* Hacquebard and Barss, Geol. Sur. Canada, Bull. 40, p. 25, pl. 3, fig. 8.
1962. *Non Cincturasporites altilis* (Hacquebard and Barss), Bharadwaj and Venkatachala, The Palaeobotanist, vol. 10, No. 1, pp. 36,37, pl. 8, figs. 120, 121.

Remarks. — Specimens of excellent preservation herein referred to *C. altilis* compare favorably with the illustration and description of the holotype. The morphologic feature described as overlap of the cingulum is probably not a true overlap as shown in figure 2 of Hacquebard and Barss (1957) but relates to light transmitting properties of a thick massive cingulum.

Genus **CIRRATRIRADITES** Wilson and Coe, 1940

Type species, *Cirratriradites maculatus* Wilson and Coe, 1940.

Cirratriradites cf. **C. saturni** (Ibrahim), Schopf, Wilson, and Bentall, 1944 Pl. 24, figs. 1-4

1932. *Sporonites saturni* Ibrahim *in* Potonié, Ibrahim and Loose, N. Jahrb. f. Min. Geol., Paläont., Beilage-Band, Abt. B. vol. 67, p. 448, pl. 15, fig. 14.
1933. *Zonales-sporites saturni* (Ibrahim), Ibrahim, Dissertation. Tech. Hochschule Berlin, Würzberg, Triltsch, p. 30, pl. 2, fig. 14.
1944. *Cirratriradites saturni* (Ibrahim), Schopf, Wilson, and Bentall, Illinois Geol. Sur., Report of Investigations, No. 91, pp. 43,44.

Remarks. — The morphology of those specimens compared to this species suggest they are conspecific. However, some notable differences in morphology can be observed with transmitted light

as well as the scanning electron microscope. Neither the original description of the species by Ibrahim (1932) or the redescription of Potonié and Kremp (1954) mentioned a differentiation of ornamentation on the proximal and distal surfaces. The ornamentation is considered to be granular.

Specimens encountered in this study are punctate to scabrate on the proximal surface as a result of removal of parts of the outer exoexine on the contact figure. The proximal surface of the flange is laevigate. The distal surface is ornamented with small blunt spines that may join to form rugae. The distal ornamentation is finest on the flange and becomes coarser toward the distal fovea. The ornamentation inside the fovea is much finer with a cluster of spines in the center. Specimens observed in the slides used for the Springer Formation study of Felix and Burbridge (1967) also exhibit these morphologic characteristics. Smith and Butterworth (1967) expressed the opinion that the number of distal fovea was not significant for assignment to this species. Consequently, the specimens in this investigation may represent an undescribed species. However, examination of other species is desirable to establish proper taxonomic criteria.

Genus **CONVOLUTISPORA** Hoffmeister, Staplin, and Malloy, 1955

Type species, *Convolutispora florida* Hoffmeister, Staplin, and Malloy, 1955.

Convolutispora ampla Hoffmeister, Staplin, and Malloy, 1955
Pl. 24, figs. 5, 6

1955. *Convolutispora ampla* Hoffmeister, Staplin, and Malloy, Jour. Paleont., vol. 29, p. 384, pl. 38, fig. 12.

Convolutispora florida Hoffmeister, Staplin, and Malloy, 1955
Pl. 24, figs. 7-9

1955. *Convolutispora florida* Hoffmeister, Staplin, and Malloy, Jour. Paleont., vol. 29, p. 384, pl. 38, fig. 6.

Convolutispora mellita Hoffmeister, Staplin, and Malloy, 1955
Pl. 24, figs. 10, 11

1955. *Convolutispora mellita* Hoffmeister, Staplin, and Malloy, Jour. Paleont., vol. 29, p. 384, pl. 38, fig. 10.

Convolutispora tortuosa, Urban, n. sp. Pl. 24, fig. 12; Pl. 25, figs. 1-3

Derivation of name. — *L. tortuosa* = intricate. Referring to the complex ornament of the convolutions.

Description. — Spores radial, trilete; equatorial outline roundly triangular to circular; trilete structure tectate, commissure rays are equal to the radius of the spore body. The rays are partially, or entirely obscured by the ornamentation. The entire spore is ornamented with a tightly packed convolute ornament. The convolutions are variable in form, appearing as anastomosing, botryoidal clumps. The individual convolutions are coarsely punctate and wrinkled on the surface. Wall ± 3 microns thick.

Size. — Holotype 38 microns. Variation in size of spore 31 to 50 microns, mean 42 microns; 20 specimens measured.

Types. — Holotype, 147F20-1; paratype 147F17-2.

Type locality. — Brooks Quarry, NE cor., sec. 3 and NW cor. sec. 2, T88N, R9W along side of Highway 20, Buchanan County, Iowa.

Remarks. — The appearance of the convolutions characterize this species. These spores were commonly found in tetrads.

Genus **COSTATASCYCLUS** Felix and Burbridge, emend.

Type species *Costatascyclus crenatus* Felix and Burbridge, 1967.

Emended description. — Spores bilateral, monolete with occasional vestigial third ray; monosaccate, may appear bisaccate. Central body is circular to elliptical in outline. The saccus is closely appressed to the proximal side of the central body. The proximal surface exhibits a botryoidal sculpturing which may be aligned in rows. The saccus covers the distal surface and is attached at the central part of the distal surface. Radiating ribs are formed on the distal surface, originating in the central part of the distal surface and diverging ouward.

Remarks. — Examination of the holotype of *C. crenatus* verifies that the proximal surface is not free but is covered by the saccus which is closely attached and modified into the botryoidal sculpturing. In addition, the distal surface is completely covered by the saccus which would suggest that the monolete is functional.

Costatascyclus crenatus Felix and Burbridge, emend. Pl. 25, figs. 4-9

1967. *Costatascyclus crenatus* Felix and Burbridge, Palaeontology, vol. 10, pt. 3, p. 411, pl. 64, fig. 6.

Emended description. — Spores bilateral, monolete with occasional vestigal third ray; monosaccate, may appear bisaccate due to

orientation. Central body circular to elliptical and laevigate. Saccus is intrareticulate. The saccus is closely appressed to the proximal side of the central body. The proximal surface exhibits a botryoidal sculpturing which may be oriented in rows paralleling the monolete suture and appear somewhat ribbed. The saccus covers the distal surface and is attached at the central part of the distal surface. Radiating ribs are formed on the distal surface as a result of the expansion of the saccus where it becomes free from the point of attachment causing it to be folded. The folds are numerous, 20 to 30 in number.

Remarks. — Comparison of specimens of this study with the holotype description suggest some fundamental differences. The saccus is closely appressed to the proximal side of the spore. The proximal area exhibits a botryoidal sculpturing which may be oriented in rows paralleling the monolete suture and appear somewhat ribbed. This latter condition can be readily observed in the holotype of *C. crenatus* using phase contrast optics.

The saccus wall covers the central part of the distal surface. The folds originate from the point of attachment and radiate outward.

Genus **DENSOSPORITES** (Berry), Schopf, Wilson, and Bentall, 1944

Type species, *Densosporites covensis* Berry, 1937.

Remarks. — Numerous emendations of this genus have been proposed since that of Schopf, Wilson, and Bentall (1944). Wilson stated (1959a, p. 48) that "*Densosporites* as a genus is in need of critical study and monographing." The emendation of Potonié and Kremp (1954) has been recognized as invalid because it would place the type species *D. covensis* in an invalid genus, *Annulatisporites*. The circumscription proposed by Bharadwaj and Venkatachala (1962) does not clarify the generic concepts significantly more than that of Schopf, Wilson and Bentall. While they do recognise the importance of the thickened equatorial region, they restrict ornament type to . . . "smooth or faintly granulose." Restriction on this basis makes the genus too narrow.

The emendation proposed in Staplin and Jansonius (1964, p. 98) is inconsistent and somewhat confusing. These authors define a zona . . . "In a two-layered spore, the outer layer (exoexine) as

seen in polar view, appearing as a relatively wide rim extending beyond the margin of the inner layer (intexine), including equatorial centrifugal extensions in excess of the normal exoexinal thickness. . . . If the outer layer is dark (not necessarily a function of thickness) it produces the typical 'densospore' structure. If it is light, it produces the 'flanged' lycospore structure. Inappropriately, many authors apply the terms cingulum and flange, respectively, to these structural configurations."

In checking the use of the term *cingulum* as applied to spores, no use of the term was found predating the use of Potonié and Kremp (1955) in which they cite examples of *Lycospora* and *Densosporites* as having the typical cingulum. Therefore, as a matter of definition, cingulum seems quite appropriately used with densospores. Since the holotype of *Densosporites* has been lost and a neotype has not been designated, it seems that assigning a particular morphographic character defined as specifically as the "zona" might be somewhat misleading.

Staplin and Jansonius (1964, p. 99) in considering the original description of *Densosporites* remarked that "The key words are 'smooth and even'." Yet Berry (1937) did not mention ornamentation in characterizing the genus but instead obviously considered it as a species character. He did describe *D. covensis* as . . . "very smooth and even." In comparison with *D. densus,* he distinguished *D. covensis* by "being more oval and with a much smoother surface." The words "smooth and even" are somewhat misleading for an understanding of the genus as it was originally intended.

In addition, Staplin and Jansonius (*loc. cit.,* p. 99) stated that they were emending *Densosporites* Berry "to include spores with the following characteristics . . . : central distal sculpture differentiated from zonal sculpture; zonal portion of outer layer thicker than central proximal or distal portions." Without a type, the sculpture differentiation is not substantiated or justified. It is noteworthy that the thickened zonal portion is mentioned.

Furthermore, Butterworth, Jansonius, Smith, and Staplin, *in* Staplin and Jansonius (1964, pp. 101, 102) made no mention in their emendation of the thicker zonal portion. Yet, this thicker zonal portion is fundamental to the generic concepts as indicated by the fact that Berry (1937, p. 157) described the thick outer wall.

Schopf, Wilson, and Bentall (1944, p. 39) in redescribing the type stated that . . . "The proximal and distal walls are usually membranous or at least significantly thinner than the equatorial portion of the coat." Finally, Wilson (1959, p. 47) reaffirmed Berry's original description.

As previously stated, a monographic study of *Densosporites* is needed for maintaining the usefulness of the genus. However, it is also essential to maintain the type concepts as long as they exist. Otherwise, total confusion will exist.

Densosporites aculeatus Playford, 1962b Pl. 25, figs. 10-12

1962b. *Densosporites aculeatus* Playford, Part II. Palaeontology, vol. 4, pt. 4, p. 631, pl. 88, figs. 16, 17.

Remarks. — Although this species is described with indistinct laesurae, it seems obvious from the scanning electron micrographs that the proximal exoexine is thin and very susceptible to removal or collapse into the void in the center of the cingulum. Either situation may make the laesurae difficult or impossible to observe.

Densosporites hispidus Felix and Burbridge, 1967 Pl. 26, figs. 1-5

1967. *Densosporites hispidus* Felix and Burbridge, Palaeontology, vol. 10, pt. 3, p. 389, pl. 59, fig. 9.

Remarks. — Specimens observed in this study differ from the original description by having spines over the entire distal surface. However, examination of the holotype and other individuals in the type material indicates that they also possess spines over the entire distal surface rather than granules on the spore body. The preferential proximal-distal orientation of the spores plus the small size of the spines generally results in the distal ornament appearing granular.

D. hispidus differs from *D. spitsbergensis* by having much finer spines that are uniform in length and density.

Densosporites rarispinosus Playford, 1962b Pl. 26, figs. 6-9

1962. *Densosporites rarispinosus* Playford, Part II. Palaeontology, vol. 5, pt. 4, p. 630, pl. 89, figs. 18-21.

Remarks. — Specimens referred to this species compare in every respect with the type description except the cingulum does taper to the equator.

Densosporites cavus Urban, n. sp. Pl. 26, figs. 10-12; Pl 27, figs. 1-5

Derivation of name. — *L. cavus* = a hollow or cavity; referring to the cavities around the margin on the distal side.

Description. — Spores radial, trilete; equatorial outline roundly triangular. Triradiate structure is tectate, commissure rays are simple and extend to or slightly onto the cingulum. Exine is two-layered. Exoexine is thin, less than 1 micron, often appearing virtually transparent; proximal exoexine is laevigate or slightly roughened; distal exoexine is ornamented with scattered, blunt, coni. Intexine is of variable thickness and forms a cingulum, proximal side of the cingulum is generally continuous. The distal side is excavated resulting in channels about the margin, the channels beginning near the inner margin of the cingulum and becoming broader toward the equatorial margin. The channels occasionally extend through the entire cingulum and are reflected as indentations in the proximal surface. The channels are variable in number, often numerous and coalescing toward the equator with thin ridges between. The distal exoexine is ornamented in the central region, the interchannel area and the equatorial margin. The proximal exoexine is thinned over the cingulum and extends beyond the cingulum as a flange; the undistorted shape is a steep sided pyramid on the proximal surface and a hemispherical distal surface.

Size. — Holotype 41 microns. Variation in size of spore 30 to 48 microns, mean 42 microns; 44 specimens measured.

Types. — Holotype, 147F7-1; paratypes 147F2-1, 147F6-1, 147F28-1, 147F20-2.

Type locality. — Brooks Quarry, NE cor. sec. 3 and NW cor. sec. 2, T88N, R9W along side of Highway 20, Buchanan County, Iowa.

Remarks. — The exoexine of the central region exhibits a number of variations. It commonly collapses into the central region or it may be completely removed. Either situation causes difficulty in resolving the true form. This species exhibits a marked resemblance to *Densosporites irregularis* Hacquebard and Barss. However, *D. irregularis* does not have coni or any ornament, the trilete rays extend to or nearly to the equatorial margin and the size is much larger.

D. cavus exhibits variations that encompass two other genera, *Cingulizonates* and *Radiizonates*. Some specimens have few distal excavations and appear as the typical *Densosporites*. However, certain differences that are perhaps ontogenetic as well as preservational phenomena may alter the appearance. The holotype (Plate 26, figures 10, 11) has a few large distal excavations and the equatorial structure appears bizonate. The specimen illustrated on Plate 27, figure 2 shows the distal excavations and "cuesta" considered characteristic of *Cingulizonates*. A consideration of ontogenetic development in the tetrad as well as comparison with figure 1 of Plate 27 indicates that the "cuesta" is a function of preservation. The proximal exine sags into the interspace of the cingulum. If the distal excavations become more numerous (Plate 27, figure 3), the positive areas between have the appearance of radial ribs. Also, the deterioration of the specimen may emphasize such things as the ribs. The specimen shown in Plate 27, figures 4 and 5 has had the outer exoexine of the proximal surface removed. Thus, the specimen takes on the typical *Radiizonates* appearance. The intergrading of these specimens plus the lack of a type for *Densosporites* suggests further study is necessary to justify the genera, *Cingulizonates* and *Radiizonates*.

Genus **DICTYOTRILETES** Naumova, emend. Potonié and Kremp, 1954

Type species, *Dictyotriletes bireticulatus* (Ibrahim) Potonié and Kremp, 1954.

Dictyotriletes clatriformis (Artuz), Sullivan, 1964 Pl. 27, figs. 6-9

1957. *Reticulatisporites clatriformis* Artuz, Istanbul Univ. Fen. Fak. Mecm, Series B, Tome XXII, Fasc. 4, p. 248, pl. 4, fig. 25.
1964. *Dictyotriletes* cf. *clatriformis* (Artuz), Sullivan, Palaeontology, vol. 7, pt. 3, p. 367, pl. 58, fig. 20; pl. 59, figs. 1, 2.

Genus **DORHEIMISPORITES** Urban, n. gen.

Type species, *Dorheimisporites inflatus* Urban, n. sp.

Derivation of name. — Named in honor of Mr. Fred Dorheim, Geologist, Iowa Geologic Survey.

Description. — Spores radial, trilete; equatorial outline roundly triangular, circular or scalloped circular. Triradiate structure is complex, tectate; commissure rays extend to the equatorial margin and covered by a thin exine ridge. The commissure is bounded by

discontinuous convoluted lips. A hollow (cavate?), equatorial ring is present and frequently becomes greatly expanded (saccate-like A distal ring is present concentric to the equator and exhibiting the same peculiarities as the equatorial ring. The distal and equatorial rings are ornamented with rugae and grana. The spore body is covered with a convolute ornament.

Remarks. — No morphologically similar fossils are known. The varients with the greatly expanded equatorial ring may occasionally appear similar to *Alatisporites* in outline. The more common, non-expanded specimens exhibit gross shape similarities to some species of *Knoxisporites*. However, the cingulum and distal ring of *Knoxisporites* are solid structures whereas the structures on *Dorheimisporites* are hollow.

Dorheimisporites inflatus Urban, n. sp. Pl. 28, figs. 1-12

Derivation of name. — *L. inflatus* = a blowing into. Referring to the tendency of the equatorial and distal structures to become greatly enlarged like a saccus.

Description. — Spores, radial, trilete; equatorial outline roundly triangular, circular or scalloped circular. Triradiate structure complex, tectate; commissure rays extend to the equatorial margin and covered by a thin, stout exine ridge. The triradiate ridges are most commonly bounded by thick, discontinuous convoluted lips. The lips are an enlargement of the proximal ornamentation (1-2 microns wide) adjacent to the commissure and extend to the equator where they fuse with the equatorial structure. The interradial areas of the proximal surface are covered with a convolute ornamentation. Individual convolutions are approximately 1 micron wide, discontinuous and apparently randomly dispersed. At the edge of the contact figure the convolutions fuse with the equatorial structure. The equatorial structure is a hollow (cavate?) ring most commonly of uniform width, but occasionally becomes greatly inflated and in transmitted light appears to have multiple sacci attached at the equator. The equatorial structure is ornamented with minute (less than 1 micron wide) rugae and grana. The distal surface is covered with a convolute ornament that is essentially identical to the proximal interradial areas. A hollow ring concentric to the equator is present on the distal surface. The distal ring is structurally identical to the

equatorial ring. When the equatorial ring is inflated, the distal is also. The distal ring is ornamented the same as the equatorial ring. Occasionally the distal and equatorial rings are continuous with each other by exine expansions ornamented as the rings. Distal exine is relatively thick (2-3 microns in the holotype).

Size. — Holotype 50 microns. Variation in size of spores 41 to 57 microns, mean 51 microns; 27 specimens measured.

Types. — Holotype, 147F31-1; paratypes, 147F20-3, 147F27A1 -1, 147F27A1-2.

Type locality. — Brooks Quarry, NE cor. sec. 3 and NW cor. sec. 2, T88N, R9W along side of Highway 20, Buchanan County, Iowa.

Remarks. — The spores representative of this species exhibit considerable variation in the morphology of the equatorial and distal ring structure. The expansion of these structures can probably be considered a cavate condition.

Genus **FLORINITES** Schopf, Wilson, and Bentall, 1944

Type species, *Florinites antiquus* Schopf, *in* Schopf, Wilson, and Bentall, 1944 [syn. *F. pellucidus* (Wilson and Coe), Wilson, 1958].

Florinites visendus (Ibrahim), Schopf, Wilson, and Bentall, 1944 Pl. 29, figs. 1, 2

1933. *Reticulata-sporites visendus* Ibrahim, Dissertation. Tech. Hochschule Berlin, Würzberg, Triltsch, p. 39, pl. 8, fig. 66.
1944. *Florinites* (?) *visendus* (Ibrahim), Schopf, Wilson, and Bentall, Illinois Geol. Sur., Report of Investigations, No. 91, p. 60.
1956. *Florinites visendus* (Ibrahim), Potonié and Kremp, Teil II, Palaeontographica, Abt. B., Bd. 99, p. 170, pl. 21, figs. 476, 477.

Florinites guttatus Felix and Burbridge, 1967 Pl. 29, figs. 3-6

1967. *Florinites guttatus* Felix and Burbridge, Palaeontology, vol. 10, pt. 3, pp. 409, 410, pl. 64, figs. 1-3.

Genus **FOVEOSPORITES** Balme, 1957

Type species, *Foveosporites canalis* Balme, 1957.

Foveosporites insculptus Playford, 1962 Pl. 27, figs. 10-12

1962. *Foveosporites insculptus* Playford, Part I. Palaeontology, vol. 5, pt. 3, p. 601, pl. 85, figs. 3-5.

Genus **GORGONISPORA*** Urban, n.gen.

Types species, *Gorgonispora** *magna* (Felix and Burbridge), Urban, comb. new.

*This genus was named *Funisporites* in the original manuscript. However, *Funisporites* was found to be preoccupied after the paper was in press. Although the name has been changed in the text, Tables 2, 3, and 4 had been printed and the name appears as *Funisporites magnus*.

Derivation of name. — *L. Gorgonis* = daughter of Phorcus. Referring to the tangled convolute ornament of the type species.

Description. — Spores radial, trilete; equatorial outline circular to rounded triangular; trilete structure tectate, commonly bordered by large convolutions, contact figure may be ornamented. Equatorial structure present which may be variable in width and is formed by an equatorial extension of an exine fold. Distal side of spore is ornamented with irregular ropelike convolutions that may branch and or short convolution segments that appear as rounded protuberances. The distal ornamentation continues onto the equatorial structure.

Remarks. — The morphology of the equatorial structure in conjunction with the prominent convolute ornament is considered to be diagnostic of this genus. *Simozonotriletes* (Naumova) Potonié and Kremp and *Murospora* Somers are interpreted as having a solid cingulum around a distinct central body. Neither have any extensive ornament developed. *Tendosporites* Hacquebard and Barss has a solid equatorial extension of the exine which tapers to a membranous edge and does not have any prominent ornament. *Cincturasporites* (Hacquebard and Barss) emend Urban (this paper) has a massive, thick bizoned equatorial structure and is unornamented. *Orbisporis* Bharadwaj and Venkatachala has similar characteristics but does not have the equatorial structure of *Gorgonispora.* Species previously assigned to *Murospora* should be examined for assignment to this genus.

Gorgonispora magna (Felix and Burbridge), Urban, comb. new emend.
Pl. 29, figs. 7-12

1967. *Cincturasporites magnus* Felix and Burbridge, Palaeontology, vol. 10, pt. 3, pp. 399,400, pl. 61.
1969. *Cincturasporites intestinalis* Hibbert and Lacey, Palaeontology, vol. 12, pt. 3, pp. 429,430, pl. 81, figs. 1-13; pl. 82, figs. 1-3.

Original description. — Holotype 112x121 m. Cingulum, distinct, laevigate, undulating to give a variable width of 8-12 m. Distal surface with muri 6-12 m. wide, forming irregular convolutions but not reticulate. Rounded protuberances averaging 10 m. in diameter scattered about distal surface. No. discernible wall ornamentation. Laesurae distinct, 35 m. long extending three-fourths distance to body margin, and with ray muri 7.5-10 m. wide [Felix and Burbridge 1967, p. 399.]

Emended description. — Spores radial, trilete, equatorial outline is irregularly circular to rounded triangular; trilete structure tec-

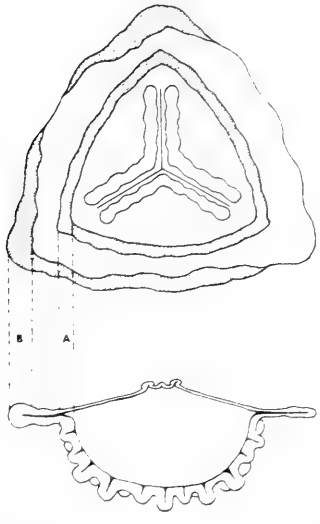

Text-figure 1. — Diagrammetic representation of *Gorgonispora magna*: A. Inner band is an optical representation of the distal wall; B. Outer band is an optical representation of the convolute ornament on the equatorial margin.

tate, consisting of a thin erect ridge over the commissure. Length of commissure ± ¾ the spore radius. The triradiate structure is commonly bordered by large convolutions 7.5-10 microns wide. Interradial contact areas are sometimes ornamented but when present the ornament is considerably reduced in comparison with ornament on the distal side. An equatorial structure is present. The equatorial structure may be variable in width and is formed by a centrifugal extension of an exine fold, that is analagous to an arcuate rim. The distal side of the spore is ornamented with irregular convolutions that occasionally branch. A variable number of short convolution segments may also be present and appear as rounded protuberances. The distal convolutions continue onto the equatorial structure. The undistorted form is a low pyramidal proximal side and a pronounced hemispherical distal side. Orientation preference is proximal-distal and in compressed specimens the distal side tend to compress eccentrically.

Size. — Holotype 112-121 microns. Variation in size 85 to 131 microns; mean size 111 microns; 62 specimens measured.

Types. — Holotype. Slide 03V16-10 (B-1), location 50x111 (Ref. 32.5x117.9) Sun Oil Company Palynology Laboratory. Figured specimens; 147F31-2, 147F31-3, 147F32-1.

Remarks. — There is no discrete central body in this species. The central area is outlined by a point where the proximal and distal exine come in contact. The inner peripheral band of thickening of the equatorial structure (Hibbert and Lacey, 1969), is an optical representation of the edge of the distal wall (text-fig. 1). The outer band is not always present.

Hibbert and Lacey (1969) refer to the equatorial structure as a cingulum. However, the equatorial structure commonly appears dark and infragranular suggesting a separation of the exine layers. The distal convolutions occasionally show a similar condition which suggest they are also formed by folding the exine.

Some minor differences exist with the interpretations of Hibbert and Lacey (1969) but comparison with their illustrations suggest *C. intestinalis* is a junior synonym of *F. magnus.*

Orbisporis convolutus Butterworth and Spinner, 1967 is very similar. *O. convolutus* is described as having a thickened band on the proximal side of the equator and lacking any proximal sculpture. There is no mention of any equatorial structure although the authors propose assignment of the spores to the Infraturma Cingulati which would presuppose a cingulum. Therefore comparison with the holotype description of *O. convolutus* leaves no choice but to consider *G. magna* a separate species. However reexamination of *O. convolutus* may show that *G. magna* is a junior synonym.

Genus **GRANULATISPORITES** Ibrahim, emend. Potonié and Kremp, 1954

Type species, *Granulatisporites granulatus* Ibrahim, 1933.

Granulatisporites granulatus Ibrahim, emend. Potonié and Kremp Pl. 30, figs. 1,2

1933. *Granulatisporites granulatus* Ibrahim, Dissertation. Tech. Hochschule Berlin, Wüzburg, Triltsch, p. 22, pl. 6, fig. 51.
1944. *Granulatisporites granulatus* Ibrahim, Schopf, Wilson, and Bentall, Illinois Geol. Sur., Report of Investigations, No. 91, p. 33.
1954. *Granulatisporites granulatus* Ibrahim, Potonié and Kremp, Geologisches Landestanstalten, Bundesrepublik Deutschlands, Geol. Jahrbuch, vol. 69, p. 58, pl. 12, figs. 157-160.

Granulatisporites microgranifer Ibrahim, 1933 Pl. 30, figs. 3-5

1933. *Granulatisporites microgranifer* Ibrahim, Dissertation. Tech. Hochschule Berlin, Würzburg, Triltsch, p. 22, pl. 5, fig. 32.

1938. *Azonotriletes microgranifer* (Ibrahim), Luber *in* Luber and Waltz, Trans. Cent. Geol. and Prosp. Inst., Fasc. 105, pl. 7, fig. 92.
1955. *Granulatisporites microgranifer* Ibrahim, Potonié and Kremp, Teil I. Palaeontographica, Abt. B, Bd. 98, pl. 12, figs. 149-151.

Granulatisporites tuberculatus Hoffmeister, Staplin, and Malloy, 1955
Pl. 30, figs. 6, 7

1955. *Granulatisporites tuberculatus* Hoffmeister, Staplin, and Malloy, Jour. Paleont., vol. 29, No. 3, p. 389, pl. 36, fig. 12.

Genus **HYMENOSPORA** Neves, 1961

Type species, *Hymenospora palliolata* Neves, 1961.

Hymenospora cf. **H. caperata** Felix and Burbridge, 1967 Pl. 30, figs. 8, 9
1967. *Hymenospora caperata* Felix and Burbridge, Palaeontology, vol. 10, pt. 3, pp. 405,406, pl. 62, fig. 12.

Remarks. — Specimens compare favorably to *H. caperata* except the outer covering is not so thin and membranous as those of the Springer Formation.

Genus **KNOXISPORITES** Potonié and Kremp, emend.
Neves and Playford, 1961

Type species, *Knoxisporites hageni* Potonié and Kremp, 1954.

Knoxisporites stephanephorus Love, 1960
Pl. 30, figs. 10-12; Pl. 31, figs. 1-3

1960. *Knoxisporites stephanephorus,* Love, Roy. Soc. Edinburgh, Proc. vol. 67., Sect. B, pp. 118,119, pl. 2, fig. 1, text fig. 8.

Remarks. — The specimens in the present study compared to the types of this species are quite deceptive in their morphology. The specimens invariably collapse with a proximal-distal orientation. The thickenings between the distal ring and the proximal surface result in the spore body wall between the contact figure and the distal ring being folded out rather than inward. Consequently, compressed specimens appear to have an equatorial "extension" that is an exine fold.

Love (1960, p. 119) compared this species with *K. rotatus* Hoffmeister, Staplin, and Malloy. *K. stephanephorus* differed in having thicker lips and the distal thickening. Felix and Burbridge (1967, p. 395) reported forms showing considerable variation and combinations of the two species which they interpreted as developmental transitions.

Forms studied were not completely in agreement with the

descriptions of either *K. stephanephorus* or *K. rotatus*. The thickened lips of *K. stephanephorus* are not present but the conspicuous distal boss is.

Knoxisporites triradiatus Hoffmeister, Staplin, and Malloy, 1955
Pl. 31, figs. 4-7

1955. *Knoxisporites triradiatus* Hoffmeister, Staplin, and Malloy, Jour. Paleont., vol. 29, p. 391, pl. 37, fig. 12, text fig. 4B.

Knoxisporites sp. Pl. 31, figs. 8, 9

Description. — Spores radial, trilete; equatorial outline is circular. Triradiate ridges locate the tetrad juncture. The ridges are thin at the proximal apex and are approximately 1/3 the radius length. The ridges widen toward the equatorial margin and blend with a proximal extension of the cingulum. The triradiate ridges and cingulum protrusions define pronounced contact figures. The cingulum is thick, 6+ microns in the holotype specimen. The distal side is characterized by a thick ring essentially parallel to the equator with five or six struts extending to the equator (most comconly six). The surface between the struts and inside the distal ring tends to sag inward. The distal ring is only slightly thinner than the cingulum.

The entire surface is laevigate. Definite proximal-distal orientation preference.

Figured specimen. — 147F28-2.

Size. — 55 microns. Variation in size of spore, 41 to 63 microns, mean 58 microns; 18 specimens counted.

Remarks. — These specimens compare most closely to *K. rotatus* Hoffmeister, Staplin, and Malloy. The major difference being the number of struts connecting the distal ring and the cingulum. *K. rotatus* was described as having three while the specimens described here have five or six.

Genus **KOCHISPORITES,** Urban, n. gen.

Type species, *Kochisporites dentatus* Urban, n. sp.

Derivation of name. — Named in honor of Mr. Donald Koch, Geologist, Iowa Geologic Survey.

Description. — Spores radial, trilete; equatorial outline rounded triangular. Triradiate structure is tectate. Commissure is simple

and rays extend to the arcuate rim. Exine is variable in thickness with the distal wall approximately twice as thick as the proximal wall. A dentate arcuate rim is present which may be incised forming lobes. The arcuate rim is best developed in the interradial areas nearest the commissure rays. Least development of the rim is directly at the end of the rays. Ornamentation is present on proximal and distal surfaces, but is reduced in size and density and is much simpler on the proximal side. Types of ornamentation present are spines, flat-topped baculae and baculae with hook-like protrusions at the top.

Remarks. — *Neoraistrickia* has similar type of sculpture but does not have the prominent dentate arcuate rim.

Kochisporites dentatus Urban, n. sp. Pl. 31, figs. 10-12; Pl. 32, figs. 1-5

Derivation of name. — *L. dentatus* = toothed. Referring to the toothed arcuate rim around the equator of the spore.

Description. — Spores radial, trilete; equatorial outline rounded triangular. Triradiate structure is tectate. Commissure is simple and rays extend to the arcuate rim. The commissure is bordered by thickened exine that supports the commissure in a rigid, low pyramidal form. Exine is variable in thickness, proximal wall is ± 2.5 microns and the distal wall is approximately twice the thickness of the proximal. The thinner proximal wall tends to sag inward in the interradial areas. A dentate arcuate rim is present. The arcuate rim is of variable width up to ± 8 microns, but is always a prominent feature. The edge of the rim is most commonly serrate with teeth 1-2 microns high and 1-2 microns broad at the base but any of the distal ornament types may be present. Occasionally the arcuate rim is deeply incised forming an isolated lobe. The arcuate rim exhibits maximum development in the area between the midpoint of the interradial area and the end of the commissure causing the spores to often appear to have prominent auriculae similar to *Tripartites*. The rim is least developed across the apex. Ornamentation is variable in type and density. The proximal surface is ornamented with a few (9-15) narrow (1-2 microns) baculae. The baculae are only slightly irregular on the ends. The distal surface is ornamented with spines, baculae with dentate tops or flat tops and baculae that are widest at the base and have hooklike

protrusions from the top. Ornamentation elements vary in length from 2-8 microns. The undistorted shape is a low pyramidal proximal side and a hemispherical distal side.

Size. — Holotype 60 microns. Variation in size of spore 43 to 67 microns; mean 55 microns; 27 specimens measured.

Types. — Holotype, 147F20-4; paratypes, 147F31-4; 147F21-1.

Type locality. — Brooks Quarry, NE cor. sec. 3 and NW cor. sec. 4, T88N, R9W along side of Highway 20, Buchanan County, Iowa.

Genus **LEIOTRILETES** Naumova, emend. Potonié and Kremp, 1954

Type species, *Leiotriletes sphaerotriangulus* (Loose) Potonié and Kremp, 1954.

Leiotriletes pyramidatus Sullivan, 1964 Pl. 32, fig. 6

1964. *Leiotriletes pyramidatus* Sullivan, Palaeontology, vol. 7, pt. 3, p. 357, pl. 57, fig. 2.

Remarks. — There were no specimens recovered for SEM examination.

Leiotriletes subintortus (Waltz), Ischenko, 1952 Pl. 32, figs. 7-9

1941. *Azonotriletes subintortus* Waltz var. *rotundatus* Waltz *in* Luber and Waltz, Trans. Cent. and Prosp. Inst., Fasc. 105, pp. 13,14, pl. 2, fig. 15b.
1952. *Leiotriletes subintortus* (Waltz), Ischenko var. *rotundatus* Waltz, 1952, Izd. Akad. Nauk. Ukr. S.S.R., Inst. Geol. Nauk., p. 11, pl. 1, fig. 7.

Leiotriletes cf. **L. tumidus** Butterworth and Williams, 1958 Pl. 32, figs. 10-12

1958. *Leiotriletes tumidus* Butterworth and Williams, Roy. Soc. Edinburgh, Trans., vol. 63, pp. 359,360, pl. 1, figs. 5,6.

Leiotriletes angulatus Urban, n. sp. Pl. 33, figs. 1-3

Derivation of name. — *L. angulatus* = angular. Referring to the definite angular form.

Description. — Spores radial, trilete; equatorial outline is triangular with straight to slightly convex edges. Triradiate structure tectate, commissure simple, rays one-half to two-thirds the radius, frequently appear to be bifurcate toward the equatorial margin, the actual suture is at the base of a triradiate ridge formed by an exine fold. The tetrad contact point of the top of the ridge appears rod-like. The exine layers of the ridge separate into an open fold at the corners. The exine of the proximal interradial areas is consider-

ably thinner than the remainder of the spore wall and frequently collapses. Remainder of exine is uniformly ± 1 micron thick.

The proximal interradial areas appear somewhat scabrate, remainder of spore body is laevigate. Definite proximal-distal orientation preference.

Size. — Holotype 46 microns. Variation in size of spore 46 to 67 microns, mean 55 microns; 24 specimens measured.

Types. — Holotype, 147F3-1; paratype, 147F20-5.

Type locality. — Brooks Quarry, NE cor. sec. 3 and NW cor. sec. 2, T88N, R9W along side of Highway 20, Buchanan County, Iowa.

Remarks. — Specimens referred to this species have a characteristic appearance of rigidity and angularity. The most nearly comparable species is believed to be *L. tumidus* Butterworth and Williams, 1958. *L. tumidus* typically has a swollen proximal side. *L. angulatus* occasionally exhibits a similar character but not frequently enough to be diagnostic. Most commonly the proximal is collapsed. *L. tumidus* frequently has prominent ray folds that may not be developed to the same extent of each ray. *L. angulatus* has a precise development of the triradiate ridges and the broadly folded corners.

Leiotriletes labrum Urban, n. sp. Pl. 33, figs. 4-6

Derivation of name. — *L. labrum* = lip. Referring to the thick, stout triradiate structure.

Description. — Spores radial trilete; equatorial outline is consistently triangular with straight sides and smoothly rounded corners. Triradiate structure tectate, commissure simple, rays extend to the equatorial margin, the suture is not apparent at the surface but is obvious in transmitted light. Suture appears to be bordered by prominent, thick lips 4-5 microns wide in transmitted light which is an optical section of the edge of the exine. Contact figure is a rigid triradiate structure which holds the proximal surface into a steep pyramid. Equatorial ends of the triradiate structure blend very smoothly into the equatorial margin. Occasionally the "lips" appear to be thicker at the equatorial margin. Frequently, the spore collapses in the interradial margins parallel to the triradiate structure. Distal exine uniformly 4-5 microns thick. Entire surface is laevigate.

Size. — Holotype 60 microns. Variation in size of spore 43 to 67 microns, mean 55 microns; 16 specimens measured.

Types. — Holotype, 147F2-2; paratype, 147F20-6.

Type locality. — Brooks Quarry, NE cor. sec. 3 and NW cor. sec. 2, T88N, R9W along side of Highway 20, Buchanan County, Iowa.

Remarks. — *L. labrum* appears somewhat similar to *L. ornatus* Ischenko, but has thicker exine and never has the rounded triangular form of the latter.

Leiotriletes sp. Pl. 33, figs. 7, 8

Description. — Spores radial, trilete; equatorial outline triangular with straight sides and rounded corners. Triradiate structure tectate, commissure simple, rays extend to the equatorial margin. Suture appears to be partially bordered by thin lips which are optical sections of upturned exine which usually folds parallel to the suture. The point of contact of the sutures is marked by a thin welt or roll. The exine along the contact figure is rigid enough to maintain straight triradiate folds elevated above the equatorial margin. The proximal interradial areas exhibit pronounced collapsing. Distal exine uniformly 1-2 microns thick. Ornamentation faintly granular to scabrate and visible with oil immersion. Definite proximal-distal orientation preference.

Size. — 41 microns.

Figured specimen. — 147F10-1.

Remarks. — There were not sufficient specimens to justify erecting a new taxon.

Genus **LOPHOTRILETES** Naumova, emend. Potonié and Kremp, 1954

Type species, *Lophotriletes gibbosus* (Ibrahim), Potonié and Kremp, 1954.

Lophotriletes fatihi Artuz, 1957 Pl. 33, figs. 9-12

1957. *Lophotriletes fatihi* Artuz, Istanbul Universite. Fen Fakultesi. Mecmuasi. S. B. Jabii Ilimer. vol. 22, p. 244, pl. 2, fig. 14.

Lophotriletes labiatus Sullivan, 1964 Pl. 34, figs. 1, 2

1964. *Lophotriletes labiatus* Sullivan, Palaeontology, vol. 7, pt. 3, pp. 360,361, pl. 57, fig. 19.

Lophotriletes obtusus Felix and Burbridge, 1967 Pl. 34, figs. 3, 4

1967. *Lophotriletes obtusus* Felix and Burbridge, Palaeontology, vol. 10, pt. 3, pp. 365,366, pl. 55, figs. 5-7.

Genus **LYCOSPORA** Schopf, Wilson and Bentall, 1944

Type species, *L. micropapillata* (Wilson and Coe), Schopf, Wilson, and Bentall, 1944.

Remarks. — Potonié and Kremp (1954) proposed an emendation of *Lycospora.* The emendation replaced the Schopf, Wilson, and Bentall (1944) reference to an equatorial ridge with a cingulum. There does not appear to be any fundamental difference in the two as described. Consequently, the emendation is considered unnecessary.

Lycospora uber (Hoffmeister, Staplin, and Malloy), Staplin, 1960
Pl. 34, figs. 5-12

1955. *Cirratriradites uber* Hoffmeister, Staplin, and Malloy, Jour. Paleont., vol. 29, No. 3, p. 383, pl. 36, fig. 24.
1957. *Cirratriradites uber* Hoffmeister, Staplin, and Malloy, Hacquebard and Barss, Geol. Sur. Canada, Bull. 40, p. 39, pl. 5, fig. 11.
1960. *Lycospora uber* (Hoffmeister, Staplin, and Malloy), Staplin, Palaeontographica Abt. B, Bd. 107, No. 1-3, p. 20, pl. 4, figs. 13, 17, 18, 20.

Description. — Spores radial, trilete; equatorial outline is roundly triangular. Triradiate structure is tectate and commissure is simple. Exine is two-layered. Triradiate ridges formed by a folding of the outer exoexine. The folds are prominent over the central region and are reduced onto the "flange." The ridges are thickened as indicated by their tendency to remain straight and erect. The flange is produced by a thinned fold of outer exoexine and is analogous to an arcuate ridge. A thickened ring of inner exoexine (cingulum) is concentric to the equator of the spore. The outer exoexine is evidently attached to the cingulum as suggested by exine folds not continuing from the central region and onto the "flange." The cingulum is also responsible for the preferential proximal-distal orientation of the forms when flattened. The ornamentation is sparsely to densely granulose on the central proximal region and becomes smooth on the flange. The distal surface is verrucate to slightly vermiculate. The distal ornamentation is much coarser in the central region and often becomes granular outside the cingulum.

Remarks. — Numerous difficulties in taxonomic assignment are inherent in the observed morphology. The ornamentation is different on the proximal and distal surfaces. The ornamentation in both instances is predominantly contained within the central region [? spore body, (Staplin, 1960) central body (Hoffmeister, Staplin,

and Malloy, 1955)]. The flange is an exine fold that thins toward the equator. A thickened "ring" (cingulum or crassitude) is present inside the central region. The "ring" is responsible for the preferential (proximal-distal) orientation of flattened specimens. It is also reponsible for the arcuate folding parallel to the equator. This folding is due to the exine being attached to the "ring," therefore, a flattening of the hemispherical distal side will result in "wrinkles" adjacent to the point of attachment.

Specimens compared to this species demonstrate the problems of inadequate descriptions that are present in palynologic taxonomy today. The holotype description *L. uber* Hoffmeister, Staplin, and Malloy (1955, p. 383) is purely morphographic according to standard practice of the times. A flange is reported as being present, but no diagnosis of the morphology of the flange. The same is true for "the central body." Ornamentation is reported as present on the "central body" and consisting of granules.

Staplin (1960, p. 20) redescribed the species and transferred the species to the genus *Lycospora*. The new description referred to ". . . ; flange variable, smooth to striate, margin tapered to limbate, sometimes faintly zonate, margin entire or unevenly indented; . . ." Mention of a central body is absent and perhaps replaced by reference to spore body. The ornamentation is reported as . . . "slightly roughened to granulose to finely verrucose and microvermiculate; . . ." The intent of the redescription being to demonstrate variability within the species. In addition, the author suggested several possible synonyms and also called attention to the fact that most published descriptions and illustrations are inadequate to show the range of variation.

Genus **MICRORETICULATISPORITES** Knox, emend.

Potonié and Kremp, 1954

Type species, *Microreticulatisporites lacunosus* (Ibrahim), Knox, 1950

Microreticulatisporites concavus Butterworth and Williams, 1958
Pl. 35, figs. 1-4

1958. *Microreticuatisporites concavus* Butterworth and Williams, Roy. Soc. Edinburgh, Trans., vol. 63, p. 367, pl. 1, figs. 55,56.

Remarks. — Variation of shape and ornamentation is believed

to encompass forms assigned to *M. concavus* Butterworth and Williams and *M. densus* (Love), Sullivan.

Cf. Microreticulatisporites punctatus Knox, 1950 Pl. 35, figs. 5-7

1950. *Microreticulatisporites punctatus* Knox, Bot. Soc. Edinburgh, Trans. vol. 33, pt. 3, p. 321.
1958. *Microreticulatisporites punctatus* Knox, Butterworth, and Williams, 1958. Roy. Soc. Edinburgh, Trans., vol. 63, pp. 367,368, (Neotype, pl. 11, figs. 12,13).

Genus **MONOLETES** Ibrahim, emend. Schopf, Wilson, and Bentall, 1944

Type species, *Monoletes ovatus* Schopf, 1936.

Monoletes cf. **M. ovatus** Schopf, 1936 Pl. 35, figs. 8-10

Monoletes ovatus Schopf, 1936, Illinois Acad. Sci., Trans., vol. 28, No. 2, p. 176.

Remarks. — The holotype has been described as having two longitudinal grooves. Comparable specimens of this investigation appear (in transmitted light) to have the two longitudinal grooves, but the scanning electron micrograph shows that the two longitudinal "grooves" are actually fold edges that border on a single wide groove that extends the entire length of the "spore."

Monoletes winslowi Urban, n. sp. Pl. 35, figs. 11, 12; Pl. 36, figs. 1-3

Derivation of name. — In honor of Mrs. Marcia Winslow, particularly for her contribution to an understanding of this genus.

Description. — Bilateral, monolete; outline circular to oval; monolete suture medially deflected, tectate, ray length is one-half the spore-body length. Lips adjacent to the suture two to three microns in width. Spore body enveloped in a cavate membrane that is attached to the proximal and distal surfaces but is free around the equator. The membrane often makes prominent ridges along the suture. The central body wall is ± 2.5 microns thick and laevigate. The enclosing membrane is thin (less than 1 micron) and infragranular.

Size. — Holotype 109 microns, central body 65 microns. Variation in size 91 to 124 microns; mean 106 microns; 29 specimens studied.

Types. — Holotype, 147F38-1; paratype, 147F36A-1.

Type locality. — Brooks Quarry, NE cor. sec. 3 and NW cor. sec. 2, T88N, R9W along side of Highway 20, Buchanan County, Iowa.

Remarks. — This species is identical to *Monoletes* sp. reported from the Springer Formation by Felix and Burbridge, (1967). They agreed with Winslow's (1959) suggestion that they may be "sports" referable to *M. ovatus*. However, the prominent extension of the exoexine and the lack of the distal groove is fundamentally quite different from *M. ovatus*.

Genus **MOOREISPORITES** Neves, 1958

Type species, *Mooreisporites fustus* Neves, 1958.

Mooreisporites fustus Neves, 1958 Pl. 36, figs. 4-6

1958. *Mooreisporites fustus* Neves, Geol. Mag. vol. 90, No. 1, p. 7, pl. 1, figs. 1,2, text fig. 2.

Mooreisporites bicornis Urban, n. sp. Pl. 36, figs. 7-11

Derivation of name. — *L. bicornis* = two-horned. Referring to the paired baculae on the proximal side below the auriculae.

Description. — Spores radial, trilete; equatorial outline is triangular with markedly concave sides. Triradiate structure is tectate, commissure is simple and rays are approximately ½ the length of the spore radius. Exine appears to be a single layer and uniformly thin (1-2 microns) except at the apices. The exine becomes thickened at the corners forming auriculae which become divided into baculate processes. Auriculae are six to eight times the thickness of the remainder of the exine and are arched distally (open to distal side). Two clavate processes occur on opposite sides of the proximal-equatorial surface approximately 2/3 the distance from the proximal pole to the ends of the auriculae. Frequently an additional clavate process occurs near the center of the interradial-equatorial region. The clavate processes are typically flat-topped and partate. Remainder of exine is laevigate.

The shape of the proximal side of the spore is gently pyramidal and the distal side is steeply pyramidal.

Size. — Holotype 46 microns measured along the longest arm from the interrradial margin to the tip of the auriculum. Variation in size of spore 42 to 51 microns; mean 47 microns; 28 specimens measured.

Types. — Holotype, 147F32-2; paratype, 147F25-1.

Type locality. — Brooks Quarry, NE cor. sec. 3 and NW cor.

sec. 2, T88N, R9W along side of Highway 20, Buchanan County, Iowa.

Remarks. — The two clavate processes specifically located on the proximal-equatorial margin readily distinguish this species from any previously described. *M. fustus* may have processes scattered on the surface but characteristically has prominent distal processes.

Genus **MUROSPORA** Somers, 1952

Type species, *Murospora kosankei* Somers, 1952.

Cf. Murospora sp. Pl. 36, fig. 12; Pl. 37, figs. 1, 2

Description. — Spores radial, trilete; equatorial outline is irregularly rounded triangular. Triradiate structure is tectate, consisting of a thin elevated ridge above a commissure. The triradiate ridges and commissures are confined to the central body and terminate against rounded protuberances ± 5 microns in diameter. The interradial areas are ornamented with smaller, less prominent protuberances. The central body radius is ± ½ the total spore diameter. The outline is definitely triangular with slightly convex sides and pointed apices. The cingulum extends beyond the interradial areas as a flat shelf for ± ½ its width and the outer half is irregularly thickened around the periphery. The distal surface is ornamented with rounded protuberances up to 10 microns in diameter. The distal part of the spore is located beneath the central area but the ornament may extend onto the cingulum. Wall is ± 5 microns thick.

Size. — 62-68 microns.

Figured specimens. — 147F22-1; 147F38-2.

Remarks. — These fossils compared to *Murospora* are believed to represent the capsulate condition referred to by Staplin (1960). They appear somewhat like *M. aurita* (Waltz) Playford but do not have the prominent lips. They also have distal ornament not reported for *M. aurita*.

Genus **NEORAISTRICKIA** Potonié, 1956

Type species, *Neoraistrickia truncatus* (Cookson), Poton'é, 1956.

Neoraistrickia variornamenta Urban, n. sp. Pl. 37, figs. 3-6

Derivation of name. — *L. varius* = diverse; *L. ornamentum* = ornament. Referring to the variation of ornament type on each specimen.

Description. — Spores radial, trilete; equatorial outline triangular with rounded corners and concave sides. Triradiate structure is tectate, commissure rays are simple and extend to or almost to the equatorial margin. Ornamentation is varied, consisting of rounded coni, elongate baculae, short, squat baculae and occasional digitate elements. The ornamentation is reduced or absent adjacent to the trilete mark and is reduced on the remainder of the proximal surface but exhibits all the variety of forms. Maximum development of the ornamentation occurs on the distal surface where the baculae may be ± 6 microns high and ± 6 microns wide. Exine is uniformly ± 2 microns thick.

Size. — Holotype 46 microns exclusive of ornament. Variation in size of spore 41-65 microns; mean 49 microns; 27 specimens measured.

Types. — Holotype, 147F32-3; paratype, 147F22-2.

Type locality. — Brooks Quarry, NE cor. sec. 3 and NW cor. sec. 2, T88N, R9W along side of Highway 20, Buchanan County, Iowa.

Remarks. — *Neoraistrickia inconstans* Neves, 1961, has a variety of ornament similar to this species but the ornament is less dense. *N. variornamenta* Urban, n. sp. has ornament distribution patterns not present in *Neoraistrickia inconstans.*

Neoraistrickia drybrookensis Sullivan, 1964 has larger ornament that is more widely distributed.

Genus **POTONIESPORITES,** Bharadwaj, 1954

Type species, *Potoniesporites novicus* Bharadwaj, 1954.

Potonieisporites elegans (Wilson and Kosanke), Wilson and Venkatachala, 1964 — Pl. 37, figs. 7, 8

1944. *Florinites elegans* Wilson and Kosanke, Iowa Acad. Sci., vol. 51, p. 330, fig. 3.
1964. *Potonieisporites elegans* (Wilson and Kosanke), Wilson and Venkatachala, pp. 67,68, figs. 1,2.

Genus **PROCORONASPORA** (Butterworth and Williams) emend. Smith and Butterworth, 1967

Type species, *Procoronaspora ambigua* Butterworth and Williams, 1958.

Procoronaspora fasciculata Love, 1960 — Pl. 37, figs. 9-11

1960. *Procoronaspora fasciculata* Love, Roy. Soc. Edinburgh, Proc., vol. 67, Sect. B, pp. 112,113, pl. 1, fig. 2, text fig. 2.
1966. *Non Tricidarisporites fasciculatus* (Love), Sullivan and Marshall, Micropaleontology, vol. 12, No. 3, pp. 268,269, pl. 1, fig. 16.

Remarks. — Sullivan and Marshall (1966) transferred *P. fasciculata* to the genus *Tricidarisporites* but gave no reason for the transfer. The original diagnosis of Butterworth and Williams (1958) and the emendation of Smith and Butterworth (1967) will identify this species.

Genus **PROPRISPORITES** Neves, 1958

Type species, *Proprisporites rugosus* Neves, 1958.

Proprisporites cf. **P. laevigatus** Neves, 1961 Pl. 37, fig. 12

1961. *Proprisporites laevigatus* Neves, Palaeontology, vol. 4, pp. 269,270, pl. 33, figs. 9,10.

Remarks. — The figured specimen was lost after examination with the SEM and consequently could not be photographed with transmitted light.

Genus **PUNCTATISPORITES** Ibrahim, emend. Potonié and Kremp, 1954

Type species, *Punctatisporites punctatus* (Ibrahim), Potonié and Kremp, 1954.

Punctatisporites heterofiliferus Felix and Burbridge, 1967 Pl. 38, figs. 1-3

1967. *Punctatisporites heterofiliferus* Felix and Burbridge, Palaeontology, vol. 10, pt. 3, pp. 356,357, pl. 53, figs. 10,11.

Punctatisporites incomptus Felix and Burbridge, 1967 Pl. 38, figs. 7, 8

1967. *Punctatisporites incomptus* Felix and Burbridge, Palaeontology, vol. 10, pt. 3, p. 357, pl. 53, fig. 12.

Remarks. — The "lips" originally described for this species are actually optical sections of the exine. Collapse of the interradial contact areas results in prominent folds which widen as they approach the equatorial margin. The bifurcating suture is an optical illusion relating to the manner in which the triradiate folds merge into the equatorial margin.

Punctatisporites cf. **P. obesus** (Loose), Potonié and Kremp, 1955 Pl. 38, figs. 4-6

1932. *Sporonites obesus* Loose, *in* Potonié, Ibrahim, and Loose, N. Jahrb. f. Min., Geol., Paläont., Beilage-Band, Abt. B, vol. 67, p. 451, pl. 19, fig. 49.
1934. *Laevigatisporites obesus* Loose, Inst. Paläobot. u. Petrog. d. Brennsteine Arb., vol. 4, No. 3, p. 145.
1944. *Calamospora* (?) *obesus* (Loose), Schopf, Wilson, and Bentall, Illinois Geol. Sur., Report of Investigations No. 91, p. 52.
1955. *Punctatisporites obesus* (Loose), Potonié and Kremp, Paläontographica, Abt. B, Bd. 98, No. 1-3, p. 43, pl. 11, fig. 124.
1967. *Punctatisporites obesus* (Loose), Potonié and Kremp, Smith and Butterworth, Special Paper Palaeontology, No. 1, pp. 127, 128, pl. 1, fig. 23.

Description. — Spores radial, trilete; outline roundly triangular to circular. Triradiate structure tectate, commissure rays are approximately ½ the radius of the spore. The commissure is situated on large folds which extend to the equatorial margin and result in the rays appearing to bifurcate toward the interradial areas near the arcuate rim. The exine of the proximal interradial areas is thinner than the remainder of the spore and sags causing the triradiate folds to appear as thick lips adjacent to the commissure. Distal exine ± 5 microns thick, finely punctuate in the contact areas, laevigate on the remainder of the spore. Proximal-distal orientation preference.

Size. — Variation in size of spore, 71 to 96 microns; mean 91 microns; 27 specimens measured.

Remarks. — These fossils are consistent in having folds along the triradiate mark and compare very favorably with the specimen figured by Smith and Butterworth (1967) as *P. obesus*. The type specimen figured by Potonié and Kremp (1955) appears to be more inflated overall and has no orientation preference.

Punctatisporites planus Hacquebard, 1957 Pl. 38, figs. 9-10

1957. *Punctatisporites planus* Hacquebard, Micropaleontology, vol. 3, No. 4, p. 308, pl. 1, fig. 12.

Punctatisporites validus Felix and Burbridge, 1967 Pl. 38, figs. 11-12

1967. *Punctatisporites validus* Felix and Burbridge, Palaeontology, vol. 10, pt. 3, p. 359, pl. 34, fig. 2.

Remarks. — Felix and Burbridge (1967, p. 359) referred to a difference in length of the "sutural opening and the lips as well as the fact that they do not always overlie each other." Examination of the type and comparison with specimens (believed to be conspecific) encountered in this study indicate that the "lips" might be more properly thought of as a ridge formed by an exine fold. The exine layers of the ridge are united throughout the length corresponding to the "sutural opening" or the tetrad scar. Beyond the extremities of the tetrad scar the layers become separated but the fold continues to the equator. In flattened specimens the ridge becomes flattened along its entirety, therefore, it is displaced with regard to lower point of contact of the layers which is what appears optically to be a "sutural opening."

Genus **RAISTRICKIA** Schopf, Wilson, and Bentall, 1944

Type species, *Raistrickia grovensis* Schopf *in* Schopf, Wilson, and Bentall, 1944.

Raistrickia cf. **R. saetosa** (Loose), Schopf, Wilson, and Bentall, 1944
Pl. 39, figs. 1, 2

1932. *Sporonites saetosus* Loose *in* Potonié, Ibrahim, and Loose, N. Jahrb. f. Min., Geol. Paläont., Beilage-Band, Abt. B, vol. 67, p. 452, pl. 19, fig. 56.
1933. *Setosi-sporites saetosus* (Loose), Ibrahim, Dissertation, Tech. Hochschule Berlin, Würzberg, Triltsch, p. 26.
1944. *Raistricka saetosus* (Loose), Schopf, Wilson, and Bentall, Illinois Geol. Sur., Report of Investigations, No. 91, p. 56.
1967. *Raistrickia saetosa* (Loose), Schopf, Wilson, and Bentall, Smith and Butterworth, Special Paper Paleontology, No. 1, pp. 181, 182, pl. 8, fig. 21.

Raistrickia densa Urban, n. sp. Pl. 39, figs. 3-8

Derivation of name. — *L. densa* = thick, stout, dense. Referring to the relatively thick wall, and stout ornament of the species.

Description. — Spores radial, trilete; roundly triangular to circular. Triradiate structure is tectate. Commissure is simple and ray length is equal to the spore radius. Exine is variable in thickness among different specimens and frequently showing some variation in a single specimen. Maximum thickness observed was four microns on the distal side of a specimen. The spores are ornamented with numerous crested or partate bacula. A variety of forms of bacula are present. Some bacula are widest at the base and narrow toward the top, some have parallel sides throughout their length, others have approximately equal widths at the base and top with a constriction approximately at mid-length, but the most common form is a baculum expanded toward the top. Some specimens show an exceptionally wide baculum that is evidently a result of two or more bacula being joined. All baculae are crested with minute apiculae. The length and width of bacula as well as length/width ratio is extremely variable. Maximum length observed was 9.5 microns, maximum width 14.5 microns, length/width ratios 2.5/1 to 3/5. The bacula are absent or essentially so on the contact area while the maximum development occurs on the distal surface. The undistorted shape was a low pyramidal proximal surface and a hemispherical distal surface.

Size. — Holotype 36 microns. Variation in size of spore 30 to 41

microns exclusive of processses; mean 34.2 microns; 41 specimens measured.

Types. — Holotype, 147F27-1; paratypes, 147F29-1, 147F33-1.

Type locality. — Brooks Quarry, NE cor. sec. 3 and NW cor. sec. 2, T88N, R9W along side of Highway 20, Buchanan County, Iowa.

Remarks. — The lack of ornamentation of the proximal surface, the marked increase in size of bacula on the distal surface and the tendency for many individuals to be rounded triangular in shape distinguish this species of *Raistrickia.*

Genus **REINSCHOSPORA** Schopf, Wilson, and Bentall, 1944

Type species, *Reinschospora speciosa* (Loose), Schopf, Wilson, and Bentall syn. *R. bellitas* Bentall, 1944.

Reinschospora cf. **R. speciosa** (Loose), Schopf, Wilson, and Bentall, 1944
Pl. 39, figs. 9-12; Pl. 40, figs. 10-12

1934. *Alati-sporites speciosus* Loose, Inst. Paläobot. u. Petrog. d. Brennsteine, Arb., vol. 4, No. 3, p. 151, pl. 7, fig. 1.
1938. *Non Zonotriletes speciosus* (Loose), Waltz *in* Luber and Waltz, Trans. Cent. Geol. and Prosp. Inst., Fasc. 105, pl. 4, fig. 48; pl. 5, fig. 9.
1944. *Reinschospora bellitas* Bentall *in* Schopf, Wilson, and Bentall, Illinois, Geol. Sur., Report of Investigations, No. 91, p. 53, fig. 2.

Remarks. — Specimens compared to *R. speciosa* appear very similar to the forms previously illustrated by various investigators as representing the species. However, there are some differences that should be considered. Descriptions of the species commonly refer to the corona being composed of setae and attached to the spore body just proximally of the equator. The "corona" or "flange" is actually a continuation of the outer layer (exoexine) which totally encompasses a triangular spore body.

In addition, specimens studied have an exine ornament which is different than the holotype description. Ornament is very finely scabrate to granular and may appear punctate in transmitted light. Felix and Burbridge (1967) reported the Springer specimens were minutely punctate. The Springer specimens were examined and they appear to be identical with those in this study.

Genus **RETICULATISPORITES** Ibrahim, emend Potonié and Kremp, 1954

Type species, *Reticulatisporites reticulatus,* Ibrahim, 1933.

Remarks. — Neves (1964) proposed an emendation of *Reticulatisporites* in which he maintained the holotype, *R. reticulatus,* is

cingulate. This emendation was based on an examination of photographs of the holotype. The muri were interpreted as ". . . restricted almost entirely to the distal hemisphere. Occasional reduced muri pass onto the proximal face, but for the large part, terminate by fusion with the equatorially placed cingulum . . ." He also stated, "the persistence of the equatorial extension of the exine is a striking feature of the specimen which cannot be reconciled with «chance» compression of muri of the distal reticulum in the equatorial plane . . ." Smith and Butterworth (1967) supported this emendation. However, their photomicrograph (pl. 14, fig. 15) illustrated morphologic features that are similar to those noted in this study and must be considered before this emendation is accepted.

Examination of reticulate spores with the SEM demonstrates a tendency for ornamentation to be missing or greatly reduced on the proximal surface. This is consistent with observations of other spore groups as previously discussed in this paper. The SEM examination suggests that the "distal" muri of many reticulate species is morphologically identical to the "equatorial structure." The photograph of Smith and Butterworth (1967) suggests that is true in *R. reticulatus*. The above information is interpreted as indicating the "equatorial structure" is muri along the periphery of the contact faces and is simply part of the ornamentation.

The concept of what constitutes a cingulum commonly relates to *Densosporites* in which the cingulum is a discrete equatorial structure. Another concept of cingulum is suggested by Couper (1958, p. 102) and Couper and Grebe (1961, p. 5) that the cingulum is a structure confined to the equator. Consequently, it appears that *R. reticulatus* does not possess a cingulum or any specific equatorial structure.

Reticulatisporites danzei Agrali, Urban, comb. new emend. Pl. 40, figs. 1-6

1965. *Knoxisporites danzei* Agrali *in* Agrali, Akyol, Konyali, Corsin, and Laveine, Société Géologique du Nord, Annales, Tome LXXV, p. 174, pl. 15, fig. 22.

Description. — Spores radial trilete; outline circular to polygonal. Triradiate structure tectate; commissure rays are simple and ray length is equal to spore body radius; triradiate ridges are commonly well developed over the commissure. The ridges when present

will be lowest at the center of the trilete mark and increase in height outward where they fuse with the muri surrounding the contact faces. Occasionally low muri extend onto the proximal face of some individuals while others are devoid of any triradiate ridges or muri. The distal side of the spore is covered with muri enclosing polygonal lumina. The muri are thickest at the top and thinnest between the top and the base. Height of the muri is consistent on an individual (as much as 10 microns observed) but varies among different individuals. The center of the lacunae are most commonly ornamented with grana, pustules, coni, and clavae. The clavate condition is most common with the clavae being variable in height (two microns maximum observed).

The proximal interradial areas are only ornamented if the triradiate ridges are developed. Occasionally, some lumina are unornamented while in others the ornament may consist of grana only. The undistorted shape is a low pyramidal proximal side and a hemispherical distal side.

Remarks. — These specimens compare closely with those of Agrali (1965) except he reported the "equatorial" muri to be higher than those on the distal. He also described the sculpture in the lumina as occurring on the distal side only. This latter condition is most common among individuals of this study but is not the only manner in which the ornament occurs. Neville (1968) described *Dictyotriletes equigranulatus* from the Visean of Scotland. The fossils of this investigation show considerable overlap between the two species and are probably related.

Reticulatisporites peltatus Playford, 1962 Pl. 40, figs. 7-9

1962. *Reticulatisporites peltatus* Playford, Part I. Palaeontology, vol. 5, pt. 3, pp. 599, 600, pl. 84, figs. 1-4.

Genus **SAVITRISPORITES** Bhardwaj, 1955

Type species, *Savitrisporites triangulus* Bhardwaj, 1955.

Savitrisporites nux (Butterworth and Williams), Smith and Butterworth, 1967 Pl. 41, figs. 1-5

1958. *Callisporites nux* Butterworth and Williams, Roy. Soc. Edinburgh, Trans., vol. 63, p. 377, pl. 3, figs. 24, 25.
1964. *Savitrisporites nux* (Butterworth and Williams), Sullivan, Palaeontology, vol. 7, pt. 3 pp. 373, 374, pl. 60, figs. 1-5.
1967. *Savitrisporites nux* (Butterworth and Williams), Smith and Butterworth, 1967, Special Paper Palaeontology, No. 1, pp. 223, 224 (lectotype, pl. 15, figs. 1,2).

Remarks. — Sullivan (1964) illustrated several variations of *S. nux*. He also described the species as having no proximal ornament. Smith and Butterworth (1967) reported the holotype missing and designated a lectotype. They described proximal ornament consisting of a low band of thickening on either side of each commissure.

Specimens of this study compare closely to the published descriptions and illustrations but exhibit considerable variation in the proximal ornament as well. However, the proximal ornament is always more reduced than that on the distal surface and is difficult to observe with transmitted light.

Genus **SCHULZOSPORA** Kosanke, 1950

Type species, *Schulzospora rara* Kosanke, 1950.

Schulzospora elongata Hoffmeister, Staplin, and Malloy, 1955
Pl. 41, figs. 6, 9

1955. *Schulzospora elongata* Hoffmeister, Staplin, and Malloy, Jour. Paleont. vol. 29, No. 3, p. 396, pl. 39, fig. 2.

Genus **SECARISPORITES** Neves, 1961

Type species, *Secarisporites lobatus* Neves, 1961.

Secarisporites remotus Neves, 1961 Pl. 41, figs. 7, 8, 10

1961. *Secarisporites remotus* Neves, Palaeontology, vol. 4, p. 262, pl. 32, figs. 8,9.

Genus **SIMOZONOTRILETES** Naumova, emend. Potonié and Kremp, 1954

Type species, *Simozonotriletes intortus* (Waltz), Potonié and Kremp, 1954.

Remarks. — The work of Smith and Butterworth (1967) in retaining the genus *Simozonotriletes* is accepted. Staplin (1960) referred to a single genus (*Murospora*) containing patellate and capsulate forms. He also expressed the opinion that the forms originally assigned to *Murospora* are capsulate. The difference between patellate and capsulate is considered to be significant enough for generic distinction. Consequently, *Simozonotriletes* is retained until the genus *Murospora* can be more thoroughly studied.

Simozonotriletes intortus (Waltz), Potonié and Kremp, 1954
Pl. 41, figs. 11, 12; Pl. 42, fig. 1

1938. *Zonotriletes intortus* Waltz, *in* Luber and Waltz, Tr. All-Union Geol. Sci. Res. Inst. (U.S.E.G.E.I.), vol. 139, p. 22, pl. 2, fig. 24.
1954. *Simozonotriletes intortus* (Waltz), Potonié and Kremp, Geologisches Landesanstalten, Bundesrepublik Deutschlands, Geol., Jahrbuch, vol. 69, p. 159.

1962a. *Murospora intorta* (Waltz), Playford, Part 1. Palaeontology, vol. 5, pt. 3, p. 609, pl. 86, figs. 12, 13.
1967. *Simozonotriletes intortus* (Waltz), Potonié and Kremp, Smith and Butterworth, Special Paper Palaeontology, No. 1, pp. 237, 238, pl. 15, figs. 18-23.

Remarks. — Staplin (1960) described specimens compared to this species from the Golata Formation of Alberta, Canada, as having a distal patella or being "acorn like." He also examined fossils identified as *Simozonotriletes intortus* by Hacquebard and Barss (1957) and stated that they had a similar structure.

Playford (1962a) described a species of *Murospora, M. dupla* (Ischenko), as having a cingulum with two zones separated by a groove. Playford (1962a) also described *M. sublobata* (Waltz) as having a cingulum that exhibits thickening around the spore apices.

The fossils compared to *Simozonotriletes intortus* definitely exhibit an "acorn like" structure. However, in transmitted light they exhibit an outer and inner zone that are separated by a groove. The inner zone represents an optical section of the inner spore body. The ?cingulum does show some thickening about the apices. Consequently, these spores exhibit morphology that can be related to several described taxa. The variations of these spores are consistent with the findings of Sullivan (1958) and others.

Genus **STENOZONOTRILETES** Naumova, emend. Potonié, 1958

Type species, *Stenozonotriletes conformis* Naumova, 1953.

Stenozonotriletes lycosporoides (Butterworth and Williams), Smith and Butterworth, 1967 Pl. 42, figs. 2-6

1958. *Anulatisporites lycosporoides* Butterworth and Williams, Roy. Soc. Edinburgh, Trans., vol. 63, p. 378, pl. 3, figs. 28,29.
1967. *Stenozonotriletes lycosporoides* (Butterworth and Williams), Smith and Butterworth, Special Paper Palaeontology, No. 1, p. 218, pl. 14, figs. 5, 6.

Genus **TANTILLUS** Felix and Burbridge, 1967

Type species, *Tantillus triquetrus* Felix and Burbridge, 1967.

Tantillus triquetrus Felix and Burbridge, 1967 Pl. 42, figs. 7, 8

1967. *Tantillus triquetrus* Felix and Burbridge, Palaeontology, vol. 10, pt. 3, p. 383, figs. 4, 5.

Genus **TRIMONTISPORITES** Urban, n. gen.

Type species. — *Trimontisporites granulatus* Urban, n. sp.
Derivation of name. — *L. tri* = three, *montis* = ridge. Referring

to the prominent triradiate ridges and proximal exine rolls that terminate the ridges.

Description. — Spores radial, trilete; equatorial outline roundly triangular to circular. Triradiate structure is tectate, commissure rays are short and lie beneath prominent exine folds or ridges. The triradiate ridges terminate against exine folds involving all layers. The large folds extend to the equatorial margin and are open to the interior of the spore body. Ornamentation is varied, laevigate, granulate to rugulate.

Remarks. — The tectate condition is common among spores, but the condition where the triradiate ridges terminate against the prominent open folds does not appear to be. Since all the diagnostic characters of the genus are haptotypic, it would appear to be well founded. The separation of species on the basis of ornamentation may ultimately prove too broad and a later reappraisal may be necessary. *Iugisporis* Bhardwaj has labra forming rays not reaching the equator and is apiculate. *Iugisporis* does not have the prominent open folds terminating the triradiate ridges. The following species are believed to be more properly assigned to *Trimontisporites*:

Trimontisporites divaricatus (Felix and Burbridge), Urban comb. new

1967. *Punctatisporites divaricatus* Felix and Burbridge, Palaeontology, vol. 10, pt. 3, p. 355, pl. 53, fig. 8.

Trimontisporites flexuosus (Felix and Burbridge), Urban comb. new

1967. *Punctatisporites flexuosus* Felix and Burbridge, Palaeontology, vol. 10, pt. 3, p. 356, pl. 53, fig. 9.

Trimontisporites trifidus (Felix and Burbridge), Urban comb. new

1967. *Punctatisporites trifidus* Felix and Burbridge, Palaeontology, vol. 10, pt. 3, p. 358, pl. 53, fig. 15.

Trimontisporites triarcuatus (Staplin), Urban comb. new

1960. *Cyclogranisporites triarcuatus* Staplin, Palaeontographica, Abt. B, Bd. 107, No. 1-3, p. 10, pl. 1, fig. 30.

Trimontisporites granulatus Urban, n. sp.
Pl. 42, figs. 9-12; Pl. 43, figs. 1-4

Derivation of name. — *L. granulata* = granular. Referring to the granular ornamentation of the exine.

Description. — Spores radial, trilete; equatorial outline roundly triangular to circular. Triradiate structure is tectate, consisting of

commissure with individual ray length ± ½ the radius of the spore. Rays of the commissure beneath thin exoexine folds which form ridges which stand two to four microns high. The thin ridges terminate abruptly against large folds involving all exine layers and open to the interior. The large folds continue to the equatorial margin. In transmitted light, the commissure rays appear to bifurcate at the point of juncture of the thin ridge and large fold, but the "bifurcation" is an optical illusion due to the folds being open to the interior of the spore. Ornamentation is uniformly and densely granular on the proximal and distal surfaces. Ornament is present on the triradiate ridges. Exine uniformly 4.5 microns thick in the holotype. Thickness varies with size, smaller forms are thinner and larger, thicker. Definite proximal-distal orientation preference. Noncompressed forms tend to be roundly triangular, compressed forms are circular.

Size. — Holotype 70 microns. Variation in size of spore 53 to 70 microns, mean 66 microns; 27 specimens measured.

Types. — Holotype, 147F21-2; paratype, 147F29-2, 147F31-5.

Type locality. — Brooks Quarry, NE cor. sec. 3 and NM cor. sec. 2, T88N, R9W along side of Highway 20, Buchanan County, Iowa.

Remarks. — *T. granulatus* is distinguished from *T. rugosus* by ornamentation differences plus a more abrupt change from the triradiate ridge to the terminal folds.

Trimontisporites contortus Urban, n. sp. Pl. 43, figs. 5-8

Derivation of name. — *L. contortus* = twist, contort. Referring to the varied configuration of the arcuate rim.

Description. — Spores radial, trilete; outline roundly triangular to subcircular. Triradiate structure is tectate, consisting of a commissure with individual ray lengths of 1/3 to 1/2 the radius of the spore. Rays of the commissure lie beneath relatively thick exoexine folds which form ridges approximately two microns high. The triradiate ridges enlarge beyond the apex of the commissure rays into prominent wide folds, ± 10 microns wide, which are open to the interior. In uncompressed specimens, the folds are seen to be continuous with the radial margin of the contact figure. In compressed forms, the folds widen slightly toward the equator. In trans-

mitted light, the commissure rays appear to bifurcate at the point of juncture of the triradiate ridge and the fold. Exine laevigate, occasionally scabrate in the contact areas, ± 4 microns thick on the distal side of the spore, the contact areas are thinner and commonly sag. The region of the arcuate rim is somewhat thicker than the distal exine. In proximal-distal compressions, this appears as thicker exine along the equatorial margin. Undistorted shape is a steeply pyramidal proximal surface and a hemispherical distal surface.

Size. — Holotype 53 microns. Variation in size of spore 47 to 61 microns, mean 52 microns; 19 specimens measured.

Types. — Holotype, 147F3-1; paratype, 147F20-7.

Type locality. — Brooks Quarry, NE cor. sec. 3 and NW cor. sec. 2, T88N, R9W alongside of Highway 20, Buchanan County, Iowa.

Trimontisporites rugosus Urban, n. sp. Pl. 43, figs. 9-12

Derivation of name. — *L. rugosus* = wrinkled. Referring to the ornamentation of the exine.

Description. — Spores radial, trilete; outline roundly triangular to circular; triradiate structure is tectate, consisting of commissure with individual ray length ± ½ the radius of the spore. Rays of the commissure lie beneath relatively thick exoexine folds which form ridges approximately 2 microns high. The triradiate ridges gradually enlarge beyond the apex of the commissure rays into prominent wide folds that are open to the interior of the spore. The large folds continue to the equatorial margin. In transmitted light the commissure rays appear to bifurcate at the point of juncture of the thin ridge and large fold, but the bifurcation is an optical illusion. Ornamentation is uniformly and densely rugulate on the proximal and distal surfaces. The rugae form a regular reticulo-punctate pattern. Exine is uniformly 2.5 microns thick in the holotype. There is a tendency for a proximal-distal orientation preference.

Size. — Holotype, 36 microns. Variation in size of spore 34 to 46 microns, mean 41 microns; 21 specimens measured.

Types. — Holotype, 147F27-2; paratype, 147F30-1.

Type locality. — Brooks Quarry, NE cor. sec. 3 and NW cor. sec. 2, T88N, R9W along side of Highway 20, Buchanan County, Iowa.

Genus **TRIQUITRITES** Wilson and Coe, 1940

Type species, *Triquitrites arculatus* Wilson and Coe, 1940.

Triquitrites tribullatus (Ibrahim), Schopf, Wilson, and Bentall, 1944
Pl. 44, figs. 1, 2

1932. *Sporonites tribullatus* Ibrahim *in* Potonié, Ibrahim, and Loose, N. Jahrb. f. Min., Geol., Paläont., Beilage-Band, Abt. B, vol. 67, p. 448, pl. 15, fig. 13.
1933. *Laevigati-sporites tribullatus* (Ibrahim), Ibrahim, Dissertation, Tech. Hochschule Berlin, Würzberg, Triltsch, pp. 20, 21, pl. 2, fig. 13.
1934. *Valvisi-sporites tribullatus* (Ibrahim), Loose, Inst. Palaobot. Arb. vol. 4, No. 3, p. 152, pl. 7, fig. 21.
1944. *Triquitrites tribullatus* (Ibrahim) Schopf, Wilson, and Bentall, Illinois Geol. Sur. Report of Investigations No. 91, p. 47.

Genus **VERRUCOSISPORITES** Ibrahim, emend. Potonié and Kremp, 1954

Type species, *Verrucosisporites verrucosus* (Ibrahim), Ibrahim, 1933.

Verrucosisporites cerosus (Hoffmeister, Staplin, and Malloy), Butterworth and Williams, 1958 Pl. 44, figs. 4-6

1955. *Punctati-sporites? cerosus* Hoffmeister, Staplin, and Malloy, Jour. Paleont., vol. 29, No. 3, p. 392, pl. 36, fig. 6.
1958. *Verrucosisporites cerosus* (Hoffmeister, Staplin, and Malloy), Butterworth and Williams, Roy. Soc. Edinburgh, Trans., vol. 63, p. 361, pl. 1, figs. 42-43.

Verrucosisporites morulatus (Knox), Smith and Butterworth, 1967
Pl. 45, figs. 1, 2

1950. *Verrucoso-sporites morulatus* Knox, Bot. Soc. Edinburgh, Trans., vol. 33, pt. 3, p. 318, pl. 17, fig. 235.
1955. *Verrucosisporites morulatus* (Knox), Potonié and Kremp, Teil I. Palaeontographica, Abt. B, Bd. 98, No. 1-3, p. 65.
1967. *Verrucosisporites morulatus* (Knox), Smith and Butterworth, Special Paper Palaeontology, No. 1, p. 152, (lectotype, pl. 5, fig. 15).

Verrucosisporites scoticus Sullivan, 1968 Pl. 44, figs. 7-9

1968. *Verrucosisporites scoticus* Sullivan, Palaeontology, vol. 11, pt. 1, p. 121, pl. 25, fig. 11.

Genus **VESTISPORA** Wilson and Hoffmeister, emend. Wilson and Venkatachala, 1963

Type species, *Vestispora profunda* Wilson and Hoffmeister, 1956.

Vestispora lucida (Butterworth and Williams), Potonié, 1960
Pl. 44, figs. 3, 10-12

1958. *Glomospora lucida* Butterworth and Williams, Roy. Soc. Edinburgh, Trans., vol. 63, p. 385, pl. 4, figs. 4-6.
1960. *Vestipora lucida* (Butterworth and Williams), Potonié Amt. für Bodenforschung, Biehefte Geol. Jahrbuch, Hanover, vol. 39, p. 52.

Genus **WALTZISPORA** Staplin, 1960

Type species, *Waltzispora lobophora* Waltz, 1938 *in* Luber and Waltz.

Waltzispora planiangulata Sullivan, 1964 Pl. 45, figs. 3, 5, 6

1964. *Waltzispora planiangulata* Sullivan, Palaeontology, vol. 7, pt. 3, p. 362, pl. 57, figs. 25-30.

Remarks. — *W. planiangulata* Sullivan may be a junior synonym of *W. sagittata* Playford. However, assignment of forms of this study to *W. planiangulata* is rationalized through strict adherance to the published descriptions of the two species. *W. sagittata* is described as being finely granulate to laevigate while *W. planiangulata* is described as variable with some forms laevigate on the proximal and granular on the distal to ornament on both. Fossils studied for this report show a similar variation. Examination of the material studied by Felix and Burbridge (1967) suggests similar characteristics.

Waltzispora politus (Hoffmeister, Staplin, and Malloy), Smith and Butterworth, 1967 Pl. 45, figs. 4, 7

1955. *Granulati-sporites politus* Hoffmeister, Staplin, and Malloy, Jour. Paleont., vol. 29, No. 3, p. 389, pl. 36, fig. 13.
1960. *Non Leiotriletes politus* (Hoffmeister, Staplin, and Malloy), Love, Roy. Soc. Edinburgh, Proc., vol. 67, Sect. B, p. 111, pl. 1, fig. 1.
1967. *Waltzispora politus* (Hoffmeister, Staplin, and Malloy), Smith and Butterworth, Special Paper Palaeontology, No. 1, pp. 159, 160, pl. 6, fig. 14.

Spore Type A Pl. 45, figs. 10-12

Description. — Spores radial, trilete; equatorial outline is roundly triangular. Triradiate structure is tectate. Commissure rays extend to the equatorial margin. Exine thickened adjacent to the commissure resulting in the proximal surface remaining in a steep pyramidal form and appearing as lips ± 2 microns wide adjacent to the commissure. Ornamentation is variable; large, squat pila, bacula and apiculae are present. The pila are the largest ornament, up to 5 microns high and 5 microns wide. Ornament is considerably reduced on the proximal surface to small apiculae and bacula less than 1 micron high. Wall 2.5 microns thick.

Size. — 41 microns.

Figured specimen. — 147F30-2.

Remarks. — Although this spore is very distinctive in form, there were not enough specimens observed to warrant describing a new taxon. It does compare reasonably well with *Raistrickia clavata* Hacquebard (1957).

Spore Type B Pl. 45, figs. 8, 9

Description. — Spores radial, trilete; equatorial outline is roundly triangular. Triradiate structure is tectate. Commissure rays extend to the equatorial margin. Exine thickened adjacent to the commissure resulting in prominent triradiate folds which appear as lips ± 3.5 microns thick on either side of the commissure. The proximal interradial contact areas are very thin and sag below the triradiate ridges. The entire exine is scabrate-punctate and the distal is ornamented with very small apiculae (less than 1 micron). Distal wall is ± 2.5 microns thick.

Size. — 46 microns.

Figured specimen. — 147F32-4.

DISCUSSION

Examination of the palynomorphs revealed an assemblage consisting of a diversity of forms, the most abundant fossil being *Tasmanites* (Table 2). Large numbers of *Tasmanites* and *Maranhites* characterize the Upper Devonian Juniper Hill Member of the Lime Creek Formation in Iowa. Therefore, the presence of *Tasmanites* would lend support to the idea of the Independence Shale consisting of solution fillings of Lime Creek Shale. However, several species of *Densosporites, Ahrensisporites, Florinites* and others were also noted. These latter species are typical Carboniferous forms.

Detailed examination of the palynomorphs in the assemblage with transmitted light microscopy suggested two conditions of preservation of the fossil material. Some specimens of spores as well as those specimens of *Tasmanites* and *Maranhites* exhibited a darkening of the inner side of the wall. Specimens figured on Plate 21, figs. 2, 4 illustrate the appearance in bright field microscopy. Phase contrast microscopy of the fossils emphasized the internal deterioration of the wall plus frequent external corrosion and pitting (Pl. 21, figs. 1, 3, 5, 6, 8, 10, 12). Finally, the surface deterioration was confirmed by examining specimens with the scanning electron microscope (Pl. 21, figs. 7, 9, 11). In addition, the specimens with the preceding characteristics were invariably flattened, also suggesting a different preservation environment. The fossils figured on Plates 22 through 45 illustrate the different preservation characteristics. They do not exhibit an exine breakdown and, with the exception of some of the saccate grains, are virtually undistorted.

Contrast between the two types of preservation is further enhanced by an apparent age difference between the two groups. As previously mentioned, *Tasmanites* and *Maranhites* are characteristic of the Lime Creek Shale (Upper Devonian age). Some identifiable specimens of *Diaphanospora* (Pl. 21, figs. 3, 9, 12) with the same preservation characteristics support the Upper Devonian age assignment for the poorly preserved fraction of the assemblage. Many other specimens of spores could not be recognized because of the amount of deterioration (Pl. 21, figs. 1, 2). The spores exhibiting the better preservation characteristics also have unifying stratigraphic distribution.

The better preserved fossils constitute an assemblage of 81 species of spores. Table 2 illustrates the relative distribution of palynomorphs in the total assemblage. The reworked complex of *Tasmanites* and *Maranhites* make up 28 percent of the counts. Reworked spores represent an additional 2.5 percent of the counts. *Lycospora uber* is the most abundant species in the principal assemblage (25.4%). Three species of *Densosporites, D. cavus* (13.5%), *D. rarispinosus* (7.3%) and *D. hispidus* (3.4%) provide the next largest abundances. These four species plus the reworked material obscured so much of the assemblage that they were omitted from the counts of an additional 450 individuals. Table 3 shows the results of the additional counting. Eight more species are reflected in the additional counts. A comparison between this assemblage and several published works is illustrated in Table 4. The listed works are believed to give an adequate comparison of the stratigraphic interval ranging from Tournaisian through Westphalian A. It is recognized that other workers have investigated the same stratigraphic interval, but a comparison could not be made in many cases because these workers failed to report the entire assemblage.

The assemblage of the Independence Shale is characterized by the great abundance of *Lycospora uber* and species of *Densosporites*. Assemblages with similar composition have been reported by Felix and Burbridge, (1967), Hoffmeister, Staplin, and Malloy (1955), Sullivan and Marshall (1966), Sullivan (1964) and Butterworth and Williams (1958). Additional similarities to Late Mississippian assemblages are the presence of species of *Convolutispora, Knoxisporites* and *Microreticulatisporites. Cincturasporites altilis, Proco-*

SPECIES	%	SPECIES	%
ACANTHOTRILETES ECHINATUS	0.2	MONOLETES OVATUS	0.4
AHRENSISPORITES BEELEYENSIS	1.3	M. WINSLOWI	
A. HALESI	0.2	MOOREISPORITES FUSTUS	
ANAPICULATISPORITES MINOR	1.0	M. BICORNIS	
CALAMOSPORA HARTUNGIANA	0.1	CF. MUROSPORA	
CAMPTOTRILETES CRISTATUS	0.4	NEORAISTRICKIA VARIORNAMENTA	
C. BACCULENTUS		POTONIESPORITES ELEGANS	0.4
CINCTURASPORITES ALTILIS		PROCORONASPORA FASCICULATA	
CIRRATRIRADITES SATURNI	0.1	PROPRISPORITES LAEVIGATUS	
CONVOLUTISPORA AMPLA		PUNCTATISPORITES HETEROFILIFERUS	0.4
C. FLORIDA	0.7	P. INCOMPTUS	
C. MELLITA	0.2	P. OBESUS	0.6
C. TORTUOSA	0.4	P. PLANUS	0.7
COSTATASCYCLUS CRENATUS		P. VALIDUS	
DENSOSPORITES ACULEATUS	0.1	RAISTRICKIA SAETOSA	
D. HISPIDUS	3.4	R. DENSA	0.2
D. RARISPINOSUS	7.3	REINSCHOSPORA SPECIOSA	
D. CAVUS	13.5	RETICULATISPORITES DANZEI	
DICTYOTRILETES CLATRIFORMIS		R. PELTATUS	
DORHEIMISPORITES INFLATUS		SAVITRISPORITES NUX	0.5
FLORINITES VISENDUS	0.2	SCHULZOSPORA ELONGATA	0.4
F. GUTTATUS	0.2	SECARISPORITES REMOTUS	0.2
FOVEOSPORITES INSCULPTUS	0.1	SIMOZONOTRILETES INTORTUS	
FUNISPORITES MAGNUS		STENOZONOTRILETUS LYCOSPOROIDES	2.1
GRANULATISPORITES GRANULATUS	0.4	TANTILLUS TRIQUETRUS	0.5
G. MICROGRANIFER	1.0	TRIMONTISPORITES GRANULATUS	
G. TUBERCULATUS	0.6	T. CONTORTUS	
HYMENOSPORA CAPERATA	0.2	T. RUGOSUS	
KNOXISPORITES STEPHANEPHORUS	0.5	TRIQUITRITES TRIBULLATUS	
K. TRIRADIATUS	0.1	VERRUCOSISPORITES SCOTICUS	
K. SP.	0.1	V. CEROSUS	
KOCHISPORITES DENTATUS		V. MORULATUS	0.1
LEIOTRILETES PYRAMIDATUS		VESTISPORA LUCIDA	
L. SUBINTORTUS	0.1	WALTZISPORA PLANIANGULATA	2.7
L. ANGULATUS	0.5	W. POLITUS	0.8
L. LABRUM	0.4	SPORE TYPE A	
L. TUMIDUS	0.1	SPORE TYPE B	
L. SP.		REWORKED TASMANITES - MARANHITES	28.3
LOPHOTRILETES FATIHI		REWORKED SPORES	2.5
L. LABIATUS			
L. OBTUSUS			
LYCOSPORA UBER	25.4		
MICRORETICULATISPORITES CONCAVUS	0.1		
M. PUNCTATUS	0.4		

Table 2. Percentage composition of the total assemblage.

SPECIES	%	SPECIES	%
ACANTHOTRILETES ECHINATUS	0.3	LYCOSPORA UBER	NC
AHRENSISPORITES BEELEYENSIS	10.1	MICRORETICULATISPORITES CONCAVUS	0.3
A. HALESI	2.7	M. PUNCTATUS	1.0
ANAPICULATISPORITES MINOR	2.0	MONOLETES OVATUS	0.5
CALAMOSPORA HARTUNGIANA	0.3	M. WINSLOWI	
CAMPTOTRILETES CRISTATUS		MOOREISPORITES FUSTUS	
C. BACCULENTUS		M. BICORNIS	
CINCTURASPORITES ALTILIS		CF. MUROSPORA	
CIRRATRIRADITES SATURNI	0.3	NEORAISTRICKIA VARIORNAMENTA	0.3
CONVOLUTISPORA AMPLA		POTONIESPORITES ELEGANS	0.3
C. FLORIDA	3.0	PROCORNASPORA FASCICULATA	
C. MELLITA	0.3	PROPRISPORITES LAEVIGATUS	
C. TORTUOSA		PUNCTATISPORITES HETEROFILIFERUS	1.2
COSTATASCYCLUS CRENATUS	1.5	P. INCOMPTUS	0.3
DENSOSPORITES ACULEATUS	0.5	P. OBESUS	1.5
D. HISPIDUS	NC	P. PLANUS	1.7
D. RARISPINOSUS	NC	P. VALIDUS	0.5
D. CAVUS	NC	RAISTRICKIA DENSA	0.3
DICTYOTRILETES CLATRIFORMIS	0.7	R. SAETOSA	0.7
DORHEIMISPORITES INFLATUS	0.3	REINSCHOSPORA SPECIOSA	
FLORINITES VISENDUS	4.7	RETICULATISPORITES DANZEI	1.2
F. GUTTATUS	2.2	R. PELTATUS	
FOVEOSPORITES INSCULPTUS	0.5	SAVITRISPORITES NUX	1.0
FUNISPORITES MAGNUS	0.5	SCHULZOSPORA ELONGATA	2.2
GRANULATISPORITES GRANULATUS	1.0	SECARISPORITES REMOTUS	1.2
G. MICROGRANIFER	3.5	SIMOZONOTRILETES INTORTUS	
G. TUBERCULATUS	4.7	STENOZONOTRILETES LYCOSPOROIDES	6.2
HYMENOSPORA CAPERATA	0.3	TANTILLUS TRIQUETRUS	1.5
KNOXISPORITES STEPHANEPHORUS	1.2	TRIMONTISPORITES GRANULATUS	
K. TRIRADIATUS	0.5	T. CONTORTUS	
K SP	0.5	T. RUGOSUS	
KOCHISPORITES DENTATUS		TRIQUITRITES TRIBULLATUS	
LEIOTRILETES PYRAMIDATUS	0.7	VERRUCOSISPORITES CEROSUS	1.2
L. SUBINTORTUS	2.5	V. MORULATUS	1.2
L. ANGULATUS	1.5	V. SCOTICUS	
L. LABRUM	1.2	VESTISPORA LUCIDA	
L. TUMIDUS	0.5	WALTZISPORA PLANIANGULATA	22.0
L. SP.	1.0	W. POLITUS	
LOPHOTRILETES FATIHI	1.5	SPORE TYPE A	
L. LABIATUS	0.7	SPORE TYPE B	
L. OBTUSUS	0.5		

Table 3. Percentage composition of the assemblage with the reworked fossils and four overrepresented species omitted.

ronaspora fasciculata and *Reticulatisporites peltatus* have been reported only from Late Mississippian sections.

The absence of species of *Laevigatosporites* is also believed to be significant. Early Pennsylvanian assemblages of the mid-continent area typically have species of *Laevigatosporites* in abundance. Therefore, it is the opinion of this investigator that this assemblage is Late Mississippian (Chester) in age.

Two interpretations are possible from the stratigraphic distribution of the spores. They are:

1) Deposition during Chester time recycling of the Devonian fossils at that time.

2) Reworking of the entire assemblage subsequent to the stratigraphic age indicated by any of the fossils.

The second interpretation is rejected in favor of the first on the basis of a comparison of the preservation. The Upper Devonian fossils have been flattened while the Chester fossils are virtually undistorted, thereby suggesting two cycles of deposition. *Lycospora uber* and other equally fragile spores show less deterioration of their walls than does *Tasmanites*. Also, the Devonian forms are predominantly marine palynomorphs and the Carboniferous forms are entirely continental. Reworking subsequent to Chester time is ruled out because the Carboniferous fossils do not show exine destruction. In addition, many of the spore species as *Lycospora uber, Densosporites hispidus, D. cavus* and *D. rarispinosa* commonly found dispersed in the assemblage are also found in tetrads. Almost all species except the saccate grains are found united in tetrads. Reworking would undoubtedly separate the tetrads of spores that obviously disperse readily as indicated by their abundance as individuals. The united tetrads suggest a depositional environment of very low energy. The undistorted condition of the Carboniferous forms indicate little, if any, compaction of the sediment after deposition. The blocky nature of the shale suggests a similar situation.

CONCLUSIONS

The environmental situation suggested is one of extensive development of karst topography during Late Mississippian time. Numerous sinks and caves were developed in the carbonate bedrock

MISSISSIPPIAN	PENN-

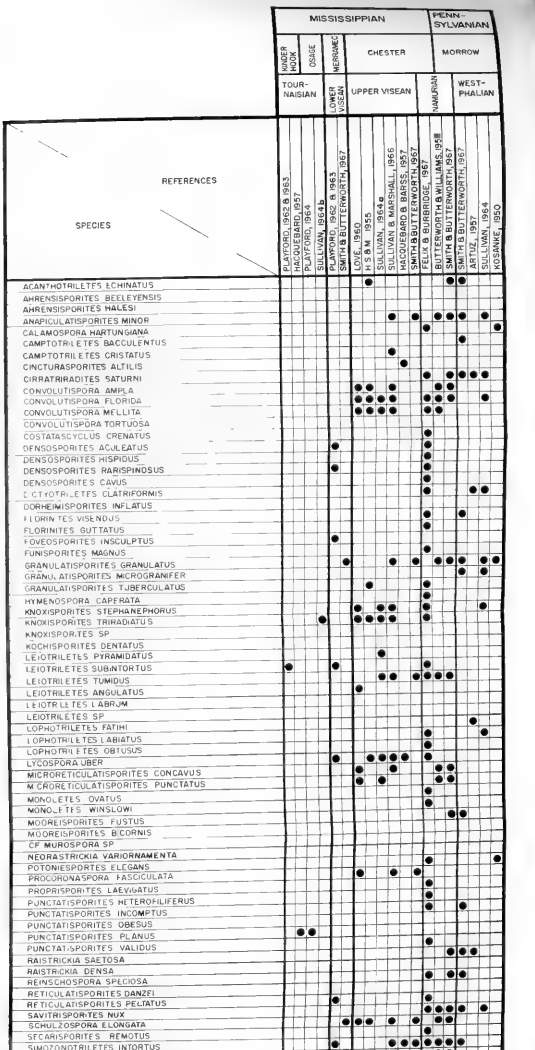

Table 4. Assemblage comparison with some published works.

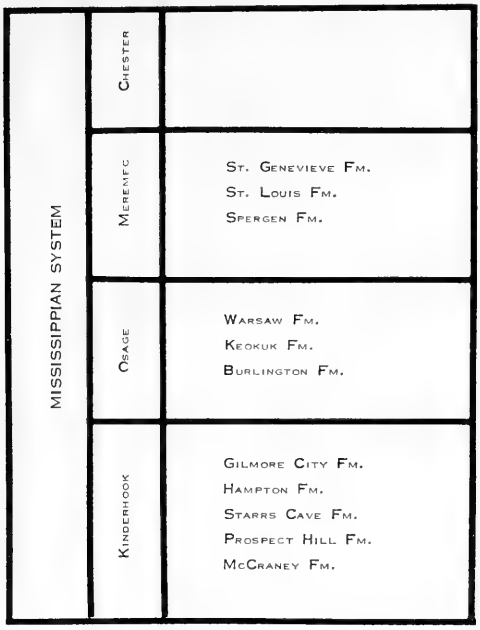

Table 5. Stratigraphic section of the Mississippian of Iowa.

of the Cedar Valley and Wapsipinicon Formations. Solution penetrated to depths of at least 175 feet, as indicated by data from other localities of equivalent age.

The soft, easily erodable shales of the Lime Creek Formation were the provenance for the detritus which was deposited during Chester (Springer) time. Little alteration of the Lime Creek Shale has taken place so that the gray-green color has been preserved and contributed to the probability of misidentification.

The Chester age determination is also significant in that it fills a gap in the geologic history of this particular region (Table 5). No Chester age sediments are known to have been reported prior to this study. Consequently, these sediments are positive evidence of an erosion cycle in this region during Late Chester time. This interpretation is also compatible with the extensive Morrow and Desmoines Karst development in this area and throughout northern Missouri.

REFERENCES CITED

Agrali, B., Akyol, E., Konyali, Y., Corsin, Paule M. and Laveine, J. P.
1965. *Nouvelles formes de spores et pollens provenant de charbons primaires et tertiaires de divers gisements turcs.* Soc. Geól. du Nord, Ann. Tt. 85V, pp. 169-182, pls. 15,16.

Artüz, S.
1957. *Die sporae dispersae der Türkischen Steinkohle vom Zonguldak-Gebeit. Istanbul Üniversitesi.* Fen Fakültesi, Mecmuasi. S. B. Jabii Ilimer, vol. 22, pp. 239-263, pls. 1-7.
1959. *Zonguldak Bölgesindeki Alimolla, Sulu ve Büyük Kömür Damarlarinin Sporolojik Etüdü.* Istanbul Universitesi. Fen Fakültesi. Monografileri Sayi 15, pp. 1-73, pls. 1-10.

Balme, B. E.
1957. *Spores and pollen grains from the Mesozoic of western Australia.* Commonwealth Sci. Ind. Res. Org., Coal Res. Sect. T.C. 25, pp. 1-48, pls. 1-7.

Berry, Willard
1937. *Spores from the Pennington coal Rhea County, Tennessee.* American Midl. Nat., vol. 18, pp. 155-160, pl. 1.

Bharadwaj, D. C.
1954. *Einige neue Sporengattungen des Saarkarbons.* N. Jahrb. Geol., Palaeont., Monatshefte, vol. 11, pp. 512-525, text-figs. 1-10.
1955. *The spore genera from the Upper Carboniferous coals of the Saar and their value in stratigraphical studies.* The Palaeobotanist, vol. 4, pp. 119-150, pls. 1,2.

Bharadwaj, D. C., and Venkatachala, B. S.
1962. *Spore assemblage out of a Lower Carboniferous Shale from Spitsbergen.* The Palaeobotanist, vol. 10, No. 1, pp. 18-47, pls. 1-10, text-figs. 1-5.

Butterworth, M. A. and Spinner, E.
1967. *Lower Carboniferous spores from Northwest England.* Palaeontology, vol. 10, pt. 1, pp. 1-24, pls. 1-5.

Butterworth, M. A., and Williams, R. W.
1958. *The small spore floras of coals in the Limestone Coal Group and Upper Limestone Group of the Lower Carboniferous of Scotland.* Roy. Soc. Edinburgh, Trans., vol. 63, pp. 353-392, pls. 1-4.

Calvin, S.
1878. *On some dark shale recently discovered below the Devonian Limestones at Independence, Iowa.* Amer. Jour. Sci., ser. 3, vol. 15, No. 90, pp. 460-462.

Cookson, I. C.
1957. *On some Australian Tertiary spores and pollen grains that extend the geological and geographical distribution of living genera.* Roy. Soc. Victoria, Proc., vol. 69, pp. 41-53, pls. 8-10.

Couper, R. A.
1958. *British Mesozoic microspores and pollen grains.* Palaeontographica, Abt. B, Bd. 103, pp. 75-179.

Couper, R. A., and Grebe, H.
1961. *A recommended terminology and descriptive method for spores.* Compte Rendu, Commission Internationale de Microflore du Paléozoïque, Krefeld, pp. 1-15.

Dorheim, Fred H.
1967. *Stratigraphic leak at Springville Quarry.* Iowa Geol. Sur., vol. 74, pp. 142-146.

Felix, C. J., and Burbridge, P. P.
1967. *Palynology of the Springer Formation of southern Oklahoma, U.S.A.*

Palaeontology, vol. 10, pt. 3, pp. 349-425, pls. 53-66, text-figs. 1-4, table 1.

Hacquebard, P. A.

1957. *Plant spores in coal from the Horton Group (Mississippian) of Nova Scotia.* Micropaleontology, vol. 3, No. 4, pp. 301-324, pls. 1-3, text-figs. 1-2, table 1.

Hacquebard, P. A., and Barss, M. S.

1957. *A Carboniferous spore assemblage, in coal from the South Nahanni River Area, Northwest Territories.* Geol. Sur. Canada, Bull. 40, pp. 1-63, pls. 1-6, text-figs. 1-4.

Hershey, H. Garland

1969. *Geologic map of Iowa.* Iowa Geological Survey.

Hibbert, F. A., and Lacey, W. S.

1969. *Miospores from the Lower Carboniferous basement beds in the Menai Straits Region of Caernarvonshire, North Wales.* Palaeontology, vol. 12, pt. 3, pp. 420-440, pls. 78-83, text-fig. 1.

Hoffmeister, W. S., Staplin, F. L., and Malloy, R. E.

1955. *Mississippian plant spores from the Hardinsburg Formation of Illinois and Kentucky.* Jour. Paleont., vol. 29, No. 3, pp. 372-399, pls. 36-39, text-figs. 1-4.

Horst, U.

1943. *Microstratigraphischer Beitrag zum Vergleich des Namur von West-Oberschlesien und Mährisch-Ostrau.* Die Mega- und Mikrosporen der hauptsächlichen Flöze beider Reviere. Techn. Hochschule Berlin, Dissertation, 243 pp., 9 pls.

1955. *Die Sporae dispersae des Namurs von Westoberschlesien und Mährisch-Ostrau.* Palaeontographica, Abt. B, Bd. 98, Nos. 4-6, pp. 137-236, pls. 17-25, text-figs. 1-7.

Hughes, N. F., and Playford, G.

1961. *Palynological reconnaissance of the Lower Carboniferous of Spitsbergen.* Micropaleontology, vol. 7, pp. 27-44, pls. 1-4, text-figs. 1,2.

Ibrahim, A.

1933. *Sporenformen des Aegirhorizonts des Ruhr-Reviers.* Dissertation. Tech. Hochschule Berlin, Würzberg, Triltsch, pp. 1-48, pls. 1-8, text-figs. 1-2.

Ishchenko, A. M.

1952. *Atlas of the microspores and pollen of the Middle Carboniferous of the western part of the Donetz Basin.* Izd. Akad. Nauk. Ukr. S.S.R., Inst. Geol. Nauk., pp. 1-83, pls. 1-22.

1956. *Spores and pollen of the Lower Carboniferous deposits of the western extension of the Donetz Basin and their stratigraphical importance.* Akad. Nauk. Ukr. S.S.R., Trudy Inst. Geol. Nauk. Ser. Strat. Palaeont., vol. 11, pp. 1-143, pls. 1-21.

Knox, E. M.

1950. *The spores of Lycopodium, Phylloglossum, Selaginella and Isoëtes and their value in the study of microfossils of Paleozoic age.* Bot. Soc. Edinburgh, Trans., vol. 33, pt. 3, pp. 211-357, pls. 8-19.

Kosanke, R. M.

1950. *Pennsylvanian spores of Illinois and their use in correlation.* Illinois Geol. Sur. Bull. 74, pp. 1-128, pls. 1-17, text-figs. 1-7.

Loose, F.

1932. *Beschreibung von Sporenformen aus Flöz Bismarck; in Potonié, R., Ibrahim, A., and Loose, F., Sporenformen aus din Flozen Agir und Bismarck des Ruhrgebietes.* N. Jahrb. f. Min., Geol., Paläontol., Beilage-Band, Abt. B, vol. 67, pp. 438-451, pls. 1-7, text-fig. 1.

1934. *Sporenformen aus dem Flöz Bismarck des Ruhrgebietes.* Arbeiten Inst. Paläobot. u. Petrog. d. Brennsteine Arb., vol. 4, No. 3, pp. 127-164.

Love, L. G.

1960. *Assemblages of small spores from the Lower Oil Shale Group of Scotland.* Roy. Soc. Edinburgh, Proc. vol. 67, Sect. B, pp. 99-126, pls. 1,2, text-figs. 1-15.

Luber, A. A., and Waltz, I. E.

1938. *Classification and stratigraphic value of spores of some carboniferous coal deposits in the U.S.S.R.* Trans. Cent. Geol. and Prosp. Inst., Fasc. 105, pp. 1-45, pls. 1-10.

1941. *Atlas of microspores and pollen grains of the Palaeozoic of the U.S.S.R.* Tr. All-Union Geol. Sci. Res. Inst. (U.S.E.G.E.I.), vol. 139, pp. 1-107, pls. 1-16.

Muller, Klaus J., and Muller, Eva M.

1957. *Early Upper Devonian (Independence) conodonts from Iowa, Part 1.* Jour. Paleont., vol. 31, No. 6, pp. 1069-1108, pls. 135-142, text-figs. 1-8.

Naumova, S. N.

1939. *Spores and pollen of the coals of the U.S.S.R.* Rept. Int. Geol. Cong., 17th Session, U.S.S.R. 1, pp. 353-364.

1953. *Sporo-pollen complexes of the Upper Devonian of the Russian Platform and their stratigraphical value.* Tr. Inst. Geol. Nauk. U.S.S.R., vol. 143, (Geol. Ser. No. 60), pp. 1-204, pls. 1-22.

Neves, R.

1958. *Upper Carboniferous plant spore assemblages from the Gastrioceras subcrenatum horizon, North Staffordshire.* Geol. Mag. vol. 90, No. 1, pp. 1-19, pls. 1-3, text-figs. 1-4, table 1.

1961. *Namurian plant spores from the Southern Pennines, England.* Palaeontology, vol. 4, pp. 247-279, pls. 30-34, text-figs. 1-6.

1964. *Knoxisporites (Potonié and Kremp) Neves, 1961.* Int. Congr. en stratigraphic and Carboniferous Geol., 5th, Compte Rendu., Tome 3, pp. 1063-1069, 1 pl., 2 text-figs.

Neves, R., and Playford, G.

1961. *'The dispersed spore' genus Knoxisporites Potonié and Kremp, 1954.* Compte Rendu, Commission Internationale de Microflore du Paléozoique, Krefeld, p. 9.

Neville, R. S. W.

1968. *Ranges of selected spores in the Upper Vissean of the East Fife coast section between St. Monance and Pittenweem.* Pollen et Spores, vol. 10, No. 2, pp. 431-462, pls. 1-3.

Playford, G.

1962a. *Lower Carboniferous microfloras of Spitsbergen. Part 1.* Palaeontology, vol. 5, pt. 3, pp. 550-618, pls. 78-87, text-figs. 1-8.

1962b. *Lower Carboniferous microfloras of Spitsbergen. Part II.* Palaeontology, vol. 5, pt. 4, pp. 619-678, pls. 88-95, text-figs. 9-12, tables 1-4.

Potonié, R.

1934. *Zur Mikrobotanik der Kohlen und ihrer Verwandten 1. Zur Morphologie der fossilen Pollen und Sporen.* Arbeiten Inst. Paläobot. u. Petrog. d. Brennsteine Arb., No. 4, pp. 5-24, 44 text-figs.

1956. *Synopsis der Gattungen der Sporae dispersae, Teil I.* Amt. fur Bodenforschung, Beihefte Geol. Jahrbuch, Hanover, vol. 23, pp. 1-103, pls. 1-11.

1958. *Synopsis der Gattungen der Sporae dispersae, Teil II.* Amt. fur Bodenforschung, Beihefte Geol. Jahrbuch, Hanover, vol. 31, pp. 1-144.

1960. *Synopsis der Gattungen der Sporae dispersae, Teil III.* Amt. fur Bodenforschung, Beihefte Geol. Jahrbuch, Hanover, vol. 39, pp. 1-189.

Potonié, R., and Kremp, G. O. W.

1954. *Die Gattungen der paläzoischen Sporae dispersae und ihre Stratigraphie.* Geologisches Landessanstalten, Bundesrepublik Deutschlands, Geol., Jahrbuch, vol. 69, pp. 111-195, pls. 4-20, text-figs. 1-5.

1955. *Die Sporae dispersae des Ruhrkarbons, ihre Morphographie und Stratigraphie mit Ausblicken auf Arten anderer Gebiete und Zeitabschnitte, Teil I.* Palaeontographica, Abt. B, Bd. 98, Nos. 1-3, pp. 1-136, pls. 1-16, text-figs. 1-37.

1956a. *Die Sporae dispersae des Ruhrkarbons, ihre Morphographie und Stratigraphie mit Ausblicken auf Arten anderer Gebiete und Zeitabschnitte, Teil II.* Palaeontographica, Abt. B, Bd. 99, Nos. 4-6, pp. 85-191.

1956b. *Die Sporae dispersae des Ruhrkarbons, ihre Morphographie und Stratigraphie mit Ausblicken auf Arten anderer Gebiete und Zeitabschnitte, Teil III.* Palaeontographica, Abt. B, Bd. 100, Nos. 1-3, pp. 65-121.

Savage, T. E.

1920. *Devonian formations of Illinois.* American Jour. Sci., ser. 4, vol. 49, pp. 169-182.

Schopf, J. M.

1936. *Spores characteristic of Illinois Coal No. 6.* Illinois Acad. Sci. Trans., vol. 28, No. 2, pp. 173-176.

Schopf, J. M., Wilson, L. R., and Bentall, Ray

1944. *An Annotated synopsis of Paleozoic fossil spores and the definition of generic groups.* Illinois Geol. Sur., Report of Investigations No. 91, pp. 1-73, pls. 1-3, text-figs. 1-5.

Scobey, Ellis H.

1940. *Sedimentary studies of the Wapsipicon Formation in Iowa.* Jour. Sed. Petr. vol. 10, No. 1, pp. 33-44, figs. 1-2, tables 1-3.

Smith, A. H. V., and Butterworth, Mavis A.

1967. *Miospores in the coal seams of the Carboniferous of Great Britain.* Special Paper Palaeontology, No. 1, pp. 1-324, pls. 1-27, text-figs. 1-72, tables 1-5.

Somers, Grace

1952. *A preliminary study of the fossil spore content of the Lower Jubilee Seam of the Sydney Coalfield, Nova Scotia.* Nova Scotia Research Found., Halifax, N.S. Canada, pp. 1-30.

Stainbrook, Merrill A.

1935. *Stratigraphy of the Devonian system of the Upper Mississippi Valley. In* Kansas Geol. Soc., Guidebook, Ninth Ann. Field Conf., Aug. 25-Sept. 1, pp. 250-260, figs. 205-206.

1944. *Devonian system in Iowa,* Illinois Geological Survey, Bull. 68, pp. 182-188.

Staplin, F. L.

1960. *Upper Mississippian plant spores from the Golata Formation, Alberta, Canada.* Palaeontographica, Abt. B, Bd. 107, Nos. 1-3, pp. 1-40, pls. 1-8, text-figs. 1,2.

Staplin, F. L., and Jansonius, Jan

1964. *Elucidation of some Paleozoic densospores.* Palaeontographica, Abt. B, Bd. 114, Nos. 4-6, pp. 95-117, pls. 18-21, text-figs. 1,2.

Stookey, S. W.

1932. *New data on the Upper Devonian of Iowa.* Iowa Acad. Sci., Proc., vol. 39, pp. 183-191.

1933. *Status of the Devonian Beds at Middle Amana.* Iowa Acad. Sci., Proc., vol. 40, pp. 133,134.

1938. *Sandstone of Des Moines in Fayette.* Iowa Acad. Sci., Proc., vol. 45, pp. 163-165.

1939. *Significance of Carbonaceous and Late Devonian material within the Iowa Devonian.* Iowa Acad. Sci., Proc., vol. 46, pp. 227-231.

Sullivan, H. J.

1958. *The Microspore genus Simozonotriletes.* Palaeontology, vol. 1, pt. 2, pp. 125-138, pls. 26-28.

1964. *Spores from the Drybrook Sandstone and associated measures in the forest of Dean Basin,* Gloucestershire. Palaeontology, vol. 7, pt. 3, pp. 251-392, pls. 57-61, text-figs. 1-6.

Sullivan, H. J., and Marshall, A. E.

1966. *Visean spores from Scotland.* Micropaleontology, vol. 12, No. 3, pp. 265-285, text-figs. 1,2, tables 1-4.

Urban, J. B., and Kline, Judith K.

1970. *Chitinozoa of the Cedar City Formation, Middle Devonian of Missouri.* Jour. Paleont., vol. 44, No. 1, pp. 69-76, pl. 1.

Urban, J. B., and Padovani, Elaine R.

1970. *A new scanning electron microscope specimen holder for palynology.* Pollen et Spores, vol. 12, No. 1, pp. 131-139, pl. 1, 6 text-figs.

Wilson, L. R.

1958. *Photographic illustrations of fossil spore types from Iowa.* Oklahoma Geol. Sur., Oklahoma Geology Notes, vol. 18, pp. 99-101, pl. 1.

1959a. *Genotype of Densosporites Berry, 1937.* Oklahoma Geol. Sur., Oklahoma Geology Notes, vol. 19, No. 3, pp. 47-50, pl. 1.

1959b. *A water-miscible mountant for palynology.* Oklahoma Geol. Sur., Oklahoma Geology Notes, vol. 19, No. 5, pp. 110,111.

Wilson, L. R., and Coe, E. A.

1940. *Descriptions of some unassigned plant microfossils from the Des Moines Series of Iowa.* American Midl. Nat., vol. 23, No. 1, pp. 182-186.

Wilson, L. R., and Kosanke, R. M.

1944. *Seven new species of unassigned plant microfossils from the Des Moines Series of Iowa.* Iowa Acad. Sci., Proc., vol. 51, pp. 329-332, 1 pl.

Wilson, L. R., and Venkatachala, B. S.

1963. *An emendation of Vestispora (Wilson and Hoffmeister, 1956).* Oklahoma Geol. Sur., Oklahoma Geology Notes, vol. 23, No. 4, pp. 94-100, pl. 1.

Wilson, L. R., and Venkatachala, B. S.

1964. *Potonieisporites elegans (Wilson and Kosanke, 1944) Wilson and Venkatachala com. nov.* Oklahoma Geol. Sur., Oklahoma Geology Notes, vol. 24, pp. 67, 68, figs. 1,2.

Winslow, Marcia R.

1959. *Upper Mississippian and Pennsylvanian megaspores and other plant microfossils from Illinois.* Illinois Geol. Sur., Bull. 86, pp. 1-101, pls. 1-16, text-figs. 1-3.

PLATES

All scanning electron micrographs were taken at magnifications twice the indicated values. The transmitted light photomicrographs were taken at a magnification of 400× then enlarged to twice the indicated values. The plates were reduced by one-half for publication.

EXPLANATION OF PLATE 21

Figure — Page

1, 2. Recycled spore (unidentifiable) 150,151
1. Phase contrast photomicrograph. Blackened areas represent deterioration of the inside of the spore wall, ×1000. 2. Transmitted light photomicrograph of specimen in Fig. 1, ×1000.

3. **Diaphanospora** sp. (recycled) 151
Phase contrast photomicrograph, ×500.

4, 5. **Tasmanites** sp. (recycled) 150
4. Transmitted light photomicrograph showing the internal wall deterioration, ×500. 5. Phase contrast photomicrograph of specimen in Fig. 4, × 500.

6. **Maranhites** sp. (recycled) 150
Phase contrast photomicrograph, ×500.

7, 8. **Tasmanites** sp. (recycled) 150
7. Scanning electron micrograph showing the corroded exterior surface and the flattened condition, ×195. 8. Phase contrast photomicrograph of specimen in Fig. 7, ×250.

9, 12. Recycled spore (unidentifiable) 150
9. Scanning electron micrograph showing the corroded exterior of the exine and the flattened condition of the spore. ×550. 12. Phase contrast photomicrograph of specimen in Fig. 9, ×500.

10, 11. **Diaphanospora** sp. (Recycled) 150
10. Phase contrast photomicrograph, ×750. 11. Scanning electron micrograph showing exterior surface and flattened condition of the spore, ×625.

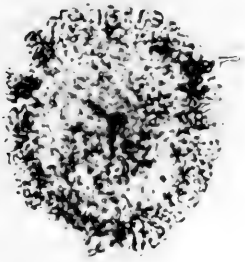

1

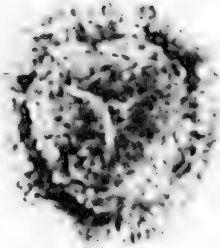

2

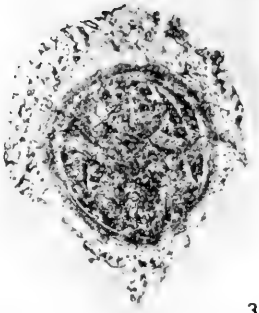

3

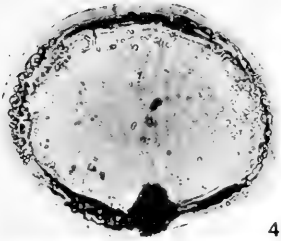

4

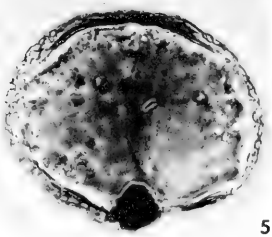

5

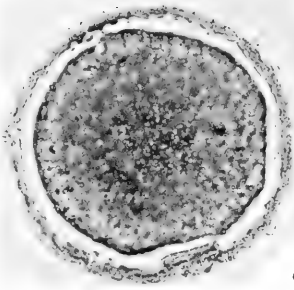

6

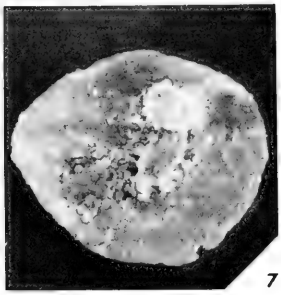

7

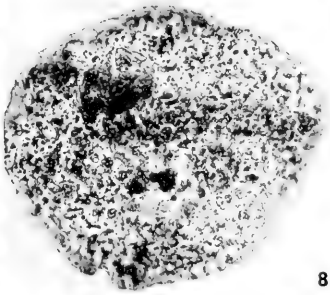

8

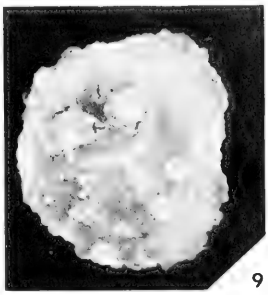

9

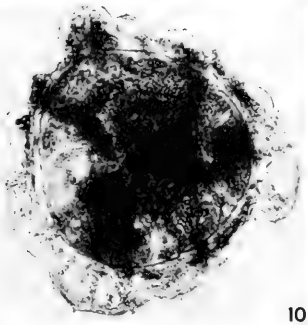

10

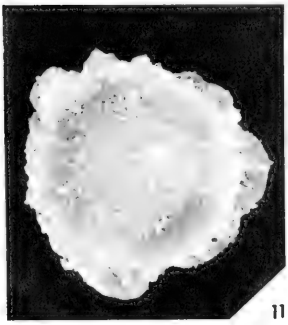

11

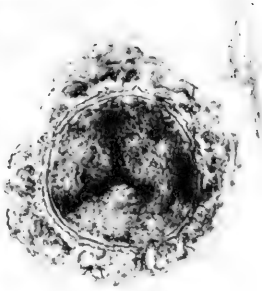

12

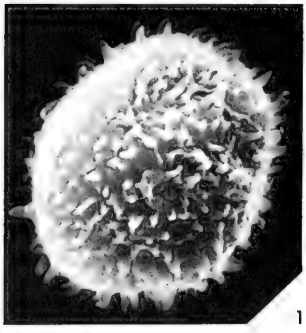
1

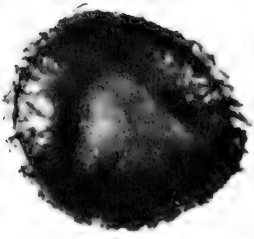
2

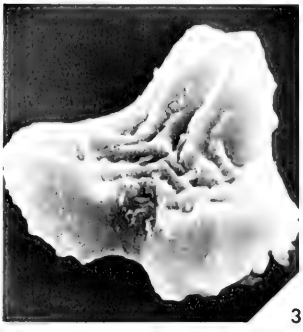
3


4

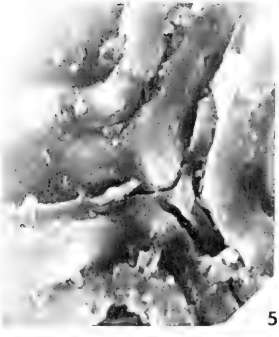
5

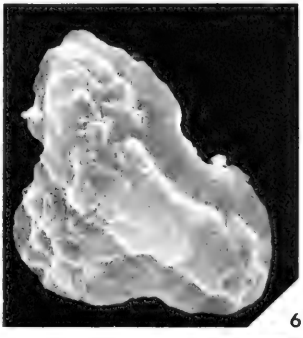
6

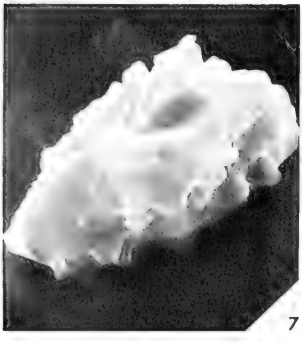
7

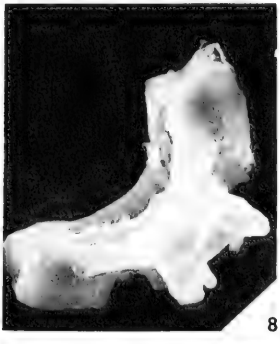
8


9


10

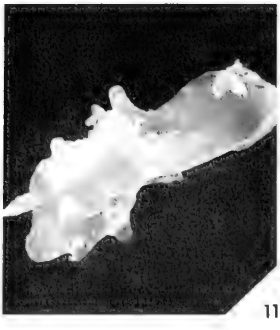
11

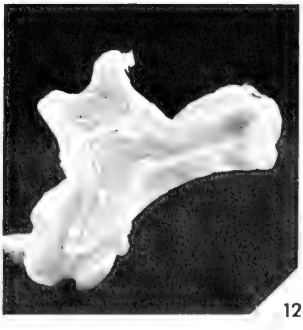
12

EXPLANATION OF PLATE 22

Figure — Page

1, 2. **Acanthotriletes echinatus** Hoffmeister, Staplin and Malloy, 1955 108

1. Scanning electron micrograph, distal surface, ×1000. 2. Transmitted light photomicrograph of specimen in Fig. 1, ×1000.

3-7. **Ahrensisporites beeleyensis** Neves, 1961 108

3. Scanning electron micrograph, proximal surface, ridges parallel to the triradiate structure, ×1250. 4. Transmitted light photomicrograph of specimen in Fig. 3, ×1000. 5. Scanning electron micrograph of specimen in Fig. 3. Tectate triradiate structure and small protuberances on the ridges parallel to the triradiate structure ×2850. 6. Scanning electron micrograph distal surface, "composite kyrtome," ×1200. 7. Scanning electron micrograph view from the end of an auricula, note the curving of the auriculum toward the distal side, and the increased development of the protuberances on the ridges parallel to the triradiate structure, ×1250.

8-12. **Ahrensisporites halesi** Urban, n. sp. 109

8. Scanning electron micrograph, proximal surface, prominent, strongly arched kyrtomes. Holotype 147F12-1, ×900. 9. Scanning electron micrograph, distal surface of specimen in Fig. 8. Serrated ridges of the kyrtome, ×900. 10. Transmitted light photomicrograph of specimen in Fig. 8, ×500. 11. Scanning electron micrograph, distal surface. Kyrtome ridges are not so prominently serrated. The protuberances are best developed near the distal pole. Paratype 147F17-1, ×900. 12. Scanning electron micrograph of specimen in Fig. 11, proximal surface, ×950.

EXPLANATION OF PLATE 23

Figure — Page

1, 4. **Calamospora hartungiana** Schopf, 1944 110
1. Scanning electron micrograph, proximal surface, ×500. 4. Transmitted light photomicrograph, ×500.

2, 3. **Anapiculatisporites minor** Butterworth and Williams, 1968 110
2. Transmitted light photomicrograph, oil immersion, ×1250. 3. Scanning electron micrograph of specimen in Fig. 2, ×1500.

5-7. **Camptotriletes cristatus** Sullivan and Marshall, 1966 111
5. Scanning electron micrograph, note absence of ornament on the proximal surface, ×800. 6. Transmitted light photomicrograph of specimen in Fig. 5, ×750. 7. Scanning electron micrograph of a specimen showing more typical ornament on the proximal surface, ×800.

8, 9. **Camptotriletes bacculentus** (Loose), Potonié and Kremp, 1955 110
8. Transmitted light photomicrograph, ×500. 9. Scanning electron micrograph of specimen in Fig. 8. Proximal surface, ×850.

10-12. **Cincturasporites altilis** Hacquebard and Barss, 1957 112
10. Scanning electron micrograph, ×500. 11. Transmitted light photomicrograph of specimen in Fig. 10. "Lips" result from the collapse of the interradial areas of the areas of the proximal surface, ×500. 12. Transmitted light photomicrograph showing a more typical "bizonate cingulum". ×500.

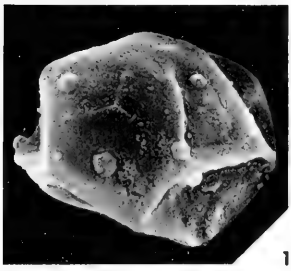
1

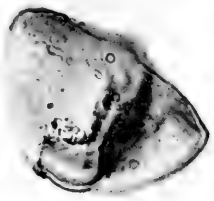
2

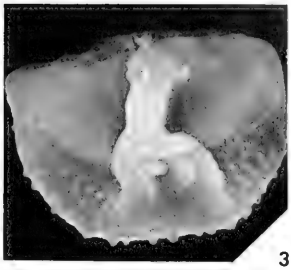
3

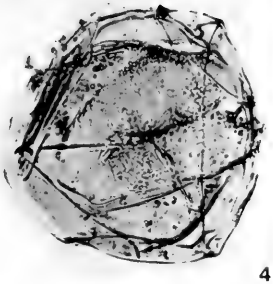
4

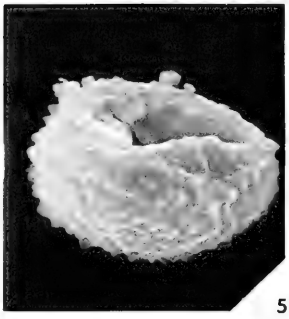
5


6

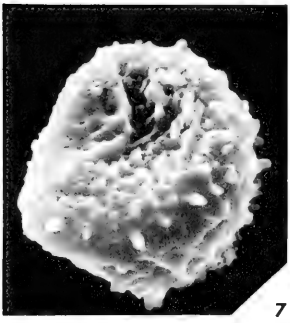
7


8

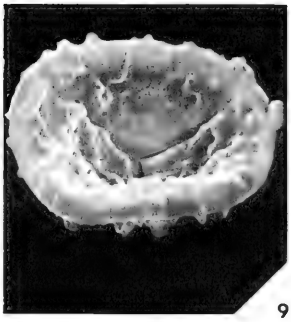
9


10

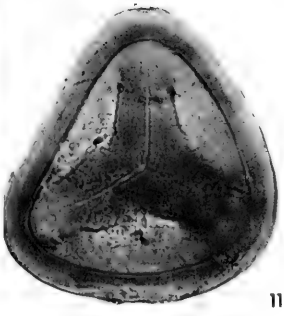
11

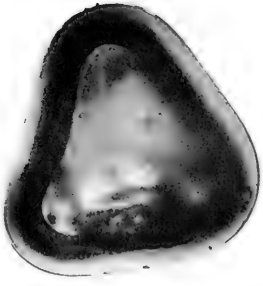
12


1

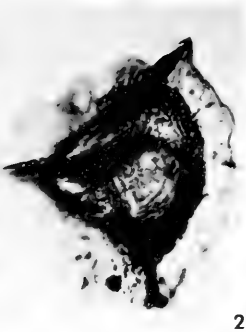
2

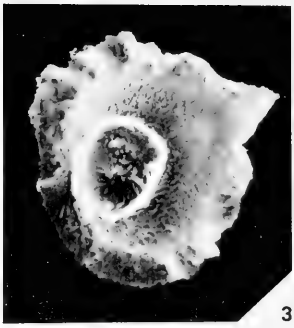
3

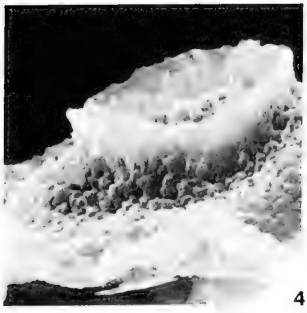
4


5

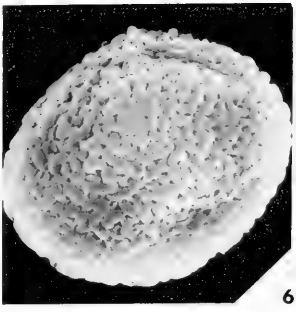
6

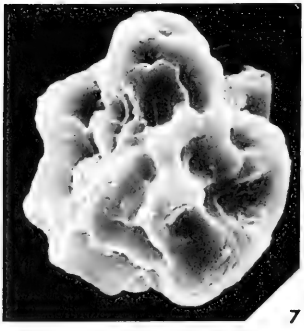
7


8

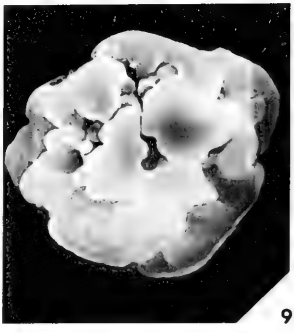
9

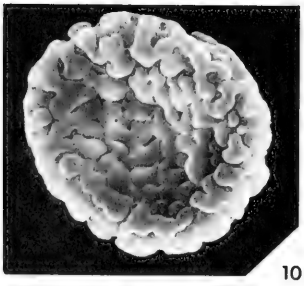
10

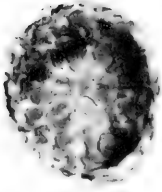
11

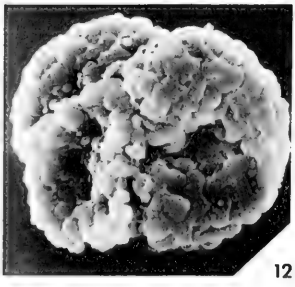
12

EXPLANATION OF PLATE 24

Figure — Page

1-4. **Cirratriradites cf. C. saturni** (Ibrahim), Schopf, Wilson and Bentall, 1944 112
1. Scanning electron micrograph, proximal surface. Note the punctate-scabrate ornament of the interradial areas and the laevigate surface of the equatorial flange, ×800. 2. Transmitted light photomicrograph, ×500. 3. Scanning electron micrograph of specimen in Fig. 2 showing the distal fovea, ×550. 4. Scanning electron micrograph. Rugate ornament of the distal surface is outside the fovea and the spines inside the fovea. ×1200.

5, 6. **Convolutispora ampla** Hoffmeister, Staplin and Malloy, 1955 113
5. Transmitted light photomicrograph, ×500. 6. Scanning electron micrograph, distal surface, ×850.

7-9. **Convolutispora florida** Hoffmeister, Staplin and Malloy, 1965 113
7. Scanning electron micrograph, proximal surface, ×1000. 8. Transmitted light photomicrograph, ×500. 9. Scanning electron micrograph of specimen in Fig. 8, distal surface, ×850.

10, 11. **Convolutispora mellita** Hoffmeister, Staplin and Malloy, 1955 113
10. Scanning electron micrograph, distal surface, ×700. 11. Transmitted light photomicrograph of specimen in Fig. 10, ×500.

12. **Convolutispora tortuosa** Urban, n. sp. 113
Scanning electron micrograph, tetrad, ×700.

EXPLANATION OF PLATE 25

Figure — Page

1-3. **Convolutispora tortuosa** Urban, n. sp. 113

1. Scanning electron micrograph, proximal surface. Tectate triradiate structure and well-developed ornament along the triradiate mark. Holotype 147F20-1, ×1200. 2. Transmitted light photomicrograph of specimen in Fig. 1, ×1000. 3. Scanning electron micrograph, proximal surface. Paratype 147F17-2, ×1150.

4-9. **Costatascyclus crenatus** Felix and Burbridge, 1967 114

4. Scanning electron micrograph, proximal surface, ×450. 5. Transmitted light photomicrograph of specimen in Fig. 8, ×500. 6. Scanning electron micrograph, distal surface of specimen in Fig. 4. "Bladder" encloses the distal side of the spore body, ×400. 7. Scanning electron micrograph showing ornament on the spore body lined in rows, ×400. 8. Scanning electron micrograph of the specimen in Fig. 5, ×450. 9. Scanning electron micrograph of a specimen showing a deflected suture suggesting a vestigial trilete condition, ×1250.

10-12. **Densosporites aculeatus** Playford, 1962 117

10. Scanning electron micrograph, proximal surface. Minute spines on the proximal surface, ×900. 11. Transmitted light photomicrograph of specimen in Fig. 10, ×900. 12. Scanning electron micrograph of specimen in Fig. 10 showing distal ornament.

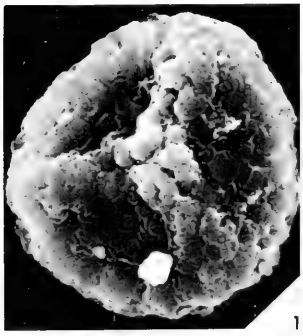
1

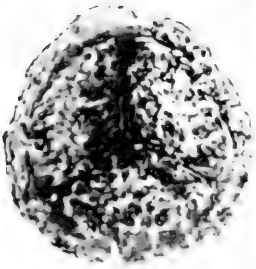
2

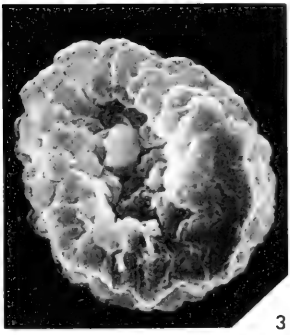
3


4

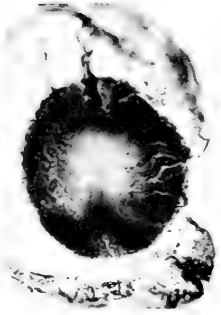
5

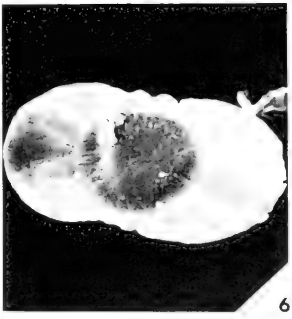
6

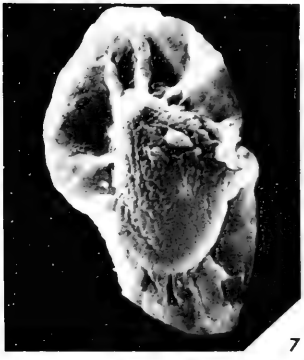
7

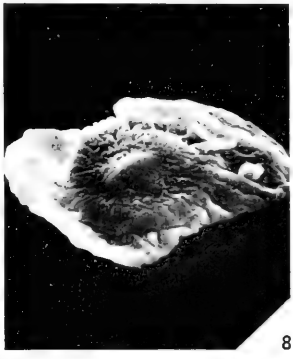
8

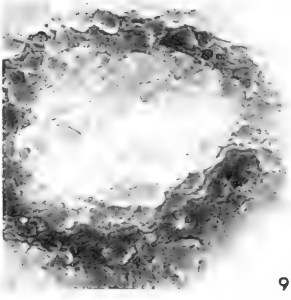
9

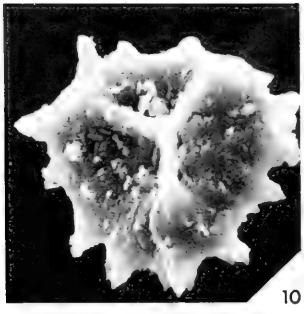
10

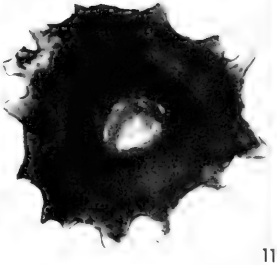
11

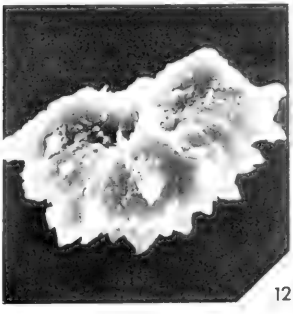
12

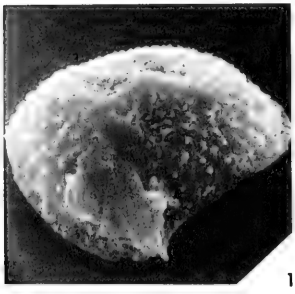
1

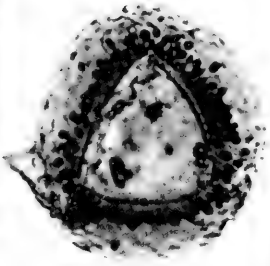
2

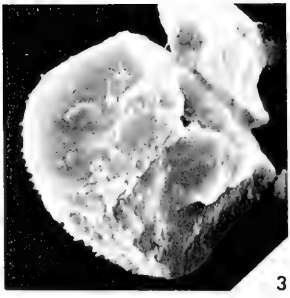
3

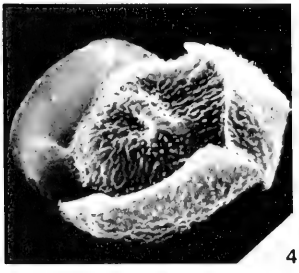
4

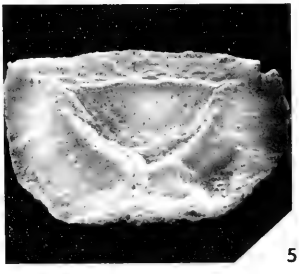
5

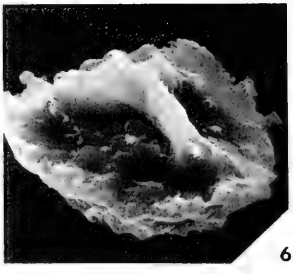
6

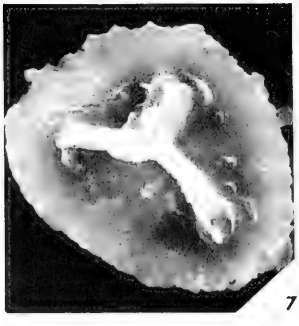
7


8

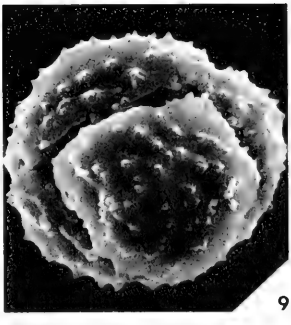
9

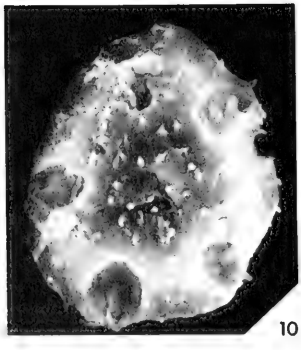
10


11

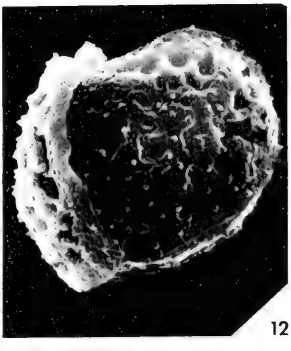
12

EXPLANATION OF PLATE 26

Figure — Page

1-5. **Densosporites hispidus** Felix and Burbridge, 1967 117

1. Scanning electron micrograph, distal surface, ×1250. 2. Transmitted light photomicrograph of specimen in Fig. 1. Vacuoles surround the central area, ×1000. 3. Scanning electron micrograph, proximal surface, ×1150. 4. Scanning electron micrograph, tetrad, ×750. 5. Scanning electron micrograph with the proximal wall of the central area removed. Vacuoles, ×1000.

6-9. **Densosporites rarispinosa** Playford, 1962 117

6. Scanning electron micrograph showing pronounced triradiate structure and distal ornament, ×1000. 7. Scanning electron micrograph of specimen in Fig. 6, proximal surface. Scattered spines on the surface, ×1000. 8. Transmitted light photomicrograph of specimen in Fig. 6, ×1000. 9. Scanning electron micrograph, tetrad. Distal ornament, ×750.

10-12. **Densosporites cavus** Urban, n. sp. 118

10. Scanning electron micrograph, distal surface. Excavations around the periphery. Holotype 147F7-1, ×1100. Transmitted light photomicrograph of specimen in Fig. 10, ×1200. 12. Scanning electron micrograph, tetrad. Variation in form of the distal excavations, ×1100.

EXPLANATION OF PLATE 27

Figure | Page

1-5. **Densosporites cavus** Urban, n. sp. 118

1. Scanning electron micrograph, proximal surface. Steep pyramidal shape of the triradiate structure and absence of proximal excavations. Paratype 147F6-1. ×1300. 2. Scanning electron micrograph edge view. Triradiate structure has collapsed into the central area and the high relief of the inner margin of the cingulum. Also note the distal excavations. Paratype 147F28-1, ×1350. 3. Scanning electron micrograph distal surface. Closely spaced excavations or channels and intervening "ribs." Paratype 147F2-1, ×1000. 4. Scanning electron micrograph of a specimen with the proximal exine removed showing the cingulum. 5. Transmitted light photomicrograph of the specimen in Fig. 4. Typical *"Radiizonates"* appearance. Paratype 147F20-2, ×1000.

6-9. **Dictyotriletes clatriformis** (Artuz), Sullivan, 1964 119

6. Scanning electron micrograph, proximal surface, ×1100. 7. Scanning electron micrograph, distal surface, ×1500. 8. Transmitted light photomicrograph of specimen in Fig. 6 ×1000. 9. Scanning electron micrograph of specimen in Fig. 6 showing detail of the triradiate structure, ×3250.

10-12. **Foveosporites insculptus** Playford, 1962 121

10. Scanning electron micrograph, proximal surface, ×850. 11. Transmitted light photomicrograph of specimen in Fig. 10, ×750. 12. Scanning electron micrograph, distal surface of the specimen in Fig. 10, ×850.


1


2

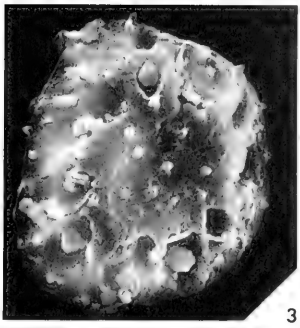
3

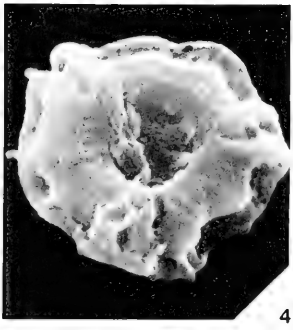
4

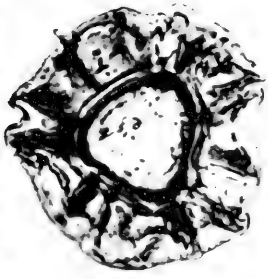
5

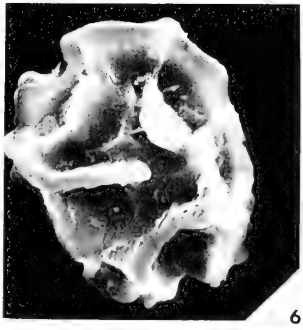
6

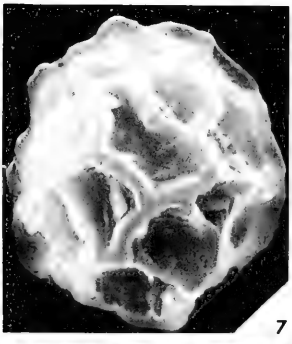
7


8


9

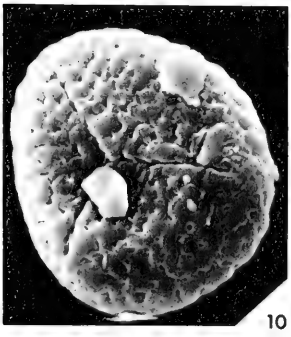
10


11

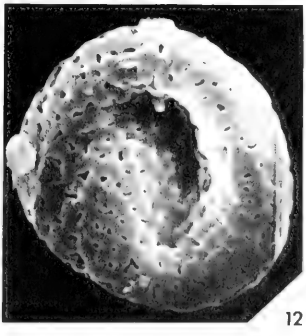
12

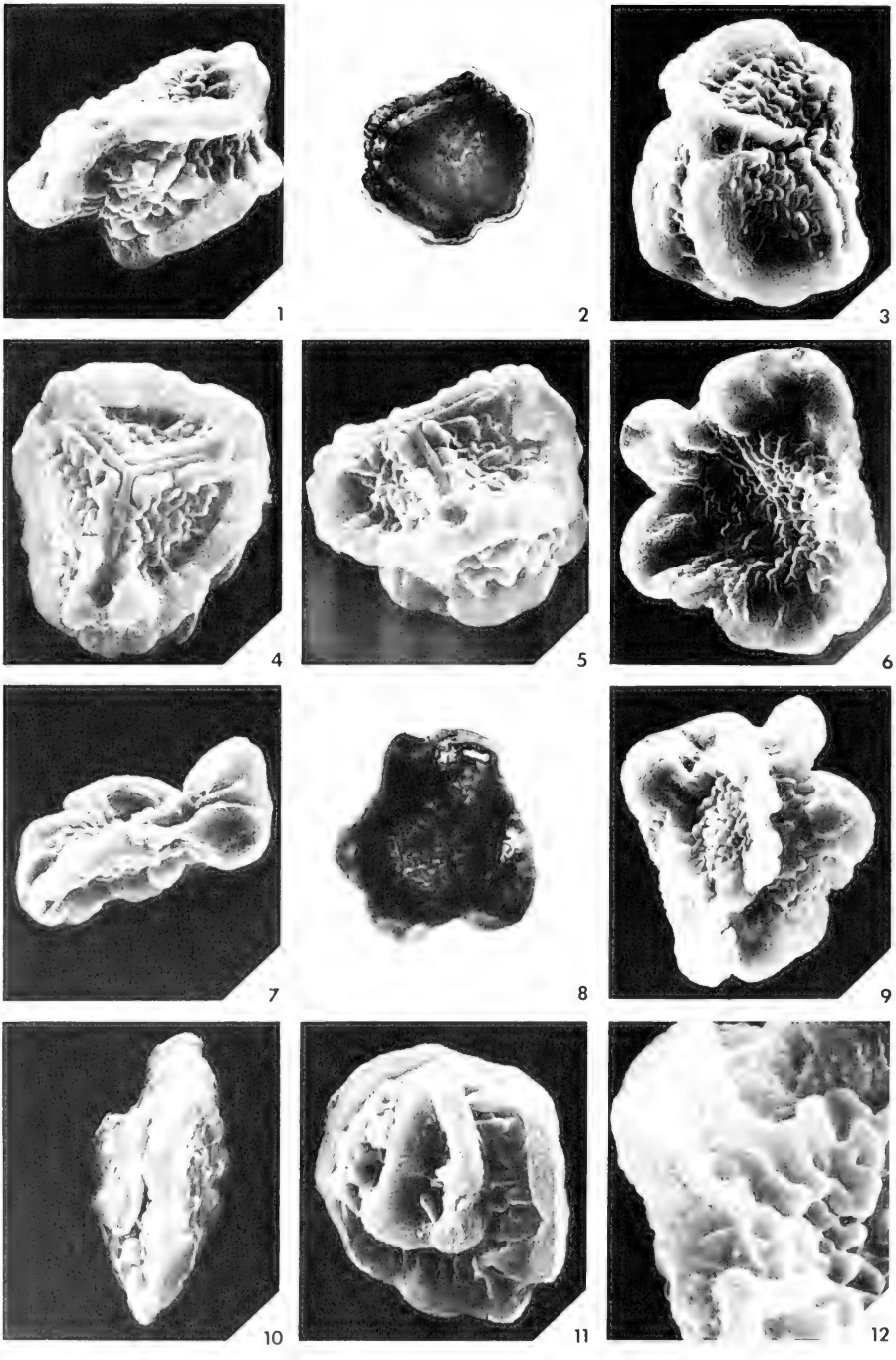
1
2
3
4
5
6
7
8
9
10
11
12

EXPLANATION OF PLATE 28

Figure | Page

1-12. **Dorheimisporites inflatus** Urban, n. gen., n. sp. 120

1. Scanning electron micrograph, edge view. Equatorial and distal structures. Holotype 147F31-1, ×850. 2. Transmitted light photomicrograph of specimen in Fig. 1, ×500. 3. Scanning electron micrograph of the proximal surface of the specimen in Fig. 1, ×850. 4. Scanning electron micrograph, proximal surface. Tectate triradiate structure. Paratype 147F20-3, ×1200. 5. Scanning electron micrograph of the specimen in Fig. 4, edge view, ×1100. 6. Scanning electron micrograph, proximal surface. See expansion of the equatorial structure. Paratype 147F27A1-1, ×750. 7. Scanning electron micrograph of specimen in Fig. 6 showing the inflated nature of the equatorial structure, ×700. 8. Transmitted light photomicrograph of specimen in Fig. 6, ×500. 9. Scanning electron micrograph of specimen in Fig. 6 showing the distal structure inflated and connecting with the equatorial structure, ×700. 10. Scanning electron micrograph, edge view. Paratype 147F27A1-2, ×950. 11. Scanning electron micrograph, distal surface of specimen in Fig. 10, ×1000. 12. Scanning electron micrograph of the specimen in Fig. 6 showing the abrupt change in character of the outer wall in the equatorial region, ×2250.

EXPLANATION OF PLATE 29

Figure — Page

1, 2. **Florinites visendus** (Ibrahim), Schopf, Wilson and Bentall, 1944 121

1. Scanning electron micrograph, distal surface, ×325. 2. Transmitted light photomicrograph of specimen in Fig. 1, ×300.

3-6. **Florinites guttatus** Felix and Burbridge, 1967 121

3. Scanning electron micrograph, proximal surface, ×500. 4. Scanning electron micrograph of the distal surface of the specimen in Fig. 3. Saccus completely encloses the proximal and distal surfaces of the spore body, ×500. 5. Transmitted light photomicrograph of the specimen in Fig. 4. 6. Scanning electron micrograph of proximal surface of spore body of specimen in Fig. 3, ×1500.

7-12. **Gorgonispora magna** (Felix and Burbridge) Urban, comb. new 122

7. Scanning electron micrograph, distal surface, 147F31, ×1500. 8. Transmitted light photomicrograph, reillustration of the holotype specimen. See Felix and Burbridge (1967, p. 399) for location designation, ×375. 9. Dark field photomicrograph. Triradiate structure, ×375. 10. Scanning electron micrograph showing the relationship of the distal ornament to the equatorial structure. 147F32-1, ×850. 11. Scanning electron micrograph of the triradiate structure of specimen in Fig. 10. Tectate triradiate ridges are bordered by the convolutions, ×2250. 12. Scanning electron micrograph, proximal surface. Note the convolution along the equator. 147F31-3, ×700.


1

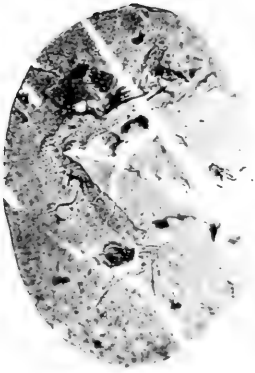
2

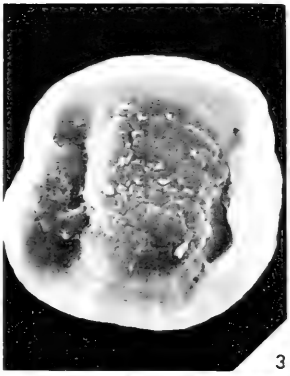
3

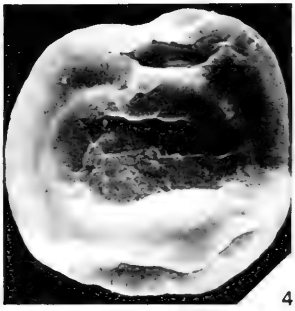
4

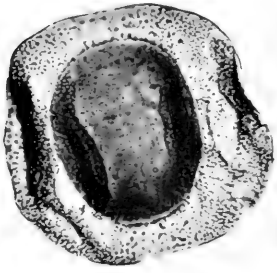
5


6

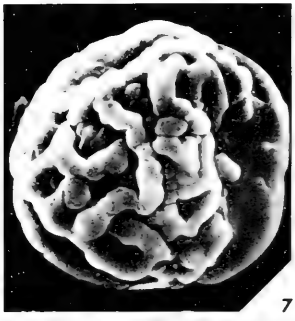
7


8


9

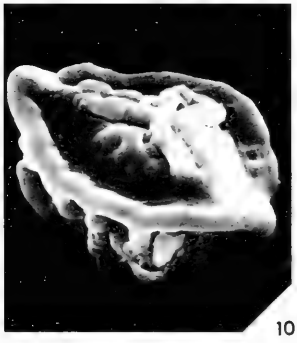
10


11


12


1


2

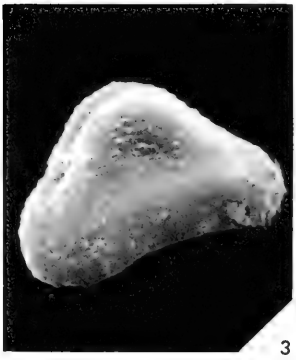
3

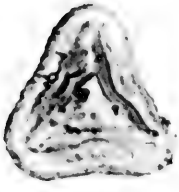
4

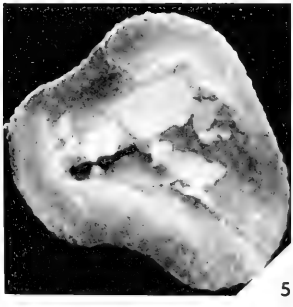
5

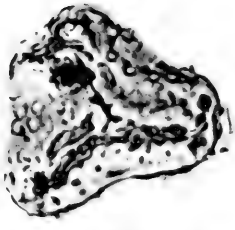
6

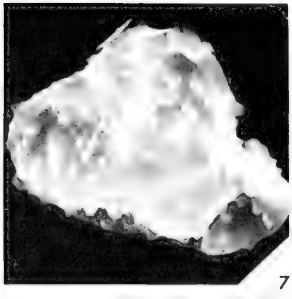
7

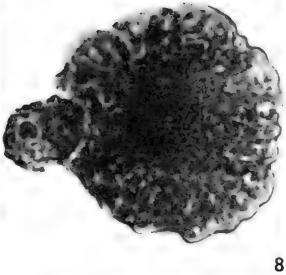
8

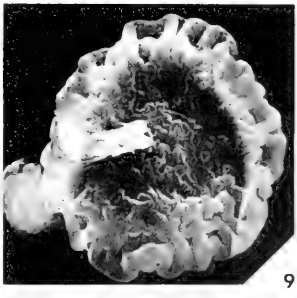
9

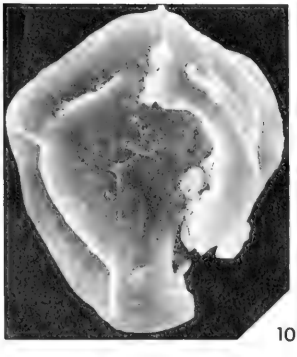
10

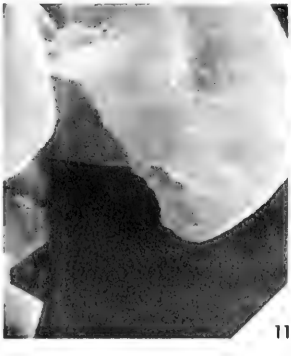
11

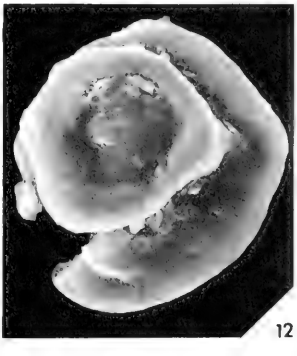
12

EXPLANATION OF PLATE 30

Figure — Page

1, 2. **Granulatisporites granulatus** (Ibrahim), Potonié and Kremp, 1954 124
1. Scanning electron micrograph, edge and distal surface, ×1400. 2. Transmitted light photomicrograph of specimen in Fig. 1, ×1000.

3-5. **Granulatisporites microgranifer** Ibrahim, 1933 124
3. Scanning electron micrograph, distal surface, ×1750. 4. Transmitted light photomicrograph of specimen in Fig. 3. ×1000. 5. Scanning electron micrograph, proximal surface, ×1500.

6, 7. **Granulatisporites tuberculatus** Hoffmeister, Staplin and Malloy, 1955 125
6. Transmitted light photomicrograph, ×1000. 7. Scanning electron micrograph of the distal surface of the specimen in Fig. 6. ×1500.

8, 9. **Hymenospora** cf. **H. caperata** Felix and Burbridge, 1967 125
8. Transmitted light photomicrograph, × 1000. 9. Scanning electron micrograph of the specimen in Fig. 8, ×1150.

10-12. **Knoxisporites stephanephorus** Love, 1960 125
10. Scanning electron micrograph, proximal surface. Tectate triradiate structure, ×850. 11. Scanning electron micrograph of the break in the equatorial region of the specimen in Figure 10. Equatorial structure is simply an exine fold, ×2250. 12. Scanning electron micrograph of the distal surface of the specimen in Fig. 10, ×700.

EXPLANATION OF PLATE 31

Figure		Page
1-3.	**Knoxisporites stephanephorus** Love, 1960 ..... 1. Scanning electron micrograph, distal surface, ×1200. 2. Transmitted light photomicrograph of specimen in Fig. 3. 3. Scanning electron micrograph, distal surfaces, ×1500.	125
4-7.	**Knoxisporites triradiatus** Hoffmeister, Staplin and Malloy, 1955 ..... 4. Scanning electron micrograph, proximal surface, ×500. 5. Transmitted light photomicrograph of the specimen in Fig. 4. 6. Scanning electron micrograph showing the relationship between the proximal and distal structures, ×1000. 7. Scanning electron micrograph of the distal surface of the specimen in Fig. 6. ×900.	126
8, 9.	**Knoxisporites** sp. ..... 8. Transmitted light photomicrograph, distal focus of specimen in Fig. 9, 147F28-2, ×500. 9. Scanning electron micrograph of the proximal surface, ×800.	126
10-12.	**Kochisporites dentatus** Urban, n. gen., n. sp. ..... 10. Scanning electron micrograph, proximal surface. Baculae on the proximal surface and tectate triradiate structure. Holotype 147F20-4, ×750. 11. Transmitted light photomicrograph of the specimen in Fig. 10, ×750. 12. Scanning electron micrograph of specimen in Fig. 10 showing a portion of the distal surface, ×750.	127

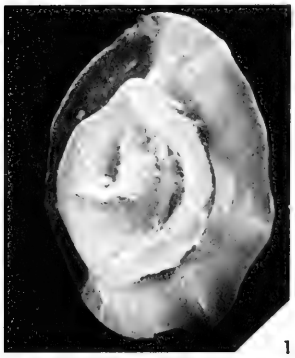
1

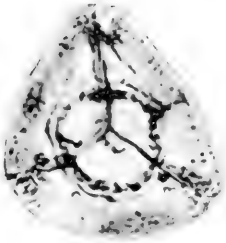
2


3

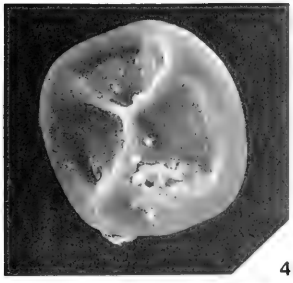
4


5

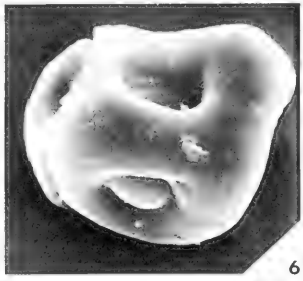
6

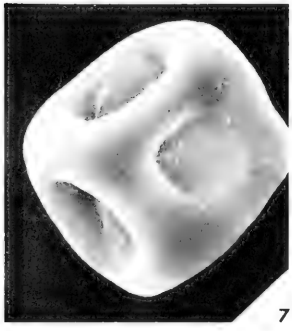
7


8

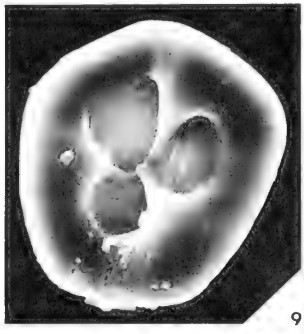
9

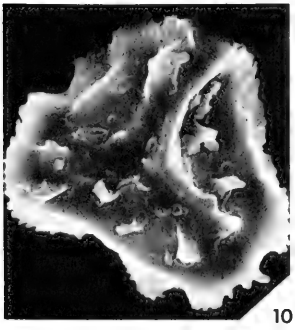
10


11

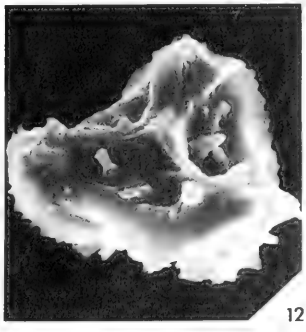
12


1

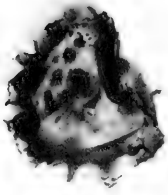
2


3

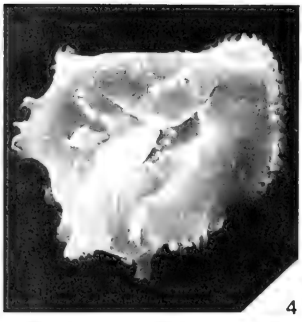
4

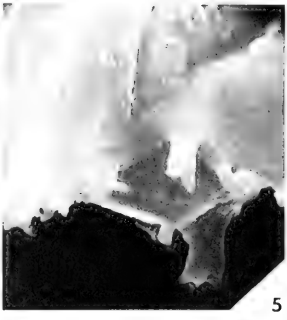
5

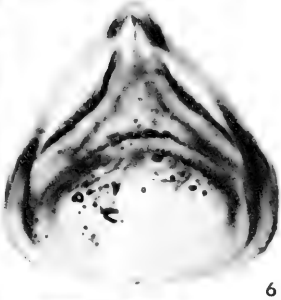
6

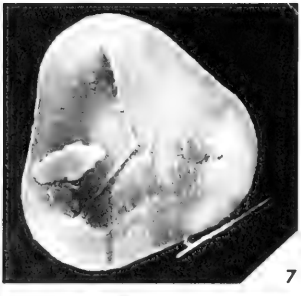
7

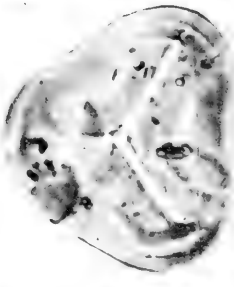
8

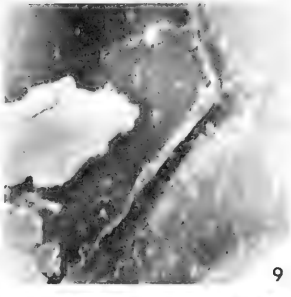
9

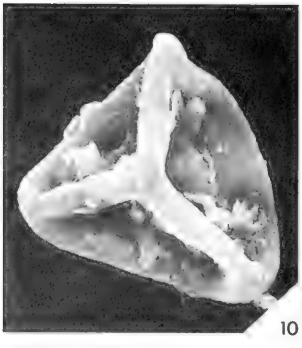
10


11


12

EXPLANATION OF PLATE 32

Figure — Page

1-5. **Kochisporites dentatus** Urban, n. gen., n. sp. 127
1. Scanning electron micrograph, distal surface, Paratype 147F31-4, ×800. 2. Transmitted light photomicrograph, distal focus of specimen in Fig. 1. 3. Scanning electron micrograph of specimen in Fig. 1 showing the morphology of the distal ornament, ×2500. 4. Scanning electron micrograph, proximal surface. Paratype 147F21-1, ×750. 5. Scanning electron micrograph of specimen in Fig. 4 showing the variable morphology of the equatorial margin, ×2100.

6. **Leiotriletes pyramidatus** Sullivan, 1964 128
Transmitted light photomicrograph, ×1000.

7-9. **Leiotriletes subintortus** (Waltz), Ischenko, 1952 128
7. Scanning electron micrograph, proximal surface, ×1000. 8. Transmitted light photomicrograph of specimen in Fig. 7, ×1000. 9. Scanning electron micrograph of specimen in Fig. 7 showing the tectate triradiate structure, ×3000.

10-12. **Leiotriletes** cf. **L. tumidus** Butterworth and Williams, 1958 128
10. Scanning electron micrograph, proximal surface, ×1000. 11. Transmitted light photomicrograph of specimen in Fig. 10, ×1000. 12. Scanning electron micrograph of specimen in Fig. 10 showing morphology of the triradiate structure, ×2850.

EXPLANATION OF PLATE 33

Figure — Page

1-3. **Leiotriletes angulatus** Urban, n. sp. 129
1. Scanning electron micrograph, proximal surface. See character of the triradiate structure and the corners of the spore. Holotype 147F3-1, ×600. 2. Transmitted light photomicrograph of specimen in Fig. 1. 3. Scanning electron micrograph, proximal surface. Paratype 147F20-5, ×1100.

4-6. **Leiotriletes labrum** Urban, n. sp. 129
4. Scanning electron micrograph, proximal surface. Holotype 147F2-2, ×500. 5. Transmitted light photomicrograph, of specimen in Fig. 4, ×500. 6. Scanning electron micrograph of a specimen showing a common variation in form, 147F20-6, ×700.

7, 8. **Leiotriletes** sp. 130
7. Scanning electron micrograph, proximal surface, Holotype 147F10-1, ×1000. 8. Transmitted light photomicrograph of specimen in Fig. 7, ×750.

9-12. **Lophotriletes fatihi** Artuz, 1957 130
9. Scanning electron micrograph, showing both proximal and distal surfaces, ×1000. 10. Scanning electron micrograph, proximal surface, ×1700. 11. Transmitted light photomicrograph of specimen in Fig. 10, ×750. 12. Scanning electron micrograph of triradiate structure of specimen in Fig. 10, ×3000.

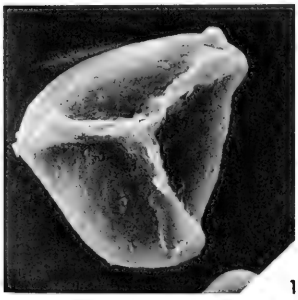
1


2

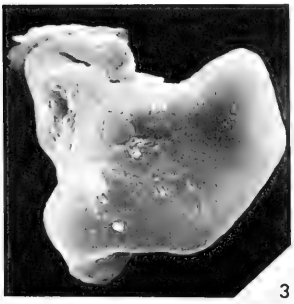
3

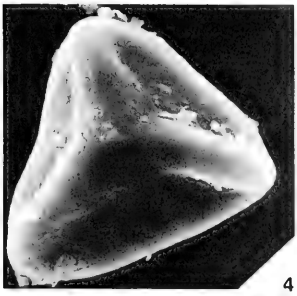
4


5

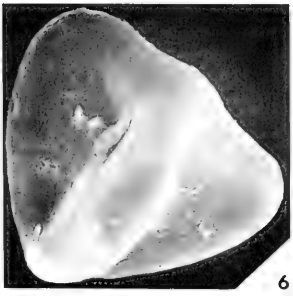
6

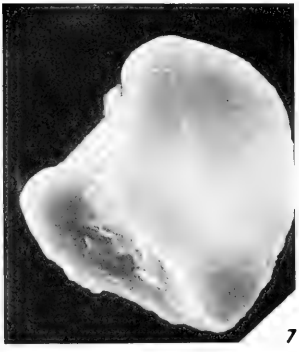
7

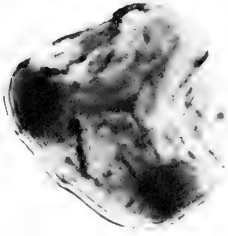
8


9

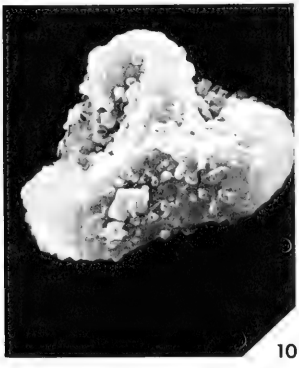
10


11


12

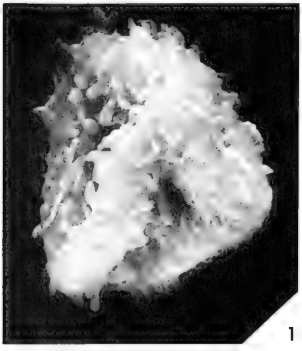
1

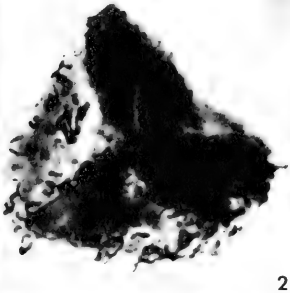
2

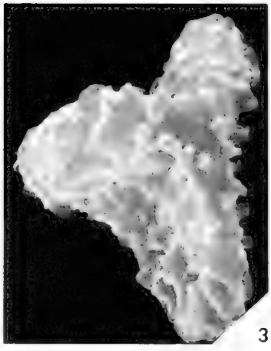
3

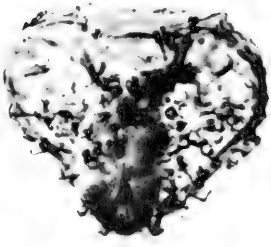
4

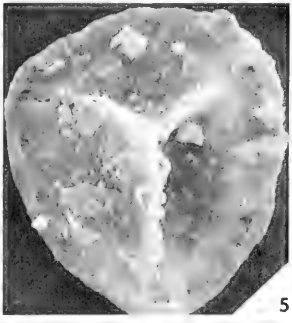
5

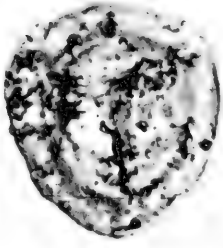
6


7

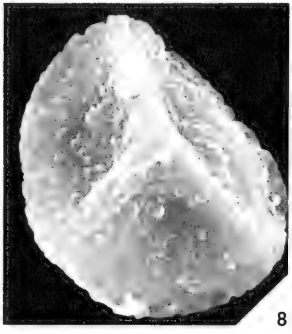
8

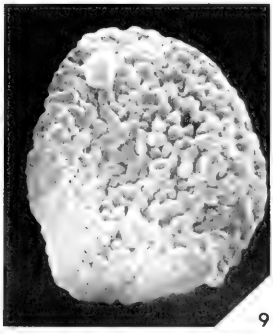
9

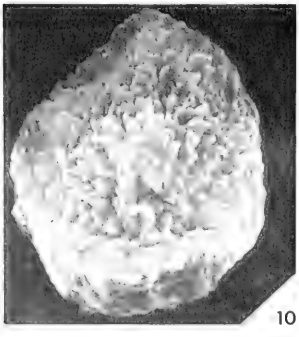
10

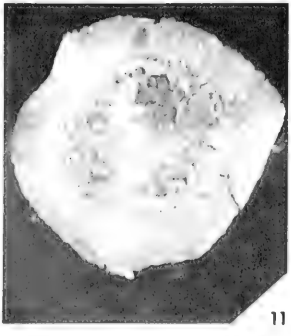
11


12

EXPLANATION OF PLATE 34

Figure — Page

1, 2. **Lophotriletes labiatus** Sullivan, 1964 130
1. Scanning electron micrograph, distal surface, ×1200. 2. Transmitted light photomicrograph of specimen in Fig. 1, ×1000.

3, 4. **Lophotriletes obtusus** Felix and Burbridge, 1967 130
3. Scanning electron micrograph, distal surface, ×1100. 4. Transmitted light photomicrograph of specimen in Fig. 3. ×750.

5-12. **Lycospora uber** (Hoffmeister, Staplin and Malloy), Staplin, 1960 131
5. Scanning electron micrograph, proximal surface, ×1500. 6. Transmitted light photomicrograph of specimen in Fig. 5, ×1000. 7. Scanning electron micrograph, proximal surface, ×1500. 8. Scanning electron micrograph, proximal surface, ×1600. 9. Scanning electron micrograph of the distal surface of the specimen in Fig. 8, ×1600. 10. Scanning electron micrograph, distal surface, ×1300. 11. Scanning electron micrograph, distal surface, ×1300. 12. Scanning electron micrograph, tetrad, ×1000.

EXPLANATION OF PLATE 35

Figure — Page

1-4. **Microreticulatisporites concavus** Butterworth and Williams, 1958 132

1. Scanning electron micrograph, distal surface, ×1000. 2. Transmitted light photomicrograph of the specimen in Fig. 1, ×1000. 3. Scanning electron micrograph, distal surface, ×1350. 4. Scanning electron micrograph, proximal surface, ×1300.

5-7. Cf. **Microreticulatisporites punctatus** Knox, 1950 133

5. Scanning electron micrograph, distal surface, ×1000. 6. Transmitted light photomicrograph of the specimen in Fig. 5, ×1000. 7. Scanning electron micrograph showing proximal and distal surfaces, ×750.

8-10. **Monoletes** cf. **ovatus** Schopf, 1936 133

8. Scanning electron micrograph, proximal surface, ×290. 9. Scanning electron micrograph of specimen in Fig. 8. Single distal groove, ×290. 10. Transmitted light photomicrograph of specimen in Fig. 8, ×375.

11, 12. **Monoletes winslowi** Urban, n. sp. 133

11. Scanning electron micrograph, proximal surface. Holotype 147F38-1, ×425. 12. Transmitted light photomicrograph of specimen in Fig. 11. Distinct spore body, ×375.

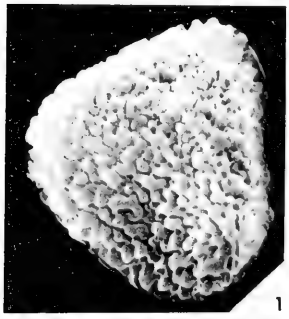
1

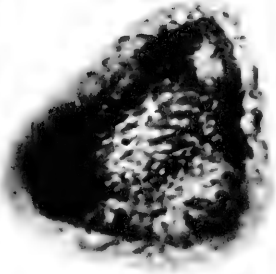
2

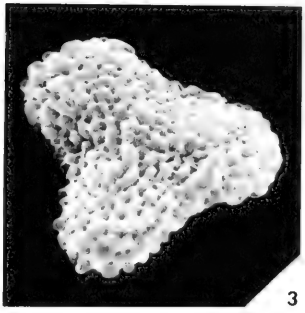
3

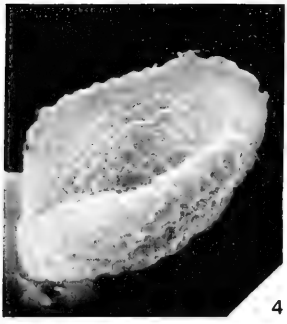
4


5

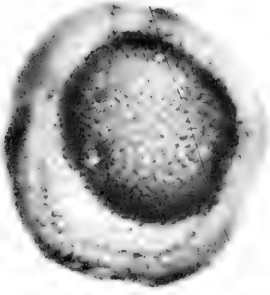
6

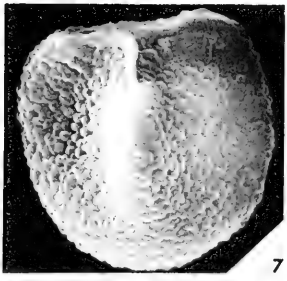
7

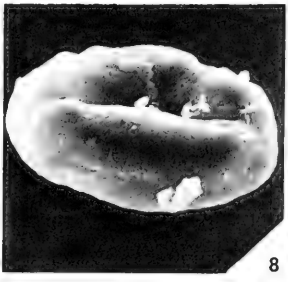
8

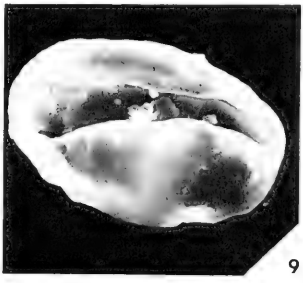
9


10

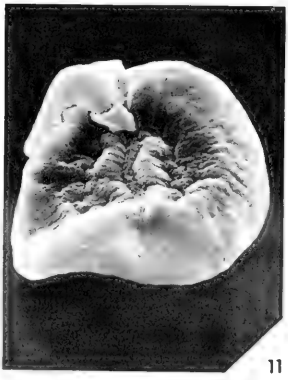
11


12


1

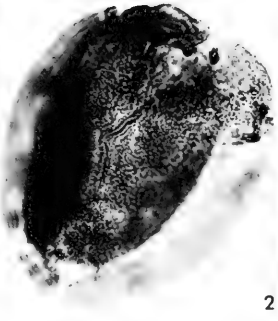
2

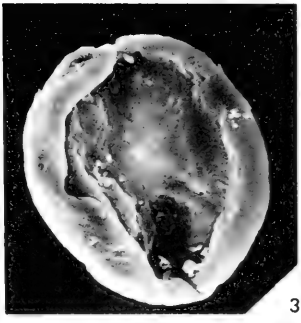
3

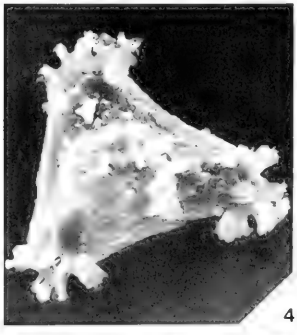
4


5

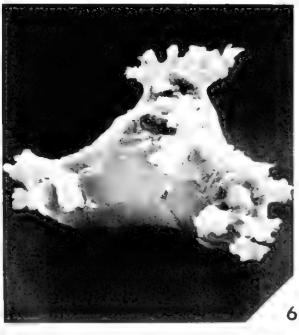
6

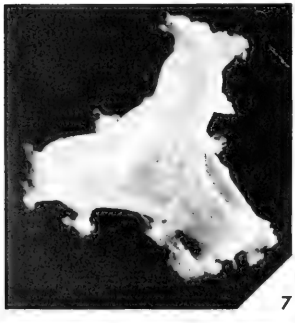
7


8

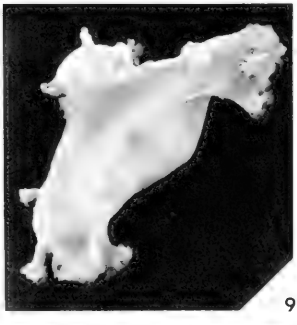
9


10


11

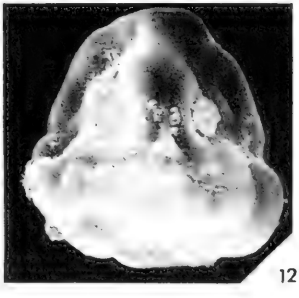
12

EXPLANATION OF PLATE 36

Figure — Page

1-3. **Monoletes winslowi** Urban, n. sp. — 133
1. Scanning electron micrograph of the monolete structure of the specimen on Plate 15, Fig. 11, ×1400. 2. Transmitted light photomicrograph, proximal focus. Deflected monolete suture. Paratype 147F36A-1, × 375. 3. Scanning electron micrograph of the distal surface of the specimen in Fig. 3.

4-6. **Mooreisporites fustus** Neves, 1958 — 134
4. Scanning electron micrograph distal surface, ×500. Distal ornament. 5. Transmitted light photomicrograph of specimen in Fig. 4 ×500. 6. Scanning electron micrograph of specimen in Fig. 4 showing a part of the proximal surface, ×550.

7-11. **Mooreisporites bicornis** Urban, n. sp. — 134
7. Scanning electron micrograph, proximal surface. Paired baculae just below the auriculae. Holotype 147F32-2. ×500. 8. Transmitted light photomicrograph of specimen in Fig. 7, ×290. 9. Scanning electron micrograph of specimen showing proximal and distal surfaces. Paratype 147F25-1, ×750. 10. Scanning electron micrograph, side view of Fig. 9, ×900. 11. Scanning electron micrograph of tectate triradiate structure of specimen in Fig. 9, ×1750.

12. Cf. **Murospora** sp. — 135
Scanning electron micrograph, distal surface, 147F38-2, ×500.

EXPLANATION OF PLATE 37

Figure — Page

1, 2. Cf. **Murospora** sp. 135
1. Scanning electron micrograph, proximal surface, 147F22-1, ×600. 2. Transmitted light photomicrograph of specimen in Fig. 1, ×500.

3-6. **Neoraistrikia variornamenta** Urban, n. sp. 135
3. Scanning electron micrograph, distal surface. Paratype 147F22-2, ×850. 4. Transmitted light photomicrograph of specimen in Fig. 3, ×1000. 5. Scanning electron micrograph of specimen showing proximal and distal surfaces. Note the variation of ornament. Holotype 147F32-3, ×900. 6. Transmitted light photomicrograph of specimen in Fig. 5, ×500.

7, 8. **Potoniesporites elegans** (Wilson and Kosanke), Wilson and Venkatachala, 1964 136
7. Scanning electron micrograph, proximal surface, ×425. 8. Transmitted light photomicrograph of specimen in Fig. 7, ×375.

9-11. **Procoronaspora fasciculata** Love, 1960 136
9. Scanning electron micrograph, distal surface, ×1100. 10. Scanning electron micrograph of specimen in Fig. 9, ×1150. 11. Transmitted light photomicrograph of specimen in Fig. 9, ×1000.

12. **Proprisporites** cf. **P. laevigatus** Neves, 1961 137
Scanning electron micrograph, distal surface, ×500.

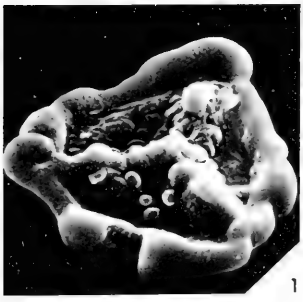
1

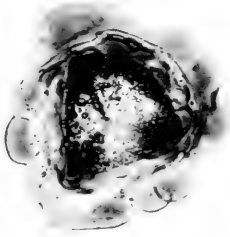
2

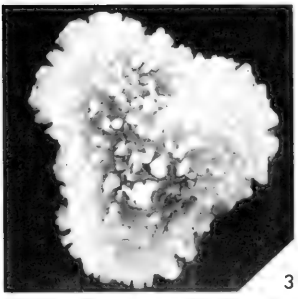
3

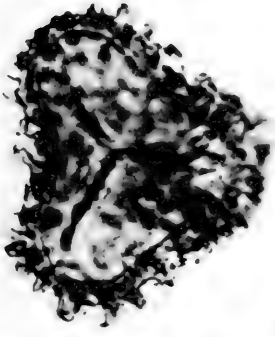
4

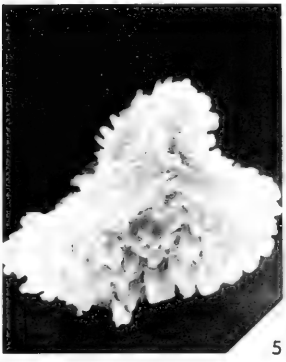
5

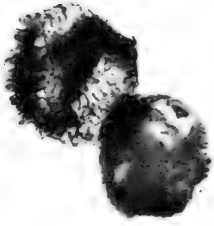
6

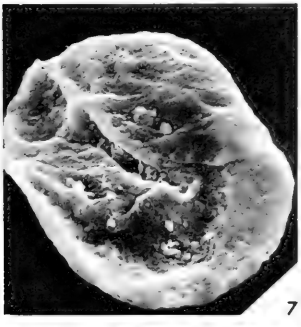
7

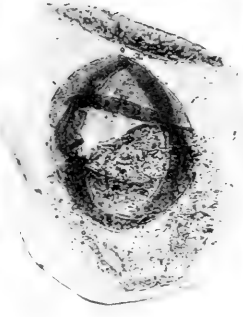
8

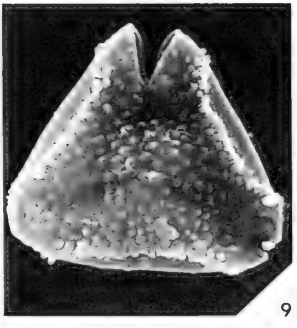
9

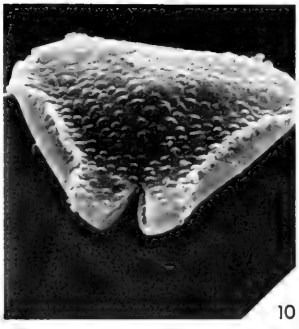
10

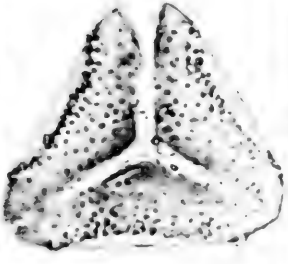
11

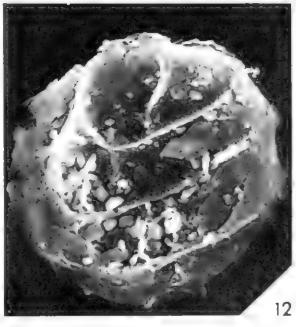
12

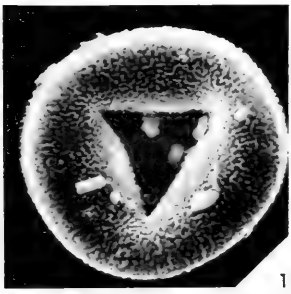
1


2

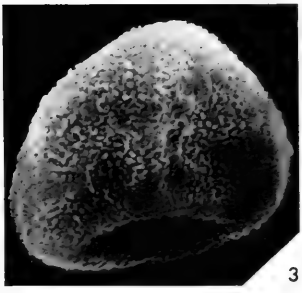
3

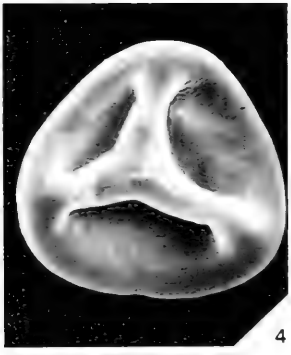
4

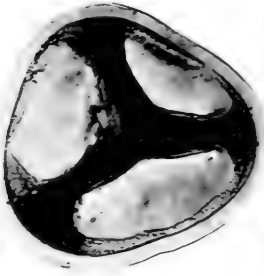
5

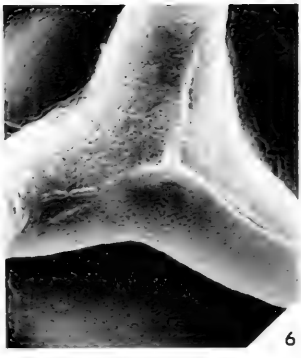
6

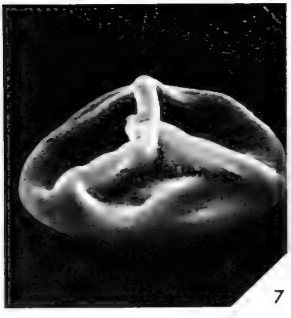
7

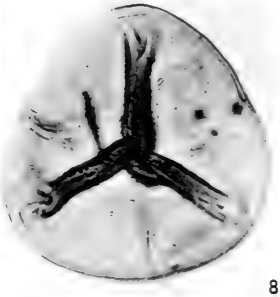
8

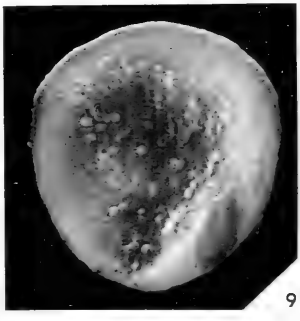
9

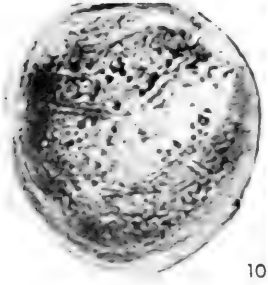
10

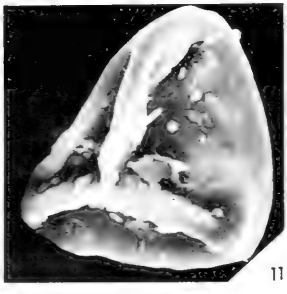
11

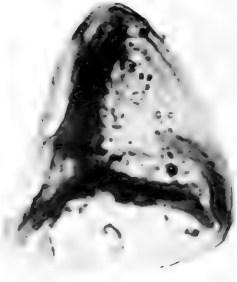
12

EXPLANATION OF PLATE 38

Figure — Page

1-3. **Punctatisporites heterofiliferus** Felix and Burbridge, 1967 ..137
1. Scanning electron micrograph, proximal surface, ×850. 2. Transmitted light photomicrograph of specimen in Fig. 1, ×500. 3. Scanning electron micrograph showing proximal and distal surfaces, ×1000.

4-6. **Punctatisporites** cf. **P. obesus** (Loose), Potonié and Kremp, 1955 137
4. Scanning electron micrograph, proximal surface, ×500. 5. Transmitted light photomicrograph of specimen in Fig. 4, ×500. 6. Scanning electron micrograph showing details of the triradiate structure, ×1500.

7, 8. **Punctatisporites incomptus** Felix and Burbridge, 1967 137
7. Scanning electron micrograph, proximal surface, ×500. 8. Transmitted light photomicrograph of the specimen in Fig. 7.

9, 10. **Punctatisporites planus** Hacquebard, 1957 138
9. Scanning electron micrograph, distal surface. The small circular items are not part of the spore, ×1100. 10. Transmitted light photomicrograph of specimen in Fig. 9.

11, 12. **Punctatisporites validus** Felix and Burbridge, 1967 138
11. Scanning electron micrograph, proximal surface, ×550. 12. Transmitted light photomicrograph of specimen in Fig. 11, ×500.

EXPLANATION OF PLATE 39

Figure — Page

1, 2. **Raistrickia** cf. **R. saetosa** (Loose), Schopf, Wilson and Bentall, 1944 139

1. Scanning electron micrograph, distal surface, ×650. 2. Transmitted light photomicrograph of specimen in Fig. 1, ×500.

3-8. **Raistrickia densa** Urban, n. sp. 139

3. Scanning electron micrograph, distal surface. Paratype 147F33-1, ×1200. 4. Scanning electron micrograph, proximal surface, Holotype 147F27-1, ×1000. 5. Transmitted light photomicrograph of specimen in Fig. 4, ×1000. 6. Scanning electron micrograph, proximal surface. Note the reduction of ornament on the proximal surface, Paratype 147F29-1. 7. Scanning electron micrograph, edge view ×100. 8. Scanning electron micrograph showing detail of the partate baculae, ×3500.

9-12. **Reinschospora** cf. **R. speciosa** (Loose), Schopf, Wilson and Bentall, 1944 140

9. Scanning electron micrograph, proximal surface, ×600. 10. Scanning electron micrograph showing details of the corona on the specimen in Fig. 9, ×1750. 11. Transmitted light photomicrograph of the specimen in Fig. 9, ×500. 12. Scanning electron micrograph showing details of the trilete of the specimen in Fig. 9, ×1750.

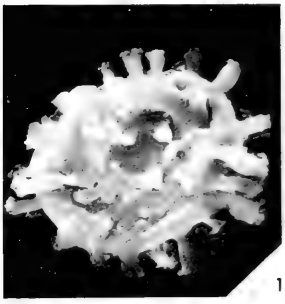
1

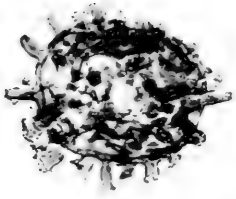
2

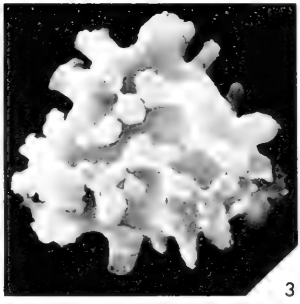
3

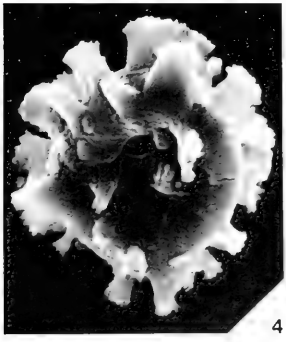
4


5

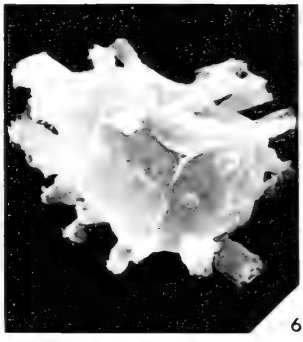
6


7


8


9


10


11


12

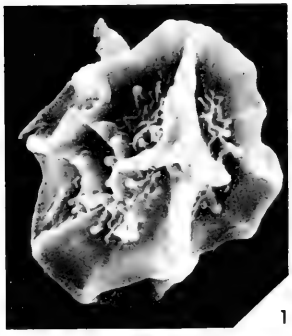
1


2

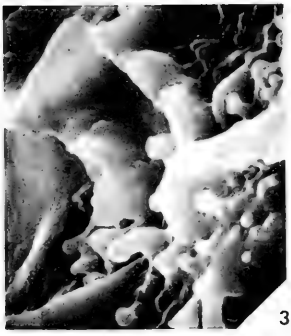
3

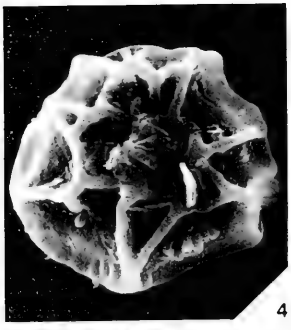
4


5


6

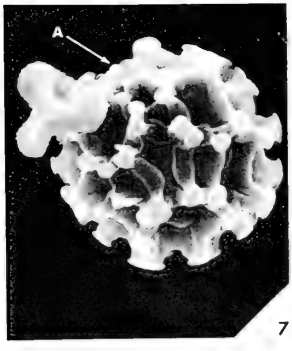

7


8


9

10

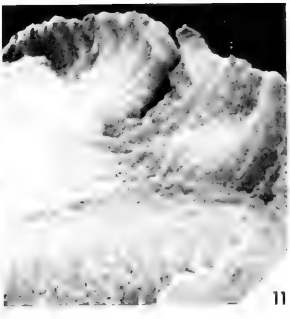
11

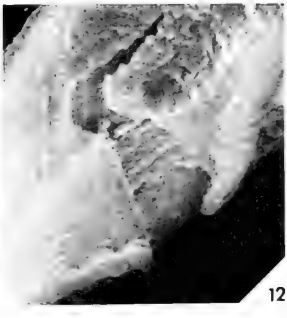
12

EXPLANATION OF PLATE 40

Figure — Page

1-6. **Reticulatisporites danzei** Agrali, 1965, comb. new 141

1. Scanning electron micrograph showing the proximal surface and a part of the distal surface. Note the tectate triradiate ridges, proximal ornament, and distal and equatorial muri. ×800. 2. Transmitted light photomicrograph of the specimen in Fig. 1, ×750. 3. Scanning electron micrograph showing details of the triradiate structure and proximal surface ornament. 4. Scanning electron micrograph distal surface. Sparseness of ornament inside the lumina, ×850. 5. Transmitted light photomicrograph of the specimen in Fig. 4. "Zoned" appearance of the muri, ×500. 6. Scanning electron micrograph, distal surface, ×500.

7-9. **Reticulatisporites peltatus** Playford, 1962 142

7. Scanning electron micrograph. The triradiate structure is located just to the right of the small spore (point A), ×600. 8. Transmitted light photomicrograph of the specimen in Fig. 7, ×600. 9. Scanning electron micrograph showing detail morphology of the ornament, ×2100.

10-12. **Reinschospora speciosa** (Loose), Schopf, Wilson and Bentall, 1944 140

10. Scanning electron micrograph, distal surface. Note the break in the corona and outer exoexine at point A, ×750. 11. Scanning electron micrograph showing detail of the distal ornament, ×1300. 12. Scanning electron micrograph showing the corona is formed by an extension of the outer exoexine which encompasses the entire spore, ×2100.

EXPLANATION OF PLATE 41

Figure — Page

1-5. **Savitrisporites nux** (Butterworth and Williams), Smith and Butterworth, 1967 142

1. Scanning electron micrograph, proximal surface, ×700. 2. Transmitted light photomicrograph of the specimen in Fig. 1, ×500. 3. Scanning electron micrograph, showing the tectate triradiate structure and the ornament on the proximal surface, ×2050. 4. Scanning electron micrograph, distal surface. This specimen compares closely to the holotype illustration of Butterworth and Williams (1958), ×850. 5. Transmitted light, photomicrograph of the specimen in Fig. 4, ×500.

6, 9. **Schulzospora elongata** Hoffmeister, Staplin and Malloy, 1955 143

6. Scanning electron micrograph, distal surface, ×500. 9. Transmitted light photomicrograph of specimen in Fig. 6, ×1000.

7, 8, 10. **Secarisporites remotus** Neves, 1961 143

7. Transmitted light photomicrograph of specimen in Fig. 10, ×1000. 8. Scanning electron micrograph, distal surface, ×1100. 10. Scanning electron micrograph of the proximal surface of specimen in Fig. 7, ×1250.

11, 12. **Simonozonotriletes intortus** (Waltz), Potonié and Kremp, 1954 143

11. Transmitted light photomicrograph, ×500. 12. Scanning electron micrograph of the proximal surface of the specimen in Fig. 11, ×900.

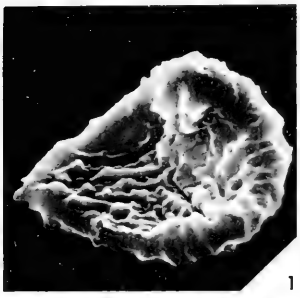
1


2

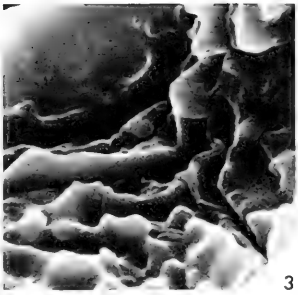
3

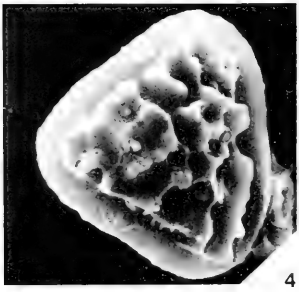
4


5

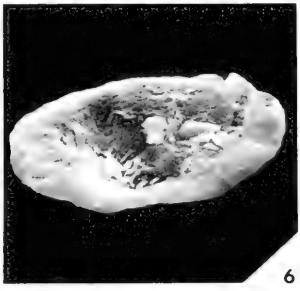
6


7

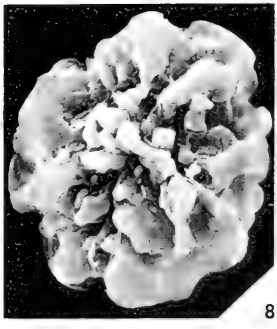
8

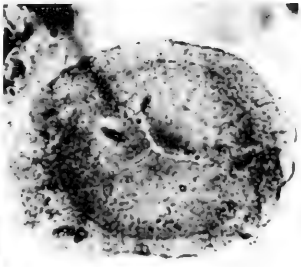
9

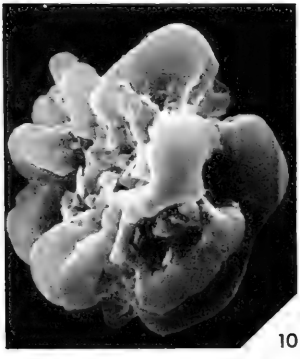
10


11

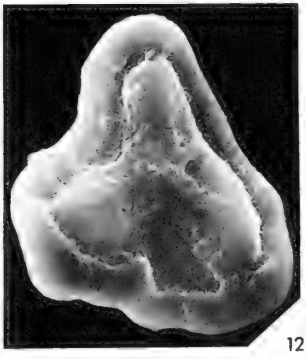
12

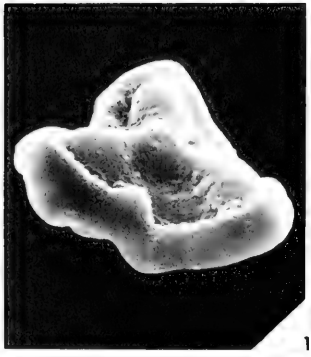
1

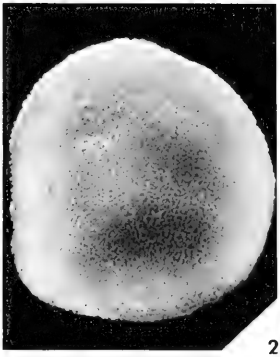
2

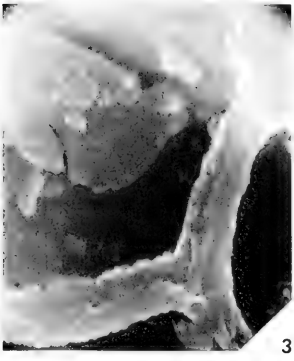
3

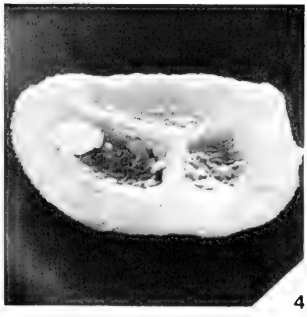
4


5

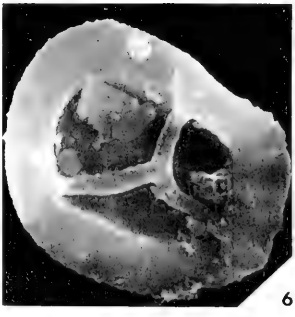
6


7

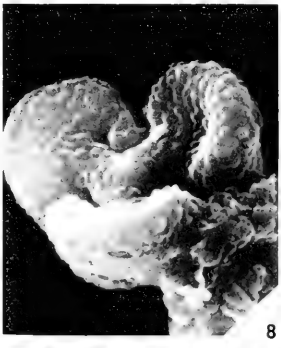
8

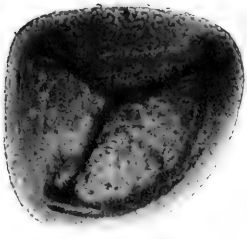
9

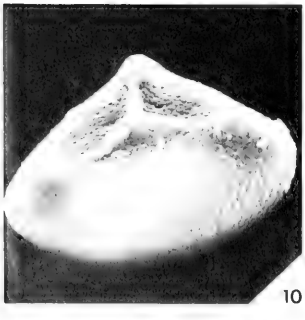
10

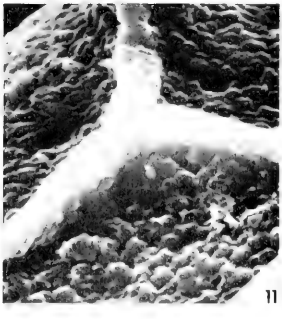
11

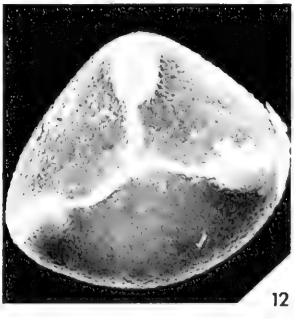
12

EXPLANATION OF PLATE 42

Figure — Page

1. **Simozonotriletes intortus** (Waltz), Potonié and Kremp, 1954 143
   Scanning electron micrograph showing the nature of the equatorial structure, ×950.

2-6. **Stenozonotriletes lycosporoides** (Butterworth and Williams), Smith and Butterworth, 1967 144
   2. Scanning electron micrograph, distal surface, ×1400. 3. Scanning electron micrograph of the tectate triradiate structure of the specimen in Fig. 6, ×4250. 4. Scanning electron micrograph, ×1500. 5. Transmitted light photomicrograph of specimen in Fig. 4. 6. Scanning electron micrograph, proximal surface, ×400.

7, 8. **Tantillus triquetrus** Felix and Burbridge, 1967 144
   7. Transmitted light photomicrograph, of specimen in Fig. 9, ×1500. 8. Scanning electron micrograph, proximal surface, ×1600.

9-12. **Trimontisporites granulatus** Urban, n. gen., n. sp. 145
   9. Transmitted light photomicrograph of specimen in Figs. 10-12. Holotype 147F21-2, ×500. 10. Scanning electron micrograph showing the nature of the triradiate structure, ×600. 11. Scanning electron micrograph of the triradiate structure of Fig. 10, ×2250. 12. Scanning electron micrograph, proximal surface, ×1200.

EXPLANATION OF PLATE 43

Figure — Page

1-4. **Trimontisporites granulatus** Urban, n. gen., n. sp. 145

1. Transmitted light photomicrograph of specimen in Fig. 2. Paratype 147F29-2, ×500. 2. Scanning electron micrograph, proximal surface, ×650. 3. Transmitted light photomicrograph of specimen in Fig. 4. Paratype 147F31-5, ×500. 4. Scanning electron micrograph, proximal surface, ×500.

5-8. **Trimontisporites contortus** Urban, n. sp. 146

5. Transmitted light photomicrograph of specimen in Fig. 6. Holotype 147F3-1, ×500. 6. Scanning electron micrograph, proximal surface, ×750. 7. Transmitted light photomicrograph of specimen in Fig. 9. Paratype 147F20-7, ×500. 8. Scanning electron micrograph, proximal surface, ×850.

9-12. **Trimontisporites rugosus** Urban, n. sp. 147

9. Transmitted light photomicrograph of specimen in Fig. 12. Holotype 147F27-2, ×1000. 10. Scanning electron micrograph, distal surface of specimen in Fig. 11. Paratype 147F30-1, ×1050. 11. Transmitted light photomicrograph, proximal focus, ×1000. 12. Scanning electron micrograph proximal surface, ×1100.

1

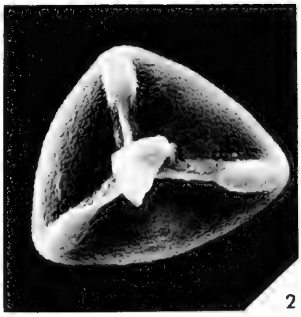

2

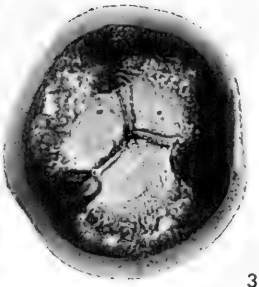

3

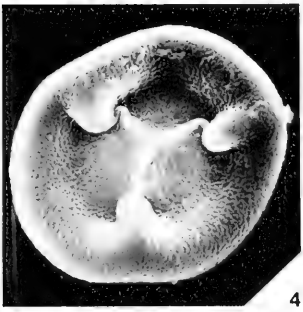

4

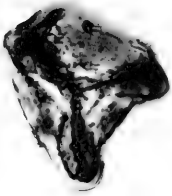

5

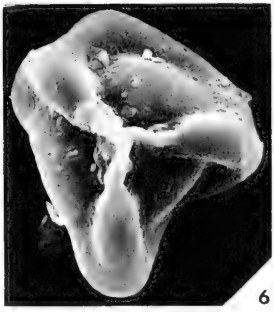

6

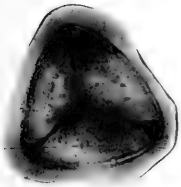

7

8

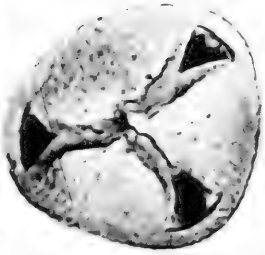

9

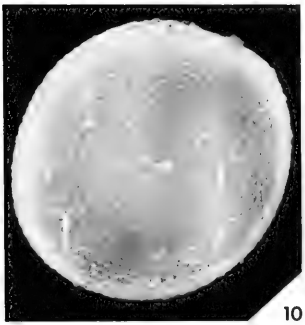

10

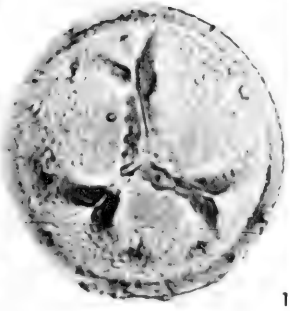

11

12

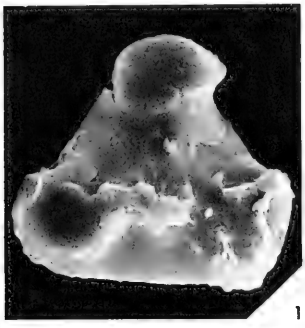
1

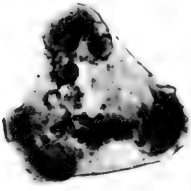
2

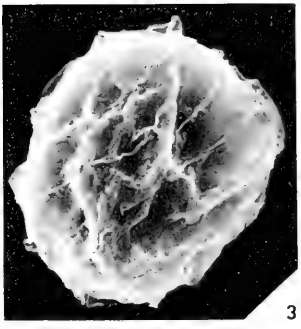
3


4


5

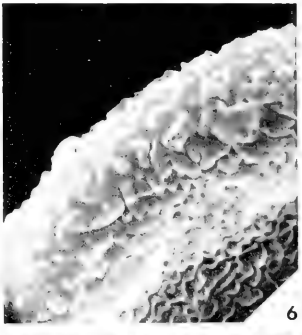
6

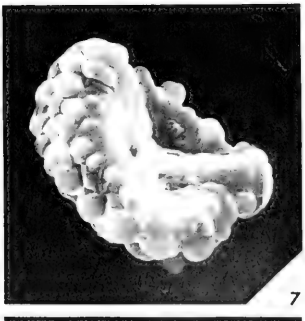
7


8

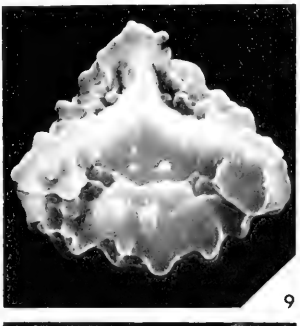
9


10


11


12

EXPLANATION OF PLATE 44

Figure — Page

1, 2. **Triquitrites tribullatus** (Ibrahim), Schopf, Wilson and Bentall, 1944 148

1. Scanning electron micrograph, distal surface, of specimen in Fig. 2, ×900. 2. Transmitted light photomicrograph, ×750.

3, 10-12. **Vestispora lucida** (Butterworth and Williams), Potonié, 1960 148

3. Scanning electron micrograph, distal surface, ×550. 10. Scanning electron micrograph showing both proximal and distal surfaces, ×600. 11. Transmitted light photomicrograph of specimen in Fig. 10, ×500. 12. Scanning electron micrograph of specimen in Fig. 10, showing the "operculum", ×1100.

4-6. **Verrucosisporites cerosus** (Hoffmeister, Staplin and Malloy), Butterworth and Williams, 1958 148

4. Scanning electron micrograph, distal surface, ×750. 5. Transmitted light photomicrograph of specimen in Fig. 4, ×500. 6. Scanning electron micrograph showing detail of ornament on specimen in Fig. 4, ×2500.

7-9. **Verrucosisporites scoticus** Sullivan, 1968 148

7. Scanning electron micrograph showing proximal and distal surfaces, ×850. 8. Transmitted light photomicrograph of specimen in Fig. 7, ×1000. 9. Scanning electron micrograph, proximal surface, ×1200.

EXPLANATION OF PLATE 45

Figure — Page

1, 2. **Verrucosisporites morulatus** (Knox), Smith and Butterworth, 1967 148
1. Scanning electron micrograph, distal surface, ×900. 2. Transmitted light photomicrograph, ×750.

3, 5, 6. **Waltzispora planiangulata** Sullivan, 1964 149
3. Scanning electron micrograph, distal surface of specimen in Fig. 6, ×1500. 5. Scanning electron micrograph, proximal surface, ×1750. 6. Transmitted light photomicrograph, ×1000.

4, 7. **Waltzispora politus** (Hoffmeister, Staplin and Malloy), Smith and Butterworth, 1967 149
4. Transmitted light photomicrograph, ×1000. 7. Scanning electron micrograph, proximal surface of specimen in Fig. 4, ×1200.

8, 9. Spore Type B 150
8. Transmitted light photomicrograph, 147F32-4, ×500. 9. Scanning electron micrograph, proximal surface of specimen in Fig. 8, ×950.

10-12. Spore Type A 149
10. Scanning electron micrograph, proximal surface of specimen in Fig. 11. 147F30-2, ×1000. 11. Transmitted light photomicrograph, ×1000. 12. Scanning electron micrograph, distal surface of specimen in Fig. 11, ×1000.

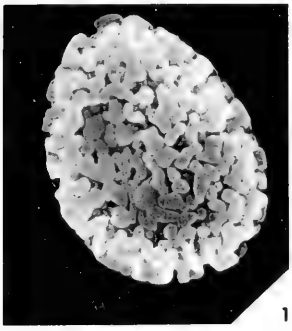
1

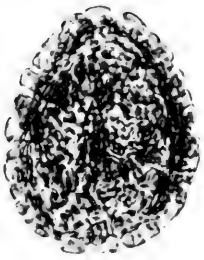
2

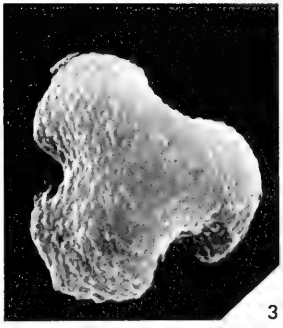
3


4

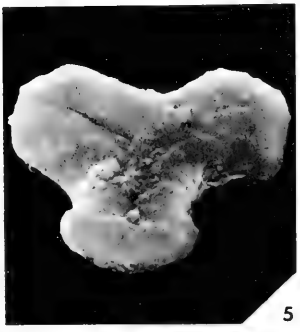
5


6

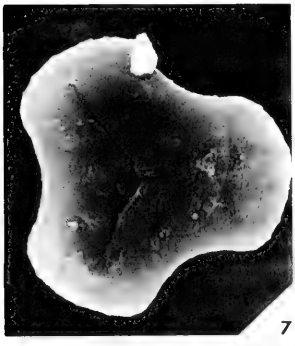
7

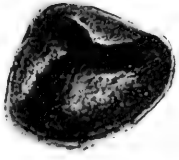
8


9

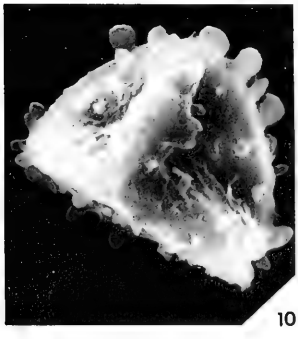
10

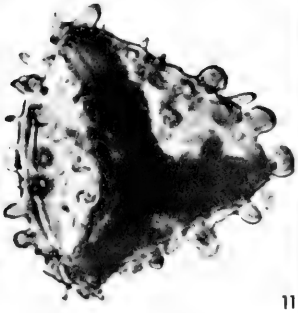
11

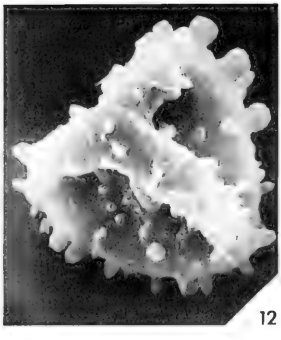
12

INDEX

Note: Light face figures refer to the page numbers. Bold face figures refer to the plate numbers.

A

Acanthotriletes 108-110
aculeatus, Densosporites **25** 117, 166
Ahrensisporites 108-110, 150
altilis, Cincturasporites **23** 112, 151, 164
ampla, convolutispora **24** 113, 165
Anapiculatisporites 110
angulatus, Leiotriletes **33** 128, 129, 174
Aplington Formation 104

B

bacculentus Camptotriletes **23** 110, 164
beeleyensis, Ahrensisporites **22** 108, 109, 163
bicornis, Mooreisporites **36** 134, 135, 177

C

Calamospora 110
Camptotriletes 110
caperata, Hymenospora **30** 125, 171
cavus, Densosporites **26, 27** 118, 119, 151, 154, 167, 168
Cedar Valley Limestone 103-105
cerosus, Verrucosisporites **44** 148, 185
Chester Series 154, 155
Cincturasporites 111, 112
Cirratriradites 108, 112
clatriformis, Dictyotriletes **27** 119, 168
concavus, Microreticulatisporites **35** 132, 122, 176
contortus, Trimontisporites **43** 146, 147, 184
Convolutispora 113, 151
Costatascyclus 114
crenatus, Constatascyclus **25** 114, 115,166
cristatus, camptotriletes **23** 111, 164

D

danzei, Reticulatisporites **40** 141, 142, 181
densa, Raistrickia **39** 139, 140, 180
Densosporites 107, 115, 116, 117, 150
dentatus, Rochisporites **31, 32** 127, 128, 172, 173
Desmoines Series 155
Devonian System of Iowa 104
Diaphanospora **21** 162
Dictyotriletes 119
divaricatus, Trimontisporites 145
Dorheim, Fred 105
Dorheimisporites 119, 120

E

echinatus, Acanthotriletes **22** 108, 163
fasciculata, Procoronaspora **37** 136, 137, 154, 178
elegans, Potonieisporites **37** 136, 178
elongata, Schulzospora **41** 143, 182
English River Formation 104

F

fatihi, Lophotriletes **33** 130, 174
Felix, Charles 105
flexuosus, Trimontisporites 145
florida convolutispora **24** 113, 165
Florinites 121, 150
Foveosporites 121
Funisporites 121
fustus, Mooreisporites **36** 134, 177

G

Gorgonispora 121
Granulatisporites 124

granulatus, Granulatusporites **30** 124, 171
granulatus, Trimontisporites **42, 43** 145, 146, 183, 184
guttatus, Florinites **29** 121, 170

H

halesi, Ahrensisporites **22** 109, 110, 163
hartungiana, Calamospora **23** 110, 164
Hershey, Garland 105
heterofiliferus, Punctatisporites **38** 137, 179
hispidus, Densosporites **26** 117, 151, 154, 167
Hymenospora 125
Hypothyridina 103

I

incomptus, Punctatisporites **38** 137, 179
Independence Shale 103, 105
inflatus, Dorheimisporites **28** 120, 121, 169
insculptus, Foveosporites **27** 121, 168
intortus, Simozonotriletes **41, 42** 143, 144, 182, 183
Iowa 103

K

Knoxisporites 125
Kochisporites 126, 127

L

labiatus, Lophotriletes **34** 130, 175
labrum, Leiotriletes **33** 129, 130, 174
Laevigatosporites 154
Laevigatus, Proprisporites **37** 137, 178
La Porte City Formation 104
Leiotriletes 128
Lime Creek Shale 103, 104, 151, 155
Lophotriletes 130
lucida, Vestispora **44** 148, 185
Lycospora 107, 131
Lycosporoides, stenozonotriletes **42** 144, 183

M

magna, Gorgonispora **29** 122, 123, 124, 170
Manticoceras 103
Maple Mill Formation 104
Maranhites **21** 150, 151, 152, 162
mellita, Convolutispora **24** 113, 165
microgranifer, Granulatisporites **30** 124, 125, 171
Microreticulatisporites 132, 151
minor, Anapiculatisporites **23** 110, 164
Mississippian, Late 154
Mississippian System of Iowa 155
Monoletes 133
Mooreisporites 134
Morrow Series 155
morulatus, Verrucosisporites **45** 148, 186
Murospora 135

N

Neoraistrickia 135
nux, Savitrisporites **41** 142, 143, 182

O

obesus, Punctatisporites **38** 137, 179
obtusus, Lophotriletes **34** 130, 175
ovatus, Monoletes **35** 133, 176

P

peltatus, Reticulatisporites **40** 142, 154, 181
planiangulata, Waltzispora **45** 149, 186

planus, Punctatisporites **38** 138
politus, Waltzispora **45** 149, 186
Potonieisporites 136
Procoronaspora 136
Proprisporites 137
Punctatisporites 137
punctatus, Microreticulatisporites **35** 133, 176
pyramidatus, Leiotriletes **32** 128, 173

R

Raistrickia 139
rarispinosus, Densosporites **26** 117, 151, 154, 167
Reinschospora 140
remotus, Secarisporites **41** 143, 182
Reticulatisporites 140
rugosus, Trimonti - sporites **43** 147, 184

S

saetosa, Raistrickia **39** 139,180
saturni, Cirratriradites **24** 112, 113, 165
Savitrisporites 142
Schulzospora 143
scoticus, Verrucosisporites **44** 148, 185
Secarisporites 143
Sheffield Formation 104
Shell Rock Formation 104
Simozonotriletes 143
Solon Member 104, 105
speciosa, Reinschospora **39, 40** 140, 180, 181
sp., Knoxisporites **31** 126, 172
sp., Leiotriletes **33** 130, 174
sp., Murospora **36, 37** 135, 177, 178
Spore Type A **45** 149
Spore Type B **45** 150
Stainbrook, M. A. 103
Stenozonotriletes 144
stephanephorus, Knoxisporites **30, 31** 125, 126, 171, 172
subintortus, Leiotriletes **32** 128, 173

T

Tantillus 144
Tasmanites **21** 150, 151, 152, 154, 162
tortuosa, Convolutispora **24, 25** 113,114, 165, 166
Tournaisian 151
triarcuatus, Trimontisporites 145
tribullatus, Triguitrites **44** 148, 185
trifidus, Trimontisporites 145
Trimontisporites 144, 145
triradiatus, Knoxisporites **31** 126, 172
triquetrus Tantillus **42** 144, 183
Triquitrites 148
tuberculatus, Granulatisporites **30** 125, 171
tumidus, Leiotriletes **32** 128, 173

U

uber, Lycospora **34** 131, 132, 151, 154, 175

V

validus, Punctatisporites **38** 138, 139, 179
variornamenta, Neoraistrickia **37** 135, 136, 178
Verrucosisporites 148
Vestispora 148
visendus, Florinites **29** 121, 170

W

Waltzispora 148
Wapsipinicon Formation 103-105
Westphalian A 151
winslowi, Monoletes **35, 36** 133, 134, 176, 177

Y

Yellow Spring Group 104

XLV. (No. 204). 564 pp., 63 pls. 18.00
Venezuela Cenozoic pelecypods

XLVI. (Nos. 205-211). 419 pp., 70 pls. 16.00
Large Foraminifera, Texas Cretaceous crustacean, Antarctic Devonian terebratuloid, Osgood and Paleocene Foraminifera, Recent molluscan types.

XLVII. (Nos. 212-217). 584 pp., 83 pls. 18.00
Eocene and Devonian Foraminifera, Venezuelan fossil scaphopods and polychaetes, Alaskan Jurassic ammonites, Neogene mollusks.

XLVIII. (No. 218). 1058 pp., 5 pls. 18.00
Catalogue of the Paleocene and Eocene Mollusca of the Southern and Eastern United States.

XLIX. (Nos. 219-224). 671 pp., 83 pls. 18.00
Peneroplid and Australian forams, North American carpoids, South Dakota palynology, Venezuelan Miocene mollusks, *Voluta*.

L. (Nos. 225-230). 518 pp., 42 pls. 18.00
Venezuela and Florida cirripeds, Antarctic forams, Linnaean Olives, Camerina, Ordovician conodonts, Niagaran forams.

LI. (Nos. 231-232). 420 pp., 10 pls. 18.00
Antarctic bivalves, Bivalvia catalogue.

LII. (Nos. 233, 236). 387 pp., 43 pls. 18.00
New Zealand forams, Stromatoporoidea, Indo-Pacific, Miocene-Pliocene California forams.

LIII. (Nos. 237-238). 488 pp., 45 pls. 18.00
Venezuela Bryozoa, Kinderhookian Brachiopods.

LIV. (Nos. 239-245). 510 pp., 50 pls. 18.00
Dominican ostracodes, Texan pelecypods, Wisconsin mollusks, Siphocypraea, Lepidocyclina, Devonian gastropods, Miocene Pectens Guadaloupe.

LV. (Nos. 246-247). 657 pp., 60 pls. 18.00
Cenozoic corals, Trinidad Neogene mollusks.

LVI. (Nos. 248-254). 572 pp., 49 pls. 18.00
American Foraminifera, North Carolina fossils, coral types, Belanski types, Venezuelan Cenozoic Echinoids, Cretaceous Radiolaria, Cymatiid gastropods.

LVII. (Nos. 255-256). 321 pp., 62 pls. 18.00
Alaskan Jurassic ammonites, Pt. II, Jurassic Ammonitina New Guinea.

LVIII. (Nos. 257-262). 305 pp., 39 pls. 18.00
Cretaceous Radiolaria, Cretaceous Foraminifera, Pacific Silicoflagellates, North American Cystoidea, Cincinnatian Cyclonema, new species Vasum.

LIX. (No. 263). 314 pp. 18.00
Bibliography of Cenozoic Echinoidea.

LX. (Nos. 264-265). 97 pp., 20 pls. 4.55
Jurassic-Cretaceous Hagiastridae, Venezuela cirriped.

Palaeontographica Americana

Volume I. See Johnson Reprint Corporation, 111 Fifth Ave., New York, N. Y. 10003
Monographs of Arcas, Lutetia, rudistids and venerids.

II. (Nos. 6-12). 531 pp., 37 pls. 23.00
Heliophyllum halli, Tertiary turrids, Neocene Spondyli, Paleozic cephalopods, Tertiary Fasciolarias and Paleozoic and Recent Hexactinellida.

III. (Nos. 13-25). 513 pp., 61 pls. 28.00
Paleozoic cephalopod structure and phylogeny, Paleozoic siphonophores, Busycon, Devonian fish studies, gastropod studies, Carboniferous crinoids, Cretaceous jellyfish, Platystrophia and Venericardia.

IV. (Nos. 26-33). 492 pp., 72 pls. 28.00
Rudist studies Busycon, Dalmanellidae, Byssonychia, Devonian lycopods, Ordovican eurypterids, Pliocene mollusks.

V. (Nos. 34-37). 445 pp., 101 pls. 32.00
Tertiary Arcacea, Mississippian pelecypods, Ambonychiidae, Cretaceous Gulf Coastal forams.

VI. (Nos. 38-41). 444 pp., 83 pls. 35.00
Lycopsids and sphenopsids of Freeport Coal, Venericardia, Carboniferous crinoids, Trace fossils.

VII. (Nos. 42-44). 153 pp., 26 pls. 15.00
Torreites Sanchezi, Cancellariid Radula, Ontogeny, sexual dimorphism trilobites.

Vols. I-XXIII. See Kraus Reprint Corp., 16 East 46th St., New York, N. Y. 10017, U.S.A.

XXIV. (Nos. 80-87). 334 pp., 27 pls. 12.00
Mainly Paleozoic faunas and Tertiary Mollusca.

XXV. (Nos. 88-94B). 306 pp., 30 pls. 12.00
Paleozoic fossils of Ontario, Oklahoma and Colombia, Mesozoic echinoids, California Pleistocene and Maryland Miocene mollusks.

XXVI. (Nos. 95-100). 420 pp., 58 pls. 14.00
Florida Recent marine shells, Texas Cretaceous fossils, Cuban and Peruvian Cretaceous, Peruvian Eogene corals, and geology and paleontology of Ecuador.

XXVII. (Nos. 101-108). 376 pp., 36 pls. 14.00
Tertiary Mollusca, Paleozoic cephalopods, Devonian fish and Paleozoic geology and fossils of Venezuela.

XXVIII. (Nos. 109-114). 412 pp., 34 pls. 14.00
Paleozoic cephalopods, Devonian of Idaho, Cretaceous and Eocene mollusks, Cuban and Venezuelan forams.

XXIX. (Nos. 115-116). 738 pp., 52 pls. 18.00
Bowden forams and Ordovician cephalopods.

XXX. (No. 117). 563 pp., 65 pls. 16.00
Jackson Eocene mollusks.

XXXI. (Nos. 118-128). 458 pp., 27 pls. 16.00
Venezuelan and California mollusks, Chemung and Pennsylvanian crinoids, Cypraeidae, Cretaceous, Miocene and Recent corals, Cuban and Floridian forams, and Cuban fossil localities.

XXXII. (Nos. 129-133). 294 pp., 39 pls. 16.00
Silurian cephalopods, crinoid studies, Tertiary forams, and Mytilarca.

XXXIII. (Nos. 134-139). 448 pp., 51 pls. 16.00
Devonian annelids, Tertiary mollusks, Ecuadoran stratigraphy paleontology.

XXXIV. (Nos. 140-145). 400 pp., 19 pls. 16.00
Trinidad Globigerinidae, Ordovician Enopleura, Tasmanian Ordovician cephalopods and Tennessee Ordovician ostracods and conularid bibliography.

XXXV. (Nos. 146-154) 386 pp., 31 pls. 16.00
G. D. Harris memorial, camerinid and Georgia Paleocene Foraminifera, South America Paleozoics, Australian Ordovician cephalopods, California Pleistocene Eulimidae, Volutidae, and Devonian ostracods from Iowa.

XXXVI. (Nos. 155-160). 412 pp., 53 pls. 16.00
Globotruncana in Colombia, Eocene fish, Canadian Chazyan Antillean Cretaceous rudists, Canal Zone Foraminifera, fossils, foraminiferal studies.

XXXVII. (Nos. 161-164). 486 pp., 37 pls. 16.00
Antillean Cretaceous Rudists, Canal Zone Foraminifera, Stromatoporoidea.

XXXVIII. (Nos. 165-176). 447 pp., 53 pls. 18.00
Venezuela geology, Oligocene Lepidocyclina, Miocene ostracods, and Mississippian of Kentucky, turritellid from Venezuela, larger forams, new mollusks, geology of Carriacou, Pennsylvanian plants.

XXXIX. (Nos. 177-183). 448 pp., 36 pls. 16.00
Panama Caribbean mollusks, Venezuelan Tertiary formations and forams, Trinidad Cretaceous forams, American-European species, Puerto Rico forams.

XL. (No. 184). 996 pp., 1 pls. 18.00
Type and Figured Specimens P.R.I.

XLI. (Nos. 185-192). 381 pp., 35 pls. 16.00
Australian Carpoid Echinoderms, Yap forams, Shell Bluff, Ga. forams. Newcomb mollusks, Wisconsin mollusk faunas, Camerina, Va. forams, Corry Sandstone.

XLII. (No. 193). 673 pp., 48 pls. 18.00
Venezuelan Cenozoic gastropods.

XLIII. (Nos. 194-198). 427 pp., 29 pls. 16.00
Ordovician stromatoporoids, Indo-Pacific camerinids, Mississippian forams, Cuban rudists.

XLIV. (Nos. 199-203). 365 pp., 68 pls. 16.00
Puerto Rican, Antarctic, New Zealand forams, Lepidocyclina, Eumalacostraca.

BULLETINS
OF
AMERICAN
PALEONTOLOGY

(Founded 1895)

Vol. 60

No. 267

TREPOSTOMATOUS ECTOPROCTA (BRYOZOA) FROM THE LOWER CHICKAMAUGA GROUP (MIDDLE ORDOVICIAN), WILLS VALLEY, ALABAMA

By

FRANK KENNETH MCKINNEY

1971

Paleontological Research Institution
Ithaca, New York 14850, U.S.A.

BULLETINS
OF
AMERICAN
PALEONTOLOGY

(Founded 1895)

Vol. 60

No. 267

TREPOSTOMATOUS ECTOPROCTA (BRYOZOA) FROM THE LOWER CHICKAMAUGA GROUP (MIDDLE ORDOVICIAN), WILLS VALLEY, ALABAMA

By

Frank Kenneth McKinney

November 18, 1971

Paleontological Research Institution
Ithaca, New York 14850, U.S.A.

Library of Congress Card Number: 70-171462

Printed in the United States of America
Arnold Printing Corporation

CONTENTS

Abstract 195
Introduction 195
Purpose of study 195
Previous studies 196
Repositories 196
Acknowledgments 197
Collecting localities 197
Stratigraphy 199
Physical stratigraphy 199
Faunal correlation 211
Procedures 212
Analysis of the fauna and phylogenetic implications 219
Systematic descriptions 222
Monticuliporidae 222
Heterotrypidae 244
Amplexoporidae 250
Trematoporidae 259
Caloporidae 279
Diplotrypidae 287
Incertae sedis 290
References cited 304
Plates 309

TEXT-FIGURES

1. Index map 198
2-18. Stratigraphic section I-XVIII 200-207
19. Section showing facies relationships 210
20. Acanthopores per mm in *Amplexopora winchelli* Ulrich 256

TREPOSTOMATOUS ECTOPROCTA (BRYOZOA) FROM THE LOWER CHICKAMAUGA GROUP (MIDDLE ORDOVICIAN), WILLS VALLEY, ALABAMA

Frank Kenneth McKinney

Trepostomatous ectoprocts from the lower part of the Chickamauga Group of the Ordovician include 24 species in 12 genera: *Monticulipora, Prasopora, Homotrypa, Mesotrypa, Heterotrypa, Eridotrypa, Amplexopora, Batostoma, Hemiphragma, Calopora, Nicholsonella,* and *Diplotrypa.* Fifteen of the species are previously known and the following nine are new: *Prasopora megacystata, Homotrypa vacua, Mesotrypa sparsa, Eridotrypa arcuata, Calopora ovata, Nicholsonella acanthobscura, N. parafrondifera, N. inflecta* and *Diplotrypa anchicatenulata.* In addition, specimens that cannot be referred to a definite species are included in *Prasopora, Amplexopora, Batostoma,* and *Nicholsonella.*

A thick bentonite (T-3) which occurs near the base of Trentonian deposits serves as the upper limit of collections and forms a natural time plane. The lowermost extent of exposed beds of the Chickamauga Group governs the lower limit of collections, so that the lower limit does not coincide with a time plane. The trepostomes have a predominantly Wilderness aspect. They give no evidence of Porterfieldian or older age.

The early age of the fauna relative to most described trepostomes may contribute to the apparent transitional nature of some species between two different genera but suggests possible phylogenetic lines from *Homotrypa* to *Heterotrypa,* and *Mesotrypa* to *Stigmatella.*

INTRODUCTION

PURPOSE OF STUDY

This study was undertaken to determine trepostomatous ectoproct species and their geographic and stratigraphic distribution in the lower part of the Chickamauga Group, as exposed in Wills Valley between the vicinities of Gadsen, Etowah County, and Fort Payne, De Kalb County, Alabama. The Ordovician stratigraphy of northern Alabama was studied by Butts (1926, pp. 119-133), Cooper (1956, pp. 53-56) and Rogers (1961a, b). In the works of Butts and of Rogers, fossils were used only as stratigraphic tools; consequently detailed thin-section studies of ectoprocts were not undertaken. Cooper's 1956 work dealt with the description and biostratigraphy of brachiopods.

When this project began, it was hoped that the trepostomes would be sufficiently abundant and well zoned to allow more detailed correlation and subdivision of the lower part of the Chickamauga Group in northern Alabama. Within the area studied, vertical zonation of the trepostomes basically corresponds to the three superposed, essentially time-parallel lithologic units exposed in the lower part of the Chickamauga Group and to subdivisions of the lithologic units. Although occurrence and relative abundance of trepostomes have a recognizable vertical zonation, the zonation may be due as much or more to facies control as to sequential evolu-

tionary development. The most predominant and easily recognized trepostome zone corresponds to the only lithologic unit in the lower Chickamauga Group characterized by interlayered calcareous shale and biomicrudite. Facies and paleoenvironments of the lower Chickamauga Group in northern Alabama are being currently investigated by A. O. Wilson.

PREVIOUS STUDIES

Only one study of Middle Ordovician ectoproct faunas south of Kentucky has been published — a study of the ectoprocts of the Stones River Group in central Tennessee (Coryell, 1921). Incidental reports of Middle Ordovician ectoproct species in the southeastern United States have been made in several stratigraphic works, notably works by Butts (1926, 1940), Bassler (1932), and Wilson (1949). Ulrich and Bassler (1904) named several new species of Ordovician trepostomes from Tennessee. Allen and Lester (1954) figured several species of ectoprocts from the Middle Ordovician of northwestern Georgia.

Rogers (1961b) worked on biostratigraphy of the Chickamauga Group in Alabama. He listed the ectoprocts *Amplexopora* from his Units I (Chazyan to Blackriveran) (p. 24) and IV (Trentonian) (p. 29) and *Pachydictya robusta, Mesotrypa* sp., and *Dekayell ridleyana* from his Unit II (Blackriveran) (pp. 27, 28).

Several papers dealing either entirely or to a large extent with Middle Ordovician trepostomatous ectoprocts of the Midcontinent include Ulrich (1886, 1893), Sardeson (1935a-c, 1936a-f), Loeblich (1942), Perry (1962), Sparling (1964), Brown (1965), and Bork and Perry (1967, 1968a, b). In addition, Fritz (1957, 1966) worked on Middle Ordovician trepostomes from Ottawa, Quebec, and Newfoundland, and Ross (1963a-c, 1967a, b, 1969, 1970) published on Middle Ordovician trepostomes of New York.

No thin-section study of Middle Ordovician ectoprocts from the Chickamauga Group in Alabama has been reported in the literature.

REPOSITORIES

Holotypes, hypotypes, and designated paratypes are deposited in the United States National Museum (USNM). Unfigured specimens of previously described species and designated paratypes

are deposited in the paleontological collections of the Geological Survey of Alabama (GSATC) and the University of North Carolina at Chapel Hill (UNC).

ACKNOWLEDGMENTS

I wish to thank Richard S. Boardman, Curator of Invertebrate Paleontology at the U.S. National Museum, for access to collections in his care and for the loan of numerous type specimens. T. G. Perry and A. S. Horowitz, Indiana University Department of Geology, and Lois Kent, Geological Survey of Illinois, graciously loaned the author type specimens in their care.

This study was begun while the author held a National Defense and Education Act Title IV Fellowship. A Sigma Xi Grant-in-Aid-of-Research, a grant from the Smith Fund of the University of North Carolina, and receipt of maps and photographic supplies from the Geological Survey of Alabama facilitated completion of the project.

Most of the field work, including compilation of the measured sections, was done in conjunction with A. O. Wilson, who is studying the facies and paleoenvironments of the lower Chickamauga Group in northern Alabama. Stratigraphic interpretation and discussion benefited from a field discussion and examination with R. C. Milici, who has worked extensively with the Chickamauga in northwestern Georgia and eastern Tennessee, and its equivalents in the Central Basin of Tennessee.

Arnold McEntire, former director of the Computer Center at Appalachian State University, assisted in tailoring a program to facilitate compilation of data acquired in the study.

Special thanks are due Joseph St. Jean, Jr., who guided and advised the author during all stages of the study. Richard S. Boardman, U.S. National Museum of Natural History, and Thomas G. Perry, Indiana University, read the manuscript and made many suggestions for improvement. Thanks are also due John Dennison, Daniel A. Textoris and Walter H. Wheeler of the University of North Carolina, who read and criticized portions of the manuscript.

COLLECTING LOCALITIES AND PROCEDURES

Specimens were collected from 17 measured stratigraphic sections and one unmeasured section along the base of Big Ridge on

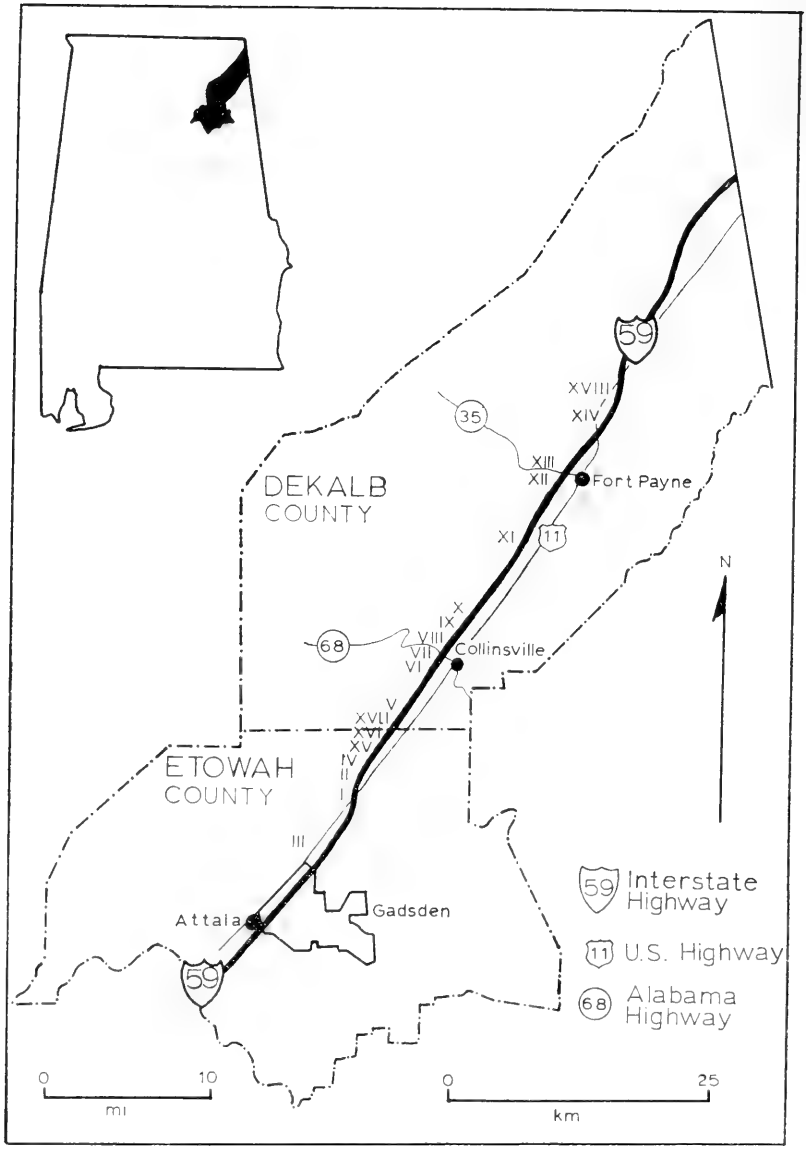

Text-figure 1. — Index map showing localities of measured sections in Wills Valley, Alabama.

the southeastern side of Wills Valley (Text-figure 1). Collecting intervals are variable in size; in each measured section collecting intervals correspond to discrete lithologic units that vary in thickness from less than 0.1 meter to over 20 meters. Within each collecting interval all available specimens were collected and mixed, so that thin zones or subtle evolutionary changes within the thicker intervals may have been missed.

In the columnar sections all types of ectoprocts — trepostomes, cryptostomes, cystoporates, and cyclostomes — are represented by the branched stick figure. Therefore, some ectoproct zones, such as the ectoproct zones in the upper 6.7 meters of section 1, do not contain trepostomes.

All but one of the sections are located along Interstate Highway 59. Text-figures 2-18 are columnar sections, data for which were collected in the summer of 1967 by the author and A. O. Wilson.

STRATIGRAPHY

PHYSICAL STRATIGRAPHY

Ectoprocts were collected from the lowest exposed portions of the Chickamauga Group up to the thick bentonite near the base of a series of 13 or more bentonite beds that are exposed in fresh road cuts along Interstate Highway 59. The thick bentonite in Wills Valley is sticky clay approximately 1.2 m thick. This bentonite appears to be correlative with the "T-3" bed of Wilson (1949, p. 64), based on lithologic similarity and thickness. The "T-3" bentonite was described from the Central Basin of Tennessee by Wilson as ". . . extremely sticky, green to olive-yellow clay." The same bed had been reported by Fox and Grant (1944, p. 366) as the "B-3" bentonite in the Tyrone Limestone (basal Trentonian) of eastern Tennessee. Other bentonites described by Wilson and by Fox and Grant lack the thickness of the "T-3" ("B-3"). None of the other bentonites in the Middle Ordovician sequence of Wills Valley is as thick as the easily recognizable bentonite here correlated with the "T-3". Approximately 4 m above the thick clayey "T-3" bentonite in Wills Valley is a bentonite that varies from 0.2 m to 0.9 m thick and is coarse-grained, containing fresh biotite grains up to 2 mm in diameter. This coarse-grained, biotite-bearing bentonite is an equivalent of the "T-4" bentonite of Wilson (1949, p. 63), which

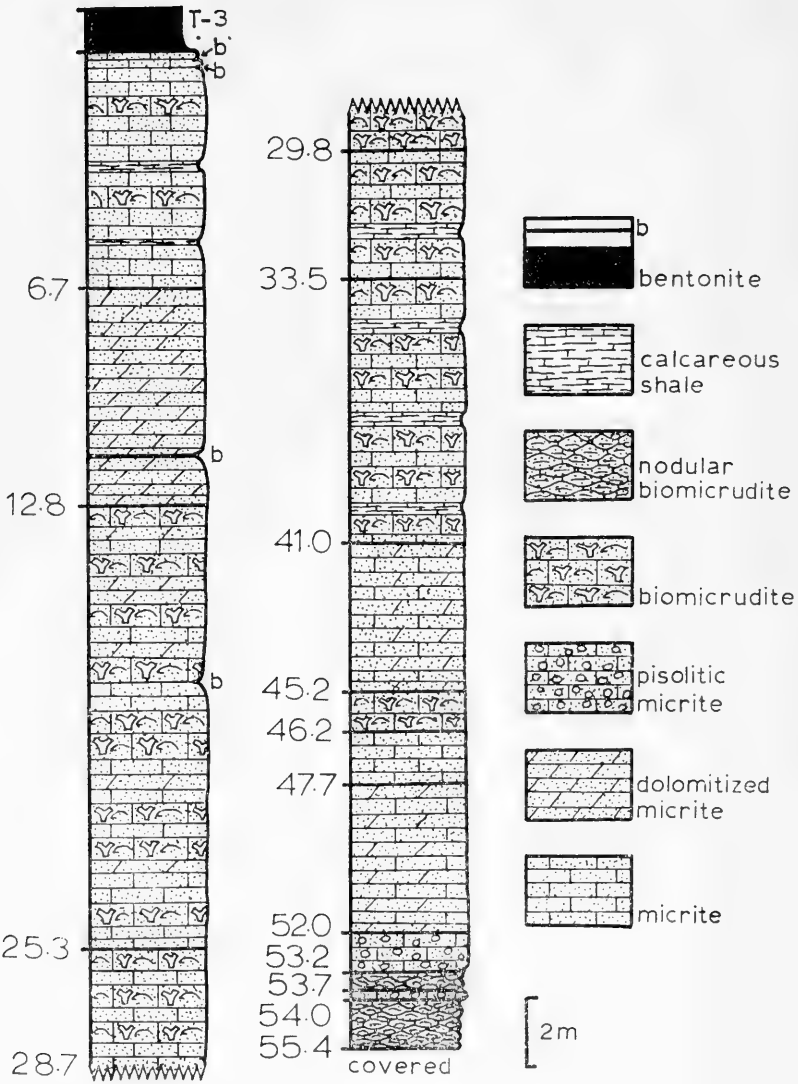

Text figure 2. — Stratigraphic section I, lower part of the Chickamauga Group. E ½ NW ¼, sec. 27, T. 10 S., R. 6 E., Keener Quad., Ala., where Interstate Highway 59 crosses Big Ridge. Numbers along the left side of stratigraphic sections I-XVII refer to distances in meters below the T-3 bentonite or below the top of the section. Sticklike figures in the biorudites represent occurrence of trepostome and cryptostome ectoprocts.

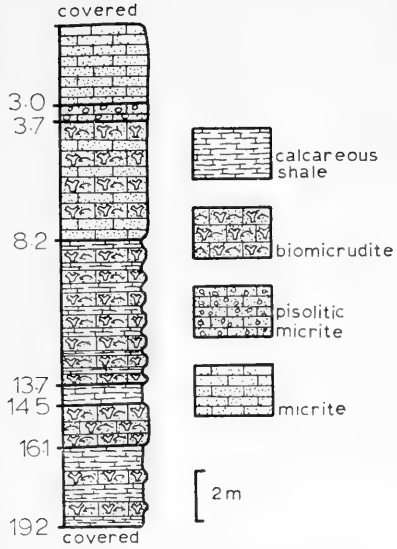

Text-figure 3. — Stratigraphic section II, portion of lower part of the Chickamauga Group. SE¼ NE ¼, sec. 22, T. 10 S., R. 6 E., Keener Quad., Ala., along Interstate Highway 59.

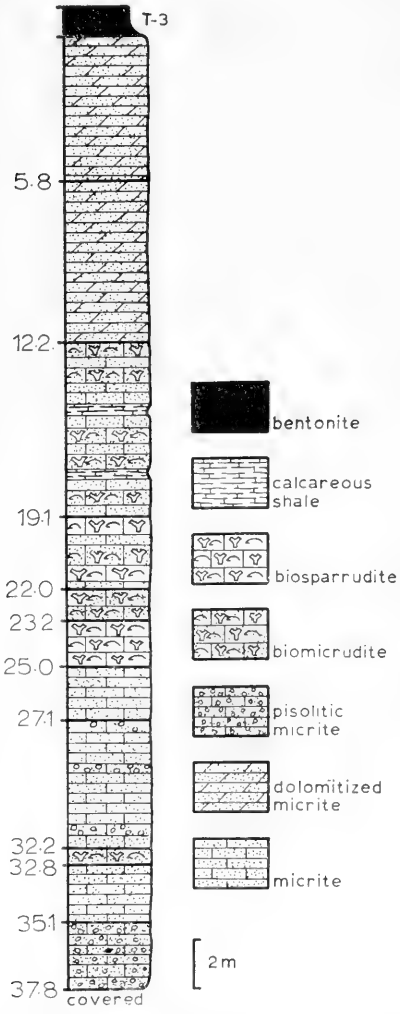

Text-figure 4. — Stratigraphic section III, lower part of Chickamauga Group. SE ¼ NW ¼ and SW ¼ NE ¼, sec. 7, T. 11 S., R 6 E., Bruton Gap, Gadsden Quad., Ala.

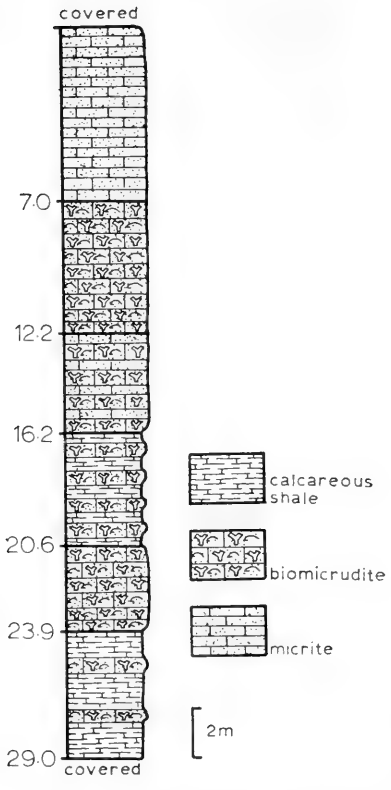

Text-figure 5. — Stratigraphic section IV, portion of lower part of the Chickamauga Group. NW ¼ NW ¼, sec. 23, T. 10 S., R. 6 E., Keener Quad. Ala., along the east side of Interstate Highway 59.

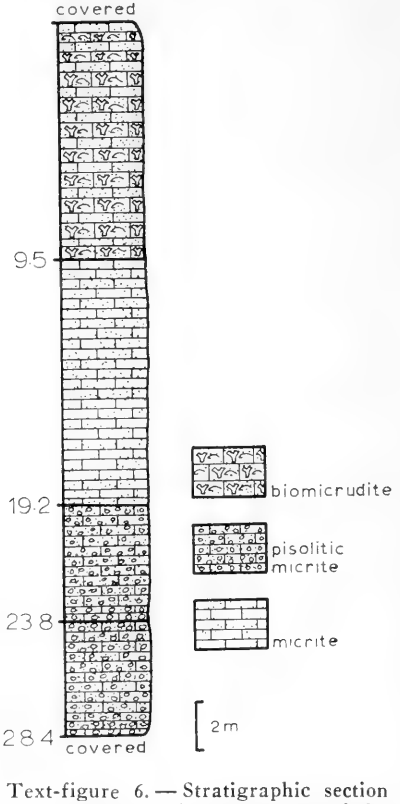

Text-figure 6. — Stratigraphic section V, a portion of the lower part of the Chickamauga Group. SE ¼ SW ¼, sec. 29, T. 9 S., R. 7 E., Keener Quad., Ala., along Interstate Highway 59, 9.1 km south of the intersection with Alabama 68.

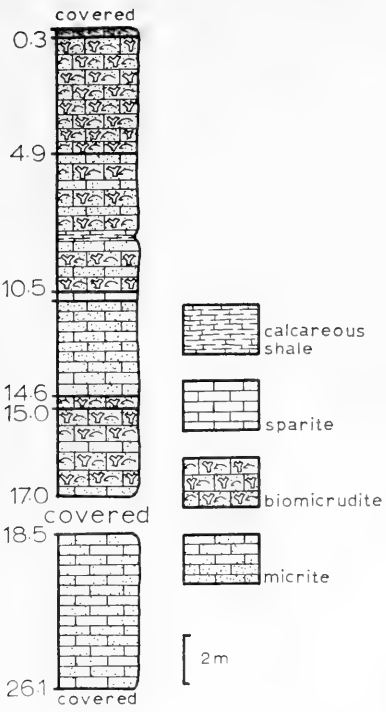

Text-figure 7. — Stratigraphic section VI, a portion of the lower part of the Chickamauga Group. SE ¼ SW ¼, sec. 10, T. 9 S., R. 7 E, Crossville Quad., Ala., along Interstate Highway 59, 1.8 km south of Alabama 68.

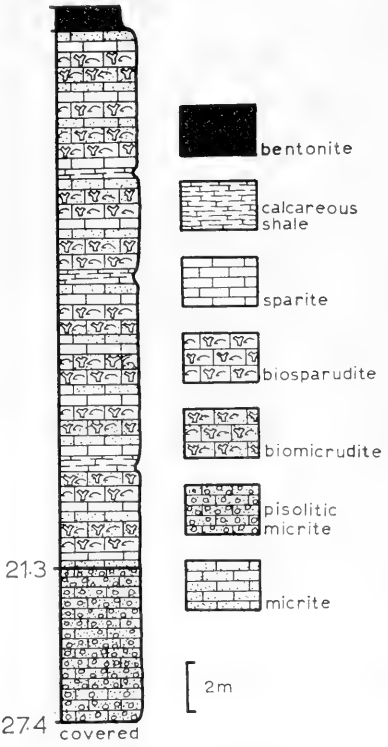

Text-figure 8. — Stratigraphic section VII, a portion of the lower part of the Chickamauga Group. SE ¼ NE ¼, sec. 10, T. 9 S., R. 7 E., Crossville Quad., Ala., along Interstate Highway 59, 0.7 km south of the intersection with Alabama 68.

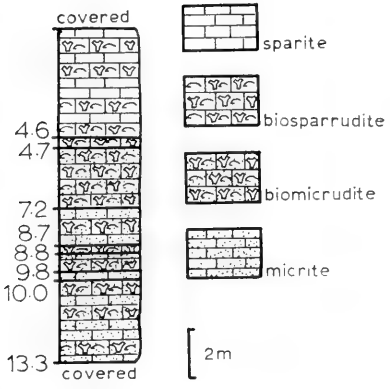

Text-figure 9. — Stratigraphic section VIII, a portion of the lower part of the Chickamauga Group. NE ¼ SW ¼, sec. 2, T. 9 S., R. 7 E., Portersville Quad., Ala., along Interstate Highway 59, 0.7 km north of the intersection with Alabama 68.

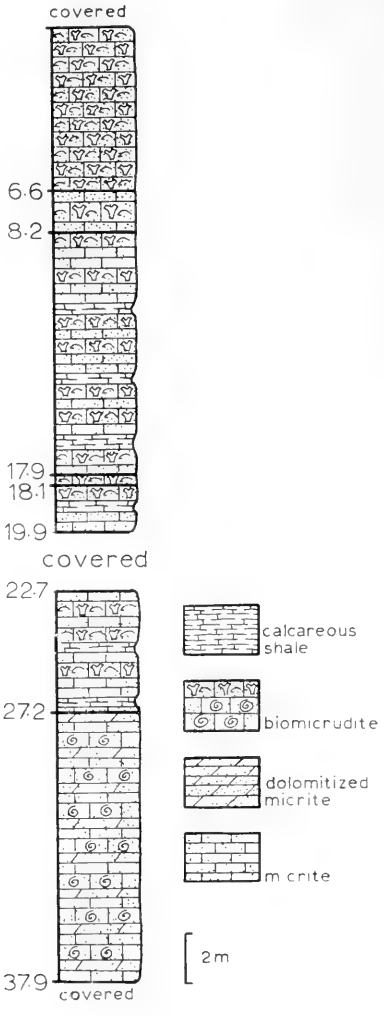

Text-figure 10. — Stratigraphic section IX, a portion of the lower part of the Chickamauga Group. NE ¼ NE ¼, sec. 2, T. 9 S., R. 7 E., Portersville Quad., Ala., along Interstate Highway 59, 1.5 km north of the intersection with Alabama 68.

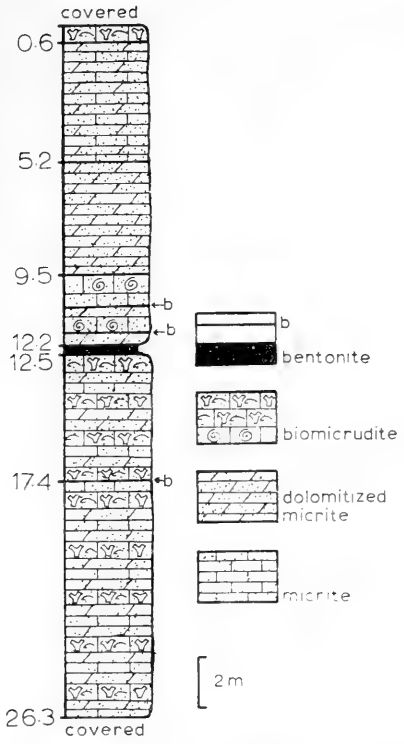

Text-figure 11. — Stratigraphic section X, a portion of the lower part of the Chickamauga Group. SE ¼ NW ¼, sec. 19, T. 8 S., R. 8 E., Portersville Quad., Ala., along Interstate Highway 59, 6.1 km north of the intersection with Alabama 68.

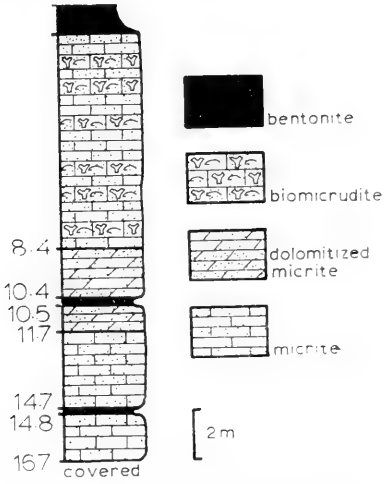

Text-figure 12. — Stratigraphic section XI, a portion of the lower part of the Chickamauga Group. NW ¼ NW ¼, sec. 9, T. 8 S., R. 8 E., Portersville Quad., Ala., along Interstate Highway 59, 7.7 km south of the intersection with Alabama 35.

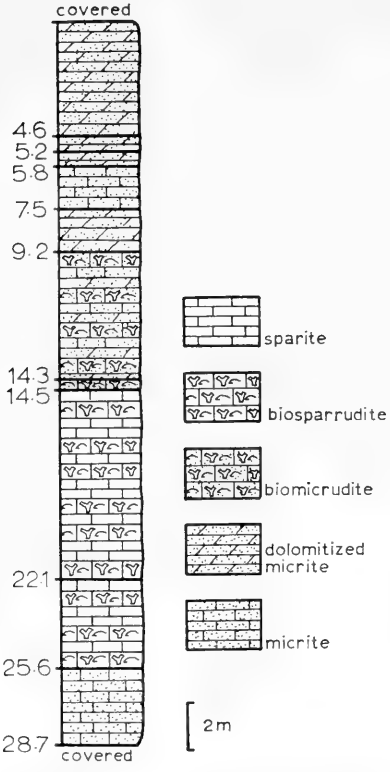

Text-figure 13. — Stratigraphic section XII, a portion of the lower part of the Chickamauga Group. SW ¼ SE ¼, sec. 12, T. 7 S., R. 8 E., Ft. Payne 7½′ Quad., Ala., along the southeastern part of the intersection of Interstate Highway 59 and Alabama 35.

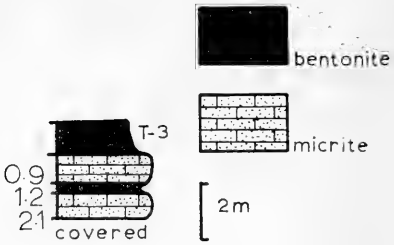

Text-figure 14. — Stratigraphic section XIII, a portion of the lower part of the Chickamauga Group. SE ¼ NE ¼, sec. 12, T. 7 S., R. 8 E., Ft. Payne 7½′ Quad., Ala., along Interstate Highway 59, 0.5 km north of the intersection with Alabama 35.

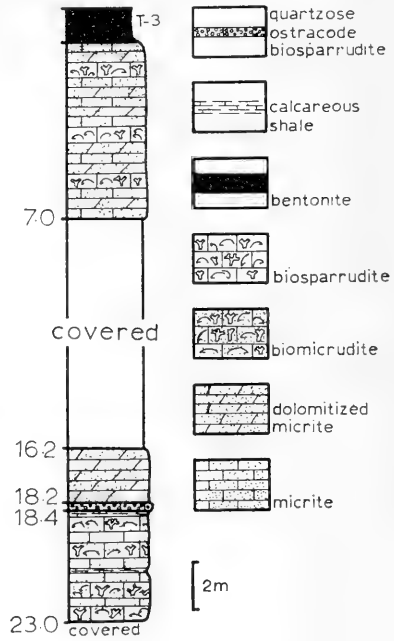

Text-figure 15. — Stratigraphic section XIV, a portion of the lower part of the Chickamauga Group. SE ¼ SE¼, sec. 29, T. 6 S., R. 9 E., Ft. Payne 7½′ Quad., Ala., along the northeastern part of the intersection of Interstate Highway 59 and U.S. 11.

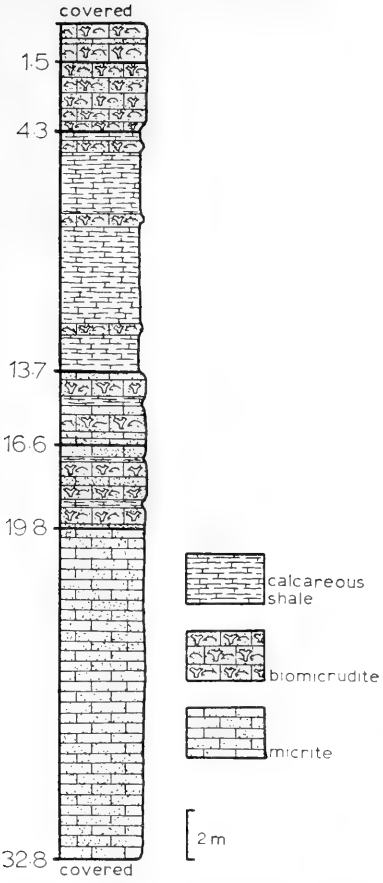

Text-figure 16. — Stratigraphic section XV, a portion of the lower part of the Chickamauga Group. NE ¼ NE ¼, sec. 14, T. 10 S., R. 6 E., Keener Quad., Ala., along Interstate Highway 59, 14.6 km south of the intersection with Alabama 68.

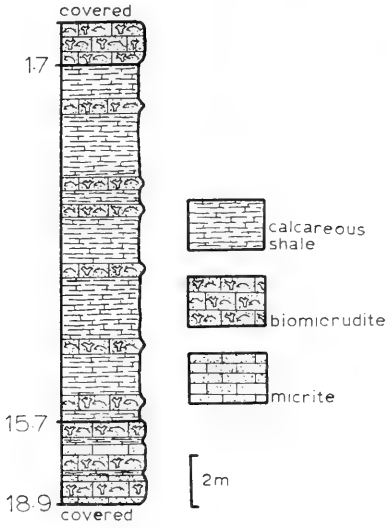

Text-figure 17. — Stratigraphic section XVI, a portion of the lower part of the Chickamauga Group. SW ¼ SE ¼, sec. 1, T. 10 S., R. 6 E., Keener Quad., Ala., along Interstate Highway 59, 11.0 km south of the intersection with Alabama 68.

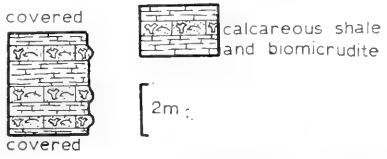

Text-figure 18. — Stratigraphic section XVII, a portion of the lower part of the Chickamauga Group. NW ¼ NW ¼, sec. 32, T. 9 S., R. 7 E., Keener Quad., Ala., along Interstate Highway 59, 8.0 km south of the intersection with Alabama 68.

he described as ". . . sticky, green to olive and yellow clay, parts of which are coarse-grained and micaceous." Firm correlation of the overlying bentonite with the "T-4" of the Central Basin further supports correlation of the thick bentonite in Wills Valley with the "T-3" of the Central Basin.

The thick "T-3" bentonite serves as the upper limit of trepostome collections because it is widespread in Wills Valley, is easily recognized and is the best time plane available in the measured sections. Also, ectoprocts are scarce for several meters immediately above the thick clayey bentonite. In Tennessee the "T-3" bentonite occurs in the eastern part of the Central Basin ". . . at the contact between the Upper and Lower members of the Carters." Limestone, the uppermost member of the Stones River Group (Wilson, 1949, p. 64). Age of the Carters Limestone is apparently lowermost Trentonian (Twenhofel *et al.*, 1954, chart 2) or uppermost Wilderness (Cooper, 1956, chart 1) and the lower members of the Stones River Group (Murfreesboro, Pierce, Ridley and Lebanon Limestones) are Wilderness in age with the exception of the Murfreesboro Limestone, which is uppermost Porterfieldian in age (Cooper, 1956, chart 1). Allen and Lester (1957, pp. 1, 6, 102) used one of the more prominent bentonites as the boundary between Middle and Upper Ordovician deposits in Georgia which is younger than other workers place the bentonite sequence.

W. S. Rogers (1961a) formally introduced the designation Chickamauga Group for the unit previously designated Chickamauga Limestone, although Cooper (1956, p. 55) had suggested that ". . . the name really is not that of a formation, but is a group term embracing several distinguishable formations." Rogers (1961a) also subdivided the newly established group into four units (Units I-IV) in Alabama to correspond with John Rodgers' units 1-4 in east Tennessee. John Rodgers recognized two bentonites near the top of unit 3. He considered units 1-3 to represent Stones River and other Blackriveran equivalents. (Rodgers, 1953, pp. 87-90). A thin bentonite (which may be any one of several exposed by Interstate Highway 59 cuts in the Chickamauga Group of Wills Valley) occurs at the upper limit of W. S. Rogers' Unit III (Rogers, 1961a, p. 242), which he assigned to the Blackriveran. Rogers 1961a, p. 217) considered Unit I to be Chazyan and Unit II to be

Blackriveran. In the present study no attempt was made to follow W. S. Rogers' terminology for subdivision of the Chickamauga Group, although a rough three-fold division exists below the thick bentonite — a lower local calcareous shale with thin interbeds of biomicrudite, a median lithologic complex of variously fossiliferous biomicrudite, micrite, and biosparrudite and an upper unit typically of more sparsely fossiliferous beds of dolomitized micrite and micrite (Text-figure 19). These three divisions may belong to Rogers' Units I, II and a portion of Unit III.

Milici and Smith (1969) recognized components of the Middle Ordovician Stones River and Nashville Groups in the Chickamauga at its type section and, therefore, considered the Chickamauga as a Supergroup. In a subsequent paper Milici (1969) further strengthened inclusion of the Stones River and Nashville Groups in the Chickamauga Supergroup by tracing the various members through the Chickamauga of Sequatchie Valley in Tennessee, which has an intermediate geographical position between the Central Basin of Tennessee (type area of the Stones River and Nashville Groups) and the type section of the Chickamauga in northwestern Georgia.

Three major lithologic units exist in the lower Chickamauga Group in Wills Valley. The lowest unit is dominated by calcareous shale. The calcareous shale varies from sparsely to abundantly fossiliferous. Light gray micrite occurs along the base of the lower unit, and toward the northeastern limit of outcrop of the lower unit, the basal micrite contains numerous gastropods. Biomicrudite beds become increasingly numerous toward the top of the lower unit.

The dominant rock type in the median lithologic unit is micrite. Biomicrudite that contains ectoprocts, brachiopods, nautiloids, tabulate corals, and trilobites is also prominent. The two lithologies are frequently interbedded (Text-figure 19). A few beds of algal pisolites occur at various levels in the median unit, especially in the south-western half of the study area. A minor amount of calcareous shale is present. Toward the northeast the upper part of the median unit grades to interbeds of sparite and biosparrudite.

The highest unit in the lower Chickamauga Group in Wills Valley is composed of sparsely fossiliferous biomicrudite, micrite, and dolomitized micrite. The sparsely fossiliferous biomicrudite is

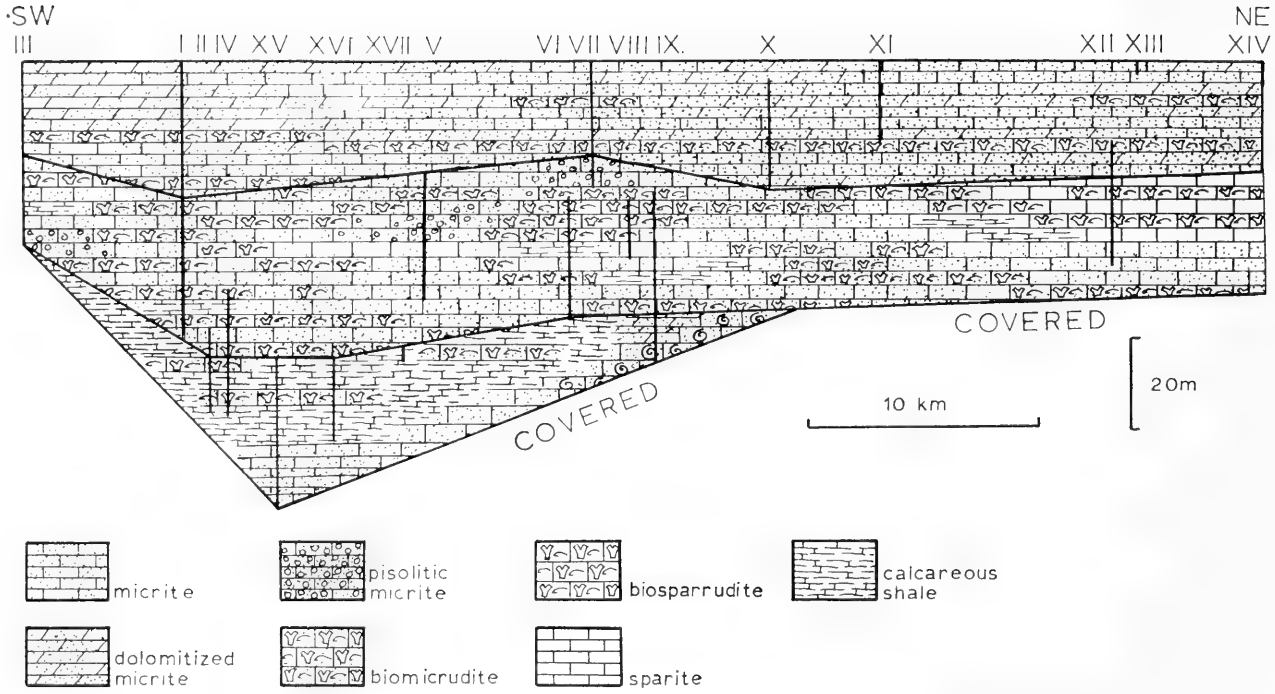

Text-figure 19. — Section showing facies relationships in the lower Chickamauga Group from Fort Payne, DeKalb Co., Alabama, to Bruton Gap, west of Reid City, Etowah Co., Alabama. Upper datum is the T-3 bentonite. Heavy vertical lines, including the ends of the diagram, represent measured sections; roman numerals at the top indicate measured section numbers. Heavy horizontal lines represent approximate boundaries between major lithologic units.

	[illegible] Shales"	"Middle third of Trenton shales"	"Upper third of Trenton shales"	UNDIFFERENTIATED MIDDLE ORDOVICIAN: Kuckers Shale	"Orthoceras Limestone" (B3)	Wegenberg Limestone	Middle Ordovician of Baltic and Western Arctic provinces	Middle Ordovician of Prebaltics
Prasopora d								
Homotrypa s		U	U	R				
Heterotrypa								
Heterotrypa								
Eridotrypa			U			R		A
Eridotrypa								
Eridotrypa								
Amplexopora		U						
Batostoma v		U						
Batostoma i								
Hemiphragma		U	U		R			
Calopora du			U	R,H			A	
Calopora sp								
Nicholsonel								
Nicholsonel								

1
called Pr

Table 1. (Letters refer to authors who reported the species:

A = Astrov S = Sardeson; U = Ulrich; W = Wilson and Mather.

Species	WILDERNESS								TRENTONIAN							UNDIFFERENTIATED MIDDLE ORDOVICIAN				
	Bromide Formation	Guttenberg Formation	Lebanon Limestone	Lowville beds of Ottawa Formation	Mifflin Formation	Pierce Limestone	Ridley Limestone	Specht's Ferry Shale	Decorah Shale	Galena Shale	Ion Formation	Logana or Jessamine Limestone	"Lower third of Trenton Shales"	"Middle third of Trenton shales"	"Upper third of Trenton shales"	Kuckers Shale	"Orthoceras Limestone" (B3)	Wegenberg Limestone	Middle Ordovician of Baltic and Western Arctic provinces	Middle Ordovician of Prebaltics
Prasopora discula (Coryell, 1921)	L[1]					C														
Homotrypa subramosa Ulrich, 1886											B			U	U	R				
Heterotrypa ridleyana (Coryell, 1921)							C													
Heterotrypa patera Coryell, 1921						C														
Eridotrypa minor Ulrich, 1893									S	U		G			U			R		A
Eridotrypa abrupta Loeblich, 1942	L																			
Eridotrypa libana (Safford, 1869)			C																	
Asplexopora winchelli Ulrich, 1886				F	B			P						U						
Batostoma varium Ulrich, 1893											B			U						
Batostoma increbescens Bork and Perry, 1967											B									
Hemiphragma irrasum (Ulrich, 1886)	L	B								U			U	J	U		R			
Calopora dumalis (Ulrich, 1893)										S,J					U	R,H			A	
Calopora spissata (Coryell, 1921)						C														
Nicholsonella parafrondifera, n. sp.						C[2]														
Nicholsonella pulchra Ulrich, 1893						U,C[2]														

1 called Prasopora fritzae by Loeblich

2 called Nicholsonella frondifera (in part) by Coryell

Table 1. Occurrence of previously named trepostomes collected from the lower Chickamauga Group, Wills Valley, Alabama. Letters refer to authors who reported the species: A = Astrova; B = Bork and Perry; C = Coryell; F = Fritz, G = Brown; H = Bekker; L = Loeblich; P = Perry; R = Bassler; S = Sardeson; U = Ulrich; W = Wilson and Mather.

S
Monticulipor
Prasopora di
Prasopora me
Prasopora sp
?Prasopora s
Homotrypa su
Homotrypa va
Mesotrypa sp
Heterotrypa
Heterotrypa
Eridotrypa n
Eridotrypa a
Eridotrypa a
Eridotrypa
Amplexopora
Amplexopora
Amplexopora
Batostoma va
Batostoma in
Batostoma sp
Hemiphragma
Calopora du
Calopora ova
Calopora spi
Diplotrypa
Nicholsonel
Nicholsonel
Nicholsonel
Nicholsonel
Nicholsonel
Nicholsonel

* Does not

Table 2.

Chickamau

indicate

SECTION

Species	I									II					III			IV			V	VI					VIII			IX		X	XII				XIV		XV					XVI			XVII	XVIII*
	54.0-55.4	53.7-54.0	53.2-53.7	47.7-52.0	45.2-46.2	33.5-41.0	28.7-29.8	25.3-28.7	12.8-25.3	16.1-19.2	14.5-15.1	13.7-14.5	8.2-13.7	3.2-8.2	32.2-32.8	22.0-23.2	19.1-22.0	20.6-23.9	16.2-20.6	7.0-12.2	23.8-28.4	15.0-17.0	14.6-15.0	10.7-14.6	4.9-10.5	0.3-4.9	10.0-13.3	7.2-8.7	0-4.6	18.1-27.2	17.9-18.1	17.4-26.3	22.1-25.6	14.5-22.1	14.3-14.5	9.2-14.3	16.2-18.2	0-7.0	16.6-19.8	13.7-16.6	4.3-13.7	1.5-4.3	0-1.5	15.7-18.9	1.7-15.7	0-1.7	0-4.0	
Monticulipora parallela									2				1												1	2								1														
Prasopora discula				2								1	22						2		2		1		1														3					2			22	
Prasopora megacystata			1	1																																				2								
Prasopora sp.						1																																										
?Prasopora sp.																																															1	
Homotrypa subramosa					6				1				2								1							1																			1	
Homotrypa vacua															1								4				7	11			1							1										5
Mesotrypa sparsa								1	8						1	6	2					1	1		3	10	1	4	2	1		2		1				1				1			1			3
Heterotrypa ridleyana									2																																							
Heterotrypa patera				1	4					2	2		101					5	5	1	3											3		1				2	1	5	9	10	1		11	2	38	
Eridotrypa minor										1					1								1				1																		2			
Eridotrypa abrupta						1											1										2																	1				
Eridotrypa arcuata																	9																	1														
Eridotrypa libana													1																																			
Amplexopora winchelli				1			3	9	61				44			26	47		1			5	4	2	1	66		14	8				12	20	17	1	101											7
Amplexopora aff. A. winchelli													1																																			
Amplexopora sp.										2																												1										
Batostoma varium									3							2	7									2						1								1				1	1			
Batostoma increbescens																					1					1							1	1														
Batostoma sp.											1																															1		1				
Hemiphragma irrasum													3								3												1							1								
Calopora dumalis																	1																									1			1			
Calopora ovata																																		1					2	4					2			1
Calopora spissata			1																	2	2																										2	
Diplotrypa anchicatenulata																																												4				
Nicholsonella parafrondifera					1		1					1		2											1																							
Nicholsonella pulchra													2																																	1		
Nicholsonella acanthobscura	2		1									1	6	1						4	1														1				1			1			2		4	
Nicholsonella inflecta												3	2					1																														
Nicholsonella aff. N. mariae													2																																			
Nicholsonella sp.		2																		1																												

* Does not include a measured section--collected along Interstate Highway 59, 1.5 km north of the intersection with U.S. 11 in NW ¼, sec. 28, T. 6 S., R. 9 E., Ft. Payne 7½' Quadrangle, Alabama.

Table 2. Distribution of trepostomatous ectoprocts within the Wills Valley sections of the Chickamauga Group, with number thin-sectioned from each unit. Numbers at the top of the chart indicate number of meters below the top of the measured section.

the least common of the three lithologies in the highest part of the lower Chickamauga Group and occurs primarily in the lower part of the highest unit, although it is locally prominent in the uppermost parts of the unit. Dolomitized micrite is the dominant rock type.

The upper division of the lower Chickamauga Group shown in Text-figure 19 is the lithologic equivalent of the lower Carters Limestone, but the lower two units shown in Text-figure 19 cannot be matched lithologically with the Ridley and Lebanon Limestones because of interfingering characteristic Ridley and Lebanon lithologies. Measured sections from which trepostomes were collected apparently do not extend below stratigraphic equivalents of the Ridley Limestone (Milici, personal communication). Since differentiation between some of the members of the Stones River Group appears to break down in northeastern Alabama, the term Chickamauga Group is retained here in preference to Chickamauga Supergroup. Only more detailed lithostratigraphic work can establish presence or absence of distinguishable groups and formations within the Chickamauga in Wills Valley of Alabama.

FAUNAL CORRELATION

Of the 15 previously named trepostome species collected from the lower Chickamauga (including *Nicholsonella parafrondifera,* n. sp. which includes two paratypes of *N. frondifera* Coryell), eight are known exclusively from Wilderness deposits, five are known exclusively from Trentonian deposits and two are known from both Wilderness and Trentonian deposits (Table 1). Table 2 is arranged to show the distribution of trepostomes collected from the lower part of the Chickamauga Group in Wills Valley and Table 3 is arranged to show the vertical range of the trepostomes in the area studied. The trepostome fauna reinforces Cooper's (1956, chart 1) assignment of the portion of the Chickamauga Group concerned within this report to the Wilderness stage of the Middle Ordovician.

The lower lithologic unit, as seen in Table 3, is characterized by abundant *Heterotrypa patera* Coryell, *Prasopora discula* (Coryell), and by the occurrence of *Calopora ovata,* n. sp. *Nicholsonella inflecta,* n.sp., *Diplotrypa anchicatenulata,* n. sp., *Nicholsonella pulchra* Ulrich, *Eridotrypa libana* (Safford), and *Nicholsonella* aff. *N.*

mariae Astrova are restricted to the upper part of the lower lithologic unit. As seen in Table 3, the most significant faunal break is between the middle and upper parts of the lower lithologic unit. The break probably results from more diversified environmental conditions as reflected by intertonguing of shale and biomicrudite, which thereby allows greater diversity of fauna. *Amplexopora winchelli* Ulrich, *Mesotrypa sparsa,* n. sp., *Homotrypa vacua,* n. sp., *Calopora spissata* Coryell, and *Homotrypa subramosa* Ulrich are most common in the median lithologic unit of the lower Chickamauga. *Batostoma varium* Ulrich and *Eridotrypa arcuata,* n. sp., have their greatest abundance in the upper lithologic unit, although *Amplexopora winchelli* Ulrich is the most abundant species in the upper lithologic unit. *Heterotrypa ridleyana* Coryell was found only in the upper lithologic unit of the lower part of the Chickamauga Group in Wills Valley. *Eridotrypa minor* Ulrich, *Nicholsonella acanthobscura,* n.sp., *Prasopora megacystata,* n. sp., and *Hemiphragma irrasum* Ulrich occur in approximately equal numbers in the lower two units, and *Amplexopora winchelli* is abundant from the uppermost biomicrudite beds in the lower unit up into dolomitic beds near the "T-3" bentonite. Sparsity of trepostomes just below the "T-3" bentonite probably results from unfavorable environmental conditions since the beds are dolomitic, and formation of dolomite requires hypersaline water.

Although trepostomes in the lower Chickamauga Group in Wills Valley can be vertically zoned, the zonation is probably in large part determined by the superposition of the three major lithofacies, whose contacts are essentially time-parallel within the area of study. The best developed zone, in the upper third of the lower lithologic unit, probably results from transition from an environment in which shale was predominant to an environment in which deposition of shale alternated with deposition of biomicrudite.

PROCEDURES

This study is based on the internal characters of 1133 trepostome specimens, most of which were examined by means of acetate peels, following the procedure given by Boardman and Utgaard (1964). The acetate peels are useful for taking quantified data, for making species groups, and, in most cases, for making generic assign-

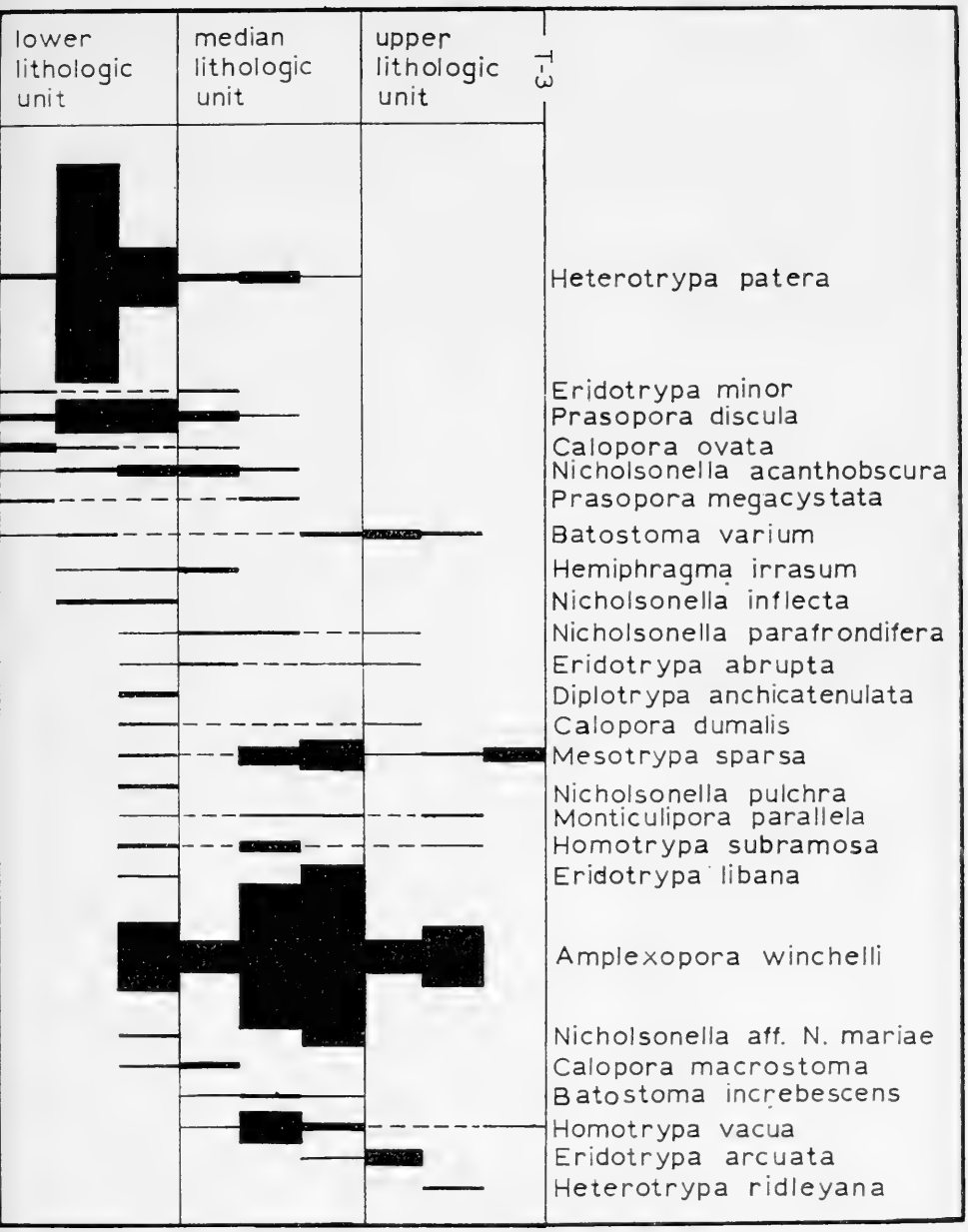

Table 3. Vertical distribution of trepostomes within the lower Chickamauga Group, Wills Valley, Alabama. Each 0.2 mm thickness of distribution lines indicates one sectioned specimen of the species.

ments. However, details of wall microstructure do not show in acetate peels of all species. Thin-sections of several specimens were necessary in some species groups before a generic assignment could be made. Because of their obscure structure, acetate peels are inadequate for *Nicholsonella;* therefore, thin-sections of all specimens of *Nicholsonella* were prepared for study. All photomicrographs are of thin-sections because thin-sections have better contrast which brings out details of microstructure more clearly.

Where applicable, standard measurements made in this study include maximum and minimum mature zooecial diameters and maximum and minimum mature zooecial tube diameters, both in monticules or maculae and in intermonticular or intermacular areas, maximum and minimum mesopore tube diameter, wall thickness, acanthopore diameter, diaphragms per mm in the mature zone, acanthopores per 1-mm square and mesopores per 2-mm square (McKinney, text-fig. 2, Alabama Geol. Survey Bull., *in press*). Less commonly, counts of cystiphragms per mm in mature zones, diaphragms per mm in immature zones, diaphragms per mm in mesopores and diaphragms per mm in proximal zooecial tips were made.

Most contemporary students of Trepostomata recognize the importance of quantifying data as an aid in species interpretation, and the application of quantified data on trepostomes is being explored especially by T. G. Perry and his students (*e.g.* Perry, 1962, Utgaard and Perry, 1964, Cuffey, 1967, Bork and Perry, 1967, 1968a, b). Most quantified data compiled from measurements of trepostomes are slightly to moderately skewed. Anstey and Perry (1968, p. 243) noted that distribution of taxonomic characters in Paleozoic ectoprocts commonly approximates a normal curve, and in a later paper (Anstey and Perry, 1969, pp. 249, 250) approached the problems of comparison of data that are not normally distributed. Data that are only slightly skewed, however, may in most cases be treated as normally distributed (Simpson, Roe, and Lewontin, 1960, p. 56).

Approaches toward biometric studies of Paleozoic ectoprocts were put forward by Anstey and Perry in 1970, in which they recommended that specimens should be coded for two-state characters and recommended that multivariate techniques be used. Cheetham (1968, pp. 23-48) in his monographic study of the cheilostome

ectoproct *Metrarabdotos,* successfully used multivariate techniques in phenetic comparison and phylogenetic interpretation.

An easily computed statistic, the coefficient of variation, gives a measure of relative variability that should help taxonomists decide characters that are most stable (*i.e.,* that have relatively low dispersion) in ectoproct species. Horowitz (1968, pp. 368, 369) and Anstey and Perry (1970, p. 392) commented on application of the coefficient of variation to Paleozoic ectoprocts. The coefficient of variation, V, is the standard deviation multiplied by a hundred and divided by the mean; it is, therefore, a measure of relative variation about the mean. A lower number for the V corresponds to a lower degree of relative variability, and a higher number corresponds to a higher degree of relative variability. As indicated by Simpson, Roe, and Lewontin (1960, p. 90), "The comparison of values of *V* derived from different distributions is almost invariably valid and useful if the variates are homologous. If they are not, experience suggests that the comparison is still generally valid if the variates are analogous and belong to the same category — for instance, if they are all linear dimensions of anatomical elements, the usual case. It is also helpful that the units of measurement have no influence on the comparison as long as they are in one category . . . As a rule, however, coefficients of variation for variates of essentially different categories cannot be usefully compared . . . unless this is shown to be warranted by logic and by experience."

Simpson, Roe, and Lewontin (1960, p. 91) indicated that the majority of V's for measured characters in Recent mammals lies between 4 and 10, and higher values indicate an impure sample, possibly including animals of different ages or different minor taxonomic divisions. Trepostomes are fossil colonial marine invertebrates in which one would expect individual characters to be more variable than individual characters in mammals. Since there is no control over the age structure of the population and little control over ecology and precise geologic age of trepostomes, a higher value for the V is expected.

Ross (1967a, p. 404; 1969, p. 260) suggested that numerical data in paleontology have been inadequately handled and that variability in ectoprocts is so great that she gave no particular importance to measurements made on ectoprocts. However, in Ross'

1969 paper the largest number of measurements on any one character is 22, which is lower than the ideal number of measurements for the most meaningful interpretations. Nevertheless even small sample numbers can contribute to valuable interpretation. For example, taking Ross' own data for *Amplexopora minnesotensis,* the species for which she had the maximum data, significance can be demonstrated by an analysis of the coefficients of variation. Table 4 contains calculations of the V for measurements presented by Ross (1969, p. 263, Table 2).

Zooecial and zooecial tube diameters, acanthopore diameters, diaphragms and cystiphragms per mm, and acanthopores per 1-mm square are traditionally considered taxonomically important and result in V values of 30 or less for most species population samples in the lower Chickamauga Group of Wills Valley (Table 7). Taxonomic importance of mesopore tube diameters, mesopores per 2-mm square, and zooecial wall thickness is questionable, and these characters result in V values of more than 30 for the most species population samples in the lower Chickamauga Group of Wills Valley.

Measured character	*Coefficient of variation (V)*
Diameter of zoarial branch	101.7
Zooecia in a 1-sq. mm area	13.3
Zooecial opening	
Length	13.0
Width	18.2
Mesopore	
Length	57.1
Width	50.0
Mesopores in a 1-sq. mm area	100

Table 4. Coefficient of variation for data by Ross (1969, p. 263, Table 2) on *Amplexopora minnesotensis* Ulrich.

Therefore, V values of approximately 30 or lower for characters in population samples of trepostomes are considered indicative of relatively constant characters that have a potential use in taxonomy; these V values for population samples generally correspond to values of approximately 20 or lower for characters in single trepostome zoaria (see discussion at the bottom of this page.).

As seen in Table 4, V values for zooecia in a 1-sq. mm area, length of the zooecial opening, and width of the zooecial opening

are all below 30 for Ross' measurements on *Amplexopora minnesotensis* Ulrich. Characters with V values well over 30 include diameter of zoarial branch, length of mesopore opening, width of mesopore opening and mesopores in a 1-sq mm area. Zoarial branch diameter is controlled by genetic capacity for growth, number of overgrowths, stage of astogenetic development, and, especially, environment. A high V value should be expected for zoarial branch diameter, which has been recognized for many years as variable and relatively unimportant taxonomically. Variation in size and abundance of mesopores is less easily explained. If, as tentatively suggested by Boardman (1969, pp. 213, 214 *in* Boardman and Cheetham) mesopores were not inhabited by individuals but were structural fills secreted by the colony between zooecia, a large degree of variation may result from slight differences in the way zooecia are packed in the zoaria.

Tables 6 and 7 list the range, median, mode, mean, and number of values used for coefficients of variation based on data given in Tables 8-53 of this paper. Table 5 lists and explains the abbrevia-

Abbreviation	Term
MxZD	Maximum zooecial diameter
MnZD	Minimum zooecial diameter
MxTD	Maximum zooecial tube diameter
MnTD	Minimum zooecial tube diameter
MxZDm	Maximum zooecial diameter in monticules or maculae
MnZDm	Minimum zooecial diameter in monticules or maculae
MxTDm	Maximum zooecial tube diameter in monticules or maculae
MnTDm	Minimum zooecial tube diameter in monticules or maculae
ZWT	Zooecial wall thickness
DBZT	Distance between adjacent zooecial tubes
MxMTD	Maximum mesopore tube diameter
MnMTD	Minimum mesopore tube diameter
M/2-mmsq	Mesopores per 2-mm square
AD	Acanthopore diameter
A/1-mmsq	Acanthopores per 1-mm square
D/mm	Diaphragms per mm
C/mm	Cystiphragms per mm
D/mmI	Diaphragms per mm in immature zone
D/mmM	Diaphragms per mm in mesopores
D/mmPT	Diaphragms per mm in proximal zooecial tips
DBM	Distance between monticules or maculae

Table 5. Abbreviations used Tables 6-53 and explanations of the abbreviations. All terms refer to the mature zone unless otherwise indicated.

tions used in Tables 6-53. Table 6 is based on multiple measurements on single zoaria, and Table 7 is based on measurements made on population samples of species. As would be expected, V values

SUMMARIZATION OF V VALUES FOR SINGLE SPECIMENS

Character	Range	Median	Mode	Mean	Number of V values used[1]
MxZDm	4-7	—	—	6.0	2
MxTDm	3-17	5	5	6.7	12
MnZD	3-9	6	—	6.7	5
MxTD	2-15	6	6	6.9	21
MnZDm	5-8	—	—	7.0	2
MnTDm	2-13	6	6	7.3	12
MxZD	5-10	7	—	7.7	5
MnTD	3-18	7	7	7.7	21
DBM	7-20	10	10	12.9	7
C/mm	12-18	14	14	15.0	4
AD	3-25	18	14,19	16.6	11
D/mm	7-56	14	8	16.7	17
ZWT	4-34	17	17	18.6	13
A/1-mmsq	6-80	15	14	21.6	13
MxMTD	11-56	32	23,38	31.5	16
MnMTD	9-54	34	41	32.5	16
M/2-mmsq	6-80	36	55	36.9	9

[1]Data on single specimens taken from Tables 10, 11, 13, 14, 18-20, 22, 23, 25, 26, 29, 31, 32, 35, 41, 42, 47-50.

Table 6. Range, median, mode, and mean of V values calculated for characters of individual zoaria, arranged in order of increased variability as indicated by the mean.

based on measurements from single zoaria are lower than corresponding V values from population samples. The V values are arranged in Tables 6 and 7 from least variable to most variable characters. It appears that, in general, measurements of diameters of zooecia and zooecial tubes, both in and between monticules or maculae, are most reliable in species distinction; other useful characters are the number of internal zooecial structures in a 1-mm distance and the abundance and size of acanthopores. Fine distinctions in wall thickness and abundance and size of mesopores appear generally unjustifiable as criteria for species separation. Distance between monticules or maculae, although of low variability, is too similar between species to serve as a widespread basis for taxonomic distinction.

SUMMARIZATION OF V VALUES FOR SPECIES POPULATION SAMPLES

Character	Range	Median	Mode	Mean	Number of V values used[1]
MnZDm	9-12	10	9	10.0	4
MxZD	4-28	11	11	11.4	16
MnTDm	7-16	11	7,13	11.6	8
MnZDm	11-13	11	11	12.0	4
MnZD	8-20	11	11	12.8	16
MxTDm	10-15	12	12	13.0	8
MxTD	6-26	12	12	13.7	26
DBM	10-18	15	16	14.8	7
MnTD	8-36	14	15	15.9	26
C/mm	15-28	25	—	23.2	3
AD	16-46	24	24,27	27.0	14
D/mm	9-52	32	26	32.9	18
A/1-mmsq	17-84	32	33	36.3	12
MxMTD	21-48	37	37,44	39.2	24
MnMTD	19-54	37	37	40.7	24
ZWT	29-55	45	50	46.0	12
M/2-mmsq	14-146	47	—	54.3	13

[1]Data on population samples taken from Tables 8, 9, 12, 15-17, 21, 24, 27, 28, 30, 33, 34, 36-40, 43-46, 51-53.

Table 7. Range, median, mode, and mean of V value calculated for characters of species population samples, arranged in order of increased variability as indicated by the mean.

ANALYSIS OF THE FAUNA AND PHYLOGENETIC IMPLICATIONS

The Trepostomata from the lower part of the Chickamauga Group in Wills Valley are dominated in number of specimens by robust representatives of *Heterotrypa* and *Amplexopora*. *Prasopora, Mesotrypa, Calopora, Nicholsonella*, and, locally, *Eridotrypa*, are also abundant. Fewer specimens of *Monticulipora, Homotrypa, Batostoma, Hemiphragma*, and *Diplotrypa* were collected.

Some species in the fauna appear close to the transitional stage between two genera, frequently two genera in separate families. The apparent transitional status of some of the species is in part a probable function of the early evolutionary age of the fauna compared to most other faunas of trepostomes. But, apparent transitions also lead to several unanswered questions: 1) What characters are truly phylogenetic and useful in classification? 2) What characters are ecologically controlled? 3) What characters result from convergent evolution? 4) Are the criteria for genera adequate?

and 5) A question asked previously by several workers (*e.g.* Boardman, 1960a, pp. 26, 27; Ross, 1963a, p. 57; 1963c, p. 857; Bork and Perry, 1967, p. 1367; Cuffey, 1967, p. 40) and being much discussed today, what are adequate bases for natural families in the trepostomes?

Boardman and Cheetham (1969a, p. 208; 1969b) discussed the problem of separating genetic from extragenetic influences in variation within an ectoproct species. Within a single colony, they recognized four areas of contribution to variation (astogeny of the colony, ontogeny of the individual, polymorphism, and microhabitat). All variation in ectoprocts can be assigned to two basic sources: differences in genotype and differences in environment. As Boardman and Cheetham (1969a, p. 208; 1969b) indicated, all individuals within an ectoproct zoarium have the same genotype, with the exception of scattered somatic crossovers (and other chromosomal aberrations) that generally have a negligible effect. If the chromosomal aberration occurs in an early embryonic stage, the effect may be more profound than if it occurs in the adult. Therefore, most variation between zooecia within a zoarium is due to the environmental effect on the individuals' uniform genetic potential of response. Astogeny, ontogeny, and polymorphism vary within a zoarium only because of interaction of genetic capacity to assume certain forms with environmental factors. The phenotype is the resultant expression of structures we observe in a specimen, which through environmental influences cause some particular form from within the genetic capacity to occur. At equal astogenetic and ontogenetic levels within a zoarium, nearly all variation of one kind of polymorph within the zoarium at the specified levels is due to environment. Apparent variation due to astogeny and ontogeny occurs only when comparing different levels of astogenetic or ontogenetic development. When thin-section characters of trepostomes are compared, differences in astogenetic and ontogenetic stages of development and polymorphic differences should be kept in mind, and, as stated by Boardman and Cheetham (1969a, p. 208), ". . . genetic calibration within a population is possible only through comparison of individuals that occupy similar astogenetic, ontogenetic, polymorphic, and, as closely as determinable, microenvironmental positions in different colonies."

After sufficient data and procedures have accumulated, future separation of environmental variation, both within and between colonies, from genetic variation between colonies could be aided by comparisons and interpretations of coefficients of variation of individual colonies with coefficients of variation of populations within and between carefully delineated environments.

Heterotrypa patera Coryell has a distinct zone of cystose diaphragms and cystiphragms at the base of the mature zone which indicates possible origin of *Heterotrypa* from *Homotrypa*. *Mesotrypa sparsa,* n. sp., has widely spaced cystiphragms and rare mesopores, which are atypical of *Mesotrypa,* and a zonal development of acanthopores and wide spacing of internal partitions which are attributes of *Stigmatella*. Possibly *M. sparsa* is in, or close to, a phylogenetic line leading from *Mesotrypa* to *Stigmatella*. It should be noted that this interpretation gives a polyphyletic origin to the Heterotrypidae, with lineages from *Homotrypa* to *Heterotrypa* and from *Mesotrypa* to *Stigmatella*. Acceptance of the above suggested lineages depends upon the acceptance of criteria used as their bases as true indicators of close phylogenetic relationship and not independent products of convergent evolution or response to environment. The character most often involved in the hypothetical lineages above is cystiphragms. The apparent function of cystiphragms is to restrict lateral space in zooecial tubes without causing the functional portion of the tube to become shorter, whereas diaphragms completely close zooecial tubes and cause a reduction in length of the tubes available as living chambers. However, there is a complete gradation between diaphragms, cystose diaphragms which are essentially tilted, bulbous, complete diaphragms (see Boardman, 1960a, p. 21, pl. 20, fig. 4b), and cystiphragms, which overlap on the next lower cystiphragm or diaphragm without completely closing the zooecial tube. Complete or partial gradation between diaphragms and cystiphragms is observed in many specimens belonging to several different species and genera, which may indicate an ecologic response rather than a genetic one. If a potential to form cystiphragms is widespread in trepostomes and development is ecologically controlled, then the hypothetical lineages given above have little or no foundation.

Several contemporary workers (Boardman, 1960a, pp. 26, 27;

Ross, 1963a, p. 57; 1963c, p. 857; Bork and Perry, 1967, p. 1367; Cuffey, 1967, p. 40) recognized problems with the classification of the Trepostomata at the family level and have, therefore, generally discarded previously erected families, whereas others (Morozova *in* Astrova, *et al.*, 1960, p. 65; Dunaeva, 1964b; Dunaeva and Morozova, 1967) are actively establishing additional names. Basically, the traditional family groups, as presented in the Treatise on Invertebrate Paleontology (Bassler, 1953) are followed in this report. It appears to me that most traditional families are essentially phylogenetic groups, although as currently recognized they may at a later time be placed at some other level in the classification scheme. An exception, as noted above, may be found in what may be a polyphyletic origin of the Heterotrypidae.

SYSTEMATIC DESCRIPTIONS

Phylum ECTOPROCTA

Class GYMNOLAEMATA

Order TREPOSTOMATA

Family **MONTICULIPORIDAE**

Genus **MONTICULIPORA**

Monticulipora parallela McKinney, n. sp. Pl. 46, figs. 1-5

Diagnosis. — Zoaria are encrusting; zooecial tubes average 0.25 mm by 0.20 mm in diameter, with closely spaced single or opposed rows of cystiphragms that produce an elongate, parallel-sided zooecial void in cross-section; walls locally thickened, especially in monticules; mesopores concentrated in monticules, typically absent in intermonticular areas; acanthopores small, scattered.

Description. — Zoaria are encrusting laminate, with single laminae up to 4 mm thick.

Zooecia and zooecial tubes are irregularly polygonal in cross-section, most typically five- or six-sided. Zooecial tubes are subrounded locally with average diameters of 0.25 mm by 0.20 mm. Internal zooecial structures include strongly curved, overlapping, bulbous cystiphragms of two basic types: one which consists of a

combination of several cystiphragms that extend around approximately 80% of the tube periphery, and another which occurs in pairs. Each of the paired cystiphragms covers about 40% of the tube periphery on opposite sides of the tube, which results in a parallel-sided median zooecial void. Cystiphragms that extend over halfway around the tube periphery result in a zooecial void that touches the periphery on the side of the tube that lacks cystiphragms. Such zooecial voids are typically elongate perpendicular to the zooecial axis, have slightly convergent, planar sides as seen in the tangential sections and are similar to zooecial voids produced by paired cystiphragms except that they are surrounded on three sides by a single cystiphragm or a composite of cystiphragms. There is an average of 16 cystiphragms in a 1 mm vertical distance. Zooecial voids are crossed by irregularly spaced, thin, planar or slightly concave to cystose diaphragms that average six per 1 mm distance.

Local groups of mesopores and enlarged zooecia, presumed to be monticules, are spaced about 3 mm apart. Diameters of zooecial tubes in the enlarged zooecia average 0.36 mm by 0.28 mm.

Zooecial walls are for the most part 0.02 mm or less thick, but in local areas they are slightly thickened by irregularly granular and laminar deposits. Wall laminae dip steeply. Where sufficiently thick, walls have a dark median plane due to steeply dipping laminae. The laminae are poorly defined in most places, but locally they are distinct. Walls have numerous granular dark spots where they are thickened.

Mesopores are concentrated in monticules and are essentially absent in intermonticular areas of most specimens. Mesopore tube diameters average 0.12 mm by 0.08 mm. Abundance of mesopores in a 2-mm square area varies from one to 54, with modal values of two and three and a mean of 13.

Scattered, small acanthopores, most of which occur in zooecial corners, average 0.03 mm in diameter and three per 1-mm square. The acanthopores cause a slight inflection of adjacent zooecial tubes where they are located along zooecial boundaries.

Discussion. — *Monticulipora parallela* most closely resembles *M. arborea* Ulrich, 1893 (pp. 220, 221, pl. 20, figs. 1-9, 13, 14). *M. arborea* has less closely spaced cystiphragms in the immature portion of the zooecial tubes, more acanthopores, and prominent monti-

cules. Also, syntypes of *M. arborea* are ramose and the holotype and paratypes of *M. parallela* are encrusting, although the growth forms are probably controlled by the environment.

The trivial name, *parallela,* refers to the parallel- sided zooecial voids as seen in cross-section.

Material. — Seven sectioned specimens from stratigraphic sections I, II, VI, XII.

Holotype. — USNM 167765.

Paratypes. — USNM 167766, GSATC 201, UNC 4150.

Measurements. — Table 8.

Genus **PRASOPORA**

Discussion. — Ross (1967a, pp. 409-411) recognized that the most significant evolutionary trend in *Prasopora* consists of changes in cystiphragms, which early in the Trentonian are strongly overlapping, crescentic-shaped in longitudinal section, and extend around three-fourths to four-fifths the circumference of the zooecial tube (cystiphragm type 1 of Ross). Later during the Trentonian the cystiphragms gradually became more restricted horizontally and

Character	Range	Mode	Mean	Standard Deviation	Number of Measurements	Number of Specimens Measured
MxTD	0.22-0.32	0.24	0.250	0.022	70	7
MnTD	0.16-0.30	0.20	0.204	0.022	70	7
MxTDm	0.29-0.45	0.34	0.361	0.046	41	7
MnTDm	0.24-0.32	0.30	0.281	0.022	41	7
MxMTD	0.03-0.24	0.10	0.116	0.043	43	5
MnMTD	0.03-0.14	0.10	0.116	0.030	43	5
M/2-mmsq	1-54	2	12.6	18.8	24	5
AD	0.02-0.04	0.03	0.028	0.005	10	1
A/1-mmsq	1-3	3	2.4	0.7	9	1
C/mm	10-21	18	16.5	2.6	33	5
D/mm	1-11	8	5.7	3.0	15	2
DBM	2.0-3.5	3.0	2.8	0.3	25	6

Table 8. Quantitative data on characters of *Monticulipora parallela* McKinney, n. sp. Type suite from the lower Chickamauga Group.

more separated vertically, which results in one lineage with completely isolated, bulbous, vesicle-like cystiphragms (cystiphragm type 3 of Ross). *P. discula* (Coryell) gives the above evolutionary trend an even earlier base, in the Wilderness. *P. discula* has more closely spaced cystiphragms than Trentonian species. Cystiphragms in *P.*

discula form doubly overlapping series locally and extend completely around the perimeter of the zooecial tubes in many specimens. *P. discula* evolved to *P. falesi* (James, 1884, p. 138, pl. 7, figs. 2-20) apparently by increased vertical separation of cystiphragms which are reduced to extend only part way around the zooecial tubes in *P. falesi.*

Prasopora discula (Coryell, 1921) Pl. 46, figs. 6-8; Pl. 47, figs. 1-7

1921. *Monticulipora discula* Coryell, Indiana Acad. Sci., Proc., vol. 29, p. 283, pl. 4, figs. 3, 4.
1942. *Prasopora fritzae* Loeblich, Jour. Paleont., vol. 16, p. 426, pl. 63, figs. 10, 11.

Diagnosis. — Zoaria uniformly low discoidal; intermacular zooecial tube diameters average 0.25 mm by 0.21 mm, with about 15 overlapping cystiphragms per mm; diaphragms variable, about nine per mm; average of 15 mesopores per 2-mm square; acanthopores present or absent, and where present average four per mm square.

Description. — Zoaria are low discoidal in shape with a ratio of diameter to height about 10:3. Of 70 zoaria of *Prasopora discula* whose dimensions were measured, the range in ratio of diameter to height is approximately 7:1 to 3:2. Almost all zoaria began growth by encrusting the pedicle valve of *Sowerbyella,* and this substrate controlled zoarial form until zoaria reached about 10 mm diameter, at which stage they began growing beyond the edges of the shells. The 10:3 ratio is attained where the zoaria are about 10 mm in diameter and is approximately maintained from that point. Where exposed beyond the shell perimeters of *Sowerbyella,* the zoarial bases are shallow concave with concentric rugae indicating growth stages and radial striations marking the zooecial bases. Maculae cannot be detected on the weathered zoarial surfaces.

Zooecial tubes are elongate polygonal in cross-section with an average maximum and minimum tube diameter of 0.25 mm by 0.21 mm between maculae. Diameters of the largest zooecial tubes in maculae average 0.35 mm by 0.28 mm. Almost all cystiphragms lining zooecial tubes extend over halfway around the tubes and may extend all the way around. Cystiphragms restrict the zooecial void to a space whose cross-section is roughly oval or subcircular and which is located either subcentrally or laterally (Ross' "type 1" cystiphragms, 1967a, pp. 406-408, text-fig. 2A). Cystiphragms

strongly overlap and locally form doubly overlapping series. They are closely appressed, an average of 15 in 1 mm. Flat to slightly concave diaphragms are less regularly spaced than cystiphragms and average nine per mm. In isolated places in several specimens, two zooecia are merged laterally to form "twins" with an open figure-eight cross-sectional shape.

Zooecial walls are thin, in most places 0.01 mm or less in thickness except at zooecial corners, where they are slightly thickened. Small, round, clear spots which may represent tubules are frequently found in zooecial corners. Walls appear vaguely laminar with a central band where laminae of adjacent zooecia meet at zooecial boundaries (see Pl. 48, fig. 3). Walls are locally thickened to over 0.04 mm.

Mesopore abundance is variable; they average 17 per 2-mm square including maculate areas, with a standard deviation of 11 per 2-mm square. Mesopore diameters average 0.12 mm by 0.08 mm, including mesopores located both in and between maculae. Mesopores in maculae are typically larger than mesopores between maculae. All mesopores are irregularly polygonal; those in maculae have straight sides and those between maculae generally have concave sides due to their position between zooecia. Diaphragm spacing in mesopores is equal to cystiphragm spacing in zooecia so that mesopores are difficult to distinguish in vertical sections.

Forty percent of the specimens examined in thin-sections and by acetate peels have acanthopores. Specimens with acanthopores have density ranges from three acanthopores in a section of about 16 sq. mm to 12 per 1-mm square, with an average of four per 1-mm square. Acanthopores are typically 0.03 mm in diameter. They have the usual cone-in-cone structure that appears as concentric rings in tangential zoarial sections and as outwardly pointing chevrons in vertical sections. The axial area of acanthopores may be either central or eccentric.

Discussion. — Measurements made on the holotypes of *Monticulipora discula* Coryell and *Prasopora fritzae* Loeblich are given in Tables 10 and 11. *P. fritzae* is here considered synonymous with *M. discula* because characters typical of both are contained in the single population from Wills Valley and visual and data compari-

sons of the holotypes indicated no major difference other than more robust zoarial size of *P. fritzae*.

Prasopora discula resembles *P. falesi* (James, 1884) (p. 138, pl. 7, figs. 2-2d) but differs in that *P. falesi* has fewer cystiphragms per mm, typically more mesopores in intermaculate areas, and maculae are spaced farther apart.

Specimens of the discoidal species of *Prasopora* from Wills Valley that possess acanthopores fit well into *P. discula* (Coryell). Al-

Character	Range	Mode	Mean	Standard Deviation	Number of Measurements	Number of Specimens Measured
MxTD	0.19-0.31	0.25	0.251	0.023	510	51
MnTD	0.15-0.30	0.20	0.212	0.022	510	51
MxTDm	0.29-0.50	0.35	0.351	0.035	96	35
MnTDm	0.23-0.33	0.28	0.287	0.021	96	35
MxMTD	0.04-0.41	0.15	0.125	0.057	342	35
MnMTD	0.02-0.25	0.05	0.085	0.040	354	36
M/2-mmsq	0-54	9	17.4	10.6	134	34
AD	0.02-0.03	0.03	0.025	0.004	7	4
A/1-mmsq[1]	1-12	1	3.8	3.2	26	6
C/mm	3-28	17	15.4	3.9	391	46
D/mm	4-13	10	8.7	2.4	79	9
D/mmM	14-26	17	18.7	3.3	15	2
DBM	2.0-3.5	2.5	2.58	0.33	122	23

[1]Includes only counts that include acanthopores per 1-mm square, thereby excluding the majority of specimens, since most specimens lack acanthopores.

Table 9. Quantitative data on characters of *Prasopora discula* (Coryell) from the lower Chickamauga Group.

Character	Range	Mode	Mean	Standard Deviation	Number of Measurements	Number of Specimens Measured
MxTD	0.24-0.29	0.28	0.265	0.016	10	1
MnTD	0.20-0.24	0.22	0.220	0.011	10	1
MxTDm	0.33-0.40	0.35	0.355	0.017	10	1
MnTDm	0.26-0.32	0.27	0.283	0.018	10	1
MxMTD	0.08-0.20	0.13	0.146	0.036	10	1
MnMTD	0.04-0.15	0.12 0.15	0.100	0.035	10	1
M/2-mmsq	5-7	—	6.0	1.0	2	1
C/mm	13-23	17	17.2	3.1	6	1
D/mm	14-18	15	15.4	1.3	8	1
DBM	2.0-2.5	2.5	2.3	0.24	3	1

Table 10. Quantitative data on characters of *Monticulipora discula* Coryell, 1921. Holotype, USNM 92162.

Character	Range	Mode	Mean	Standard Deviation	Number of Measurements	Number of Specimens Measured
MxTD	0.26-0.29	0.26 0.29	0.274	0.012	10	1
MnTD	0.20-0.25	0.24	0.227	0.017	10	1
MxTDm	0.34-0.40	0.37	0.367	0.021	10	1
MnTDm	0.27-0.33	0.30 0.33	0.307	0.018	10	1
MxMTD	0.04-0.20	0.13	0.129	0.042	10	1
MnMTD	0.03-0.16	0.09	0.090	0.037	10	1
M/2-mmsq	1-3	1	1.7	0.94	3	1
AD	0.02-0.04	0.03	0.027	0.005	10	1
A/1-mmsq	4-11	9	8.0	1.84	10	1
C/mm	13-23	18 21	18.6	2.73	10	1
D/mm	5-14	9 12	9.6	2.50	10	1
DBM	3	3	3	—	1	1

Table 11. Quantitative data on characters of *Prasopora fritzae* Loeblich, 1942. Holotype, USNM 114625.

though over half the *Prasopora* zoaria sectioned lack acanthopores, they are also assigned to *P. discula* because, in the population and even at a single locality, all gradations exist between absent and common acanthopores (as at stratigraphic sections II and XVII). Specimens both with and without acanthopores were collected alongside one another in the same bed and in identical matrices. Since there is no evidence that environment contributed to absence or presence of acanthopores, it is concluded that the presence or absence of acanthopores in *P. discula* is due most likely to the genotype of individual clones within the species and should not be relied upon in this case as a species characteristic.

Material. — Fifty-eight sectioned specimens from stratigraphic sections I, II, IV, V, VI, XVI, XVII.

Hypotypes. — USNM 167767-167769, 167839.

Measurements. — Table 9.

Prasopora megacystata McKinney, n. sp. Pl. 48, figs. 1-3

Diagnosis. — Zoarial form variable; maculae present; zooecial diameters 0.24 mm by 0.20 mm; large, bulbous cystiphragms 12 per mm and diaphragms nine per mm; about 20 mesopores per 2-mm square.

Description. — Zoaria are encrusting and free laminate to

massive and ramose. Greatest observed zoarial thickness is 12 mm, and greatest laminate width is 34 mm. Maculae are from 1.5 to 3 mm apart, most typically 2.5 mm to 3 mm apart, measured from center to center.

Zooecia are irregularly polygonal in cross-section. Intermacular zooecial tube diameters average 0.24 mm by 0.20 mm, but there are local groups of smaller zooecia in one specimen. Mean zooecial tube diameters are 0.36 mm by 0.29 mm in maculae. There is an average of nine diaphragms per mm and 12 cystiphragms per mm in zooecia. Diaphragms are thin and most are slightly concave or slightly convex; few are planar. Cystiphragms are thin also; they overlap and are bulbous-appearing in vertical sections. In tangential sections they can be seen to extend a half to three-fourths, infrequently all the way, around zooecial peripheries, surrounding a central to subcentrally placed void. Cystiphragms in macular zooecia extend all or almost all the way around the periphery, surrounding a void with a highly elliptical cross-section. Long axes of the elliptical voids extend from the center to the periphery of the zooecial tube in most places.

Walls are thin, 0.01 mm or less in thickness. Walls are finely laminated, as seen under magnifications of $\times 100$ or greater.

Mesopores are abundant and average 20 per 2-mm square. The mesopores appear to originate at various levels within zoaria but are most abundant near the zoarial margin. Mesopore cross-sections are angular, most typically four-sided, but in some places three-, five-, or six-sided. Size is variable; mesopore tube diameters average 0.11 mm by 0.07 mm. Diaphragms are spaced two to three times closer in mesopores than in zooecia. Some mesopores swell slightly between diaphragms, which results in a vaguely beaded appearance.

Where proximal mesopore tips are cut in tangential sections, mesopores have an acanthopore-like appearance because of the small size of mesopore tubes. No true acanthopores were observed.

Discussion. — *Prasopora megacystata* most closely resembles *Prasopora compacta* (Coryell, 1921, p. 283, pl. 4, figs. 5, 6) but has more widely spaced, bulbous cystiphragms and lacks abundant, prominent acanthopores. The specimens identified by Astrova (1965, p. 197, pl. 34, fig. 1a, b) as *Monticulipora compacta* Coryell lack

Character	Range	Mode	Mean	Standard Deviation	Number of Measurements	Number of Specimens Measured
MxTD	0.21-0.28	0.24	0.244	0.015	40	4
MnTD	0.16-0.24	0.20	0.201	0.018	40	4
MxTDm	0.30-0.43	0.38	0.363	0.040	17	4
MxMTD	0.20-0.35	0.28 0.32	0.290	0.039	17	4
MnMTD	0.03-0.31	0.10 0.14	0.109	0.051	40	4
M/2-mmsq	0.03-0.15	0.10 12	0.074	0.030	40	4
	7-38	15 29	19.9	9.4	17	4
C/mm	5-20	12	11.8	3.4	40	4
D/mm	6-16	11	9.0	2.4	30	3
DBM	1.5-3.0	2.5	2.50	0.45	18	4

Table 12. Quantitative data on characters of *Prasopora megacystata*, n. sp. Type suite from the lower Chickamauga Group.

abundant, prominent acanthopores and have more widely spaced, bulbous cystiphragms than the holotype of *M. compacta* (USNM 92163). Astrova's specimens more closely resemble *P. megacystata* than *P. compacta* (Coryell).

The four specimens that form the basis for *Prasopora megacystata* differ distinctly from specimens of *P. discula* (Coryell, 1921, p. 283, pl. 4, figs. 3, 4), the dominant *Prasopora* species in the Chickamauga fauna, primarily in nature of cystiphragms. Cystiphragms in *P. megacystata* are more bulbous, more widely spaced, and occupy a much greater portion of the zooecial diameter than do cystiphragms of *P. discula*.

The trivial name, *megacystata*, refers to the large, bulbous cystiphragms characteristic of the species.

Material. — Four sectioned zoaria from stratigraphic sections I and XV.

Holotype. — USNM 167770.

Paratypes. — USNM 167771, GSATC 202, UNC 4152.

Measurements. — Table 12.

Prasopora sp. Pl. 48, figs. 4-6

Description. — The zoarium is low discoidal, 17 mm in diameter and 5.5 mm high. The zoarium is composed of two to four laminae and is 4 mm in maximum thickness; it was originally thicker, but the base has been dissolved and has a stylolitic contact with under-

lying micrite. Small maculae are 2.5 mm apart, measured from center to center.

Zooecia are irregularly polygonal in cross-section. Most are five- or six-sided. Zooecial tube diameters average 0.26 mm by 0.21 mm. Most cystiphragms extend three-fourths to entirely around the periphery of zooecia, surrounding a subcircular peripheral or subperipheral void. Cystiphragms strongly overlap, appear bulbous in vertical section and average 16 per mm. Diaphragm spacing is approximately equal to or slightly less than the cystiphragm spacing. Most diaphragms are essentially planar, but some are strongly tilted. Both cystiphragms and diaphragms are thin. Zooecial tube diameters in maculae average 0.37 mm by 0.31 mm.

Walls are 0.01 mm to 0.02 mm thick. They are composed of laminae that are so steeply dipping that they are essentially parallel to the zooecial border, in both vertical and tangential sections. Contact between two adjacent zooecia is marked by a thin dark line.

Mesopores are present but are moderately sparse. An average of four mesopores occurs in a 2-mm square. Most mesopores are four-sided in cross-section, with mean maximum and minimum tube diameters 0.14 mm by 0.10 mm. Diaphragm spacing in mesopores is approximately equal to cystiphragm spacing in zooecia.

Acanthopores are abundant and average 15 per 1-mm square. There is an acanthopore at most zooecial corners. Acanthopores originate at or near the base of zoarial laminae. They have a large axial area and range from 0.02 mm to 0.07 mm in diameter; most are about 0.04 mm in diameter.

Discussion. — The specimen described above cannot be readily placed in any previously recognized species, but the single specimen collected does not give sufficient information, due to the small amount of material available for sectioning, to erect a new species.

Material. — One thin-sectioned colony from stratigraphic section I.

Hypotype. — USNM 167772.

Measurements. — Table 13.

?Prasopora sp. Pl. 48, figs. 7, 8; Pl. 49, figs. 1-3

Description. — Zoarial form varies from encrusting to irregularly ramose. Maximum thin-section diameter is 21 mm.

Character	Range	Mode	Mean	Standard Deviation	Number of Measurements	Number of Specimens Measured
MxTD	0.23-0.33	0.23	0.262	0.034	10	1
MnTD	0.19-0.23	0.20	0.209	0.014	10	1
MxTDm	0.32-0.49	0.36	0.373	0.062	10	1
MnTDm	0.27-0.42	0.30	0.309	0.042	10	1
MxMTD	0.03-0.23	0.23	0.143	0.068	10	1
MnMTD	0.03-0.15	0.12	0.097	0.037	10	1
M/2-mmsq	1-8	—	4.0	3.2	4	1
A/1-mmsq	13-21	15	16.0	2.6	10	1
C/mm	14-21	15	15.6	2.0	10	1
DBM	2.0-3.0	2.5	2.5	0.5	5	1

Table 13. Quantitative data on characters of *Prasopora* sp. from the lower Chickamauga Group.

In immature regions, large, bulbous cystiphragms are spaced about one-half to one tube diameter apart. Due to the crowded nature of zoarial growth in an interlobate area, local groups of immature zooecia are restricted to about half the mature zooecial diameters. Zooecia in the mature region are irregularly polygonal, most typically five- or six-sided. Most zooecial tubes are also polygonal but some are subrounded where walls are thickened in mature areas. Mature zooecial tube diameters average 0.26 mm by 0.22 mm. Where zooecia pass into the mature region, cystiphragms become smaller, more closely spaced and more strongly overlapping, and thin, essentially planar diaphragms in the zooecial void become more numerous. In the mature zone there are averages of 27 cystiphragms and 15 diaphragms per mm. Cystiphragms in the mature zone are locally thickened and typically extend around approximately 30-40% of the zooecial periphery. Several cystiphragms per zooecium are cut in the plane of shallow tangential sections so that there is a small, rounded zooecial void located in most cases on one side of the zooecial periphery. Deeper tangential sections that cut the larger cystiphragms in the immature zone show individual cystiphragms that extend around approximately 90% of the zooecial periphery and leave a small, rounded zooecial void similar to those in shallower section.

Mesopores and enlarged zooecia are locally grouped into monticules that are spaced 2 mm to 3 mm apart, measured from center to center. Zooecial tube diameters in monticules average 0.42 mm by 0.31 mm.

Zooecial walls are thin and planar in the immature region but are abnormally and abruptly thickened by curved, steeply dipping laminae in the mature zone. Laminae from adjacent zooecia meet along a distinct plane that appears as a dark, finely serrate line in longitudinal sections and as a well- to moderately defined dark line in tangential sections. In the area where they are thickest, mature walls average 0.04 mm.

Mesopores are concentrated in monticules and are apparently absent in intermonticular areas. Mesopore tube diameters average 0.14 mm by 0.09 mm and are surrounded by walls that are similar to zooecial walls. Slightly thickened, closely spaced, planar diaphragms are present in mesopores. Including monticules, mesopores average six per 2-mm square.

Short acanthopores that originate in the mature and outer immature zones are located mostly in zooecial corners, with a few located along zooecial borders. The acanthopores average 0.03 mm in diameter and two per 1-mm square.

Discussion. — The single specimen on which the above description is based is tentatively assigned to the genus *Prasopora.* It resembles *Monticulipora* in growth form and differentiation into distinct mature and immature zones, which is closely related to trepostome growth form since discoidal or encrusting zoaria usually have the immature region restricted to a thin basal zone, and massive, frondose and ramose zoaria typically have well-developed immature zones. The specimen is not placed in *Monticulipora* because it lacks the granular-laminar structure that is a fundamental character of *Monticulipora.* The laminar wall structure in the specimen is like that in *Prasopora,* and because other characters except growth form are similar to characteristic features of *Prasopora,* the specimen is placed in that genus.

Material. — One thin-sectioned specimen from stratigraphic section XVII.

Hypotype. — USNM 167773.

Measurements. — Table 14.

Character	Range	Mode	Mean	Standard Deviation	Number of Measurements	Number of Specimens Measured
MxTD	0.24-0.28	—	0.261	0.014	10	1
MnTD	0.19-0.24	0.20 0.23	0.215	0.017	10	1
MxTDm	0.38-0.45	0.43	0.418	0.018	5	1
MnTDm	0.27-0.32	—	0.312	0.022	5	1
MxMTD	0.06-0.32	0.06 0.14	0.138	0.078	10	1
MnMTD	0.05-0.20	0.05	0.086	0.047	10	1
M/2-mmsq	1-11	7	6.4	3.6	5	1
AD	0.02-0.04	0.03	0.031	0.006	10	1
A/1-mmsq	1-4	1	2.0	1.6	10	1
C/mm	21-33	23 29	26.6	3.9	10	1
D/mm	12-20	14	15.3	2.7	10	1
DBM	2.0-3.0	2.5	2.4	0.39	10	1

Table 14. Quantitative data on characters of *?Prasopora* sp. from the lower Chickamauga Group.

Genus **HOMOTRYPA**

Homotrypa subramosa Ulrich, 1886 Pl. 49, figs. 4-8; Pl. 50, fig. 1

1886. *Homotrypa subramosa* Ulrich, Minnesota Geol. and Nat. Hist. Sur., 14th Ann. Rept., p. 81.
1886. *Homotrypa insignis* Ulrich, Minnesota Geol. and Nat. Hist. Sur., 14th Ann. Rept., p. 82.
1893. *Homotrypa subramosa* Ulrich, Ulrich, extract from Minnesota Geol. and Nat. Hist. Sur., Final Rept., Paleont., vol. 3, pp. 239, 240, pl. 19, figs. 21-28.
1893. *Homotrypa subramosa* var. *insignis* Ulrich, Ulrich, extract from Minnesota Geol. and Nat. Hist. Sur., Final Rept., Paleont., vol. 3, p. 240.
1911. *Homotrypa subramosa* Ulrich, Bassler, U. S. Nat. Mus., Bull. 77, p. 187, text-figs. 99a-e.
1968b. *Homotrypa subramosa* Ulrich, Bork and Perry, Jour. Paleont., vol. 42, pp. 1053-1055, pl. 136, figs. 1-3.

Diagnosis. — Zoarial form variable; mature zooecial diameters average 0.26 mm by 0.21 mm, diaphragms typically absent to sparse in immature zone but intergrade with cystiphragms in mature zone and average 11 per mm; wall thickness variable; monticules prominent in thin-section; mesopores 0.11 mm by 0.07 mm in mean diameter and eight per 2-mm square, mostly in monticules; acanthopores average 15 per 1-mm square.

Description. — Zoaria are encrusting, multilaminar massive or ramose. The greatest observed diameter of a fragmented massive zoarium is 25 mm and the greatest observed branch diameter is 12 mm.

Zooecia are variable. In ramose forms they bend continuously out from the axial region and enter the mature zone with a distinct bend or with no increase in curvature. Cross-sections of mature zooecia are polygonal, typically five- or six-sided. Mature zooecial diameters are 0.26 mm by 0.21 mm and corresponding zooecial tube diameters are 0.22 mm by 0.18 mm on the average. Thin, essentially planar diaphragms are absent to most typically sparse in the immature zone. There is an apparent gradation in the mature zone from well-defined, slightly domal diaphragms near the base to cystose diaphragms to small, tightly overlapping bulbous or slightly curved cystiphragms higher within the mature zone. Thin, essentially planar diaphragms are distributed throughout the mature zone along with progressively changing cystiphragms. There is an average of 11 internal zooecial structures in a 1 mm line in the mature zone. Some cystiphragms and diaphragms are slightly thickened.

Monticules composed of enlarged zooecia and mesopores are distributed at approximately 2.5 mm intervals measured from center to center. Zooecia in monticules have average mature diameters of 0.35 mm by 0.27 mm, and corresponding zooecial tube diameters average 0.32 mm by 0.25 mm. Mesopores in monticules are also slightly larger than mesopores between monticules.

Zooecial walls in immature zones are thin and smooth. Mature zooecial walls are variable, with an overall mean thickness of 0.05 mm; the average within each zoarium varies from 0.02 mm to 0.08 mm. Even where mature walls are thin, there is a distinct plane of contact between walls of adjacent zooecia. Along the zooecial cavity, wall laminae are subparallel to the zooecial axis. They bend imperceptably toward the zooecial boundary until they have an angle of about 15° with the boundary. As the laminae approach the boundary, they curve abruptly to meet it at an approximate 45° angle.

Mesopores are irregularly polygonal in cross-section. Mesopore tubes are subangular where walls are thin to rounded oval in cross-section where walls are thicker; tube diameters average 0.11 mm by 0.07 mm. There is an average of eight mesopores, most of which are located in monticules, per 2-mm square. About 10 mesopore diaphragms occur in 1 mm.

Acanthopores average 15 per 1-mm square and are 0.04 mm

in diameter. They are located in zooecial corners and typically inflect adjacent zooecial tubes to a small degree. At least some acanthopores originate at the base of the mature zone, although some may originate higher within the mature zone.

Discussion. — Because cystiphragms are locally difficult to differentiate from diaphragms, the number of all internal zooecial structures crossing a 1 mm straight line was counted rather than cystiphragms per mm and diaphragms per mm. Ulrich's original description (1886, p. 81) of *Homotrypa subramosa* included a subramose growth form, moderately thin walls, well-developed acanthopores ("spiniform tubuli"), occurrence of diaphragms in parallel convex lines at unequal intervals in the immature zone, and more or less closely spaced cystiphragms in the mature zone. Ulrich subsequently gave illustrations and a modified description (1893, pp. 239, 240, pl. 19, figs. 21-28), in which he noted that acanthopores are variable in both number and size. The Chickamauga Group specimens here assigned to *H. subramosa* agree in all aspects with the early descriptions except that diaphragms in the immature region are more sparse and growth form is more variable. The specimen illustrated in Plate 50, figure 5 has an abnormal number of diaphragms in the immature area and is not typical of the Chickamauga representatives of *H. subramosa*. Plate 50, figure 4, depicts a more nearly typical area in the same zoarium. Measurements and counts of mean maximal zooecial tube diameter, zooecia in a 2 mm line, mean maximum zooecial tube diameter in monticules, mesopores per unit area, acanthopore size and acanthopores per 1-mm square are within one standard deviation range in the Chickamauga specimens and the specimen that Bork and Perry (1968b, pp. 1053-1055, pl. 136, figs. 1-3, table 9) assigned to *H. subramosa*.

Bassler (1911, pp. 187-189, text-fig. 100), Troedsson (1929, p. 98, pl. 53, figs. 1, 2), Sardesson 1935c, p. 353), and Astrova (1965, pp. 201, 202, pl. 36, fig. 1a, b) reported *Homotrypa subramosa* but their specimens were not reexamined in this study and their descriptions do not allow a firm decision that their specimens belong to *H. subramosa*.

Homotrypa subramosa is similar to *H. dickeyvillensis* Perry, 1962 (pp. 13, 14, pl. 2, figs. 5-9) and *H. minnesotensis* Ulrich, 1886 (pp. 79, 80), both from the Middle Ordovician. The Chickamauga

Character	Range	Mode	Mean	Standard Deviation	Number of Measurements	Number of Specimens Measured
MxZD	0.22-0.34	0.26	0.264	0.026	47	5
MnZD	0.17-0.28	0.20	0.214	0.025	47	5
MxTD	0.13-0.30	0.25	0.223	0.036	117	12
MnTD	0.10-0.25	0.20	0.182	0.036	117	12
MxZDm	0.27-0.44	0.32	0.350	0.040	27	4
MnZDm	0.19-0.34	0.27	0.269	0.027	27	4
MxTDm	0.22-0.44	0.35	0.317	0.050	85	11
MnTDm	0.13-0.33	0.25	0.250	0.040	85	11
ZWT	0.02-0.10	0.02	0.047	0.026	90	9
MxMTD	0.05-0.23	0.10	0.113	0.041	100	10
MnMTD	0.03-0.15	0.05 0.08	0.073	0.026	100	10
M/2-mmsq	1-15	11	8.0	4.2	41	10
AD	0.02-0.05	0.03	0.035	0.007	70	7
A/1-mmsq	7-33	12	15.2	5.2	68	9
C&D/mm	7-27	8	11.1	4.1	67	7
DBM	2.0-3.5	2.0 2.5	2.37	0.37	70	8

Table 15. Quantitative data on characters of *Homotrypa subramosa* Ulrich from the lower Chickamauga Group.

specimens of *H. subramosa* differ from *H. dickeyvillensis* in having smaller zooecia, generally more sparse diaphragms in the immature region, more abundant acanthopores, and apparent mesopores. Perry (1962, p. 13) indicated a probable lack of mesopores in *H. dickeyvillensis*, and in subsequent work, Bork and Perry (1968b, p. 1045) indicated a mean maximum zooecial tube diameter of 0.30 mm and recognized mesopore-like apertures which they interpreted as partially developed zooecia.

Ulrich (1886, pp. 79, 80; 1893, pp. 235, 236) indicated a lack of diaphragms in the immature region, oblique zooecial apertures, and near the surface, zooecia that ". . . are flattened and their size considerably reduced" in *Homotrypa minnesotensis*. Chickamauga specimens of *H. subramosa* differ from *H. minnesotensis* in that some specimens have sparse diaphragms in the immature zone, the mature walls in most zooecia are thicker, zooecial apertures are at a higher angle to the zoarial surface and the zooecia do not narrow in the submature zone.

Material. — Twelve sectioned specimens from stratigraphic sections I, II, V, VIII, XVII.

Hypotypes. — USNM 167774, 167775.

Measurements. — Table 15.

Homotrypa vacua McKinney, n. sp. Pl. 50, figs. 2-7

Diagnosis. — Zoaria ramose; branches typically 1.5 mm to 2 mm in diameter; zooecia constricted in submature zone, with diaphragms only in submature and mature zones and cystiphragms only in mature zone, mean mature zooecial diameters 0.23 mm by 0.15 mm; mesopores common, 0.08 mm by 0.05 mm mean diameter; small acanthopores average 23 per 1-mm square.

Description. — Zoaria are ramose, typically with branches 1.5 mm to 2 mm in diameter but some approximately 5 mm in diameter.

Zooecia are long, essentially parallel with the branch axis in the immature zone. They gradually diverge from the axial region to an angle of about 15° in the submature zone, where zooecial diameters are noticeably constricted. Passage into the mature zone is marked by a slight increase in angle of divergence, appearance of cystiphragms, and thickened wall deposits. Mature zooecial diameters are small and average 0.23 mm by 0.15 mm, with corresponding average zooecial tube diameters of 0.16 mm by 0.09 mm. Mature zooecial cross-sections are irregularly polygonal, and mature zooecial tube cross-sections are subrounded oval. Diaphragms are lacking in the immature zone but are present in the submature and mature zones. Diaphragms are typically thin, essentially planar and are oriented at right angles to zooecial axes. Strongly bulbous cystiphragms, present in the mature zone, are typically thickened and overlap each other. The thickest portion of the cystiphragms is distal with respect to zooecial tubes, where they merge with zooecial walls. Cystiphragm spacing averages six per mm.

Small monticules are composed of larger than normal zooecia. In them, zooecial diameters average 0.32 mm by 0.24 mm and corresponding zooecial tube diameters average 0.24 mm by 0.18 mm. Distances between monticules could not be determined because of the small size of tangential sections and the fact that all specimens are buried in matrix.

Immature zooecial walls are thin and, in some specimens, slightly crinkled. Mature walls are thick, average 0.05 mm in thickness, and are composed of laminae which dip about 45° to zooecial borders. The plane of contact between adjacent zooecia is distinct. Laminae in mature walls pass frequently into cystiphragms within zooecial tubes.

Mesopores are small and common. Mesopore tubes average 0.08 mm by 0.05 mm in diameter. Due to the small area of tangential sections, only one count of mesopore abundance was obtained, which is 18 per 2-mm square. Mesopores originate in the submature zone and are confined to zooecial corners. They have thin diaphragms spaced less than a tenth of a mm apart. Mesopore walls may be thin or may be thickened similar to zooecial walls.

Acanthopores are small, 0.03 mm in mean diameter, and most are confined to zooecial corners. They originate at the base of the mature zone and average 23 per 1-mm square.

Discussion. — *Homotrypa vacua* resembles *H. exilis* Ulrich, 1886 (p. 80) in small branch diameter, wall thickness, lack of diaphragms in the axial region, and constriction of zooecia in the submature zone. (See Ulrich, 1893, pl. 19, fig. 12; Perry, 1962, pl. 1, fig. 1.) However, *H. vacua* differs in possessing abundant, prominent acanthopores, distinctly smaller zooecial tubes (based on my measurements of Ulrich's 1893 pl. 19, fig. 14), and more arcuate cystiphragms. In two different studies of population samples of *H. exilis,* Perry (1962, p. 6, text-fig. 1) measured zooecial tube diameters averaging 0.21 mm in the Middle Ordovician Spechts Ferry Shale specimens and Bork and Perry (1968b, p. 1046, table 4) found an average of 0.22 mm for the same character of specimens from the Middle Ordovician Quimbys Mill and Guttenberg Formations. The longitudinal sections figured by Perry (1962, pl. 1, figs. 1, 6) and by Bork and Perry (1968b, pl. 133, fig. 10) appear to have more abundant diaphragms in both submature and mature zones than does the longitudinal section first figured by Ulrich (1893, pl. 19, fig. 12).

Homotrypa vacua differs from the type description of *H. lowvillensis* Fritz, 1957 (p. 22) in possessing distinct acanthopores and abundant, prominent cystiphragms. All species of *Homotrypa* originally described by Loeblich in 1942 (*H. callitoecha,* pp. 420, 421, pl. 62, figs. 18-20; *H. multitabulata,* p. 421, pl. 63, figs. 1-3; *H. sagittata,* pp. 421, 422, pl. 63, figs. 7-9; *H. ulrichi,* p. 422, pl. 63, figs. 4-6) differ from *H. vacua* because they possess abundant diaphragms in the immature zone and do not have zooecia constricted in the submature zone.

One associated taxon that is superficially similar to *Homotrypa vacua* is *Eridotrypa minor* Ulrich, 1893 (p. 266, pl. 26, figs. 20, 21,

29, 30). Zoarial fragments of *E. minor* have branch diameters of 2 mm to 4 mm and a lack of diaphragms in the axial zone. A few cystiphragms or cystose diaphragms occur in the mature zone, zooecial constrictions occur in the submature zone, and zooecial tube diameters average 0.18 mm by 0.11 mm in the mature zone of the Chickamauga specimens of *E. minor*. However, *H. vacua* has more numerous, prominent cystiphragms, smaller zooecia, and more prominent, abundant acanthopores. The granular, zigzag zooecial boundaries in the mature zone of *E. minor*, a diagnostic generic character of *Eridotrypa*, further differentiates the two taxa.

Constricted zooecia in the submature zone, a characteristic of both *Homotrypa exilis* and *H. vacua*, is a family characteristic of Aisenvergiidae Dunaeva, 1964 (1964b, p. 39). However, as with

Character	Range	Mode	Mean	Standard Deviation	Number of Measurements	Number of Specimens Measured
MxZD	0.14-0.29	0.25	0.232	0.038	98	10
MnZD	0.10-0.23	0.15	0.154	0.030	98	10
MxTD	0.09-0.28	0.13	0.159	0.036	129	13
MnTD	0.05-0.15	0.08	0.089	0.028	128	13
MxZDm	0.28-0.38	—	0.318	0.037	8	3
MnZDm	0.19-0.28	—	0.238	0.023	8	3
MxTDm	0.20-0.30	0.25	0.238	0.023	8	3
MnTDm	0.14-0.20	0.17 0.19	0.177	0.019	8	3
ZWT	0.02-0.12	0.04	0.049	0.016	130	13
MxMTD	0.04-0.17	0.05 0.08	0.078	0.027	55	9
MnMTD	0.02-0.10	0.04	0.049	0.016	55	9
AD	0.02-0.05	0.03	0.032	0.006	69	7
A/1-mmsq	12-34	—	22.8	7.5	15	6
D/mm	2-14	5	5.8	2.5	18	6

Table 16. Quantitative data on characters of *Homotrypa vacua*, n. sp. Type suite from the lower Chickamauga Group.

Eridotrypa the constriction is not as severe as in Devonian and Carboniferous genera originally placed in the Aisenvergiidae and probably does not indicate a close phylogenetic relationship. The possibility of a close relationship between *Homotrypa* and *Eridotrypa* has been discussed further.

The trivial name, *vacua*, refers to the characteristic lack of diaphragms and cystiphragms in the immature region.

Material. — Thirty sectioned zoarial fragments from stratigraphic sections III, VI, VIII, IX, XIV, XVIII.

Holotype. — USNM 167776.

Paratypes. — USNM 167777, 167778, GSATC 203, UNC 4154.

Measurements. — Table 16.

Genus **MESOTRYPA**

Mesotrypa sparsa McKinney, n. sp. Pl. 50, fig. 8; Pl. 51, figs. 1-7

Diagnosis. — Zoarial form variable; mature zooecial tube diameters average 0.23 mm by 0.19 mm, diaphragms sparse in immature zones, diaphragms and cystiphragms are variably developed in mature zones and average nine per mm; mature walls typically thin; mesopores sparse, concentrated in monticules; acanthopores in longitudinal bands, 15 per 1-mm square on the average where present in tangential sections.

Description — Zoaria are encrusting, free laminate, ramose, or most typically low to high domal with a moderately concave base. Most specimens are 10 mm to 20 mm in diameter and 3 mm to 10 mm high.

In ramose specimens, zooecia curve gently out from the axial region to a more pronounced bend at the base of the mature zone, beyond which they extend with little curvature and at a high angle to the zoarial surface. Where walls are thin, mature zooecia are irregularly polygonal in cross-section, most typically five- or six-sided. Maximum and minimum mature zooecial tube diameters average 0.23 mm by 0.19 mm. Thin, planar diaphragms are present in the immature zone. In the mature zone, development of zooecial tube partitions is variable. In most zooecia of some colonies, there is an intergradation between planar to slightly domal diaphragms, cystose diaphragms, and large cystiphragms which occupy over half the tube diameter. In these colonies the cystiphragms may be located either at the base or well up into the mature zone. In most specimens, however, the majority of the zooecia have cystiphragms distributed more or less continuously throughout the mature zone. In specimens which have zooecial tubes partially closed by cystiphragms, diaphragms may or may not close off the remainder of each such zooecial tube. Locally within mature zooecia, diaphragms extend all the way across the zooecial tubes and cystiphragms are

absent, but this appearance may be due to lateral cuts through large cystiphragms so that downward curvature of the large cystiphragms is not exhibited in the sections. Most cystiphragms are large and overlapping and a large majority are closely spaced. Locally the cypstiphragms may occupy less than half the zooecial tube diameter, but most extend well over half the diameter across the zooecial tubes. Combined cystiphragm and diaphragm spacing in the mature zone of most zoaria averages from six to eight per mm. In three zoaria the spacing averages from 14 to 18 per mm. The overall mean cystiphragm spacing in the mature zone is nine per mm. All cystiphragms and diaphragms are thin.

Monticules composed of enlarged zooecia and few mesopores are spaced 1.5 mm to 3 mm apart, measured from center to center. Most are about 3 mm apart. Zooecial tube diameters in monticules average 0.34 mm by 0.27 mm.

Walls are thin in the immature zone and, for the most part, equally thin in the mature zone. Most are under 0.01 mm thick. Small, local areas of wall thickening are present in some zoaria, where their thickness is 0.03 mm or less, frequently 0.02 mm or less. Thick walls have an amalgamate appearance, with curved laminae that appear superficially to pass continuously, through the walls of adjacent zooecia.

Mesopores are few and are concentrated in monticules. They are polygonal and angular in cross-section, being most commonly three- or four-sided. Mesopores are restricted to the mature zone and their tube diameters average 0.11 mm by 0.07 mm. They are infrequently cut in longitudinal section, but where cut they may be recognized by diaphragm spacing which is close relative to spacing in adjacent zooecia. Including monticules, there is an average of seven mesopores per 2-mm square.

Acanthopores are restricted to the mature zone, where they are developed in more or less definite zones parallel to the zoarial surface, as is well illustrated in longitudinal sections (Pl. 52, fig. 4). Where tangential sections pass through the acanthopore zones, acanthopore density may be as high as 24 per 1-mm square, but where tangential sections miss such zones acanthopores may be lacking completely. Where acanthopores are present they average 15 per 1-mm square. Although acanthopores are rod-shaped through most

of their length, diminished diameters in deeper portions of tangential sections indicate that they taper at their proximal ends. Some specimens tend to have slightly larger acanthopores than other specimens. Combination of the two characters just mentioned causes a greater than usual variation in acanthopore diameters in tangential sections. The largest and smallest acanthopore diameters are 0.10 mm and 0.03 mm; the mean in 0.05 mm. Acanthopores are restricted to zooecial corners and cause adjacent zooecial tubes to be inflected.

Discussion.—*Mesotrypa sparsa* is not a typical species of *Mesotrypa* in that it lacks abundant mesopores. The most similar species is *M. augularis* Ulrich and Bassler, 1904 (p. 23, pl. 7, figs. 7-9). *M. sparsa* has smaller zooecial diameters and better developed cystiphragms than *M. angularis*. Also, mesopores in *M. angularis* are ". . . comparatively numerous in the immature region, but pinch out as growth continues . . ." (Ulrich and Bassler, 1904, p. 23). The few mesopores in *M. sparsa* occur in the mature zone.

Mesotrypa sparsa has smaller zooecia in monticules, better developed cystiphragms, and lacks the numerous mesopores characteristic of *M. infida* (*Diplotrypa infida* Ulrich, 1886, pp. 88-90). Also, the mesopores are not ". . . more conspicuous in the lower half of the section than in the upper . . ." (Ulrich, 1886, p. 89) as in *M. infida*.

Mesotrypa sparsa can be as closely compared with species of *Stigmatella* as with species of *Mesotrypa,* with the primary difference that cystiphragms are not typical of *Stigmatella* but are well developed in *M. sparsa*. The zonal development of acanthopores, which is observed in *M. sparsa,* was considered by Ulrich and Bassler (1904, pp. 33, 34) to be a generic character of *Stigmatella* and is not a characteristic of *Mesotrypa*. *Stigmatella* typically has crenulate immature walls and a sparsity of diaphragms, although some atypical species assigned to *Stigmatella* have abundant diaphragms and straight immature walls, such as *S. multispinosa* Brown, 1965 (pp. 996, 997, pl. 115, figs. 9-11).

Assignment of the above described new species to *Mesotrypa* is based on presence of well-developed cystiphragms and, although sparse, mesopores. Such an assignment is arbitrary inasmuch as equal or greater phylogenetic consideration should be given possibly to the zonal development of acanthopore, which would place the species

in *Stigmatella*. The three characters listed above, cystiphragms, mesopores, and zonation of acanthopores, are probably good phylogenetic indicators. The presence of these indicators in a single species suggests a direct link between *Mesotrypa* and *Stigmatella,* and, by extension, a direct link between the families Monticuliporidae and Heterotrypidae. The typically thin walls and variable zoarial shape, although displayed by members of both families, is taken to be an environmental adaptation that has little or no phylogenetic significance at the family level.

The trivial name, *sparsa,* refers to the sparsity of mesopores.

Material. — Fifty sectioned zoaria from stratigraphic sections I, III, VI, VIII, IV, X, XII, XIV, XVI, XVIII.

Holotype. — USNM 167779.

Paratypes. — USNM 167780-167782, GSATC 204, UNC 4155.

Measurements. — Table 17.

Character	Range	Mode	Mean	Standard Deviation	Number of Measurements	Number of Specimens Measured
MxTD	0.16-0.29	0.24	0.232	0.024	170	17
MnTD	0.15-0.27	0.20	0.187	0.022	170	17
MxTDm	0.20-0.46	0.33	0.339	0.044	118	15
MnTDm	0.16-0.35	0.25	0.270	0.030	118	15
ZWT	0.01-0.05	0.02	0.018	0.008	120	12
MxMTD	0.05-0.24	0.10	0.108	0.046	158	16
MnMTD	0.02-0.15	0.05	0.071	0.030	158	16
M/2-mmsq	1-29	4 6	6.8	4.7	67	16
AD	0.03-0.10	0.05	0.050	0.013	150	15
A/1-mmsq	6-24	11 14	15.1	4.6	149	17
C&D/mm	4-25	7	9.1	3.8	138	15
DBM	1.5-3.0	3.0	2.65	0.36	68	14

Table 17. Quantitative data on characters of *Mesotrypa sparsa,* n. sp. Type suite from the lower Chickamauga Group.

Family **HETEROTRYPIDAE**

Genus **HETEROTRYPA**

Heterotrypa ridleyana (Coryell, 1921) Pl. 51, fig. 8; Pl. 52, figs. 1, 2

1921. *Dekayella ridleyana* Coryell, Indiana Acad. Sci., Proc., vol. 29, pp. 286, 287, pl. 6, figs. 3, 4.

Diagnosis. — Zoaria massive to subramose; zooecia have diaphragms in immature zone and diaphragms, large bulbous cysti-

phragms, and some cystose diaphragms in mature zone; mature zooecial tubes average 0.22 mm by 0.18 mm in diameter; mesopores common, small; acanthopores average 25 per 1-mm square, confined to zooecial corners.

Description. — Zoaria are massive to subramose with an encrusting basal expansion. Greatest observed dimensions are 24 mm diameter for the basal expansion, 12 mm for subramose branch diameter and 23 mm for colony height.

Zooecia diverge gradually in the axial portions of the immature zone with curvature becoming stronger in the distal submature zone. Curvature continues strong in the base of the mature zone, with zooecia oriented perpendicular to the zoarial surface through the remainder of the mature zone. Both specimens show resumed growth similar to the immature zone after development of a well-defined mature zone. Rejuvenation apparently involved all zooecia since there is no basal lamina between the base of the reformed immature portion and the mature zooecia below. Mature zooecia below the plans of rejuvenation are in direct communication with the same immature zooecia above. Mature zooecial tube diameters average 0.22 mm by 0.18 mm. Mature zooecial cross-sections are irregularly polygonal with zooecial tube cross-sections subangular to subrounded polygonal to oval. Thin, planar to moderately convex or concave diaphragms, some of which are tilted, are spaced about two to three zooecial diameters apart in the immature zone. Typically diaphragms in the immature portion of the rejuvenated zone are spaced farther apart than in the mature zone and are more inclined to be tilted. Internal zooecial structures in the mature zone include diaphragms, cystose diaphragms, and cystiphragms, with an average of eight such structures in a 1 mm distance. Cystiphragms are bulbous, moderately overlapping, and extend one-half to two-thirds across the zooecial tube diameter.

Monticules of mesopores and enlarged zooecia are present. Zooecial tube diameters in monticules average 0.28 mm by 0.24 mm.

Zooecial walls are thin and straight in the immature zone. In the mature zone walls are locally integrate in appearance with laminae steeply inclined so that they appear almost parallel to the zooecial border. In other places walls are obscurely integrate or amalgamate. Mature walls average 0.02 mm thick.

Mesopores are common but the sections are insufficient to allow a count per unit area. Mesopore tube diameters average 0.09 mm by 0.06 mm. Mesopores are three- to four-sided with flat walls but tubes are subrounded and are frequently oval in cross-section. Diaphragm spacing in mesopores is similar to diaphragm spacing in mature zooecia.

Acanthopores average 25 per 1-mm square and 0.03 mm in diameter. They originate at the base of the mature zone and appear to terminate anywhere within the mature zone.

Discussion. — The mature zone is not so well developed in Chickamauga Group specimens of *Heterotrypa ridleyana* as it is in the holotype (IU 9245-6 and 9245-10). Consequently the heterotrypid walls are not as prominent in the Chickamauga specimens, although they can be seen locally. Integrate-appearing walls, which are more common in the Chickamauga specimens, are developed along the base of the mature zone of the holotype of *H. ridleyana* and at the same position in other *Heterotrypa* species (Boardman and Utgaard, 1966, p. 1105).

Boardman and Utgaard (1966, pp. 1087, 1090-1092) discussed the history of the role of acanthopores in distinguishing *Dekayia, Dekayella,* and *Heterotrypa,* followed by emended definitions and descriptions of *Dekayia* and *Heterotrypa (ibid.,* pp. 1103, 1105) which includes revised bases for the determination of the two genera. They agreed with Cumings and Galloway (1913, pp. 413, 414) in discarding the generic term *Dekayella.* As first recognized by Cumings (1902, p. 206), the appearance of two sizes of acanthopores results from cutting them at different levels of development. Therefore, the basis for *Dekayella* has no taxonomic significance. Based on an extensive study of specimens in the U.S. National Museum, Boardman and Utgaard (1966, p. 1103) gave, among others, the following characteristics of *Dekayia*: 1) zooecial walls undulatory to crenulated throughout their length, 2) zooecial linings never well developed, 3) diaphragms commonly absent in immature region (endozone) and distant or lacking in mature zone (exozone) and 4) mesopores rare in intermonticular areas.

Contrasting characteristics of *Heterotrypa* are *(ibid.,* p. 1105) 1) zooecial linings common in thick-walled specimens, 2) diaphragms convex or cystose, few to abundant in the immature

region and in many places closely spaced to locally more separated in the mature zone, and 3) intermonticular mesopores abundant to essentially absent. Since Coryell's species *Dekayella ridleyana*

Character	Range	Mode	Mean	Standard Deviation	Number of Measurements	Number of Specimens Measured
MxTD	0.20-0.25	0.21	0.215	0.012	10	1
MnTD	0.16-0.19	0.18	0.177	0.007	10	1
MxTDm	0.26-0.31	—	0.282	0.017	5	1
MnTDm	0.22-0.25	0.23 0.25	0.235	0.012	5	1
ZWT	0.01-0.03	0.02	0.020	0.005	10	1
MxMTD	0.08-0.11	0.10	0.094	0.011	6	1
MnMTD	0.05-0.07	0.06	0.061	0.006	6	1
AD	0.02-0.04	0.03	0.029	0.006	10	1
A/1-mmsq	15-31	—	25.0	5.5	5	1
D/mm	7-10	8	8.3	0.9	10	1

Table 18. Quantitative data on characters of *Heterotrypa ridleyana* (Coryell) from the lower Chickamauga Group.

Character	Range	Mode	Mean	Standard Deviation	Number of Measurements	Number of Specimens Measured
MxTD	0.18-0.22	0.20	0.197	0.011	10	1
MnTD	0.13-0.17	0.16	0.156	0.012	10	1
MxTDm	0.25-0.30	0.30	0.280	0.021	10	1
MnTDm	0.21-0.25	0.23	0.236	0.013	10	1
ZWT	0.03-0.05	0.03	0.035	0.006	10	1
MxMTD	0.03-0.19	0.05	0.092	0.047	10	1
MnMTD	0.03-0.12	0.04	0.066	0.032	10	1
M/2-mmsq	2-6	2	3.4	1.3	10	1
AD	0.04-0.06	0.05	0.047	0.007	10	1
A/1-mmsq	12-19	13	14.6	2.0	10	1
D/mm	8-11	10	9.8	1.0	10	1
DBM	2.0-3.0	2.5	2.55	0.27	10	1

Table 19. Quantitative data on characters of *Dekayella ridleyana* Coryell. Holotype slides, IU 9245-6.

Character	Range	Mode	Mean	Standard Deviation	Number of Measurements	Number of Specimens Measured
MxTD	0.21-0.26	0.24	0.239	0.015	10	1
MnTD	0.18-0.21	0.21	0.202	0.008	10	1
ZWT	0.02-0.03	0.02	0.023	0.004	10	1
AD	0.03-0.05	0.05	0.040	0.008	10	1
A/1-mmsq	16-21	18	18.2	1.4	10	1
D/mm	10-14	12	12.1	1.0	10	1

Table 20. Quantitative data on characters of *Dekayella ridleyana* Coryell. Holotype slides, IU 9245-10.

has smooth walls, a few zooecial linings in the holotype, diaphragms in the immature region, closely spaced diaphragms (some of which are cystose) in the mature zone, and common mesopores in intermonticular areas, it is here assigned to *Heterotrypa*.

Material. — Two thin-sectioned specimens from stratigraphic section I.

Hypotypes. — USNM 167783, 167784.

Measurements. — Table 18 (see also Tables 19 and 20).

Heterotrypa patera Coryell, 1921 Pl. 52, figs. 3-9; Pl. 53, figs. 1-4

1921. *Heterotrypa patera* Coryell, Indiana Acad. Sci. Proc., vol. 29, pp. 287, 288, pl. 6, figs. 5, 6.
1921. *Heterotrypa stonensis* Coryell, Indiana Acad. Sci. Proc., vol. 29, p. 288, pl. 7, figs. 1, 2.

Diagnosis. — Zoaria ramose to subpalmate; zooecia with or without pronounced bend at the base of mature zone; mature zooecial tube diameters average 0.21 mm by 0.17 mm, cystiphragms at the base of the mature zone, diaphragms in the mature zone average 13 per mm; monticules of mesopores and enlarged zooecia spaced 2.5 mm apart; walls average 0.05 mm thick; mesopores rare in intermonticular areas; acanthopores small, originate near the base of mature zone, average 14 1-mm square, located in zooecial corners.

Description. — Zoaria are ramose to subpalmate, with cylindrical to flattened branches typically about 8 mm to 12 mm in diameter, but varying to over 20 mm in diameter.

Zooecia bend out gradually from the axial region to a generally, though not universally, pronounced angle at the base of the mature zone, beyond which they extend at a right angle to the zoarial surface. Immature zooecia are irregularly polygonal in cross-section, but mature zooecia are more regularly polygonal, typically five- or six-sided. Zooecial tubes are rounded suboval to subrounded in cross-section. On the average mature zooecial diameters are 0.27 mm by 0.22 mm, and corresponding zooecial tube diameters are 0.21 mm by 0.17 mm. Thin, planar to slightly concave and convex diaphragms are widely spaced to sparse in the immature zone. Diaphragms in the mature zone average 13 per mm, where they may be locally thickened by superimposed laminae. Mature zone diaphragms vary from planar or slightly concave to moderately convex. Because of crowding of diaphragms, many convex di-

aphragms are cystose. In addition, there are true cystiphragms present, most of which are restricted to the base of the mature zone. Many zooecia apparently lack cystiphragms and where developed there are typically only a few per zooecium.

Low monticules are present, regularly spaced from 2 mm to 3 mm apart, most typically about 2.5 mm apart measured from center to center. Mature zooecial diameters in monticules average 0.37 mm to 0.30 mm, and corresponding average zooecial tube diameters are 0.31 mm by 0.25 mm. Due to the large size of zooecia, monticules are prominent in tangential sections. Most monticules have one or more mesopores associated with them, but some monticules apparently lack mesopores.

Immature zooecial walls are thin and appear linear to locally crinkled in longitudinal section. Walls thicken abruptly at the base of the mature zone. Walls in the mature zone average 0.05 mm thick and vary from integrate-appearing to amalgamate-appearing. Wall laminae are broadly curved and meet the zooecial borders at a high angle. Where the zooecial border has a granular, irregular appearance walls have an integrate aspect. In other places laminae meet with no conspicuous contact between adjacent zooecia, producing an amalgamate appearance. Laminae curve proximally along zooecial tubes to produce a locally prominent lining.

Mesopore walls are similar to zooecial walls although frequently less thick. Mesopore tube diameters average 0.09 mm by 0.07 mm. They are sparse, located mostly in monticules and are more rare in intermonticular areas. Including monticules there is an average of five mesopores per 2-mm square. Mesopores were not recognized in longitudinal sections, indicating that either no mesopores were cut or diaphragm spacing in mesopores is similar to diaphragm spacing in zooecia.

Acanthopores are restricted to zooecial corners and a few are offset toward zooecial axes. Acanthopores originate in the submature zone near the base of the mature zone. They originate at about the level that cystiphragms are first formed. Acanthopores average 0.04 mm in diameter and 14 per 1-mm square.

Discussion. — Holotypes of *Heterotrypa patera* Coryell, 1921 (pp. 287, 288, pl. 6, figs. 5, 6) and *H. stonensis* Coryell, 1921 (p. 288, pl. 7, figs. 1, 2) are both from the same locality and formation,

the Pierce Limestone two miles northwest of Murfreesboro, Tennessee. Coryell's original distinction between the two species (1921, p. 288) was based on, "The scarcity of diaphragms in the axial region, the thinner cingulum and inconspicuousness and zooecial composition of the maculae of *Heterotrypa stonensis* . . ." in relation to *H. patera.* Measured characteristics of the holotypes of the two species are given in Tables 22 and 23. The population sample of 207 specimens studied for this report includes variations of diaphragm spacing in the immature region, composition of monticules and measured characters listed in Table 21 that encompass characters originally used to differentiate between *H. patera* and *H. stonensis* as well as differences in measured parameters given in Tables 22 and 23. Because of variations noted in the current population study and because holotypes of *H. patera* and *H. stonensis* were collected from the same locality and probably belonged to a single population, the two species are here considered synonymous. *Heterotrypa patera* is the senior synonym by page priority.

Since the generic characters of *Heterotrypa* are well developed in *H. patera,* the few cystiphragms at the base of the mature zone are regarded as unimportant in generic assignment. However, the basal cystiphragms may be important in relating the heterotrypids to the monticuliporoids by indication of close phylogenetic relationship between *Heterotrypa* and *Homotrypa.* If such a relation is real, and if the principle of ontogenetic recapitulation holds in this case, then *Heterotrypa* may be a descendent of *Homotrypa,* or they may both be descended from a common ancestor.

Heterotrypa patera is one of the most common species in the lower Chickamauga Group.

Material. — Two hundred seven sectioned specimens from stratigraphic sections I, II, IV, V, X, XII, XIV, XV, XVI, XVII.

Hypotypes. — USNM 167785-167790.

Measurements. — Table 21.

Family **AMPLEXOPORIDAE**

Genus **AMPLEXOPORA**

Amplexopora winchelli Ulrich, 1886 Pl. 54, figs. 1-8; Pl. 55, figs. 1-3

1886. *Amplexopora winchelli* Ulrich, Minnesota Geol. and Nat. Hist. Sur., 14th Ann. Rept., p. 91.

1893. *Batostoma winchelli (Ulrich),* Ulrich, extract from Minnesota Geol. and Nat. Hist. Sur., Final Rept., Paleont., vol. 3, pp. 295, 296, pl. 26, figs. 33-37, pl. 27, figs. 1-6.
1893. *Batostoma winchelli* var. *nodosa* Ulrich, extract from Minnesota Geol. and Nat. Hist. Sur., Final Rept., Paleont., vol. 3, p. 295, pl. 26, fig. 35.
1911. *Batostoma winchelli* (Ulrich), Bassler, U. S. Nat. Mus., Bull. 77, pp. 278, 279, text-figs. 166a-g.
1942. *Batostoma winchelli* (Ulrich), Loeblich, Jour. Paleont., vol. 16, pp. 432, 433, pl. 64, figs. 8-10.
1962. *Batostoma winchelli* (Ulrich), Perry, Illinois Geol. Sur., Circ. 326, pp. 26-28, pl. 6, figs. 4-11.
1965. *Amplexopora winchelli* Ulrich, Brown, Jour. Paleont., vol. 39, pp. 1002, 1003, pl. 118, figs. 8-10.
1967. *Amplexopora winchelli* Ulrich, Bork and Perry, Jour. Paleont., vol. 41, pp. 1374, 1375, pl. 173, figs. 1, 2, 7-9.
1967. *Amplexopora winchelli spinulosum* (Ulrich), Bork and Perry, Jour. Paleont,. vol. 41, pp. 1374-1377, pl. 173, figs. 3-6, pl. 174, fig. 1.
1969. *Amplexopora winchelli* Ulrich, Ross, Jour. Paleont., vol. 43, p. 265, pl. 37, figs. 2-4.

Diagnosis. — Zoaria typically ramose; mature zooecial tube diameters average 0.26 mm by 0.21 mm; diaphragms average two per mm in immature zone and eight per mm in mature zone but tend to develop in zones of more closely spaced diaphragms in large specimens; low monticules present; walls average 0.06 mm thick; mesopores sparse, with an average of four per 2-mm square; acanthopores about 0.04 mm in diameter, with a mean of 13 per 1-mm square.

Character	Range	Mode	Mean	Standard Deviation	Number of Measurements	Number of Specimens Measured
MxZD	0.24-0.34	0.27	0.272	0.021	163	17
MnZD	0.15-0.28	0.23	0.223	0.021	163	17
MxTD	0.15-0.28	0.20	0.209	0.026	217	22
MnTD	0.12-0.25	0.15	0.173	0.026	217	22
MxZDm	0.31-0.50	0.35	0.372	0.041	125	17
MnZDm	0.25-0.44	0.30	0.299	0.029	125	17
MxTDm	0.22-0.44	0.30	0.312	0.041	192	22
MnTDm	0.17-0.33	0.25	0.251	0.031	184	22
ZWT	0.01-0.15	0.04	0.050	0.025	211	22
MxMTD	0.02-0.20	0.05	0.094	0.046	217	22
MnMTD	0.01-0.15	0.03	0.066	0.035	217	22
M/2-mmsq	1-26	2	4.7	4.3	153	21
AD	0.02-0.11	0.04	0.040	0.010	211	22
A/1-mmsq	3-35	13	13.5	5.9	200	20
D/mm	5-25	11	13.2	4.0	196	20
DBM	1.0-4.0	2.5	2.44	0.41	182	20

Table 21. Quantitative data on characters of *Heterotrypa patera* Coryell from the lower Chickamauga Group.

Character	Range	Mode	Mean	Standard Deviation	Number of Measurements	Number of Specimens Measured
MxTD	0.17-0.20	0.18	0.179	0.008	10	1
MnTD	0.13-0.17	0.15	0.152	0.011	10	1
MxTDm	0.22-0.25	—	0.233	0.012	3	1
MnTDm	0.18-0.19	0.18	0.183	0.004	3	1
ZWT	0.07-0.12	0.10	0.094	0.014	10	1
MxMTD	0.08-0.16	0.13	0.126	0.021	10	1
MnMTD	0.06-0.13	—	0.101	0.019	10	1
M/2-mmsq	3-8	—	6.0	2.2	3	1
AD	0.04-0.05	0.05	0.048	0.003	5	1
A/1-mmsq	8-17	14	11.9	3.1	10	1
D/mm	10-12	11	11.0	0.8	10	1

Table 22. Quantitative data on characters of *Heterotrypa patera* Coryell Holotype, IU 9242-4.

Character	Range	Mode	Mean	Standard Deviation	Number of Measurements	Number of Specimens Measured
MxTD	0.18-0.20	0.19	0.188	0.005	10	1
MnTD	0.16-0.18	0.16	0.168	0.008	10	1
MxTDm	0.24-0.31	0.27	0.276	0.018	10	1
MnTDm	0.20-0.27	0.24	0.232	0.017	10	1
ZWT	0.04-0.07	0.06	0.052	0.010	10	1
MxMTD	0.06-0.16	0.10 0.12	0.111	0.029	10	1
MnMTD	0.04-0.15	0.10	0.091	0.032	10	1
AD	0.04-0.06	0.05	0.047	0.007	10	1
A/1-mmsq	9-18	10	13.6	3.5	10	1
D/mm	7-15	12 14	11.7	2.4	10	1
DBM	2.0-3.0	2.5	2.4	0.30	10	1

Table 23. Quantitative data on characters of *Heterotrypa stonensis* Coryell. Holotype, IU 9242-5.

Description. — Zoaria are ramose to encrusting, most typically ramose with branches about 5 mm in diameter. Largest ramose specimen has a maximum branch diameter of 19 mm and is 26 mm long.

Zooecia in the immature zone bend out gently from the axial zone to a stronger curve at the base of the mature zone, beyond which zooecia extend directly at right angles to the zoarial surface where the mature zone is thick. Zooecia are slightly less than perpendicular where the mature zone is thin. Mature zooecia are sharply polygonal in cross-section, typically five- or six-sided. Zooecial tubes are rounded oval to subrounded polygonal in cross-section. Mature

zooecial diameters average 0.33 mm by 0.26 mm, and corresponding zooecial tube diameters average 0.26 mm by 0.21 mm. Diaphragm spacing in the immature zone is variable, as close as one tube diameter apart or locally absent, but most typically they are two to four diameters apart with an average of two diaphragms per mm. Diaphragms in the immature zone are thin, planar, or slightly concave or convex and are oriented at right angles to the zooecial axis. Diaphragms in the mature zone average eight per mm, and although most are oriented essentially perpendicular to the zooecial axis, many are inclined, some greater than 45°. Most mature diaphragms are planar or slightly concave, but some, particularly those that are steeply inclined, are convex. Cystose diaphragms are present. Diaphragm spacing within the mature zone of some large zoaria is zoned, with zones of crowded diaphragms and zones of sparse, frequently inclined and cystose, diaphragms. Thickening of diaphragms also occurs in bands. Most diaphragms in mature zones are thin, but some are thickened by addition of laminae continuous with wall laminae.

Small groups of slightly enlarged zooecia and a few mesopores represent low monticules. Distance between monticules averages 3 mm. Mature zooecial diameters in monticules average 0.42 mm by 0.34 mm, with corresponding zooecial tube diameters of 0.36 mm by 0.29 mm.

Mature zooecial walls have a mean thickness of 0.06 mm. They are composed of steeply dipping planar laminae that typically form thin linings along the zooecial tube. The linings extend into the diaphragms and are reformed below each diaphragm. In at least one specimen (USNM 167791), the zooecial lining does not extend all the way around the perimeter of zooecial tubes, but occurs as restricted spots in adjacent zooecia, forming bulbous structures superficially resembling acanthopores at low magnifications. Plane of contact between adjacent zooecia is seen in thin-section as a dark, locally crenulate line in longitudinal section.

Mesopores are sparse and are concentrated in monticules. Including monticules, mesopores average four per 2-mm square. They are polygonal, typically three- or four-sided in cross-section with walls as thick as those in zooecia. Mesopore tubes are rounded suboval in cross-section and average 0.12 mm by 0.09 mm. Di-

aphragm spacing in mesopores is unknown. They apparently originate near the base of the mature zone.

Acanthopores most typically occur in zooecial corners, but some are offset along zooecial borders. They have an average diameter of 0.04 mm. Acanthopores occur throughout the mature zone and average 13 per 1-mm square.

Discussion. — Diaphragm spacing, diaphragm thickness, and wall thickness in the mature zone are related to growth rate, which is environmentally controlled. Zonation of the three above-mentioned characters in specimens of *Amplexopora winchelli* in Wills Valley indicates variation in the environmental influence which affects growth rate. Since there is a strong external control on these characters through variation in growth rate, then caution should be used in giving taxonomic significance to them.

The respective descriptions of "*Batostoma winchelli*" given by Bassler (1911, pp. 278, 279) for Baltic specimens, by Wilson and Mather (1916, pp. 49, 55), and by Sardeson (1936c, pp. 104-108) are insufficient for recognition of the species. Fritz (1957, pp. 12, 13, pl. 3, figs. 1, 2) reported "*Batostoma winchelli spinulosum* Ulrich" from the Blackriveran of Ontario, but the specimen figured by her has too many mesopores that locally almost surround entire zooecia to fit the concept of *Amplexopora winchelli* or *Amplexopora winchelli spinulosa*. Of the specimens described and figured as *A. winchelli spinulosa* or *B. winchelli spinulosa* since Ulrich's original description and figures (1893, p. 296, pl. 27, figs. 7, 8), only the description and figures given by Perry (1962, pp. 25, 26, pl. 5, figs. 4-6) closely match Ulrich's.

Text-figure 20 is a histogram of acanthopores per 1-mm square based on averages from 59 specimens. The distribution is slightly leptokurtic normal with a kurtosis value (Ks) of +0.21 and seems to represent a single population (see Simpson, Roe, and Lewontin, 1960, pp. 146, 147). Ulrich (1893, p. 296) originally based *Batostoma winchelli spinulosa* on the presence of ". . . stronger and more abundant acanthopores" than in *Amplexopora winchelli*. Bork and Perry (1967, p. 1374) reported a range of zero to 15 acanthopores per 1-mm square for *Amplexopora winchelli* and a range of 12 to 21 acanthopores per 1-mm square, with a mean of 17.5 *(ibid.,* p. 1375), for *Amplexopora winchelli spinulosa*. Since the ranges of acantho-

pore abundance used by Bork and Perry to distinguish *A. winchelli spinulosa* from *A. winchelli* are encompassed by the single population from the lower Chickamauga Group, the specimens reported as *Amplexopora winchelli spinulosa* by Bork and Perry should be included in *A. winchelli.*

Amplexopora winchelli is the most abundant trepostome species in the lower Chickamauga Group in Wills Valley.

Material. — Four hundred fifty sectioned specimens from stratigraphic sections I, II, III, IV, VI, VIII, XII, XIV, XVIII.

Hypotypes. — USNM 167791-167793.

Measurements. — Table 24.

Character	Range	Mode	Mean	Standard Deviation	Number of Measurements	Number of Specimens Measured
MxZD	0.21-0.45	0.32	0.333	0.038	309	32
MnZD	0.18-0.35	0.25	0.255	0.031	309	32
MxTD	0.15-0.35	0.26	0.262	0.035	690	69
MnTD	0.13-0.30	0.20	0.207	0.031	690	69
MxZDm	0.35-0.60	0.45	0.421	0.058	80	15
MnZDm	0.21-0.46	0.35	0.336	0.043	80	15
MxTDm	0.17-0.53	0.35	0.362	0.053	368	50
MnTDm	0.15-0.38	0.30	0.286	0.039	368	50
ZWT	0.02-0.18	0.05	0.056	0.024	700	70
MxMTD	0.03-0.25	0.12 0.14	0.125	0.046	560	66
MnMTD	0.03-0.18	0.09	0.086	0.033	560	66
M/2-mmsq	0-24	3	4.1	3.8	302	61
AD	0.02-0.11	0.04	0.043	0.012	587	62
A/1-mmsq	0-27	12	12.6	4.4	451	59
D/mm	5-18	9	8.5	4.4	532	64
DBM	2.0-4.0	3.0	3.00	0.48	157	31

Table 24. Quantitative data on characters of *Amplexopora winchelli* Ulrich from the lower Chickamauga Group.

Amplexopora aff. A. winchelli spinulosa (Ulrich, 1893) Pl. 55, figs. 4-8

1893. *Batostoma winchelli* var. *spinulosum* Ulrich, extract from Minnesota Geol. and Nat. Hist. Sur., Final Rept., Paleont., vol. 3, p. 296, pl. 27, figs. 7, 8.
1911. *Batostoma winchelli spinulosum* Ulrich, Bassler, U. S. Nat. Mus., Bull. 77, pp. 279, 280, text-figs. 168a, b.

Description. — The zoarium is ramose with an abraded branch diameter of 8 mm and a fragmented length of 16 mm.

Zooecia in the immature zone bend away from the branch axis, with a gentle increase in curvature to the base of the mature zone,

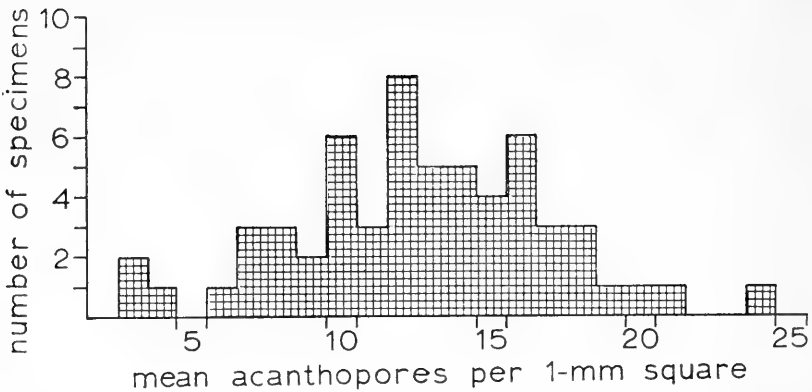

Text-figure 20. — Histogram of mean acanthopores per 1-mm square in *Amplexopora winchelli* Ulrich based on counts made on 59 zoarial fragments from the lower Chickamauga Group of Wills Valley, Alabama.

at which point the curvature locally becomes noticeably greater. New zooecia are intercalated throughout the entire immature zone. Mature zooecia are irregularly subrounded polygonal in cross-section. Mature zooecial diameters average 0.33 mm by 0.27 mm, and corresponding zooecial tube diameters are 0.24 mm by 0.19 mm. Diaphragms are crowded at proximal zooecial tips, where they average nine per mm, which is slightly greater than the mature diaphragm spacing. Where immature zooecia have reached their full diameter, diaphragms are spaced one or more, in most places two to four, tube diameters apart. Diaphragms in the immature zone are thin, typically planar, and oriented perpendicular to the zooecial axis, but a few are slightly domal and tilted or tilted up to 45° with respect to the zooecial axis. Diaphragms in the mature zone average six per mm. Mature zone diaphragms are slightly thickened and represent an extension of a group of wall laminae. Diaphragms in the mature zone are mostly planar and normal to the zooecial axis, although a few are slightly domal or concave and some are slightly tilted.

Walls thicken gradually at the base of the mature zone. Mature wall thickness averages 0.09 mm. Thin immature walls appear to be continuous with a thin, dark divisional line in the mature zone

that represents the plane of contact between wall laminae of adjacent zooecia. Wall laminae diverge from the zooecial borders at an approximate 30° angle, continue as a lining along the zooecial tube, and extend into thickened diaphragms.

Mesopores originate in the submature zone just below the zone of increase in wall thickness and resemble proximal zooecial tips in diaphragm spacing. They do not have a strong increase in diameter like the zooecia, but are of small diameter throughout their length. Mesopore tube diameters average 0.13 mm by 0.08 mm. Most mesopore tubes are subrounded polygonal or oval. Mesopore walls are thick and are similar to zooecial walls. Diaphragms are slightly thickened and represent an extension of groups of wall laminae in many mesopores. There is an average of 31 mesopores per 2-mm square.

Acanthopores originate at the base of the mature zone where increase in wall thickness occurs. Acanthopores average 0.04 mm in diameter with a mean of 27 per 1-mm square. They are frequently offset from the median plane between zooecia and occur both in corners and along zooecial walls. Acanthopores that are most highly offset strongly inflect zooecial tubes and stand out well in longitudinal section (see especially Pl. 55, fig. 5).

Discussion. — The specimen described above resembles *Amplexopora winchelli* Ulrich, 1886 (p. 91) but has much more abundant acanthopores, many of which are offset along zooecial borders. In nature of acanthopores, the specimen resembles *A. winchelli spinulosa* (Ulrich, 1893, p. 296, pl. 27, figs. 7, 8). The tangential thin-section of the Chickamauga specimen is too thick and too poorly oriented for accurate comparison with the figured type specimen of *A. winchelli spinulosa.*

Material. — One thin-sectioned specimen from stratigraphic section II.

Hypotype. — USNM 167794.

Measurements. — Table 25.

Character	Range	Mode	Mean	Standard Deviation	Number of Measurements	Number of Specimens Measured
MxZD	0.31-0.35	0.33	0.330	0.011	10	1
MnZD	0.25-0.30	0.25	0.267	0.015	10	1
MxTD	0.21-0.26	0.25	0.240	0.015	10	1
MnTD	0.16-0.23	0.19	0.192	0.019	10	1
ZWT	0.05-0.13	—	0.090	0.022	10	1
MxMTD	0.10-0.20	0.10	0.130	0.030	10	1
MnMTD	0.07-0.13	0.08	0.084	0.018	10	1
M/2-mmsq	13-43	—	30.6	9.6	7	1
AD	0.03-0.06	0.04	0.041	0.008	10	1
A/1-mmsq	25-30	28	27.4	1.7	5	1
D/mm	4-7	5	5.5	0.8	10	1
D/mmM	8-11	9	9.2	0.9	10	1

Table 25. Quantitative data on characters of *Amplexopora* aff. *A. winchelli spinulosa* (Ulrich) from the lower Chickamauga Group.

Amplexopora sp. Pl. 56, figs. 1-4

Description. — Zoaria are encrusting to ramose, with branch diameters 2 mm to 6 mm.

Zooecia extend with little curvature through the immature zone and bend outward more strongly in the mature zone to meet the zoarial surface at an oblique to right angle. Mature zooecia are polygonal, five- or six-sided or rounded with average diameters of 0.25 mm by 0.20 mm. Mature zooecial tubes are oval, with mean diameters of 0.19 mm by 0.16 mm. Diaphragms in the immature zone are spaced approximately two or more diameters apart. Based on 0.5 mm segments, counts of 11 and 13 diaphragms per mm in the mature zone were made. Diaphragms in the mature zone are frequently composed of a basal dark lamina overlain by several light-colored laminae that extend in from the wall. The basal dark portion apparently represents the basic part of the diaphragm as it is similar in appearance to unthickened diaphragms. Two local groups of enlarged zooecia may represent monticules. The enlarged zooecia average 0.26 mm by 0.21 mm in diameter.

Immature walls are thin. Mature walls are thick, composed of laminae that dip away from zooecial boundaries at a 30° to 45° angle and gradually become less inclined along the interior of the zooecial tube. As noted above, many wall laminae are continuous with laminae of thickened diaphragms. Boundaries between adjacent zooecia appear as distinct, dark lines in both longitudinal and tangential sections.

Mesopores originate at the base of the mature zone, are abundant, but the tangential section is too small to obtain a count per 2-mm square. Mesopores are polygonal with concave sides, and mesopore tubes are suboval in cross-section. Mesopore walls are

Character	Range	Mode	Mean	Standard Deviation	Number of Measurements	Number of Specimens Measured
MxZD	0.21-0.30	—	0.252	0.030	10	1
MnZD	0.18-0.21	0.20	0.199	0.007	10	1
MxTD	0.16-0.22	0.19	0.189	0.019	10	1
MnTD	0.13-0.19	0.17	0.158	0.016	10	1
MxZDm	0.27-0.34	—	0.311	0.024	5	1
MnZDm	0.22-0.26	0.26	0.245	0.014	5	1
MxTDm	0.24-0.29	0.27	0.265	0.016	5	1
MnTDm	0.20-0.23	0.21	0.213	0.010	5	1
ZWT	0.03-0.05	0.04	0.040	0.009	10	1
D/mm	11-13	—	12.0	1.0	2	1

Table 26. Quantitative data on characters of *Amplexopora* sp. from the lower Chickamauga Group.

similar to zooecial walls. Mesopore tube diameters are about one-third zooecial tube diameters. Diaphragm spacing in mesopores is unknown.

Small acanthopores, 0.02 mm in diameter, are present in some zooecial corners. Acanthopores originate at the base of the mature zone. Because of the small size of the tangential sections and the small size of the few specimens collected, acanthopore abundance could not be determined.

Material. — Three thin-sectioned specimens from stratigraphic sections II and XIV.

Hypotype. — USNM 167795.

Measurements. — Table 26.

Family **TREMATOPORIDAE**

Genus **ERIDOTRYPA**

Discussion. — Ross (1967b, p. 635) placed the genus *Eridotrypa* in the Aisenvergiidae Dunaeva, 1964, on the basis of restriction of the zooecial tubes in the submature region. *Eridotrypa* is here retained in the Trematoporidae which is the current practice followed by Russian ectoproctologists (*e.g.* Astrova, 1965). Relative to *Aisenvergia, Volnovachia,* and *Polycylindricus,* the genera comprising the original concept of Aisenvergiidae (Dunaeva, 1964b, p. 39), the

characteristic submature constriction of zooecia in *Eridotrypa* is slight. Ross (1967b, p. 635) believed that increased restriction of zooecia is an evolutionary trend of the Aisenvergiidae from Ordovician to Carboniferous. I prefer to believe restriction of zooecia in *Eridotrypa* (as well as in *Homotrypa similis* and *H. vacua*) is convergent with the much more severe restriction characteristic of the Aisenvergiidae.

Eridotrypa minor Ulrich, 1893 Pl. 56, figs. 5-8

1893. *Eridotrypa mutabilis* var. *minor* Ulrich, extract from Minnesota Geol. and Nat. Hist. Sur., Final Rept., Paleont., vol. 3, p. 266, pl. 26, figs. 20, 21, 29, 30.
1911. *Eridotrypa aedilis minor* Ulrich, Bassler, U. S. Nat. Mus., Bull. 77, p. 245, text-figs. 139a-f.
1965. *Eridotrypa aedilis minor* Ulrich, Brown, Jour. Paleont., vol. 39, pp. 998, 999, pl. 117, figs. 1, 2.

Diagnosis. — Zoaria ramose, with thin branches; mature zone thin, with zooecia at a low angle to the zoarial surface; diaphragms average seven per mm in mature and submature zones but are absent throughout most of immature zone; zooecial tube diameters in mature zone average 0.18 mm by 0.11 mm.

Description. — Zoaria are ramose, with most branches about 2 mm in diameter, but some up to 4 mm in diameter.

Zooecia have long immature portions that essentially parallel the branch axis in the proximal portions, after which they diverge only slightly. The mature zone is thin and is marked by slight outward curvature of zooecia and thickened zooecial walls. Diaphragms are absent in the immature zone except in the portion immediately adjacent to the mature zone. Diaphragms occur in the mature and submature zones and average seven per mm. Most diaphragms are thin, but some are laminar and thickened. Scattered thickened cystiphragm-like diaphragms and cystiphragms are present. In the mature zone, zooecia are circular or oval to irregularly polygonal in cross-section; rounded zooecia determine the presence of mesopores in zooecial corners. Zooecial diameters average 0.26 mm by 0.18 mm in the mature zone, and corresponding zooecial tube diameters average 0.18 mm by 0.11 mm.

Mesopores are common, but tangential sections are insufficient for a count. Mesopores are short, sharply polygonal in cross-section, mostly four-sided, and they originate at or just above the base of

the mature zone. As seen in cross-section, some mesopores have planar sides but most have slightly to strongly concave sides due to their association with rounded zooecia. Mesopore tubes are mostly circular or oval. A few mesopores are partially filled by wall deposits. Mesopores average 0.12 mm by 0.08 mm in diameter, and 0.06 mm by 0.04 mm in tube diameter. Closely spaced diaphragms are present in the mesopores and may or may not be thickened.

Walls are thin and apparently granular in the immature region and thicken gradually at the base of the mature region. Both mesopore and zooecial walls are thickened in the mature region, averaging 0.09 mm thick. In the mature zones, wall laminae lining zooecial tubes are essentially parallel to the zooecial axis, but they gradually turn toward the zooecial boundary, becoming more and more inclined until they meet the zooecial boundary at close to a 90° angle. Laminae therefore appear narrowly U-shaped in longitudinal section, especially in the thickest, most distal part of the wall. Zooecial boundaries appear granular and have a finely zigzag pattern in longitudinal section.

Small acanthopores, 0.01 mm to 0.02 mm in diameter, are present in zooecial corners in some specimens. They range from absent to common.

Discussion. — Specimens of *Eridotrypa minor* from the lower Chickamauga Group were compared with Ulrich's holotype (USNM 43537), and no essential differences were discovered. Zooecia in the holotype average slightly greater in minimum diameter and zooecial tubes are slightly less in minimum diameter. Therefore, zooecial walls are thicker in the holotype than in the specimens here described.

Eridotrypa minor differs from *Eridotrypa mutabilis* Ulrich, 1893 (pp. 265, 266, pl. 26, figs. 22-28, 31, 32) in the lack of diaphragms in the immature region and has smaller zooecia. Bassler (1911, p. 245) transferred *Eridotrypa mutabilis minor* to *E. aedilis minor* when he placed Ulrich's species *E. mutabilis* in synonymy with *E. aedilis* (Eichwald, 1855). However, as indicated by Ross (1967b, p. 638) Bassler did not figure or describe the Baltic material that he assigned to *E. aedilis*, and its taxonomic position is not clear. Also, the early descriptions and figures of *E. aedilis* are not sufficient to distinguish it from several other described species of

Eridotrypa. Therefore, until type specimens of *E. aedilis* are restudied or until topotypes are made available, *E. aedilis* must not be considered synonymous with *E. mutabilis*. Kopaevich (1968, p. 21), in his study of the genus *Eridotrypa*, retained *E. aedilis* as the senior synonym of *E. mutabilis*, although he gave no indication of restudy of type specimens or examination of topotypes.

Specimens assigned to *Eridotrypa aedilis minor* by Wilson and Mather (1916, p. 55) are not portrayed in sufficient detail to allow exact determination of the species.

Eridotrypa minor is here treated as a species rather than as a subspecies of *E. mutabilis* because the two may be readily distinguished by presence or absence of diaphragms in the axial region. Taxonomic value of diaphragms in the axial region in this case cannot be precisely determined. Since *E. minor* and *E. mutabilis* are not always found together, and there is a distinctive morphologic difference the two are regarded here as autonomous species.

Character	Range	Mode	Mean	Standard Deviation	Number of Measurements	Number of Specimens Measured
MxZD	0.18-0.43	0.24 0.30	0.261	0.073	36	4
MnZD	0.14-0.25	0.18	0.184	0.037	36	4
MxTD	0.10-0.26	0.15	0.181	0.047	36	4
MnTD	0.05-0.20	0.10	0.114	0.041	36	4
ZWT	0.03-0.16	0.07	0.091	0.039	40	4
MxMTD	0.02-0.10	—	0.060	0.029	6	1
MnMTD	0.02-0.05	0.03	0.035	0.010	6	1
D/mm[1]	2-10	8	6.9	2.4	29	3

[1]Most based on 0.5 mm measurements.

Table 27. Quantitative data on characters of *Eridotrypa minor* Ulrich from the lower Chickamauga Group.

Material. — Six sectioned zoarial fragments from stratigraphic sections II, III, VI, VIII, XVI.

Hypotype. — USNM 167796.

Measurements. — Table 27.

Eridotrypa abrupta Loeblich, 1942 Pl. 57, figs. 1-6

1942. *Eridotrypa abrupta* Loeblich, Jour. Paleont., vol. 16, pp. 429, 430, pl. 63, figs. 20, 21.

Diagnosis. — Zoaria ramose, branches about 2.5 mm diameter;

zooecia near zoarial axis diverge gradually, each making a sharp angle at the base of the mature zone so that mature zooecia are perpendicular to the zoarial surface; average tube diameters average 0.18 mm by 0.15 mm; zooecia subcircular to oval in cross-section.

Description. — Zoaria are ramose with thin branches about 2.5 mm in diameter.

Zooecia are long, some originate near the zooarial axis, and others are intercalated nearer the branch periphery. Zooecia near the zoarial axis are large and diverge gently, becoming slightly more divergent and smaller nearer to the mature zone. They make a sharp angular bend at the base of the mature zone so that mature portions are normal or almost normal to the zoarial surface. Mature zones are narrow, about 0.2 mm to 0.3 mm thick in most specimens. Mature zooecia are oval to subcircular in cross-section. In the mature zone, zooecial diameters average 0.25 mm by 0.20 mm, with corresponding zooecial tube diameters of 0.18 mm by 0.15 mm. Distance between adjacent zooecial tubes averages 0.05 mm. Thin diaphragms, planar or slightly concave to slightly convex, are common to sparse in the immature zone. They are more closely spaced in the mature zone and in the submature zone, averaging six per mm. In the mature zone, some diaphragms are thickened and cystiphragms are infrequent in the mature zone.

Mesopores are abundant, but the areas of the tangential sections are insufficient to count the mesopores in a 2-mm square. One mesopore occurs in almost every corner caused by the junction of three or more zooecia in the mature zone. As a consequence, most mesopores are three- or four-sided, although some are five- or six-sided. Due to smooth oval to subcircular zooecial cross-sections, mesopore sides are concave. Mesopores originate at the base of the mature zone. They contain closely spaced diaphragms, and some mesopores are closed by calcareous deposits. Many mesopore diaphragms are thickened and laminar. Most mesopore tubes are transversely angular, though a few tubes have rounded cross-sections. Mesopore diameters average 0.10 mm by 0.07 mm. Mesopore tube diameters were not measured because their boundaries are not sharp in tangential sections due to the presence of closely spaced diaphragms and calcareous deposits.

Zooecial walls are about 0.04 mm to 0.05 mm thick in the mature zone, where they are composed of laminae that are gently inclined upward toward the zooecial boundary. Laminae from adjacent zooecia form walls that appear V-shaped in longitudinal sections and concentrically laminated in zoarial tangential sections. The line of contact between adjacent zooecial walls is slightly crenulated in longitudinal section and appears granular. Mesopore walls are similar to zooecial walls but are typically thinner.

Discussion. — Lower Chickamauga Group specimens of *Eridotrypa abrupta* are similar to Loeblich's holotype (USNM 114580). Observed differences are that mature zooecia in the holotype are not as evenly oval or subcircular is cross-section as are zooecia in lower Chickamauga specimens, possibly resulting from the tangential section of the holotype passing near the base of the mature zone. In the holotype there are larger average zooecial diameters, larger average zooecial tube diameters and greater average wall thickness (Table 29). The greater average size of these features is interpreted as individual differences of a specimen, the holotype, that belongs to the same species as the suite from the lower Chickamauga Group. The differences could be caused by different environmental conditions or within-species genetic differences. A third alternative, which I consider less likely, is that specimens from the lower Chickamauga Group belong to a species other than *E. abrupta.* The diagnostic character that relates the Chickamauga specimens of *E. abrupta* with the holotype is the distinct, abrupt bend at the base of the mature zone that causes the mature zooecia to be perpendicular to the zoarial surface. Such an abrupt bend is found in no other known species of *Eridotrypa;* all others are characterized by oblique mature zooecia.

Material. — Five sectioned zoarial fragments from stratigraphic sections I, III, VIII, XVI.

Hypotypes. — USNM 167797, 167798.

Measurements. — Table 28 (see also Table 29).

Eridotrypa arcuata McKinney, n. sp. Pl. 57, figs. 7, 8; Pl. 58, figs. 1-5

Diagnosis. — Zoaria ramose, branches 2 mm to 3 mm diameter; zooecia curve smoothly from immature zone into mature zone, with sparse diaphragms in immature zone and about two to three di-

aphragms per 0.5 mm in mature and submature zones; mature zooecial tube diameters average 0.21 mm by 0.13 mm; mature zone thin; mesopores few.

Descriptions. — Zoaria are ramose, with branches ranging from 2 mm to 3 mm in diameter.

Zooecia originate at a slight angle to the branch axis, then bend smoothly out into the mature zone, rarely with a strong increase in curvature at the base of the mature zone. Walls in immature parts of the zooecia vary from smooth, to broadly crinkled, to irregularly crinkled. Zooecia meet the zoarial surface at an angle from about 30° to 60°, but in most places the angle is about 45°. The mature walls begin to thicken gradually at the base of the mature zone, which in conjunction with the even curvature of zooecia, makes the border between the immature and the thin mature zone gradational. Mature zooecial cross-sections are five- and six-sided, subrounded to angular. Mature zooecial diameters average 0.31 mm by 0.21 mm, and corresponding zooecial tube diameters average 0.21 mm by 0.13 mm. Diaphragms are rare in the immature zone, but most zooecia have up to four diaphragms in the mature and submature zones, two to three contained within a 0.5 mm distance. Infrequent cystiphragms are also present. One specimen has anastomozing branches. On the inside of the rejoined branches, zooecia are sharply reflected, the mature zone is locally thickened, and several zooecia contain up to 12 thin to slightly thickened planar diaphragms (Pl. 57, fig. 7).

Mature walls average 0.08 mm in thickness and are composed of extended laminae that curve gently outward at a low angle toward the zooecial border. The walls appear vaguely concentric in tangential sections and have a slightly bowed, outwardly pointing V-shape in longitudinal sections. Zooecial borders are irregular in the mature zone, appearing granular in both longitudinal and tangential sections. At least part of the granular appearance is due to tiny, short tubules along the zooecial borders (Pl. 58, fig. 3).

Mesopores are scarce, mostly four-sided in cross-section, small and filled by wall deposits. They originate at the base of the mature zone and have closely spaced diaphragms.

Discussion. —*Eridotrypa arcuata* may be distinguished from *E. crownensis* Ross, 1967c (pp. 638, 639, pl. 69, figs. 8, 10; pl. 70,

Character	Range	Mode	Mean	Standard Deviation	Number of Measurements	Number of Specimens Measured
MxZD	0.20-0.29	0.25	0.251	0.018	40	3
MnZD	0.15-0.24	0.20	0.204	0.023	40	3
MxTD	0.14-0.24	0.16	0.182	0.029	40	3
MnTD	0.10-0.21	0.14	0.146	0.022	40	3
ZWT	0.02-0.13	0.02	0.054	0.028	30	3
		0.04				
MxMD	0.07-0.14	0.08	0.098	0.021	14	2
		0.10				
MnMD	0.05-0.10	0.07	0.071	0.014	14	2
D/mm[1]	3-10	4	5.8	1.9	23	3

[1]Based on 0.5 mm measurements.

Table 28. Quantitative data on characters of *Eridotrypa abrupta* Loeblich from the lower Chickamauga Group.

Character	Range	Mode	Mean	Standard Deviation	Number of Measurements	Number of Specimens Measured
MxZD	0.26-0.35	0.29	0.306	0.027	10	1
MnZD	0.20-0.28	0.25	0.246	0.020	10	1
MxTD	0.20-0.26	0.20	0.222	0.021	10	1
MnTD	0.12-0.20	—	0.168	0.022	10	1
ZWT	0.07-0.08	0.07	0.074	0.004	5	1
MxMTD	0.06-0.25	0.17	0.150	0.052	10	1
MnMTD	0.03-0.14	0.08	0.078	0.032	10	1
M/2-mmsq	7	7	7	—	2	1
D/mm	3-5	5	4.5	0.7	10	1

Table 29. Quantitative data on characters of *Eridotrypa abrupta* Loeblich. Holotype, USNM 114580.

figs. 1-10) by the more gentle curvature of zooecia from the immature to the mature zone, less oblique approach of zooecia to the mature zone, less distinct boundary between immature and mature zones, more widely spaced diaphragms in the mature zone and fewer cystiphragms.

The trivial name, *arcuata,* refers to the arcuate nature of zooecia where they pass from the immature zone to the mature zone.

Material. — Ten thin-sectioned zoarial fragments from stratigraphic sections III and XV.

Holotype. — USNM 167799.

Paratypes. — USNM 167800-167802, GSATC 205, UNC 4161.

Measurements. — Table 30.

Character	Range	Mode	Mean	Standard Deviation	Number of Measurements	Number of Specimens Measured
MxZD	0.24-0.40	0.30	0.310	0.035	63	7
MnZD	0.13-0.29	0.21	0.214	0.034	63	7
MxTD	0.12-0.30	0.20	0.206	0.043	63	7
MnTD	0.06-0.21	0.15	0.128	0.036	63	7
ZWT	0.03-0.13	0.08	0.077	0.023	67	7

Table 30. Quantitative data on characters of *Eridotrypa arcuata,* n. sp. Type suite from the lower Chickamauga Group.

Eridotrypa libana (Safford, 1869) Pl. 58, figs. 6-9

1869. *Stenopora Libana* Safford, Geol. Tennessee, p. 285.
1921. *Batostoma libana* (Safford), Coryell, Indiana Acad. Sci., Proc., vol. 29. p. 293, pl. 8, figs. 5-7.

Diagnosis. — Zoarium ramose, branches about 8 mm thick; zooecia with about four diaphragms per mm in mature zone, mature zooecial tube diameters average 0.48 mm by 0.35 mm; mature wall thickness averages 0.07 mm.

Description. — The zoarium is ramose. The eroded branch diameter is 7.7 mm.

Zooecia diverge from the branch axis at about 10° to 15° and extend linearly to the base of the mature zone, where there is a distinct bend where the mature zooecia extend at about a 60° angle through the short mature zone to the zoarial surface. In the immature zone some zooecia are locally constricted in the longitudinal section, which may be due to slight zooecial meandering which causes the zooecia to pass in and out of the section. All zooecia are constricted in the submature portion or at the base of the mature zone. The latter type of constriction is inherent and of taxonomic significance. Zooecia originate throughout the immature zone, some at the periphery of the immature zone. Mature zooecial diameters average 0.57 mm by 0.44 mm, and corresponding zooecial tube diameters average 0.48 mm by 0.35 mm. Zooecial cross-sections in the mature zone are polygonal, in most cases five- or six-sided. Diaphragms are scarce in the immature zone and average four per mm in the submature and mature zones. Diaphragms are slightly thickened. A few are indistinctly laminate, but the majority appear granular. Diaphragms are variously planar, slightly concave or slightly convex.

Mature walls average 0.07 mm thick and are indistinctly laminate. As seen in longitudinal section the laminae are steep, forming a slight angle with the zooecial border. Laminae are concentric in tangential sections. Zooecial borders are obscure in longitudinal section but vary from well-defined, thin, dark lines to broad, clear zones in tangential section. Immature walls are thin, mostly straight, but locally flexuous.

Mesopores and acanthopores are absent.

Discussion. — Safford (1869, p. 285) described "*Stenopora Libana*" from the Glade Limestone (now the Lebanon Limestone, part of the Stones River Group) of central Tennessee as "Like *fibrosa* but with cell-tubes much larger." Coryell (1921, p. 293) designated a "holotype" of *Batostoma libana* (Safford) and gave adequate description and figures. However, the specimen designated by Coryell cannot be a holotype because it was not designated at the time the species was described; nor is there evidence that Coryell's specimen came from the specimens or from the same locality as the specimens on which Safford based his initial description. Therefore, Coryell's specimen ought to be considered a neotype.

The only specimen of *Eridotrypa libana* (Safford) collected for this study from the lower Chickamauga Group was compared with Coryell's neotype specimen. Coryell's description is accurate except that he interpreted dark, acanthopore-like areas where zooecia meet in the zooecial corners as true acanthopores. The acanthopore-like areas lack the cone-in-cone structure typical of acantho-

Character	Range	Mode	Mean	Standard Deviation	Number of Measurements	Number of Specimens Measured
MxZD	0.52-0.64	0.52 0.55	0.572	0.039	10	1
MnZD	0.40-0.48	—	0.436	0.025	10	1
MxTD	0.40-0.51	0.51	0.477	0.036	10	1
MnTD	0.31-0.43	0.35	0.351	0.036	10	1
ZWT	0.04-0.09	0.08	0.074	0.013	10	1
D/mm	3-6	4	4.1	0.8	10	1

Table 31. Quantitative data on characters of *Eridotrypa libana* (Safford) from the lower Chickamauga Group.

Character	Range	Mode	Mean	Standard Deviation	Number of Measurements	Number of Specimens Measured
MxTD	0.40-0.48	0.45	0.443	0.025	10	1
MnTD	0.32-0.40	—	0.362	0.027	10	1
ZWT	0.04-0.08	0.05	0.054	0.013	10	1
MxMTD	0.05-0.21	0.11	0.122	0.047	10	1
MnMTD	0.03-0.15	0.09 0.07	0.074	0.032	10	1
M/2-mmsq	4-5	—	4.5	0.5	2	1
D/mm	3-4	4	3.7	0.5	10	1

Table 32. Quantitative data on characters of *Batostoma libana* (Safford). Coryell's neotype, USNM 44693.

pores, but are clear structures that are irregular in cross-section. There is an apparent misprint (Coryell, 1921, p. 293) in which "7 to 8 maculae are present in one sq. mm, . . ." should probably read ". . . 7 to 8 maculae are present in one sq. cm. . . ." Coryell did not mention constriction of zooecia at the base of the mature zone. Because he failed to take into account zooecial constrictions and interpreted the dark areas as acanthopores, Coryell considered that the species fitted the concept of *Batostoma* as the genus was then known. The species is here transferred to *Eridotrypa* because of zooecial constrictions at the base of the mature zone and abundance of diaphragms in the mature area. Measurements made on Coryell's type (USNM 44693) are given in Table 32.

Material. — One thin-sectioned specimen from stratigraphic section II.

Hypotype. — USNM 167803.

Measurements. — Table 31 (see also Table 32).

Genus **BATOSTOMA**

Batostoma varium Ulrich, 1893 Pl. 59, figs. 1-8; Pl. 60, figs. 1-4

1893. *Batostoma varium* Ulrich, extract from Minnesota Geol. and Nat. Hist. Sur., Final Rept., Paleont., vol. 3, pp. 292, 293, pl. 25, figs. 16-25.
1967. *Batostoma varium* Ulrich, Bork and Perry, Jour. Paleont., vol. 41, pp. 1388-1390, pl. 177, figs. 6-9.

Diagnosis. — Zoaria ramose; zooecia without diaphragms in immature zone, diaphragms present in mature and submature zones, zooecial tube diameters average 0.24 mm by 0.18 mm; mesopores abundant, most with calcareous deposits; acanthopores small to typically large, averaging 12 per 1-mm square.

Description. — Zoaria are ramose, with most branch diameters about 5 mm to 6 mm. Branch division is irregular and a few branches anastomose. Some overgrowths are present.

The zooecia bend out gradually from the axial region to an abrupt bend at the base of the mature zone, beyond which they extend almost at a right angle to the zoarial surface. Zooecial cross-sections are polygonal in the immature zone and are rounded oval in the mature zone. Mature zooecial diameters, including the ring-like wall, average 0.31 mm by 0.24 mm, and corresponding zooecial tube diameters average 0.24 mm by 0.18 mm. The distance between adjacent zooecial tubes averages 0.10 mm. Diaphragms are absent to rare in the immature region except for the peripheral submature zone, where thin diaphragms are present. Diaphragms are abundant in the mature zone, averaging six per mm. Most diaphragms in the zooecia are thin and planar to slightly concave or convex. A few are thickened by laminar deposits extending out from the walls.

Zooecial walls begin to thicken abruptly at the base of the mature zone, producing a ringlike or girdle-like band around mature zooecia. The mature walls average 0.07 mm thick. Mature walls are laminated. Laminae appear as fine concentric rings in tangential sections and are inclined from about 20° to 45° to the zooecial border in longitudinal sections. The line of contact between adjacent zooecia in longitudinal sections is thin, dark, and smooth to finely crenulate or granular-appearing.

Polygonal mesopores with concave walls originate at the base of the mature zone and expand rapidly to average tube diameters of 0.17 mm by 0.09 mm. They occupy spaces between zooecia and arise from an abrupt bend of zooecia at the base of the mature zone. Mesopores have thin walls in contrast with thickened zooecial walls. Mesopore diaphragms are moderately thickened and are abundant. Only two measurements of diaphragm spacing, yielding 14 and 15 diaphragms per mm, were possible in the mesopores. Most mesopores are partially to entirely filled by vaguely laminated calcareous deposits, and the number per 2-mm square was not counted because calcareous filling causes borders between adjacent mesopores to be obscured.

Acanthopores also originate at the base of the mature zone and may be located anywhere around the periphery of the girdle-like

zooecial walls. The size of acanthopores varies from specimen to specimen, but the average diameter is 0.06 mm. The maximum observed acanthopore diameter is 0.14 mm. Most acanthopores extend in the same direction as adjacent mature zooecia, but some are directed at a slight angle to the zooecia. Acanthopores have inverted, cone-shaped laminae surrounding a large clear axial area. The average acanthopore density is 12 per 1-mm square.

Discussion. — The syntypes of *Batostoma varium* Ulrich (USNM 43510) contain more variation than included in the specimens from the lower Chickamauga Group. With the possible exception of one of the specimens illustrated by Ulrich (1893, pl. 25, fig. 22), the syntypes form a cohesive group. The specimen illustrated by Ulrich (1893, pl. 25, fig. 23) is here designated the lectotype.

Character	Range	Mode	Mean	Standard Deviation	Number of Measurements	Number of Specimens Measured
MxZD	0.25-0.38	0.30	0.307	0.035	70	8
MnZD	0.19-0.31	0.23	0.233	0.019	70	8
MxTD	0.15-0.36	0.25	0.238	0.038	136	13
MnTD	0.10-0.28	0.17	0.179	0.034	136	13
ZWT	0.02-0.21	0.10	0.104	0.041	130	13
MxMTD	0.04-0.40	0.15	0.168	0.073	68	7
MnMTD	0.02-0.27	0.10	0.093	0.044	68	7
AD	0.01-0.14	0.03	0.064	0.030	11	12
A/1-mmsq	3-24	14	11.9	4.3	54	12
D/mm	3-8	5	5.6	1.5	10	2

Table 33. Quantitative data on characters of *Batostoma varium* Ulrich from the lower Chickamauga Group.

Calcareous deposits that partially or completely fill most mesopores are probably extreme examples of thickened diaphragms. Where calcareous deposits occur, vague laminae extend across the mesopores and turn outward slightly toward the zoarial surface just before reaching the mesopore border. Possibly the vague horizontal laminae in the filled mesopores are analogous with diaphragms and upturned edges represent mesopore walls.

Material. — Eighteen thin-sectioned zoarial fragments from stratigraphic sections I, III, VI, X, XV, XVI.

Hypotypes. — USNM 167804-167808, 167799.

Measurements. — Table 33.

Batostoma increbescens Bork and Perry, 1967 Pl. 60, figs. 5-8; Pl. 61, figs. 1, 2

1967. *Batostoma increbescens* Bork and Perry, Jour. Paleont., vol. 41, pp. 1386-1388, pl. 177, figs. 1-5.

Diagnosis. — Zoaria encrusting to ramose; zooecial tubes with diaphragms throughout, average diameter 0.18 mm by 0.14 mm; a ringlike band is present around zooecia where walls are thickened; mesopores average 80 per 2-mm square, similar to zooecia in longitudinal sections; acanthopores average 29 per 1-mm square, highly variable in length.

Description. — The zoaria are ramose to encrusting, with branch diameters about 3 mm, and encrusting portions up to 4 mm thick.

The zooecia are small, with average diameters of 0.21 mm by 0.18 mm, and corresponding zooecial tube diameters average 0.18 mm by 0.14 mm. The distance between adjacent zooecial tubes averages 0.08 mm. Zooecial cross-sections are subrounded polygonal in the proximal portions and change to rounded oval or subcircular in the distal portions. Ramose forms have well-defined immature and mature zones with a gentle increase in curvature at the base of the mature zone. In encrusting portions, however, zooecia extend vertically to the surface through most of their length. Increases in wall thickness are confined to a narrow zone along the zoarial surface and below positions of former zoarial surfaces. Zooecial diaphragms are abundant in the entire tube in encrusting specimens, but are more abundant within the mature periphery in ramose specimens. Diaphragms average 10 per mm in mature zooecia. Diaphragms in both zooecia and mesopores vary from thin to slightly thickened and laminar.

The walls are thin throughout most of the zooecial length. Where thickened, they form a girdle-like band around each zooecium. The bands average about 0.03 mm in thickness. They appear concentrically laminated in tangential sections, and in longitudinal sections they have laminae that vary from steeply and uniformly inclined, making an angle of about 15° with the zooecial border, to laminae that are less steeply inclined and that curve toward the zooecial boundary. The zooecial boundary is a thin, granular-appearing line in thin-section.

Mesopores are abundant; they average 80 per 2-mm square.

In tangential sections, mesopores are irregularly polygonal with concave sides due to the curvature of zooecia. Mesopore walls vary from thin to a thickness and appearance similar to zooecial walls. Diameters of mesopore tubes average 0.16 mm by 0.10 mm. Due to similarity in size, diaphragm spacing, wall structure, and wall thickness, and because the mesopores originate near the base of encrusting portions and within the axial zone of ramose forms, they are difficult to differentiate from zooecia in longitudinal sections.

Acanthopores are also abundant and average 29 per 1-mm square. They are located along the outer periphery of the girdle-like bands surrounding the zooecia. Acanthopores average 0.04 mm in diameter and frequently cause small inflections into zooecial tubes and greater inflections into adjacent mesopore tubes. They are located from the base to the surface of encrusting portions of the zoaria and are variable in length. Some acanthopores extend through the entire thickness of the crust but others are less than a tenth of a mm long and may be located anywhere within the encrusting zoarium except along the basal lamina where zooecia are inclined. They are restricted to the mature and submature portions of ramose zoaria.

Discussion. — Specimens here included in *Batostoma increbescens* have been compared with Bork's and Perry's holotype and paratype (IGS 12P700 and 12P701). The greatest difference noted is that the Chickamauga Group specimens have an average of 29 acanthopores per 1-mm square. The range of acanthopores per 1-mm square in the Chickamauga specimens overlaps that of the types. This difference in acanthopore abundance is the only major discrepancy between the two sets of specimens, which is not considered to be sufficiently great to warrant the distinction of a new species.

The number of mesopores per 2-mm square also differs between type specimens of *Batostoma increbescens* and the lower Chickamauga Group specimens, but the mean number in the type specimens (59 per 2-mm square) is included within the range (59 to 90) of mesopores per 2-mm square in the Chickamauga specimens. Mesopore size and abundance is highly variable, and the variation observed here is not considered taxonomically important. Also, the slight difference in average number of diaphragms per mm in the

Character	Range	Mode	Mean	Standard Deviation	Number of Measurements	Number of Specimens Measured
MxZD	0.19-0.25	0.20	0.208	0.018	10	1
MnZD	0.15-0.21	0.18	0.180	0.020	10	1
MxTD	0.14-0.25	0.15 0.20	0.180	0.027	30	3
MnTD	0.12-0.17	0.14	0.139	0.013	30	3
ZWT	0.03-0.12	0.08	0.075	0.026	30	3
MxMTD	0.05-0.26	—	0.160	0.055	30	3
MnMTD	0.04-0.19	0.10	0.096	0.038	30	3
M/2-mmsq	59-90	87	80.4	12.2	7	2
AD	0.02-0.07	0.03	0.037	0.011	30	3
A/1-mmsq	17-36	30	28.8	6.1	20	4
D/mm	9-11	9	9.8	0.9	11	2
D/mmI	4-7	6	5.5	1.0	10	1

Table 34. Quantitative data on characters of *Batostoma increbescens* Bork and Perry from the lower Chickamauga Group.

mature zone (14 per mm in the type specimens and 10 per mm in the Chickamauga specimens) may be attributed to different growth rates.

All other characters compared — maximum and minimum zooecial diameter, maximum and minimum zooecial tube diameter, distance between adjacent zooecial tubes, zooecial wall thickness, acanthopore diameters, inflected acanthopores and their placement, and maximum and minimum mesopore tube diameter — are essentially identical.

Material. — Four thin-sectioned specimens from stratigraphic section V, VI, and XII.

Hypotypes. — USNM 167809, 167810.

Measurements. — Table 34.

Batostoma sp. Pl. 61, figs. 3-6

Description. — The zoaria are encrusting to ramose and measure 4 mm in maximum thickness.

Most zooecia in encrusting specimens extend to the zoarial surface at a 60° angle. In a few places in the encrusting specimens, such as the thickest part of the zoarium, and in ramose forms, zooecia meet the zoarial surface at about 90°. Zooecial cross-sections vary from polygonal and angular to, in most cases, smoothly oval or subcircular. Zooecial tube diameters average 0.18 mm by 0.16 mm. Adjacent zooecial tubes are separated by an average distance

of 0.06 mm. Sparse, thin planar to concave and tilted diaphragms occur in some zooecial tubes but are completely lacking in others. There is an average of two diaphragms per mm in the zooecia.

The zooecial walls are thin but are locally thickened slightly (less than 0.02 mm) into a narrow, ringlike band surrounding zooecia.

Mesopores are abundant; about two or three times more mesopores than zooecia occur in a given area. No counts of mesopore abundance were made due to the small size of the only tangential section. Mesopores are thin-walled, tube diameters average 0.09 mm by 0.05 mm. In cross-section they are polygonal, three- to six-sided, and have concave walls where adjacent to the zooecia. Mesopore diaphragms are abundant, with an average of seven per mm, thin, and in most cases planar. Mesopores typically swell between diaphragms, to produce a beaded appearance in vertical sections.

Acanthopores are also abundant, but thickness and insufficient size of the tangential section prevented counts. Acanthopores are about 0.02 mm in diameter. They occur along zooecial borders but are large enough to cause some of the adjacent zooecial tubes to be inflected.

Discussion. — Sections of the specimens described above do not give sufficient information to warrant erection of a new species, although the specimens do not appear to match any previously described *Batostoma* species.

The specimens here assigned to *Batostoma* sp. have many characters, especially the encrusting nature and thin walls, originally though to be diagnostic of *Stromatotrypa*. As shown by Boardman (1960b, pp. 6, 7), *Stromatotrypa* is actually the encrusting, thin-walled form of *Batostoma*.

Character	Range	Mode	Mean	Standard Deviation	Number of Measurements	Number of Specimens Measured
MxTD	0.15-0.20	0.18	0.183	0.016	10	1
MnTD	0.15-0.17	0.15	0.159	0.10	10	1
DBZT	0.02-0.08	0.02	0.056	0.026	10	1
MxMTD	0.03-0.15	0.07	0.088	0.034	10	1
MnMTD	0.03-0.08	0.05	0.051	0.015	10	1
D/mm	0-4	3	2.3	1.3	10	1
D/mmM	6-10	7	7.2	0.5	10	1

Table 35. Quantitative data on characters of *Batostoma* sp. from the lower Chickamauga Group.

Locally, as shown in figure 3 of Plate 62, rapid growth caused diaphragms to be widely spaced in the mesopores. Where this rapid growth occurs, mesopores appear to grade upward into zooecia and apparent zooecia grade upward into mesopores. Therefore, some apparent mesopores in the area of rapid growth may be zooecia, or mesopores may be occupied by polymorphic individuals that possess the ability to build typical zooecia under certain environmental conditions.

Material. — Three thin-sectioned zoarial fragments from stratigraphic sections II, XV, XVI.

Hypotype. — USNM 167811.

Measurements. — Table 35.

Genus **HEMIPHRAGMA**

Hemiphragma irrasum (Ulrich, 1886) Pl. 61, figs. 7, 8; Pl. 62, figs. 1-6

1886. *Batostoma irrasa* Ulrich, Minnesota Geol. and Nat. Hist. Sur., Ann. Rept. 14, pp. 94, 95.
1893. *Hemiphragma irrasum* (Ulrich), Ulrich, extract from Minnesota Geol. and Nat. Hist. Sur., Final Rept., Paleont., vol. 3, pp. 299, 300, pl. 24, figs. 5-19.
1911. *Hemiphragma irrasum* (Ulrich), Bassler, U. S. Nat. Mus., Bull. 77, pp. 284-286, text-figs. 172a-f.
1919. *Hemiphragma irrasum* (Ulrich), Bassler, Maryland Geol. Sur., Cambrian and Ordovician, pp. 218, 219, pl. 44, figs. 1-5.
1942. *Hemiphragma irrasum* (Ulrich), Loeblich, Jour. Paleont., vol. 16, pp. 433, 434, pl. 63, fig. 19.
1968a. *Hemiphragma irrasum* (Ulrich), Bork and Perry, Jour. Paleont., vol. 42, pp. 342, 343, pl. 44, figs. 1-3, 5.

Diagnosis. — Zoaria irregularly ramose and encrusting; zooecial diameters in mature zone, including cingulum, average 0.36 mm by 0.29 mm; zooecial tube diameters are 0.26 mm by 0.20 mm in the mature zone; acanthopores average 13 per 1-mm square; mesopores average about 18 per 2-mm square.

Description. — The zoaria are irregularly ramose with branches up to 6 mm in diameter, less frequently encrusting. Branch bifurcation is frequent.

The zooecia have sparse, thin diaphragms in the thin-walled axial region. As the zooecial walls thicken outward in the mature zone, hemiphragms, which are restricted to the mature region, become progressively thicker. Most hemiphragms are spaced so that four occur in one mm, but vary from three to rarely six. Maximum

zooecial diameters, including cingulum, average 0.36 mm and minimum zooecial diameters average 0.29 mm; corresponding zooecial tube diameters are 0.26 mm by 0.20 mm. Distances between adjacent zooecial tubes average 0.14 mm. Both zooecia and zooecial tubes are smoothly oval to subcircular in cross-section in the mature zone.

Mesopores originate at the base of the mature zone and widen within a short distance to their maximum diameter. Their average tube diameters are 0.19 mm by 0.10 mm. Mesopores are angular to subangular. In tangential sections their sides have the shape of one or more concave curves where they are adjacent to zooecia; less frequently, where mesopores contact one another, the common side is straight. Mesopore walls remain thin for a short distance distal to the zone at which the zooecial walls begin to thicken, beyond which they too thicken. Near the surface of the zoarium mesopores are frequently filled by a dense deposit of calcareous material so that, in the most extreme case, mesopore boundaries are not discernible in tangential section. Mesopores contain diaphragms spaced two or three times more closely than hemiphragms in the mature zones of the zooecia. There are 15 to 26 mesopores per 2-mm square in tangential sections, with an average of about 18 per 2-mm square.

Acanthopores average 13 per 1-mm square in tangential sections and range from 6 to 19 per 1-mm square. They are typically 0.03 mm to 0.04 mm in diameter, but in one specimen in which mesopores are completely obscured by calcareous deposits, acanthopores are 0.05 mm by 0.09 mm in diameter. Acanthopore axial areas are atypically large relative to other trepostomes. Acanthopores originate at or near the base of the mature zone and are located most typically at zooecial-mesopore corners. They frequently inflect the cingulum but rarely cause the zooecial tube to be inflected. Some acanthopores appear to be within the mesopores where the mesopores are filled by calcarous laminae, have vague borders, and are difficult to discern from one another, but careful observation indicates that such acanthopores are actually located along mesopore borders.

Discussion. — In the one specimen on which comparative measurements between the mature and submature zooecia can be made, average mature zooecial tube diameters are 0.24 mm by 0.19 mm, and zooecial tube diameters immediately below the thick-walled

mature zone average 0.39 mm by 0.28 mm. Comparison of the two sets of averages strongly indicates that zooecal tubes are restricted in the mature zone. Restriction appears to result possibly from two factors: intercalation of rapidly widening mesopores between zooecia and thickening of zooecial walls to develop a cingulum around each zooecial tube. Since the zooecial diameters, including the cingulum, in the mature zone are approximately equal to zooecial tube diameters just below the thick-walled mature zone, it appears that development of a cingulum is the major cause of restriction of zooecial tubes. Appearance of mesopores is probably more intimately related to increased outward divergence of zooecia in the mature region than to a decrease in zooecial tube diameter.

The specimens identified and figured by Bassler (1911, p. 284, text-fig. 173a-d) as *Hemiphragma irrasum* from Estonia, differ from Ulrich's type description and figures, which Bassler reproduced *(op. cit.,* pp. 284-286, text-fig. 172a-f). Bassler's Estonian specimens have less pronounced curvature of the zooecia at the base of the mature zone, more widely spaced hemiphragms, smaller acanthopores, and abundant diaphragms in the immature region. Bassler's Estonian specimens probably do not belong to *H. irrasum.*

The specimen of *Hemiphragma irrasum* described and illustrated by Bork and Perry, 1968a, pp. 342, 343, pl. 44, figs. 1-3, 5) from the Guttenberg Formation of Iowa, appears most similar to Chickamauga representatives of *H. irrasum.*

Character	Range	Mode	Mean	Standard Deviation	Number of Measurements	Number of Specimens Measured
MxZD	0.29-0.45	0.33 0.35	0.357	0.039	40	4
MnZD	0.20-0.33	0.30	0.289	0.027	40	4
MxTD	0.17-0.36	0.28	0.257	0.047	60	6
DBZT	0.03-0.26	—	0.137	0.054	50	5
MxMTD	0.06-0.34	0.20 0.25	0.189	0.071	50	5
MnMTD	0.04-0.17	0.10	0.100	0.037	50	5
M/2-mmsq	11-26	—	17.8	4.9	9	3
AD	0.03-0.09	0.03	0.047	0.018	40	4
A/1-mmsq	6-19	15	13.1	3.3	37	4

Table 36. Quantitative data on characters of *Hemiphragma irrasum* (Ulrich) from the lower Chickamauga Group.

Material. — Eight sectioned specimens from stratigraphic sections II, V, XII, XV.

Hypotypes. — USNM 167812, 167813.

Measurements. — Table 36.

Family **CALOPORIDAE**

Genus **CALOPORA***

Calopora dumalis (Ulrich, 1893) Pl. 62, figs. 7, 8; Pl. 63, figs. 1, 2

1893. *Callopora dumalis* Ulrich, extract from Minnesota Geol. and Nat. Hist. Sur., Final Rept., Paleont., vol. 3, p. 282, pl. 23, figs. 1-8.
1911. *Hallopora dumalis* (Ulrich), Bassler, U. S. Nat. Mus., Bull. 77, pp. 331, 332, text-figs. 207a-h.

Diagnosis. — Zoaria ramose, branches about 2 mm in diameter; zooecia curve gently outward to zoarial surface, with diaphragms sparse to questionably common in full-sized zooecia and abundant in proximal zooecial tips; mature zooecial tube diameters average 0.25 mm by 0.18 mm; mesopores are numerous, with closely spaced diaphragms; mature zooecial walls slightly thickened.

Description. — The zoaria are ramose with branches about 2 mm in diameter. All specimens collected have one bifurcation each, with the longest specimen 11 mm long.

In the axial region zooecia are slightly curved to sinuous. Zooecia bend smoothly into the mature zone, in which they are more strongly curved. At their proximal tips zooecia have closely spaced thin, planar diaphragms averaging eight per mm. Where zooecia have reached their full diameter, both in the immature and mature zones, diaphragm spacing is variable, with diaphragms closely spaced in one zoarium (Plate 63, fig. 8) and rare in others. There is an average of five diaphragms per mm in full-sized zooecia in the specimen figured in Plate 63, figure 8. Zooecia have subrounded cross-sections in the immature region because of intercalated zooecial tips and mesopores in corners. In the mature zone zooecia are subcircular to oval in cross-section with almost all zooecial corners occupied by a mesopore. Mature zooecial diameters average 0.27 mm by 0.22 mm, and the corresponding zooecial tube diameters average 0.25 mm by 0.18 mm.

Mesopores are moderately short and originate in the outer im-

*For discussion of *Calopora* and *Callopora* see Ross, J. P., 1969, pp. 270, 271.

mature zone and in the basal portion of the mature zone. Most are quadrangular in cross-section and a few are triangular or pentagonal in cross-section. The sides of mesopores are essentially flat, but some are slightly concave or convex as seen in zoarial tangential sections. Diaphragms within mesopores are thin and closely spaced, with an average of 13 per mm based on segmented measurements in one specimen. Diaphragms vary from planar to less commonly strongly curved and where combined with the mesopore wall undulation, especially in the proximal ends, give a few mesopores a slightly beaded appearance. Mesopore tube diameters average 0.11 mm by 0.06 mm. There are about 50 to 80 mesopores in a 2-mm square area.

The zooecial wall thickness averages 0.03 mm. Where the walls are slightly thickened, a dark median line separates adjacent zooecia. The dark line between zooecia varies from smooth to slightly irregular in longitudinal sections. Wall laminae appear concentric in zoarial tangential sections. In longitudinal sections most wall laminae form an approximate 15° angle with the zooecial border, which results in a narrow, outwardly directed "V" with laminae from the adjacent zooecia. Laminae curve distally into zooecial borders, resulting in a U-shaped appearance in a few zooecia.

Discussion. — Ulrich's original description and drawings of *Calopora dumalis* (1893, p. 282, pl. 23, figs. 1-8) give a misleading impression of internal characters due to Ulrich's interpretation of some crystal boundaries as zooecial diaphragms. I have examined the thin section (USNM 44501) originally figured by Ulrich: the section is thick and the zooecia are filled by coarse calcite spar. Some of the flat, inclined crystal faces that extend across zooecial tubes at low magnifications resemble diaphragms and were so interpreted by Ulrich. Bassler (1911, pp. 331, 332, text-fig. 207a-h) reproduced Ulrich's original figures with no comment on internal structures, and subsequent authors have interpreted *Calopora dumalis* as characterized by numerous diaphragms in the zooecia. Although this interpretation by subsequent authors does not agree with the sparsity of diaphragms in the lectotype (USNM 43517, here designated) and originally figured section (USNM 44501), moderately abundant diaphragms is accepted here as characteristic of a variation found in some specimens. Two specimens of *C. dumalis*

collected from the lower Chickamauga Group are similar to the lectotype. A third specimen, USNM 167814, agrees with the lecto-

Character	Range	Mode	Mean	Standard Deviation	Number of Measurements	Number of Specimens Measured
MxZD	0.25-0.29	0.28	0.272	0.012	10	1
MnZD	0.18-0.24	—	0.215	0.021	10	1
MxTD	0.23-0.28	0.23	0.249	0.019	20	2
MnTD	0.15-0.20	0.17	0.175	0.016	20	2
ZWT	0.02-0.04	0.03	0.020	0.009	20	2
MxMTD	0.05-0.21	0.06 0.08	0.110	0.043	20	2
MnMTD	0.04-0.11	0.05	0.063	0.020	20	2
D/mm	4-6	5	4.9	0.7	8	2
D/mmPT	6-11	8	8.4	1.8	18	2
D/mmM	11-17	11 13	13.2	2.3	10	1

Table 37. Quantitative data on characters of *Calopora dumalis* (Ulrich) from lower Chickamauga Group.

Character	Range	Mode	Mean	Standard Deviation	Number of Measurements	Number of Specimens Measured
MxZD	0.24-0.37	0.30	0.314	0.031	12	2
MnZD	0.17-0.26	0.19	0.194	0.034	14	2
MxTD	0.21-0.30	0.25	0.246	0.025	12	2
MnTD	0.10-0.20	0.13	0.133	0.028	14	2
DBZT	0.03-0.09	0.06	0.063	0.016	16	2
MxMTD	0.05-0.30	0.06	0.102	0.071	10	1
MnMTD	0.03-0.08	0.05	0.045	0.013	10	1
D/mmPT	6-8	6	6.3	0.7	7	1
D/mmM	9-19	12	13.3	2.7	12	2

Table 38. Quantitative data on characters of *Callopora dumalis* Ulrich. Type suite, USNM 43517.

type in all aspects except that within the specimen there are abundant diaphragms in the zooecia, even more than in Ulrich's misinterpreted figure of specimen USNM 44501. Further studies on larger numbers of specimens may prove that specimens with abundant diaphragms that have been assigned to *C. dumalis* by Bekker (1921, pp. 42, 43, pl. 6, figs. 9-13), Kiepura (1962, pp. 386, 387, pl. 4, fig. 1), Astrova (1965, pp. 177, 178, pl. 24, fig. 1a-d), and Ross (1969, pp. 273, 274, pl. 44, figs. 2-4, 7-9, pl. 45, fig. 4), and USNM 167816 assigned here, belong to a different species. On the other hand, further studies may show a complete intergradation of forms with from few to common diaphragms. Most probably, since no inter-

mediate forms have yet been found, specimens with more abundant diaphragms belong to a different species.

Material. — Three thin-sectioned zoarial fragments from stratigraphic sections III, XV, XVI.

Hypotypes. — USNM 167816, 167817.

Measurements. — Table 37 (see also Table 38).

Calopora ovata McKinney, n. sp. Pl. 63, figs. 3-8

Diagnosis. — Zoaria ramose, branches about 3 mm in diameter; zooecia are smoothly oval in tangential sections and are directed gradually outward from the axial zone with a smooth bend; about eight diaphragms per mm in proximal zooecial tips, but diaphragms are rare in full-diameter zooecia; mature zooecial tube diameters average 0.24 mm by 0.17 mm; walls are thickened in mature zone; mesopores are abundant with about 15 diaphragms per mm.

Description. — The zoaria are ramose, with branch bifurcations at close intervals. Branches are 2.5 mm to 4 mm in diameter, and most are 3 mm in diameter.

Most zooecia originate in the axial zone, although some originate in more peripheral parts of the immature zone. Beyond their point of origin zooecia gradually increase in diameter. They bend slightly outward with smooth curvature that gradually increases into the mature zone. Depending partially on the growth stage, mature zooecia meet the zoarial surface at 45° to 90° angle, typically about 60°. Zooecia in the immature zone have polygonal cross-sections, but in the mature zone zooecia have oval cross-sections with mesopores partially surrounding them. Mature zooecial diameters average 0.30 mm by 0.22 mm, and the corresponding zooecial tube diameters average 0.24 mm by 0.17 mm. Diaphragms are rare except in proximal zooecial tips where thin, planar to shallow concave diaphragms average eight per mm. The distance between adjacent zooecial tubes averages 0.07 mm; most measurements include a mesopore between zooecia.

The mature zooecial walls are about 0.04 mm to 0.06 mm thick. Wall laminae begin subparallel to the zooecial axis then diverge outward at a maximum angle of about 35° from the zooecial border. Distal to the point at which laminae bend toward the zooecial border, most laminae appear linear in longitudinal sections, but

some have a distal bend so that they meet the zooecial border at a higher angle. Zooecial borders appear as a thin dark line defining zooecia in both tangential and longitudinal sections. Near the base of the mature zone slightly thickened zooecial walls appear as girdle-like bands around the zooecial tubes. Mesopore walls are thin. Groups of laminae in the mesopores extend down the wall only a short distance before extending directly across the mesopore as a thickened diaphragm.

Mesopores are abundant and average 66 per 2-mm square. They originate in the outer part of the immature zone and are polygonal in cross-section. As seen in cross-sections (zoarial tangential

Character	Range	Mode	Mean	Standard Deviation	Number of Measurements	Number of Specimens Measured
MxZD	0.26-0.34	0.30	0.302	0.023	30	3
MnZD	0.18-0.26	0.21	0.220	0.019	30	3
MxTD	0.16-0.37	0.24	0.242	0.045	100	10
MnTD	0.13-0.25	0.18	0.172	0.026	90	9
DBZT	0.02-0.16	0.04	0.070	0.036	83	9
MxMTD	0.03-0.20	0.13	0.097	0.042	76	8
MnMTD	0.02-0.11	0.05	0.058	0.022	76	8
M/2-mmsq	48-85	—	65.6		5	4
D/mmPT	5-6	8	7.6	1.8	46	6
D/mmM	9-22	12	14.7	3.6	47	7

Table 39. Quantitative data on characters of *Calopora ovata,* n. sp. Type suite from the lower Chickamauga Group.

sections) most borders between mesopores and zooecia are slightly concave into mesopores, to follow the more dominant curvature of zooecia. Borders between adjacent mesopores appear planar. Mesopore tube diameters average 0.10 mm by 0.06 mm. There is an average of 15 diaphragms per mm in the mesopores. Almost all mesopore diaphragms are thickened by laminar deposits.

Discussion. — *Calopora ovata* differs from *C. dumalis* in having thicker mature zooecial walls, more oval mature zooecial cross-sections, and more abundant mesopores. *C. ovata* differs from *C. incontroversa* (Ulrich, 1886, pp. 96, 97; see also Ulrich, 1893, pp. 278, 279, pl. 22, figs. 33-36) because *C. ovata* has smaller zooecia, fewer diaphragms in the mature zooecia and more abundant mesopores, based on my measurements of the paratypes of *C. incontroversa* in the U.S. National Museum of Natural History.

Character	Range	Mode	Mean	Standard Deviation	Number of Measurements	Number of Specimens Measured
MxZD	0.35-0.55	0.45	0.454	0.052	42	5
MnZD	0.29-0.46	0.34	0.351	0.042	46	5
MxTD	0.29-0.44	—	0.355	0.045	53	6
MnTD	0.20-0.36	0.25	0.275	0.038	59	6
ZWT	0.02-0.18	0.05	0.079	0.040	70	7
MxMTD	0.02-0.23	0.09	0.116	0.048	43	6
MnMTD	0.02-0.18	0.05	0.073	0.034	43	6
M/2-mmsq	3-32	27	17.6		12	3
D/mmPT	2-11	6	6.4	1.9	40	4
D/mmM	10-22	13 16	14.2	2.7	47	5

Table 40. Quantitative data on characters of *Calopora spissata* (Coryell) from the lower Chickamauga Group.

Character	Range	Mode	Mean	Standard Deviation	Number of Measurements	Number of Specimens Measured
MxZD	0.41-0.48	—	0.457	0.023	10	1
MnZD	0.34-0.41	0.34	0.364	0.024	10	1
MxTD	0.25-0.31	—	0.278	0.018	10	1
MnTD	0.20-0.26	0.23	0.227	0.018	10	1
MxZDm	0.51-0.60	0.57	0.562	0.025	10	1
MnZDm	0.40-0.50	0.40	0.438	0.038	10	1
MxTDm	0.30-0.40	0.35	0.354	0.025	10	1
MnTDm	0.23-0.30	0.30	0.280	0.034	10	1
ZWT	0.15-0.21	0.15	0.171	0.024	10	1
MxMTD	0.08-0.11	—	0.095	0.015	2	1
MnMTD	0.18-0.09	—	0.085	0.004	2	1
M/2-mmsq	1	1	1	—	2	1
D/mmPT	8-14	—	11.0	2.2	10	1
D/mmM	16-18	17	16.8	0.7	5	1
DBM	2.0-3.0	2.0	2.33	0.37	6	1

Table 41. Quantitative data on characters of *Hallopora spissata* Coryell. Holotype, USNM 44519.

Character	Range	Mode	Mean	Standard Deviation	Number of Measurements	Number of Specimens Measured
MxZD	0.45-0.57	0.55	0.511	0.040	10	1
MnZD	0.35-0.49	0.38	0.389	0.037	10	1
MxTD	0.27-0.45	—	0.334	0.052	10	1
MnTD	0.20-0.38	0.25	0.258	0.048	10	1
ZWT	0.07-0.19	0.08	0.120	0.041	10	1
MxMTD	0.10-0.29	—	0.172	0.061	10	1
MnMTD	0.08-0.18	0.10	0.100	0.033	10	1
M/2-mmsq	24	24	24	—	1	1
D/mmPT	7-10	10	8.8	1.1	10	1
D/mmM	15-19	15	16.0	1.5	5	1

Table 42. Quantitative data on characters of *Hallopora macrostoma* Loeblich. Holotype, USNM 114603.

The trivial name, *ovata,* refers to the pronounced predominant oval nature of the zooecial tubes in zoarial tangential sections.

Material. — Ten thin-sectioned zoarial fragments from stratigraphic sections XII, XV, XVI, XVIII.

Holotype. — USNM 167816.

Paratypes. — USNM 167817-167819, GSATC 206, UNC 4166.

Measurements. — Table 39.

Calopora spissata (Coryell, 1921) Pl. 64, figs. 1-6

1921. *Hallopora spissata* Coryell, Indiana Acad. Sci., Proc., vol. 29, pp. 291-292, pl. 8, figs. 1, 2.

Diagnosis. — Zoaria ramose, branches about 5 mm in diameter; zooecia curve gently outward from axial region; diaphragms are abundant in mesopores and proximal zooecial tips, absent to scarce in full-sized zooecia; mature zooecial tube diameters average 0.36 mm by 0.28 mm with relatively thin walls; mesopores are common, most prevalent at base of mature zone and are pinched out or filled by calcareous tissue higher in the mature zone.

Description. — The zoaria are ramose, bifurcate, with branches 3 mm to 6 mm in diameter, most about 4 mm to 5 mm in diameter.

Within the immature zone, zooecia bend gently outward toward the zoarial surface and pass into the mature zone with no abrupt change in curvature. The mature zone is marked by a gradual thickening of zooecial walls. Diaphragms are closely spaced in proximal zooecial tips, where they average six per mm. As zooecia increase in diameter, diaphragms become more widely spaced and are absent to rare in full-sized zooecia. Some zoaria with thick mature zones have closely spaced diaphragms in the most distal portion of a few zooecia. Zooecia have subrounded cross-sections in the axial region and the lower mature zone, becoming polygonal or subrounded polygonal in cross-section in the distal-most mature zone, where zooecia are four- to six-sided. Zooecial diameters are 0.45 mm by 0.35 mm, and corresponding zooecial tube diameters average 0.36 mm by 0.28 mm. Zooecial tube cross-sections in the mature zone are rounded and oval to subcircular.

Most mesopores originate in the outer immature zone and are frequently closed by calcareous deposits in the outer mature region. Other mesopores become reduced in cross-sectional diameter and are pinched out before they reach the outer mature zone. Most meso-

pores are four-sided in cross-section although some have rounded cross-sectional outlines. Mesopore tube diameters average 0.12 mm by 0.07 mm. Mesopore walls are thin to slightly thickened. Diaphragms are closely spaced in the mesopores and average 14 per mm. Where mesopore walls are thin, mesopore diaphragms are also thin; but where mesopore walls are slightly thickened, mesopore diaphragms are laminar, slightly thickened, and bend sharply upward to pass into mesopore walls from the diaphragm periphery. There is an average of 18 mesopores per 2-mm square in tangential sections.

Zooecial wall thickness averages 0.08 mm. Wall laminae in the mature zone bend toward the zooecial border at an angle that varies from close to 0° along the periphery of the zooecial tubes to about 15° to 30° near the zooecial boundary. Laminae from adjacent zooecia meet along a well defined, irregularly crenulated boundary to form outwardly-directed V-shaped structures in longitudinal section. In the zoarial tangential sections, walls have a concentric appearance around zooecia to form a well-defined ring about the zooecial tubes and a well-defined line of contact between adjacent zooecia. Near the base of the mature zone, the concentric nature of moderately thickened zooecial walls and thin-walled mesopores cause zooecial walls to have the appearance of a girdle-like band in tangential sections.

Discussion. — Specimens of *Calopora spissata* from the lower Chickamauga Group are similar to the holotype of *C. spissata* (Coryell, 1921, p. 291, pl. 8, figs. 1, 2) but differ in that most mesopores in the holotype are closed by zooecial wall deposits throughout most of the mature zone, zooecial walls are significantly thicker (Table 41) than the average in Chickamauga specimens, and there is a distinct angle at the base of the mature zone so that mature zooecia are directed more perpendicularly toward the zoarial surface in the holotype. Differences in wall thickness and relative length of mesopores is probably due to different stages of maturity between the Chickamauga specimens of *C. spissata* and the holotype, and the difference in degree of curvature at the base of the mature zone may be due to individual variation.

The holotype of *Calopora macrostoma* (Loeblich, 1942, pp. 430, 431, pl. 62, figs. 12-14) has much more abundant diaphragms in

full-sized zooecia in the axial region, slightly larger zooecia, and slightly thicker mature zooecial walls (Table 42) than do lower Chickamauga specimens of *C. spissata*. The same degree of difference exists between the holotypes of *C. spissata* and *C. macrostoma*, which may be sufficiently minor to consider *C. macrostoma* to be a junior synonym of *C. spissata*. Conventionally, differences in abundance or presence or absence of diaphragms have been interpreted to be of at least specific significance and, therefore, the two species are here kept separate.

Material. — Eight thin-sectioned zoarial fragments from stratigraphic sections I, IV, V, XVII.

Hypotypes. — USNM 167820, 167821.

Measurements. — Table 40 (see also Tables 41 and 42).

Family DIPLOTRYPIDAE

Discussion. — Nicholson established *Diplotrypa* in 1879 and, in 1881 (pp. 101, 102, 155, 156) included it as a subgenus of *Monticulipora*. Ulrich (1882, p. 153) retained *Diplotrypa* in the family Monticuliporidae, but in 1890 (p. 378) he erected the Diplotrypidae for the reception of *Diplotrya, Basostoma,* and *Monotrypa*. Ulrich originally characterized the Diplotrypidae as, "Zoaria hemispheric, massive or ramose. Zooecia forming comparatively large tubes of which the walls are more or less flexous and mostly very thin. Mesopores and acanthopores present or wanting. Diaphragms very thin, developed at rather irregular intervals. No cystiphragms." The Diplotrypidae was retained by Ulrich in 1893 (p. 285) with the addition of *Hemiphragma* and *Stromatotrypa*. By 1900, however, Nickles and Bassler (pp. 16, 35, 36) placed the genera that composed the Diplotrypidae into the Trematoporidae. Subsequently, Vinassa de Regny (1920, p. 217) reintroduced Diplotrypidae as a junior homonym, and he included *Diplotrypa, Diplotrypella, Hallopora, Diazipora, Constellaria,* and *Stellipora* in the family.

The family Diplotrypidae is revived in this report as a monogeneric family containing only *Diplotrypa*. As defined here, the Diplotrypidae are characterized by originally tripartite walls that consist of a finely granular median plane that represents the zooecial border, surrounded on either side by vaguely fibrous-appearing walls with the fibers directed at right angles to the median plane. The fibers may represent vague, planar laminae.

Genus **DIPLOTRYPA**

Diplotrypa anchicatenulata McKinney, n. sp. Pl. 64, figs. 7-9; Pl. 65, fig. 1

Diagnosis. — Zoaria massive to hemispherical; zooecia large, irregularly polygonal and angular to suboval in cross-section with average tube diameters 0.44 mm by 0.37 mm; mesopores common, beaded, variable in length; walls appear structureless to fibrous, with a dark median line locally developed near zoarial surfaces.

Description. — The zoaria are massive; some tend toward a hemispherical shape. The greatest observed diameter of fragments is 12 mm. All zoaria are fragmentary and none retain the base; therefore whether the colony has a basically radial growth pattern with new zooecia intercalated between older zooecia or whether the base spread as new zooecia were added laterally cannot be determined. Zooecia are essentially parallel in some zoaria and divergent in others.

The zooecia are large, with average zooecial tube diameters of 0.44 mm by 0.37 mm. Zooecial cross-sections are irregularly polygonal and angular to suboval, depending on zooecial packing, mesopore abundance, and wall thickness. Zooecial angularity is increased by more irregular zooecial packing, decrease in mesopore abundance, and thinner walls. Zooecia locally have smooth walls in longitudinal sections, but in most places the wall is crinkled or is indented by mesopores. Diaphragms are thin, planar to slightly curved. They are spaced from one to slightly more than one zooecial diameter apart and average two per mm. Zooecial space beyond the most distally placed diaphragm is, in most cases, one and a half or two times greater than the space between adjacent diaphragms.

Where zooecial walls are in contact with micrite matrix along the zoarial surface, walls are about 0.04 mm thick, composed of a central, apparently structureless dark line with a clear band of finely crystalline, vaguely fibrous calcite on either side (see Pl. 66, fig. 1). Except for areas of recrystallization and the zone of variable thickness just below the zoarial surface, zooecial walls appear thin (less than 0.01 mm thick) and apparently structureless in nonpolarized light (Pl. 65, fig. 8). In polarized light, a finely crystalline zone 0.03 mm by 0.04 mm thick surrounds the thin, structureless wall visible in nonpolarized light. The finely crystalline material apparently represents the same part of the wall as

does the light-colored, vaguely fibrous wall material near the zoarial surface. Beyond the zone of fine crystals, zooecial tubes are filled by coarse calcite spar. Contact between the finely crystalline wall and the coarse spar is slightly diffuse but is discernible in polarized light.

Mesopores are strongly moniliform; in some places mesopores are so strongly constricted that they are completely closed, only to reappear again immediately above. Diaphragms are present where constrictions are not complete. In longitudinal sections mesopores are variable in length, but are in all cases short. A mean value of 27 was obtained for mesopores in a 2-mm square. In tangential sections mesopores are three- or four-sided and have an average maximum tube diameter of 0.14 mm and an average minimum tube diameter of 0.08 mm. Mesopores occur in zooecial corners.

Discussion. — *Diplotrypa anchicatenulata* appears to be closely related to *D. catenulata* Coryell (1921, p. 296, pl. 10, figs. 6, 7). Comparison with the holotype of *D. catenulata* (USNM 44658) indicates that *D. anchicatenulata* differs primarily in having more abundant and more regularly spaced zooecial diaphragms, more numerous mesopores, and smaller average zooecial tube diameters. Average maximum zooecial tube diameter equals 0.44 mm for *D. anchicatenulata* and 0.56 mm for *D. catenulata* (based on measurements of *D. catenulata* by Bork and Perry, 1968a, p. 341). *D. anchicatenulata* and *D. catenulata* are most similar in extreme catenulation or moniliform nature of mesopores. *D. moniliformis* Bassler

Character	Range	Mode	Mean	Standard Deviation	Number of Measurements	Number of Specimens Measured
MxTD	0.34-0.54	0.45	0.443	0.052	30	3
MnTD	0.28-0.45	0.40	0.371	0.047	40	4
ZWT	0.03-0.10	0.03	0.040	0.015	39	4
MxMTD	0.05-0.24	0.10 0.18	0.142	0.050	31	4
MnMTD	0.03-0.17	0.04	0.077	0.036	31	4
M/2-mmsq	19-32	26 32	26.6	4.7	8	3
D/mm	1-3	2	2.0	0.7	40	4

Table 43. Quantitative data on characters of *Diplotrypa anchicatenulata*, n. sp. Type suite from the lower Chickamauga Group.

(1911, pp. 321, 322, text-fig. 199a-d) is also similar to *D. anchicatenulata* but differs in having more abundant mesopores, mesopores

that change into typical zooecia, and less moniliform mesopores. *D. anchicatenulata* has more abundant, more regularly spaced, and more horizontally planar diaphragms than *D. moniliformis argutus* Astrova (1948, pp. 21-23, pl. 3, fig. 4; pl. 4, figs. 1, 2, text-figs. 9, 10a-e), and strongly moniliform mesopores do not develop into typical zooecia as in the subspecies described by Astrova.

The trivial name, *anchicatenulata,* is derived from the Greek word *anchi,* meaning near, and *catenula,* the Greek diminuitive of chain, referring to beaded mesopores. The trivial name refers to nearness of this species to *Diplotrypa catenulata* Coryell.

Material. — Four thin-sectioned colonies from stratigraphic section XVI.

Holotype. — USNM 167822.

Paratypes. — USNM 167823.

Measurements. — Table 43.

INCERTAE SEDIS

Genus **NICHOLSONELLA**

Discussion. — *Nicholsonella* is included in *Incertae Sedis* because the genus has a recrystallized wall structure that does not allow its inclusion in previously recognized families, and not enough is yet known about its original wall structure to allow erection of a new, well-defined family. The apparently ubiquitous recrystallization of *Nicholsonella* suggests an original composition of aragonite, which is less stable than calcite and frequently recrystallizes to calcite.

Nicholsonella Ulrich (1890, p. 374), was assigned by him to the family Trematoporidae *(op. cit.,* p. 373), which he erected for the reception of *Trematopora, Nicholsonella, Constellaria, Stellipora,* and *Idiotrypa.* Ulrich *(op. cit.,* p. 421) commented on the apparent affinities of *Nicholsonella* to *Constellaria,* and noted that an absence of stellate maculae distinguishes *Nicholsonella. Trematopora,* the type genus of the Trematoporidae, has laminate walls with well-defined zooecial boundaries caused by convergent laminae that form a narrow V-shaped pattern, whereas walls between zooecia and mesopores are formed by more broadly curved laminae that result in a U-shaped pattern (Boardman, 1959, pp. 5, 6). With current emphasis on wall microstructure as a family-group phylogenetic indicator, the poorly defined, typically altered and recrystallized

walls of *Nicholsonella* remove it from close relationship with *Trematopora.*

Concerning *Nicholsonella,* Ulrich noted in 1893 (p. 313) that, "This a Lower Silurian genus with rather uncertain affinities. So far as our knowledge goes the position of the genus in classification seems to be in a measure intermediate between *Constellaria* and *Leioclema.*" and it ". . . appears to occupy a rather isolated position with respect to contemporaneous types of structure." In 1900 Ulrich (p. 276) erected the family Constellariidae to include *Constellaria, Stellipora, Nicholsonella, Idiotrypa,* and questionably *Dittopora.* (The date of authorship of Constellariidae is widely cited as 1890, but even as late as 1893 Ulrich included *Constellaria* in the Trematoporidae.) *Nicholsonella* remained in the Constellariidae from 1900 to 1960, when it was included by Astrova (*et al.,* 1960, p. 69) in the Heterotrypidae. Removal of *Nicholsonella* from the Constellariidae was further strengthened when Astrova (1964) included the Constellariidae in her new order Cystoporata. *Nicholsonella* does not share the granular-fibrous calcitic walls and inter-zooecial vesicles characteristic of the Cystoporata. I feel that assignment of *Nicholsonella* to the Heterotrypidae as was done by Astrova (*et al.,* 1960, p. 69) is also in error, because *Nicholsonella* is recrystallized in all known occurrences, which suggests aragonitic walls. The heterotrypid wall structure consists of broadly U-shaped, calcitic laminae and common zooecial tube linings.

Vinassa de Regny (1920, p. 224) erected the new family Nicholsonellidae for the reception of *Nicholsonella, Idiotrya,* and *Stromatotrypa.* However, *Idiotrypa* belongs to the Constellariidae, and *Stromatotrypa* is a junior synonym of *Batostoma* (see Boardman, 1960b, pp. 2, 6, 7), a member of the family Trematoporidae. As stated previously (p. 100), not enough is yet known about the original wall structure of *Nicholsonella* for it to stand at present as the basis for a family. Therefore, Vinassa de Regny's Nicholsonellidae is not used in this report, although a modified understanding of the family may well be considered valid at some time in the future.

Where zooecia are partially filled by micrite matrix, the walls of *Nicholsonella* appear thinner and are more sharply delineated. However, where sparry calcite infills zooecia, walls have more obscure borders and appear somewhat thicker than where bounded by

micrite. Walls are recrystallized in both situations, but where micrite is present more accurate measurements of wall thickness can be made because the presence of micrite prevented spread and diffusion of zooecial walls during recrystallization. Since measurements of wall thickness in most *Nicholsonella* species are made where sparry calcite infillings exist, reported average wall thickness is probably biased upward.

Nicholsonella acanthobscura McKinney, n. sp. Pl. 65, figs. 2-8

Diagnosis. — Zoaria ramose or laminate; zooecial tube diameters average 0.21 mm by 0.16 mm, diaphragms sparse to abundant in immature zone, three per mm in mature zone; mesopores are abundant, some filled by calcareous deposits; acanthopores are obscured in most zoaria and are vague in other zoaria.

Description. — The zoaria are ramose, encrusting, or free laminate. Maximum diameter of the ramose branches is 17 mm, including conspecific overgrowths, but most branches are about 5 mm to 6 mm in diameter. Encrusting and free laminate forms are up to at least 15 mm in diameter and 2 mm thick.

The zooecia curve smoothly out from the axial region in ramose forms. The degree of curvature increases slightly in the mature zone in some specimens, and in others there is a distinct bend at the base of the mature zone, from which zooecia extend at a right angle to the zoarial surface. Mature zooecial tube diameters average 0.21 mm by 0.16 mm. Distance between adjacent zooecial tubes averages 0.10 mm and in most specimens includes a mesopore. In some specimens the mesopores are filled by calcareous deposits, in other specimens either filled or open mesopore tubes occur locally. Zooecia in the mature zone have rounded to subrounded circular to oval cross-sections. In sections that cut along the base of the mature zone, zooecia have increased diameters and have polygonal rather than oval cross-sections. Diaphragms vary from rare to common in in the immature zone. There is an average of three diaphragms per mm in the mature zooecia. Zooecial diaphragms are most typically planar and have a granular appearance. Some specimens have diaphragms in the mature zone that are thickened by deposits underlain by a dark granular line that represents the original diaphragm. The dark line is missing in some thickened diaphragms. Some zooecia have a mature part occupied by continuous calcareous deposits.

Mesopores originate at the base of the mature zone. They are abundant and average 70 per 2-mm square. Mesopore tube diameters average 0.14 mm by 0.09 mm near the base of the mature zone. Mesopores are polygonal in cross-section, three- to five-sided, with flat to concave sides. Higher in the mature zone, walls common to mesopores and zooecia are convex toward the mesopores, resulting in concave sides for the mesopores. Entire mesopores in some areas are filled with dense calcareous deposits, but in most areas deposits are either lacking or are restricted to distal portions of mesopores. Where obscuring deposits are not present, mesopores contain closely spaced diaphragms. Mesopore diaphragms average eight per mm. A few of the mesopores swell slightly between diaphragms, resulting in a vaguely beaded aspect.

Original structure of the walls has been obscured. Mature walls are only slightly thickened.

Acanthopores are present but can be seen only after critical examination and only in a few sections. Within most zoaria, infilled materials and alteration have totally obscured acanthopore structure. In sections where acanthopores can be observed, they average 0.06 mm in diameter. There were no areas suitable for making counts of acanthopores per 1-mm square. Acanthopores show up best where thin-sections pass through matrix just above the zoarial surface.

Discussion. — Depending on depth of sections and local nature of zoaria, tangential sections may have four different appearances: 1) polygonal zooecia surrounded by slightly smaller polygonal mesopores; 2) oval zooecia surrounded by polygonal mesopores with concave sides; 3) oval zooecia surrounded by calcareous deposits, and 4) sheetlike calcareous deposits with zooecia filled in and obscured. Local irregularities in cross-sectional shape of zooecial tubes, most typically caused by acanthopore inflections, results in a superficial appearance of lunaria. However, the typical structure of inset lunaria is missing and the structures are isolated, variable, and asymmetrical.

Nicholsonella acanthobscura is most similar to *N. irregularis* Loeblich (1942, p. 428, pl. 64, figs. 5-7) but may be distinguished by the presence or greater abundance of diaphragms in the immature zone, lack of beaded appearance in proximal portions of mesopores, and by more abundant mesopores. *N. acanthobscura*

Character	Range	Mode	Mean	Standard Deviation	Number of Measurements	Number of Specimens Measured
MxTD	0.15-0.31	0.20	0.210	0.031	197	22
MnTD	0.10-0.25	0.15	0.163	0.027	197	22
DBZT	0.01-0.23	0.15	0.105	0.044	187	20
MxMTD	0.05-0.26	0.15	0.139	0.046	116	12
MnMTD	0.03-0.17	0.10	0.087	0.033	116	12
M/2-mmsq	58-91	64	69.5	9.9	10	6
AD	0.03-0.14	0.05	0.065	0.026	40	4
D/mm	0-5	2	2.6	1.0	142	16
D/mmM	5-10	8	7.5	1.3	81	12

Table 44. Quantitative data on characters of *Nicholsonella acanthobscura,* n. sp. Type suite from the lower Chickamauga Group.

differs from *N. parafrondifera* McKinney in having smaller zooecia and slightly larger and less numerous acanthopores.

The trivial name, *acanthobscura,* refers to the generally obscure nature of acanthopores.

Material. — Twenty-five thin-sectioned zoarial fragments from stratigraphic sections I, II, IV, V, XII, XV, XVI, XVII.

Holotype. — USNM 167824.

Paratypes. — USNM 167825-167828, GSATC 207, UNC 4168.

Measurements. — Table 44.

Nicholsonella parafrondifera McKinney, n. sp. Pl. 66, figs. 1-7

1921. *Nicholsonella frondifera* (part) Coryell, Indiana Acad. Sci., Proc., vol. 29, p. 290 (IU 9244-4 and IU 9244-5, not pl. 7, figs. 6, 7).

Diagnosis. — Zoaria laminar to ramose; mature zooecia are subcircular to suboval; zooecial tube diameters average 0.23 mm by 0.20 mm, diaphragms average three per mm in mature zone; mesopores abundant, small; acanthopores average 30 per 1-mm square, locally inflect zooecial tubes.

Description. — The zoaria are free and encrusting, laminar to ramose. The greatest diameter of laminar zoaria is 25 mm and the greatest thickness is 5 mm. Ramose forms have branches up to 5 mm in diameter.

The zooecia are subcircular to oval in cross-section and in some zoaria there are areas in which zooecial tubes are strongly indented by adjacent acanthopores. Zooecial tube diameters average 0.23 mm by 0.20 mm. The distance between adjacent zooecial tubes averages

0.11 mm and typically includes a mesopore. Zooecial diaphragms are planar or slightly convex and are either at right angles or are slightly inclined to the zooecial axis.

Mature walls are thin or slightly thickened, 0.03 mm or less. Original structure has been destroyed by recrystallization. Some walls retain a dark median line.

Mesopores occupy spaces between zooecia. They are polygonal, typically three- or four-sided. In laminar forms, mesopores originate near the base of the zoarium. Slight constrictions occur at diaphragms causing the mesopores to appear beaded. An average of eight mesopore diaphragms occur in 1 mm. Mesopore tube diameters average 0.15 mm by 0.09 mm. Although mesopores are abundant, wall alteration and infilling obscures so many boundaries that an accurate count per 2-mm square was not possible.

Acanthopores are numerous; they average 30 per 1-mm square and 0.06 mm in diameter. Acanthopores are located along zooecial peripheries, inflect mesopores, and, where mesopores are small or absent, they cause inflections into adjacent zooecial tubes.

Discussion. — *Nicholsonella parafrondifera* is distinguished from the holotype of *N. frondifera* Coryell (1921, p. 290, pl. 7, figs. 6, 7) by larger zooecia and larger and slightly less numerous acanthopores. Examination of Coryell's type specimens indicates that two paratypes of *N. frondifera* (IU 9244-4 and 9244-5) differ distinctly from the holotype (USNM 54043) and another paratype (IU 9244-3), and are indistinguishable from the lower Chickamauga Group specimens that form the type suite of *N. parafrondifera*. Therefore specimens IU 9244-4 and 9244-5 are assigned to the here named new species *N. parafrondifera*. Measurements made on IU 9244-4 and 9244-5 are given in Tables 49 and 50. The holotype USNM 54043 and paratype IU 9244-3 of *N. frondifera* Coryell, 1921, form a junior synonym of *N. pulchra* Ulrich, 1893.

The trivial name, *parafrondifera*, refers to the similarity of the new species to the species intended by Coryell (1921, p. 290) in his description of *N. frondifera*, which he described as, ". . . similar to *Nicholsonella pulchra* with the exception that diaphragms are more numerous in the mesopores of the mature region and the longitudinal tubuli are larger, fewer, and more clearly defined in *N. frondifera*."

Material. — Six thin-sectioned zoarial fragments from stratigraphic sections I, II, VI.

Holotype. — USNM 167829.

Paratypes. — USNM 167830, 167831, GSATC 208, UNC 4169.

Measurements. — Table 45 (see also Tables 49 and 50).

Character	Range	Mode	Mean	Standard Deviation	Number of Measurements	Number of Specimens Measured
MxTD	0.16-0.30	0.23	0.234	0.029	60	6
MnTD	0.12-0.26	0.18	0.195	0.031	60	6
DBZT	0.02-0.20	0.10	0.108	0.043	60	6
MxMTD	0.05-0.28	0.14	0.154	0.056	28	3
MnMTD	0.03-0.19	—	0.090	0.038	28	3
AD	0.02-0.10	0.06	0.057	0.014	60	6
A/1-mmsq	12-52	—	30.3	12.3	26	5
D/mm	1-4	3	2.9	0.9	25	3
M/mmM	5-11	7	7.8	1.9	8	2

Table 45. Quantitative data on characters of *Nicholsonella parafrondifera,* n. sp. Type suite from the lower Chickamauga Group.

Nicholsonella pulchra Ulrich, 1893 Pl. 67, figs. 1-4

1893. *Nicholsonella pulchra* Ulrich, extract from Minnesota Geol. and Nat. Hist. Sur., Final Rept., Paleont., vol. 3, p. 314, pl. 21, figs. 8-12.
1921. *Nicholsonella frondifera* (part) Coryell, Indiana Acad. Sci., Proc., vol. 29, p. 290, pl. 7, figs. 6,7 (not paratypes IU 9244-4 and 9244-5).
1937. *Nicholsonella pulchra* Ulrich, Shrock and Raasch, American Midland Nat., vol. 18, pp. 543, 544, pl. 3, fig. 8.

Diagnosis. — Zoaria ramose to encrusting; most zooecia are oval in cross-section, zooecial tube diameters average 0.19 mm by 0.15 mm, with diaphragms abundant; mesopores abundant, small, beaded, with eight diaphragms per mm, some with dense deposits; acanthopores average 38 per 1-mm square.

Description. —The zoaria are ramose to encrusting. Maximum branch diameter is 8.5 mm.

In ramose forms, zooecia bend out gently from the axial region to a slightly greater curvature at the base of the mature zone, beyond which zooecia tend to straighten out. Mature zooecial cross-sections are subrounded to rounded oval. Zooecial tube diameters average 0.19 mm by 0.15 mm. The distance between adjacent zooecial tubes averages 0.12 mm. Diaphragms are present in both mature and submature zones, but are most abundant in the mature zone, where they average three per mm. Most diaphragms are planar

but some are slightly concave, slightly convex or tilted with respect to the zooecial axis. Some zooecial tubes are slightly indented by adjacent acanthopores.

The walls are thin to slightly thickened, not over 0.02 mm thick. Original wall, diaphragm, and acanthopore structure has been destroyed by recrystallization.

Abundant mesopores have polygonal cross-sections, with concave sides where they are adjacent to zooecia, and average tube diameters of 0.11 mm by 0.07 mm. Mesopores originate in the outer immature zone and along the base of the mature zone. Proximal portions of mesopores are beaded, resulting from constrictions in mesopores at diaphragms. Distally the constrictions become less obvious and in many places disappear. Planar mesopore diaphragms average eight per mm. Mesopores in one specimen are obscured locally by infilled calcareous deposits. Alteration is too advanced to allow counts of mesopores per 2-mm square.

Acanthopores are abundant, averaging 38 per 1-mm square. Average diameter of acanthopores is 0.05 mm. Most zooecial and zooecial-mesopore corners are occupied by an acanthopore.

Discussion. — Coryell (1921, p. 290) distinguished the new species *Nicholsonella frondifera* from *N. pulchra* on the basis of growth form, more closely spaced diaphragms in mesopores, and ". . . larger, fewer, and more clearly defined . . ." acanthopores than in *N. pulchra*. However, growth form is environmentally controlled in *Nicholsonella* and numerous other trepostome genera, and small variations in diaphragm spacing may be due to rapidity of growth. A recent comparison of Ulrich's tangential section of *N. pulchra* (1893, pl. 21, fig. 10) and Coryell's tangential section of the holotype of *N. frondifera* (1921, pl. 7, fig. 7) indicates similarity in all characters, including equal size and abundance of acanthopores. Moreover, types of both species were collected from the Pierce Limestone of Murfreesboro, Tennessee. *Nicholsonella frondifera* is here considered a junior synonym of *N. pulchra*.

Measurements made on the four sectioned specimens which form the type suite of "*Nicholsonella frondifera*" Coryell indicate two distinct pairs within the suite (Tables 47-50). One pair contains the holotype (USNM 54043) and one paratype (IU 9244-3) (here considered to form a junior synonym of *N. pulchra* Ulrich),

Character	Range	Mode	Mean	Standard Deviation	Number of Measurements	Number of Specimens Measured
MxTD	0.15-0.24	0.18	0.188	0.023	30	3
MnTD	0.13-0.19	0.15	0.148	0.013	30	3
DBZT	0.06-0.18	0.12	0.119	0.030	30	3
MxMTD	0.05-0.20	0.09	0.113	0.052	10	1
MnMTD	0.04-0.14	0.04	0.074	0.039	10	1
AD	0.03-0.08	0.05	0.048	0.013	20	2
A/1-mmsq	32-42	—	37.7	4.8	3	2
D/mm	2-4	3	3.2	0.6	10	1
D/mmM	6-10	8	7.8	1.3	10	1

Table 46. Quantitative data on characters of *Nicholsonella pulchra* Ulrich from the lower Chickamauga Group.

Character	Range	Mode	Mean	Standard Deviation	Number of Measurements	Number of Specimens Measured
MxTD	0.16-0.19	0.19	0.177	0.011	10	1
MnTD	0.13-0.17	0.15	0.146	0.010	10	1
DBZT	0.08-0.19	0.12	0.127	0.032	10	1
MxMTD	0.10-0.22	0.11	0.145	0.040	10	1
MnMTD	0.06-0.14	0.08	0.092	0.024	10	1
AD	0.03-0.05	0.05	0.040	0.006	10	1
A/1-mmsq	47-76	69	64.2	9.3	10	1
D/mm	7-10	7	8.2	1.3	6	1

Table 47. Quantitative data on the holotype of Coryell's *"Nicholsonella frondifera"* (= *N. pulchra* Ulrich). USNM 54043.

Character	Range	Mode	Mean	Standard Deviation	Number of Measurements	Number of Specimens Measured
MxTD	0.18-0.23	0.20	0.204	0.013	10	1
MnTD	0.15-0.19	0.15	0.161	0.014	10	1
DBZT	0.07-0.16	0.15	0.124	0.033	10	1
AD	0.05-0.06	0.05	0.051	0.002	10	1
A/1-mmsq	31-47	31 47	39.0	6.0	10	1
D/mm	3-4	3	3.4	0.5	10	1
D/mmM	7-9	7	7.8	0.7	5	1

Table 48. Quantitative data on characters of a paratype of Coryell's *"Nicholsonella frondifera"*. Paratype, IU 9244-3. (= *N. pulchra* Ulrich)

Character	Range	Mode	Mean	Standard Deviation	Number of Measurements	Number of Specimens Measured
MxTD	0.23-0.29	0.25	0.259	0.017	10	1
MnTD	0.20-0.25	0.24	0.233	0.016	10	1
MxTDm	0.29-0.32	0.29	0.301	0.010	6	1
MnTDm	0.23-0.29	0.27	0.266	0.018	6	1
DBZT	0.04-0.13	0.09	0.082	0.027	10	1
MxMTD	0.09-0.14	0.13	0.122	0.019	10	1
MnMTD	0.06-0.10	0.10	0.084	0.015	10	1
M/2-mmsq	44-50	—	47.0	3.0	2	1
AD	0.03-0.07	0.05	0.048	0.012	10	1
A/1-mmsq	17-25	—	20.9	3.1	10	1

Table 49. Quantitative data on characters of a paratype of Coryell's *"Nicholsonella frondifera"*. Paratype, IU 9244-4. (= *N. parafrondifera,* n. sp.)

Character	Range	Mode	Mean	Standard Deviation	Number of Measurements	Number of Specimens Measured
MxTD	0.25-0.29	0.25	0.266	0.013	10	1
MnTD	0.19-0.23	0.23	0.220	0.012	10	1
DBZT	0.06-0.17	0.10	0.107	0.032	10	1
MxMTD	0.10-0.21	0.16	0.154	0.036	6	1
MnMTD	0.07-0.15	—	0.106	0.027	6	1
AD	0.05-0.08	0.07	0.069	0.008	10	1
A/1-mmsq	12-20	15	15.6	2.2	10	1
D/mm	3-5	5	4.3	0.7	6	1
D/mmM	7-8	8	7.7	0.5	7	1

Table 50. Quantitative data on characters of a paratype of Coryell's *"Nicholsonella frondifera"*. Paratype, IU 9244-5 (= *N. parafrondifera,* n. sp.)

and the other group contains paratypes IU 9244-4 and 9244-5 (here assigned to *N. parafrondifera* McKinney). Before examination of the type specimens, separation of specimens of *Nicholsonella* from the lower Chickamauga Group into apparent species groups yielded, among others, one group that later proved to be *N. pulchra* and another group that forms the type suite of *N. parafrondifera.*

Material. — Three thin-sectioned zoarial fragments from stratigraphic sections II and XVI.

Hypotype. — USNM 167832.

Measurements. — Table 46 (see also Tables 47 and 48).

Nicholsonella inflecta McKinney, n. sp. Pl. 67, figs. 5-8; Pl. 68, figs. 1, 2

Diagnosis. — Zoaria ramose to laminar; zooecia polygonal in cross-section, tube diameters average 0.25 mm by 0.20 mm, di-

aphragms common; mesopores average 22 per 2-mm square, with closely spaced diaphragms; zooecial walls about 0.04 mm thick; acanthopores average 21 per 1-mm square, producing numerous inflections into zooecial walls.

Description. — Zoaria are ramose to free laminate. Greatest branch diameter in ramose fragments is 7 mm.

Zooecia are angular to subrounded polygonal in cross-section. In ramose forms they bend smoothly out from the axial region to a slightly more pronounced bend at the base of the mature zone, beyond which curvature is diminished. In some zoaria, proximal portions of zooecia are elongate moniliform. Zooecial tube diameters average 0.25 mm by 0.20 mm. Distance between adjacent zooecial tubes (most commonly including only wall deposits) averages 0.06 mm. Diaphragms are common but widely spaced in the immature region; in the mature region zooecial diaphragms average three per mm. Diaphragms are planar, slightly concave or slightly convex, and are oriented at a right angle or are slightly tilted with respect to the zooecial axis.

Walls, diaphragms, and acanthopores are altered and now contain fine-grained calcite. However, a dark median line can be seen locally in walls and diaphragms in longitudinal section. Original character of altered walls is obscured in many places but in other places a dark median line and remnants of sharply defined zooecial tube boundaries indicate an original integrate character of zooecial walls. Modal thickness of walls is 0.04 mm.

Mesopores average 22 per 2-mm square in tangential sections. They are polygonal, three- or most frequently four-sided. Mesopore tube diameters average 0.14 mm by 0.08 mm. Origin of mesopores is in the outer immature region, where they begin as a series of elongate, thin beadlike structures. Where they enter the mature zone the beadlike nature becomes less pronounced and in most cases disappears completely. Mesopore diaphragms are planar and average eight per mm.

Acanthopores originate near the base of the mature zone. They average 0.05 mm in diameter, with an average of 21 per 1-mm square. In most places they cause a conspicuous inflection of adjacent zooecial tubes.

Discussion. — *Nicholsonella inflecta* most closely resembles *N.*

Character	Range	Mode	Mean	Standard Deviation	Number of Measurements	Number of Specimens Measured
MxTD	0.20-0.30	0.24	0.248	0.029	60	6
MnTD	0.15-0.26	0.20	0.204	0.025	60	6
DBZT	0.02-0.15	0.04	0.060	0.027	60	6
MxMTD	0.03-0.25	0.10	0.141	0.053	40	4
MnMTD	0.03-0.15	0.07	0.083	0.031	40	4
M/2-mmsq	12-48	—	22.5	10.2	13	4
AD	0.03-0.08	0.05	0.052	0.012	60	6
A/1-mmsq	11-30	27	21.1	5.6	24	5
D/mm	2-5	3	3.0	0.8	27	3
D/mmM	6-12	6	8.1	2.0	12	3

Table 51. Quantitative data on characters of *Nicholsonella inflecta,* n. sp. Type suite from the lower Chickamauga Group.

irregularis Loeblich (1942, p. 428, pl. 64, figs. 5-7) but differs primarily in having slightly larger zooecia, more abundant diaphragms in the axial region, and the mesopores are not filled distally by calcareous deposits and are less strongly beaded.

The trivial name, *inflecta,* is given because of the numerous moderate inflections made into zooecial tubes by acanthopores.

Material. — Six thin-sectioned specimens from stratigraphic sections II and IV.

Holotype. — USNM 167833.

Paratypes. — USNM 167834, 167835, GSATC 209, UNC 4171.

Measurements. — Table 51.

Nicholsonella aff. **N. mariae** Astrova, 1965 Pl. 68, figs. 3-5

1965. *Nicholsonella mariae* Astrova, Akad. Nauk SSSR, Paleont. Inst. Trudy, vol. 106, p. 214, pl. 44, fig. 2a-d.

Description. — Zoaria are ramose, with branch diameters up to at least 6 mm.

Zooecia are irregularly polygonal in cross-section and have four to six sides. They curve smoothly out from the axial region with no obvious increase in curvature at the base of the mature zone. Zooecial tube diameters average 0.27 mm by 0.21 mm. In most places, zooecia are separated only by walls, with mesopores confined to zooecial corners. Diaphragms in zooecia are planar to slightly concave and are oriented at right angles or are slightly tilted with respect to the zooecial axis. Diaphragms average three per mm.

Recrystallization has obscured the original structure of walls and diaphragms, which now contain fine-grained calcite. Many diaphragms retain a thin, clear median line in longitudinal section. Walls average 0.03 mm in thickness.

Mesopores originate in the outer immature zone. They have abundant diaphragms and are somewhat constricted at the diaphragms, resulting in a vaguely moniliform appearance. There is an average of 17 mesopores per 2-mm square. Mesopore tube diameters average 0.11 mm by 0.07 mm.

Acanthopores are sparse, and in at least some areas have been obscured by alteration. Where observable, acanthopores average 0.05 mm in diameter and three per 1-mm square.

Discussion. — Two specimens from the lower Chickamauga Group have affinities with *Nicholsonella mariae* Astrova, 1965 (p. 214, pl. 44, fig. 2a-d). They resemble *N. mariae* in zooecial size, curvature of zooecia, and in abundance and shape of diaphragms. The main differnece is that acanthopores in the holotype and paratype of *N. mariae* are smaller and much more abundant.

Material. — Two thin-sectioned zoarial fragments from stratigraphic section II.

Hypotype. — USNM 167836.

Measurements. — Table 52.

Character	Range	Mode	Mean	Standard Deviation	Number of Measurements	Number of Specimens Measured
MxTD	0.24-0.34	0.28	0.273	0.024	20	2
MnTD	0.17-0.25	0.21	0.208	0.023	20	2
ZWT	0.01-0.08	0.03	0.030	0.016	20	2
MxMTD	0.05-0.18	0.08	0.113	0.043	18	2
MnMTD	0.02-0.11	0.08	0.068	0.028	18	2
M/2-mmsq	16-19	16	17.2	1.3	5	1
AD	0.03-0.06	0.05	0.046	0.011	10	1
D/mm	1-3	3	2.7	0.7	10	1

Table 52. Quantitative data on characters of *Nicholsonella* aff. *N. mariae* Astrova from the lower Chickamauga Group.

?Nicholsonella sp. Pl. 68, figs. 6-8

Description. — Zoaria are massive to free laminar. Greatest diameter of massive zoaria is 24 mm. Greatest thickness of the laminar zoarium is 6 mm.

Zooecia are subrounded to angular in cross-section. Most polygonal zooecia are six-sided. Zooecial tube diameters average 0.26 mm by 0.20 mm. Distance between zooecial tubes averages 0.12 mm and is in most places occupied by a mesopore. Most zooecial diaphragms are planar and horizontal. A few diaphragms are steeply inclined, slightly concave, or slightly convex. There is an average of three diaphragms per mm.

Walls are about 0.01 mm thick. Original structure has been destroyed by recrystallization.

Mesopores are polygonal, with planar to slightly concave sides as seen in tangential sections. They vary from three- to five-sided, with average tube diameters of 0.16 mm by 0.10 mm. Essentially planar diaphragms average four per mm. Mesopores are slightly to severely constricted at diaphragms, resulting in a moderate to pronounced beaded appearance. There is an average of 59 mesopores per 2-mm square.

Acanthopores are evident in only one specimen (USNM 167838), which is questionably assigned to this group. Acanthopore diameters average 0.04 mm, and there is an average of 20 per 1-mm square.

Discussion. — These specimens are questionably assigned to *Nicholsonella* because two of the specimens apparently lack acanthopores, and the mesopores lack the obscuring calcareous deposits thought to be a characteristic of *Nicholsonella*. The criteria that indicate the specimens may belong to *Nicholsonella* are the abundant, slightly beaded mesopores, and the altered walls.

Character	Range	Mode	Mean	Standard Deviation	Number of Measurements	Number of Specimens Measured
MxTD	0.20-0.32	0.25	0.260	0.026	30	3
MnTD	0.17-0.25	0.23	0.202	0.029	30	3
DBZT	001-0.28	—	0.117	0.065	30	3
MxMTD	0.06-0.24	0.18	0.157	0.051	30	3
MnMTD	0.03-0.19	0.10	0.099	0.039	30	3
M/2-mmsq	39-82	—	59.2	14.3	20	3
AD	0.03-0.05	0.05	0.040	0.008	10	1
A/1-mmsq	16-27	19	20.3	3.6	10	1
D/mm	1-5	4	3.0	1.0	30	3
D/mmM	2-8	5	4.4	1.2	29	3

Table 53. Quantitative data on characters of ?*Nicholsonella* sp. from the lower Chickamauga Group.

Material. — Three thin-sectioned zoarial fragments from stratigraphic sections I and IV

Hypotypes. — USNM 167837, 167838.

Measurements. — Table 53.

REFERENCES CITED

Allen, A. T., and Lester, J. G.

1954. *Contributions to the paleontology of northwest Georgia.* Georgia Geol. Sur., Bull. 62, vi + 166 pp., 42 pls.

1957. *Zonation of the Middle and Upper Ordovician strata in northwestern Georgia.* Georgia Geol. Sur., Bull. 66, vii + 110 pp., 9 pls., 12 text-figs.

Anstey, R. L., and Perry, T. G.

1968. *Biometric procedures in taxonomic studies of Paleozoic Bryozoa.* Atti Soc. It. Sci. Nat., vol. 108, pp. 241-244.

1969. *Redescription of cotypes of Peronopora vera Ulrich, a Cincinnatian (Late Ordovician) ectoproct species.* Jour. Paleont., vol. 43, No. 2, pp. 245-251, pls. 31, 32, 1 text-fig.

1970. *Biometric procedures in taxonomic studies of Paleozoic bryozoans.* Jour. Paleont., vol. 44, No. 2, pp. 383-398, 3 text-figs.

Astrova, G. G.

1948. *Nizhnesiluriiskie Trepostomata Pai-Khoya.* Moskovsky Gosud. Ped. Inst., Uchenye Zapiski, vol. 52, Kafedra Géol., no. 3, pp. 3-35, 4 pls.

1964. *O novom otryade Paleozoyskikh mshanok.* Paleont. Zhurnal, No. 2, pp. 22-31, 3 text-figs.

1965. *Morfologiya, istoriya razvitiya i sistema ordovikskikh i siluriiskikh mshanok.* Akad. Nauk SSSR Paleont. Inst. Trudy, vol. 106, 432 pp., 84 pls., 52 text-figs.

Astrova, G. G., et al.

1960. *Tip Bryozoa,* in Sarycheva, T. G. (ed.), *Mshanki, brakhiopody,* in Orlov, Yu. A. (ed.), *Osnovy paleontology.* Akad. Nauk SSSR, pp. 13-112, 7 pls., 208 text-figs.

Bassler, R. S.

1906. *A study of the James types of Ordovician and Silurian Bryozoa.* U. S. Nat. Mus., Proc., vol. 30, pp. 1-66, pls. 1-7.

1911. *The early Paleozoic Bryozoa of the Baltic provinces.* U. S. Nat. Mus., Bull. 77, xxi + 382 pp., 13 pls., 226 text-figs.

1932. *The stratigraphy of the central basin of Tennessee.* Tennessee Div. Geol., Bull. 38, x + 268 pp., frontispiece + 49 pls., 4 text-figs.

1953. *Bryozoa* in Moore, R. C. (ed.), *Treatise of invertebrate paleontology,* Pt. G. Geol. Soc. America and Kansas Univ. Press, 253 pp., 175 text-figs.

Bekker, H.

1921. *The Kuckers stage of the Ordovician rocks of N. E. Esthonia.* Acta et Commen. Univ. Dorpatensis, vol. A2, 92 pp., 12 pls.

Boardman, R. S.

1959. *A revision of the Silurian bryozoan genus Trematopora.* Smithsonian Misc. Coll., vol. 139, No. 6, 14 pp., 2 pls.

1960a. *Trepostomatous Bryozoa of the Hamilton Group of New York State.* U. S. Geol. Sur., Prof. Paper 340, pp. i-iii, 1-87, 22 pls., 27 text-figs.

1960b. *A revision of the Ordovician bryozoan genera Batostoma, Anaphragma, and Amplexopora.* Smithsonian Misc. Coll., vol. 140, No. 5, 28 pp., 7 pls.

Boardman, R. S., and Cheetham, A. H.

1969a. *Skeletal growth, intracolony variation, and evolution in Bryozoa: a review.* Jour. Paleont., vol. 43, No. 2, pp. 205-233, pls. 27-30, 8 text-figs.

1969b. *Intracolony variability, a determining factor in the genus concept in Bryozoa.* (Abstract) Jour. Paleont., vol. 43, No. 4, p. 882.

Boardman, R. S., and Utgaard, John

1964. *Modifications of study methods for Paleozoic Bryozoa.* Jour. Paleont., vol. 38, No. 4, pp. 768-770.

1966. *A revision of the Ordovician bryozoan genera Monticulipora, Peronopora, Heterotrypa, and Dekayia.* Jour. Paleont., vol. 40, No. 5, pp. 1082-1108, pls. 133-142, 9 text-figs.

Bork, K. B., and Perry, T. G.

1967, 1968a, 1968b. *Bryozoa (Ectoprocta) of Champlainian age (Middle Ordovician) from northwestern Illinois and adjacent parts of Iowa and Wisconsin.* 1967. *Part I. Amplexopora, Monotrypella, Hallopora, and Batostoma.* Jour. Paleont., vol. 41, No. 6, 1365-1392, pls. 173-177. 1968a. *Part II. Bythotrypa, Diplotrypa, Hemiphragma, Heterotrypa, Stigmatella, Eridotrypa, and Nicholsonella.* Jour. Paleont., vol. 42, No. 2, pp. 337-355, pls. 44-48. 1968b. *Part III. Homotrypa, Orbignyella, Prasopora, Monticulipora, and Cyphotrypa.* Jour. Paleont., vol. 42, No. 4, pp. 1042-1065, pls. 133-138.

Brown, G. D.

1965. *Trepostomatous Bryozoa from the Logana and Jessamine Limestones (Middle Ordovician) of the Kentucky Bluegrass region.* Jour. Paleont., vol. 39, No. 5, pp. 974-1006, pls. 111-118, 2 text-figs.

Butts, Charles

1926. *The Paleozoic rocks* in Adams, G. I., *et al., Geology of Alabama.* Alabama Geol. Sur., Special Rept. 14, pp. 41-230, pls. 3-76, text-figs. 2-4.

1940, 1941. *Geology of the Appalachian Valley in Virginia.* Virginia. Geol. Sur., Bull. 52, pt. 1 (1940), xxxii + 568 pp., 63 pls., 10 text-figs.; pt. 2 (1941), iv + 271 pp., pls. 64-135.

Cooper, G. A.

1956. *Chazyan and related brachiopods.* Smithsonian Misc. Coll., vol. 127, pt. 1, xvi + 1024 pp., 3 text-figs.

Cheetham, A. H.

1968. *Morphology and systematics of the bryozoan genus Metrarabdotos.* Smithsonian Misc. Coll., vol. 153, No. 1, 121 pp., 18 pls., 24 text-figs.

Coryell, H. N.

1921. *Bryozoan faunas of the Stones River Group of central Tennessee.* Indiana Acad. Sci., Proc., vol. 29, pp. 261-339, 14 pls., 3 text-figs.

Cuffey, R. J.

1967. *Bryozoan Tabulipora carbonaria in Wredford megacyclothem (Lower Permian) of Kansas.* Kansas Univ. Paleont. Contr., Bryozoa, art. 1, 96 pp., 9 pls., 33 text-figs.

Cumings, E. R.

1902. *A revision of the bryozoan genera Dekayia, Dekayella, and Heterotrypa of the Cincinnati Group.* Amer. Geologist, vol. 29, pp. 197-217, pls. 9-12.

Cumings, E. R., and Galloway, J. J.

1913. *The stratigraphy and paleontology of the Tanner's Creek section of the Cincinnati series of Indiana.* Indiana Dept. Geol. Nat. Res., Ann. Rept. 37, pp. 353-478, 20 pls., 18 text-figs.

Dunaeva, N. N.

1964a. *K faune nizhnekamennougol'nykh trepostomat Donetzkogo basseina* in Aizenverg, D. E., *et al., Materialy k faune verkhnego paleozoya Donbassa.* Akad. Nauk Ukrainskoi SSR Inst. Geol. Trudy, ser. strat. i paleont., No. 48, pp. 104-143, 9 pls., 20 text-figs.

1964b. *Novye mshanki otryada Trepostomata iz nizhnego karbona Donetzkogo basseina.* Paleont. Zhurnal, No. 2, pp. 39-44, pls. 4, 5, 4 text-figs.

Dunaeva, N. N., and Morozova, I. P.

1967. *Osobennosti razvitiya i sistematicheskoe nolozhenie nekotorykh pozdnepaleozoiskikh trepostomat.* Paleont. Zhurnal, No. 4, pp. 86-94, pl. 5, text-fig. 1.

Fox, P. P., and Grant, L. F.

1944. *Ordovician bentonites in Tennessee and adjacent states.* Jour. Geol., vol. 52, pp. 319-332, 5 text-figs.

Fritz, M. A.

1957. *Bryozoa (mainly Trepostomata) from the Ottawa Formation (Middle Ordovician) of the Ottawa-St. Lawrence lowland.* Canada Geol. Sur., Bull. 42, v + 75 pp., 30 pls.

1966. *Diplotrypa schucherti, a new bryozoan species from the Long Point Formation (Ordovician), western Newfoundland.* Jour. Paleont., vol. 40, No. 6, pp. 1335-1337, pls. 165, 166.

Horowitz, A. S.

1968. *The ectoproct (bryozoan) genus Actinotrypa Ulrich.* Jour. Paleont., vol. 42, No. 2, pp. 356-373, pls. 49-52, 6 text-figs.

James, U. P.

1884. *Descriptions of four new species of fossils from the Cincinnati Group.* Jour. Cincinnati Soc. Nat. Hist., vol. 7, pp. 137-139, pl. 7.

Kiepura, Maria

1962. *Bryozoa from the Ordovician erratic boulders of Poland.* Acta Paleont. Polonica, vol. 7, pp. 347-428, 11 pls. 17 text-figs.

Kopaevich, G. V.

1968. *Rod Eridotrypa i ego istoricheskoe razvitie.* Paleont. Zhurnal, No. 1, pp. 18-26, pl. 4, 3 text-figs.

Loeblich, A. R.

1942. *Bryozoa from the Ordovician Bromide Formation, Oklahoma.* Jour. Paleont., vol. 16, No. 4, pp. 413-436, pls. 61-64.

Milici, R. C.

1969. *Middle Ordovician stratigraphy in central Sequatchie Valley, Tennessee.* Southeastern Geol., vol. 11, pp. 111-127, 4 text-figs.

Milici, R. C., and Smith, J. W.

1969. *Stratigraphy of the Chickamauga supergroup in its type area* in Milici, R. C., *et al., Precambrian-Paleozoic Appalachian problems.* Georgia Geol. Sur., Bull. 80, pp. 1-35, 4 text-figs.

Nicholson, H. A.

1881. *On the structure and affinities of the genus Monticulipora and its sub-genera.* William Blackwood and Sons, Edinburgh and London. xvi + 240 pp., 6 pls., 50 text-figs.

Nickles, J. M., and Bassler, R. S.

1900. *A synopsis of American fossil Bryozoa including bibliography and synonymy.* U. S. Geol. Sur., Bull. 173, pp. 1-663.

Owen, D. E.

1965. *Silurian Polyzoa from Benthall Edge, Shropshire.* British Mus. (Nat. Hist.), Bull., Geol., vol. 10, pp. 93-117, 6 pls.

Perry, T. G.

1962. *Specht's Ferry (Middle Ordovician) bryozoan fauna from Illinois, Wisconsin, and Iowa.* Illinois Geol. Sur., Circ. 326, 36 pp., 7 pls., 4 tex-figs.

Perry, T. G., and Horowitz, A. S.
1963. *Bryozoans from the Glen Dean Limestone (Middle Chester) of southern Indiana and Kentucky.* Indiana Geol. Sur., Bull. 26, pp. 1-51, 9 pls., 1 text-fig.

Rodgers, John
1953. *Geologic map of East Tennessee with explanatory text.* Tennessee Div. Geol., Bull. 58, pt. 2, vi + 168 pp., 7 text-figs.

Rogers, W. S.
1961a. *Middle Ordovician stratigraphy of the Red Mountain area, Alabama.* Southeastern Geol., vol. 2, pp. 217-249, 4 text-figs.
1961b. *The stratigraphic paleontology of the Chickamauga Group of the Red Mountain area, Birmingham.* Southeastern Geol., vol. 3, pp. 21-35, 5 text-figs.

Ross, J. P.
1961. *Ordovician, Silurian, and Devonian Bryozoa of Australia.* Australia Bur. Min. Res., Geol. Geophys., Bull. 50, 172 pp., 28 pls., 13 text-figs.
1963a. *New Ordovician species of Chazyan trepostome and cryptostome Bryozoa.* Jour. Paleont., vol. 37, No. 1, pp. 57-63, pls. 7, 8, 2 text-figs.
1963b. *Chazyan (Ordovician) leptotrypellid and atactotoechid Bryozoa.* Palaeont., vol. 5, pp. 727-739, pls. 105-108, 6 text-figs.
1963c. *The bryozoan trepostome Batostoma in Chazyan (Ordovician) strata.* Jour. Paleont., vol. 37, No. 4, pp. 857-866, pls. 106-109, 6 text-figs.
1967a. *Evolution of ectoproct genus Prasopora in Trentonian time (Middle Ordovician) in northern and central United States.* Jour. Paleont., vol. 41, No. 2, pp. 403-416, pls. 46-50, 3 text-figs.
1967b. *Champlainian Ectoprocta (Bryozoa), New York State.* Jour. Paleont., vol. 41, No. 3, pp. 632-648, pls. 67-74, 4 text-figs.
1969. *Champlanian (Ordovician) Ectoprocta (Bryozoa), New York State, Part II.* Jour. Paleont., vol. 43, No. 2, pp. 257-284, pls. 35-49, 1 text-fig.
1970. *Distribution, paleoecology and correlation of Champlainian Ectoprocta (Bryozoa), New York State, Part III.* Jour. Paleont., vol. 44, No. 2, pp. 346-382, pls. 67-74, 8 text-figs.

Safford, J. M.
1869. *Geology of Tennessee.* S. C. Mercer, Publisher, Nashville. xi + 550 pp., illus.

Sardeson, F. W.
1935a. *Behavior of the bryozoan Prasopora simulatrix.* Pan-Amer. Geologist, vol. 63, pp. 173-188, pl. 21.
1935b. *Behavior of Monticulipora.* Pan-Amer. Geologist, vol. 64, pp. 43-54, pl. 10.
1935c. *Behavior of Homotrypa of Decorah shales.* Pan-Amer. Geologist, vol. 64, pp. 343-354, pl. 16.
1936a. *Behavior of Dekayella of Decorah shales.* Pan-Amer. Geologist, vol. 65, pp. 19-30, pl. 1.
1936b. *Bryozoan Hallopora behavior.* Pan-Amer. Geologist, vol. 65, pp. 97-112, pl. 6.
1936c. *Early Batostoma behavior and Hemiphragma.* Pan-Amer. Geologist, vol. 66, pp. 95-111, pl. 10.
1936d. *Early bryozoans: Monotrypa to Eridotrypa.* Pan-Amer. Geologist, vol. 66, pp. 179-190, pl. 15.
1936e. *Fossil bryozoans: Leptotrypa to Fistulipora.* Pan-Amer. Geologist, vol. 66, pp. 251-263, pl. 23.
1936f. *Early bryozoans; Batostoma to Fenestella.* Pan-Amer. Geologist, vol. 66, pp. 329-346, pl. 30.

Shrock, R. R., and Raasch, G. O.
1937. *Paleontology of the disturbed Ordovician rocks near Kentland, Indiana.* American Midland Nat., vol. 18, pp. 532-607, 11 pls.

Simpson, G. G., Roe, Anne, and Lewontin, R. C.
1960. *Quantitative Zoology.* Harcourt, Brace and Co., New York. vii + 440 pp., 64 text-figs.

Sparling, D. R.
1964. *Prasopora in a core from the Northville area, Michigan.* Jour. Paleont., vol. 38, No. 6, pp. 1072-1981, pls. 161, 162, 3 text-figs.

Troedsson, G. T.
1929. *On the Middle and Upper Ordovician faunas of Northern Greenland. Part II.* Medd. on Grønland, vol. 72, 197 pp., 56 pls., 12 text-figs.

Twenhofel, W. H., et al.
1954. *Correlation of the Ordovician formations of North America.* Geol. Soc. Amer. Bull., vol. 65. pp. 247-298.

Ulrich, E. O.
1882. *American Paleozoic Bryozoa.* Jour. Cincinnati Soc. Nat. Hist., vol. 5, pp. 121-175, pls. 6-8.
1886. *Report on the Lower Silurian Bryozoa with preliminary descriptions of some of the new species.* Minnesota Geol. Nat. Hist. Sur., Ann. Rept. 14, pp. 57-103.
1890. *Paleozoic Bryozoa.* Illinois Geol. Sur., vol. 8, pp. 283-688, pls. 29-78.
1893. *The Bryozoa of the Lower Silurian in Minnesota.* Minnesota Geol. Nat. Hist. Sur., Final Rept., vol. 3, pp. 96-332, 28 pls., text-figs. 8-20.
1900. *Bryozoa* in Zittel, K. A., *Text-book of Palaeontology, vol. 1.* Macmillan and Co., London, and New York. pp. 257-291, text-figs. 411-488.

Ulrich, E. O., and Bassler, R. S.
1904. *A revision of the Paleozoic Bryozoa. Part II — On genera and species of Trepostomata.* Smithsonian Misc. Coll., vol. 47, pp. 15-55, pls. 6-14.

Utgaard, John, and Perry, T G.
1964. *Trepostomatous bryozoan fauna of the upper part of the Whitewater Formation (Cincinnatian) of eastern Indiana and western Ohio.* Indiana Geol. Sur., Bull. 33, pp. 1-111, 23 pls., 1 text-fig.

Vinassa de Regny, P. E.
1920. *Sulla classificazione dei treptostomide* Italiana Soc. Sci. Nat. Atti, vol. 59, pp. 212-231.

Wilson, A. E., and Mather, K. F.
1916. *Synopsis of the common fossils of the Kingston area.* Ontario Bur. Mines, Ann. Rept., vol. 25, pt. 3, pp. 45-66, 3 pls.

Wilson, C. W.
1949. *Pre-Chattanooga stratigraphy in central Tennessee.* Tennessee Div. Geol., Bull. 56, xviii + 407 pp., 28 pls., 89 text-figs.

PLATES

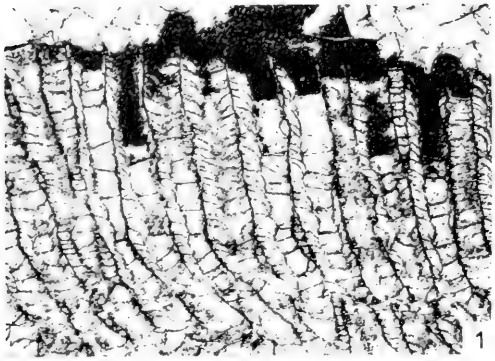
1

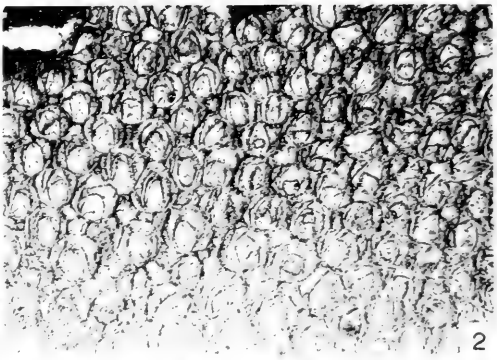
2

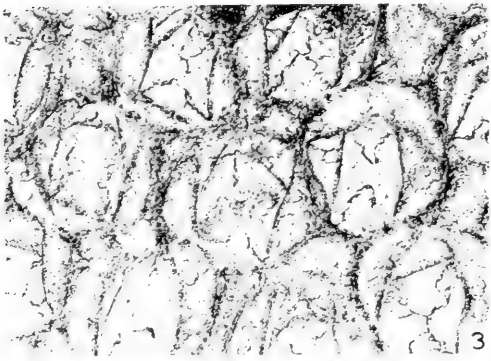
3

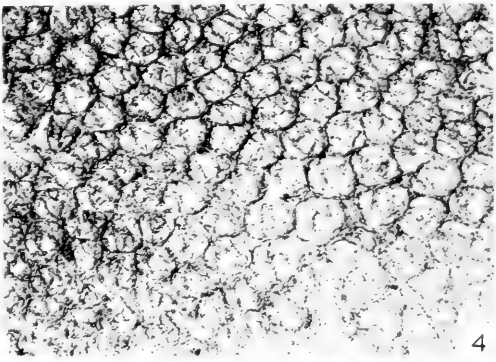
4

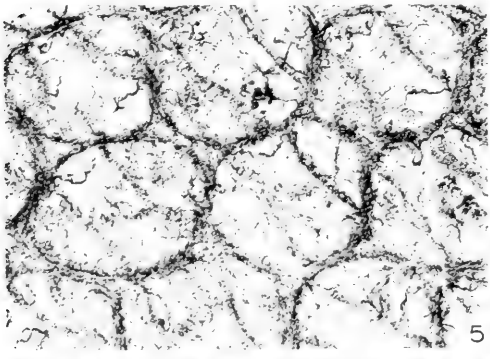
5

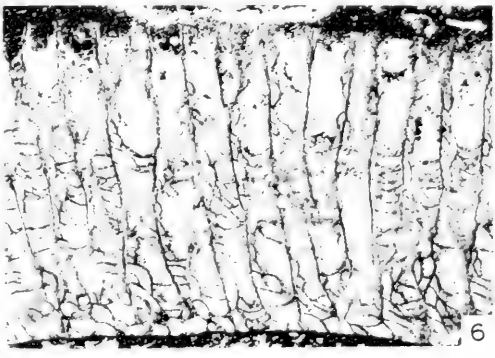
6

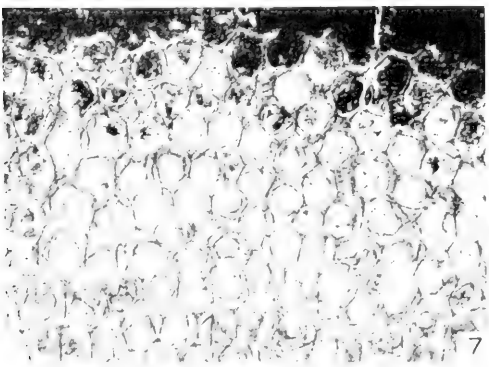
7

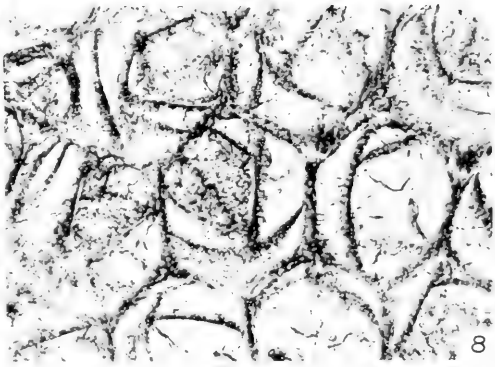
8

Explanation of Plate 46

Figure *Page*

1-5. **Monticulipora parallela** McKinney, n. sp. 222

1. Longitudinal section, × 20, which shows overlapped cystiphragms, irregularly spaced diaphragms, and mesopores. Holotype, USNM 167765. Locality II, 3.2-13.7 m. 2. Tangential section, × 20, which shows cystiphragms on three sides of subparallel-sided zooecial voids. Holotype, USNM 167765. Locality II, 3.2-13.7 m. 3. Tangenital section, × 80, which illustrates granular-laminar walls and cross-cutting relation between cystiphragms that overlap. Holotype, USNM 167765. Locality II, 3.2-13.7 m. 4. Tangential section × 20, which shows paired cystiphragms that form elongate parallel-sided zooecial voids. Paratype, USNM 167766. Locality XII, 14.5-22.1 m. 5. Tangential section, × 80, which shows detail from figure 4 above. Paratype, USNM 167766. Locality XII, 14.5-22.1 m.

6-8. **Prasopora discula** (Coryell) 225

6. Vertical section, × 20, of specimen with fewer than typical cystiphragms and irregularly spaced diaphragms. Hypotype, USNM 167767. Locality XVI, 15.7-18.9 m. 7. Tangential section, × 20, of same specimen as in figure 6 above, which exhibits local variation in density of cystiphragms. Hypotype, USNM 167767. Locality XVI, 15.7-18.9 m. 8. Tangential section, × 80, which illustrates acanthopores in zooecial corners and irregular zooecial voids due to variable density and placement of cystiphragms. Hypotype, USNM 167767. Locality XVI, 15.7-18.9 m.

Explanation of Plate 47

Figure *Page*

1-7. **Prasopora discula** (Coryell) 225

1. Vertical section, × 20, which shows strongly overlapped, narrow cystiphragms and irregularly spaced diaphragms. Hypotype, USNM 167768. Locality XVII, 0-4.0 m. 2. Vertical section, × 20, which shows cystiphragms that overlap and that increase in size towards base of the colony. Hypotype, USNM 167769. Locality II, 3.2-13.7 m. 3. Vertical section, × 80, which shows obscurely laminar walls with median dark line, cystiphragms continuous with wall deposits, and diaphragms that terminate against cystiphragms. Hypotype, USNM 167839. Locality XVII, 0-4.0 m. 4. Tangential section, × 20, which shows central to subcentral, oval zooecial voids and monticules of enlarged zooecia and mesopores in bottom center and top left of photograph. Hypotype, USNM 167769. Locality II, 3.2-13.7 m. 5. Tangential section, × 80, which illustrates central, oval zooecial voids caused by complete and nearly complete cystiphgrams. Hypotype, USNM 167769. Locality II, 3-2.13.7 m. 6. Tangential section × 20, which shows central, oval zooecial voids and monticule of mesopores and enlarged zooecia in bottom center of photograph. Hypotype, USNM 167768. Locality XVII, 0-4.0 m. 7. Tangential section, × 80, which exhibits central, oval zooecial voids caused by several incomplete cystiphragms. Hypotype, USNM 167768. Locality XVII, 0-4.0 m. As seen in figure 8 of Plate 46 and in figures 5 and 7 of this plate, the differences in aspect of tangential sections of *Prasopora discula* are due to the number and completeness of cystiphragms cut by the section.

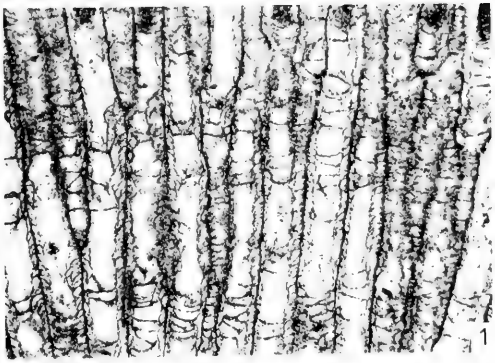
1

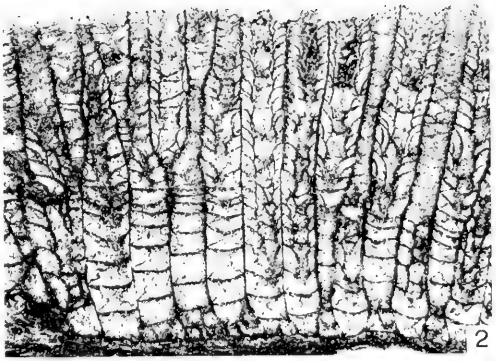
2

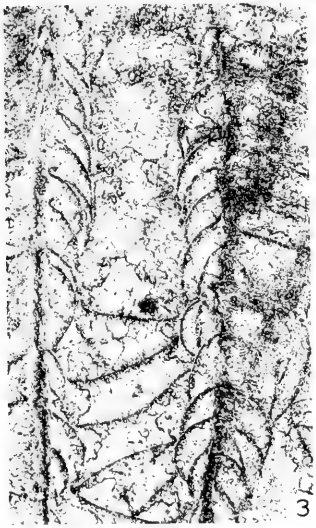
3

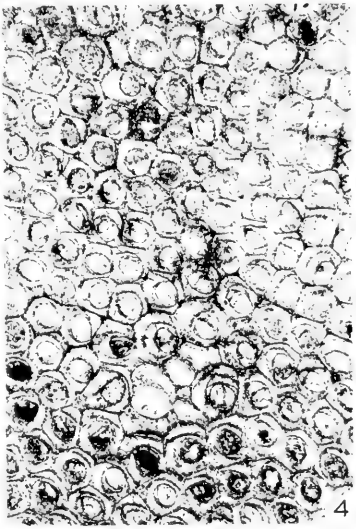
4

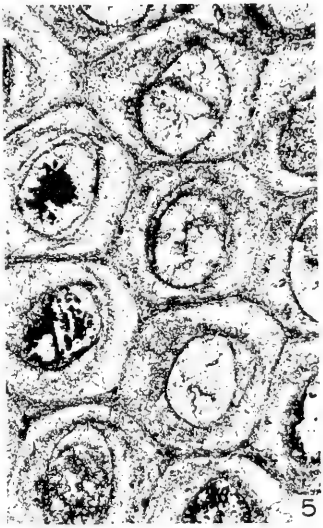
5

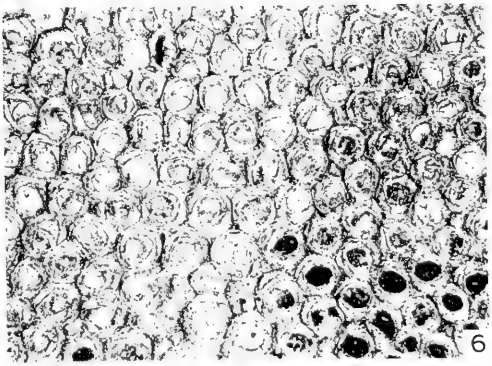
6

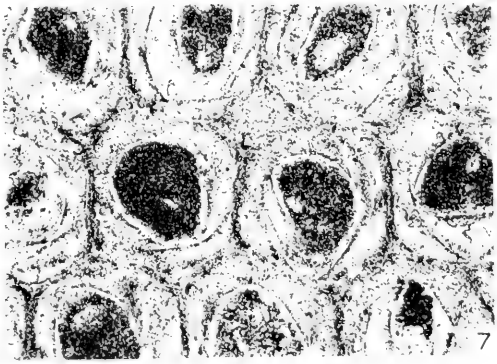
7

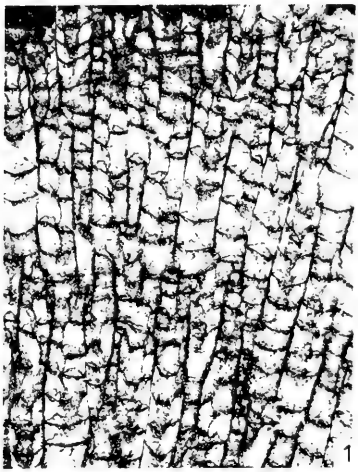
1

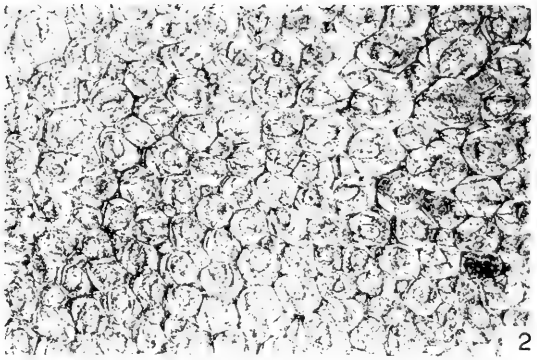
2

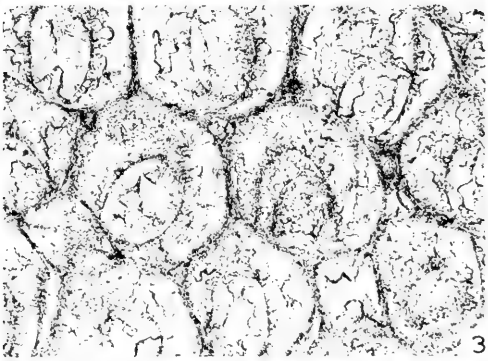
3

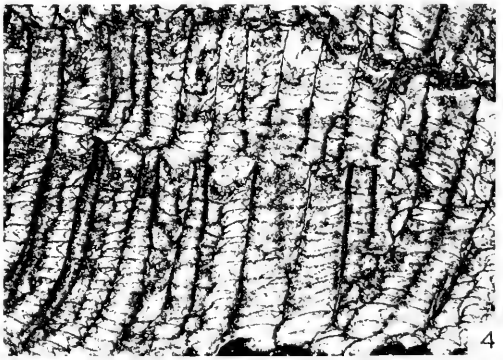
4

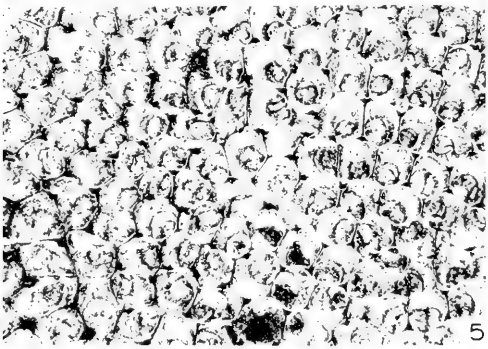
5

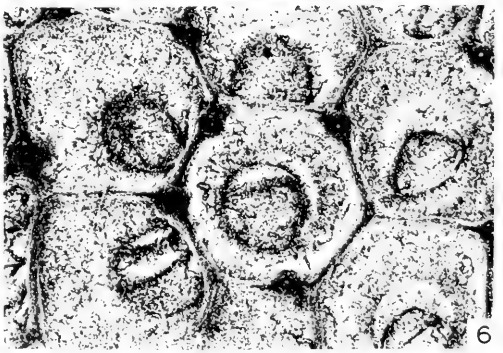
6

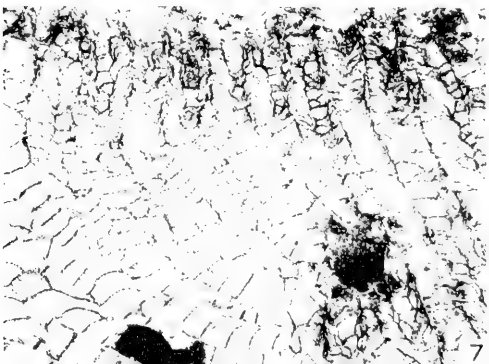
7

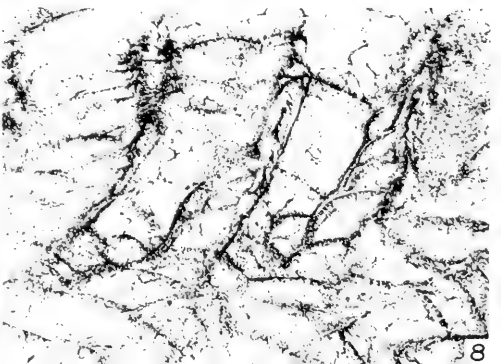
8

Explanation of Plate 48

Figure *Page*

1-3. **Prasopora megacystata** McKinney, n. sp. 228

1. Vertical section, × 20, which shows large, bulbous cystiphragms. Holotype, USNM 167770. Locality I, 53.2-53.7 m. 2. Tangential section, × 20, which shows peripheral zooecial void, common mesopores, and monticules of mesopores and enlarged zooecia in both upper left and upper right corners of photograph. Holotype, USNM 167770. Locality I, 53.2-53.7 m. 3. Tangential section, × 80, which shows mesopores, proximal tips of mesopores, and large, almost 360° cystiphragms that result in a peripheral zooecial void. Holotype, USNM 167770. Locality I, 53.2-53.7 m.

4-6. **Prasopora** sp. 230

4. Vertical section, × 20, which shows generally wide cystiphragms and closely spaced diaphragms. Hypotype, USNM 167772. Locality I, 33.5-41.0 m. 5. Tangential section, × 20, which shows acanthopores in lower left corner especially and peripheral to subcentral zooecial voids. Hypotype, USNM 167772. Locality 33.5-41.0 m. 6. Tangential section, × 80, which shows laminar zooecial walls, cystiphragms that extend entirely or almost entirely around zooecial periphery, peripheral to subcentral zooecial voids and most acanthopores situated in zooecial corners. Hypotype, USNM 167772. Locality I, 33.5-41.0 m.

7, 8. ?**Prasopora** sp. 231

7. Longitudinal section, × 20, which illustrates large cystiphragms in definite immature zone and smaller, more closely cystiphragms in mature zone. Hypotype, USNM 167773. Locality XVII, 0-4.0 m. 8. Longitudinal section, × 80, which illustrates thickened, laminar mature walls with median dark line zooecial borders, and thickened cystiphragms continuous with wall laminae especially clear in the right hand wall. Hypotype, USNM 167773. Locality XVII, 0-4.0 m.

Explanation of Plate 49

Figure *Page*

1-3. ?**Prasopora** sp. 231

1. Tangential section, × 20, which shows thickened zooecial walls, peripheral oval zooecial voids, and monticules of enlarged zooecia in bottom left, right center, and top center of photograph. Hypotype, USNM 167773. Locality XVII, 0-4.0 m. 2. Tangential section, × 80, which shows slightly thickened walls, acanthopores in zooecial corners and along zooecial borders, and cystiphragms which extend around 30% to over 50% of the zooecial periphery and form peripheral zooecial voids. Hypotype, USNM 167773. Locality XVII, 0-4.0 m. 3. Tangential section, × 80, which illustrates thickened walls with definite median line and vague laminae. Hypotype, USNM 167773. Locality XVII, 0-4.0 m.

4-8. **Homotrypa subramosa** Ulrich 234

4. Longitudinal section, × 20, which shows diaphragm spacing in immature zone, large bulbous cystiphragms in mature zone, and slightly thickened mature walls. Hypotype, USNM 167774. Locality XVII, 0-4.0 m. 5. Longitudinal section, × 20, of the same specimen as figure 4 above, which shows less distinction between mature and immature zones, with diaphragms more numerous in immature zone than is typical. Hypotype, USNM 167774. Locality XVII, 0-4.0 m. 6. Tangential section, × 20, which illustrates monticule in center of photograph and a preferred orientation of peripheral zooecial voids. Hypotype, USNM 167775. Locality I, 45.2-46.2 m. 7. Tangential section, × 80, which illustrates cystiphragms with small peripheral zooecial voids, acanthopores in zooecial corners, and slightly thickened zooecial walls. Hypotype, USNM 167775. Locality I, 45.2-46.2 m. 8. Longitudinal section, × 20, showing multilaminar zoarial form which encrusts a pelecypod shell, cystiphragms, cystose and regular diaphragms, and a mesopore with closely spaced diaphragms. Hypotype, USNM 167774. Locality XVII, 0-4.0 m.

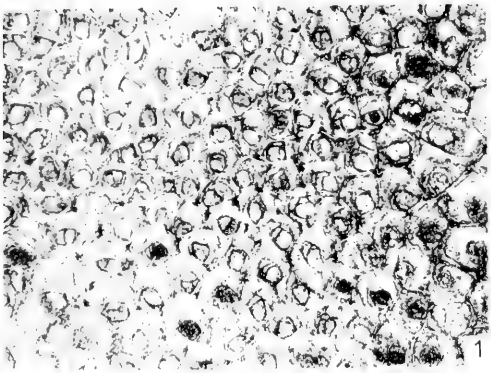
1

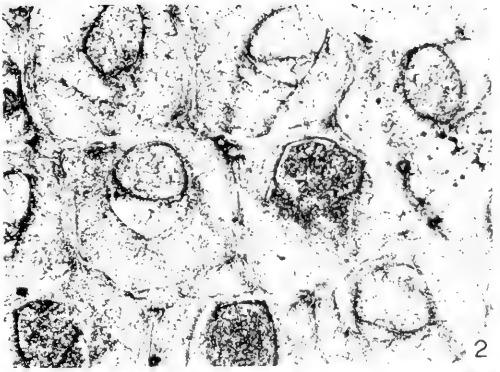
2

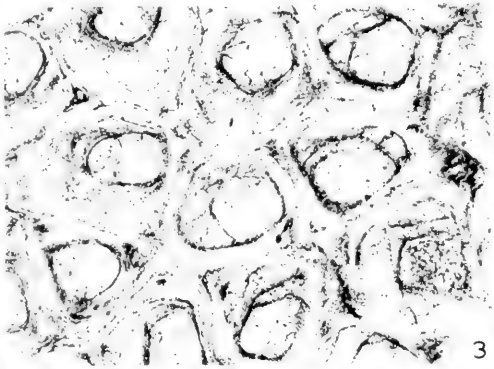
3

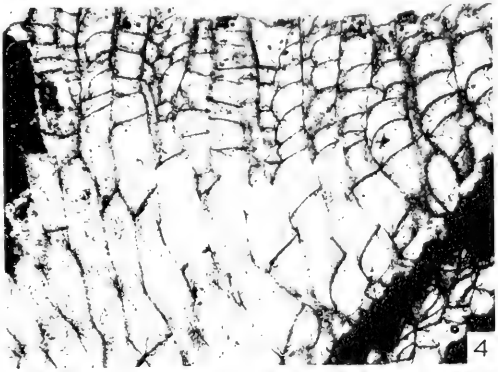
4

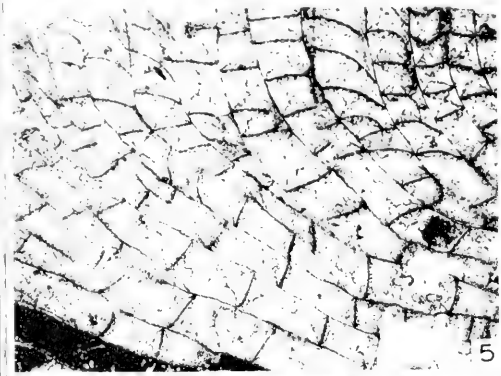
5

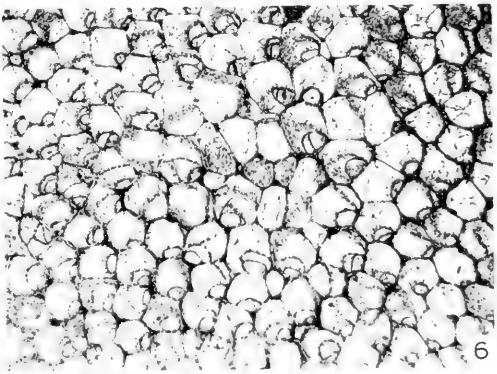
6

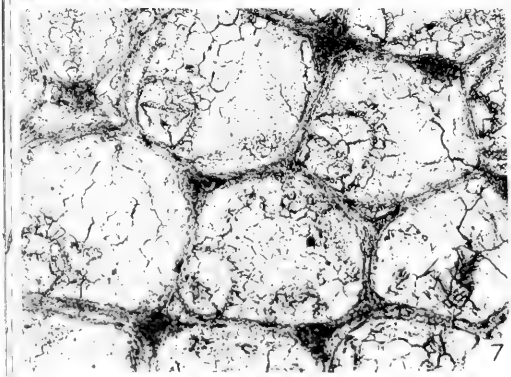
7

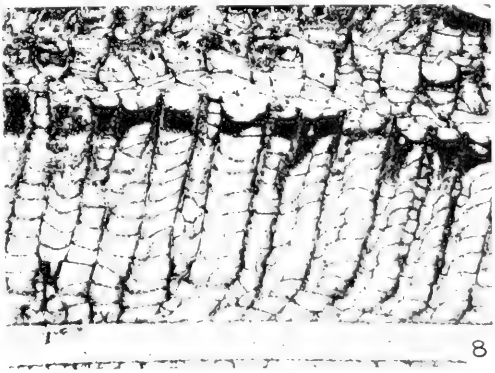
8

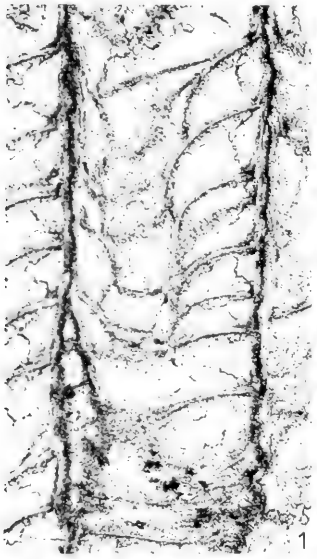
1

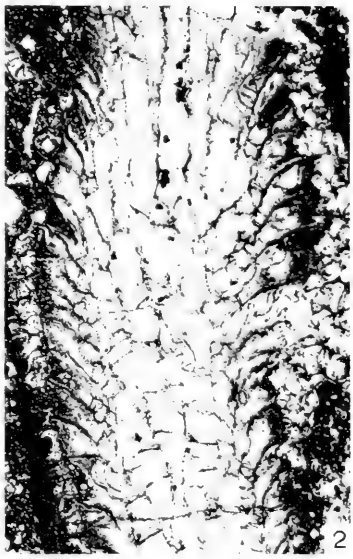
2

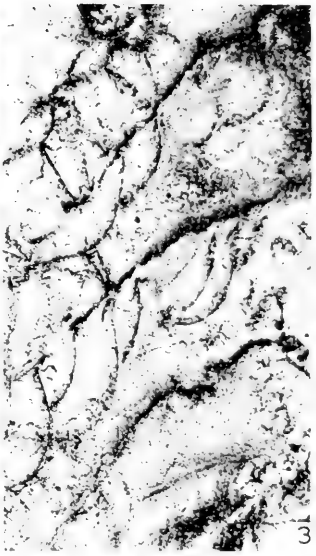
3

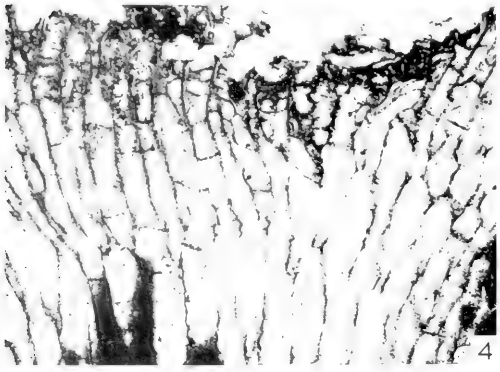
4

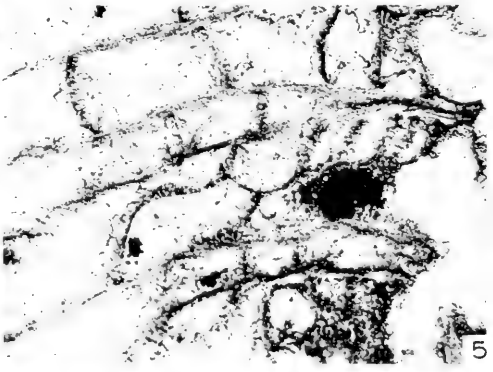
5

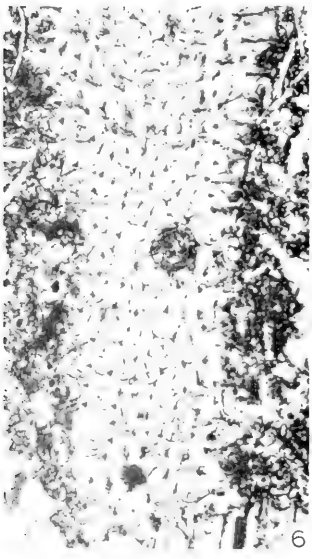
6

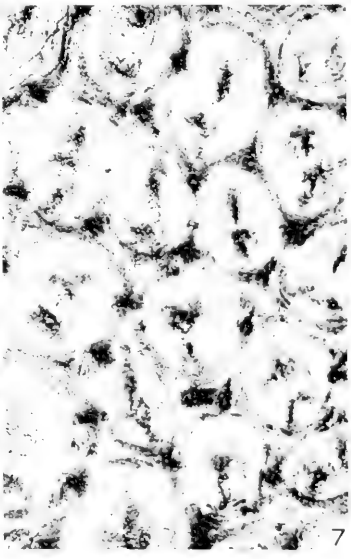
7

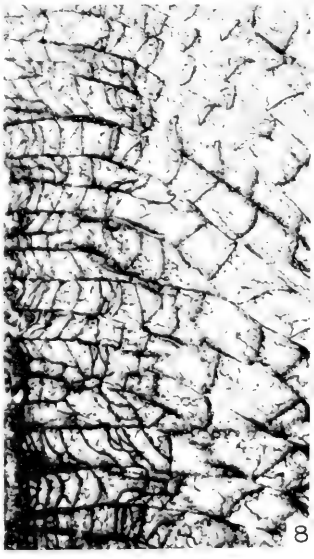
8

Explanation of Plate 50

Figure *Page*

1. **Homotrypa subramosa** Ulrich 234

Longitudinal section, × 80, which shows thickened cystiphragms that pass into V-shaped laminae of the zooecial wall and median dark lines which represent zooecial boundaries. Hypotype, USNM 167774. Locality XVII, 0-4.0 m.

2-7. **Homotrypa vacua** McKinney, n. sp. 238

2. Longitudinal section, × 20, which shows sparse diaphragms in immature zone concentrated in the submature zone, numerous small cystiphragms in the mature zone (best seen in right half of photograph), and thickened mature zooecial walls. Holotype, USNM 167776. Locality XVI, 0-1.7 m. 3. Longitudinal section, × 80, which shows overlapped, locally thickened diaphragms which pass into V-shaped laminae of thickened zooecial walls and median dark line which represents zooecial boundaries. Holotype, USNM 167776. Locality XVI, 0-1.7 m. 4. Longitudinal section, × 20, of branch bifurcation, which illustrates same characters as figure 2 above. Paratype, USNM 167777. Locality VIII, 10.0-13.3 m. 5. Longitudinal section, × 80, which shows same characters as figure 3 above and a prominent diaphragm. Paratype, USNM 167777. Locality VIII, 10.0-13.3 m. 6. Tangential section, × 20, which shows zooecial tubes almost closed by abnormal calcareous deposits. Holotype, USNM 167776. Locality XVI, 0-1.7 m. 7. Tangential section, × 80, which illustrates laminar nature of calcareous deposits that close zooecial tubes and prominent acanthopores both in zooecial corners and along boundaries. Holotype, USNM 167776. Locality XVI, 0-1.7 m.

8. **Mesotrypa sparsa** McKinney, n. sp. 241

Longitudinal section, × 20, which shows closely spaced diaphragms, cystose diaphragms, and cystiphragms in mature zone, more widely spaced diaphragms in immature zone, and zonal development of short acanthopores. Paratype, USNM 167780. Locality I, 12.8-25.3 m.

Explanation of Plate 51

Figure *Page*

1-7. **Mesotrypa sparsa** McKinney, n. sp. 241

1. Tangential section, × 20, which passes through zone of abundant acanthopores and contains a monticule of enlarged zooecia in upper right center. Paratype, USNM 167780. Locality I, 12.8-25.3 m. 2. Tangential section, × 20, which passes through zone with few acanthopores and contains a monticule in upper left corner. Paratype, USNM 167781. Locality I, 12.8-25.3 m. 3. Longitudinal section, ×20, which shows numerous curved and cystose diaphragms in immature zone. Paratype, USNM 167781. Locality I, 12.8-25.3 m. 4. Longitudinal section, × 20, which illustrates a more typical reduced definition between mature and immature zones and a zonal development of short acanthopores at the base of the mature zone. Holotype, USNM 167779. Locality III, 19.1-22.0 m. 5. Longitudinal section, × 80, which exhibits cone-in-cone structure of short acanthopores. Holotype, USNM 167779. Locality III, 19.1-22.0 m. 6. Tangential section, × 20, which shows good development of large acanthopores at zooecial corners and typically thin zooecial walls. Holotype, USNM 167779. Locality III, 19.1-22.0 m. 7. Tangential section, × 80, which illustrates locally thickened, obscurely laminate zooecial walls with a dark median line shown in lower left corner, variability of zooecial cross-sections, and large, strongly laminate acanthopores with large axial zones in zooecial corners. Holotype, USNM 167779. Locality III, 19.1-22.0 m.

8. **Heterotrypa ridleyana** (Coryell) 244

Tangential section, × 20, which cuts through mature zone only in a narrow band just below the center of the photograph. Hypotype, USNM 167783. Locality I, 12.8-25.3 m.

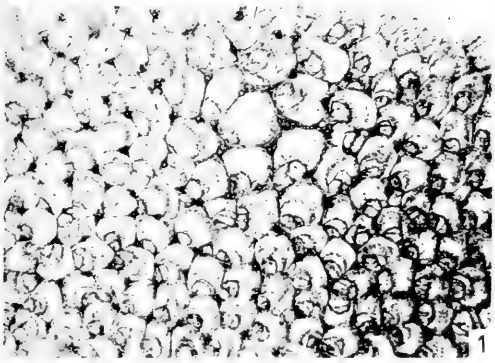
1

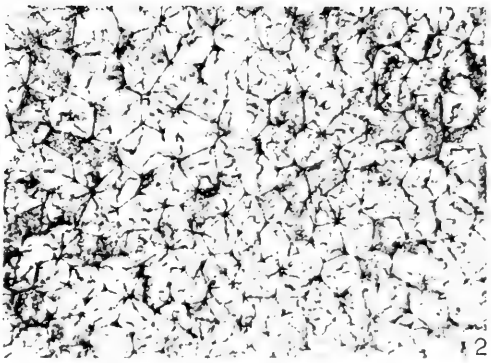
2


3


4

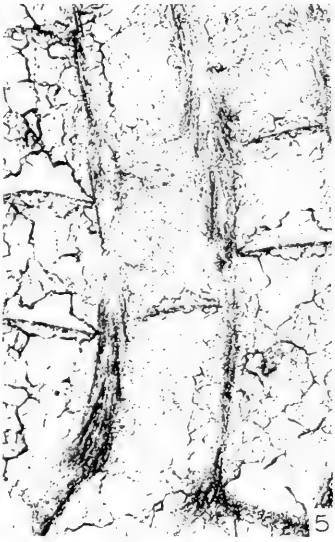
5

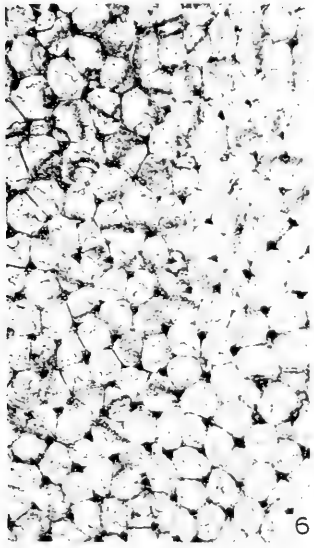
6

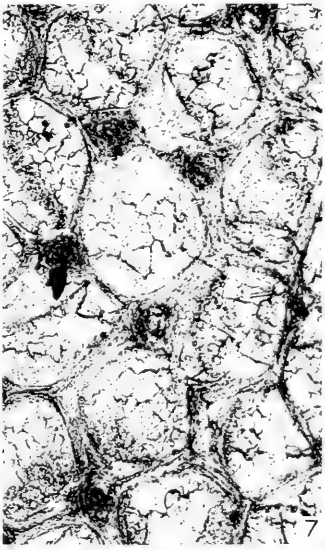
7

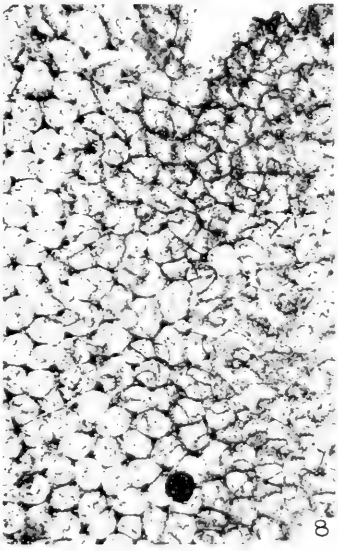
8

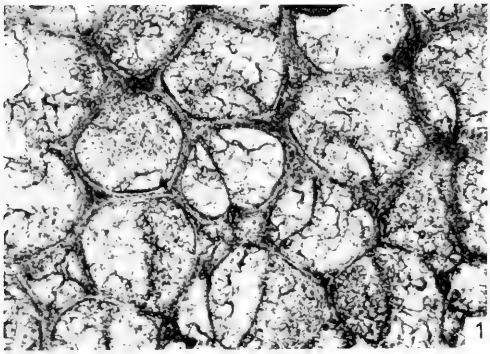
1

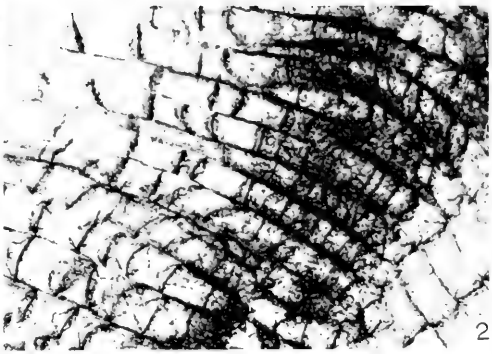
2

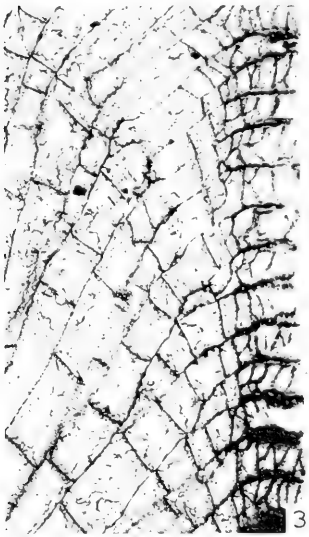
3

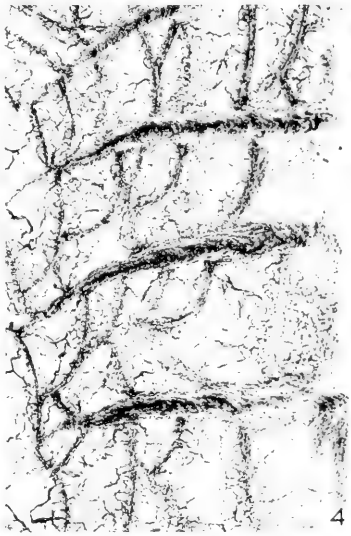
4

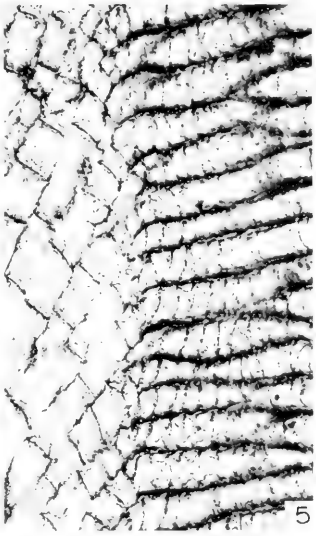
5

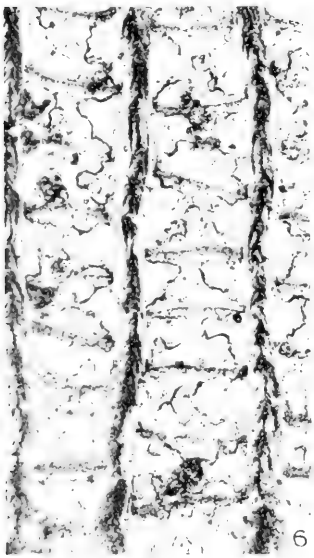
6

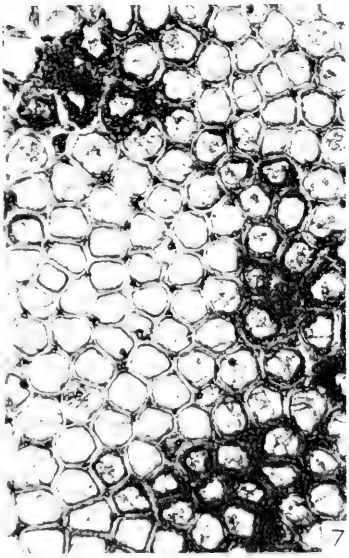
7

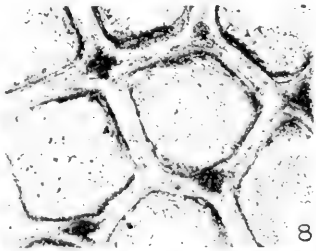
8

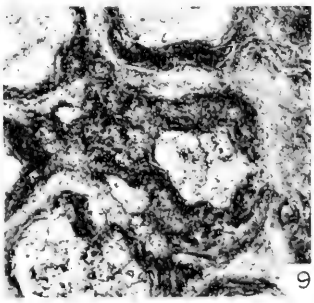
9

Explanation of Plate 52

Figure *Page*

1, 2. Heterotrypa ridleyana (Coryell) 244

1. Tangential section, × 80, which illustrates mesopores, sparse, small acanthopores located both in zooecial corners and along borders, and thickened zooecial walls. Hypotype, USNM 167783. Locality I, 12.8-25.3 m. 2. Longitudinal section, × 20, which shows mature zone in right bottom corner, some cystiphragms in lower portion of mature zone where diaphragms are closely spaced, and more widely spaced diaphragms in the outermost part of the mature zone. Hypotype, USNM 167784. Locality I, 12.8-25.3 m.

3-9. Heterotrypa patera Coryell 248

3. Longitudinal section, × 20, which exhibits diaphragm spacing in immature zone, gentle to pronounced bend at base of mature zone, and cystiphragms at base of mature zone. Hypotype, USNM 167785. Locality XVII, 0-4.0 m. 4. Longitudinal section, × 80, which illustrates diaphragms, cystose diaphragms, and cystiphragms that continue into wall laminae, and lower integrate type wall structure which passes outward into typical two-part heterotrypid walls. Hypotype, USNM 167785. Locality XVII, 0-4.0 m. 5. Longitudinal section, × 20, which shows same characters as figure 3 above, but with distinct bend at base of thicker mature zone and more obvious restriction of cystiphragms to the base of the mature zone. Hypotype, USNM 167786. Locality II, 14.5-16.1 m. 6. Longitudinal section, × 80, which shows typical heterotrypid wall structure. Hypotype, USNM 167787. Locality II, 14.5-16.1 m. 7. Tangential section, × 20, with abnormal, irregularly crenulated deposits in monticules. Hypotype, USNM 167788. Locality XVII, 0-4.0 m. 8. Tangential section, × 80, which illustrates amalgamate walls due to curved wall laminae, thin zooecial linings, and acanthopores that slightly inflect the zooecial tubes located in zooecial corners. Hypotype, USNM 167788. Locality XVII, 0-4.0 m. 9. Tangential section, × 80, of zooecium in a monticule lined by irregularly crenulated wall deposits. Hypotype, USNM 167788. Locality XVII, 0-4.0 m.

Explanation of Plate 53

Figure *Page*

1-4. **Heterotrypa patera** Coryell 248

1. Reconstructed specimen, × 2/3, with frondose, parallel, intergrown branches. Hypotype, USNM 167789. Locality II, 16.1-19.2 m. 2. Tangential section, × 20, which exhibits typical tangential aspect of well developed mature zone, with monticules in upper left and lower right corners. Hypotype, USNM 167790. Locality II, 8.2-13.7 m. 3. Tangential section, × 80, which illustrates amalgamate wall structure, thick zooecial lining, and local absence of acanthopores. Hypotype, USNM 167790. Locality II, 8.2-13.7 m. 4. Tangential section × 80, which shows same features as figure 3 above, but with acanthopores in most zooecial corners. Hypotype, USNM 167787. Locality II, 14.5-16.1 m.


1

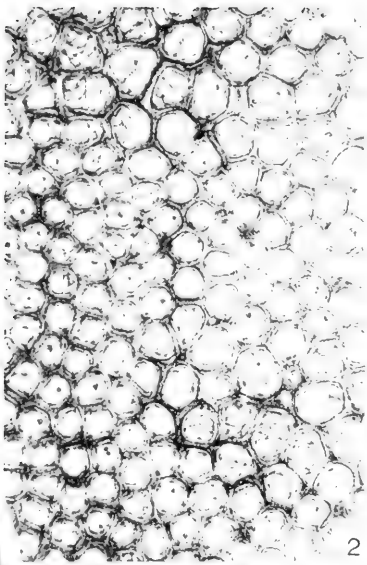
2

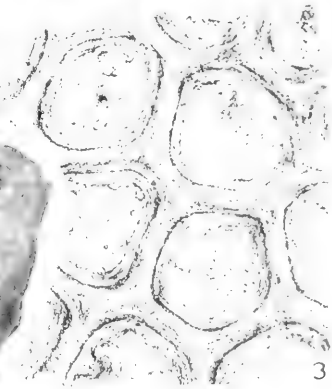
3


4

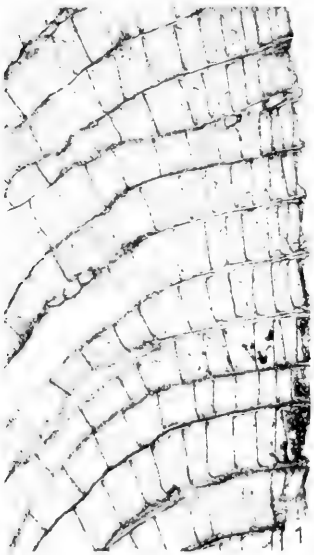
1

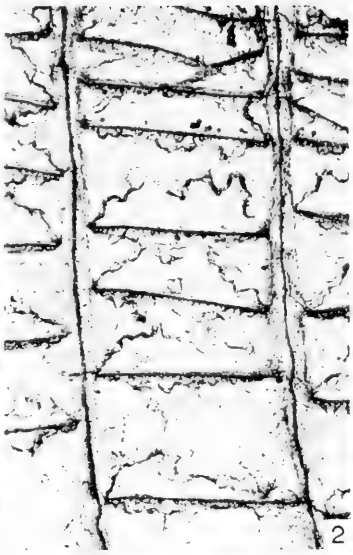
2

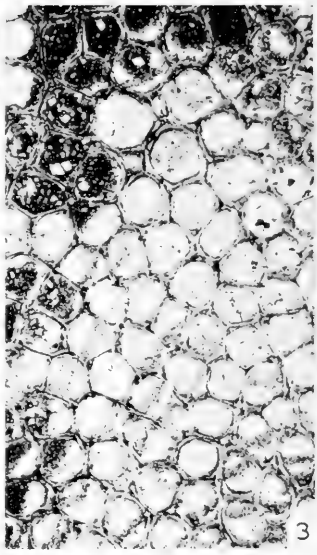
3

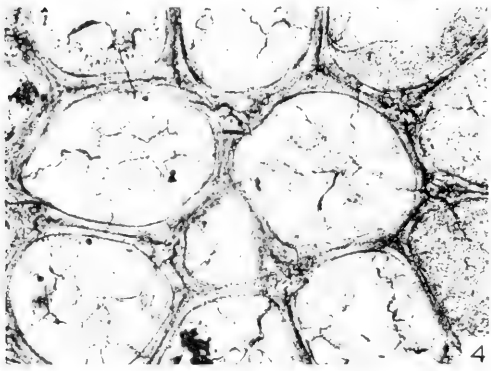
4

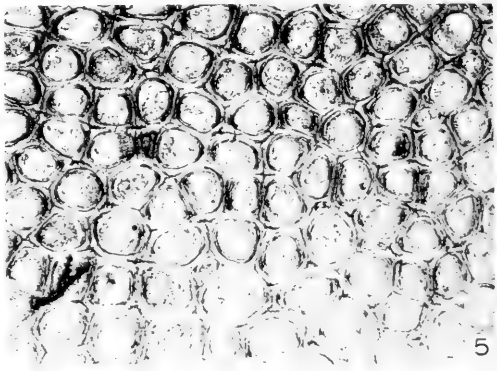
5


6


7


8

Explanation of Plate 54

Figure *Page*

1-8. **Amplexopora winchelli** Ulrich 250

1. Longitudinal section, × 20, which illustrates gentle curvature of zooecia into mature zone and moderately spaced diaphragms in mature zone. Hypotype, USNM 167792. Locality XIV, 16.2-18.2 m. 2. Longitudinal section, × 80, which shows two slightly thickened diaphragms near the top of the photograph, with basal dark layer and overlying lighter laminae continuous with wall laminae, and absence of zooecial lining. Hypotype, USNM 167792. Locality XIV, 16.2-18.2 m. 3. Tangential section, × 20, which shows monticule in lower left corner, sparse mesopores, and integrate walls. Hypotype, USNM 167792. Locality XIV, 16.2-18.2 m. 4. Tangential section, × 80, which illustrates acanthopores at zooecial corners, dark line which represents zooecial boundaries, and slightly thickened mature zooecial walls with no internal lining. Hypotype, USNM 167792. Locality XIV, 16.2-18.2 m. 5. Tangential section, × 20, of specimen with well-developed zooecial lining. Hypotype, USNM 167793. Locality XIV, 16.2-18.2 m. 6. Tangential section, × 80, which shows dark line between adjacent zooecia, acanthopores and mesopores in some zooecial corners, and thick zooecial linings. Hypotype, USNM 167793. Locality XIV, 16.2-18.2 m. 7. Longitudinal section, × 20, of locally thin-walled mature zone. Hypotype, USNM 167793. Locality XIV, 16.2-18.2 m. 8. Longitudinal section, × 80, which illustrates thickened diaphragm and cystose diaphragm continuous with wall laminae. Hypotype, USNM 167793. Locality XIV, 16.2-18.2 m.

Explanation of Plate 55

Figure *Page*

1-3. **Amplexopora winchelli** Ulrich 250

1. Longitudinal section, × 80, which illustrates slightly thickened diaphragms continuous with laminae of well developed zooecial linings. Hypotype, USNM 167793. Locality XIV, 16.2-18.2 m. 2. Longitudinal section, × 80, of zooecium with large acanthopore to left. Hypotype, USNM 167791. Locality XIV, 16.2-18.2 m. 3. Tangential section, × 80, which shows same characters as figure 6 of Plate 54, with zooecial lining developed only as local bulbous thickenings. Hypotype, USNM 167791. Locality XIV, 16.2-18.2 m.

4-8. **Amplexopora** aff. **A. winchelli** Ulrich 255

4. Tangential section, × 20, which exhibits abundant acanthopores both in zooecial corners and along zooecial borders. Hypotype, USNM 167794. Locality II, 8.2-13.7 m. 5. Longitudinal section, × 80, which shows short acanthopores developed along zooecial borders. Hypotype, USNM 167794. Locality II, 8.2-13.7 m. 6. Longitudinal section, × 20, which illustrates transition from immature to mature zone and closely spaced diaphragms in proximal tips of short zooecia. Hypotype, USNM 167794. Locality II, 8.2-13.7 m. 7. Longitudinal section, × 80, which shows change from immature to mature portions of a short zooecium. Hypotype, USNM 167794. Locality II, 8.2-13.7 m. 8. Tangential section, × 80, which illustrates acanthopores both in zooecial corners and along zooecial boundaries that inflect zooecial tubes. Hypotype, USNM 167794. Locality II, 8.2-13.7 m.

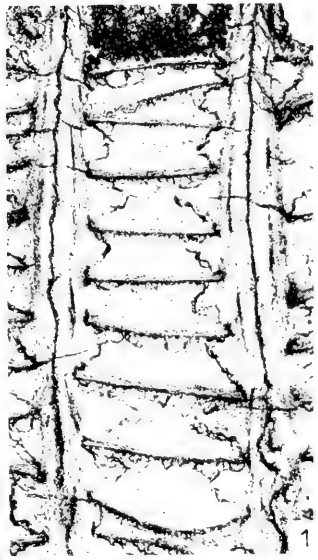
1

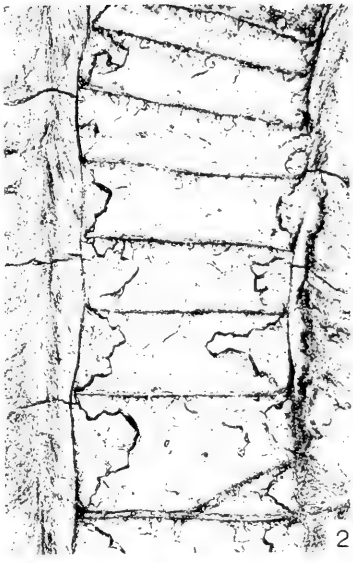
2

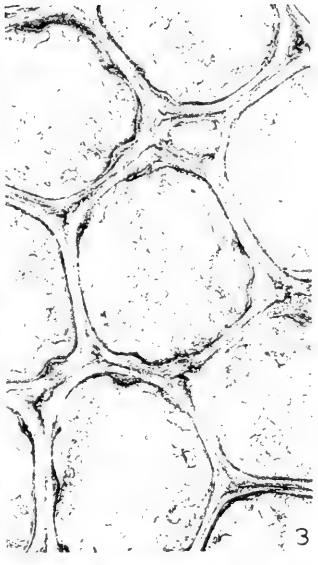
3

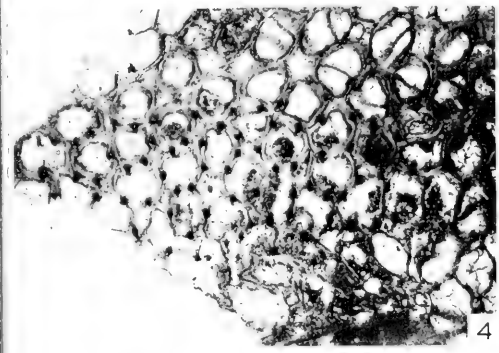
4


5

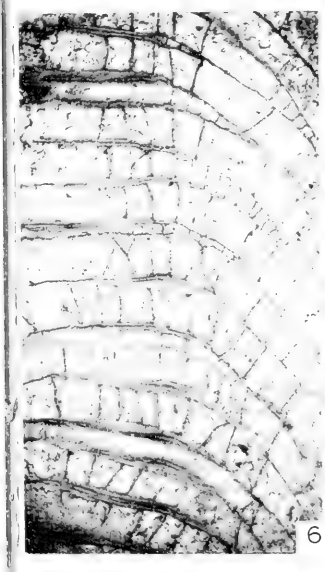
6

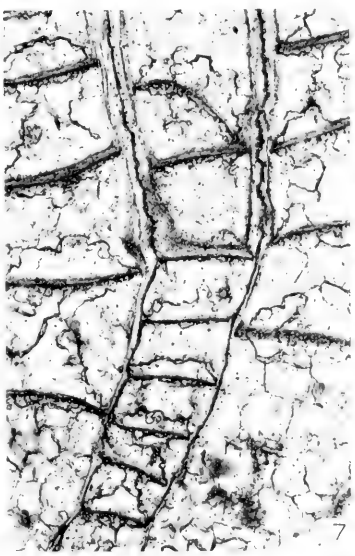
7

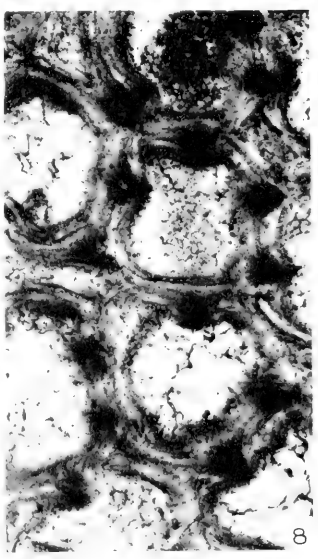
8

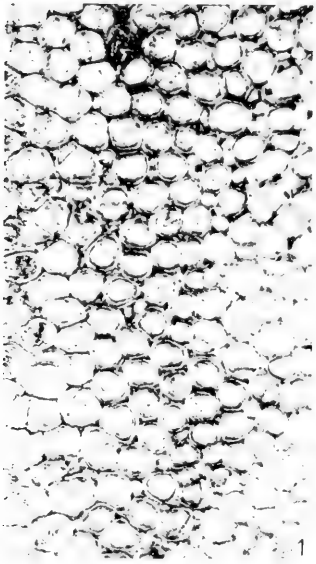
1

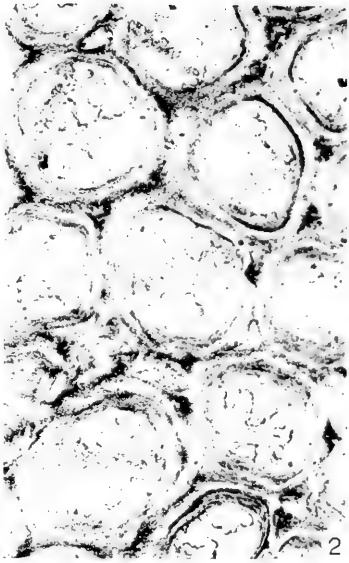
2

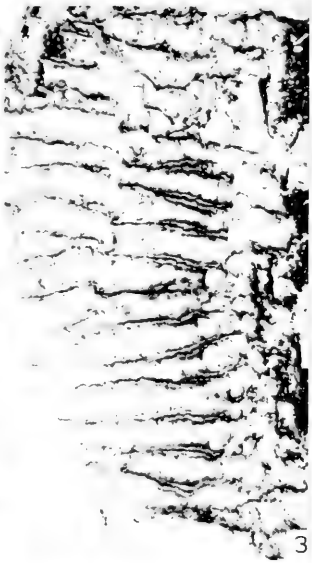
3

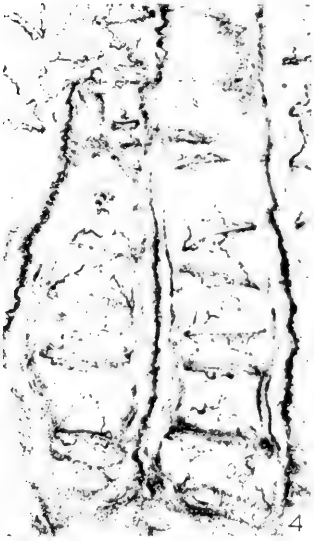
4


5


6

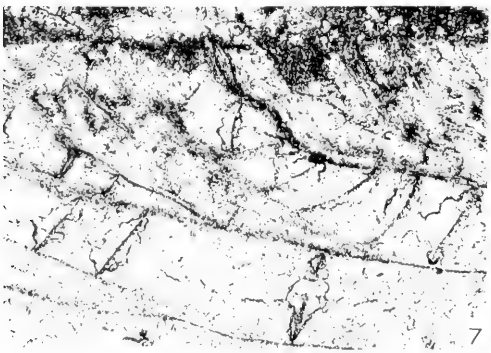
7

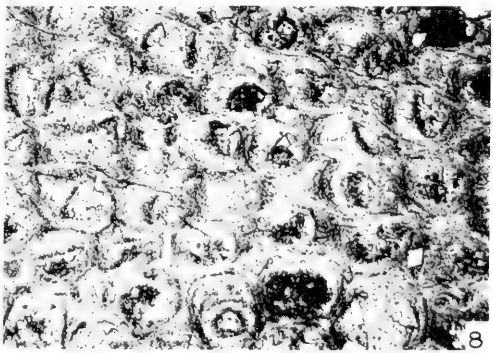
8

Explanation of Plate 56

Figure *Page*

1-4. **Amplexopora** sp. 258

1. Tangential section, × 20, which exhibits small zooecia, abundant mesopores, and a questionable monticule in the upper right corner of the photograph. Hypotype, USNM 167795. Locality II, 16.1-19.2 m. 2. Tangential section, × 80, which shows abundant small acanthopores in mesopore and zooecial corners and laminar zooecial walls. Hypotype, USNM 167795. Locality II, 16.1-19.2 m. 3. Vertical section, × 20, which illustrates thickened mature walls and prominent crenulate dark line between adjacent zooecia. Hypotype, USNM 167795. Locality II, 16.1-19.2 m. 4. Longitudinal section, × 80, which illustrates a crenulate dark line of contact between adjacent mature zooecia, V-shaped laminae in zooecial walls, and slightly thickened diaphragms continuous with zooecial linings. Hypotype, USNM 167795. Locality II, 16.1-19.2 m.

5-8. **Eridotrypa minor** Ulrich 260

5. Longitudinal section, × 40, which illustrates relationship of mature, submature, and immature zones. Hypotype, USNM 167796. Locality III, 19.1-22.0 m. 6. Longitudinal section, × 20, which shows a thin mature zone and absence or sparsity of diaphragms in the immature zone except in the submature region and in a plane of rejuvenation. Hypotype, USNM 167796. Locality III, 19.1-22.0 m. 7. Longitudinal section, × 80, which illustrates mature and submature diaphragms continuous with wall laminae and dark line that represents plane of contact between adjacent zooecia. Hypotype, USNM 167796. Locality III, 19.1-22.0 m. 8. Tangential section, × 40, which illustrates slightly thickened walls in thin mature zone. Hypotype, USNM 167796. Locality III, 19.1-22.0 m.

Explanation of Plate 57

Figure *Page*

1-6. **Eridotrypa abrupta** Loeblich 262

1. Tangential section, × 40, which illustrates rounded to subrounded, typically oval or polygonal mature zooecial cross-sections. Hypotype, USNM 167797. Locality XVI, 15.7-18.9 m. 2. Tangential section, × 80, which illustrates dark line in walls between adjacent zooecia, laminar walls, and mesopores at zooecial corners. Hypotype, USNM 167797. Locality XVI, 15.7-18.9 m. 3. Longitudinal section, × 20, which exhibits unusual lack of diaphragms in immature zone except in plane of rejuvenation just above lower edge of photograph and in submature zone and abrupt bend at base of thin mature zone. Hypotype, USNM 167797. Locality XVI, 15.7-18.9 m. 4. Longitudinal section, × 80, which shows submature diaphragms continuous with wall laminae (best seen in lower right corner) and dark line which represents zooecial borders. Hypotype, USNM 167797. Locality XVI, 15.7-18.9 m. 5. Tangential section, × 20, which illustrates subcircular mature zooecial cross-sections and abundant mesopores. Hypotype, USNM 167798. Locality I, 33.5-41.0 m. 6. Longitudinal section, × 20, which shows scattered diaphragms in immature zone and abrupt bend at base of mature zone. Hypotype, USNM 167798. Locality I, 33.5-41.0 m.

7, 8. **Eridotrypa arcuata** McKinney, n. sp. 264

7. Longitudinal section, × 20, of two anastomosed branches that result in a locally thickened and reflexed mature zone. Paratype, USNM 167800. Locality III, 19.1-22.0 m. 8. Longitudinal section, × 40, which exhibits gentle curvature into mature zone, faintly suggested V-shaped laminae in mature walls, planar diaphragms in mature zone, and dark line which represents plane of contact between adjacent zooecia. Holotype, USNM 167799. Locality III, 19.1-22.0 m.

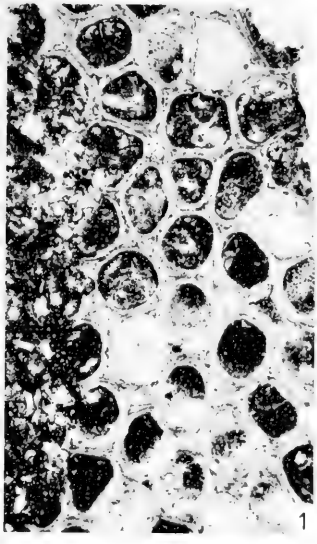
1

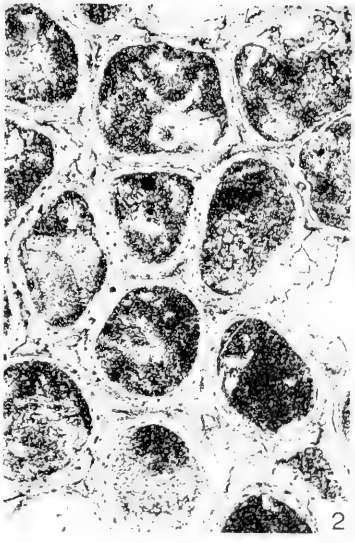
2


3


4

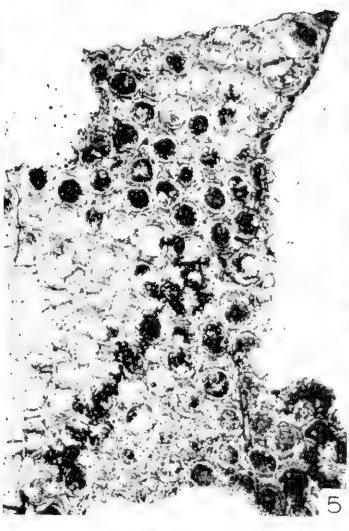
5


6

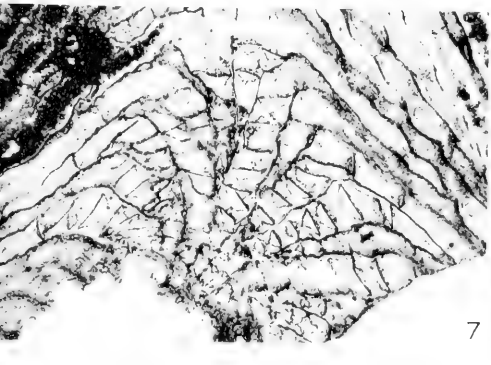
7


8

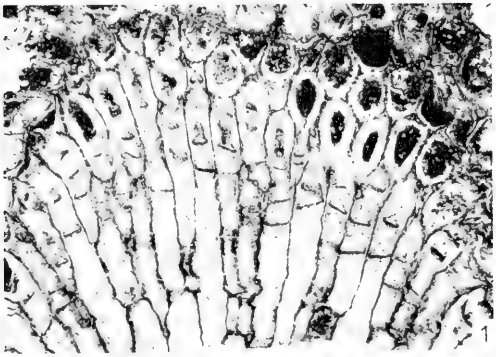
1

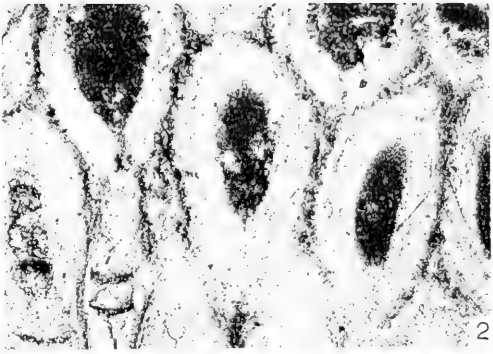
2

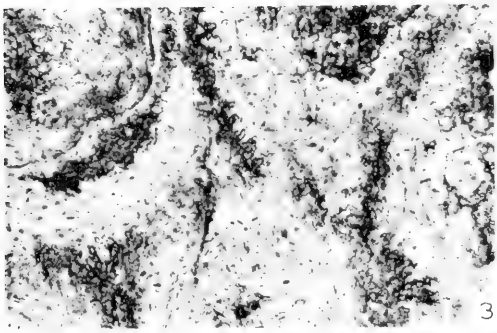
3

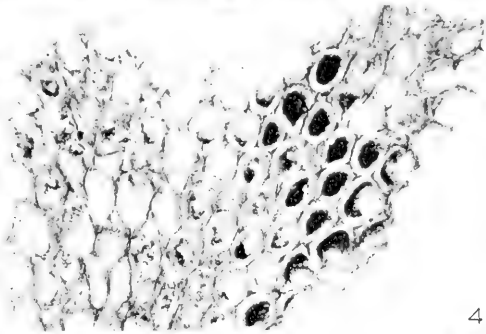
4


5

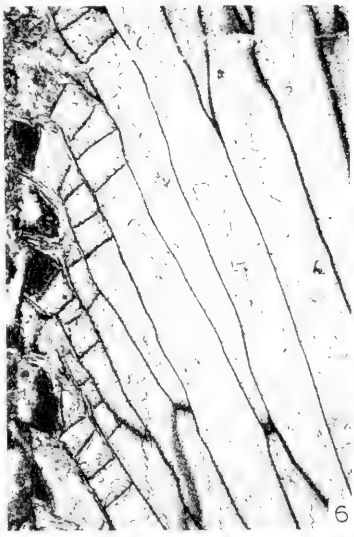
6


7

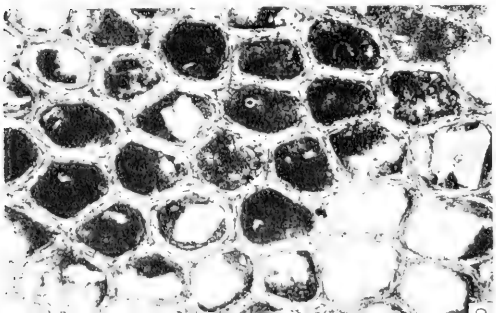
8

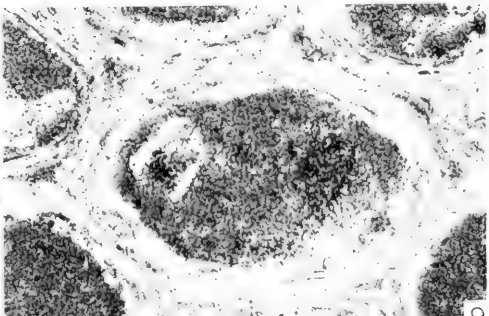
9

Explanation of Plate 58

Figure *Page*

1-5. Eridotrypa arcuata McKinney, n. sp. 264

1. Tangential section, × 20, which cuts from mature zone near top of photograph into immature zone in bottom center of photograph. Holotype, USNM 167799. Locality III, 19.1-22.0 m. 2. Tangential section, × 80, which illustrates thickened mature walls, "granular" contact between zooecia, and elongate oval zooecial tubes. Holotype, USNM 167799. Locality III, 19.1-22.0 m. 3. Tangential section, × 200, which illustrates minute tubules that cause "granular" appearance of zooecial borders at lower magnifications. Holotype, USNM 167799. Locality III, 19.1-22.0 m. 4. Tangential section, × 20, of branch bifurcation. Paratype, USNM 167801. Locality III, 19.1-22.0 m. 5. Longitudinal section, × 20, which shows lack of diaphragms in immature zone and gentle curvature into mature zone. Paratype, USNM 1677800. Locality III, 19.1-22.0 m.

6-9. Eridotrypa libana (Safford) 267

6. Longitudinal section, × 20, which shows zooecia that diverge steeply in immature zone, lack of diaphragms in immature zone, and presence of diaphragms in submature and thin mature zones. Hypotype, USNM 167803. Locality II, 8.2-13.7 m. 7. Longitudinal section, × 80, which shows slightly thickened diaphragms continuous with vague laminae of walls. Hypotype, USNM 167803. Locality II, 8.2-13.7 m. 8. Tangential section, × 20, which illustrates irregularly polygonal cross-sectional shape of mature zooecia. Hypotype, USNM 167803. Locality II, 8.2-13.7 m. 9. Tangential section, × 80, which exhibits laminae of indistinctly integrate walls. Hypotype, USNM 167803. Locality II, 8.2-13.7 m.

Explanation of Plate 59

Figure *Page*

1-8. **Batostoma varium** Ulrich 269

1. Longitudinal section, × 20, which illustrates lack of diaphragms in immature zone except in outer immature zone and gradual curvature of zooecia into thin mature zone. Hypotype, USNM 167804. Locality I, 12.8-25.3 m. 2. Tangential section, × 20, which illlustrates oval mature zooecial cross-sections, large acanthopores in a band that extends from the center top to center bottom of the photograph, and vague mesopores. Hypotype, USNM 167805. Locality I, 12.8-25.3 m. 3. Tangential section, × 80, which exhibits well-developed zooecial lining, large acanthopores with large axial outside of zooecial linings, and mesopores masked by calcareous deposits. Hypotype, USNM 167805. Locality I, 12.8-25.3 m. 4. Longitudinal section, × 80, which cuts large axial area of two notched acanthopores, thin diaphragms in zooecial tube, and thickened diaphragms which partially to completely fill mesopores. Hypotype, USNM 167806. Locality VI, 0.3-4.9 m. 5. Longitudinal section, × 80, which illustrates thickened wall deposits, acanthopores with moderately large axial areas, and mesopore with slightly thickened diaphragms. Hypotype, USNM 167807. Locality XVI, 1.7-15.7 m. 6. Tangential section, × 80, which shows well-developed zooecial linings, relatively small acanthopores with large axial areas, and mesopores partly obscured by calcareous deposits. Hypotype, USNM 167807. Locality XVI, 1.7-15.7 m. 7. Tangential section, × 20, of specimen with large acanthopores that can best be seen just below the center of the photograph. Hypotype, USNM 167799. Locality III, 19.1-22.0 m. 8. Tangential section, × 80, which illustrates variable size of axial areas in large acanthopores, vague wall laminae, zooecial linings in upper left of photograph, and obscure mesopores. Hypotype, USNM 167799. Locality III, 19.1-22.0 m.


1

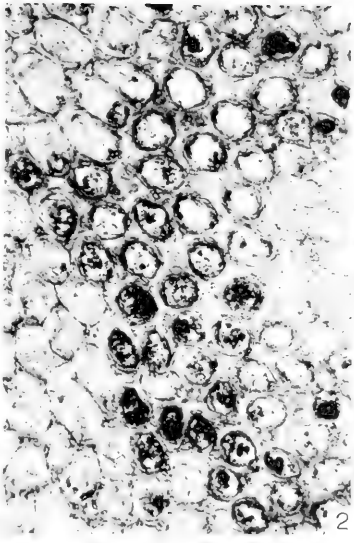
2


3

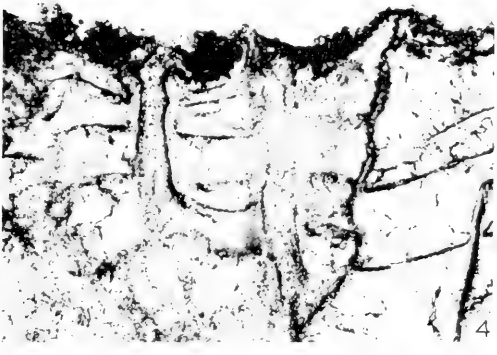
4

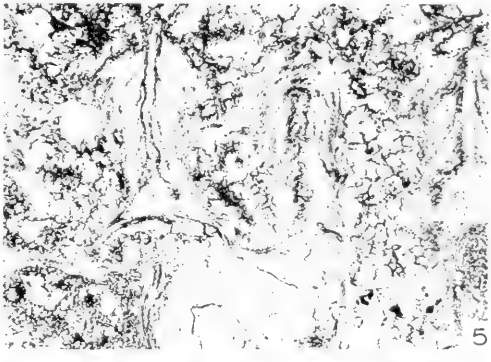
5

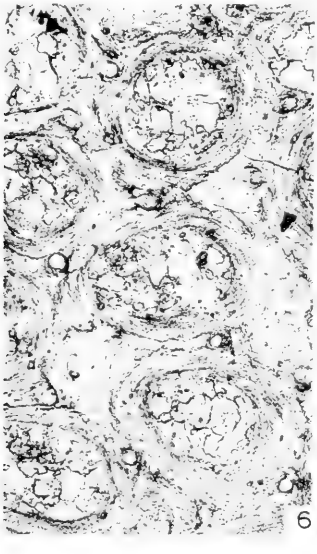
6

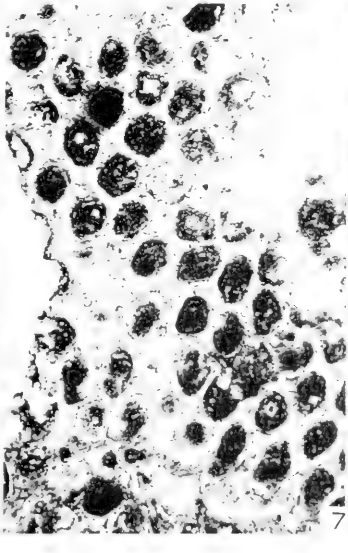
7


8


1

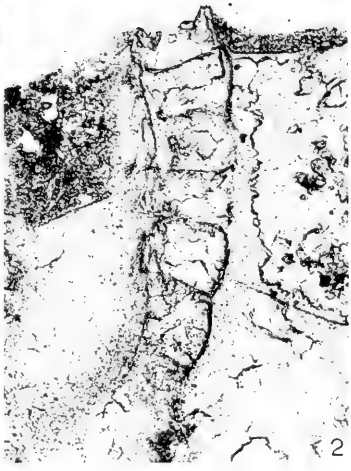
2

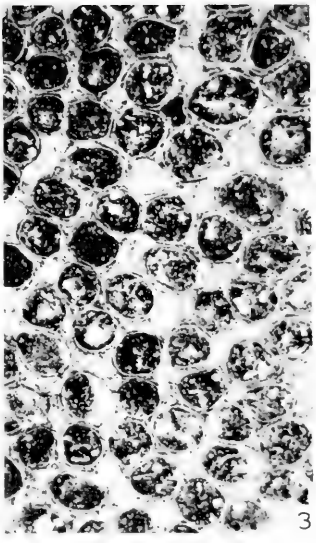
3

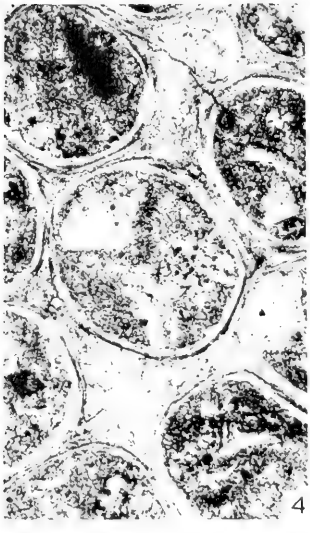
4

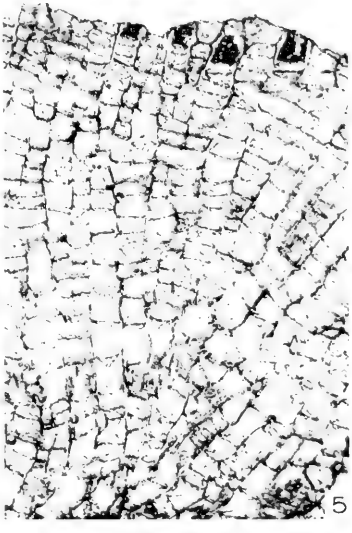
5


6

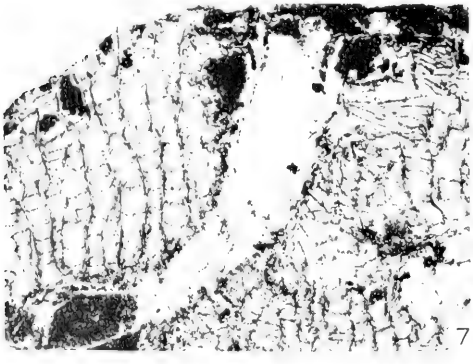
7

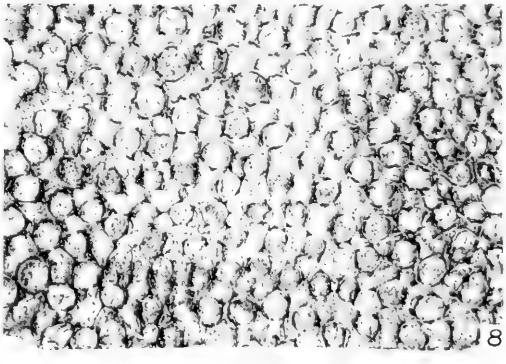
8

Explanation of Plate 60

Figure *Page*

1-4. **Batostoma varium** Ulrich 269

1. Longitudinal section, × 20, of thin-walled specimen with large zooecia. Hypotype, USNM 167808. Locality XV, 13.7-16.6 m. 2. Longitudinal section, × 80, which shows a slightly moniliform mesopore with thin diaphragms. Hypotype, USNM 167808. Locality XV, 13.7-16.6 m. 3. Tangential section, × 20, which exhibits a monticule in the upper right corner. Hypotype, USNM 167808. Locality XV, 13.7-16.6 m. 4. Tangential section, × 80, which illustrates thin zooecial linings relative to other specimens of *B. varium,* small acanthopores in the zooecial-mesopore corners, and well-defined mesopores. Hypotype, USNM 167808. Locality XV, 13.7-16.6 m.

5-8. **Batostoma increbescens** Bork and Perry 272

5. Longitudinal section, × 20, which illustrates abundant diaphragms and moderately thin walls. Hypotype, USNM 167809. Locality XII, 22.1-25.6 m. 6. Longitudinal section, × 80, which shows long acanthopores in zooecial corners and short acanthopores along zooecial borders. Hypotype, USNM 167809. Locality XII, 22.1-25.6 m. 7. Longitudinal section, × 20, of area penetrated by boring organism. Distortion of zooecia to the right of the bore hole may indicate an adjustment of the ectoproct colony while or after it was invaded by the boring organism. Hypotype, USNM 167809. Locality XII, 22.1-25.6 m. 8. Tangential section, × 20, which exhibits subcircular zooecia and abundant mesopores. Hypotype, USNM 167809. Locality XII, 22.1-25.6 m.

Explanation of Plate 61

Figure *Page*

1, 2. **Batostoma increbescens** Bork and Perry 272

1. Tangential section, × 80, which illustrates well-developed zooecial linings indented by numerous small acanthopores. Most mesopores are filled by calcareous deposits. Hypotype, USNM 167809. Locality XII, 22.1-25.6 m. 2. Tangential section, × 20, which cuts both mature and immature zones. Hypotype, USNM 167810. Locality VI, 0.3-4.9 m.

3-6. **Batostoma** sp. 274

3. Longitudinal section, × 20, of an area with relatively widely spaced diaphragms in mesopores and zooecial walls that are thinner than typical. Hypotype, USNM 167811. Locality II, 14.5-16.1 m. 4. Longitudinal section, × 20, of a more generally typical area of the same specimen shown in figure 3 above. Hypotype, USNM 167811. Locality II, 14.5-16.1 m. 5. Longitudinal section, × 80, illustrating curved diaphragms in zooecia, abundant diaphragms in somewhat moniliform mesopores and an acanthopore. Holotype, USNM 167811. Locality II, 14.5-16.1 m. 6. Deep tangential section, × 20, cutting subcircular zooecia, abundant mesopores and abundant acanthopores. Hypotype, USNM 167811. Locality II, 14.5-16.1 m.

7, 8. **Hemiphragma irrasum** (Ulrich) 276

7. Vertical section, × 20, of encrusting specimen on brachiopod shell, which shows decreased diameter of zooecia in the mature zone and hemiphragms that project into zooecial tubes from one side of the zooecial walls. Hypotype, USNM 167812. Locality II, 8.2-13.7 m. 8. Vertical section, × 20, which shows thick-walled mature zone and numerous hemiphragms. Hypotype, USNM 167812. Locality II, 8.2-13.7 m.

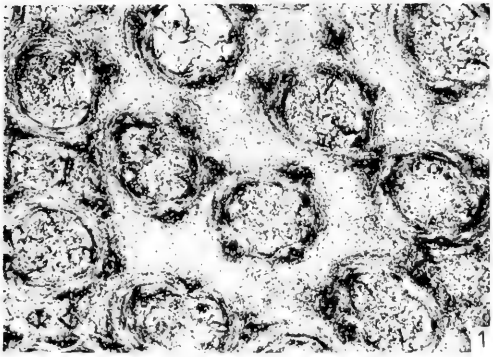
1

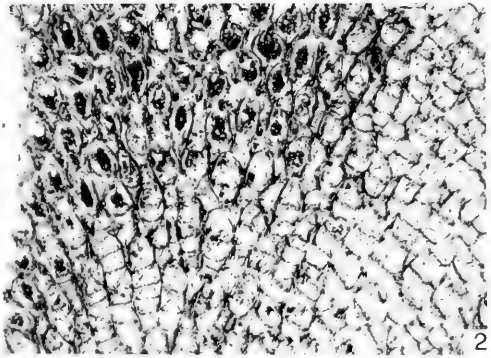
2

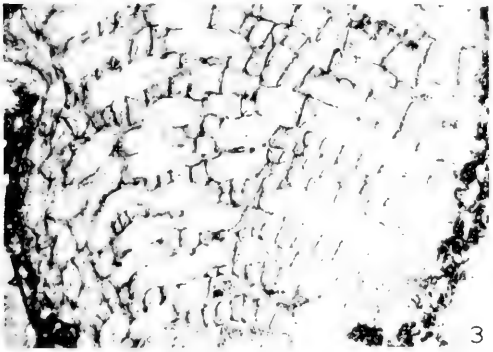
3

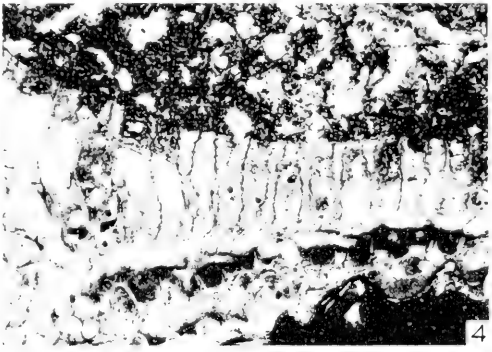
4

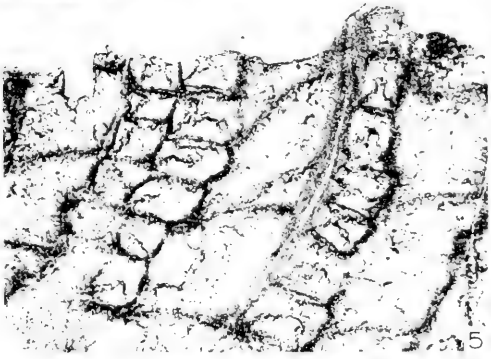
5

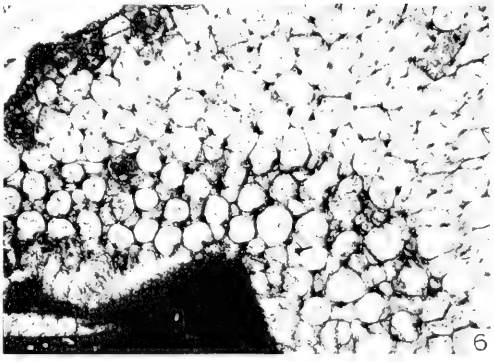
6

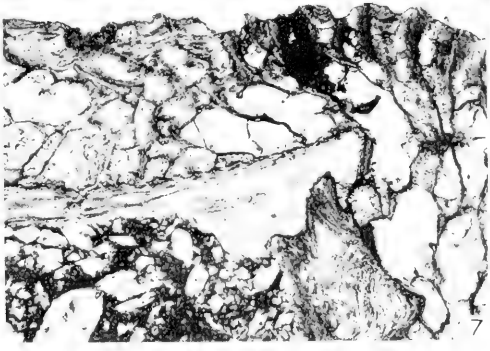
7

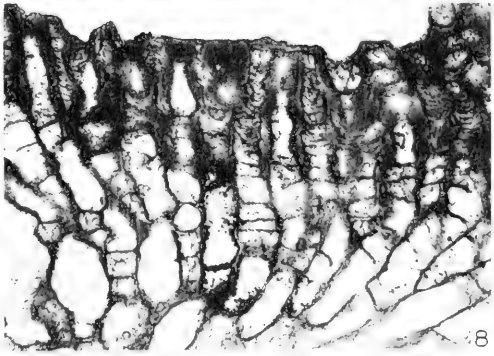
8


1


2

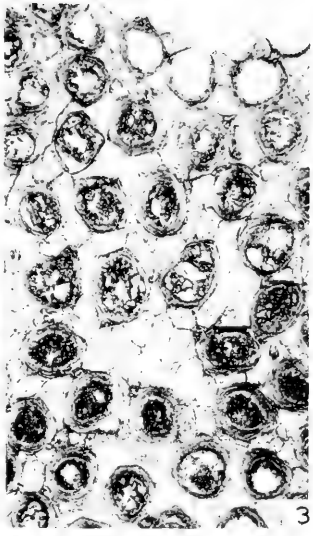
3

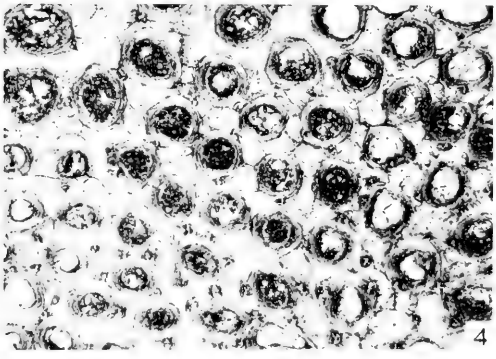
4

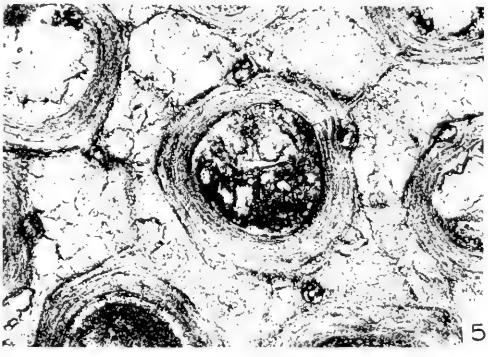
5


6

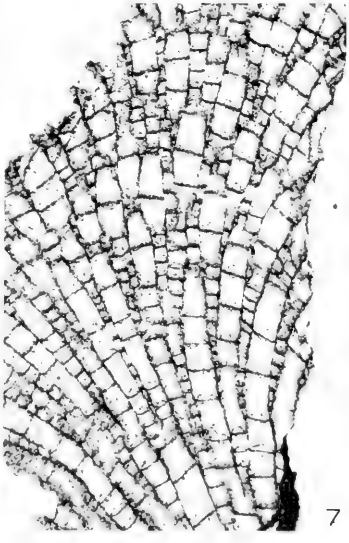
7

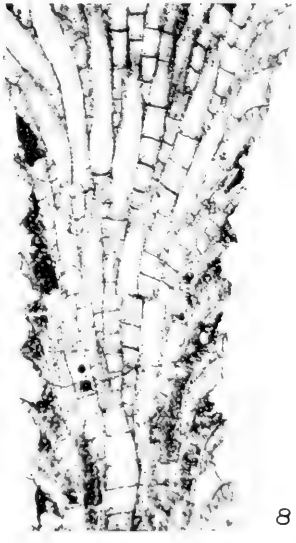
8

Explanation of Plate 62

Figure *Page*

1-6. Hemiphragma irrasum (Ulrich) 276

1. Longitudinal section, × 20, with hemiphragms in submature zone and in thick-walled mature zone. Hypotype, USNM 167813. Locality V, 23.8-28.4 m. 2. Longitudinal section, × 80, which cuts small mesopore, prominent inclined wall laminae that meet along dark median plane of contact, and hemiphragms continuous with wall laminae. Hypotype, USNM 167812. Locality II, 8.2-13.7 m. 3. Tangential section, × 20, which illustrates well-developed girdle-like bands around zooecia, mesopores in lower part of photograph filled by calcareous deposits, and a monticule in center of photograph. Hypotype, USNM 167812. Locality II, 8.2-13.7 m. 4. Tangential section, × 20, which shows prominent acanthopores, most of which are located along the peripheries of girdle-like bands around zooecia, and local areas with mesopores filled by calcareous deposits. Hypotype, USNM 167812. Locality II, 8.2-13.7 m. 5. Tangential section, × 80, which illustrates thick girdle-like bands around zooecia indented by small acanthopores and thin-walled, polygonal mesopores. Hypotype, USNM 167812. Locality II, 8.2-13.7 m. 6. Tangential section, × 80, which cuts area of calcareous deposits in mesopores. Hypotype, USNM 167812. Locality II, 8.2-13.7 m.

7, 8. Calopora dumalis (Ulrich) 279

7. Longitudinal section, × 20, of a specimen with atypically abundant diaphragms in zooecia that have reached full diameter. Hypotype, USNM 167814. Locality III, 19-1-22.0 m. 8. Longitudinal section, × 20, which shows abundant diaphragms in proximal portions of zooecia, sparse diaphragms in zooecia that have reached full diameter, and oblique zooecia at the zoarial surface. Hypotype, USNM 177815. Locality, XV, 1.5-4.3 m.

Explanation of Plate 63

Figure *Page*

1, 2. **Calopora dumalis** (Ulrich) 279

1. Tangential section, × 20, which shows subround to suboval zooecia and polygonal mesopores. Hypotype, USNM 167814. Locality III, 19.1-22.0 m. 2. Tangential section, × 80, which illustrates thin walls with median dark line. Hypotype, USNM 167814. Locality III, 19.1-22.0 m.

3-8. **Calopora ovata** McKinney, n. sp. 282

3. Longitudinal section, × 20, which illustrates the common occurrence of diaphragms in proximal portions of zooecia and the abundant occurrence of diaphragms throughout most mesopores, and widely spaced diaphragms in zooecia that have reached their full diameter. Paratype, USNM 167818. Locality XV, 13.7-16.6 m. 4. Longitudinal section, × 20, which shows smooth curvature of zooecia into thick-walled mature zone. Holotype, USNM 167816. Locality XV, 13.7-16.6 m. 5. Longitudinal section, × 80, which exhibits V-shaped wall laminae, dark median line between adjacent zooecia, and close diaphragm spacing in mesopore. Holotype, USNM 167816. Locality XV, 13.7-16.6 m. 6. Tangential section, × 20, which shows thick-walled, oval zooecia and abundant mesopores. Holotype, USNM 167816. Locality XV, 13.7-16.6 m. 7. Tangential section, × 20, which illustrates well-developed, thick walls of mature zooecia, thin walls of immature zooecia in lower right of photograph, and abundant mesopores. Paratype, USNM 167817. Locality XV, 13.7-16.6 m. 8. Tangential section, × 80, which illustrates thick laminar walls, oval zooecial tubes, and irregularly polygonal mesopores. Paratype, USNM 167817. Locality XV, 13.7-16.6 m.

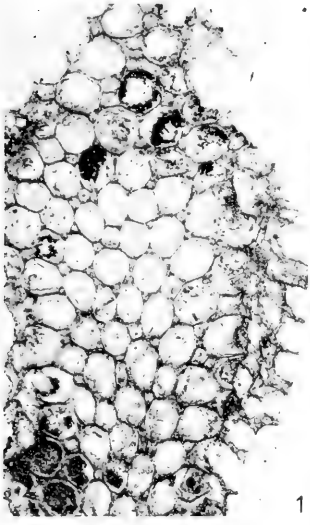
1

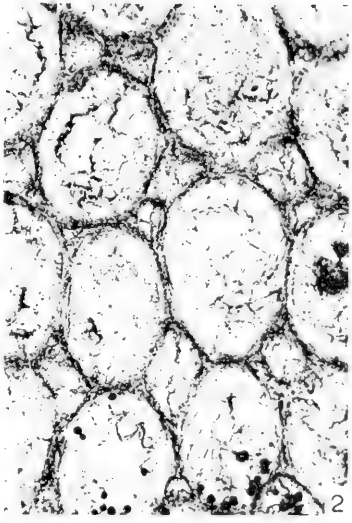
2


3


4


5

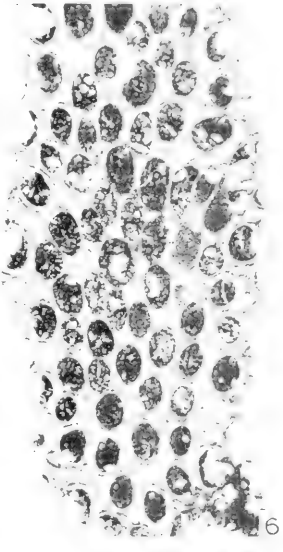
6

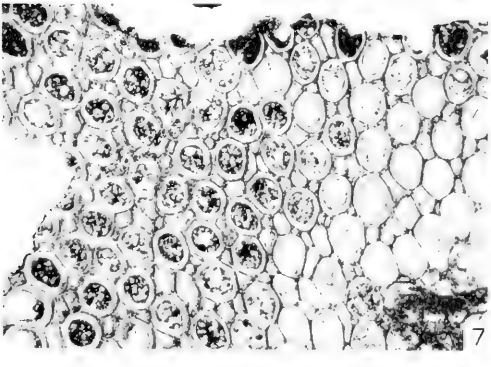
7

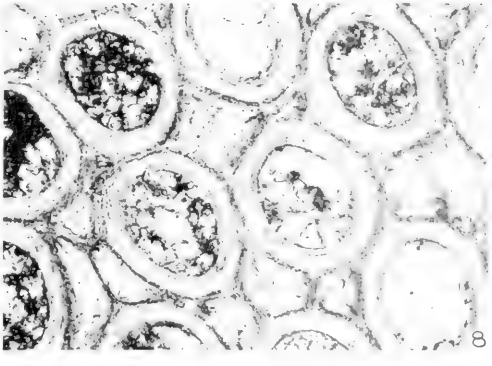
8


1


2


3


4

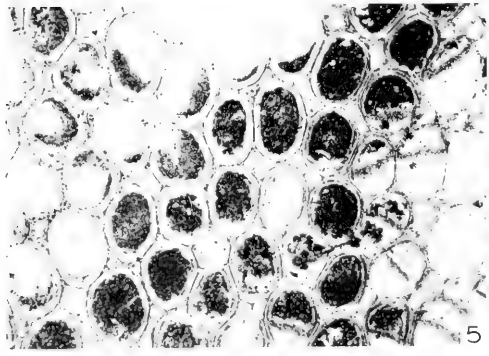
5

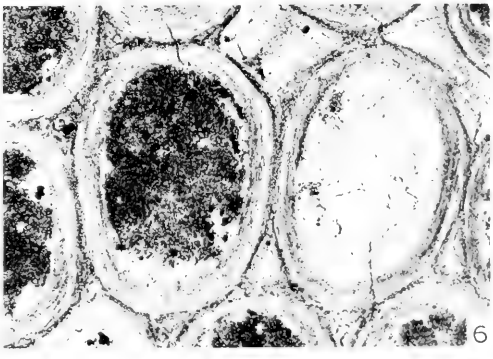
6

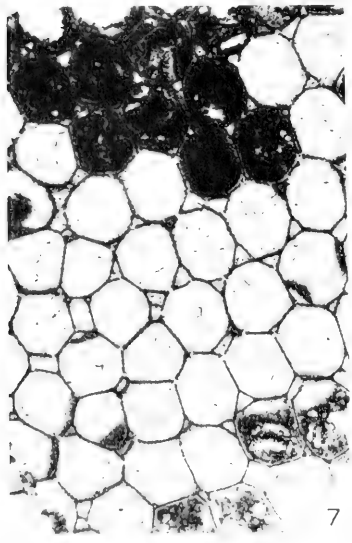
7


8

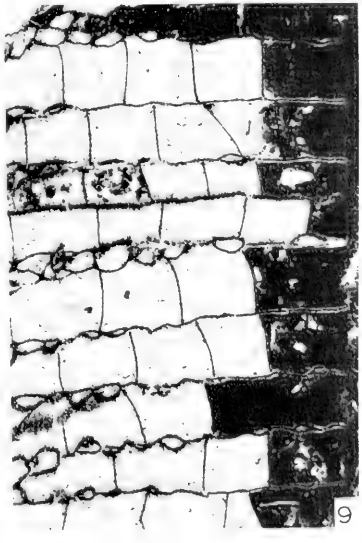
9

Explanation of Plate 64

Figure *Page*

1-6. **Calopora spissata** Coryell 285

1. Longitudinal section, × 20, which illustrates closely spaced diaphragms in proximal portions of zooecia, lack of diaphragms in immature zooecia that have reached full diameter, rare diaphragms in mature zooecia, mesopores that are restricted to basal part of mature zone, and thick mature zooecial walls. Hypotype, USNM 167820. Locality XVII, 0-4.0 m. 2. Longitudinal section, × 80, which shows diaphragms in mesopore that is closed distally by wall deposits, wall laminae which dip steeply, and dark lines which represent zooecial borders. Hypotype, USNM 167820. Locality XVII, 0-4.0 m. 3. Longitudinal section, × 80, which illustrates a mesophore that pinches out distally. Hypotype, USNM 167820. Locality XVII, 0-4.0 m. 4. Longitudinal section, × 20, similar to figure 1 above but with slightly thinner mature walls. Hypotype, USNM 167821. Locality IV, 7.0-12.2 m. 5. Tangential section, × 20, which shows large size of zooecia that are oval in cross-section and abundant mesopores in zooecial corners. Hypotype, USNM 167821. Locality IV, 7.0-12.2 m. 6. Tangential section, × 80, which illustrates thick, laminar zooecial walls and mesopores that lack walls or have thin walls between zooecia. Hypotype, USNM 167821. Locality IV, 7.0-12.2 m.

7-9. **Diplotrypa anchicatenulata** McKinney, n. sp. 288

7. Tangential section, × 20, which illustrates suboval to polygonal zooecial cross-sections and mesopores at most zooecial corners. Holotype, USNM 167822. Locality XVI, 15.7-18.9 m. 8. Longitudinal section, × 80, which shows moniliform mesopore and thin zooecial walls where zooecial tubes are filled by sparry calcite. Holotype, USNM 167822. Locality XVI, 15.7-18.9 m. 9. Longitudinal section, × 20, which shows uniform diaphragm spacing in zooecia and moniliform mesopores, some of which consist of isolated vesicles. Holotype, USNM 167822. Locality XVI, 15.7-18.9 m.

Explanation of Plate 65

Figure *Page*

1. **Diplotrypa anchicatenulata** McKinney, n. sp. 288

Longitudinal section, × 80, which exhibits three-part nature of walls where protected by micrite matrix, with thin, median dark band surrounded by fibers oriented perpendicular to surface of walls. Holotype, USNM 167822. Locality XVI, 15.7-18.9 m.

2-8. **Nicholsonella acanthobscura** McKinney, n. sp. 292

2. Longitudinal section, × 80, which illustrates mesopores with recrystallized, vague laminae and infilled zooecial tubes. Holotype, USNM 187824. Locality XVI, 1.7-15.7 m. 3. Longitudinal section, × 20, with widely spaced diaphragms in zooecia and mesopores in thin mature zone with closely spaced diaphragms. Holotype, USNM 167824. Locality XVI, 1.7-15.7 m. 4. Tangential section, × 20, of specimen which has larger zooecia and fewer mesopores than typical. Paratype, USNM 167825. Locality XVII, 0-4.0 m. 5. Tangential section, × 20, which shows typical state of small, suboval zooecial tubes separated by abundant mesopores, some of which are infilled. Holotype, USNM 167824. Locality XVI, 1.7-15.7 m. 6. Tangential section, × 80, which exhibits small zooecial tubes and altered walls that obscure zooecial and mesopore boundaries; vague, large acanthopores may be distinguished with difficulty, especially in the lower part of the figure and around the upper of the two median zooecia. Holotype, USNM 167824. Locality XVI, 1.7-15.7 m. 7. Longitudinal section, × 20, of ramose specimen with moderately spaced diaphragms in zooecia and closely spaced diaphrams in mesopores. Paratype, USNM 167826. Locality V, 23.8-28.4 m. 8. Vertical section, × 20, of multilaminar specimen with same internal features as in figure 7 above. Paratype, USNM 167827. Locality V, 23.8-28.4 m.

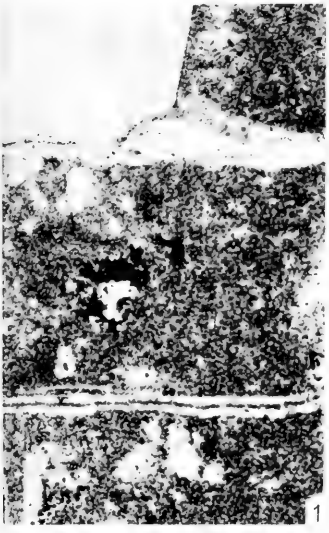
1


2

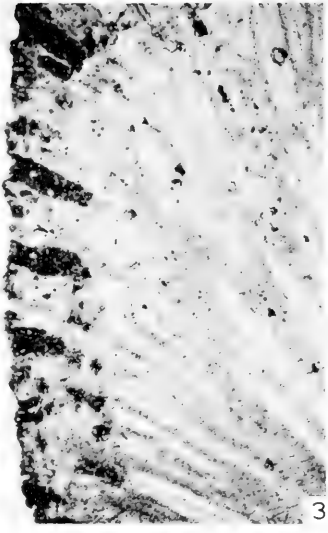
3

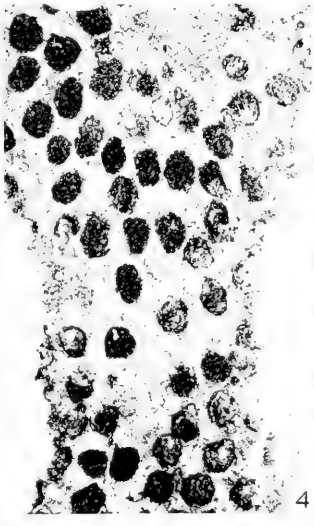
4

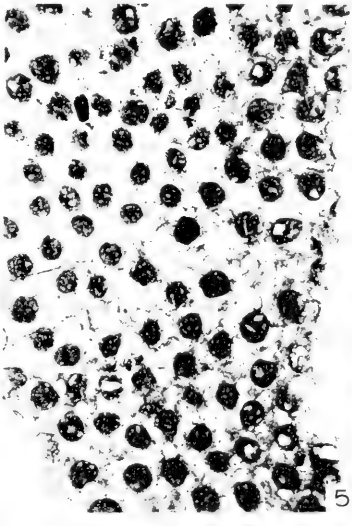
5

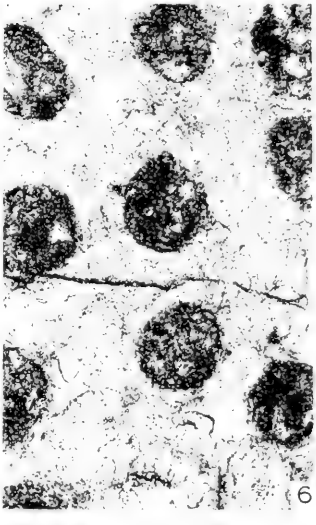
6


7

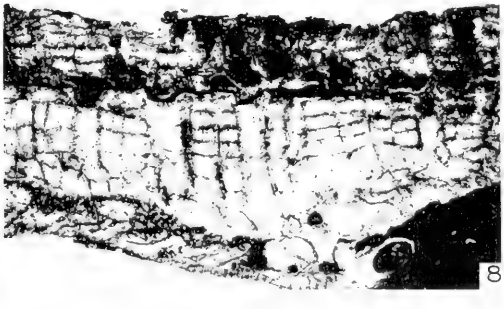
8


1


2

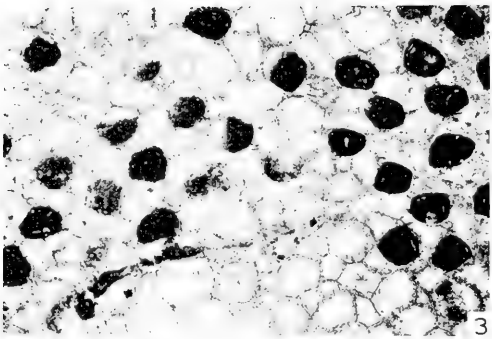
3

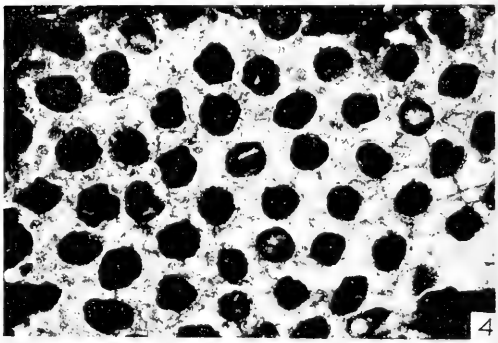
4


5

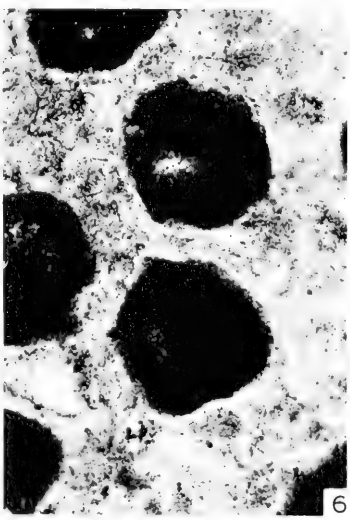
6


7

Explanation of Plate 66

Figure *Page*

1-7. **Nicholsonella parafrondifera** McKinney, n. sp. 294

1. Longitudinal section, × 20, which illustrates laminate growth form, recrystallized walls, and abundant mesopores with closely spaced diaphragms. Holotype, USNM 167829. Locality II, 3.7-8.2 m. 2. Longitudinal section, × 80, which shows zooecial tubes infilled by matrix and almost obscured walls and diaphragms in both zooecia and mesopores. Holotype, USNM 167829. Locality II, 3.7-8.2 m. 3. Tangential section, × 20, which illustrates thin-walled region in center of photograph, with open polygonal mesopores and few acanthopores. Holotype, USNM 167829. Locality II, 3.7-8.2 m. 4. Tangential section, × 20, which illustrates suboval zooecia, abundant mesopores, and large, abundant acanthopores, especially in the lower right corner of the figure. Holotype. USNM 167829. Locality II, 3.7-8.2 m. 5. Tangential section, × 80, of thin-walled region with distinct walls bounded by a diffuse, recrystallized zone. Holotype, USNM 167829. Locality II, 3.7-8.2 m. 6. Tangential section, × 80, of more thick-walled area than in figure 5 above which contains common acanthopores. Holotype, USNM 167829. Locality II, 3.7-8.2 m. 7. Longitudinal section, × 20, which shows moderately spaced diaphragms in zooecia, gentle curvature of zooecia into mature zone, and mesopores in mature zone. Paratype, USNM 167830. Locality VI, 4.9-10.5 m.

Explanation of Plate 67

Figure *Page*

1-4. **Nicholsonella pulchra** Ulrich 296

1. Longitudinal section, × 20, which shows gentle curvature of zooecia into mature zone, characterized by abundant diaphragms and mesopores. Hypotype, USNM 167832. Locality II, 8.2-13.7 m. 2. Tangential section, × 20, which exhibits suboval zooecia, abundant mesopores and acanthopores, and altered zooecial walls. Hypotype, USNM 167832. Locality II, 8.2-13.7 m. 3. Tangential section, × 20, which shows same characters as in figure 2 above but with slightly larger zooecia and some mesopores cut below the zone of infilled material. Wall thickness and clearly defined mesopores and acanthopores in zooecial and mesopore corners are best illustrated in the lower portion of the figure. Hypotype, USNM 167832. Locality II, 8.2-13.7 m. 4. Tangential section, × 80, of same specimen as in figures 2 and 3 above, which shows details of suboval zooecia, mesopores, some of which are infilled, acanthopores which slightly inflect zooecial tubes in a few places, and altered walls. Hypotype, USNM 167832. Locality II, 8.2-13.7 m. Number is missing on fig. 5 of pl. 67.

5-8. **Nicholsonella inflecta** McKinney, n. sp. 299

5. Tangential section, × 20, which illustrates irregularly subcircular zooecia and swollen areas in altered walls which inflect zooecial tubes and which represent acanthopores (number missing on plate). Holotype, USNM 167833. Locality IV, 20.6-23.9 m. 6. Tangential section, × 80, which suggests vaguely concentric swollen areas in zooecial walls that represent acanthopores. Holotype, USNM 167833. Locality IV, 20.6-23.9 m. 7. Longitudinal section, × 20, which shows diaphragms in zooecia, gentle curvature of zooecia into mature zone, and mesopores in mature zone. Holotype, USNM 167833. Locality IV, 20.6-23.9 m. 8. Longitudinal section, × 20, which shows thicker mature zone than in figure 7 above and elongate moniliform nature of proximal portions of some zooecia. Paratype, USNM 167834. Locality II, 8.2-13.7 m.


1

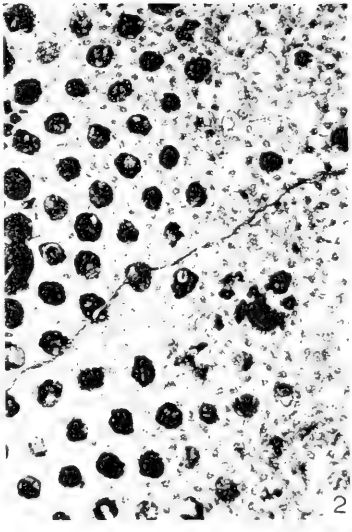
2

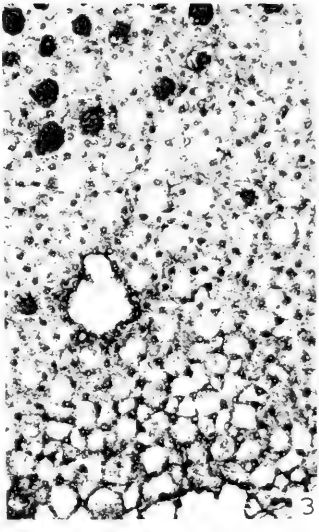
3

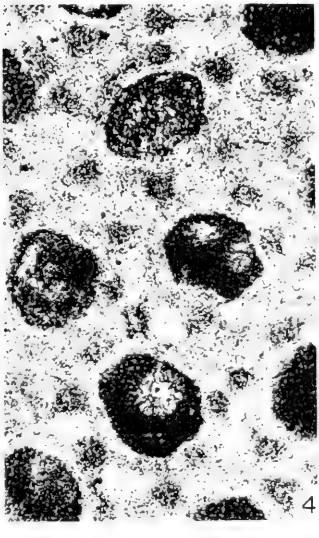
4

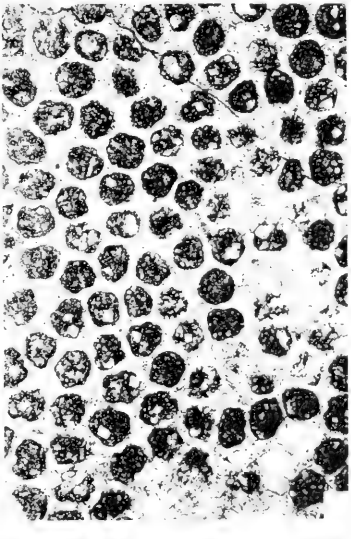

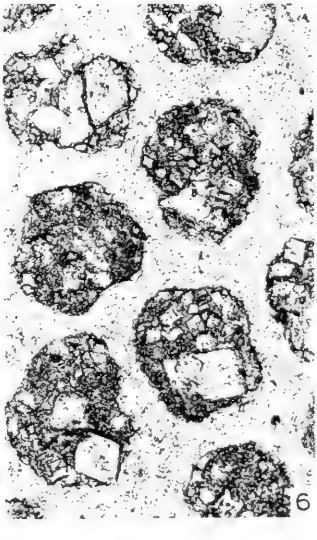
6

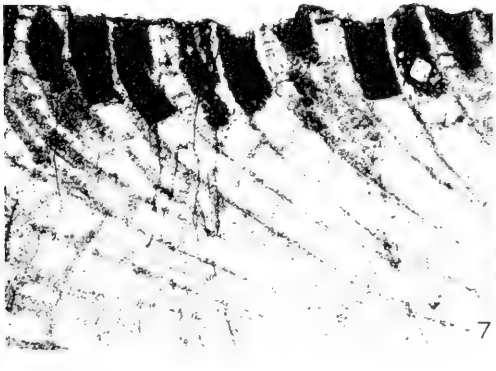
7


8

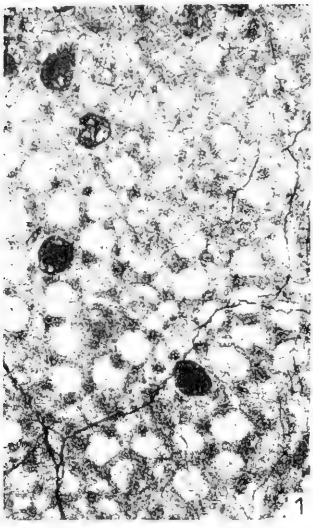
1

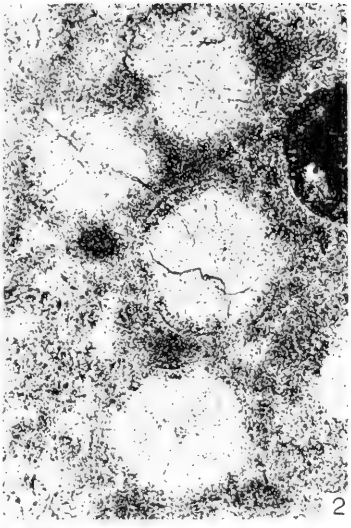
2

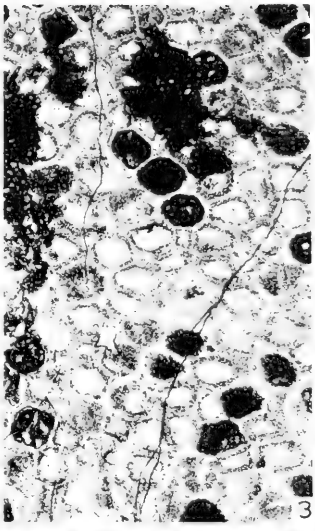
3

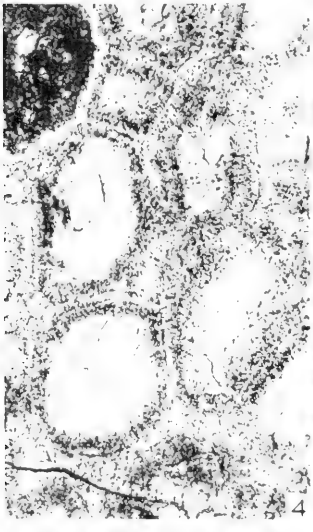
4


5


6

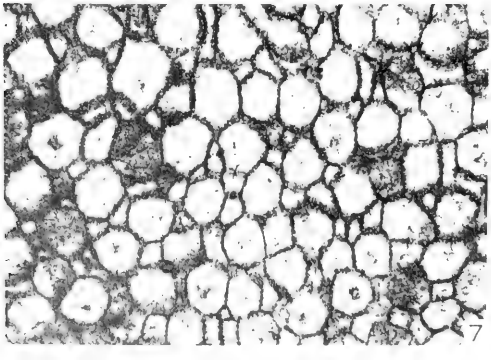
7

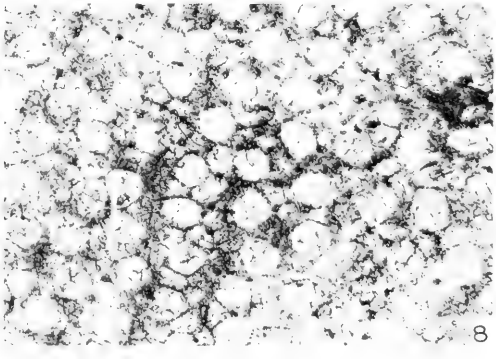
8

Explanation of Plate 68

Figure *Page*

1, 2. **Nicholsonella inflecta** McKinney, n. sp. 299

1. Tangential section, × 20, which shows more distinct acanthopores than in figure 5 of Plate 67. Paratype, USNM 167834. Locality II, 8.2-13.7 m. 2. Tangential section, × 80, which shows acanthopores and locally preserved distinct contact between altered zooecial walls and zooecial tubes. A diffuse median dark line is present in the wall on the upper left of the center zooecium. Paratype, USNM 167834. Locality II, 8.2-13.7 m.

3-5. **Nicholsonella** aff. **N. mariae** Astrova 301

3. Tangential section, × 20, which illustrates polygonal zooecia and sparse mesopores. Hypotype, USNM 167836. Locality II, 8.2-13.7 m. 4. Tangential section, × 80, which exhibits thin, altered zooecial walls with edges of walls fairly well preserved. Hypotype, USNM 167836. Locality II, 8.2-13.7 m. 5. Longitudinal section, × 20, which exhibits uniform spacing of diaphragms and gentle curvature of zooecia into mature zone. Hypotype, USNM 167836. Locality II, 8.2-13-7 m.

6-8. ?**Nicholsonella** sp. 302

6. Longitudinal section, × 20, which shows diaphragms in zooecia and slightly moniliform mesopores. Hypotype, USNM 167837. Locality XVII, 0-4.0 m. 7. Tangential section, × 20, which illustrates thin-walled, polygonal zooecia, and abundant mesopores. Hypotype, USNM 167837. Locality XVII, 0-4.0 m. 8. Tangential section, × 20, of specimen with acanthopores and more mesopores and smaller zooecia than in figure 7 above. Hypotype, USNM 167838. Locality IV, 7.0-12.2 m.

INDEX

Note: Light face type refers to page numbers. Bold face type refers to plate numbers.

A

abrupta, Eridotrypa **57,** 262-264, 266
acanthobscura, Nicholsonella **65,** 212, 292-294
aedilis, Eridotrypa 261, 262
Aisenvergia 259
Allen, A. T. & Lester, J. G. 196, 208
Amplexopora 196, 219, 250
Amplexopora sp. **56,** 258, 259
anchicatenulata, Diplotrypa **64, 65,** 211, 288-290
angularis, Mesotrypa 243
Anstey, R. L. & Perry, T. G. 214, 215
arborea, Monticulipora 223, 224
arcuata, Eridotrypa **57, 58,** 212, 264-267
Astrova, G. G. 229, 230, 236, 281, 290, 291

B

Baltic 254, 261
Bassler, R. S. 196, 222, 236, 254, 261, 278
Batostoma 219, 269, 287, 291
Batostoma sp. **61,** 274-276
Bekker, H. 281
Big Ridge, Wills Valley, Alabama 197
Blackriveran 208, 209, 254
Boardman, R. S. 217, 220, 221, 275, 290, 291
Boardman, R. S. & Cheetham, A. H. 220
Boardman, R. S. & Utgaard, John 212, 246
Bork, K. B. & Perry, T. G.
..... 196, 214, 220, 222, 236, 237, 239, 254, 273, 278, 289
Brown, G. D. 196
Butts, Charles 195, 196

C

callitoecha, Homotrypa 239
Calopora 219, 279
Carters Limestone 208, 211
catenulata, Diplotrypa 289, 290
Central Basin, Tennessee 199, 209, 268
Chazyan 208
Cheetham, A. H. 214
Chickamauga Group 195, 196, 199, 208, 209, 210, 211, 212, 216, 236, 264
compacta, Prasopora 229, 230
Constellaria 287, 290, 291
Cooper, G. A. 195, 208, 211
Coryell, H. N. 196, 268, 269, 295, 297
crownensis, Eridotrypa 265
Cuffey, R. J. 214, 220, 222
Cumings, E. R. 246
Cumings, E. R. & Galloway, J. J. 246
Cystoporata 291

D

Dekayella 246
Dekayia 246
Diazipora 287
dickeyvillensis, Homotrypa 236, 237

INDEX

Diplotrypa 219, 287, 288
Diplotrypella 287
discula, Prasopora **46, 47,** 211, 225-228, 230
Dittopora 291
dumalis, Calopora **62, 63,** 279-282, 283
Dunaeva, N. N. 222, 240, 259
Dunaeva, N. N. & Morozova, I. P. 222

E

Eridotrypa 219, 240, 259
Estonia 278
exilis, Homotrypa 239, 240

F

falesi, Prasopora 225, 227
Fort Payne, Alabama 195
Fox, P. P. & Grant, L. F. 199
Fritz, M. A. 196, 254
fritzae, Prasopora 225-228
frondifera, Nicholsonella 211, 295, 297, 298

G

Gadsden, Alabama 195
Geological Survey of Alabama 197
Georgia, northwestern 209
Glade Limestone 268
Guttenberg Formation 239, 278

H

Hallopora 287
Hemiphragma 219, 276, 287
Heterotrypa 219, 221, 244
Homotrypa 219, 221, 234, 250
Horowitz, A. S. 215

I

Idiotrypa 290, 291
incontroversa, Calopora 283
increbescens, Batostoma **60, 61,** 272-274
infida, Mesotrypa 243
inflecta, Nicholsonella **67, 68,** 211, 299-301
Iowa 278
irrasum, Hemiphragma **61, 62,** 212, 276-279
irregularis, Nicholsonella 293, 301

J

James, U. P. 225

K

Kiepura, Maria 281
Kopaevich, G. P. 262

L

Lebanon Limestone 208, 211, 268
Leioclema 291
libana, Eridotrypa **58,** 211, 267-269
Loeblich, A. R. 196, 239, 264
lowvillensis, Homotrypa 239

M

macrostoma, Hallopora 284, 286, 287
mariae, Nicholsonella 302
aff. mariae, Nicholsonella **68,** 211, 301, 302
megacystata, Prasopora **48,** 212, 228-230
Mesotrypa 219, 221, 241
Mesotrypa sp. 196
Metrarabdotos 215
Milici, R. C. 197, 209, 211
Milici, R. C. & Smith, J. W. 209
minnesotensis, Amplexopora 216
minnesotensis, Homotrypa 236, 237
minor, Eridotrypa **56,** 212, 239, 240, 260-262
moniliformis, Diplotrypa 289
moniliformis argutus, Diplotrypa 290
Monotrypa 287
Monticulipora 219, 222, 233, 287
Morozova, I. P. 222
multispinosa, Stigmatella 243
multitabulata, Homotrypa 239
Murfreesboro Limestone 208
Murfreesboro, Tennessee 297
mutabilis, Eridotrypa 261, 262

N

Nashville Group 209
Newfoundland 196
New York 196
Nicholson, H. A. 287
Nicholsonella 214, 219, 290
?Nicholsonella sp. **68,** 302-304
Nickles, J. M. & Bassler, R. S. 287
North Carolina, University of 197

O

Ontario 254
Ordovician 195, 196
Ottawa 196
ovata, Calopora **63,** 211, 282, 283, 285

P

parafrondifera, Nicholsonella **66,** 211, 294-296, 299
parallela, Monticulipora **46,** 222-224
patera, Heterotrypa **52, 53,** 211, 221, 248-252
Perry, T. G. 196, 214, 237, 239, 254
Pierce Limestone 208, 297
Polycylindricus 259
Porterfieldian 208
Prasopora 219, 224, 225
Prasopora sp. **48,** 230, 231
?Prasopora sp. **48, 49,** 231-234
pulchra, Nicholsonella **67,** 211, 295, 296-299

Q

Quebec 196
Quimbys Mill Formation 239

R

Ridley Limestone 208, 211
ridleyana, Dekayella 196
ridleyana, Heterotrypa **51, 52,** 212, 244-248
robusta, Pachydictya 196
Rodgers, John 208
Rogers, W. S. 195, 196, 208, 209
Ross, J. P. 196, 215-217, 220, 222, 224, 225, 259-261, 281

S

Safford, J. M. 268
sagittata, Homotrypa 239
Sardeson, F. W. 196, 236, 254
Sequatchie Valley, Tennessee 209
Simpson, G. G., *et al.* 214, 215, 254
Sowerbyella 225
Sparling, D. R. 196
sparsa, Mesotrypa **50, 51,** 212, 221, 241-244
Spechts Ferry Shale 239
spissata, Calopora **64,** 212, 284-287
Stellipora 287, 290, 291
Stigmatella 221, 243, 244
stonensis, Heterotrypa 249, 250, 252
Stones River Group 196, 208, 209, 211, 268
Stromatrypa 275, 287, 291
subramosa, Homotypa **49, 50,** 212, 234-237

T

Tennessee 196, 208
Trematopora 290, 291
Trentonian 208, 211, 224
Troedsson, G. T. 236

U

Ulrich, E. O. 196, 223, 236, 237, 239, 243, 254, 261, 271, 278, 280, 281, 287, 290, 291, 297
Ulrich, E. O. & Bassler, R. S. 196, 243
ulrichi, Homotrypa 239
United States National Museum 196, 246, 283
Utgaard, John & Perry, T. G. 214

V

vacua, Homotrypa **50,** 212, 238-241
varium, Batostoma **59, 60,** 212, 269-271
Vinassa deRegny, Paolo 287, 291
Volnovachia 259

W

Wilderness 208, 211
Wills Valley, Alabama 195, 198, 199, 208, 209, 211, 212, 216, 226, 227
Wilson, A. E. & Mather, K. F. 254, 262
Wilson, A. O. 196, 197, 199
Wilson, C. W. 196, 199, 208
winchelli, Amplexopora **54, 55,** 212, 250-255, 257
winchelli spinulosa, Amplexopora 254, 255, 257
aff. winchelli spinulosa, Amplexopora **55,** 255-258

XLV. (No. 204). 564 pp., 63 pls. 18.00
Venezuela Cenozoic pelecypods

XLVI. (Nos. 205-211). 419 pp., 70 pls. 16.00
Large Foraminifera, Texas Cretaceous crustacean, Antarctic Devonian terebratuloid, Osgood and Paleocene Foraminifera, Recent molluscan types.

XLVII. (Nos. 212-217). 584 pp., 83 pls. 18.00
Eocene and Devonian Foraminifera, Venezuelan fossil scaphopods and polychaetes, Alaskan Jurassic ammonites, Neogene mollusks.

XLVIII. (No. 218). 1058 pp., 5 pls. 18.00
Catalogue of the Paleocene and Eocene Mollusca of the Southern and Eastern United States.

XLIX. (Nos. 219-224). 671 pp., 83 pls. 18.00
Peneroplid and Australian forams, North American carpoids, South Dakota palynology, Venezuelan Miocene mollusks, *Voluta*.

L. (Nos. 225-230). 518 pp., 42 pls. 18.00
Venezuela and Florida cirripeds, Antarctic forams, Linnaean Olives, Camerina, Ordovician conodonts, Niagaran forams.

LI. (Nos. 231-232). 420 pp., 10 pls. 18.00
Antarctic bivalves, Bivalvia catalogue.

LII. (Nos. 233, 236). 387 pp., 43 pls. 18.00
New Zealand forams, Stromatoporoidea, Indo-Pacific, Miocene-Pliocene California forams.

LIII. (Nos. 237-238). 488 pp., 45 pls. 18.00
Venezuela Bryozoa, Kinderhookian Brachiopods.

LIV. (Nos. 239-245). 510 pp., 50 pls. 18.00
Dominican ostracodes, Texan pelecypods, Wisconsin mollusks, Siphocypraea, Lepidocyclina, Devonian gastropods, Miocene Pectens Guadaloupe.

LV. (Nos. 246-247). 657 pp., 60 pls. 18.00
Cenozoic corals, Trinidad Neogene mollusks.

LVI. (Nos. 248-254). 572 pp., 49 pls. 18.00
American Foraminifera, North Carolina fossils, coral types, Belanski types, Venezuelan Cenozoic Echinoids, Cretaceous Radiolaria, Cymatiid gastropods.

LVII. (Nos. 255-256). 321 pp., 62 pls. 18.00
Alaskan Jurassic ammonites, Pt. II, Jurassic Ammonitina New Guinea.

LVIII. (Nos. 257-262). 305 pp., 39 pls. 18.00
Cretaceous Radiolaria, Cretaceous Foraminifera, Pacific Silicoflagellates, North American Cystoidea, Cincinnatian Cyclonema, new species Vasum.

LIX. (No. 263). 314 pp. 18.00
Bibliography of Cenozoic Echinoidea.

LX. (Nos. 264-266). 189 pp., 45 pls. 11.55
Jurassic-Cretaceous Hagiastridae, Venezuela cirriped, Palynology of Iowa.

Palaeontographica Americana

Volume I. See Johnson Reprint Corporation, 111 Fifth Ave., New York, N. Y. 10003
Monographs of Arcas, Lutetia, rudistids and venerids.

II. (Nos. 6-12). 531 pp., 37 pls. 23.00
Heliophyllum halli, Tertiary turrids, Neocene Spondyli, Paleozic cephalopods, Tertiary Fasciolarias and Paleozoic and Recent Hexactinellida.

III. (Nos. 13-25). 513 pp., 61 pls. 28.00
Paleozoic cephalopod structure and phylogeny, Paleozoic siphonophores, Busycon, Devonian fish studies, gastropod studies, Carboniferous crinoids, Cretaceous jellyfish, Platystrophia and Venericardia.

IV. (Nos. 26-33). 492 pp., 72 pls. 28.00
Rudist studies Busycon, Dalmanellidae, Byssonychia, Devonian lycopods, Ordovican eurypterids, Pliocene mollusks.

V. (Nos. 34-37). 445 pp., 101 pls. 32.00
Tertiary Arcacea, Mississippian pelecypods, Ambonychiidae, Cretaceous Gulf Coastal forams.

VI. (Nos. 38-41). 444 pp., 83 pls. 35.00
Lycopsids and sphenopsids of Freeport Coal, Venericardia, Carboniferous crinoids, Trace fossils.

VII. (Nos. 42-45). 257 pp., 58 pls. 23.50
Torreites Sanchezi, Cancellariid Radula, Ontogeny, sexual dimorphism trilobites, Jamaican Rudists.

Vols. I-XXIII. See Kraus Reprint Corp., 16 East 46th St., New York, N. Y. 10017, U.S.A.

XXIV. (Nos. 80-87). 334 pp., 27 pls. 12.00
Mainly Paleozoic faunas and Tertiary Mollusca.

XXV. (Nos. 88-94B). 306 pp., 30 pls. 12.00
Paleozoic fossils of Ontario, Oklahoma and Colombia, Mesozoic ehinoids, California Pleistocene and Maryland Miocene mollusks.

XXVI. (Nos. 95-100). 420 pp., 58 pls. 14.00
Florida Recent marine shells, Texas Cretaceous fossils, Cuban and Peruvian Cretaceous, Peruvian Eogene corals, and geology and paleontology of Ecuador.

XXVII. (Nos. 101-108). 376 pp., 36 pls. 14.00
Tertiary Mollusca, Paleozoic cephalopods, Devonian fish and Paleozoic geology and fossils of Venezuela.

XXVIII. (Nos. 109-114). 412 pp., 34 pls. 14.00
Paleozoic cephalopods, Devonian of Idaho, Cretaceous and Eocene mollusks, Cuban and Venezuelan forams.

XXIX. (Nos. 115-116). 738 pp., 52 pls. 18.00
Bowden forams and Ordovician cephalopods.

XXX. (No. 117). 563 pp., 65 pls. 16.00
Jackson Eocene mollusks.

XXXI. (Nos. 118-128). 458 pp., 27 pls. 16.00
Venezuelan and California mollusks, Chemung and Pennsylvanian crinoids, Cypraeidae, Cretaceous, Miocene and Recent corals, Cuban and Floridian forams, and Cuban fossil localities.

XXXII. (Nos. 129-133). 294 pp., 39 pls. 16.00
Silurian cephalopods, crinoid studies, Tertiary forams, and Mytilarca.

XXXIII. (Nos. 134-139). 448 pp., 51 pls. 16.00
Devonian annelids, Tertiary mollusks, Ecuadoran stratigraphy paleontology.

XXXIV. (Nos. 140-145). 400 pp., 19 pls. 16.00
Trinidad Globigerinidae, Ordovician Enopleura, Tasmanian Ordovician cephalopods and Tennessee Ordovician ostracods and conularid bibliography.

XXXV. (Nos. 146-154) 386 pp., 31 pls. 16.00
G. D. Harris memorial, camerinid and Georgia Paleocene Foraminifera, South America Paleozoics, Australian Ordovician cephalopods, California Pleistocene Eulimidae, Volutidae, and Devonian ostracods from Iowa.

XXXVI. (Nos. 155-160). 412 pp., 53 pls. 16.00
Globotruncana in Colombia, Eocene fish, Canadian Chazyan Antillean Cretaceous rudists, Canal Zone Foraminifera, fossils, foraminiferal studies.

XXXVII. (Nos. 161-164). 486 pp., 37 pls. 16.00
Antillean Cretaceous Rudists, Canal Zone Foraminifera, Stromatoporoidea.

XXXVIII. (Nos. 165-176). 447 pp., 53 pls. 18.00
Venezuela geology, Oligocene Lepidocyclina, Miocene ostracods, and Mississippian of Kentucky, turritellid from Venezuela, larger forams, new mollusks, geology of Carriacou, Pennsylvanian plants.

XXXIX. (Nos. 177-183). 448 pp., 36 pls. 16.00
Panama Caribbean mollusks, Venezuelan Tertiary formations and forams, Trinidad Cretaceous forams, American-European species, Puerto Rico forams.

XL. (No. 184). 996 pp., 1 pls. 18.00
Type and Figured Specimens P.R.I.

XLI. (Nos. 185-192). 381 pp., 35 pls. 16.00
Australian Carpoid Echinoderms, Yap forams, Shell Bluff, Ga. forams. Newcomb mollusks, Wisconsin mollusk faunas, Camerina, Va. forams, Corry Sandstone.

XLII. (No. 193). 673 pp., 48 pls. 18.00
Venezuelan Cenozoic gastropods.

XLIII. (Nos. 194-198). 427 pp., 29 pls. 16.00
Ordovician stromatoporoids, Indo-Pacific camerinids, Mississippian forams, Cuban rudists.

XLIV. (Nos. 199-203). 365 pp., 68 pls. 16.00
Puerto Rican, Antarctic, New Zealand forams, Lepidocyclina, Eumalacostraca.